LAYER STRIPPING SOLUTIONS OF INVERSE SEISMIC PROBLEMS

by

Andrew Emil Yagle

B.S.E., University of Michigan
(1978)

S.M., Massachusetts Institute of Technology
(1981)

E.E., Massachusetts Institute of Technology
(1982)

SUBMITTED IN PARTIAL FULFILLMENT

OF THE REQUIREMENTS FOR THE DEGREE OF

DOCTOR OF PHILOSOPHY

at the

MASSACHUSETTS INSTITUTE OF TECHNOLOGY

February, 1985

Signature of Author _____
Department of Electrical Engineering
and Computer Science, January 18, 1985

Certified by _____
Bernard C. Levy,
Thesis Supervisor

Accepted by _____
Arthur C. Smith, Chairman
Departmental Committee on Graduate Students

LAYER STRIPPING SOLUTIONS OF INVERSE SEISMIC PROBLEMS

by

Andrew Emil Yagle

Submitted to the Department of Electrical Engineering and Computer Science on January 18, 1985, in partial fulfillment of the requirements for the Degree of Doctor of Philosophy.

ABSTRACT

The inverse scattering theory concept of layer stripping is applied to a variety of inverse seismic problems. This results in fast algorithms that solve these problems more simply and quickly than techniques used previously on these problems, and also admit physical insight into their operation.

A layer stripping algorithm works by recursively identifying and stripping away differential layers of the medium. As the wave front of the excitation passes through a given depth z, the first non-zero value of the medium response at depth z yields information about the medium at depth z. Then the excitation and response can be propagated through the known differential layer at depth z to depth $z + \Delta$, where the process is repeated.

The inverse seismic problems for which layer stripping fast algorithm solutions are obtained include: (1) the reconstruction of layered acoustic and elastic media from their reflection responses to impulsive plane waves at non-normal incidence; (2) the reconstruction of a layered acoustic medium from its reflection response to a point impulsive or harmonic source; and (3) the reconstruction of a two-dimensionally inhomogeneous medium from its plane wave reflection response. None of these algorithms has appeared previously in the literature.

Computer runs of some of these algorithms are included, and their performance is quite satisfactory. Several procedures for improving their performance on noisy data are given. Some results on general inverse scattering theory, and relations between these fast algorithms and fast algorithms that exploit structure in matrices or the kernels of integral equations, are also presented.

Thesis Supervisor: Dr. Bernard C. Levy
Title: Associate Professor of Electrical Engineering and Computer Science.

ACKNOWLEDGMENTS

It is impossible to overstate the importance of the role my thesis supervisor, Professor Bernard Levy, has played throughout all phases of my experiences at MIT. His widespread interests, insights, comments, and suggestions for avenues of research have contributed enormously in making this thesis what it is. Without his encouraging support and invaluable guidance through the mazes of the EECS doctoral program, I would still be looking for a topic for my Master's Thesis.

I would also like to thank the other members of my thesis committee, Professor Arthur Baggeroer, Professor Sanjoy Mitter, Professor Alan Willsky, and Dr. George Frisk, for their interest in my work and for their helpful comments.

Without the generous support of the Exxon Education Foundation, in the form of an Exxon Teaching Fellowship, I would still be struggling to finish this research, even as you read this. I must also express my gratitude to the MIT Department of Electrical Engineering and Computer Science, not only for bestowing this fellowship on me, but also for supporting me throughout my stay at MIT with teaching assistantships and a Departmental Fellowship.

Special thanks go to the inimitable Professor Alvin Drake, who suffered me as a teaching assistant for three terms, allowing me to gain teaching experience. Teaching under Al was an experience not to be missed.

Thanks also to Becky Bayerl for a fine job of typing this thesis, to Arthur Giordani for drafting the figures, and to Helene George for typing countless papers and revisions over the last year and a half.

Finally, I would like to thank my parents, who in the most fundamental way made this thesis possible. To them I dedicate this thesis.

TABLE OF CONTENTS

CHAPTER I: Introduction 15

1.1 Motivation 15

1.2 Literature Survey. 20

1.3 Contributions of Thesis. 28

References 31

CHAPTER II: Layer Stripping and Inverse Scattering Theory . . 34

2.1 Introduction 34

2.2 Inverse Scattering Problems 35

2.3 Differential Methods for Inverse Scattering--Layer Stripping 45

2.3.1 The Continuous-Time Schur and Fast Cholesky Algorithms 46

2.3.2 Example: The Lossless Non-Uniform Transmission Line 53

2.3.3 Inverse Scattering for Asymmetric Two-Component Wave Systems 59

2.3.4 Example: The Non-Uniform Transmission Line with Losses 64

2.3.5 Other Differential Methods 68

2.4 Integral Equation Methods for Solving Inverse Scattering Problems. . 74

2.4.1 The Marchenko, Gel'fand-Levitan, and Krein Integral Equations . . . 75

2.4.2 The Krein-Levinson Algorithm 80

2.4.3 Inverse Scattering as Orthonormalization 84

2.5 Relations Between Differential and Integral Methods . . . 87

2.5.1 Differential vs. Integral Methods 87

2.5.2 Fast Cholesky vs. Krein-Levinson Algorithms . . . 90

2.5.3 Example: Linear Least-Squares Estimation of a Stochastic Process 93

References 102

CHAPTER III: The One-Dimensional Inverse Problem at Normal Incidence . . 106

3.1 Introduction 106

3.2 Solution of the Inverse Problem for a Continuous Medium . . 109

3.2.1 Basic Concepts of Acoustics 111

3.2.2 Mathematical Physics Solution for a Continuous Medium 120

3.2.3 Layer Stripping Solutions for a Continuous Medium 123

3.3 Solution of the Inverse Problem for a Discrete Medium . . . 129

3.3.1 Matrix Equation Solutions for a Discrete Medium. . . 132

3.3.2 Layer Stripping Solutions for a Discrete Medium. . . 142

3.4 Relations Between Discrete and Continuous Problems and Solutions . . . 146

3.4.1 Discrete to Continuous Transformation 146

3.4.2 Continuous to Discrete Transformation 149

References 153

CHAPTER IV: The One-Dimensional Inverse Problem. at Non-Normal Incidence 155

4.1 Introduction 155

4.2 Plane Waves at Oblique Incidence 162

4.2.1 Integral Equation Solutions. 162

4.2.2 Layer Stripping Solution for a Continuous Medium . . 167

4.2.3 Layer Stripping Solution for a Discrete Medium . . . 174

4.3 Impulsive Point Source 176

4.3.1 The Radon and Hankel Transforms 177

4.3.2 Layer Stripping Solution 183

4.4 Turning Points 186

4.4.1 Turning Points 186

4.4.2 Propagation of the Layer Stripping Algorithm Through a Turning Point . . . 198

References 202

CHAPTER V: Performance of the Non-Normal Incidence Inversion Algorithms . 203

5.1 Introduction 203

5.1.1 Forward vs. Backward Stability 203

5.1.2 Previous Work 207

5.1.3 Summary 209

5.2 Performance of the Algorithms in the Absence of Noise . . 211

5.2.1 Forward Problem Algorithms. 212

5.2.2 Inversion Algorithms 215

5.2.3 Frequency-Domain Layer Stripping Algorithms . . . 230

5.3 Performance of the Algorithm in the Presence of Noise . . 234

5.4 Modifications of the Algorithm for Dealing with Noisy Data . 254

5.4.1 Zeroing Out Reflection Coefficients Using the Condition Number 254

5.4.2 Use of Reflection Responses at More Than Two Angles of Incidence 256

5.4.3 Reconstruction of Slightly Lossy Media 268

5.5 Summary 274

References 278

CHAPTER VI: The Inverse Problem for a One-Dimensional Elastic Medium . . . 279

6.1 Introduction 279

6.2 Layer Stripping Solution for a Continuous Elastic Medium . . . 284

6.3 Alternative Formulations of the Algorithm 304

6.3.1 Dynamic Deconvolution 304

6.3.2 Elastic Medium with an Overlying Liquid Half-Space 306

6.3.3 Some Comments on Discrete Elastic Media 311

6.4 Computational Results 315

References 326

CHAPTER VII: The Inverse Problem for a Layered Acoustic Medium Probed by Spherical Harmonic Waves . 327

7.1 Introduction 327

7.2 The Half-Space Problem 333

7.2.1 Formulation of the Problem 333

7.2.2 Layer Stripping Solution of the Half-Space Problem . . . 339

7.3 The Free Surface Problem 351

7.4 Simple Illustrations of the Algorithms 359

7.4.1 Free Surface Problem--Analytic Example 360

7.4.2 Half-Space Problem--Computer Run 363

7.5 The Inverse Resistivity Problem 364

7.5.1 Formulation of the Problem. 364

7.5.2 Solution by Fast Algorithms 369

7.5.3 The Inverse Problem of Determining Reservoir Transmissivities 374

References 377

CHAPTER VIII: Higher Dimensional Inverse Seismic Problems 379

8.1 Introduction 379

8.2 Reconstruction of $\rho(x,y,z)$ for Constant Wave Speed 387

8.3 Reconstruction of $c(x,z)$ for Constant Density. 391

8.4 Generalizations of One-Dimensional Results to Higher Dimensions 399

8.4.1 The Two-Dimensional Non-Normal Incidence Problem. . . 400

8.4.2 The Two-Dimensional Normal Incidence Problem 404

References 408

CHAPTER IX: Conclusion 409

9.1 Summary 409

9.2 Suggestions for Further Research. 416

References 419

APPENDIX: Computer Programs 420

LIST OF FIGURES

CHAPTER II: Layer Stripping and Inverse Scattering Theory

2.1 Elementary scattering sections obtained by discretizing the two-component wave equations. . . . 38

2.2a Scattering for an impulsive wave incident from the left . . . 40

2.2b Scattering for an impulsive wave incident from the right. . . 40

2.3a Recursion pattern for updating the downgoing waves in the fast Cholesky algorithm. . . 49

2.3b Recursion pattern for updating the upgoing waves in the fast Cholesky algorithm. . . . 49

2.4 Infinitesimal section of a lossless non-uniform transmission line. . 54

2.5 The perceived load to the right of x. 57

2.6 Infinitesimal section of a lossy non-uniform transmission line. . . 65

2.7a Recursion pattern for updating $m_{11}(x,t)$ in the Krein-Levinson algorithm. . . . 83

2.7b Recursion pattern for updating $m_{21}(x,t)$ in the Krein-Levinson algorithm. . . . 83

2.8a Aggregate modelling filter for $y(\cdot)$. 97

2.8b Infinitesimal ladder sections associated with the Krein-Levinson algorithm. . . . 97

CHAPTER III: The One-Dimensional Inverse Problem at Normal Incidence

3.1 Scattering formulation of the inverse seismic problem. . . . 110

3.2 The discrete, Goupillaud, equal-traveltime layered medium . . 131

3.3 Notation for upgoing and downgoing waves at the top and bottom of each layer. . . . 133

3.4 Interaction of the downgoing and upgoing waves in layers i and i+1. . . 134

CHAPTER IV: The One-Dimensional Inverse Problem at Non-Normal Incidence

4.1 The non-normal incidence inverse problem 157

4.2 The point source inverse problem 158

CHAPTER V: Performance of the Non-Normal Incidence Inversion Algorithms

5.1a Result of running the frequency-domain method forward program FOR1 with the inverse program INVDISC, using 512 points. . . . 216

5.1b Result of running the time-domain method forward program BREM with INVDISC. Both forward programs work well if 512 points are used. . . 217

5.2a Result of running FOR1 with INVDISC on the medium used in Figure 5.1, using 256 points. . . . 218

5.2b Result of running BREM with INVDISC on the medium used in Figure 5.1, using 256 points. FOR1 is breaking down while BREM is still working. . . . 219

5.3a Result of running FOR1 with INVDISC on a more sharply varying medium than the one used in Figures 5.1 and 5.2. 220

5.3b Result of running BREM with INVDISC on the medium used in Figure 5.3a. FOR1 has trouble synthesizing the larger primary reflections, while BREM does not. . . . 220

5.4 Result of running BREM with INVDISC on a sharply varying medium. The failure of BREM to generate tertiary reflections (second-order multiple reflections) causes errors. 221

5.5a Result of running BREM with INVDISC while reading the reflection coefficient from a single value of the upgoing wave. Errors in the computed wave speeds soon cause the algorithm to miss primary reflections. 224

5.5b Result of running BREM with INVDISC while reading the reflection coefficient from three neighboring values of the upgoing wave. This corrects the instability revealed in Figure 5.5a. 225

5.6 Result of running BREM with INVDISC showing the double reading of primary reflections that can occur from the alteration used in Figure 5.5b. 226

5.7a Result of running BREM with the continuous medium inversion program INV1 for a fairly smooth medium. This shows INV1 works fairly well for such a medium. 227

5.7b Result of running BREM with INVDISC on the medium used in Figure 5.7a. Both inversion programs work well on fairly smooth media. 227

5.8a Result of running BREM with INVDISC on a more sharply varying medium than the one used in Figures 5.7. INVDISC still works well. 228

5.8b Result of running BREM with INV1 on the medium used in Figure 5.8a. INV1 now breaks down, as expected. 228

5.9a Result of running BREM with INVDISC on the medium used in Figures 5.8, showing the actual (r1,r2) and computed (rc1,rc2) reflection coefficients. 229

5.9b Result of running BREM with INV1 on the medium used in Figures 5.8. Note that even though the reflection coefficients are read perfectly through ten layers, the computed wave speed and densities are in error, showing that the problem lies in the medium parameter updates. 229

5.10 Result of running FOR1, without its inverse Fourier transform, with the Schur algorithm inversion program SCHUR. 232

5.11 Result of running FOR1, without its inverse Fourier transform, with the dynamic deconvolution inversion program DYNDEC. 235

5.12a Result of running BREM with NOISE, which adds noise to the results of BREM and then uses INVDISC on the noisy data. Here a high SNR is used. 237

5.12b Plots of the actual (2) and reconstructed (3) wave speeds. 238

5.12c Plots of the actual (4) and reconstructed (5) densities. . . .239

5.12d Plot of the noisy waveform used as data for INVDISC, for p = p1. 240

5.12e Plot of the noisy waveform used as data for INVDISC, for p = p2. 241

5.13a Result of running BREM with NOISE for a moderate SNR. 242

5.13b Plots of the actual (2) and reconstructed (3) wave speeds. 243

5.13c Plots of the actual (4) and reconstructed (5) densities. . . .244

5.13d Plots of the noiseless (3) and noisy (4) wave forms used as data for INVDISC, for p = p1. 245

5.13e Plots of the noiseless (1) and noisy (2) wave forms used as data for INVDISC, for p = p2. 246

5.14a Result of running BREM with NOISE for a low SNR 247

5.14b Plots of the actual (2) and reconstructed (3) wave speeds. 248

5.14c Plots of the actual (4) and reconstructed (5) densities . . . 249

5.14d Plots of the noiseless (3) and noisy (4) wave forms used as data for INVDISC, for p = p1. 250

5.14e Plots of the noiseless (1) and noisy (2) wave forms used as data for INVDISC, for p = p2. 251

5.15 Result of running BREM with NOISE for a low SNR showing how the algorithm breaks down after 20 layers. 253

5.16a Result of running BREM with NOISE using the condition number modification. . . 257

5.16b Result of running BREM with NOISE without the condition number modification. In this case the modification improves the performance of INVDISC. 258

5.17a Result of running BREM with NOISE using the condition number modification. . . 259

5.17b Result of running BREM with NOISE without the condition number modification. Again the modification improves the performance of INVDISC. 260

5.18a Result of running BREM with NOISE using the condition number modification. . . 261

5.18b Result of running BREM with NOISE without the condition number modification. In this case the modification hampers the performance of the algorithm. 262

5.19a Result of running MULTFOR, which runs BREM using several different angles of incidence, with MULT1, which adds noise and uses a least-squares fit to compute the updated wave speed and density at each depth. Note the low SNR's. . . . 265

5.19b Result of running BREM with NOISE, for comparison with 5.19a. . . . 267

5.20 Result of running MULTFOR with MULTINV, which adds noise and averages the updated wave speeds and densities computed by using the discrete medium updates on every pair of experiments. 269

CHAPTER VI: The Inverse Problem for a One-Dimensional Elastic Medium

6.1 An infinitesimal section of the ladder filter which implements the elastic wave equation. 292

6.2a Recursion pattern for updating the downgoing waves 301

6.2b Recursion pattern for updating the upgoing waves 301

6.3 Wave notations for downgoing and upgoing P and SV waves in a discrete elastic medium. 312

6.4a P→P impulse response, scaled by $1/\Delta t$ for convenience. . . .317

6.4b P→S impulse response, scaled by $1/\Delta t$ for convenience. . . .318

6.4c S→S impulse response, scaled by $1/\Delta t$ for convenience. . . .319

6.5a Comparison between actual and computed P wave speed profiles (2 = actual, 3 = computed). 321

6.5b Comparison between actual and computed SV wave speed profiles (4 = actual, 5 = computed). 322

6.5c Comparison between actual and computed density profiles (6 = actual, 7 = computed). 323

6.6 Computer output of a run of the layer stripping algorithm on a smoothly varying medium (p = 0.1). 324

6.7 Computer output of a run of the layer stripping algorithm on the layered medium used in Clarke (1984) (p = 0.4). 325

CHAPTER VII: The Inverse Problem for a Layered Acoustic Medium Probed by Spherical Harmonic Waves

7.1 Experimental set-up for the inverse problem 330

7.2 The half-space inverse problem. 335

7.3 Regions where $R(k_z)$ may be computed from data 340

7.4a Recursion pattern for updating the downgoing waves 345

7.4b Recursion pattern for updating the upgoing waves 345

7.5 $\overset{\vee}{\pi}(z,\zeta)$ interpreted as a sequence of image sources emitting spherical waves. 348

7.6 The free surface inverse problem 352

7.7 Comparison between actual and computed density profiles (2 = actual, 3 = computed). 365

CHAPTER VIII: Higher Dimensional Inverse Seismic Problems

8.1 Definition of coordinates s and e. 392

8.2 Derivation of update equation for ϕ. 397

CHAPTER I

Introduction

1.1 Motivation

The inverse seismic problem can be defined roughly as follows. The medium to be probed (i.e., the earth or the ocean floor) is excited by some sort of source, generally explosive in nature. The response of the medium to this source is measured, and from this response some properties of the medium are determined. The importance of this problem in locating oil and mineral deposits should be evident.

The above definition is vague because the problem can be specialized in many different ways. The experiment may take place entirely on land, in which case the medium response is measured by seismometers as the (particle) displacement, velocity, or acceleration at a given point. Alternately, the experiment may take place at sea, in which case the medium being probed is the sea bottom, and the medium response is measured by hydrophones as the pressure in the ocean water. The medium itself may be assumed to consist of homogeneous layers of varying thicknesses, horizontally stratified, or lateral variation in medium properties may be permitted. The medium may support the propagation of elastic (P and S) waves, or of acoustic (P) waves only.

A particular case of the inverse seismic problem that has been the focus of considerable attention in recent years is the case where the medium is parametrized by profiles of local density $\rho(z)$ and local acoustic wave speed $c(z)$, and these two quantities vary continuously

with depth. Since any medium discontinuity likely to occur in the real world could be modelled by a fast-changing continuous function, this is in a sense the most general case of a one-dimensional acoustic medium. In addition, the difficulty of the general problem necessitates some simplifying assumptions; this case (henceforth referred to as the "1-D problem") is specialized enough to admit an exact (in principle) analytic solution, while still being general enough to be of some practical use.

Starting with the landmark paper of Ware and Aki (1969), solutions to the 1-D problem have generally employed a mathematical physics approach. This is because the basic acoustic and stress-strain equations of the 1-D problem may be transformed into a Schrodinger equation, to which exact inverse scattering solutions are already known (See Section 3.2.2). However, these solutions require the solution of a Marchenko integral equation, which is computationally unattractive since the amount of computation involved for a discretization of order N is $0(N^3)$. In addition, the medium parameter profiles are required to be twice differentiable.

In searching for computationally faster ways of solving the 1-D problem, the general inverse scattering problem concept of layer-stripping suggests itself. A layer-stripping algorithm applied to the 1-D problem works conceptually as follows. The basic equations for the 1-D problem are transformed into a coupled set of partial differential equations which describe the propagation of up- and down-going waves as they interact with the medium and with each other. If the downgoing wave is assumed to contain a leading impulse (representing an explosive source), then the first reflection of this impulse into the upgoing wave

at a given depth reveals information about the medium at that depth. This information is then used to propagate the waves downward, where information about the medium at this (lower) depth is obtained. Proceeding recursively in this manner, differential layers of the medium are "peeled away" as the algorithm penetrates deeper and deeper. Mathematical details of this procedure are given in Chapter II; the physical interpretation of the workings of such an algorithm should be quite apparent. The advantage of such an algorithm is that it requires only $0(N^2)$ computation--a considerable savings.

How can the layer-stripping algorithm get by with $0(N^2)$ computation? Details are given in Chapter II and are too complicated to recount here, but the special structure (identity-plus-Hankel kernel) of the Marchenko integral equation allows a fast algorithm solution to the discretized version of this equation in the same manner that the special structure of a Toeplitz matrix allows a fast algorithm solution to a Toeplitz system of equations by the Levinson algorithm. In fact, the layer-stripping algorithm consists in part of a continuous-parameter version of the fast Cholesky algorithm encountered in studying the factorization of Toeplitz matrices, and there is a close relationship between this algorithm and the Levinson algorithm.

Thus, layer-stripping is more than just a technique for solving inverse scattering problems. In addition to admitting an unusually vivid physical interpretation of its operation, it ties in quite readily with factorization of matrices and solutions of integral equations whose kernels have specific forms. This in turn is related to the capacity of this procedure to exploit these forms to generate faster and simpler algorithms for solving these inverse scattering problems. This suggests that layer-stripping might be a powerful technique to bring to bear on various

inverse seismic problems--more so than has generally been recognized.

The subject of this thesis is the theoretical development of the layer-stripping methodology, and the application of layer-stripping methods to a wider variety of inverse seismic problems than has been dealt with so far. Among the major problems considered are:

(1) The "offset" problem in which the medium is probed with impulsive plane pressure waves at non-normal incidence. This allows the recovery of density and wave speed profiles separately as functions of depth, which is not possible for the 1-D problem described above;

(2) The "point-source" problem in which the medium is probed with spherical waves emanating from an impulsive point source, or from a point harmonic source. This is a situation far more likely to be encountered in practice than infinite plane waves, which must be simulated by stacking data;

(3) The "elastic" problem in which the medium supports the propagation of both P and S waves, with continual interconversion between the two types of waves. The goal is to recover profiles of the Lamé parameters $\lambda(z)$ and $\mu(z)$ as well as the density $\rho(z)$;

(4) Higher-dimensional problems in which lateral variations of density and wave speed are allowed, viz. $\rho(x,z)$ and $c(x,z)$.

The goal of this thesis is not merely to obtain algorithms that solve these problems, but to interpret these algorithms physically and

relate them to past work done in solving these problems, insofar as possible. It is also noted how the various algorithms generalize from one problem to another, pointing out mathematical similarities in the problems themselves that may not be immediately apparent.

Comparison with Other Inversion Methods

The inversion algorithms given in this thesis are all amplitude-based procedures, since the amplitude of the measured medium response is used to reconstruct the medium. ("Amplitude" here refers to the amplitude and phase of the reflection response.) Ths is in contrast to travel time inversion methods, which use only the arrival times of various modes or converted waves. It should be noted that travel time inversion methods such as the Herglotz-Wiechert formula (Aki and Richards, 1980) generally have difficulty with low-velocity zones in the medium, require the assumption of geometrical seismics (i.e., high frequencies), and are unable to reconstruct the density of the medium. None of these difficulties applies to the layer stripping inversion procedures given in this thesis.

However, the requirement of measuring the amplitude of the reflection response introduces noise into the inversion problem. In Chapter V, some study is made of the behavior of the offset problem layer stripping algorithms of Chapter IV in the presence of noise. The results of this study show that the algorithms work well in the presence of small amounts of additive noise, but break down at some depth for higher noise levels. This is due in part to the poor conditioning of the inverse problem at this depth, and does not reflect an inherent fault in the algorithms themselves, as is commonly believed. This issue is

discussed in more detail in Chapter V.

The presence of a significant amount of noise in the data suggests the use of deconvolution methods in which the medium is modelled as an autoregressive (AR) filter. In using this approach, it is necessary to assume that the medium reflection coefficients constitute a white (i.e., completely uncorrelated) random process, which is tantamount to neglecting all multiple reflections within the medium. Thus deconvolution methods are inherently inexact. Further, Lash (1982) reports that multiple reflections can constitute a significant part of the reflection response, particularly for sedimentary, layered media.

This last point is particularly important, since sedimentary, layered media constitute a likely milieu for deposits of petroleum. Petroleum deposits tend to be found in "traps" about half a square mile in extent and about four miles deep. Such traps tend to arise in layered media generally formed by sedimentary processes. Since searching for these traps by inverse seismic methods is of great interest to oil companies, the relevance of the approach used in this thesis should be evident.

1.2 Literature Survey

Details of past work done on each of the problems considered in this thesis are given in the introductions to each chapter. In this section, the most important references are collected and summarized.

Application of the Layer-Stripping Principle

The concept of layer stripping has been developed only recently, and not many references are available on the application of this concept to inverse scattering problems. Although the concept of dynamic

deconvolution (e.g., Robinson, 1982) can be considered to be a precursor to the results of application of the layer-stripping idea, application of the layer-stripping concept itself has occurred only recently.

Bruckstein et al. (1983) is a good survey paper on the concept and its relations to other means of solving inverse scattering problems, i.e., integral equations. Chapter II of this thesis contains most of the important ideas of this paper, with more emphasis on applications. Symes (1981), Santosa and Schwetlick (1982), Symes and Zimmerman (1982), and Bube and Burridge (1983) have all applied layer stripping ideas to the 1-D problem at normal incidence, and the latter two report satisfying results for numerical tests on synthetic data. Corones et al. (1983) used the time-domain version of a Riccati equation as an invariant embedding equation, which can be considered to be a layer stripping approach. This also solved the one-dimensional problem at normal incidence.

Carrion (1983) has recently applied layer stripping ideas to the one-dimensional problem at non-normal incidence (i.e., the "offset" problem). However, Carrion's procedure is much more complicated than the alogrithm specified in Chapter IV, and lacks the physical interpretability of that algorithm. Carrion's procedure is also not easily related to layer stripping algorithms for the one-dimensional problem at normal incidence, and does not generalize to algorithms for the elastic problem and higher-dimensional problems, as does the algorithm of Chapter IV.

Similar objections apply to the layer stripping algorithm given in Clarke (1984) for the elastic problem. In particular, the medium

parameter updates are far too complicated to consider this algorithm a "fast" algorithm. Although Clarke's (1984) algorithm, unlike the algorithm given in Chapter VI, does in principle furnish an exact solution for a discrete medium (i.e., a medium whose properties change sharply at each interface between layers), the numerical results presented in Chapter VI indicate that the more complicated discrete medium updates may not be worth the added computation time they require.

Mendel and Habibi-Ashrafi (1980) and Habibi-Ashrafi and Mendel (1982) have utilized the principle of layer stripping in a somewhat different manner from the approach taken in this thesis. Their approach is to perform a maximum-likelihood estimation of the time and strength of each primary reflection, using a matched filter and a transversal equalizing filter, and then use this data to propagate the waves downward. This a posteriori approach is in contrast to the a priori approach used in this thesis. Although it is more complex and time-consuming, it may well work better on noisy data. Shiva and Mendel (1983) apply this approach to the elastic problem, but as in Clarke (1984) the use of discrete medium updates results in a very complicated procedure.

The One-Dimensional Problem at Normal Incidence

The landmark paper of Ware and Aki (1969) stimulated interest in the 1-D problem, in which an infinite impulsive plane pressure wave is normally incident on a medium supporting the propagation of acoustic (sound) waves and having depth-dependent density $\rho(z)$ and wave speed $c(z)$. By suitable transformations (see Chapter III), the basic acoustic and stress-strain equations of the 1-D problem are transformed into a Schrodinger equation. The inverse scattering problem for a

Schrodinger equation is well known both in mathematical physics and in inverse scattering theory, and its solution requires the solution of a Marchenko integral equation, as discussed in Chapter II. This approach, which may be termed the "classical" approach to the 1-D problem, has been employed by many authors.

The result of solving the 1-D problem is the impedance $\rho c(\tau)$ as a function of travel time τ. Gerver (1970) showed that the impedance is all that can be reconstructed for an excitation by plane waves at normal incidence, and that the reconstruction is unique, subject to mild assumptions.

Other methods for solving the 1-D problem have been given by Burridge (1980), who derives the Marchenko integral equation and several related integral equations directly in the time domain, bypassing the Schrodinger equation formulation. Gray (1983) derives a Marchenko equation directly in terms of a reflectivity function $r(\tau)$, bypassing the Schrodinger potential. This allows discontinuities in $r(\tau)$ and requires only that the impedance be continuous, unlike the Schrodinger formulation for which the impedance must be twice differentiable. The excellent review paper by Newton (1981) summarizes several different ways of solving the 1-D problem.

The discrete version of the 1-D problem consists of a layered medium being probed by a discrete impulsive plane wave. The layered medium is assumed to be composed of horizontally stratified homogeneous layers whose thicknesses are such that the travel time $\Delta\tau$ through each layer is the same. Then all events (reflections at or transmissions through any interface, or arrivals at the surface) occur at integer multiples of $\Delta\tau$, making the problem a digital signal processing problem.

This model of the medium was first proposed by Goupillaud (1961), and is often referred to in the literature as a "Goupillaud medium." Analysis of wave propagation through such a medium has been performed in Kunetz (1962), Berryman and Greene (1980), Aki and Richards (1980), and Robinson (1982), among others, and it is shown that the impedance of the layers may be recovered by solving an identity-plus-Hankel system of equations. It is shown further in the above references that this system can be solved by a fast, Levinson-like algorithm that exploits the structure of the system matrix. Berryman and Greene (1980) showed that discretizations of the Marchenko integral equation and the Schrodinger equation lead to the same identity-plus-Hankel system, so that discretization of the medium is equivalent to discretization of the equations.

The Offset and Point-Source Problems

The offset problem is a variation on the 1-D problem described above in that the probing impulsive plane wave is not incident normally on the medium, but arrives at the top of the medium at a slant or offset (see Figure 4.1). Although the density and wave speed are still functions of depth only, the medium itself is now assumed to be two-dimensional in extent--the waves no longer propagate only along a single vertical ray path. Since the offset experiment may be performed at two different angles of incidence, resulting in two different ray paths through the medium, the density and wave speed profiles $\rho(z)$ and $c(z)$ can be recovered separately as functions of depth. This is unlike the 1-D experiment, for which only the impedance as a function of travel time $\rho c(\tau)$ can be recovered.

The offset problem was first analyzed by Ware (1969), who showed how it could be transformed into a 1-D problem parametrized by the angle of incidence. Coen (1981) used a different transformation to obtain a Schrodinger equation which, upon solution of a Marchenko integral equation, yields the index of refraction. Coen's procedure requires the solution of two Marchenko integral equations (one for each experiment) and some algebra to recover $\rho(z)$ and $c(z)$.

Howard (1983) gives still another procedure that results in a matrix Marchenko integral equation. The profiles $\rho(z)$ and $c(z)$ are then recovered using a rather messy reconstruction procedure. Although Howard uses the transformation into upgoing and downgoing waves used in Chapter IV, his procedure is not at all well suited for computation.

In the point-source problem the medium is probed with spherical impulsive waves emanating from a single point source. This is a more realistic set-up than supposing an infinite plane wave, which cannot exist in the real world and must be simulated by stacking data. Although transformations between plane waves (actually cylindrical waves) and spherical waves are well known (e.g., the Sommerfeld integral; see Aki and Richards, 1980), surprisingly little work has been done on the inverse problem with a point-source excitation.

Coen (1982) uses the Hankel transform of order zero to transform the point source problem to the offset problem. A Hankel transform must be performed on the original data (vertical particle velocity at the surface), and Coen notes that this can be interpreted as a Radon transform. However, the resulting (synthetic) offset problem may involve an impulsive plane wave incident at a post-critical angle, which must be dealt with in a manner different from that of the case of

pre-critical incidence.

Coen (1982) and Stickler (1983) consider the inverse problem in which the medium is excited by a point harmonic source. By performing this experiment at two different source frequencies, the profiles $\rho(z)$ and $c(z)$ are recovered separately. Coen posits an experiment run on land, obtains a Schrodinger-like equation, and requires the solution of two Marchenko integral equations. Stickler posits an experiment run at sea, and requires the solution of a Schrodinger equation inverse potential problem by trace methods.

The Elastic Problem

The elastic problem is a variation on the offset problem in which the medium is now assumed to support the propagation of both P waves and S waves. This is a more realistic assumption for the earth than the assumption of acoustic (P) wave propagation only, which is tantamount to treating the earth as a fluid. The problem is difficult in that the two wave types are being continually interconverted as they propagate through an inhomogeneous medium. The goal of the elastic problem is recovery of profiles of the Lamé parameters $\lambda(z)$ and $\mu(z)$, and the density $\rho(z)$.

Previous work on this problem has yielded methods of solution that are computationally arduous to implement. Blagoveschenskii (1967) exhibited several integral equations whose solutions yielded the parameter profiles, and by combining the Gel'fand-Levitan inverse scattering procedure with the solution of a Volterra-type equation, Carroll and Santosa (1982) were able to recover the parameter profiles more simply. Baker (1982) solved the related problem of reconstructing radially-varying parameters by using spherical harmonics

and Marchenko integral equations.

Kennett and Illingworth (1981) gave a very complicated procedure involving approximations by Airy functions and propagator matrices, which "propagate" displacements and stresses from one depth to another as a state transition matrix propagates the state of a system from one time to another. Frasier (1969) gave a treatment of the discrete elastic problem analogous to Berryman and Greene's (1980) treatment of the 1-D problem, although the different wave speeds of P and S waves cause problems in defining a Goupillaud medium model.

In summary, none of the methods brought to bear on the elastic problem so far can be considered to be attractive from a practical, computational perspective.

Higher Dimensional Problems

Very little work has been done in obtaining exact solutions to higher-dimensional inverse seismic problems, in which the density $\rho(x,z)$ and wave speed $c(x,z)$ are allowed to vary laterally as well as with depth. The most commonly used approach is migration, in which an observed wave field is back-propagated into the medium to determine its strength at the point of reflection, yielding the reflection coefficient at that point. This is effective if the medium consists of a few large homogeneous regions, with variation only at a few (non-horizontal) interfaces. Tomographic approaches employing the Born (weak scattering) approximation are useful only if the wave speed has little variation. Neither of these approaches can reconstruct density or account for multiple reflections.

Newton (1980) has extended the Gel'fand-Levitan potential reconstruction procedure to general 3-D media. However, this result has

proven to be of limited use in solving higher-dimensional seismic problems.

1.3 Contributions of Thesis

The major contribution of this thesis is the demonstration that layer stripping principles can be applied to a much wider variety of inverse seismic problems than has generally been realized. Other contributions include the numerical demonstration that the new algorithms do in fact work on synthetically generated data, and that the offset problem algorithm works on slightly noisy data as well.

The material of Chapter II is a synthesis of the major results of Bruckstein et al. (1983) and Yagle and Levy (1984a). The results on inverse scattering for asymmetric two-component wave systems, and on recovery of the potential of a Schrodinger equation by conversion to a symmetric two-component wave system (Section 2.3.5) have not previously appeared in the literature (save for Yagle and Levy, 1984a), although Jaulent (1982) used an approach similar to the former to solve the inverse problem for a lossy non-uniform transmission line.

The material covered in Chapter III is a compendium of results from a variety of sources, including Ware and Aki (1969), Berryman and Greene (1980), Robinson (1982), Bube and Burridge (1983), and Yagle and Levy (1984b). The results on the use of the continuous-parameter fast Cholesky algorithm to reconstruct a continuous layered medium were obtained concurrently with and independently of the work of Bruckstein et al. (1983) and Bube and Burridge (1983). The Schur and dynamic deconvolution algorithms for reconstructing a continuous medium seem to be new to the literature, although they are only a trivial generalization

of the discrete medium results. However, Chapter III does do an excellent job of linking together the various approaches to solving the one-dimensional normal incidence inverse problem, and of showing the dual nature of the layer stripping and integral equation/matrix equation methods for both continuous and discrete layered media.

The layer stripping algorithms of Chapter IV are all new, with the continuous medium algorithms for plane wave and point source excitations having appeared in Yagle and Levy (1984b). The material of Sections 4.2.1., 4.3.1, and 4.4.1 on integral equations solutions, Hankel and Radon transforms, and turning points, respectively, is necessary foundation material taken from a variety of sources (see references for Chapter IV).

Chapter V consists of a variety of modifications to the algorithms of Chapter IV, and numerical tests of the various algorithms on synthetically-generated data. The discussion of forward and backward stability is due to Stewart (1973), and the condition number threshold modification is adapted from Bruckstein et al. (1984). The modification of using a least-squares fit to compute the updates at each depth, the lossy medium algorithm, and all of the numerical results and observations are new.

All of the results of Chapter VI (save for the contents of Section 6.3.3, which are taken from Frasier, 1969) are new. The contents of Sections 6.2 and 6.4 appear in Yagle and Levy (1985). It should be noted that the 4x4 system matrix for upgoing and downgoing waves in inhomogeneous media has been derived in several papers by B.L.N. Kennett, e.g., Kennett and Illingworth (1981).

In Chapter VII two different inverse problems are treated, since

they are mathematically analogous. This analogy seems to have gone unnoticed previously. The fast algorithms for solving the two formulations of the inverse problem with a point harmonic source are new, and they appear in Yagle and Levy (1984c). The results on the inverse resistivity problem are taken from Levy (1984).

In Chapter VIII the layer stripping approach is applied to higher-dimensional inverse seismic problems, in which the density and wave speed vary laterally as well as with depth (viz. $\rho(x,z)$ and $c(x,z)$). All of the results in this chapter are new. The results of Sections 8.2 and 8.4 have appeared in Yagle (1983).

In this section the contributions of and new results in this thesis have been summarized. In the process, an overview of the thesis as a whole has been given. Since the major contribution of this thesis is the application of the layer stripping concept to a wide variety of inverse seismic problems, considerable attention is paid throughout the thesis to analogies between various problems and solutions, and to ways in which solutions to one problem generalize to those of another. In the next chapter a foundation for all of this is laid by discussing the concept of layer stripping itself, the ways in which it may be used to solve various types of inverse scattering problems, and the ways in which these methods are mathematically dual to the usual, integral-equation-based methods of solving these problems.

REFERENCES FOR CHAPTER I

K. Aki and P.G. Richards, Quantitative Seismology, Theory and Methods, W.H. Freeman and Co., San Francisco, 1980.

G.A. Baker, "Solutions of an Inverse Elastic-Wave Scattering Problem," J. Acoust. Soc. Am. 71, 785-789 (1982).

J. Berryman and R. Greene, "Discrete Inverse Methods for Elastic Waves in Layered Media," Geophys. 45(2), 213-233 (1980).

A.S. Blagoveshchenskii, "The Inverse Problem in the Theory of Seismic Wave Propagation," in Topics in Mathematical Physics v.1, pp. 55-67, ed. by M.S. Birman, Consultants Bureau, N.Y., 1967.

A. Bruckstein, B. Levy and T. Kailath, "Differential Methods in Inverse Scattering," Tech. Report, Information Systems Laboratory, Stanford University (1983), to appear in SIAM J. Applied Math.

A.M. Bruckstein, I. Koltracht, and T. Kailath, "Inverse Scattering with Noisy Data," Tech. Report, Information Systems Laboratory, Stanford University (1984).

K.P. Bube and R. Burridge, "The One-Dimensional Inverse Problem of Reflection Seismology," SIAM Review 25(4), 497-559 (1983).

R. Burridge, "The Gelfand-Levitan, the Marchenko and the Gopinath-Sondhi Integral Equations of Inverse Scattering Theory Regarded in the Context of Inverse Impulse Response Problems," Wave Motion 2, 305-323 (1980).

P.M. Carrion, "Computation of Velocity and Density Profiles of Acoustic Media with Vertical Inhomogeneities Using the Method of Characteristics Applied to the Slant Stacked Data," Tech. Report, Aldridge Laboratory of Applied Geophysics, Columbia University, 1983.

R. Carroll and F. Santosa, "On the Complete Recovery of Geophysical Data," Math. Meth. in the Appl. Sci. 4, 33-73 (1982).

T.J. Clarke, "Full Reconstruction of a Layered Elastic Medium from P-SV Slant-Stack Data," Geophys. J.R. astr. Soc. 78(3), 775-793 (1984).

S. Coen, "Density and Compressibility Profiles of a Layered Acoustic Medium from Precritical Incidence Data," Geophys. 46(9), 1244-1246 (1981).

S. Coen, "Velocity and Density Profiles of a Layered Acoustic Medium from Common Source-Point Data," Geophys. 47(6), 898-905 (1982).

J.P. Corones, M.E. Davison, and R.J. Krueger, "Direct and Inverse Scattering in the Time Domain via Invariant Imbedding Equations," J.

Acoust. Soc. Am. 74(5), 1535-1541 (1983).

C.W. Frasier, "Discrete-Time Solution of Plane P-SV Waves in a Plane Layered Medium," Ph.D. Thesis, Dept. of Earth and Planetary Sciences, MIT, May 1969.

M.L. Gerver, "The Inverse Problem for the One-Dimensional Wave Equation," Geophys. J.R. astr. Soc. 21, 337-357 (1970).

P. Goupillaud, "An Approach to Inverse Filtering of Near-Surface Layer Effects from Seismic Records," Geophys. 26(6), 754-760 (1961).

S. Gray, "Inverse Scattering for the Reflectivity Function," J. Math. Phys. 24(5), 1148-1151 (1983).

F. Habibi-Ashrafi and J. Mendel, "Estimation of Parameters in Lossless Layered Media Systems," IEEE Trans. A.C. AC-27(1), 31-48 (1982).

M. Howard, "Inverse Scattering for a Layered Acoustic Medium Using the First-Order Equations of Motion," Geophys. 48(2), 163-170 (1983).

M. Jaulent, "The Inverse Scattering Problem for LCRG Transmission Lines," J. Math. Physics 23(12), 2286-2290 (1982).

B.L.N. Kennett and M.R. Illingworth, "Seismic Waves in a Stratified Half Sapce, Part III. Piecewise Smooth Models," Geophys. J.R. astr. Soc. 66, 633-675 (1981).

G. Kunetz and I. d'Erceville, "Sur Certaines Propriétés d'une Onde Plane de Compréssion dans un Milieu Stratifié," Ann. Geophysique 18, 351-359 (1962).

C.C. Lash, "Investigation of Multiple Reflections and Wave Conversion by Means of a Vertical Wave Test in Southern Mississippi," Geophysics 47(7), 977-1000 (1982).

B. Levy, "Layer by Layer Reconstruction Methods for the Earth Resistivity from Direct Current Measurements," Tech. Report # LIDS-P-1388, Laboratory for Information and Decision Systems, MIT, 1984.

J. Mendel and F. Habibi-Ashrafi, "A Survey of Approaches to Solving Inverse Problems for Lossless Layered Media Systems," IEEE Trans. Geoscience and Remote Sensing GE-18(4), 320-330 (1980).

R.G. Newton, "Inverse Scattering. II. Three Dimensions," J. Math. Physics 21(7), 1698-1715 (1980).

R. Newton, "Inversion of Reflection Data for Layered Media: A Review of Exact Methods," Geophys. J.R. astr. Soc. 65, 191-215 (1981).

E.A. Robinson, "Spectral Approach to Geophysical Inversion by Lorentz, Fourier, and Radon Transforms," Proc. IEEE 70, 1039-1054 (1982).

F. Santosa and H. Schwetlick, "The Inversion of Acoustical Impedance Profile by Method of Characteristics," Wave Motion 4, 99-110 (1982).

M. Shiva and J. M. Mendel, "Non-Normal Incidence Inversion: Existence of Solution," Geophysical Prospecting 31, 888-914 (1983).

G. Stewart, Introduction to Matrix Computations, Academic Press, NY, 1973.

D. Stickler, "Inverse Scattering in a Stratified Medium," J. Acoust. Soc. Am. 74(3), 994-1005 (1983).

W. Symes, "Stable Solution of the Inverse Reflection Problem for a Smoothly Stratified Medium," SIAM J. Math. Anal. 12(3), 421-453 (1981).

W. Symes and G. Zimmerman, "Experiments in Impedance Profile Inversion Using Noisy and Band-Limited Data," Amoco Production Co. Research Report No. F82-C-3 (1982).

J. Ware, "Scattering and Inverse Scattering Problems in a Continuously-Varying Elastic Medium," Ph.D. Thesis, Dept. of Earth and Planetary Sciences, MIT, Aug. 1969.

J. Ware and K. Aki, "Continuous and Discrete Inverse-Scattering Problems in a Stratified Elastic Medium, Part I: Plane Waves at Normal Incidence," J. Acoust. Soc. Am. 45, 911-921 (1969).

A. Yagle, "Notes on Layer Stripping Solutions of Higher Dimensional Inverse Seismic Problems," Tech. Report # LIDS-P-1347, Laboratory for Information and Decision Systems, MIT, 1983.

A. Yagle and B. Levy, "The Schur Algorithm and its Applications," 1984, to appear in Acta Applicandae Mathematicae.

A. Yagle and B. Levy, "Application of the Schur Algorithm to the Inverse Problem for a Layered Acoustic Medium," J. Acoust. Soc. Am. 76(1), 301-308 (1984).

A. Yagle and B. Levy, "A Fast Algorithm Solution of the Inverse Problem for a Layered Acoustic Medium Probed by Spherical Harmonic Waves," 1984, to appear in J. Acoust. Soc. Am.

A. Yagle and B. Levy, "A Layer-Stripping Solution of the Inverse Problem for a One-Dimensional Elastic Medium," to appear in Geophysics 50(3), 1985.

CHAPTER II

Layer Stripping and Inverse Scattering Theory

2.1 Introduction

In this chapter we collect a variety of results on inverse scattering theory from several sources, and present a unified treatment of several methods for solving inverse scattering problems. In particular, the mathematical concept of layer stripping (Bruckstein et al, 1983) is explained and used to develop algorithms for solving inverse scattering problems.

In Section 2.2 the concept of an inverse scattering problem is quickly reviewed, and the symmetric two-component wave system inverse scattering problem is defined. Most of the inverse seismic problems dealt with in this thesis can be cast into this form, or into an analogous form. Thus approaches used to solve this problem can be (and will be) used to solve other problems in this thesis. The properties of the scattering matrix are then discussed, with attention paid to physical interpretation of these properties in terms of conservation of energy.

In Section 2.3 differential methods for solving inverse scattering problems are derived and discussed. These methods utilize the concept of layer stripping, which means that the scattering medium is reconstructed differentially, layer by layer, rather than all at once in a "batch" procedure. The continuous-parameter fast Cholesky, Schur, and dynamic deconvolution algorithms (which are all different versions of the same algorithm) are derived and applied to the inverse scattering problem for a lossless transmission line. Next, a fast algorithm for the

asymmetric two-component wave system inverse scattering problem is derived and applied to the inverse scattering problem for a lossy transmission line. Finally, other differential methods are derived, including the misnamed "method of characteristics" of Santosa and Schwetlick (1982), and two methods for recovering the potential of a Schrodinger equation. These methods will be used in Chapters VIII and VII, respectively.

In Section 2.4 integral equation methods for solving inverse scattering problems are derived and discussed. The Marchenko, Gel'fand-Levitan, and Krein integral equations are all derived using the treatment of Bruckstein et al. (1983). The Krein-Levinson algorithm, a continuous-parameter version of the famous Levinson algorithm for solving Toeplitz systems of equations, is shown to solve these integral equations. Finally, an approach due to Levy (1985) which interprets the inverse scattering problem as an orthogonalization problem is used to again obtain the Marchenko integral equation.

In Section 2.5 relations between differential and integral methods are explored. In particular, the relation between the fast Cholesky algorithm (a differential method) and the Krein-Levinson algorithm (which solves the integral equations) is discussed. The relations are then illustrated by interpreting the problem of linear least-squares estimation of a stationary stochastic process as an inverse scattering problem, and solving it using both algorithms.

2.2 Inverse Scattering Problems

In an inverse scattering problem a medium is probed with some sort of disturbance (e.g., acoustic or electromagnetic) and the effect on the

disturbance (either the scattered field or the transmitted field, or both) is measured. From this measurement an attempt is made to reconstruct the medium. Obviously a priori assumptions about the medium are necessary. For example, in Chapter IV it will be assumed that the acoustic medium being probed is lossless, layered (medium parameters vary only with depth z), isotropic (no variation with direction), linear (small strains), and completely specified by wave speed c(z) and density $\rho(z)$. The problem is then to recover two functions $\rho(z)$ and c(z) from measurement of the scattered field. This is now a mathematical problem, but in general still a difficult one.

The Symmetric Two-Component Wave System

Consider a lossless, one-dimensional scattering medium described by the coupled partial differential equations

$$\partial p/\partial x + \partial p/\partial t = -r(x)q(x,t) \qquad (2\text{-}1a)$$

$$\partial q/\partial x - \partial q/\partial t = -r(x)p(x,t) \qquad (2\text{-}1b)$$

These equations are a special case of equations discussed by Zakharov and Shabat (1972) and Ablowitz and Segur (1981). The reflectivity function r(x) completely characterizes the medium, and it is assumed that $r(x) = 0$ for $x < 0$ and $r(x) \in L_1[0,\infty)$. This means that for $x < 0$ and $x \to \infty$ p(x,t) and q(x,t) have the forms

$$p(x,t) = p(x-t), \quad q(x,t) = q(x+t). \qquad (2\text{-}2)$$

Thus p and q can be interpreted as waves propagating rightward and leftward at unit velocity. The interpretation of the medium being probed by waves at $x = 0$ and $x \to \infty$ is evident.

What measurements are necessary to recover the reflectivity function

r(x)? To answer this question, we look at the scattering matrix for the two-component system.

The Scattering Matrix

By taking the Fourier transform of (2-1), we obtain

$$\frac{d}{dx}\begin{bmatrix}\hat{p}\\ \hat{q}\end{bmatrix} = \begin{bmatrix}-j\omega & -r(x)\\ -r(x) & j\omega\end{bmatrix}\begin{bmatrix}\hat{p}\\ \hat{q}\end{bmatrix}. \qquad (2\text{-}3)$$

Now if x is discretized with discretization length Δ (i.e., $x = n\Delta$), a simple forward difference approximation to the derivative in (2-3) and noting that $1 - j\omega\Delta \approx e^{-j\omega\Delta}$ for small Δ gives the elementary scattering section described in Figure 2.1. This figure shows that $r(x)\Delta$ is the fraction of the rightgoing wave $\hat{p}$ which is reflected by a section of thickness Δ at point x inside the medium. The discrete ladder structure displayed by Figure 2.1 has been used to design signal processing architectures for speech processing (Markel and Gray, 1983), digital wave-filter synthesis (Deprettere and Dewilde, 1980), spectral estimation (Makhoul, 1977), and linear estimation (Dewilde, 1982; Dewilde and Dym, 1981; Dewilde et al., 1978).

The elementary scattering layers of Figure 2.1 can be composed by using the rules of composition for scattering layers described in Redheffer (1962). The resulting aggregate medium is described by the scattering matrix

$$S(\omega) = \begin{bmatrix}\hat{T}_L(\omega) & \hat{R}_R(\omega)\\ \hat{R}_L(\omega) & \hat{T}_R(\omega)\end{bmatrix} \qquad (2\text{-}4)$$

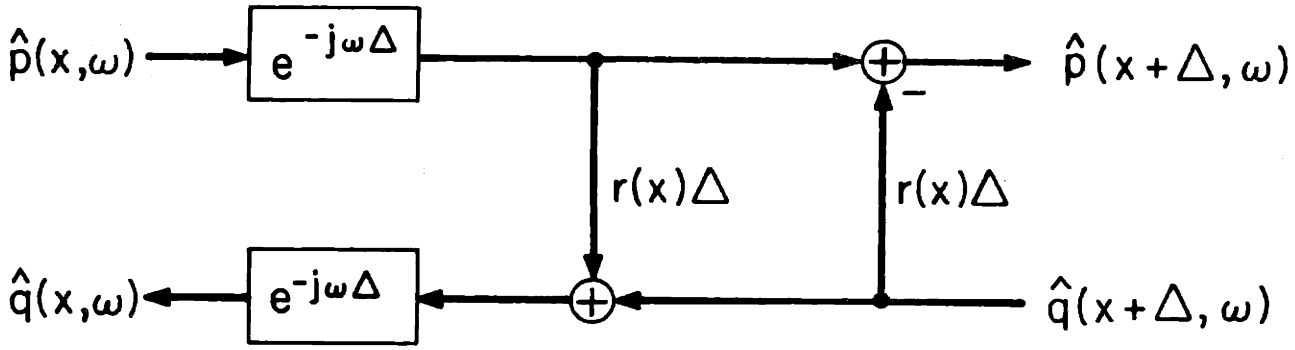

2.1 Elementary scattering sections obtained by discretizing the two-component wave equations.

which relates the incoming and outgoing waves appearing in Figures 2.2a and 2.2b. In Figure 2.2a, the medium is probed from the left by a rightward propagating wave $e^{-j\omega x}$, and $\hat{R}_L(\omega)e^{j\omega x}$ and $\hat{T}_L(\omega)e^{-j\omega x}$ are respectively the reflected and transmitted waves. Figure 2.2b corresponds to the case when the medium is probed from the right. More generally, for arbitrary waves $\hat{p}(x,\omega)$ and $\hat{q}(x,\omega)$

$$\hat{p}(x,\omega) = \hat{p}_L(\omega)e^{-j\omega x} \quad \hat{q}(x,\omega) = \hat{q}_L(\omega)e^{j\omega x} \tag{2-5a}$$

for $x < 0$, and

$$\hat{p}(x,\omega) = \hat{p}_R(\omega)e^{-j\omega x} \quad \hat{q}(x,\omega) = \hat{q}_R(\omega)e^{j\omega x} \tag{2-5b}$$

as $x \to \infty$, and

$$\begin{bmatrix} \hat{p}_R(\omega) \\ \hat{q}_L(\omega) \end{bmatrix} = S(\omega) \begin{bmatrix} \hat{p}_L(\omega) \\ \hat{q}_R(\omega) \end{bmatrix} \tag{2-6}$$

expresses the outgoing waves $(\hat{p}_R, \hat{q}_L)$ as a function of the incoming waves $(\hat{p}_L, \hat{q}_R)$.

If

$$a_i(x,\omega) = \begin{bmatrix} \hat{p}_i(x,\omega) \\ \hat{q}_i(x,\omega) \end{bmatrix} \quad i = 1,2 \tag{2-7}$$

are two arbitrary solutions of (2-3), and if $\Sigma \triangleq \text{diag}(1,-1)$, the system (2-3) has the properties that

$$\frac{d}{dx}\left(a_1^H(x,\omega)\,\Sigma\,a_2(x,\omega)\right) = 0 \tag{2-8}$$

and

$$\frac{d}{dx}\,W(a_1(x,\omega),\ a_2(x,\omega)) = 0, \tag{2-9}$$

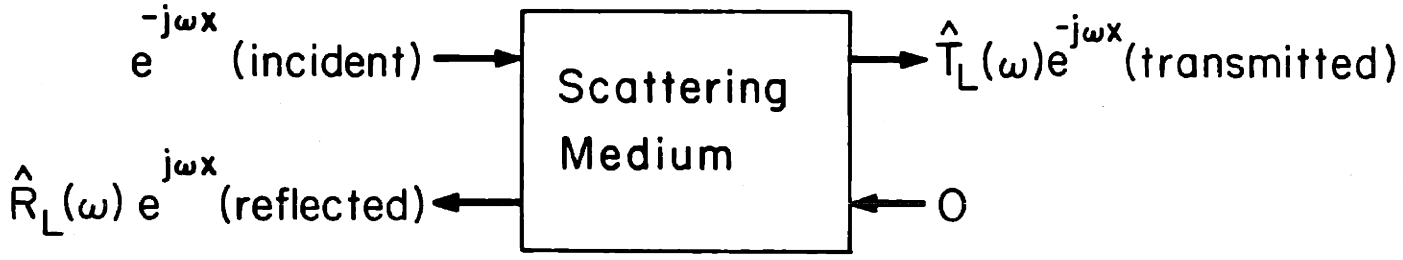

2.2a Scattering for an impulsive wave incident from the left.

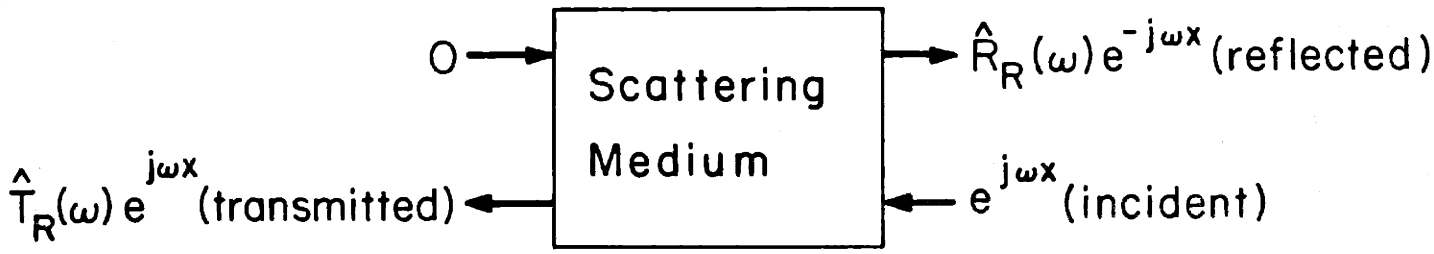

2.2b Scattering for an impulsive wave incident from the right.

where H denotes the Hermitian transpose, and where

$$W(a_1,a_2) \triangleq \hat{p}_1\hat{q}_2 - \hat{q}_1\hat{p}_2 \tag{2-10}$$

is the Wronskian of a_1 and a_2. Equations (2-8) and (2-9) may be easily verified by direct computation, but they have important implications. Equation (2-8) shows that $|\hat{p}_i(x,\omega)|^2 - |\hat{q}_i(x,\omega)|^2$ is independent of x, and employing this at $x = 0$ and $x \to \infty$ yields

$$|\hat{p}_i(0,\omega)|^2 + |\hat{q}_i(\infty,\omega)|^2 = |\hat{p}_i(\infty,\omega)|^2 + |\hat{q}_i(0,\omega)|^2. \tag{2-11}$$

The left side of (2-11) represents the incoming energy of the probing waves, and the right side of (2-11) represents the outgoing energy. Thus equation (2-11) is a statement of conservation of energy, i.e., the system is lossless.

In equation (2-9), let a_1 be the solution of (2-3) when the medium is probed from the left, and let a_2 be the solution of (2-3) when the medium is probed from the right (see Figure 2.2). Then employing the implication of (2-9) that $W(a_1,a_2)$ is the same at $x = 0$ and $x \to \infty$ yields

$$e^{-j\omega x} \cdot \hat{T}_R e^{j\omega x} - \hat{R}_L e^{j\omega x} \cdot 0 = \hat{T}_L e^{-j\omega x} \cdot e^{j\omega x} - 0 \cdot \hat{R}_R e^{-j\omega x} \tag{2-12}$$

or

$$\hat{T}_R(\omega) = \hat{T}_L(\omega) \ . \tag{2-13}$$

Physically, this means that the transmission loss through the system is the same going in either direction. This is a statement of reciprocity. Note that if time were reversed the leftgoing and rightgoing waves would switch their identities but still suffer the same transmission losses.

If T_L and T_R were different, the system would depend on the direction of time.

From equations (2-6) and (2-11) we have, for any solution,

$$[\hat{p}_L^* \; \hat{q}_R^*] \begin{bmatrix} \hat{p}_L \\ \hat{q}_R \end{bmatrix} = [\hat{p}_R^* \; \hat{q}_L^*] \begin{bmatrix} \hat{p}_R \\ \hat{q}_L \end{bmatrix} = [\hat{p}_L^* \; \hat{q}_R^*] \; S^H \; S \begin{bmatrix} \hat{p}_L \\ \hat{q}_R \end{bmatrix}. \tag{2-14}$$

Since this holds for any solution we must have

$$S^H S = I \tag{2-15}$$

i.e., the scattering matrix is unitary. Writing out (2-15) element by element yields

$$|\hat{T}(\omega)|^2 + |\hat{R}_L(\omega)|^2 = |\hat{T}(\omega)|^2 + |\hat{R}_R(\omega)|^2 = 1 \tag{2-16a}$$

$$\hat{T}(\omega)\hat{R}_L(\omega)^* + \hat{T}(\omega)^*\hat{R}_R(\omega) = 0. \tag{2-16b}$$

Equation (2-16a) is an obvious statement of conservation of energy, while equation (2-16b) is a phase relationship that can be derived by considering the following two experiments.

Let the medium be probed from both ends at once, first with two waves each of amplitude unity ($e^{-j\omega x}$ and $e^{j\omega x}$), and then with the waves $e^{-j\omega x}$ and $je^{j\omega x}$. Equating the incoming and outgoing energies for each experiment, we have

$$\begin{aligned} 1^2 + 1^2 = |\hat{T}+\hat{R}_L|^2 + |\hat{T}+\hat{R}_R|^2 &= |\hat{T}|^2 + |\hat{R}_L|^2 + |\hat{T}|^2 \\ &+ |\hat{R}_R|^2 + \hat{T}\hat{R}_L^* + \hat{T}^*\hat{R}_R + (\hat{T}\hat{R}_L^* + \hat{T}^*\hat{R}_R)^* \end{aligned} \tag{2-17a}$$

$$1^2 + |j|^2 = |j\hat{T}+\hat{R}_L|^2 + |\hat{T}+j\hat{R}_R|^2 = |\hat{T}|^2 + |\hat{R}_L|^2 + |\hat{T}|^2 + |\hat{R}_R|^2 + j(\hat{T}\hat{R}_L^*+\hat{T}^*\hat{R}_R) - j(\hat{T}\hat{R}_L^* +\hat{T}^*\hat{R}_R)^* . \quad (2\text{-}17b)$$

Subtracting off (2-16a) from (2-17a) and (2-17b), dividing (2-17b) by j, and adding (2-17a) and (2-17b) yields (2-16b). Hence (2-16b) can be obtained entirely from the principle of conservation of energy. Note that superposition of energy equations is only valid for lossless systems, so (2-16b) depends on the losslessness of the medium.

Another way of deriving (2-16) is by considering time reversal. Suppose that the medium is probed from the left, as in Figure 2.2a, and time is reversed. This is now equivalent to probing the medium with $\hat{T}(-\omega) = \hat{T}^*(\omega)$ and $\hat{R}_L(-\omega) = \hat{R}_L^*(\omega)$, and getting out $e^{j\omega x}$ at the left end of the medium and 0 at the right end. Interpreting this in terms of Figures 2.2a and 2.2b as an experiment forward in time, and equating the results of the experiments running backward and forward in time immediately yields (2-16). This interpretation, unlike the previous one, utilizes the reciprocity of the lossless system.

The relations (2-16) furnish considerable information about the scattering matrix $S(\omega)$. Indeed, it can be shown (Faddeev, 1967; Chadan and Sabatier, 1977) that if it is known a priori that $\hat{T}(\omega)$ has no poles in the lower half of the complex plane, then $\hat{T}(\omega)$ also has no zeros in the lower half-plane and is therefore minimum phase. Then, since the magnitude of $\hat{T}(\omega)$ is known from $1-|\hat{R}_L(\omega)|^2$ or $1-|\hat{R}_R(\omega)|^2$, the argument of $\hat{T}(\omega)$ can be recovered from its magnitude using the Hilbert transform and cepstrum. The other reflection coefficient can then be obtained from (2-16b). Thus $\hat{S}(\omega)$ can be completely reconstructed from knowledge of either $\hat{R}_L(\omega)$ or $\hat{R}_R(\omega)$

alone (explicit formulae are given by Chadan and Sabatier, 1977, and by Faddeev, 1967). This means that the inverse scattering problem defined by the two-component system (2-1) being probed by a wave $e^{-j\omega x}$ and knowledge of either $\hat{R}_L(\omega)$ or $\hat{R}_R(\omega)$ is well-posed.

The significance of poles of $\hat{T}(\omega)$ in the lower half-plane is that such a pole allows a localized solution to exist. Such a solution cannot be discerned from the results of this experiment. To see this, suppose there is a pole of $\hat{T}(\omega)$ at $-j\omega_p$, where ω_p is real and positive. Take Figure 2.2a and divide all three waves by $\hat{T}(\omega)$. Then there is a solution which behaves like $e^{-j(-j\omega_p)x} = e^{-\omega_p x}$ as $x \to \infty$, i.e., it vanishes. The reflected wave at $x = 0$ behaves like $1/\hat{T}(\omega_p)$, hence it is also zero. Yet there is a non-zero solution inside the medium. Such a solution is called a bound state (Chadan and Sabatier, 1977). Technically, a bound state is a square-integrable solution with negative energy. Physically, a bound state corresponds to an inverse scattering problem in which no scattering occurs. In nuclear physics, for example, this corresponds to an incident particle being captured by the nucleus. In seismology, this corresponds to a low-velocity zone in which energy is trapped in a waveguide-like effect.

Bound states can often be ruled out by causality. Suppose a medium initially at rest is probed with a causal disturbance

$$p(x,t) = \tilde{p}(x,t)1(t-x). \qquad (2\text{-}18)$$

If $p(x,t)$ is causal, its Fourier transform must be analytic in the lower half plane for all x. Then $\hat{T}(\omega) = \hat{p}(\infty,\omega)/\hat{p}(0,\omega)$ must also have this property, implying that there are no bound states (Newton, 1981).

Then the scattering matrix $S(\omega)$ can be completely reconstructed from $\hat{R}_L(\omega)$ or $\hat{R}_R(\omega)$. This is important, since in the inverse seismic problem, we have access to only one side of the scattering medium.

Note that our sign convention for the Fourier transform is the opposite of that of Faddeev (1967) and Chadan and Sabatier (1977), which explains why we use the lower half-plane to study the properties of $S(\omega)$, instead of the upper half-plane used in the mentioned references.

Having defined the inverse scattering problem for the two-component wave system, we now define procedures for solving it.

2.3 Differential Methods for Inverse Scattering--Layer Stripping

A differential or layer-stripping method for solving an inverse scattering problem works as follows. Suppose that the medium is being probed from the left, as in Figure 2.2a, and that the leftgoing and rightgoing waves $p(x,t)$ and $q(x,t)$ are known at x from previous recursions. The first reflection of the rightgoing wave $p(x,t)$ into the leftgoing wave $q(x,t)$ yields information about the medium at x. This information is then used to propagate the waves from x to $x + \Delta$. The problem has now been altered to one starting at $x + \Delta$ instead of at x. Since the waves continue to propagate through the medium, the procedure can be performed recursively, reconstructing the medium as the waves propagate through it.

This concept has been developed in some detail by Bruckstein et al (1983), and applied by Symes (1981), Santosa and Schwetlick (1982), and Bube and Burridge (1983) to the one-dimensional inverse seismic problem, and by Sondhi and Resnick (1983) to the inverse problem of

determining the shape of the human vocal tract. Note that it is a stripping principle instead of a constructive one: instead of extending the reconstructed medium from $[0,x]$ to $[0,x+\Delta]$, each recursion strips away the effect of the medium in $[x,x+\Delta)$, transforming the problem support from $[x,\infty)$ to $[x+\Delta,\infty)$. Hence the name "layer stripping."

2.3.1 The Continuous-Time Schur and Fast Cholesky Algorithms

The archetypical layer stripping algorithm is the fast Cholesky algorithm, so named because in its discrete form it performs a Cholesky factorization (LDU, or lower-triangular times diagonal times upper-triangular) of a Toeplitz matrix (Rissanen, 1973; Morf 1974; Musicus, 1981). The connection between this factorization and inverse scattering will be explored in Chapter III. The frequency-domain version of this algorithm is the Schur algorithm, and dynamic deconvolution utilizes a Riccati equation derived from the Schur algorithm. Although these three are different forms of the same algorithm, the fast Cholesky algorithm forms the most efficient procedure of the three for solving problems.

Fast Cholesky Algorithm

To obtain the fast Cholesky algorithm, we assume that the medium is quiescent at $t = 0$, and that it is probed from the left by a known rightward propagating wave

$$p(0,t) = \delta(t) + \tilde{p}(0,t)1(t) \qquad (2\text{-}19)$$

which is incident on the medium at $t = 0$. Here $\delta(\cdot)$ denotes the Dirac delta function and

$$1(t) = \begin{cases} 1 \text{ for } t \geq 0 \\ 0 \text{ for } t < 0 \end{cases} \tag{2-20}$$

is the unit step function. Note that the main feature of $p(0,t)$ is that it contains a leading impulse which can be thought of as a tag indicating the wavefront of the probing wave. The measured data is the reflected wave

$$q(0,t) = \tilde{q}(0,t)1(t) \tag{2-21}$$

recorded at $x = 0$. In the special case when $\tilde{p}(0,t) \equiv 0$, $\tilde{q}(0,t) = R_L(t)$ is the impulse response of the scattering medium and its Fourier transform $\hat{R}_L(\omega)$ is the left reflection coefficient. Note that $\hat{R}_L(\omega)$ can also be measured by sending into the medium sinusoidal waveforms at various frequencies and measuring the magnitude and phase shift of the reflected sinusoidal wave. In the following, for convenience we will omit the subscript L of $R_L(t)$ and $\hat{R}_L(\omega)$.

Since the medium is causal and originally at rest, the waves $p(x,t)$ and $q(x,t)$ inside the medium must have the form

$$p(x,t) = \delta(t-x) + \tilde{p}(x,t)1(t-x) \tag{2-22a}$$

$$q(x,t) = \tilde{q}(x,t)1(t-x) \tag{2-22b}$$

where $\tilde{p}(x,t)$ and $\tilde{q}(x,t)$ are smooth functions. By substituting (2-22) inside (2-1), and identifying coefficients of the impulse $\delta(t-x)$ on both sides of (2-16), we find that

$$r(x) = 2\tilde{q}(x,x) \tag{2-23}$$

and

$$\partial\tilde{p}/\partial x + \partial\tilde{p}/\partial t = -r(x)\tilde{q}(x,t) \tag{2-24a}$$

$$\partial\tilde{q}/\partial x - \partial\tilde{q}/\partial t = -r(x)\tilde{p}(x,t) \ . \tag{2-24b}$$

The recursions (2-23) - (2-24) constitute the fast Cholesky recursions (Bruckstein et al, 1983), and have also been called the downward continuation recursions by Bube and Burridge (1983). Note that only the smooth parts of $p(x,t)$ and $q(x,t)$ are propagated--it is not necessary to represent the impulse numerically.

The initial data for these recursions are the measured waves $\tilde{p}(0,t)$ and $\tilde{q}(0,t)$. The algorithm (2-23) - (2-24) can be viewed as using a layer stripping principle to identify the parameters of the scattering medium. Thus, assume that the waves $\tilde{p}(x,t)$ and $\tilde{q}(x,t)$ at x have been computed. The reflectivity function $r(x)$ is obtained from (2-23) and is used in (2-24) to compute the waves $\tilde{p}(x+\Delta,t)$ and $\tilde{q}(x+\Delta,t)$ at $x + \Delta$. The effect of the recursions (2-23) - (2-24) is therefore to identify and then strip away the layer $[x,x+\Delta)$.

Discretization of the Fast Cholesky Algorithm

To see how the fast Cholesky algorithm is propagated, let distance x and time t be discretized by $x = n\Delta$ and $t = m\Delta$, where n and m are positive integers. Then a forward-difference approximation to the partial derivatives in (2-24) yields the fast Cholesky recursions

$$\tilde{p}(x+\Delta,t+\Delta) = \tilde{p}(x,t) - r(x)\Delta\tilde{q}(x,t) \qquad (2\text{-}25a)$$

$$\tilde{q}(x+\Delta,t-\Delta) = \tilde{q}(x,t) - r(x)\Delta\tilde{p}(x,t) \qquad (2\text{-}25b)$$

$$\tilde{r}(x+\Delta) = 2\tilde{q}(x+\Delta,x+\Delta) \quad . \qquad (2\text{-}25c)$$

The recursion patterns for the waves are illustrated in Figures 2.3a and 2.3b. We start off knowing the waves at x for all t, and we wish to to find the waves at $x + \Delta$ for all t. Although it may seem as though information for $t < x$ is being lost, recall that by causality there can be

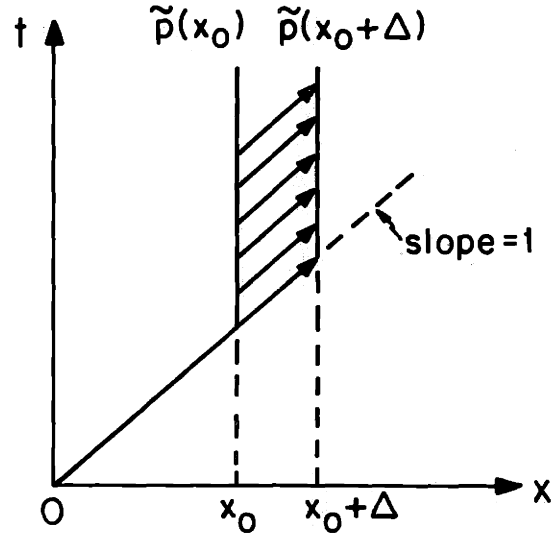

2.3a Recursion pattern for updating the downgoing waves in the fast Cholesky algorithm.

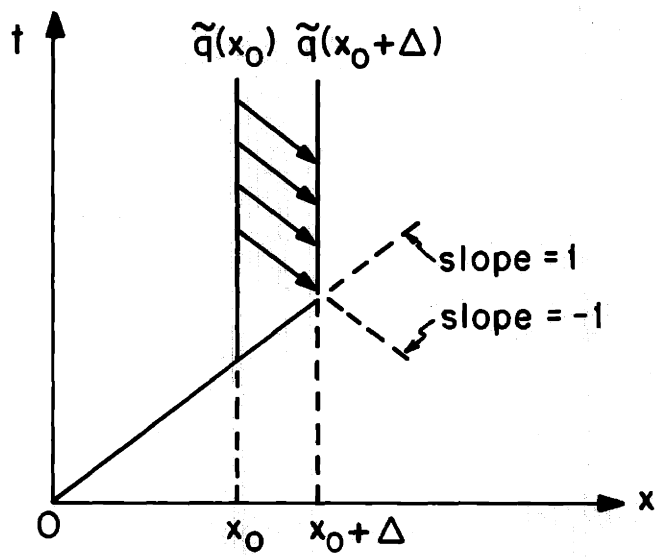

2.3b Recursion pattern for updating the upgoing waves in the fast Cholesky algorithm.

no wave at x until the initial excitation has had time to reach that far. Hence both waves are zero for $t < x$.

The Schur Algorithm

An alternative procedure for reconstructing the medium is to utilize directly the coupled differential equations (2-3) for the two-component wave system together with

$$r(x) = 2\tilde{q}(x,x) = \lim_{\omega \to \infty} 2j\omega e^{j\omega x} \tilde{q}(x,\omega) = \frac{1}{\pi}\int_0^\infty e^{j\omega x}\tilde{q}(x,\omega)d\omega \quad (2\text{-}26)$$

which follows immediately from the initial value theorem. It is still being assumed that the probing wave contains an impulse, as in (2-22). Equations (2-3) and (2-26) form the Schur algorithm.

Dynamic Deconvolution

Still another procedure is to consider the left reflection coefficient

$$\hat{R}(x,\omega) \triangleq \hat{q}(x,\omega)/\hat{p}(x,\omega) \quad (2\text{-}27)$$

which is associated with the section of the medium extending over $[x,\infty)$. $\hat{R}(x,\omega)$ is the transfer function for this section of the medium, relating the rightgoing probing wave $\hat{p}(x,\omega)$ to the leftgoing scattered wave $\hat{q}(x,\omega)$. It is easy to show, using (2-3), that $\hat{R}(x,\omega)$ satisfies the Riccati equation

$$d\hat{R}/dx = 2j\omega\hat{R} - r(x)(1-\hat{R}^2) \quad (2\text{-}28)$$

and since $\hat{R}$ and $d\hat{R}/dx$ are strictly proper we also have

$$r(x) = \lim_{\omega \to \infty} 2j\omega\hat{R}(x,\omega). \quad (2\text{-}29)$$

The dynamic deconvolution algorithm (2-28) - (2-29) is propagated in x,

yielding the left reflection coefficient $\hat{R}(x,\omega)$ and reflectivity function $r(x)$ for each x. This algorithm is a particularly dramatic illustration of the layer-stripping concept, in that each step of this algorithm transforms a complete inverse scattering problem on $[x,\infty)$, including the known medium response $\hat{R}(x,\omega)$, to an equivalent problem on $[x+\Delta,\infty)$, including the medium response $\hat{R}(x+\Delta,\omega)$.

It should be noted that many authors (e.g., Tolstoy and Clay, 1966; Pusey, 1975) have noted the Riccati equation (2-28), and in fact it is a direct consequence of the rules of composition of scattering layers (Redheffer, 1962). Gjevick et al. (1976) used this equation to develop an interative method for reconstructing $r(x)$. However, none of these results utilized (2-29) to propagate the Riccati equation in x. Corones et al. (1983) used the time-domain version of the Riccati equation as an invariant embedding equation, and Robinson (1982) and others derived the discrete form of this algorithm for the discrete one-dimensional inverse seismic problem. This is discussed in Chapter III.

It is worth noting that the $\hat{R}^2$ term in the Riccati equation accounts precisely for all multiple reflections within the scattering medium. To see this, neglect the $\hat{R}^2$ term in (2-23), leaving

$$d\hat{R}/dx = 2j\omega\hat{R} - r(x). \qquad (2\text{-}30)$$

This differential equation has the solution

$$\hat{R}(x,\omega) = \int_x^\infty r(y)e^{-2j\omega(y-x)}dy \qquad (2\text{-}31)$$

so that the reflection response of the medium is merely the superposition of the primary reflections at each depth y. These primary reflections have strength $r(y)$ and are phase-delayed by the two-way travel time

$2(y-x)$. Candel et al. (1980) used this assumption to recover $r(x)$ from $\hat{R}(0,\omega)$. This point was also noted by Corones et al. (1983) for the time-domain version of the Riccati equation.

Historical Background of the Algorithms

The fast Cholesky algorithm, as mentioned earlier, is so named because its discrete form performs a Cholesky (LDU) factorization of a Toeplitz matrix (see Musicus, 1981, for details). This algorithm, in its discrete form, seems to have appeared first in Rissanen (1973) and Morf (1974). The continuous algorithm similarly performs a causal-anticausal factorization of Toeplitz operators, a fact first brought to wide attention by Kailath et al. (1979).

The Schur algorithm (2-3) and (2-26) is the continuous version of an algorithm obtained by Schur (1917; see also Akhiezer, 1965) for testing the boundedness of a function $R(z)$ which is analytic outside the unit disk. Given $R(z)$, Schur showed that $|R(z)| \leq 1$ outside the unit disk if and only if the reflection coefficients r_n obtained from the recursions

$$R_{n+1}(z) = \frac{R_n(z)-r_n}{z(1-r_n R_n(z))} \quad , \quad R_0(z) = R(z) \tag{2-32a}$$

$$r_n = \lim_{z \to \infty} R_n(z) \tag{2-32b}$$

are such that $|r_n| \leq 1$. Some recursions similar to (2-32) can in fact be obtained by performing a backwards-difference discretization of the Riccati equation (2-28), as was done by Tolstoy and Clay (1966).

2.3.2 Example: The Lossless Non-uniform Transmission Line

In this section we study the inverse problem for the lossless non-uniform transmission line, and show that its solution is given by the Schur or fast Cholesky algorithms (see Gopinath and Sondhi, 1971, for an earlier solution of this problem). In the process, we give a scattering interpretation of transmission line phenomena such as waves, reflections, and impedances. This treatment can be found in many references, e.g., Kraus and Carver (1973) and Pusey (1975).

Consider an infinitesimal section of length Δ of a lossless non-uniform transmission line. Such a section is illustrated in Figure 2.4. Note that L(x) and C(x) represent inductance and capacitance per unit length, i.e., they are distributed quantities. Writing equations for Figure 2.4, we have

$$v(x,t) = L\Delta\,\partial i/\partial t + v(x + \Delta, t) \qquad (2\text{-}33a)$$

$$i(x,t) = C\Delta\,\partial v/\partial t + i(x + \Delta, t) \qquad (2\text{-}33b)$$

Dividing by Δ and letting $\Delta \to 0$, we obtain the telegrapher's equations

$$\partial v/\partial x + L(x)\partial i/\partial t = 0 \qquad (2\text{-}34a)$$

$$\partial i/\partial x + C(x)\,\partial v/\partial t = 0 \qquad (2\text{-}34b)$$

which also arise in acoustics (Santosa and Schwetlick, 1982) and in studies of the human vocal tract (Sondhi and Resnick, 1983; Gopinath and Sondhi, 1970) under the assumption of losslessness.

For a uniform line, it is well known (see Kraus and Carver, 1973) that (2-34) admits wave solutions, and that for such waves the ratio of the amplitudes of the voltage and current is the characteristic

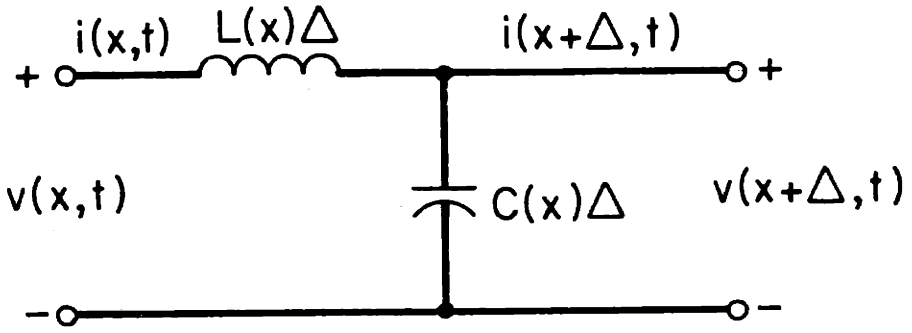

2.4 Infinitesimal section of a lossless non-uniform transmission line.

impedance

$$Z_0 \triangleq (L/C)^{\frac{1}{2}}. \tag{2-35}$$

Since the quantities p and q appearing in the two-component wave equations must be dimensionally equivalent, this suggests defining for the non-uniform line the dimensionally equivalent variables

$$V(x,t) = Z_0^{-\frac{1}{2}}\, v(x,t) \tag{2-36a}$$

$$I(x,t) = Z_0^{\frac{1}{2}}\, i(x,t) \tag{2-36b}$$

where $Z_0(x) = (L(x)/C(x))^{\frac{1}{2}}$. Substituting (2-36) in (2-34) yields

$$\partial V/\partial x + (LC)^{\frac{1}{2}}\, \partial I/\partial t = -\frac{1}{2}\frac{d}{dx} \ln Z_0\, V(x,t) \tag{2-37a}$$

$$\partial I/\partial x + (LC)^{\frac{1}{2}}\, \partial V/\partial t = \frac{1}{2}\frac{d}{dx} \ln Z_0\, I(x,t) \quad . \tag{2-37b}$$

In order to make the dependent variables x and t dimensionally equivalent, we replace x with the travel time z defined by

$$z(x) = \int_0^x (L(u)\, C(u))^{\frac{1}{2}}\, du \tag{2-38}$$

Since $(L(x)\, C(x))^{-\frac{1}{2}}$ is the local wave speed at x, z(x) is the time required for a wave, starting at x = 0, to reach position x. Making the additional change of variables

$$p(z,t) = \frac{1}{2}(V(z,t) + I(z,t)) \tag{2-39a}$$

$$q(z,t) = \frac{1}{2}(V(z,t) - I(z,t)) \tag{2-39b}$$

and defining the reflectivity function

$$r(z) = \frac{1}{2}\frac{d}{dz} \ln Z_0(z) \qquad (2\text{-}40)$$

we obtain the two-component wave system (2-1). The relations (2-39) provide an interpretation of the right and left propagating waves in terms of the normalized voltage and current.

Interpretation of the Reflection Coefficient

Suppose a uniform transmission line is terminated with a load Z_L. Then a wave travelling down the line will be reflected back by the load. Define $\hat{R}(\omega)$, the reflection coefficient for the load, to be the ratio of the Fourier transforms of the primary and reflected voltage waves, at the frequency ω. It is easy to show (see Kraus and Carver, 1973) that

$$\hat{R}(\omega) = \frac{\hat{v}_{REFL}(\omega)}{\hat{v}_{PRIM}(\omega)} = \frac{Z_L(\omega) - Z_0}{Z_L(\omega) + Z_0} \qquad (2\text{-}41)$$

where $Z_L(\omega)$ is the impedance (defined below in (2-42)).

For the non-uniform transmission line considered here, since there is a one-to-one correspondence between position x and travel time z, we will use x instead of z in the qualitative analysis to follow. Then, at point x on the line, the load perceived due to all of the line to the right of x is the impedance

$$Z_L(x,\omega) = \hat{v}(x,\omega)/\hat{i}(x,\omega) \quad . \qquad (2\text{-}42)$$

This is illustrated in Figure 2.5. By substituting this expression in (2-41), we find that for the non-uniform transmission line, the reflection coefficient at point x is

$$\hat{R}(x,\omega) = \frac{\hat{v}/\hat{i} - Z_0(x)}{\hat{v}/\hat{i} + Z_0(x)} = \frac{\hat{V}/\hat{I} - 1}{\hat{V}/\hat{I} + 1}$$

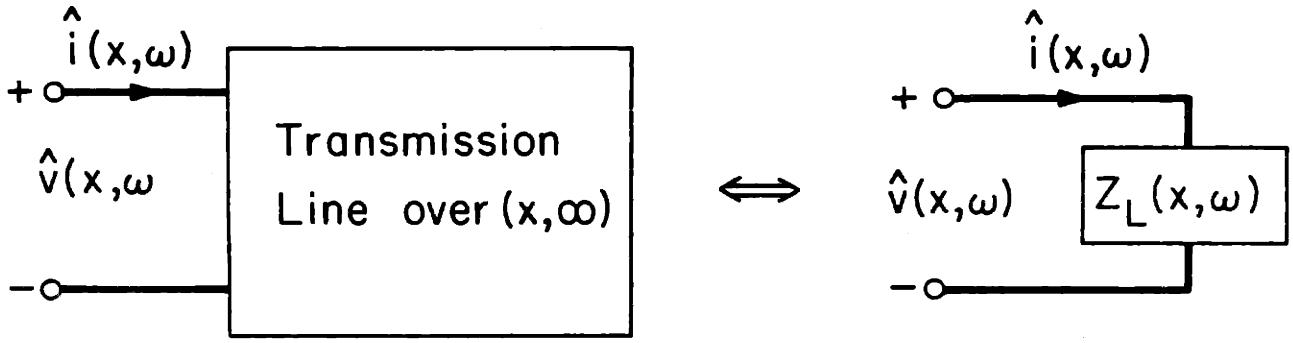

2.5 The perceived load to the right of x .

$$= \hat{q}(x,\omega)/\hat{p}(x,\omega) \qquad (2\text{-}43)$$

This is precisely the expression (2-27) for the left reflection coefficient of the section of the two-component system (2-1) extending over $[x,\infty)$.

We see therefore the meaning of $\hat{R}(z,\omega)$. For a given point x on the line, and any given frequency ω, it is the ratio of the reflected and primary voltage waves, with the reflection due to the inhomogeneity of the line at x. From Section 2.3.1, we know that $\hat{R}(z,\omega)$ satisfies the Riccati equation (2-28), and that r(x) may be found from $\hat{R}(x,\omega)$ by using (2-29). Also note that if the line is locally uniform at point x_0, we have $dZ_0/dx|_{x_0} = 0$, hence $r(x_0) = 0$ and no reflection occurs. Reflections occur only where the line is inhomogeneous.

Inverse Problem

Suppose now that the line characteristics L(x) and C(x) are unknown and that we want to determine them from the measured impedance $Z(\omega) = Z_L(0,\omega)$. This problem arises not only when we want to find the characteristics of an existing transmission line, but also if we want to synthesize a transmission line with prescribed impedance $Z(\omega)$. It is assumed here that we have access to only one end of the line. The line characteristics can be partially reconstructed as follows. First, scale $Z_0(0)$ to 1 and consider the reflection coefficient

$$\hat{R}(\omega) = \frac{Z(\omega) - 1}{Z(\omega) + 1} \cdot \qquad (2\text{-}44)$$

Then, run the Schur algorithm (2-3) - (2-26), using $\hat{R}(\omega)$ as initial condition, to obtain r(z). Alternately, we may compute the inverse Fourier transform R(t) of $\hat{R}(\omega)$, and use the fast Cholesky recursions (2-23) - (2-24) to obtain r(z). Given r(z), the expression

$$Z_0(z) = \exp 2 \int_0^z r(u)\, du \qquad (2\text{-}45)$$

enables us to recover the characteristic impedance $Z_0(z) = (L(z)/C(z))^{\frac{1}{2}}$ as a function of the travel time z. However, we cannot reconstruct L(x) and C(x) separately as functions of the position x.

The same difficulty will appear in Chapter III for the one-dimensional inverse seismic problem, except that in this case we will be able to use an additional degree of freedom, the angle of incidence of the probing waves, in order to reconstruct the medium completely.

2.3.3 Inverse Scattering for Asymmetric Two-Component Wave Systems

In this section, the inverse scattering problem for asymmetric two-component wave equations is examined, and solved by using two coupled fast Cholesky algorithms. The systems which are described by asymmetric two-component wave equations are not necessarily lossless, and we can therefore use these equations to describe a larger class of physical phenomena than those that we have studied in the previous sections. Our results will be illustrated by considering the inverse problem for a nonuniform transmission line with losses. It is worth noting that a solution of the inverse scattering problem for asymmetric two-component wave equations was presented in Ablowitz and Segur (1981) and was used by Jaulent (1982) to solve the inverse problem for lossy transmission lines. However, this method relied on the solution of two coupled Marchenko equations, whereas the solution that we present here is differential, and uses the layer stripping principle.

The system that we consider is described by the asymmetric two-component wave equations

$$\frac{d}{dx}\begin{bmatrix}\hat{p}\\ \hat{q}\end{bmatrix} = \begin{bmatrix}-j\omega & -s(x)\\ -r(x) & j\omega\end{bmatrix}\begin{bmatrix}\hat{p}\\ \hat{q}\end{bmatrix} \tag{2-46}$$

which in the time domain correspond to

$$(\partial/\partial x + \partial/\partial t)p = -s(x)\, q(x,t) \tag{2-47a}$$

$$(\partial/\partial x - \partial/\partial t)q = -r(x)\, p(x,t) \tag{2-47b}$$

It is assumed that $r(x) = s(x) = 0$ for $x < 0$, and that $r, s \in L_1[0,\infty)$, so that $r(x)$ and $s(x)$ are localized, i.e., they go to zero as $x \to \infty$.

Then, the scattering matrix $S(\omega)$ can be defined as in Section 2.2 by relating the outgoing and incoming waves appearing in Figure 2.2. In addition, the property (2-9) for the Wronskian of two independent solutions $a_i^T(x,\omega) = (\hat{p}_i(x,\omega), \hat{q}_i(x,\omega))$, $i = 1, 2$ of (2-46) remains valid, and by applying it to the waves $a_1(x,\omega)$ and $a_2(x,\omega)$ appearing in Figures 2.2a and 2.2b, respectively, we obtain again the reciprocity relation

$$\hat{T}_L(\omega) = \hat{T}_R(\omega) \ . \tag{2-48}$$

However, if $a^T(x,\omega) = (\hat{p}(x,\omega), \hat{q}(x,\omega))$ is an arbitrary solution of (2-46) we have

$$\frac{d}{dx}\left(|\hat{p}|^2 - |\hat{q}|^2\right) = 2(r(x) - s(x))\, \mathrm{Re}(\hat{p}(x,\omega)\hat{q}^*(x,\omega)) \tag{2-49}$$

so that the scattering medium associated to (2-46) is not lossless unless $r(x) = s(x)$, which corresponds to the case when the two-component wave equations are symmetric. This implies that $S(\omega)$ is not a unitary matrix, and consequently we cannot recover $S(\omega)$ from the knowledge of the left reflection coefficient $\hat{R}_L(\omega)$ alone.

Inverse Scattering Procedure

The inverse scattering method that we develop here relies on the observation that if time is reversed (i.e., t is changed to -t in (2-47), or ω is changed to $-\omega$ in (2-46)), and if the waves p and q are interchanged, we obtain a (synthetic) asymmetric two-component wave system

$$(\partial/\partial x + \partial/\partial t)p^A = -r(x)\, q^A(x,t) \qquad (2\text{-}50a)$$

$$(\partial/\partial x - \partial/\partial t)q^A = -s(x)\, p^A(x,t) \qquad (2\text{-}50b)$$

where r(x) replaces s(x) and vice-versa. The scattering matrix associated to this system is

$$S^A(\omega) = \begin{bmatrix} 0 & 1 \\ 1 & 0 \end{bmatrix} S^{-1}(-\omega) \begin{bmatrix} 0 & 1 \\ 1 & 0 \end{bmatrix}$$

$$= (S^H(\omega))^{-1} . \qquad (2\text{-}51)$$

where to obtain (2-51) we have used the reciprocity relation (2-48). The system (2-50) is a fake system, which does not really exist, but its scattering matrix is entirely specified by the knowledge of $S(\omega)$.

Then, in order to reconstruct r(x) and s(x), we assume that the true system (2-46) and the fake system (2-50) are probed simultaneously by some waves which have the form

$$p(x,t) = \delta(t-x) + \tilde{p}(x,t)\, 1(t-x)$$

$$q(x,t) = \tilde{q}(x,t)\, 1(t-x) \qquad (2\text{-}52)$$

and

$$p^A(x,t) = \delta(t-x) + \tilde{p}^A(x,t) 1(t-x)$$

$$q^A(x,t) = \tilde{q}^A(x,t)1(t-x) \quad . \tag{2-53}$$

By substituting these waves in (2-46) and (2-50), we obtain the system of coupled fast Cholesky recursions

$$\begin{aligned}(\partial/\partial x + \partial/\partial t)\tilde{p} &= -s(x)\ \tilde{q}(x,t) \\ (\partial/\partial x - \partial/\partial t)\tilde{q} &= -r(x)\ \tilde{p}(x,t)\end{aligned} \tag{2-54a}$$

and

$$\begin{aligned}(\partial/\partial x + \partial/\partial t)\tilde{p}^A &= -r(x)\ \tilde{q}^A(x,t) \\ (\partial/\partial x - \partial/\partial t)\tilde{q}^A &= -s(x)\ \tilde{p}^A(x,t)\end{aligned} \tag{2-54b}$$

with

$$r(x) = 2\tilde{q}(x,x),\ s(x) = 2\tilde{q}^A(x,x) \tag{2-54c}$$

which can be propagated recursively for increasing values of x, starting from x = 0. The specification of the initial conditions for these recursions is very important, since as noted above, the system (2-50) does not really exist, and cannot be relied upon to provide some experimental waves $\tilde{p}^A(0,t)$ and $\tilde{q}^A(0,t)$.

The initial conditions that we select are

$$\tilde{p}(0,t) = \tilde{p}^A(0,t) = 0 \tag{2-55a}$$

$$\tilde{q}(0,t) = R_L(t)\ ,\ \tilde{q}^A(0,t) = R_L^A(t) \tag{2-55b}$$

where $R_L(t)$ and $R_L^A(t)$ denote the inverse Fourier transforms of the left reflection coefficients $\hat{R}_L(\omega)$ and $\hat{R}_L^A(\omega)$. $\hat{R}_L(\omega)$ can be measured directly, and from (2-51)

$$\hat{R}_L^A(\omega) = (S^{-H}(\omega))_{21} \tag{2-56}$$

i.e., $\hat{R}_L^A(\omega)$ is the (2, 1) entry of the inverse of $S^H(\omega)$. Thus, $\hat{R}_L^A(\omega)$ can be expressed as a function of the whole scattering matrix $S(\omega)$, and it will be specified provided that we can measure all the entries of $S(\omega)$. This implies that we must have access to both ends of the scattering medium. In some cases, such as for the inverse seismic problem, this is impossible; but for some other problems, such as the reconstruction of non-uniform lossy transmission lines, the medium can be probed from both sides, and all the entries of $S(\omega)$ can be measured.

Instead of expressing our reconstruction procedure in terms of the coupled fast Cholesky recursions described above, we can also use a set of coupled Schur recursions. Let

$$\hat{R}(x,\omega) = \frac{\hat{q}(x,\omega)}{\hat{p}(x,\omega)} \quad \text{and} \quad \hat{R}^A(x,\omega) = \frac{\hat{q}^A(x,\omega)}{\hat{p}^A(x,\omega)} \tag{2-57}$$

be the left reflection coefficients for the true and fake systems over the interval $[x,\infty)$, where the waves $\hat{p}$, $\hat{q}$, $\hat{p}^A$, $\hat{q}^A$ in the definition (2-57) are assumed to have the forms (2-52) - (2-53). Then, $\hat{R}(x,\omega)$ and $\hat{R}^A(x,\omega)$ satisfy the coupled Riccati equations

$$d\hat{R}/dx = 2j\omega\hat{R} + s(x)\,\hat{R}^2 - r(x) \tag{2-58a}$$

$$d\hat{R}^A/dx = 2j\omega\hat{R}^A + r(x)(\hat{R}^A)^2 - s(x) \tag{2-58b}$$

with initial conditions

$$\hat{R}(0,\omega) = \hat{R}_L(\omega),\ \hat{R}^A(0,\omega) = \hat{R}_L^A(\omega) \tag{2-59}$$

By using the initial value theorem for the reflection coefficients (2-57),

and taking into account the form of the waves (2-52) - (2-53), we get

$$\lim_{\omega \to \infty} 2j\omega\hat{R}(x,\omega) = r(x) \qquad (2\text{-}60a)$$

$$\lim_{\omega \to \infty} 2j\omega\hat{R}^{A}(x,\omega) = s(x) \qquad (2\text{-}60b)$$

which can be combined with (2-58a) and (2-58b) to propagate $\hat{R}(x,\omega)$ and $\hat{R}^{A}(x,\omega)$ recursively, and to reconstruct $r(x)$ and $s(x)$ for all x. This algorithm constitutes the generalization of the Schur algorithm.

2.3.4 Example: The Non-uniform Transmission Line with Losses

In Section 2.3.2, the reconstruction problem for a non-uniform lossless transmission line was solved using the fast Cholesky and Schur algorithms. We now consider the more general case where some losses, in the form of series and shunt resistances per unit length have been added to the transmission line. This reconstruction problem is then solved as an asymmetric two-component inverse scattering problem, using the method obtained at the beginning of this section. The problem is set up as in Jaulent (1982).

An infinitesimal section of the line is shown in Figure 2.6. $R(x)$ is the nonuniform series resistance per unit length, representing the finite resistance of the wires, and $G(x)$ is the shunt conductance per unit length, representing leakage current between the wires. The circuit equations are

$$v(x,t) = (L\partial i/\partial t + Ri)\Delta + v(x+\Delta, t) \qquad (2\text{-}61a)$$

$$i(x,t) = (C\partial v/\partial t + Gv)\Delta + i(x+\Delta, t) \quad . \qquad (2\text{-}61b)$$

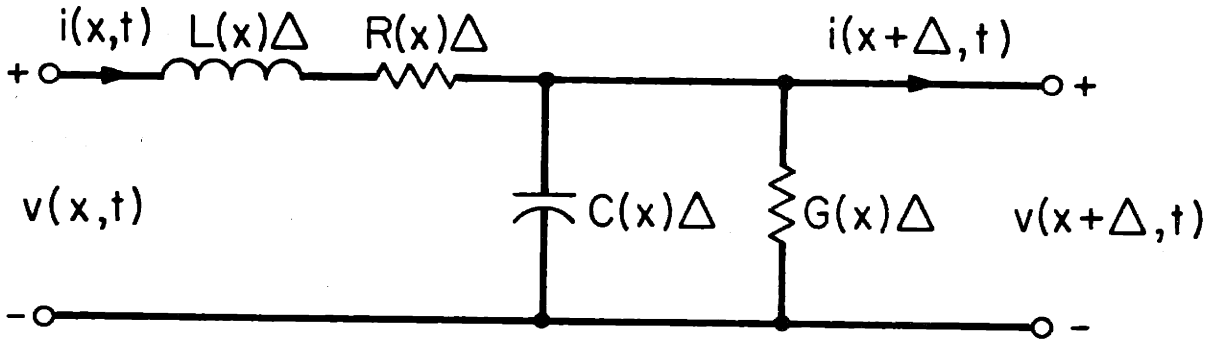

2.6 Infinitesimal section of a lossy non-uniform transmission line.

Dividing by Δ, and letting $\Delta \to 0$ yields the transmission line equations

$$\partial v/\partial x + L\, i/\partial t + Ri = 0 \qquad (2\text{-}62a)$$

$$\partial i/\partial x + C\, v/\partial t + Gv = 0 \qquad (2\text{-}62b)$$

As in Section 2.3.2, we replace the position x by the travel time z(x) given by (2-38), and we introduce the dimensionally equivalent variables

$$V(z,t) = Z^{-\frac{1}{2}} v(z,t) \qquad (2\text{-}63a)$$

$$I(z,t) = Z^{\frac{1}{2}} i(z,t) \qquad (2\text{-}63b)$$

where $Z(z) = (L(z)/C(z))^{\frac{1}{2}}$ is the characteristic impedance. Then, the equations (2-62) take the form

$$\partial V/\partial z + \partial I/\partial t = -\frac{R}{L}\, I - m(z)V \qquad (2\text{-}64a)$$

$$\partial I/\partial z + \partial V/\partial t = m(z)\, I - \frac{G}{C}\, V \qquad (2\text{-}64b)$$

where

$$m(z) = \frac{1}{2}\, \frac{d}{dz}\, \ell n\, Z(z)\ . \qquad (2\text{-}65)$$

Making the change of variables

$$p(z,t) = \frac{1}{2}\,(V+I) \qquad (2\text{-}66a)$$

$$q(z,t) = \frac{1}{2}\,(V-I) \qquad (2\text{-}66b)$$

gives

$$(\partial/\partial z + \partial/\partial t)p = -a(z)p(z,t) - (m(z) + b(z))q(z,t) \qquad (2\text{-}67a)$$

$$(\partial/\partial z - \partial/\partial t)q = -(m(z) - b(z))p(z,t) + a(z)q(z,t) \qquad (2\text{-}67b)$$

which is almost in the desired form, and where

$$a(z) = \frac{1}{2}\left(\frac{G}{C} + \frac{R}{L}\right) \tag{2-68a}$$

$$b(z) = \frac{1}{2}\left(\frac{G}{C} - \frac{R}{L}\right) \quad . \tag{2-68b}$$

Considering the scaled variables

$$p^1(z,t) = p(z,t) \exp \int_0^z a(u)\, du \tag{2-69a}$$

$$q^1(z,t) = q(z,t) \exp -\int_0^z a(u)\, du \tag{2-69b}$$

and taking the Fourier transforms yields the asymmetric two-component wave equations

$$\frac{d}{dz}\,\hat{p}^1 = -j\omega\hat{p}^1(z,\omega) - s(z)\hat{q}^1(z,\omega) \tag{2-70a}$$

$$\frac{d}{dz}\,\hat{q}^1 = -r(z)\hat{p}^1(z,\omega) + j\omega\hat{q}^1(z,\omega) \tag{2-70b}$$

where

$$r(z) = (m-b)\exp -2\int_0^z a(u)du = \left(\frac{1}{4}\,\frac{d}{dz}\,(\ell n\frac{L}{C}) - \frac{1}{2}(\frac{G}{C} - \frac{R}{L})\right)\exp\, -\int_0^z\left(\frac{R}{L} + \frac{G}{C}\right) du \tag{2-71a}$$

$$s(z) = (m+b)\exp 2\int_0^z a(u)du = \left(\frac{1}{4}\,\frac{d}{dz}\,(\ell n\frac{L}{C}) + \frac{1}{2}(\frac{G}{C} - \frac{R}{L})\right)\exp\, \int_0^z\left(\frac{R}{L} + \frac{G}{C}\right) du \tag{2-71b}$$

Thus, if we are given the scattering matrix $S(\omega)$ associated to the system (2-70), the coupled fast Cholesky (2-54) or Schur (2-58) - (2-60) algorithms may be used to reconstruct the rather bizarre quantities $r(z)$

and s(z). Further, these two quantities are the most information about the line that can be obtained from this data. Although r(z) and s(z) may seem to be peculiar quantities, this result is in agreement with Jaulent (1982).

Note that in the event

$$R(z)/L(z) = G(z)/C(z) \tag{2-72}$$

we may recover Z(z) and R(z)/L(z) by multiplying and dividing r(z) and s(z), and then solving two differential equations. Thus, in this case it is possible to recover R(z), L(z), C(z), and G(z) in various ratios quite easily. This case is referred to as the Heaviside condition for a distortionless line (Kraus and Carver, 1973), since if (2-72) holds then the true characteristic impedance $((R + j\omega L)/(G + j\omega C))^{\frac{1}{2}}$ which relates the current and voltage for a wave travelling down the line, is real. Thus, the current and voltage for such a wave are in phase, just as in the lossless line, and it is not surprising that ratios of various line parameters can be recovered, as in the lossless case.

2.3.5 Other Differential Methods

In this section we quickly cover three other differential or layer stripping algorithms. These consist of the misnamed "method of characteristics" of Santosa and Schwetlick (1982), and two procedures for recovering the potential of a Schrodinger equation. These procedures will all be applied to inverse seismic problems in Chapters VII and VIII.

The "Method of Characteristics"

This refers to the impedance reconstruction procedure used by Santosa and Schwetlick (1982). Although it is technically incorrect

terminology, it has been used both by Santosa and Schwetlick (1982) and by Bruckstein et al. (1983), and no other term has come along to replace it. Hence, to be in accord with the literature, the term "method of characteristics" will be used here and in Chapter VIII. The true method of characteristics is discussed in Courant and Hilbert (1962), and applied to the propagation of axial shear waves in Achenbach (1975).

The method will be illustrated by applying it to the problem of reconstructing the impedance of a lossless transmission line. Recall from Section 2.3.2 that this problem was transformed into a two-component wave system problem by defining the waves

$$p(z,t) = \frac{1}{2}\,(V(z,t) + I(z,t)) \tag{2-73a}$$

$$q(z,t) = \frac{1}{2}\,(V(z,t) - I(z,t)) \tag{2-73b}$$

where

$$V(z,t) = Z_0^{-\frac{1}{2}}\, v(z,t) \tag{2-74a}$$

$$I(z,t) = Z_0^{\frac{1}{2}}\, i(z,t) \tag{2-74b}$$

Here $v(z,t)$ and $i(z,t)$ are the voltage and current, $Z_0(z)$ is the characteristic impedance (which is to be recovered), and z is travel time. Suppose now that the probing wave $p(z,t)$ does <u>not</u> contain a leading impulse, contrary to equations (2-22). Then, by causality, the waves $p(z,t)$ and $q(z,t)$ have the form

$$p(z,t) = \tilde{p}(z,t)1(t-z) \tag{2-75a}$$

$$q(z,t) = \tilde{q}(z,t)1(t-z) \tag{2-75b}$$

Substituting equations (2-75) into the two-component wave system (2-1) yields

$$\tilde{q}(z,z^+) = 0 \tag{2-76}$$

and, using (2-73b), this implies that

$$V(z,z^+) = I(z,z^+) \ . \tag{2-77}$$

From definitions (2-74) we have

$$Z_0(z) = v(z,z^+)/i(z,z^+) \tag{2-78}$$

and changing variables from position x to travel time z in the telegrapher's equations (2-34) yields

$$\partial v(z,t)/\partial z + Z_0 \partial i(z,t)/\partial t = 0 \tag{2-79a}$$

$$Z_0 \partial i(z,t)/\partial z + \partial v(z,t)/\partial t = 0 \ . \tag{2-79b}$$

Equations (2-78) - (2-79) form the method of characteristics for the lossless transmission line. The voltage v(z,t) and current i(z,t) can be propagated in z, yielding the impedance $Z_0(z)$ by (2-73).

As in the fast Cholesky algorithm, $Z_0(z)$ can be recovered because in the instant after the wavefront passes v and i must be related by (2-78). Unlike the fast Cholesky algorithm, no probing impulse is necessary. However, all physical interpretations in terms of waves and scattering have been lost--the procedure is a purely mathematical technique applied to partial differential equations.

Inverse Scattering and the Schrodinger Equation

Inverse scattering problems are often formulated using the

Schrodinger equation

$$\frac{d^2}{dx^2}\hat{y} + (\omega^2 - V(x))\hat{y}(x,\omega) = 0 \qquad (2\text{-}80)$$

and a scattering matrix, which was described in Section 2.2. Here the aim is to reconstruct the potential $V(x)$. $V(x)$ is usually assumed to be localized, i.e., $V(x) = 0$ for $x < 0$ and

$$\int_0^\infty (1+x)\,|V(x)|dx < \infty. \qquad (2\text{-}81)$$

The Schrodinger equation appears frequently in the literature on inverse scattering problems in nuclear physics (e.g., Chadan and Sabatier, 1977) and seismology (Ware and Aki, 1969, and many others). In this section two layer-stripping methods for recovering $V(x)$ are presented. Both methods will be used in Chapter VII, where the inverse problem for a layered acoustic medium probed by spherical harmonic waves is formulated using the Schrodinger equation. The standard integral equation methods for recovering $V(x)$ are covered in Section 2.4.

Reformulation of the Schrodinger Equation as a Two-Component System

Any two-component wave system inverse scattering problem can be recast as a Schrodinger equation inverse scattering problem. Thus in seeking a layer stripping solution to the Schrodinger inverse problem, it seems natural to try to recast it as a two-component wave system inverse problem. This has been done in Yagle and Levy (1984), and their technique is repeated below.

Taking the derivative of the two-component system (2-3) with

respect to x, we obtain the matrix Schrodinger equation

$$\left(\left(\frac{d^2}{dx^2} + \omega^2 I_2\right) - \begin{bmatrix} r^2 & -\dot{r} \\ -\dot{r} & r^2 \end{bmatrix}\right)\begin{bmatrix} \hat{p}(x,\omega) \\ \hat{q}(x,\omega) \end{bmatrix} = 0 \qquad (2\text{-}82)$$

where I_2 denotes the 2 x 2 identity matrix and $\dot{r}(x) = dr/dx$. By making the change of variable

$$\hat{y}_1(x,\omega) = \hat{p}(x,\omega) + \hat{q}(x,\omega) \qquad (2\text{-}83a)$$

$$\hat{y}_2(x,\omega) = \hat{p}(x,\omega) - \hat{q}(x,\omega) \qquad (2\text{-}83b)$$

this equation can be decoupled into two scalar Schrodinger equations

$$\frac{d^2}{dx^2}\hat{y}_1 + (\omega^2 - V_1(x))\hat{y}_1(x,\omega) = 0 \qquad (2\text{-}84a)$$

$$\frac{d^2}{dx^2}\hat{y}_2 + (\omega^2 - V_2(x))\hat{y}_2(x,\omega) = 0 \qquad (2\text{-}84b)$$

where

$$V_1(x) = r^2(x) - \dot{r}(x) \qquad (2\text{-}85a)$$

$$V_2(x) = r^2(x) + \dot{r}(x) \qquad (2\text{-}85b)$$

This shows how any two-component wave system inverse problem can be recast as a Schrodinger inverse problem. In addition, we observe from (2-83) and from the definition of the scattering matrix $S(\omega)$ of the two-component system (2-3) that the scattering matrix associated to $V_1(x)$ is identical to that of (2-3), and that the scattering matrix

$S_2(\omega)$ associated to $V_2(x)$ is given by

$$S_2(\omega) = \begin{bmatrix} \hat{T}_L(\omega) & -\hat{R}_R(\omega) \\ -\hat{R}_L(\omega) & \hat{T}_R(\omega) \end{bmatrix} = \Sigma S(\omega) \Sigma \quad , \tag{2-86}$$

i.e., it is obtained by changing the sign of the reflection coefficients $\hat{R}_L$ and $\hat{R}_R$ of (2-3).

Consequently, given a potential $V(x)$, we can always view its left reflection coefficient $\hat{R}_L(\omega)$ as arising from a two-component system such as (2-3). Then, given $\hat{R}_L(\omega)$ or the impulse reponse $R_L(t)$, we can use the Schur or fast Cholesky recursions to reconstruct the reflectivity function $r(x)$, which in turn can be used to recover $V(x)$ from the relation (2-85a). The relation (2-85a) is known in soliton theory as the Miura transformation (Ablowitz and Segur, 1981; Lamb, 1980), and it maps solutions of the modified Korteweg-de Vries equation into solutions of the Korteweg-de Vries equation.

Direct Recovery of Potential

Bruckstein et al. (1983) have pointed out that the potential $V(x)$ may also be recovered directly, without first reconstructing the reflectivity function $r(x)$. Applying their procedure to the Schrodinger equation (2-80), we take the inverse Fourier transform of (2-80), which is

$$\partial^2 y/\partial x^2 - \partial^2 y/\partial t^2 = V(x)y(x,t). \tag{2-87}$$

Note that this is the equation for an elastically braced string. Defining

$$\psi(x,t) \triangleq (\partial/\partial x + \partial/\partial t)y(x,t) \tag{2-88}$$

equation (2-87) can be rewritten as the coupled system

$$(\partial/\partial x + \partial/\partial t)y(x,t) = \psi(x,t) \qquad (2\text{-}89a)$$

$$(\partial/\partial x - \partial/\partial t)\psi(x,t) = V(x)y(x,t) \qquad (2\text{-}89b)$$

Now, if $y(x,t)$ can be shown to contain a leading impulse, as $p(x,t)$ does in (2-22a), we have

$$V(x) = -2\,\psi(x,x^+) \; . \qquad (2\text{-}90)$$

Equations (2-89) - (2-90) can be propagated in x as a recursive algorithm. Initialization of y and ψ at $x = 0$ depends on the problem; see Chapter VII for an example.

Bruckstein et al. (1983) have pointed out that this algorithm can be interpreted as successively truncating the potential $V(x)$. If the algorithm is at point x in the medium, the current problem being solved is one in which the medium to the left of x has been replaced by free space (i.e., $V(z) = 0$ for $z < x$). Thus again we see how a layer stripping algorithm transforms at each step a problem on the interval $[x,\infty)$ to one on $[x + \Delta, \infty)$.

2.4 Integral Equation Methods for Solving Inverse Scattering Problems

In this section we switch gears and review integral equation methods for solving inverse scattering problems. None of these methods will be employed in this thesis; indeed, the purpose of this thesis is to obviate these methods. Nevertheless, it is important that integral equation methods be understood so that the dual nature of differential and integral methods be appreciated.

Recall the layer-stripping action of differential methods, in which a problem on the interval $[x,\infty)$ is transformed into one on $[x + \Delta, \infty)$ at each step of the algorithm. In contrast, integral equation methods are constructive, in that the entire medium is involved at each step, and the reconstructed portion is extended from $[0,x]$ to $[0, x + \Delta]$ at each step. The concept of adding to the reconstructed portion of medium, in contrast to stripping away from the unreconstructed portion of the medium, will be illustrated throughout this section.

2.4.1 The Marchenko, Gel'fand-Levitan, and Krein Integral Equations

In this subsection we follow Bruckstein et al. (1983) in deriving the above three integral equations for solving the two-component wave system inverse scattering problem. Other approaches are possible; Burridge (1980) derives these equations entirely in the time domain, using Green's functions, convolutions, and Green's identities. In contrast, Chadan and Sabatier (1977) and Lamb (1980) use a spectral, frequency-domain approach, while Faddeev (1963) uses an operator approach. However, the approach of Bruckstein et al. is the simplest, and fits in most readily with the material of Section 2.3.

Note that the two-component wave system in the frequency domain (2-3) can be viewed as a state equation in the state $\begin{bmatrix} \hat{p}(x,\omega) \\ \hat{q}(x,\omega) \end{bmatrix}$. Then we may define the state transition matrix $\hat{M}(x,\omega)$ for this system. $\hat{M}(x,\omega)$ is specified by

$$\frac{d}{dx}\hat{M}(x,\omega) = \begin{bmatrix} -j\omega & -r(x) \\ -r(x) & j\omega \end{bmatrix} \hat{M}(x,\omega) \qquad (2\text{-}91)$$

and

$$\hat{M}(0,\omega) = I_2 \ , \tag{2-92}$$

and has the property that

$$\begin{bmatrix} \hat{p}(x,\omega) \\ \hat{q}(x,\omega) \end{bmatrix} = \hat{M}(x,\omega) \begin{bmatrix} \hat{p}(0,\omega) \\ \hat{q}(0,\omega) \end{bmatrix} \ . \tag{2-93}$$

Taking the inverse Fourier transforms with respect to <u>time</u> yields

$$\partial M(x,t)/\partial x = \begin{bmatrix} -\partial/\partial t & -r(x) \\ -r(x) & \partial/\partial t \end{bmatrix} M(x,t) \tag{2-94}$$

$$M(0,t) = \begin{bmatrix} \delta(t) & 0 \\ 0 & \delta(t) \end{bmatrix} \tag{2-95}$$

$$\begin{bmatrix} p(x,t) \\ q(x,t) \end{bmatrix} = \begin{bmatrix} M_{11}(x,t) & M_{12}(x,t) \\ M_{21}(x,t) & M_{22}(x,t) \end{bmatrix} * \begin{bmatrix} p(0,t) \\ q(0,t) \end{bmatrix} \ . \tag{2-96}$$

Equations (2-94) and (2-95), and the principle of causality, show that $M_{11}(x,t)$ and $M_{21}(x,t)$ have the forms

$$M_{11}(x,t) = \delta(x-t) + \tilde{M}_{11}(x,t)(1(x-t) - 1(x+t)) \tag{2-97a}$$

$$M_{21}(x,t) = \tilde{M}_{21}(x,t)(1(x-t) - 1(x+t)) \ . \tag{2-97b}$$

This simply means that $M_{11}(x,t)$ contains a leading impulse (from (2-95)) $M_{11}(x,t)$ and $M_{21}(x,t)$ have support on $[-x,x]$, and $\tilde{M}_{11}$ and $\tilde{M}_{21}$ are the smooth parts of M_{11} and M_{21}. We also note that if time is reversed, the left and right propagating waves are interchanged, so that

$$M_{11}(x,t) = M_{22}(x,-t) \tag{2-98a}$$

$$M_{21}(x,t) = M_{12}(x,-t) \tag{2-98b}$$

Now, if the medium is being probed from the left, we have by causality

$$p(x,t) = q(x,t) = 0 \text{ for } t < x \ . \tag{2-99}$$

Note that we have not yet specified how the probing is to take place. Using (2-97), (2-98), and (2-99) in (2-96) yields the coupled integral equations

$$\int_{-x}^{t} p(0,t-\tau)\tilde{M}_{11}(x,\tau)d\tau \ + \ \int_{-t}^{x} q(0,t+\tau)\tilde{M}_{21}(x,\tau)d\tau = 0 \tag{2-100a}$$

$$q(0,t+x) + \int_{-t}^{x} q(0,t+\tau)\tilde{M}_{11}(x,\tau)d\tau + \int_{-x}^{t} p(0,t-\tau)\tilde{M}_{21}(x,\tau)d\tau = 0 \tag{2-100b}$$

In these equations, a change in the sign of the dummy variable τ has been made in the terms involving $q(x,t)$ in order to make use of (2-98). This explains the $t + \tau$ dependence of q.

The Marchenko, Gel'fand-Levitan, and Krein integral equations are all derived from (2-100). The particular equation obtained depends on how the medium is probed.

Marchenko equation (half-space boundary): Let the probing waves take the form

$$p(0,t) = \delta(t) \tag{2-101a}$$

$$q(0,t) = R(t) \tag{2-101b}$$

where $R(t)$ is causal. This corresponds to the case of a medium being probed from an infinite homogeneous half-space. Define

$$K(x,t) = \tilde{M}_{11}(x,t) + \tilde{M}_{21}(x,t). \tag{2-102}$$

Then, adding (2-100a) and (2-100b) and inserting (2-101) and (2-102) yields the Marchenko integral equation (Agranovich and Marchenko, 1963; Chadan and Sabatier, 1977)

$$K(x,t) + R(x+t) + \int_{-t}^{x} K(x,\tau)R(\tau+t)d\tau = 0, \quad t < x \tag{2-103}$$

Upon solving this integral equation for $K(x,t)$ we may use

$$r(x) = -2\tilde{M}_{21}(x,x^-) \tag{2-104a}$$

$$r^2(x) = 2\frac{d}{dx}\tilde{M}_{11}(x,x^-) \tag{2-104b}$$

which are obtained by substituting (2-97) into (2-94), and recall that for the Schrodinger equation associated with the two-component system (2-3) the potential $V(x)$ is given by (2-85a) as

$$V(x) = r^2(x) - \dot{r}(x) \ . \tag{2-105}$$

Then we have

$$V(x) = 2\frac{d}{dx}K(x,x^-) \tag{2-106}$$

so that the solution of the Marchenko equation yields the Schrodinger potential.

The procedure of solving the Marchenko equation (2-103) and then using (2-106) to recover the Schrodinger potential is the standard mathematical physics procedure for solving Schrodinger equation inverse scattering problems. Ware and Aki (1969) used this procedure to solve the one-dimensional inverse seismic problem.

Gel'fand-Levitan equation (free surface): Let the probing waves take the form

$$p(0,t) = \delta(t) + k(t) \tag{2-107a}$$

$$q(0,t) = k(t) \tag{2-107b}$$

$$\hat{k}(\omega) = \hat{R}(\omega)/(1-\hat{R}(\omega)) \tag{2-107c}$$

where $k(t)$ is causal. This corresponds to the case of a medium being probed from a perfectly reflecting surface ((2-107c) follows from a simple feedback argument). An example of this situation is probing the earth from an earth-air or ocean-air interface, which is quite well modelled by a pressure-release or "free" surface. Define

$$K_s(x,t) = \frac{1}{2}\,(K(x,t) + K(x,-t)). \tag{2-108}$$

Then, adding (2-100a), (2-100b), and their time-reversals, and inserting (2-107) and (2-108) yields the Gel'fand-Levitan integral equation (Gel'fand and Levitan, 1955; Faddeev, 1963)

$$K_s(x,t) + \frac{1}{2}(k(x-t) + k(x+t)) + \int_0^x \frac{1}{2}(k(|t-\tau|) + k(t+\tau))K_s(x,\tau)\,d\tau$$

$$= 0, \quad 0 < t < x. \tag{2-109}$$

Again we may use (2-106) to recover the Schrodinger potential $V(x)$.

Krein integral equation (free surface): Let the probing waves again take the form (2-107) and define

$$L(x,t) = \tilde{M}_{11}(x,t) + \tilde{M}_{12}(x,t)\ . \tag{2-110}$$

Adding (2-100a) to the time-reversal of (2-100b) and using (2-107) and

(2-110) yields the Krein integral equation (Krein, 1954)

$$k(x-t) + L(x,t) + \int_{-x}^{x} k(|t-\tau|)L(x,\tau)d\tau = 0, \quad 0 < t < x \tag{2-111}$$

By setting $t = -x$ in (2-100a) we get

$$\tilde{M}_{11}(x,-x) = 0 \tag{2-112}$$

and using this with (2-104a) and (2-98b) and adding yields

$$r(x) = -2L(x,-x) \tag{2-113}$$

so that the solution to the Krein integral equation yields $r(x)$.

2.4.2 The Krein-Levinson Algorithm

Any of the integral equations derived above can be solved numerically by discretizing x and t. If x and t are discretized by $x = n\Delta$ and $t = m\Delta$, where n and m are integers in the intervals $[0,N]$ and $[-N,N]$, respectively, then $O(N^3)$ operations are necessary to solve the integral equation and reconstruct $r(x)$.

However, the fast Cholesky algorithm in Section 2.3 requires only $O(N^2)$ operations to reconstruct $r(x)$ for the same discretization. If there is some duality between differential and integral methods for solving inverse scattering problems, then there should be some way to reduce the amount of computation required to solve the integral equations to $O(N^2)$.

In this subsection we derive the Krein-Levinson algorithm, a continuous-parameter, slightly modified version of the famous Levinson

algorithm for solving Toeplitz systems of equations (Musicus, 1981, is a thorough treatment). This algorithm solves the Marchenko integral equation using $O(N^2)$ operations by taking advantage of its Hankel structure. Slight modifications of this algorithm can be used to solve integral equations with Toeplitz or Toeplitz-plus-Hankel structure (Gohberg and Koltracht, 1983).

The continuous-parameter fast Cholesky and Krein-Levinson algorithms thus provide two different ways of solving inverse scattering problems using $O(N^2)$ computation. In Section 2.5 we shall discuss how these two algorithms are "flip sides" of each other, and why the fast Cholesky algorithm requires less storage and computation.

Inserting (2-97), which specifies the forms of M_{11} and M_{21}, into (2-94), the time-domain system satisfied by $M(x,t)$, and taking the first column of the result yields

$$\frac{\partial}{\partial x}\begin{bmatrix}\tilde{M}_{11}(x,t)\\ \tilde{M}_{21}(x,t)\end{bmatrix} = \begin{bmatrix}-\partial/\partial t & -r(x)\\ -r(x) & \partial/\partial t\end{bmatrix}\begin{bmatrix}\tilde{M}_{11}(x,t)\\ \tilde{M}_{21}(x,t)\end{bmatrix}, \quad -x \le t \le x \tag{2-114}$$

with the initial condition

$$\begin{bmatrix}\tilde{M}_{11}(0,0)\\ \tilde{M}_{21}(0,0)\end{bmatrix} = \begin{bmatrix}0\\ 0\end{bmatrix} . \tag{2-115}$$

Equations (2-114) look like the fast Cholesky algorithm dynamics, but there is an important difference. In the fast Cholesky algorithm the quantities propagated were the waves $p(x,t)$ and $q(x,t)$, which were non-zero (by causality) for $t > x$. Here the quantities propagated are elements of the transition matrix $M(x,t)$, and are non-zero for

$-x < t < x$. The update patterns are shown in Figures 2.7. These should be compared with Figures 2.3, the update patterns for the fast Cholesky algorithm.

Examination of Figure 2.7 shows that in order to propagate (2-114) it is necessary to supply values for $\tilde{M}_{11}(x,-x)$ and $\tilde{M}_{21}(x,x^-)$ independently of (2-114). Setting $t= -x$ in (2-100a) yields

$$\tilde{M}_{11}(x,-x) = 0 \ . \tag{2-116}$$

However, $\tilde{M}_{21}(x,x^-) = -r(x)/2$ from (2-104a), and we certainly need $r(x)$ to propagate (2-114). The only way we can get this is to set $t = x^-$ in (2-100b), yielding the rather unwieldly expression

$$r(x) = -2\tilde{M}_{21}(x,x^-) = 2(q(0,2x) + \int_{-x}^{x} q(0,x+\tau)\tilde{M}_{11}(x,\tau)d\tau + \int_{-x}^{x} p(0,x-\tau)\tilde{M}_{21}(x,\tau)d\tau \ ). \tag{2-117}$$

In the case of probing from a half-space, the last term in (2-117) vanishes. In this case (2-117) should be compared to the "inner product" expression in the discrete Levinson algorithm.

The Krein-Levinson algorithm thus consists of equations (2-114) and (2-117), with the additional trivial condition (2-116). Its dynamics are the same as the fast Cholesky algorithm, but the quantitites in the algorithm are different, and the inner product expression (2-117) replaces the trivial first reflection relation (2-23). Thus the Krein-Levinson algorithm requires more computation and storage than the fast Cholesky algorithm, although both algorithms require $O(N^2)$ operations.

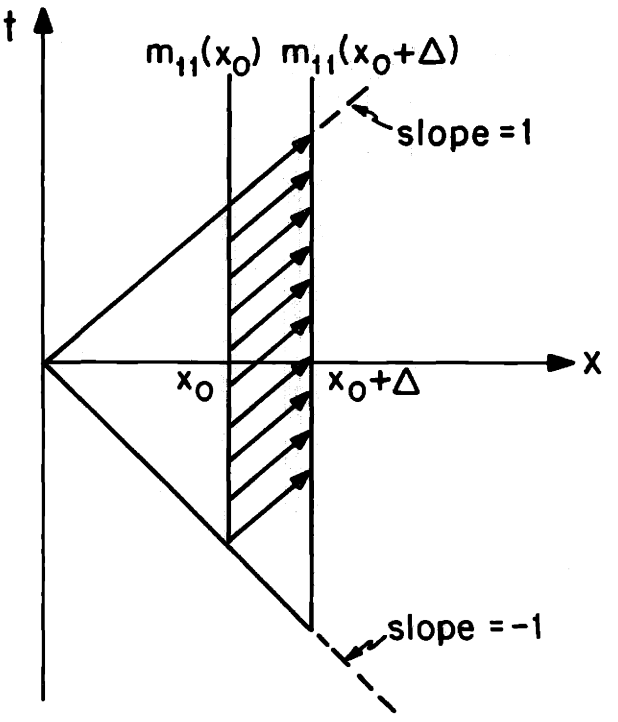

2.7a Recursion pattern for updating $m_{11}(x,t)$ in the Krein-Levinson algorithm.

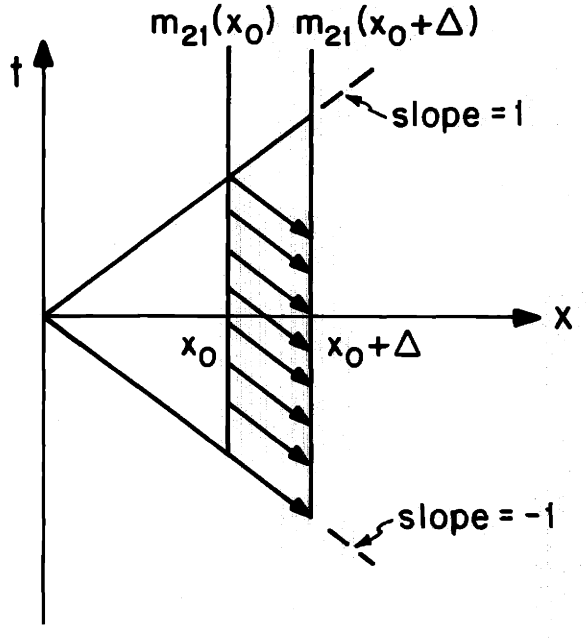

2.7b Recursion pattern for updating $m_{21}(x,t)$ in the Krein-Levinson algorithm.

2.4.3 Inverse Scattering as Orthonormalization

Levy (1985) has recently pointed out that the solution of a two-component wave system inverse scattering problem can be viewed as an orthonormalization procedure. It is well known (e.g., Kailath, 1981) that the problem of linear least-squares estimation of an autoregressive (AR) stationary stochastic process can be regarded as a polynomial orthonormalization, with the Levinson algorithm carrying out the orthonormalization and the Szego polynomials (representing the residuals) the result. For the inverse scattering problem, the orthonormalization procedure is applied to continuous analogues of matrix orthogonal polynomials. The Marchenko integral equation results from application of orthogonality to residuals, such as the Wiener-Hopf equations are derived in linear least-squares estimation theory (e.g., Kailath, 1981).

This result is presented here to give another perspective on inverse scattering, and to show similarities between inverse scattering and linear least-squares estimation theory. These two problems will be linked more tightly in Section 2.5.

Define the matrix inner product of two 2 x 2 complex-valued matrix functions $A(\omega)$ and $B(\omega)$ as

$$< A,B > \triangleq \int_{-\infty}^{\infty} A(\omega)W(\omega)B^{H}(\omega)d\omega \qquad (2\text{-}118)$$

where the Hermitian weighting matrix $W(\omega)$ is

$$W(\omega) \triangleq \frac{1}{2\pi}\begin{bmatrix} 1 & \hat{R}^{*}(\omega) \\ \hat{R}(\omega) & 1 \end{bmatrix} . \qquad (2\text{-}119)$$

Here $R(\omega)$ is the left reflection coefficient of the scattering medium.

If the medium is lossless, $|R(\omega)| < 1$ for ω real, and by Sylvester's criterion $W(\omega)$ is positive semidefinite. Hence $\langle A, A \rangle > 0$ unless the medium is perfectly reflecting.

The weighting matrix $W(\omega)$ in (2-119) was suggested by Newton (1983, p. 20) as follows. Let the matrix Jost solution $\Psi(x,\omega)$ for the two-component wave system (2-3) be that solution which behaves like

$$\Psi(x,\omega) \simeq \begin{bmatrix} e^{-j\omega x} & 0 \\ \hat{R}_L e^{j\omega x} & \hat{T} e^{j\omega x} \end{bmatrix} \quad \text{as } x \to -\infty \tag{2-120a}$$

$$\Psi(x,\omega) \simeq \begin{bmatrix} \hat{T} e^{-j\omega x} & \hat{R}_R e^{-j\omega x} \\ 0 & e^{j\omega x} \end{bmatrix} \quad \text{as } x \to \infty. \tag{2-120b}$$

Note that the first column of $\Psi(x,\omega)$ represents a scattering experiment in which the medium is probed from the left, while the second column represents a scattering experiment in which the medium is probed from the right. Now, the two columns of the state transition matrix $M(x,\omega)$ also represent two independent experiments, so $M(x,\omega)$ can be obtained from the matrix Jost solution $\Psi(x,\omega)$ by multiplying it by the Jost function $J(\omega)$,

$$M(x,\omega) = J(\omega)\Psi(x,\omega). \tag{2-121}$$

Then the spectral function

$$W(\omega) = \frac{1}{2\pi} \left(J^H(\omega)J(\omega)\right)^{-1} \tag{2-122}$$

turns out to be the weighting matrix specified by (2-119).

Note that the probing waves

$$E(x,\omega) = \begin{bmatrix} e^{-j\omega x} & 0 \\ 0 & e^{j\omega x} \end{bmatrix} \tag{2-123}$$

have the property that

$$\langle E(x,\omega),\ E(y,\omega)\rangle = \delta(x-y)I_2 + \begin{bmatrix} 0 & 1 \\ 1 & 0 \end{bmatrix} R(x+y). \tag{2-124}$$

Thus $E(x,\omega)$ and $E(y,\omega)$ are orthonormal in free space $(x,y < 0)$ since $R(t)$ is causal.

The inverse scattering problem is solved recursively by orthonormalizing $E(x,\omega)$ and $E(y,\omega)$ for successively larger x and $-\infty < y < x$. This is done by the usual Gram-Schmidt procedure: $E(x,\omega)$ is projected onto the subspace $\mathcal{E}_x \triangleq \text{SPAN}[E(y,\omega),\ -\infty < y < x]$, and the residual is then orthogonal to $\mathcal{E}_x$. The projection operator takes the form

$$\mathcal{P}[E(x,\omega)] = -\int_{-\infty}^{x} m(x,y)E(y,\omega)dy \tag{2-125}$$

where $m(x,y)$ is an unknown 2 x 2 matrix kernel. The residual $\hat{M}(x,\omega)$ is

$$\begin{aligned} \hat{M}(x,\omega) &= E(x,\omega) - \mathcal{P}[E(x,\omega)] \\ &= E(x,\omega) + \int_{-\infty}^{x} m(x,y)E(y,\omega)dy. \end{aligned} \tag{2-126}$$

Now, $\hat{M}(x,\omega)$ is orthogonal to $\mathcal{E}_x$ by construction. This means $m(x,y)$ satisfies

$$\begin{bmatrix} 0 & 1 \\ 1 & 0 \end{bmatrix} R(x+z) + m(x,z) + \int_{-z}^{x} m(x,y) \begin{bmatrix} 0 & 1 \\ 1 & 0 \end{bmatrix} R(y+z)dy = 0,\ -x<z<x. \tag{2-127}$$

2.5 Relations Between Differential and Integral Methods

In this section the dual nature of differential and integral methods of solving inverse scattering problems is discussed. These two methods are not merely related, but are complements of each other. This is illustrated in particular by the complementary nature of the fast Cholesky algorithm (a differential method) and the Krein-Levinson algorithm (which solves the integral equations). Finally, in order to furnish an example outside the usual context of inverse scattering theory, the familiar problem of linear least-squares estimation of a stationary stochastic process is interpreted as an inverse scattering problem, and solved using both algorithms. This illustrates the physical meanings of various quantities in a novel setting, adding depth to an understanding of inverse scattering concepts and quantities.

2.5.1 Differential vs. Integral Methods

In Section 2.3 it was seen that the differential or layer stripping methods operate in a stripping fashion: At each step of a layer stripping algorithm, a problem on the interval $[x,\infty)$ is replaced by one on the interval $[x + \Delta, \infty)$. This was particularly vivid for the dynamic deconvolution procedure, in which the quantity being propagated was the reflection response of the remaining unknown portion of the medium. An advantage of layer stripping methods is that they are clearly efficient: The effects of the reconstructed portion of the medium are included in a cumulative fashion at each step, while all aspects of the medium itself are discarded. And any unknown portion of the medium can have no effect until the algorithm reaches it (this is why causality is so important to these algorithms). Thus a layer stripping algorithm is only

concerned with that differential slice of the medium where the algorithm is currently operating.

In Section 2.4 it was seen that integral equation methods utilize all of the data (measured medium response) at each step. Although the medium is again reconstructed one layer at a time (the integral equation must be solved for each x), the entire medium affects the reconstruction at each step, since all of the data are being used. This is why bound states affect integral methods at the start, while not bothering layer stripping algorithms until that part of the medium is reached. No attempt is ever made to isolate the effects of part of the data or medium on reconstruction of any layer. This is why unwieldly integral equations are necessary, which might seem to require $O(N^3)$ operations to solve completely.

On the other hand, it is not necessary to account for the cumulative effect of the reconstructed medium at each step. The integral equation methods are constructive in nature: At each step, the reconstructed portion of the medium is extended from $[0,x]$ to $[0, x + \Delta]$. Note that this complements perfectly the layer stripping approach: one decreases the size of the problem at each step, while the other increases the size of the solution at each step.

The structure of the integral equations (Hankel for the Marchenko, Toeplitz-plus-Hankel for the Gel'fand-Levitan, Toeplitz for the Krein) allows fast algorithm solutions for them. This reduces the computation required to $O(N^2)$, the same as for the layer stripping methods. Nevertheless, it should be noted that the integral equation methods amount to formulating a problem mathematically and solving it from a mathematical perspective. The layer stripping methods amount to formulating a problem physically, in terms of clearly physical variables such as waves and

Since this equation is centrosymmetric, we have

$$m_{11}(x,y) = m_{22}(x,y) \text{ and } m_{12}(x,y) = m_{21}(x,y) \tag{2-128}$$

and this simplifies (2-127) to

$$m_{11}(x,z) + \int_{-z}^{x} m_{21}(x,y)R(y+z)dy = 0, \quad -x < z < x \tag{2-129a}$$

$$R(x+z) + m_{21}(x,z) + \int_{-z}^{x} m_{11}(x,y)R(y+z)dy = 0, \quad -x < z < x. \tag{2-129b}$$

Adding these two equations and recalling (2-102) yields the Marchenko integral equation (2-103).

Two comments are in order here. First, the original choice (2-123) for the probing waves $E(x,\omega)$ is tantamount to probing the medium from a half-space, as in (2-101). This is why the Marchenko equation is obtained, rather than the Gel'fand-Levitan or Krein equations. These latter equations were obtained by a choice of probing waves associated with a free surface, as in (2-107). Second, the centrosymmetric equalities (2-128) do not quite agree with the time reversal equalities (2-98). The reason for this is that $m_{22}(x,t)$ in (2-98) contains a probing impulse $\delta(x-t)$, while the probing impulse in the second component of the present experiment is $\delta(x+t)$. This cancels the time reversal in (2-98), leaving (2-128).

Operating on (2-129a) and (2-129b) respectively with the operators $(\partial/\partial x + \partial/\partial z)$ and $(\partial/\partial x - \partial/\partial z)$ yields the Krein-Levinson algorithm dynamics (2-114). Proceeding as before, the Krein-Levinson algorithm can be shown to solve (2-129). And the residual $\hat{M}(x,\omega)$ therefore satisfies (2-91) and (2-92), and is therefore the state transition matrix.

reflectivity functions. Thus a layer stripping approach is much "closer" to the problem; indeed, layer stripping methods have been described as "letting the medium perform the inversion itself" (Bruckstein and Kailath, 1983). It would seem, then, that a layer stripping approach is the "right way" to look at the problem. This is emphasized by the comparison of the fast Cholesky and Krein-Levinson algorithms to follow.

2.5.2 Fast Cholesky vs. Krein-Levinson Algorithms

For convenience these two algorithms are summarized below.

Fast Cholesky Algorithm

basic dynamics: $(\partial/\partial x + \partial/\partial t)\tilde{p}(x,t) = -r(x)\tilde{q}(x,t)$
$(\partial/\partial x - \partial/\partial t)\tilde{q}(x,t) = -r(x)\tilde{p}(x,t)$.

update patterns: See Figure 2.3.

reflectivity function update: $r(x) = 2\tilde{q}(x,x^+)$

initial conditions: half-space: $\tilde{p}(0,t)=0$, $\tilde{q}(0,t)=R(t)$;
free surface: $\tilde{p}(0,t) = \tilde{q}(0,t)=k(t)$.

quantities being propagated: rightgoing and leftgoing waves, $\tilde{p}(x,t)$ and $\tilde{q}(x,t)$, respectively.

support: $t \geq x$

factorization performed: free surface i.c.: $\delta(\tau)+k(\tau)+k(-\tau)=$(causal)(anticausal);
half-space i.c.: $\delta(\tau)-R(\tau)*R(-\tau)=$(causal)(anticausal).

The latter follows from noting in the operator domain that (using (2-52c))

$$1-\hat{R}\hat{R}^* = 1 - (\hat{k}/(1+\hat{k}))(\hat{k}^*/(1+\hat{k}^*)) = (1+\hat{k}+\hat{k}^*)/((1+\hat{k})(1+\hat{k}^*)) \quad (2\text{-}130)$$

which is clearly factored if $1 + \hat{k} + \hat{k}^*$ is.

Krein-Levinson Algorithm

basic dynamics: $(\partial/\partial x + \partial/\partial t)\tilde{M}_{11}(x,t) = -r(x)\tilde{M}_{21}(x,t)$
$(\partial/\partial x - \partial/\partial t)\tilde{M}_{21}(x,t) = -r(x)\tilde{M}_{11}(x,t).$

update patterns: See Figure 2.7.

reflectivity function update: $r(x) = 2(\tilde{q}(0,2x) + \int_{-x}^{x}\tilde{q}(0,x+\tau)\tilde{M}_{11}(x,\tau)d\tau + \int_{-x}^{x}\tilde{p}(0,x-\tau)\tilde{M}_{21}(x,\tau)d\tau)$, where $\tilde{p}(0,t)$ and $\tilde{q}(0,t)$ are the probing waves, as in the fast Cholesky algorithm.

initial conditions: $\tilde{M}_{11}(0,0) = \tilde{M}_{21}(0,0) = 0$. Also need $\tilde{M}_{11}(x,-x)=0$.

quantities being propagated: elements of the state transition matrix, i.e., the medium transmission matrix.

support: $-x \le t \le x$

factorization performed: $\delta(t-s) + H(t,s;x) = (\text{anticausal})(\text{causal})$.

In the factorization performed by the Krein-Levinson algorithm, $H(t,s;x)$ represents the Fredholm resolvent operator to $k(|\tau|)$. This operator is defined in the operator domain by the operator equation

$$(I + \hat{H})(I + \hat{k} + \hat{k}^*) = I \qquad (2\text{-}131)$$

which is equivalent to the integral equation

$$H(t,s;x) + k(|t-s|) + \int_{-x}^{x}H(t,v;x)k(|v-s|)dv = 0, \; -x \le s, \; t \le x. \qquad (2\text{-}132)$$

Note that although the dynamics of the two algorithms are the same, the quantities being propagated differ. The fast Cholesky quantities carry the clear interpretation of waves propagating leftward and rightward in the medium at the point x. The Krein-Levinson quantities carry the murkier interpretation of being one column of the transmission matrix of the medium to point x. The supports of these quantities are exactly complementary,

but the fast Cholesky algorithm supplies r(x) directly, while the Krein-Levinson algorithm requires that r(x) be computed. In Chapter III the simple equation $r(x) = 2\tilde{q}(x,x)$ will be interpreted physically as the first reflection from the medium at x having strength r(x)/2. No such interpretation of the inner product expression for r(x) is available.

It should also be noted that the Krein-Levinson algorithm requires that the original scattering data $\tilde{q}(0,t) = R(t)$ be stored in addition to the propagating quantities $\tilde{M}_{11}(x,t)$ and $\tilde{M}_{21}(x,t)$. Thus the Krein-Levinson algorithm requires a storage capacity of 3N words, while the fast Cholesky requires only 2N words. And the extra computation involved in the inner product expression for r(x) runs the total operation (multiplication-and-add) count for the Krein-Levinson algorithm to $3N^2$ vs. $2N^2$ for the fast Cholesky algorithm.

The "factorization performed" by each algorithm requires some explanation. The quantities in these algorithms can be interpreted as operators in L_2^p, the Hilbert space of square-integrable p-vector functions (Kailath et al., 1979). The action of the fast Cholesky algorithm is to perform a causal-times-anticausal factorization of the Toeplitz operator $\delta(\tau) + k(\tau) + k(-\tau)$, where $k(\tau)$ is the (causal) free surface response. The Krein-Levinson algorithm, on the other hand, performs an anticausal-times-causal factorization of the operator $\delta(t-s) + H(t,s;x)$, where $H(t,s;x)$ is the Fredholm resolvent of $k(|t-s|)$. This again illustrates the complementary nature of these two algorithms. The discretized versions of these algorithms perform LDU and UDL factorizations, respectively, of the Toeplitz matrix $I + k(|i-j|)$ and its inverse (see Musicus, 1981, for details).

2.5.3 Example: Linear Least-Squares Estimation of a Stochastic Process

In this example it is shown how this familiar problem can be posed as an inverse scattering problem and solved using integral equations, the Krein-Levinson algorithm, or the fast Cholesky algorithm. This will lend some perspective to the various inverse scattering concepts, which were already introduced in the lossless transmission line example (Pusey, 1975, shows the connections between these two examples). More details on the connection between linear estimation, inverse scattering, and fast algorithms can be found in Dewilde et al. (1981), Dewilde and Dym (1981), and Dewilde et al. (1978).

The basic problem to be considered is as follows. Let

$$y(t) = z(t) + v(t) \tag{2-133}$$

be some observations of a zero-mean stationary stochastic process $z(\cdot)$ with covariance

$$E[z(t)z(s)] = k(|t-s|), \tag{2-134}$$

where $v(\cdot)$ is a white noise process with unit intensity, i.e.,

$$E[v(t)v(s)] = \delta(t-s) \quad . \tag{2-135}$$

We assume that $z(\cdot)$ and $v(\cdot)$ are uncorrelated and that $k(\cdot) \in L_1[0,\infty)$, so that its Fourier transform

$$\hat{k}(\omega) = \int_0^\infty k(t) \exp -j\omega t \, dt \tag{2-136}$$

exists. In this case, the spectral density of $y(\cdot)$ is

$$\hat{W}(\omega) = 1 + \hat{k}(\omega) + \hat{k}(-\omega). \tag{2-137}$$

Given the Hilbert space

$$Y(t;\ x) = H[y(t+s),\ -x \le s \le x] \tag{2-138}$$

spanned by the observations over the interval $[t-x,\ t+x]$, our objective is to compute the forwards and backwards linear least-square estimates of z at the endpoints of this interval. These estimates can be denoted as

$$\hat{z}(t+x|Y(t;\ x)) = \int_{-x}^{x} A(x;\ u)\ y(t+u)du \tag{2-139a}$$

$$\hat{z}(t-x|Y(t;\ x)) = \int_{-x}^{x} B(x;\ u)\ y(t+u)du\ , \tag{2-139b}$$

where $A(x;\ \cdot)$ and $B(x;\ \cdot)$ are the optimal forwards and backwards prediction filters, respectively. Note that since the process $z(\cdot)$ is stationary the filters $A(x;\ \cdot)$ and $B(x;\ \cdot)$ do not depend on t, the center of the interval $[t-x,\ t+x]$. Then, if the forwards and backwards residuals are defined as

$$e(t,x) = y(t+x) - \hat{z}(t+x|Y(t;\ x)) \tag{2-140a}$$

$$b(t,x) = y(t-x) - \hat{z}(t-x|Y(t;\ x)), \tag{2-140b}$$

by using the orthogonality property

$$e(t,x),\ b(t,x) \perp Y(t;\ x) \tag{2-141}$$

of linear least-squares estimates, we find that the filters $A(x;\ \cdot)$ and $B(x;\ \cdot)$ satisfy the Wiener-Hopf equations

$$A(x;\ s) + \int_{-x}^{x} A(x;\ u)\ k(|u-s|)\ du = k(x-s) \qquad (2\text{-}142a)$$

$$B(x;\ s) + \int_{-x}^{x} B(x;\ u)\ k(|u-s|)\ du = k(x+s) \qquad (2\text{-}142b)$$

with $-x \leq s \leq x$. These integral equations should be compared to the Krein equation (2-111).

Applying the operators $\frac{\partial}{\partial x} + \frac{\partial}{\partial s}$ and $\frac{\partial}{\partial x} - \frac{\partial}{\partial s}$ to (2-142a) and (2-142b) respectively, and using the linearity of the resulting equations yields the Krein-Levinson algorithm

$$\left(\frac{\partial}{\partial x} + \frac{\partial}{\partial s}\right) A(x;\ s) = -\ r(x)\ B(x;\ s) \qquad (2\text{-}143a)$$

$$\left(\frac{\partial}{\partial x} - \frac{\partial}{\partial s}\right) B(x;\ s) = -\ r(x)\ A(x;\ s) \qquad (2\text{-}143b)$$

with $-x \leq s \leq x$, and where

$$r(x) = 2A(x;\ -x) = 2B(x;\ x) \qquad (2\text{-}144a)$$

$$= 2\left(k(2x) - \int_{-x}^{x} A(x,u)k(x+u)du\right) \qquad (2\text{-}144b)$$

is the reflectivity function. The fact that $r(x)$ is well-defined can be obtained by noting from a time-reversal argument that $B(x;\ s) \equiv A(x;\ -s)$.

So far this has all been routine--it is certainly well-known that the Krein-Levinson algorithm solves the Wiener-Hopf equations. We now show that an inverse scattering interpretation can be assigned to this problem, and that the fast Cholesky algorithm may be used to solve it.

If we apply the operators $\frac{\partial}{\partial t} \mp \frac{\partial}{\partial t}$ to the definition (2-140) of the forwards and backwards residuals $e(t,x)$ and $b(t,x)$ and use the Krein-

Levinson equations (2-143), we obtain the two-component wave system

$$\left(\frac{\partial}{\partial x} - \frac{\partial}{\partial t}\right) e(t,x) = - r(x)\, b(t,x) \qquad (2\text{-}145a)$$

$$\left(\frac{\partial}{\partial x} + \frac{\partial}{\partial t}\right) b(t,x) = - r(x)\, e(t,x) \quad . \qquad (2\text{-}145b)$$

This shows that the residuals satisfy a two-component wave system, where the waves $e(t,x)$ and $b(t,x)$ propagate respectively leftward and rightward, and where the waves at $x = 0$ are given by

$$e(t, 0) = b(t, 0) = y(t) \quad . \qquad (2\text{-}146)$$

As a consequence of this observation, the process $y(t)$ can be viewed as the ouput of a modeling filter driven by $e(t,x)$ as shown in Figure 2.8a. This modeling filter is obtained by aggregating infinitesimal ladder sections of the type described in Figure 2.8b. Clearly the filter problem is solved if $r(x)$ can be recovered.

The scattering matrix associated to the two-component wave system (2-145) can be identified by noting that as $x \to \infty$

$$e(t,x) = \nu_F(t+x), b(t,x) = \nu_B(t-x) \qquad (2\text{-}147)$$

where $\nu_F(\cdot)$ and $\nu_B(\cdot)$ denote respectively the forwards and backwards innovations processes associated to $y(\cdot)$ (Kailath et al., 1978). The processes $\nu_F(\cdot)$ and $\nu_B(\cdot)$ are white noise processes and are related to the observations $y(\cdot)$ through the identities

$$\hat{y}(\omega) = F(\omega)\, \hat{\nu}_F(\omega) \qquad (2\text{-}148a)$$

$$\hat{y}(\omega) = F(-\omega)\, \hat{\nu}_B(\omega) \qquad (2\text{-}148b)$$

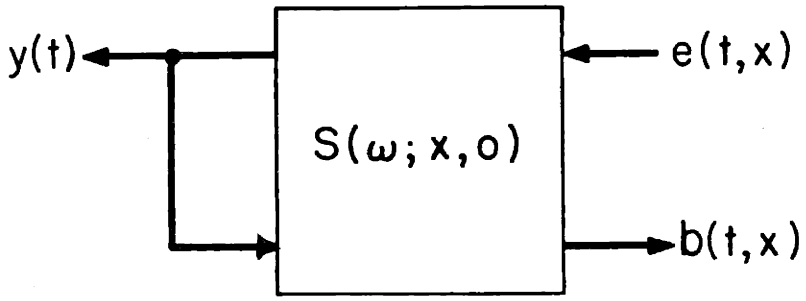

2.8a Aggregate modelling filter for y(·).

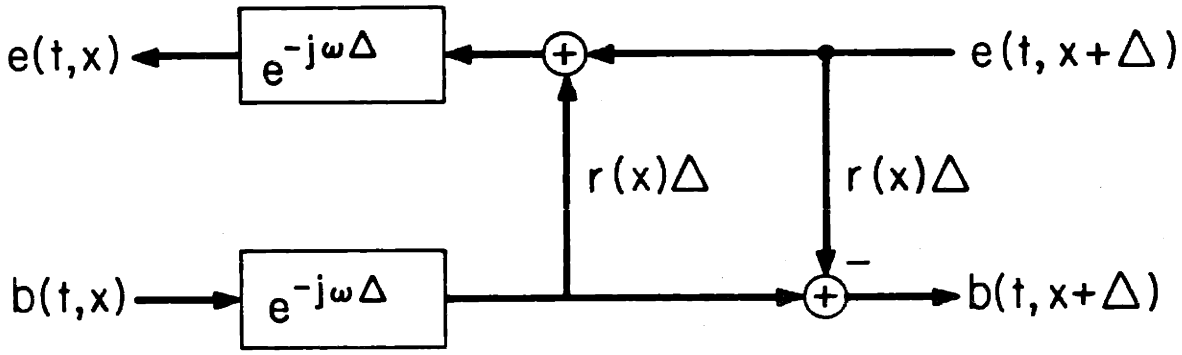

2.8b Infinitesimal ladder sections associated with the Krein-Levinson algorithm.

where $\hat{y}(\omega)$, $\hat{\nu}_F(\omega)$ and $\hat{\nu}_B(\omega)$ denote formally the Fourier transforms of $y(\cdot)$, $\nu_F(\cdot)$ and $\nu_B(\cdot)$, and where the shaping filter $F(\omega)$ is the outer or minimum phase spectral factor of $\hat{W}(\omega)$, the spectral density of $y(\cdot)$. That is,

$$\hat{W}(\omega) = 1 + \hat{k}(\omega) + \hat{k}(-\omega) = |F(\omega)|^2 \tag{2-149}$$

on the real axis, and $F(\omega)$ and $F^{-1}(\omega)$ are analytic in the lower half-plane.

The relations (2-146) and (2-147), or Figure 2.8a, imply that the scattering matrix $S(\omega)$ satisfies

$$\begin{bmatrix} \hat{\nu}_B(\omega) \\ \hat{y}(\omega) \end{bmatrix} = S(\omega) \begin{bmatrix} \hat{y}(\omega) \\ \hat{\nu}_F(\omega) \end{bmatrix}, \tag{2-150}$$

and by substituting (2-148) inside this relation and cancelling $\hat{y}(\omega)$, we obtain the identity

$$\begin{bmatrix} F^{-1}(-\omega) \\ 1 \end{bmatrix} = \begin{bmatrix} \hat{T} & \hat{R}_R \\ \hat{R}_L & \hat{T} \end{bmatrix} \begin{bmatrix} 1 \\ F^{-1}(\omega) \end{bmatrix} \tag{2-151}$$

for the entries of $S(\omega)$. Using the fact (2-15) that the scattering matrix is unitary, this gives after some algebra

$$\hat{R}_L(\omega) = \frac{\hat{k}(\omega)}{1 + \hat{k}(\omega)} \tag{2-152a}$$

$$\hat{T}(\omega) = \frac{F(\omega)}{1 + \hat{k}(\omega)} \tag{2-152b}$$

$$\hat{R}_R(\omega) = \frac{-\hat{k}(-\omega)}{1 + \hat{k}(\omega)} \quad \frac{F(\omega)}{F(-\omega)} \quad , \tag{2-152c}$$

so that the left reflection coefficient $\hat{R}_L(\omega)$ depends only on the covariance data given by $\hat{k}(\omega)$.

Thus, the linear least-squares estimation problem has now been recast as an inverse scattering problem. The two-component wave system (2-145) has been defined, with the residuals e(t,x) and b(t,x) acting as waves, and the scattering matrix for this system has been specified by (2-152). In particular, the left reflection coefficient $\hat{R}_L(\omega)$ has been specified entirely in terms of the known covariance k(t). The aim is to reconstruct r(x), and once this has been done the optimal modelling filter is specified by Figure 2.8.

Moreover, the form of (2-152a) allows the choice of probing waves (made by Dewilde et al., 1981; note that this choice corresponds to a free surface)

$$b(t,0) = \delta(t) + k(t)1(t) \tag{2-153a}$$

$$e(t,0) = k(t)1(t) \tag{2-153b}$$

which now replaces (2-146) but leaves $\hat{R}_L(\omega)$ (2-152a) unaltered. And since $\hat{R}_L(\omega)$ determines the rest of the scattering matrix, the choice (2-153) of probing waves leaves the entire inverse scattering problem unaltered. The choice of probing waves (2-153) means that the fast Cholesky algorithm

$$(\partial/\partial x - \partial/\partial t)\tilde{e}(t,x) = -r(x)\tilde{b}(t,x) \tag{2-154a}$$

$$(\partial/\partial x + \partial/\partial t)\tilde{b}(t,x) = -r(x)\tilde{e}(t,x) \tag{2-154b}$$

$$r(x) = 2\tilde{e}(x,x) \tag{2-154c}$$

$$\tilde{b}(t,0) = \tilde{e}(t,0) = k(t)1(t) \tag{2-154d}$$

(recall that only the smooth parts of the waves are propagated) can be used to reconstruct $r(x)$.

It should also be noted that this results in a causal-times-anticausal factorization of $\delta(\tau) + k(\tau) + k(-\tau)$. Furthermore, from (2-152a) and (2-152b) we have

$$\begin{bmatrix} F(\omega) \\ \hat{k}(\omega) \end{bmatrix} = S(\omega) \begin{bmatrix} 1 + \hat{k}(\omega) \\ 0 \end{bmatrix} \tag{2-155}$$

so that the choice of probing waves (2-146) implies

$$\hat{b}(x,\omega) \simeq F(\omega)\, e^{-j\omega x} \text{ as } x \to \infty. \tag{2-156}$$

Thus the fast Cholesky recursions also generate $F(\omega)$.

On the other hand, the Krein-Levinson algorithm (2-143) - (2-144) operated not on the residuals $e(t,x)$ and $b(t,x)$, but on the forwards and backwards filters $A(x,\cdot)$ and $B(x,\cdot)$. This again illustrates that the fast Cholesky algorithm operates directly on the waves in the scattering interpretation of the problem, while the Krein-Levinson algorithm operates on the transmission matrix, and is thus less physically interpretable in its operation.

In this chapter, we have investigated in detail both differential and integral equation methods for solving inverse scattering problems. In the next chapter we shall see how these methods are applied to the one-

dimensional inverse seismic problem, and derive their discrete counterparts for the discrete version of this problem.

REFERENCES FOR CHAPTER II

M.J. Ablowitz and H. Segur, Solitons and the Inverse Scattering Transform, SIAM, Philadelphia, 1981.

J.D. Achenbach, Wave Propagation in Elastic Solids, North-Holland, Amsterdam, 1975.

Z.S. Agranovich and V.A. Marchenko, The Inverse Problem of Scattering Theory, Gordon and Breach, New York, 1963.

N.I. Akhiezer, The Classical Moment Problem, Hafner Publishing Co., New York, 1965 (Russian Original, 1961).

A.M. Bruckstein and T. Kailath, "Spatio-Temporal Scattering and Inverse Problems," Tech. Report, Information Systems Laboratory, Stanford University, 1983.

A. Bruckstein, B. Levy, and T. Kailath, "Differential Methods in Inverse Scattering," Tech. Report, Information Systems Laboratory, Stanford University (1983).

K.P. Bube and R. Burridge, "The One-Dimensional Problem of Reflection Seismology," SIAM Review 25(4), 497-559 (1983).

R. Burridge, "The Gelfand-Levitan, the Marchenko and the Gopinath-Sondhi Integral Equations of Inverse Scattering Theory Regarded in the Context of Inverse Impulse Response Problems," Wave Motion 2, 305-323 (1980).

S.M. Candel, F. Defillipi, and A. Launay, "Determination of the Inhomogeneous Structure of a Medium from its Plane Wave Reflection Response, Part II: A Numerical Approximation," J. Sound and Vibration 68(4), 583-595 (1980).

K. Chadan and P.C. Sabatier, Inverse Problems in Quantum Scattering Theory, Springer-Verlag, New York-Heidelberg-Berlin, 1977.

J.P. Corones, M.E. Davison, and R.J. Krueger, "Direct and Inverse Scattering in the Time Domain via Invariant Imbedding Equations," J. Acoust. Soc. Am. 74(5), 1535-1541 (1983).

R. Courant and D. Hilbert, Methods of Mathematical Physics, v.2, Interscience Publishers, New York, 1962.

E. Deprettere and P. Dewilde, "Orthogonal Cascade Realization of Real Multiport Digital Filters," Int. J. Circuit Theory and Appl. 8(3), 245-272 (1980).

P. Dewilde, "Stochastic Modeling with Orthogonal Filters," in Mathematical Tools and Models for Control Systems Analysis and Signal Processing, I.D. Landau ed., CNRS Publication, Paris, 1982.

P. Dewilde and H. Dym, "Schur Recursions, Error Formulas, and Convergence of Rational Estimators for Stationary Stochastic Sequences," IEEE Trans. Inform. Theory IT-29(4), 446-461 (1981).

P. Dewilde, A.C. Vieira and T. Kailath, "On a Generalized Szëgo-Levinson Realization Algorithm for Optimal Linear Prodictors Based on a Network Synthesis Approach," IEEE Trans. Circuits Systems CAS-25 (9), 663-675 (1978).

P. Dewilde, J.T. Fokkema, and I. Widya, "Inverse Scattering and Linear Prediction, The Time Continuous Case," in Stochastic Systems: The Mathematics of Filtering and Identification and Applications, M. Hazewinkel and J.C. Willems eds., pp. 351-382, D. Reidel Publ. Co., Dordrecht, Holland, 1981.

L.D. Faddeev, "The Inverse Problem of Quantum Theory of Scattering," J. Math. Phys 4(1), 72-104 (1963).

L.D. Faddeev, "Properties of the S-Matrix of the One-Dimensional Schrodinger Equation," Amer. Math. Soc. Transl., Series 2, 65, 139-166 (1967).

I.M. Gelfand and B.M. Levitan, "On the Determination of a Differential Equation from its Spectral Function," Amer. Math. Soc. Transl., Series 2, 1, 253-304 (1955).

B. Gjevick, A. Nilsen, and J. Hoyen, "An Attempt at the Inversion of Reflection Data," Geophys. Prospecting 24, 492-505 (1976).

I. Gohberg and I. Koltracht, "Numerical Solutions of Integral Equations, Fast Algorithms, and the Krein-Sobolev Equations," Preprint, Weizmann Institute of Science, Rehovot 76100, Israel, 1983.

B. Gopinath and M.M. Sondhi, "Determination of the Shape of the Human Vocal Tract from Acoustical Measurements," Bell Syst. Tech. J. 49, 1195-1214 (1970).

B. Gopinath and M.M. Sondhi, "Inversion of the Telegraph Equation and the Synthesis of Nonuniform Lines," Proc. IEEE 59(3), 383-392 (1971).

M. Jaulent, "The Inverse Scattering Problem for LCRG Transmission Lines," J. Math. Phys. 23(12), 2286-2290 (1982).

T. Kailath, Lectures on Wiener and Kalman Filtering, Springer-Verlag, New York, 1981.

T. Kailath, A. Vieira and M. Morf, Inverses of Toeplitz Operators, Innovations, and Orthogonal Polynomials," SIAM Review 20(1), 106-119 (1978)

T. Kailath, B. Levy, L. Ljung and M. Morf, "The Factorization and Representation of Operators in the Algebra Generated by Toeplitz Operators," SIAM J. Appl. Math. 37(3), 467-484 (1979).

J. Kraus and K. Carver, Electromagnetics, McGraw-Hill, New York, 1973.

M.G. Krein, "On a Method for the Effective Solution of the Inverse Boundary Value Problem," Dokl. Acad. Nauk USSR 94, 987-990 (1954).

G.L. Lamb, Jr., Elements of Soliton Theory, J. Wiley & Sons, New York, 1980.

B. Levy, "An Orthonormalization Formulation of the Inverse Scattering Problem for Two-Component Wave Equations," Tech. Report, Laboratory for Information and Decision Systems, MIT, 1985.

J. Makhoul, "Stable and Efficient Lattice Methods for Linear Prediction," IEEE Trans. Acoust., Speech, Signal Proc. ASSP-25 (5), 256-261 (1977).

J.D. Markel and A.H. Gray, Linear Prediction of Speech, Springer-Verlag, New York, 1978.

M. Morf, "Fast Algorithms for Multivariable Systems," Ph.D. Dissertation, Dept. of Elec. Eng., Stanford University, Stanford, CA, Aug. 1974.

B. Musicus, "Levinson and Fast Cholesky Algorithms for Toeplitz and Almost Toeplitz Matrices," Technical Report, Research Laboratory of Electronics, MIT, Cambridge, MA, Nov. 1981.

R.G. Newton, "Inversion of Reflection Data for Layered Media: A Review of Exact Methods," Geophys. J. Royal Astr. Soc. 65(1), 191-215 (1981).

R.G. Newton, "The Marchenko and Gel'fand-Levitan Methods in the Inverse Scattering Problem in One and Three Dimensions," in Conference on Inverse Scattering: Theory and Applications, ed. by J.B. Bednar, R. Redner, E. Robinson, and A. Weglein, pp. 1-74, SIAM, Philadelphia, 1983.

L. Pusey, "An Innovations Approach to Spectral Estimation and Wave Propagation," Ph.D. Thesis, Dept. of Electrical Engineering and Computer Science, MIT, 1975.

R. Redheffer, "On the Relation of Transmission-Line Theory to Scattering and Transfer," J. Math. Phys. 41, 1-41 (1962).

J. Rissanen, "Algorithms for Triangular Decomposition of Block Hankel and Toeplitz Matrices with Applications to Factoring Positive Matrix Polynomials," Math. Comput. 27, 147-154 (1973).

E.A. Robinson, "Spectral Approach to Geophysical Inversion by Lorentz, Fourier, and Radon Transforms," Proc. IEEE 70(9), 1039-1054 (1982).

F. Santosa and H. Schwetlick, "The Inversion of Acoustical Impedance Profile by Methods of Characteristics," Wave Motion 4, 99-110 (1982).

I. Schur, "Über Potenzreihen, die in Innern des Einheitskrises Beschränkt Sind," J. für die Reine und Angewandte Mathematik, Vol. 147, Berlin, pp. 205-232 (1917).

M.M. Sondhi and J.R. Resnick, "The Inverse Problem for the Vocal Tract: Numerical Methods, Acoustical Experiments and Speech Synthesis," J. Acoust. Soc. America 73(3), 985-1002 (1983).

W.W. Symes, "Stable Solution of the Inverse Reflection Problem for a Smoothly Stratified Elastic Medium," SIAM J. Math. Anal. 12(3), 421-453 (1981).

I. Tolstoy and C.S. Clay, Ocean Acoustics, McGraw-Hill, New York, 1966.

J.A. Ware and K. Aki, "Continuous and Discrete Inverse Scattering Problems in a Stratified Elastic Medium I: Plane Waves at Normal Incidence," J. Acoust. Soc. America 45(4), 911-921 (1969).

A. Yagle and B. Levy, "The Schur Algorithm and its Applications," Tech. Report # LIDS-P-1362, Laboratory for Information and Decision Systems, MIT, 1984, to appear in Acta Applicandae Mathematicae.

V.E. Zakharov and P.B. Shabat, "Exact Theory of Two-Dimensional Self-Focusing and One-Dimensional Self-Modulation of Waves in Nonlinear Media," Soviet Phys. JETP 34, 62-69 (1972).

CHAPTER III

The One-Dimensional Inverse Problem at Normal Incidence

3.1 Introduction

In this chapter the inverse seismic problem for a one-dimensional acoustic layered medium probed by impulsive plane waves at normal incidence is reviewed. The goal is to recover the acoustical impedance $\rho c(\tau)$ as a function of travel time τ. The case of a medium with continuous variation of material parameters, and the case of a medium with variations only at discrete depths, are both covered.

A considerable body of literature exists on both of these problems; indeed, the majority of published work on theoretical methods for solving inverse seismic problems has dealt with these two problems. Newton (1981) is a good review paper for references and methods for solving the continuous medium problem. In general, these methods have employed a mathematical physics approach: the basic equations of the problem are transformed into a Schrodinger equation, and the potential of this equation is recovered by solving a Marchenko integral equation. This procedure is described in detail in Section 3.2.2 below. Ware and Aki (1969) popularized this approach, which has been employed many times since (see the list of references in Newton (1981)).

Other methods for solving the continuous medium problem have been proposed. Gray (1983) derived a Marchenko equation directly in terms of a reflectivity function $r(\tau)$, bypassing the necessity of solving for the Schrodinger potential. This allows discontinuities in $r(\tau)$ and requires

only that the impedance be continuous, unlike the Schrodinger formulation for which the impedance must be twice differentiable. Burridge (1980) derived the Marchenko integral equation and several related integral equations directly in the time domain, bypassing the Schrodinger equation formulation.

As for the discrete layered medium problem, the assumption is generally made that the medium is composed of horizontally stratified homogeneous layers whose thicknesses are such that the travel time through each layer is the same. In this case, all events (arrivals at, reflections at, or transmissions through any interface, including the surface) occur at integer multiples of $\Delta\tau$, making the problem a digital signal processing problem. This model of the medium was first proposed by Goupillaud (1961), and is generally referred to as a "Goupillaud medium." The inverse seismic problem for such a medium being probed by plane waves at normal incidence has been solved by Goupillaud (1961), Kunetz (1962), Claerbout (1968), Ware and Aki (1969), and Berryman and Greene (1980), among others. Berryman and Greene (1980) also discuss this problem for the case of unequal travel times through the layers; in this case the problem is no longer discrete in time, since arrivals can occur at any time at any depth.

Layer stripping methods have been applied to the inverse problem for a continuous medium by Symes (1981), Santosa and Schwetlick (1982), and Bube and Burridge (1983), and to the inverse problem for a discrete medium by Symes and Zimmerman (1982). The one-dimensional inverse seismic problem at normal incidence is, to our knowledge, the one inverse seismic problem to which the layer stripping concept has been applied extensively prior to this thesis. (Some work has been done on the elastic

problem covered in Chapter VI.)

In Section 3.2 the solution of the inverse problem for a continuous medium is discussed. After some basic concepts of acoustics (plane waves, impedance, reflection and transmission coefficients, energy normalization, and free and half-space surface boundary conditions) are reviewed, the standard Gel'fand-Levitan procedure (Ware and Aki, 1969) for solving this problem is presented. Then the concept of layer stripping is applied, and the fast Cholesky, Schur, dynamic deconvolution, and method of characteristics algorithms for solving this problem are obtained.

In Section 3.3 the solution of the inverse problem for a discrete Goupillaud layered medium is discussed. An approach similar to that of Claerbout (1968) and Ware and Aki (1969) is used to derive the matrix equations appearing in Ware and Aki (1969), Aki and Richards (1980), and Berryman and Green (1980). These equations are discrete analogues of the integral equations of Section 2.4. The discrete Levinson algorithm for solving these matrix equations is also derived (Berryman and Green, 1980). Next, discrete layer stripping algorithms for solving this problem are derived. The discrete Schur and dynamic deconvolution algorithms obtained here were noted by Robinson (1982). It is most instructive to compare these discrete results with their continuous counterparts.

In Section 3.4 relations between the solutions of Section 3.2 and those of Section 3.3 are discussed. In particular, it is shown how the discrete medium problem approaches the continuous medium problem in the limit of the layer thicknesses going to zero. Gerver (1970) showed that for sufficiently small layer thicknesses the discrete problem solution approximates the continuous problem solution. Other aspects

of the discrete-to-continuous and continuous-to-discrete transitions are also discussed, including transmission losses, variations in impulses, a subtle distinction between discrete inverse scattering solutions and discretization of the medium, as pointed out by Berryman and Greene (1980).

3.2 Solution of the Inverse Problem for a Continuous Medium

The inverse seismic problem for a one-dimensional acoustic medium probed by impulsive plane waves at normal incidence is formally defined as follows. An impulsive acoustic plane wave, propagating vertically downward, is incident on a layered medium from a homogeneous half-space $z < 0$ in which the density ρ_o and local speed of sound c_o are known. This half-space could, for example, be the ocean above the ocean floor. The layered medium is laterally homogeneous, so that material parameters vary only in depth. The medium is also assumed to be acoustic (i.e., a fluid), so that it is entirely characterized by the profiles of density $\rho(z)$ and wave speed $c(z)$. If the medium is continuous, then $\rho(z)$ and $c(z)$ are continuous functions of depth z. The reflection response of the medium (i.e., the reverberations making their way back to the surface) is measured at the surface; the actual physical quantity being measured depends on the surface boundary conditions, as described in Section 3.2.1 below. The goal is to recover the profile functions $\rho(z)$ and $c(z)$. The problem is clearly one-dimensional in that all action can be represented by action along the z axis. The situation is illustrated in Figure 3.1.

Several variations on this problem will be considered in this chapter. In particular, the case of a continuous medium, in which $\rho(z)$

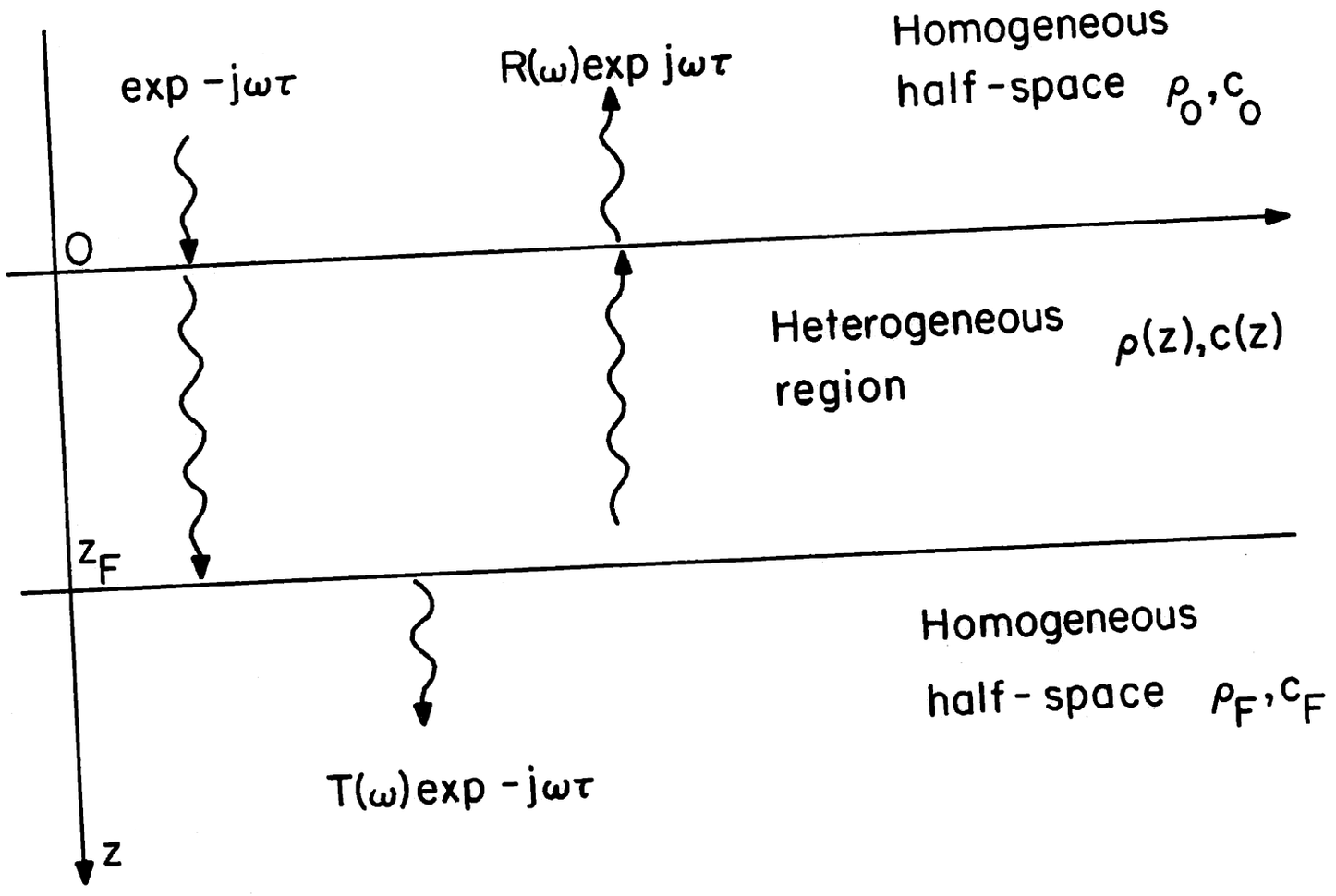

3.1 Scattering formulation of the inverse seismic problem.

and $c(z)$ are continuous functions of z, and the case of a discrete medium, in which $\rho(z)$ and $c(z)$ are piecewise constant, will both be treated. In the latter case it will be assumed, following Goupillaud (1961), that the layers have equal travel times, i.e., that the thickness of a layer is proportional to the wave speed in that layer. This makes the discrete problem a digital signal processing one. Two different sets of boundary conditions at the surface will be employed: the half-space configuration described above; and a free surface boundary condition, for which the surface pressure is zero.

For all of the above experimental configurations, Gerver (1970) has proved that it is impossible to recover $\rho(z)$ and $c(z)$ separately; all that can be obtained is their product $\rho c(\tau)$ as a function of travel time τ. Further, this reconstruction is unique, subject to mild assumptions. This is reasonable from a degrees-of-freedom point of view--the measurement of a single time function should not be expected to determine two different depth functions. In order to determine $\rho(z)$ and $c(z)$ separately, the oblique incidence experiment of Chapter IV must be employed. If the medium is not acoustic but elastic (i.e., not a liquid but a solid), then it can support shear stresses and shear wave propagation. This elastic problem is covered in Chapter VI.

3.2.1 Basic Concepts of Acoustics

In this section we quickly review some basic acoustical concepts, including plane waves, impedance, reflection and transmission coefficients, energy normalization, and surface boundary conditions. This will clear up some confusing points and lend physical insight into the meanings of various quantities appearing in the algorithms.

The two basic equations of acoustics are (Dowling and Williams, 1983)

$$p = -\rho c^2 \nabla \cdot \underset{\sim}{u} \tag{3-1a}$$

$$\partial^2 \underset{\sim}{u}/\partial t^2 = -(1/\rho)\nabla p \tag{3-1b}$$

where $\underset{\sim}{u}$ is the particle or medium displacement and p is the negative isotropic stress, i.e., pressure. Equation (3-1a) can be interpreted as an equation of conservation of mass, while equation (3-1b) is a convervation of momentum equation (compare (3-1b) to Newton's second law of motion F = ma). For a one-dimensional layered medium (3-1) becomes

$$p = -\rho c^2 \partial u/\partial z \tag{3-2a}$$

$$\partial^2 u/\partial t^2 = -(1/\rho)\, \partial p/\partial z \tag{3-2b}$$

where u(z,t) is the vertical displacement (the z-component of the vector $\underset{\sim}{u}$). Note that (3-2a) can be interpreted as Hooke's law for fluids: an applied stress -p produces the strain $\partial u/\partial z$, with the stress and strain linearly related by the elastic constant ρc^2.

Plane waves

In a homogeneous medium, insertion of (3-2a) in (3-2b) yields the wave equation

$$(\partial^2/\partial t^2 - c^2 \partial^2/\partial z^2)u(z,t) = 0 \tag{3-3}$$

which has the fundamental solutions

$$u(z,t) = u(t \pm z/c) \tag{3-4}$$

These solutions describe waves traveling upward and downward with speed c. These waves can take many forms (e.g., sinusoidal or impulsive), with some recognizable feature (an impulsive wave front, or a point of constant phase) moving through the medium at speed c. Note that there is no variation with x or y, so the wave can be thought of as a plane of constant phase or a planar impulse moving in the z or -z direction. This absence of spatial variation over a plane normal to the direction of propagation at a fixed time defines a plane wave (Aki and Richards, 1980, p. 125).

In general, if a plane wave is propagating in a space $\underset{\sim}{x}$ in direction $\underset{\sim}{n}$ with speed c, the quantity being propagated (displacement, pressure, etc.) is a function of $(t - \underset{\sim}{n} \cdot \underset{\sim}{x}/c)$. Note that the component in the direction $\underset{\sim}{y}$ of a plane wave moving in direction $\underset{\sim}{n}$ has dependence $t-(\underset{\sim}{n}\cdot\underset{\sim}{y})(\underset{\sim}{x}\cdot\underset{\sim}{y})/c$, which corresponds to an apparent speed of propagation faster than c. Since this is a phase velocity, there is no violation of causality.

Impedance

Consider the sinusoidal plane pressure wave

$$p(z,t) = p_0 e^{j\omega(t-z/c)} \tag{3-5}$$

propagating through a homogeneous medium. From (3-2) the particle or medium velocity $v(z,t) = \partial u/\partial t$ associated with the wave is

$$v(z,t) = p_0/\rho c \; e^{j\omega(t-z/c)} \tag{3-6}$$

so that

$$p(z,t)/v(z,t) \triangleq Z = \rho c \tag{3-7}$$

i.e., the pressure and velocity associated with the wave are related linearly by the impedance Z. Impedance is thus a measure of medium resistance to motion, i.e., the amount of pressure p required to set particles in motion with velocity v. Equation (3-7) should be compared to the electrical definition (2-42) of impedance as the ratio of voltage to current.

It should be noted (Aki and Richards, 1980, p. 137) that impedance depends on the type of wave. For example, a pressure wave propagating through a homogeneous medium at an angle θ from the vertical has impedance $\rho c/\cos\theta$, while a similar displacement wave has impedance $\rho c \cos\theta$, even though the waves are physically identical. How can this be true? For both waves, the ratio of stress to particle velocity in the direction of propagation is ρc. However, the impedance for the pressure wave is defined by

$$v_z \triangleq p/Z = v\cos\theta = (p/\rho c)\cos\theta \tag{3-8}$$

so $Z = \rho c/\cos\theta$. The impedance for the displacement wave is defined by

$$\tau_{zz} \triangleq Zv = p\cos\theta = (\rho c\, v)\cos\theta \tag{3-9}$$

so $Z = \rho c \cos\theta$. The reasons that impedance is defined in terms of the z-components of the produced stress or particle velocity will become apparent below. Also, the impedances for waves travelling in opposite directions have different signs.

Energy and energy normalization

It may be shown (Aki and Richards, 1980, p. 127) that the energy flux (energy per unit time per unit area normal to the direction of propagation) for a displacement plane wave is $\rho c v^2$, where v is the particle velocity amplitude of the wave. The energy flow in the z-direction is then $Zv^2 = \rho c \cos\theta\, v^2$, where θ is the angle between the direction of propagation of the plane wave and the z-axis. This can be seen by projecting a unit area of wavefront on a unit area normal to the z-axis.

Suppose now that the medium is inhomogeneous in the z-direction. Then the amplitude of the wave will be continually varying as ρc varies, in order that the energy flux $\rho c \cos\theta\, v^2$ be kept constant (save for losses due to reflections). This phenomenon has often been observed in earthquakes, when a seismic wave that had small amplitude when it was passing through hard rock (high impedance) suddenly becomes much larger (and more damaging) when it passes through landfill or sediment (low impedance).

This continual variation of the wave amplitude makes it difficult to note the effects of reflections, since the wave amplitude is varying due both to reflection losses and impedance variations. For this reason, the (energy)-normalized pressure ψ and displacement ϕ are defined by

$$\psi \triangleq p/Z^{\frac{1}{2}} \qquad (3\text{-}10a)$$

$$\phi \triangleq uZ^{\frac{1}{2}} \quad . \qquad (3\text{-}10b)$$

These quantities have the property that the energy flux in a wave is simply the square of the amplitude of the wave--it is no longer necessary to multiply or divide by Z. Thus variations in amplitude are due solely

to transmission and reflection losses. Note that normalized pressure and velocity have the same dimensions.

Reflection and transmission coefficients

Suppose a wave is propagating through a medium #1 with density ρ_1 and speed of sound c_1 and reaches an interface between medium #1 and another medium #2 with density ρ_2 and local speed of sound c_2. Some of the wave will be reflected and some transmitted. The ratios of the amplitudes of the reflected and transmitted waves to the amplitude of the incident wave are the reflection and transmission coefficients for that particular wave type.

Reflection and transmission coefficients are determined by boundary conditions at the interface: displacement and normal stress are continuous across the interface. Derivations are made in almost any seismic or acoustics text; the coefficients for various wave types are simply summarized below. These expressions are still valid for non-normal incidence on the interface if the impedance expressions (3-8) and (3-9) are used.

DEFINITIONS:
- r = reflection coefficient for a wave incident from medium #1
- $\bar{r}$ = reflection coefficient for a wave incident from medium #2
- t = transmission coefficient for a wave incident from medium #1
- $\bar{t}$ = transmission coefficient for a wave incident from medium #2

DISPLACEMENT WAVES:

$$r = \frac{Z_1 - Z_2}{Z_1 + Z_2}, \quad t = 1+r = \frac{2Z_1}{Z_1 + Z_2} \qquad (3\text{-}11a,b)$$

$$\bar{r} = \frac{Z_2 - Z_1}{Z_2 + Z_1}, \quad \bar{t} = 1+\bar{r} = \frac{2Z_2}{Z_1 + Z_2} \qquad (3\text{-}11c,d)$$

$$r = -\bar{r}, \quad t\bar{t} - r\bar{r} = 1 \qquad (3\text{-}11e,f)$$

PRESSURE WAVES:

$$r = \frac{Z_2 - Z_1}{Z_2 + Z_1}, \quad t = 1+r = \frac{2Z_2}{Z_1 + Z_2} \qquad (3\text{-}12a,b)$$

$$\bar{r} = \frac{Z_1 - Z_2}{Z_1 + Z_2}, \quad \bar{t} = 1+\bar{r} = \frac{2Z_1}{Z_1 + Z_2} \qquad (3\text{-}12c,d)$$

$$r = -\bar{r}, \quad t\bar{t} - r\bar{r} = 1 \qquad (3\text{-}12e,f)$$

NORMALIZED DISPLACEMENT WAVES:

$$r = \frac{Z_1 - Z_2}{Z_1 + Z_2}, \quad t = \bar{t} = \frac{2(Z_1 Z_2)^{\frac{1}{2}}}{Z_1 + Z_2} \qquad (3\text{-}13a,b)$$

$$\bar{r} = \frac{Z_2 - Z_1}{Z_2 + Z_1} \qquad (3\text{-}13c)$$

$$r = -\bar{r}, \quad t^2 + r^2 = 1, \quad t\bar{t} - r\bar{r} = 1 \qquad (3\text{-}13d\text{-}f)$$

NORMALIZED PRESSURE WAVES:

$$r = \frac{Z_2 - Z_1}{Z_2 + Z_1}, \quad t = \bar{t} = \frac{2(Z_1 Z_2)^{\frac{1}{2}}}{Z_1 + Z_2} \qquad (3\text{-}14a,b)$$

$$\bar{r} = \frac{Z_1 - Z_2}{Z_1 + Z_2} \qquad (3\text{-}14c)$$

$$r = -r, \quad t^2 + r^2 = 1, \quad t\bar{t} - r\bar{r} = 1 \qquad (3\text{-}14d\text{-}f)$$

Several comments are in order. Note that the reflection coefficients are the same for normalized and unnormalized waves. This is as expected; since the wave is reflected back into the same medium, normalization should have no effect. However, normalization does affect the transmission coefficients; the normalized coefficients are the same going in either direction (reciprocity), while the unnormalized coefficients must alter the

wave amplitude to preserve the energy flux through the medium.

Note that the reflection coefficients for pressure and displacement waves have opposite signs. Physically this amounts to a phase inversion; mathematically, it may be seen as follows. Recall that the amplitudes of the pressure and velocity associated with a wave are related by the impedance. Hence the reflection coefficients for pressure and velocity are related by the ratio of the impedances of upgoing and downgoing waves, since the incident and reflected waves travel in opposite directions. But these two impedances differ in sign, so their ratio is minus one.

For the normalized coefficients, we have the conservation of energy relation $t^2 + r^2 = 1$ (incoming energy = outgoing energy). For all coefficients, we have $r = -\bar{r}$ (simply exchange the media) and the relation $t\bar{t} - r\bar{r} = 1$, which should not be confused with the energy conservation relation $t^2 + r^2 = 1$.

Surface boundary conditions

In an inverse seismic problem, the medium is probed by a downgoing wave $D(0,t)$ at the surface, and the resulting upgoing wave $U(0,t)$ is measured at the surface. These waves must be specified in terms of known or measured quantities.

Half-space

If the medium is probed from a homgeneous half-space, then we set

$$D(0,t) = \delta(t) \tag{3-15a}$$

$$U(0,t) = R(t) \tag{3-15b}$$

Here $\delta(\cdot)$ is the impulse (Dirac delta) function and $R(t)$ is the measured response. This is the most common choice of boundary condition in the

literature, since the mathematical physics solution procedure described next requires this as a boundary condition. However, it is physically reasonable to make this choice when the actual physical experiment consists of detonating an explosive charge just above the ground for a land experiment, or close to the sea bottom (far away from the ocean surface) for an ocean experiment. In the latter case, the water column reverberations (reflections from the ocean surface) must be removed from the data.

Free surface

A free surface is also known as a pressure release surface, since the boundary condition is that the pressure at the surface is zero. The surface of the ocean is modelled quite well by a free surface (Claerbout, 1976), and the surface of the earth in a flat region is also modelled well by such a surface.

The effect of the free surface is to reflect the upcoming waves into the downgoing waves at the surface. It is necessary to assume that the density and wave speed are known immediately below the free surface, in lieu of specifying them in a half-space. Of course, the pressure release boundary condition is violated for an instant by the impulsive source, but as long as the source stops before any reflections return to the surface, there is no problem.

The boundary conditions for a free surface are

$$D(0,t) = \delta(t) \pm k(t) \qquad (3\text{-}16a)$$

$$U(0,t) = k(t) \qquad (3\text{-}16b)$$

where the upper sign is for displacement waves and the lower sign is for

pressure waves (to see this, set $Z_1 = 0$ in (3-11c) and (3-12c)). Note that the reflection response for a free surface can be synthesized from the response for a half-space boundary, and vice-versa, by

$$\hat{R}(\omega) = \hat{k}(\omega)/(1 \pm \hat{k}(\omega)) \qquad (3\text{-}17a)$$

$$\hat{k}(\omega) = \hat{R}(\omega)/(1 \mp R(\omega)) \qquad (3\text{-}17b)$$

where the same sign convention as in (3-16) is followed. Indeed, the entire scattering matrix for a free surface can be synthesized from the half-space scattering matrix and vice-versa; see Ware and Aki (1969).

Bottom boundary conditions

A radiation boundary condition is also assumed throughout: at sufficiently great depths, there is no upcoming wave ($U(\infty,t) = 0$). The transmitted wave at great depths is unknown. The medium is also assumed to be relaxed (quiescent) before the experiment beings. This is clearly necessary in order to use causality.

3.2.2 Mathematical Physics Solution for a Continuous Medium

Here the standard mathematical physics procedure for solving the one-dimensional inverse seismic problem for a continuous medium is presented. First popularized by Ware and Aki (1969), it has been used so often since then that it might well be termed the "classical" approach to solving this problem. The basic equations (3-2) are transformed into a Schrodinger equation, an equation often encountered in quantum mechanical scattering problems (Chadan and Sabatier, 1977). The Gel'fand-Levitan procedure for recovering the potential of the Schrodinger equation is well known (Faddeev, 1967; Chadan and Sabatier, 1977; etc.), and the

impedance is recovered by solving a differential equation involving the potential, or is recovered directly from the Schrodinger solution. A major problem with this method is that it requires the impedance profile $Z(\tau)$ to be twice differentiable, or impulses will appear in the Schrodinger potential.

Note that the travel time $\tau(z)$ from the top of the medium to depth z is given by

$$\tau(z) = \int_0^z ds/c(s), \tag{3-18}$$

and recall the definitions of impedance $Z = \rho c$ (3-7) and normalized displacement $\phi = Z^{\frac{1}{2}}u$ (3-10b). Substituting all of these in the basic acoustic equations (3-2) and Fourier transforming with respect to time yields the Schrodinger equation

$$\left(\frac{\partial^2}{\partial t^2} + \omega^2 - V\right)\hat{\phi}(\tau,\omega) = 0 \tag{3-19}$$

where $\hat{\phi}(\tau,\omega)$ is the Fourier transform of $\phi(\tau,t)$ and the potential $V(\tau)$ is defined as

$$V(\tau) = Z^{-\frac{1}{2}} \frac{d^2}{d\tau^2}(Z^{\frac{1}{2}}). \tag{3-20}$$

Note that equation (3-20) requires $Z(\tau)$ to be twice differentiable to avoid impulses in the potential $V(\tau)$.

The boundary conditions for the Gel'fand-Levitan solution procedure are those for a half-space boundary (3-15). Taking Fourier transforms of (3-15), employing the radiation condition, and recalling that $\phi = D + U$ results in

$$\hat{\phi}(\tau,\omega) = \begin{cases} e^{-j\omega\tau} + \hat{R}(\omega)e^{j\omega\tau} & , \ \tau < 0 \text{ (above surface)} \\ \hat{T}(\omega)e^{-j\omega\tau} & , \ \tau \to \infty \text{ (at great depth)} \end{cases} \tag{3-21}$$

where $e^{-j\omega\tau}$ is the source impulsive plane wave, $\hat{R}(\omega)e^{j\omega\tau}$ is the (measured) reflected plane wave response, and $\hat{T}(\omega)e^{-j\omega\tau}$ is the (unknown) transmission response of the medium. The situation is illustrated in Figure 3.1.

The Gel'fand-Levitan procedure applied to the inverse scattering problem specified by (3-19) - (3-21) results in the following procedure for solving the one-dimensional inverse seismic problem:

(1) Measure $\hat{R}(\omega)$ or its inverse Fourier transform $R(t)$;

(2) Solve the Marchenko integral equation

$$K(t,\tau) + R(t+\tau) + \int_{-t}^{\tau} K(s,\tau)R(s+t)ds = 0, \ t \leq \tau \tag{3-22}$$

(3) Compute the potential $V(\tau)$ from

$$V(\tau) = 2\frac{d}{d\tau} K(\tau,\tau) \tag{3-23}$$

(4) Solve the differential equation (3-20) for $Z(\tau)$.

Berryman and Greene (1980) have pointed out that steps (3) and (4) may be replaced by

$$Z(\tau)/Z(0) = 1 + \int_{-\tau}^{\tau} K(s,\tau)ds \tag{3-24}$$

since the differential equation (3-20) has the same form as the Schrodinger equation (3-19) with $\omega = 0$. From (3-22) it is evident that reconstruction of $Z(\tau)$ on $[0,T]$ requires $R(t)$ on $[0,2T]$, where $2T$ is the two-way travel time.

The Gel'fand-Levitan procedure is derived in Chadan and Sabatier (1977); the appearance of a Marchenko integral equation in an inverse scattering problem with a half-space boundary condition should not be surprising in light of Chapter II. It should be noted that this procedure requires that there be no bound states (see Chapter II) and that the potential $V(\tau)$ be localized, i.e.

$$\int_0^\infty (1 + \tau)|V(\tau)|d\tau < \infty \quad . \tag{3-25}$$

Neither of these conditions presents any problem for the one-dimensional problem at normal incidence, but they do present problems when the medium is probed at non-normal incidence. This is discussed in Chapter IV.

3.2.3 Layer Stripping Solutions for a Continuous Medium

To obtain layer stripping solutions, it is first necessary to obtain a two-component wave system from the basic acoustic equations (3-2). This is done as follows. Fourier transformation of (3-2) and changing variables from depth z to travel time τ using (3-18) results in the symmetrized equations

$$\hat{p} = -Z\, d\hat{u}/d\tau \tag{3-26a}$$

$$\omega^2 \hat{u} = (1/Z) d\hat{p}/d\tau \tag{3-26b}$$

which can be written as the matrix system

$$\frac{d}{d\tau} \begin{bmatrix} \hat{p} \\ \hat{u} \end{bmatrix} = \begin{bmatrix} 0 & \omega^2 Z \\ -1/Z & 0 \end{bmatrix} \begin{bmatrix} \hat{p} \\ \hat{u} \end{bmatrix} . \tag{3-27}$$

Claerbout (1976, p. 169) has pointed out that if the state vector $\begin{bmatrix} \hat{p} \\ \hat{u} \end{bmatrix}$ is

multiplied by the matrix of row eigenvectors of the system matrix, the new state variables can be interpreted as upgoing and downgoing waves. To see this, write the system (3-27) as

$$\frac{d\underline{x}}{d\tau} = A\underline{x} \tag{3-28}$$

where $\underline{x} \triangleq \begin{bmatrix} \hat{p} \\ \hat{u} \end{bmatrix}$, and let R and C be the matrices of row and column eigenvectors, respectively, of the system matrix A. Then, defining

$$\underline{w} = R\underline{x} \quad , \tag{3-29}$$

substituting (3-29) into (3-28), premultiplying by R, and using RC = I results in

$$\frac{d\underline{w}}{d\tau} = (RAC - R\frac{dC}{dz})\,\underline{w} \quad . \tag{3-30}$$

But RAC is the diagonal matrix of eigenvalues of A, i.e., RAC = DIAG[$-j\omega$, $j\omega$]. In a homogeneous medium, the second term $R\frac{dC}{dz}$ is zero, and from (3-30) it is evident that $\underline{w}$ is indeed a vector whose components are upgoing and downgoing waves.

However, in an <u>inhomogeneous</u> medium, the second term of (3-30) $R\frac{dC}{dz}$ differs from zero. But the interpretation of $\underline{w}$ as consisting of upgoing and downgoing waves will be preserved if the <u>diagonal</u> elements of $R\frac{dC}{dz}$ are zero. This can be achieved by scaling R appropriately (scaling the elements of R will not affect their status as eigenvectors). Since R is

$$R = \begin{bmatrix} 1 & j\omega Z \\ 1 & -j\omega Z \end{bmatrix} \tag{3-31}$$

resulting in the waves

resulting in the waves

$$\underline{w} = R\begin{bmatrix}\hat{p}\\ \hat{u}\end{bmatrix} = \begin{bmatrix}\hat{p} + j\omega Z\hat{u}\\ \hat{p} - j\omega Z\hat{u}\end{bmatrix} \tag{3-32}$$

the obvious scaling to try is the energy-normalized waves

$$\begin{bmatrix}\hat{D}(\tau,\omega)\\ \hat{U}(\tau,\omega)\end{bmatrix} \triangleq Z^{-\frac{1}{2}}\underline{w} = (Z^{-\frac{1}{2}}R)\begin{bmatrix}\hat{p}\\ \hat{u}\end{bmatrix} \tag{3-33}$$

$$= \begin{bmatrix}\hat{p}/Z^{\frac{1}{2}} + j\omega Z^{\frac{1}{2}}\hat{u}\\ \hat{p}/Z^{\frac{1}{2}} - j\omega Z^{\frac{1}{2}}\hat{u}\end{bmatrix} = \begin{bmatrix}\hat{\psi} + j\omega\hat{\phi}\\ \hat{\psi} - j\omega\hat{\phi}\end{bmatrix}.$$

Indeed this works and the waves $\hat{D}(\tau,\omega)$ and $\hat{U}(\tau,\omega)$ satisfy the two-component wave system

$$\frac{d}{d\tau}\begin{bmatrix}\hat{D}\\ \hat{U}\end{bmatrix} = \begin{bmatrix}-j\omega & -r\\ -r & j\omega\end{bmatrix}\begin{bmatrix}\hat{D}\\ \hat{U}\end{bmatrix} \tag{3-34}$$

where the reflectivity function $r(\tau)$ is defined as

$$r(\tau) = \frac{1}{2Z}\frac{dZ}{d\tau}. \tag{3-35}$$

Two comments are in order here. Recall the definition of impedance and the fact that impedances of waves travelling in opposite directions are opposite in sign. Then, in a homogeneous medium, the waves (3-33) both become waves in the normalized pressure $\hat{\psi}$, i.e., the normalized pressure $\hat{\psi}$ is decomposed into upgoing and downgoing waves. Next, recall the reflection coefficient (3-14a) for normalized pressure waves.

A continuous medium may be modelled by a stack of thin homogeneous layers, each with travel time Δ, and then letting Δ approach zero. This gives

$$\lim_{\Delta \to 0} \frac{r}{\Delta} = \lim_{\Delta \to 0} \frac{Z(\tau+\Delta) - Z(\tau)}{Z(\tau+\Delta) + Z(\tau)} \frac{1}{\Delta} = \frac{1}{2Z} \frac{dZ}{d\tau} = r(\tau). \qquad (3\text{-}36)$$

This will be discussed in more detail in Section 3.4. In the present context, the sign of (3-35) implies that the waves are really normalized pressure waves, rather than displacement waves. This is in accordance with the first comment.

Fast Cholesky algorithm

If the downgoing wave $D(\tau,t)$ contains an impulse, as it does in both the half-space and free surface boundary conditions, then we immediately have the fast Cholesky algorithm

$$\left(\frac{\partial}{\partial \tau} + \frac{\partial}{\partial t}\right) D(\tau,t) = -r(\tau)U(\tau,t) \qquad (3\text{-}37a)$$

$$\left(\frac{\partial}{\partial \tau} - \frac{\partial}{\partial t}\right) U(\tau,t) = -r(\tau)D(\tau,t) \qquad (3\text{-}37b)$$

$$r(\tau) = 2U(\tau,\tau) \qquad (3\text{-}37c)$$

initialized by either set of boundary conditions (3-15) or (3-16). The impedance $Z(\tau)$ is then recovered by integrating (3-35), yielding

$$Z(\tau) = Z(0) \exp 2\int_0^\tau r(s)ds. \qquad (3\text{-}38)$$

This algorithm is preferable to the Gel'fand-Levitan procedure (3-20), (3-22), (3-23) on both computational and aesthetic grounds. The

quantities in the algorithm have obvious physical interpretations, allowing the user to physically envision the inversion process, and the algorithm is guaranteed stable as long as $\int_o^\infty |r(\tau)|\,d\tau < \infty$, which merely requires that the impedance be positive and bounded. Bube and Burridge (1983) have experimented with various discretizations of this algorithm (which they call the "downward continuation" algorithm), and have gotten excellent results.

Schur algorithm

In the frequency domain we have

$$\frac{d}{d\tau}\begin{bmatrix}\hat{D}(\tau,\omega)\\ \hat{U}(\tau,\omega)\end{bmatrix} = \begin{bmatrix}-j\omega & -r\\ -r & j\omega\end{bmatrix}\begin{bmatrix}\hat{D}(\tau,\omega)\\ \hat{U}(\tau,\omega)\end{bmatrix} \tag{3-39a}$$

$$r(\tau) = \lim_{\omega\to\infty} 2j\omega\, e^{j\omega\tau}\,\hat{U}(\tau,\omega) = (1/\pi)\int_o^\infty \hat{U}(\tau,\omega)e^{j\omega\tau}\,d\omega \tag{3-39b}$$

which may be preferable if all of the waves are only known over a limited frequency range (i.e., are bandlimited in measurement). In this case, the lack of high frequency components will cause some error in (3-39b). $Z(\tau)$ is obtained from (3-38).

Dynamic deconvolution

Defining the reflection coefficient for the entire medium below depth z

$$\hat{R}(\tau,\omega) \triangleq \hat{U}(\tau,\omega)/\hat{D}(\tau,\omega) \tag{3-40}$$

we have the Riccati equation

$$\frac{d}{d\tau}\hat{R}(\tau,\omega) = 2j\omega\hat{R} - r(\tau)(1-\hat{R}^2) \tag{3-41}$$

along with

$$r(t) = \underset{\omega \to \infty}{\text{LIM}}\ 2j\omega\hat{R} = (1/\pi)\int_0^\infty \hat{R}(\omega,\tau)d\omega \quad . \tag{3-42}$$

This algorithm, in which $\hat{R}(\tau,\omega)$ is propagated in τ by (3-41), is initialized by

$$\hat{R}(0,\omega) = \hat{R}(\omega) \text{ for a half-space boundary} \tag{3-43a}$$

$$\hat{R}(0,\omega) = \hat{k}(\omega)/(1-\hat{k}(\omega)) \text{ for a free surface boundary .} \tag{3-43b}$$

Tolstoy and Clay (1966) noted the Riccati equation (3-41) for propagating the forward problem, as did Newton (1981). Corones et al. (1983) used the inverse Fourier transform of (3-41) as an invariant embedding equation, along with

$$r(\tau) = 2R(\tau,0) \tag{3-44}$$

to solve the inverse problem.

Note that $\hat{R}(\tau,\omega)$ is the Fourier transform of the seismogram at depth τ that would be obtained if all of the medium above depth τ were stripped away, and the remaining portion of the medium probed with an impulsive plane wave. Equation (3-44) then states that the first reflection from the medium is caused solely by $r(\tau)$. Equation (3-37c) in the fast Cholesky algorithm has a similar interpretation: the first reflection from the downgoing wave into the upgoing wave at depth τ is caused solely by $r(\tau)$.

Method of characteristics

The choice of variables in using the method of characteristics is dictated by the relation $Z = p/v$. Letting

$$p(\tau,t) = \tilde{p}(\tau,t)1(t-\tau) \tag{3-45a}$$

$$v(\tau,t) = \tilde{v}(\tau,t)1(t-\tau) \tag{3-45b}$$

and changing variables from z to τ in the basic acoustic equations (3-2) results in the symmetrized system

$$\partial\tilde{p}(\tau,t)/\partial\tau = -Z\partial\tilde{v}(\tau,t)/\partial t \tag{3-46a}$$

$$\partial\tilde{v}(\tau,t)/\partial\tau = -(1/Z)\partial\tilde{p}(\tau,t)/\partial t \quad . \tag{3-46b}$$

Along the wave front, which is a plane wave in (τ,t) space propagating with unit velocity, we have by the definition of impedance

$$Z(\tau) = \tilde{p}(\tau,\tau^+)/\tilde{v}(\tau,\tau^+) \quad . \tag{3-47}$$

The set of equations (3-46) - (3-47) can be propagated in τ, yielding $Z(\tau)$. However, there is no guarantee of stability, and all physical interpretation in terms of waves and reflections is gone.

Each of the above algorithms has its counterpart in the inverse seismic problem for a discrete layered medium. This is explored in the next section.

3.3 Solution of the Inverse Problem for a Discrete Medium

The inverse seismic problem for a one-dimensional acoustic discrete medium is defined as follows. The medium consists of a stack of homogeneous layers whose thicknesses are proportional to the speeds of sound within them. Such a medium is called a Goupillaud medium, after Goupillaud (1961). The medium is probed by an impulsive acoustic plane wave at normal incidence, as before, and the reflection response of the medium is measured. The goal is to recover the

impedance in each layer, which is equivalent to finding impedance as a function of travel time. The medium is illustrated in Figure 3.2.

The special structure of a Goupillaud medium causes all events (wave arrivals, reflections, and transmissions at all interfaces, including the surface) to occur at half-integer multiples of the two-way travel time $\Delta\tau$ through each layer. This means that the actual mathematical problem, involving impulses, can be replaced by a completely equivalent digital signal processing problem. This makes things much simpler mathematically, and allows much easier visualization of what is happening inside the medium.

It should be noted that the Goupillaud assumption is not as restrictive as it may first appear. Thick layers of various thicknesses may be built up by stacking various numbers of the fundamental layers, each having the same density and wave speed. This can be used to approximate a general discrete medium. For $\Delta\tau$ small, the Goupillaud medium may be a good approximation to a continuous medium. Indeed, it will be shown in Section 3.4 below that the Goupillaud medium results approach the continuous medium results as $\Delta\tau \to 0$ (this result is due to Gerver, 1970).

In the course of solving the discrete problem, discrete analogues of integral equations and of all of the layer stripping algorithms will be obtained. The approach will be similar to that of Aki and Richards (1980), with results from Kunetz (1967), Ware and Aki (1969), Berryman and Greene (1980), and Robinson (1982) also worked in. Bruckstein and Kailath (1984) gave a similar treatment for the discrete transmission line.

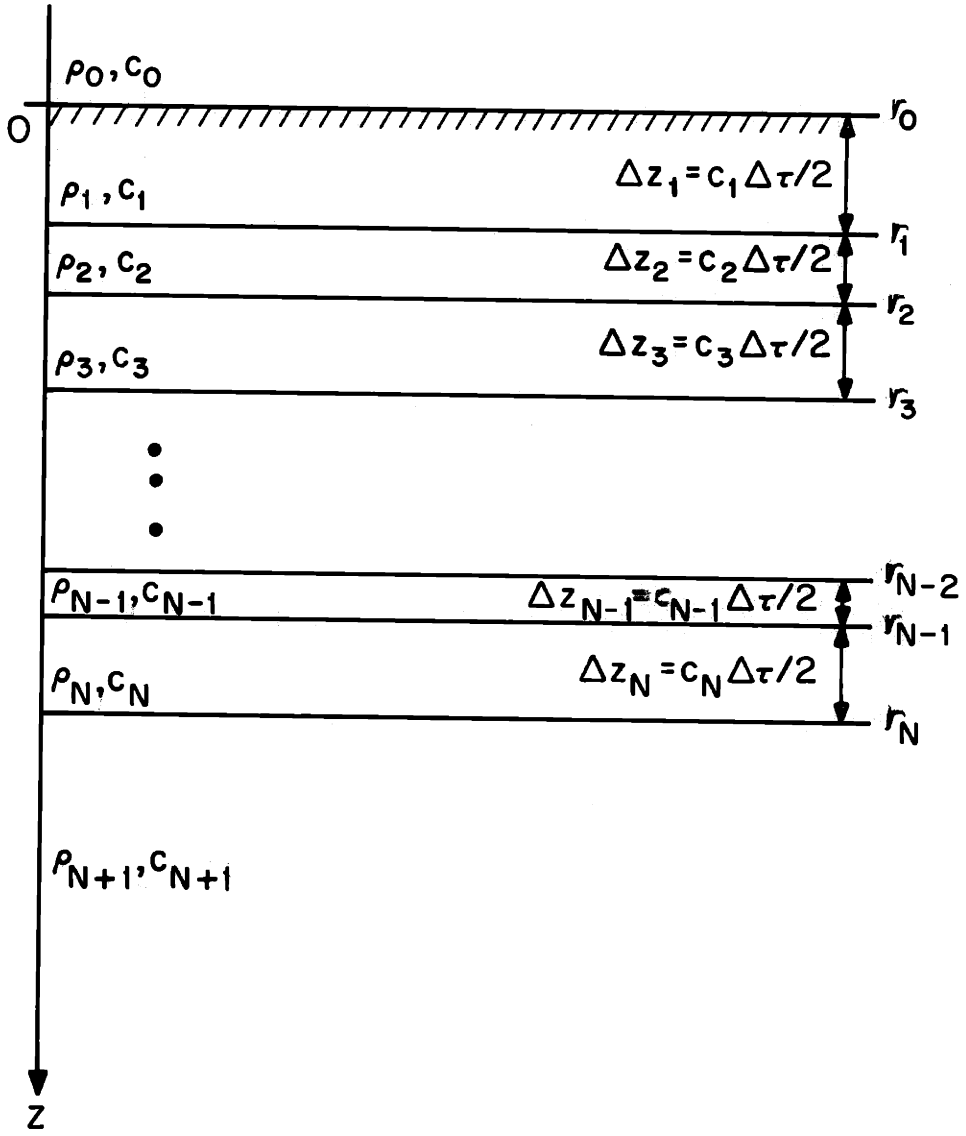

3.2 The discrete, Goupillaud, equal-traveltime layered medium .

3.3.1 Matrix Equation Solutions for a Discrete Medium

For convenience we consider the medium as consisting of N equal-traveltime layers sandwiched between two infinite half-spaces. The two-way travel time through each layer is $\Delta\tau$. Insertion of the lower half-space is simply equivalent to cutting off the data record after $N\Delta\tau$. In due course, a free surface will be introduced in lieu of the upper half-space (this can be done by setting $\rho_o = c_o = 0$). The medium is illustrated in Figure 3.2.

The medium will be probed by an impulsive displacement wave, and the problem will be treated as a digital signal processing problem. The downgoing and upgoing normalized displacement waves at the top of layer i will be designated as d_i and u_i, respectively, while the waves at the bottom of layer i will be designated as d_i' and u_i'. The wave notation is illustrated in Figure 3.3. Note that

$$d_i'(t) = d_i(t - \tfrac{1}{2}) \qquad (3\text{-}48a)$$

$$u_i'(t) = u_i(t + \tfrac{1}{2}) \quad . \qquad (3\text{-}48b)$$

It should also be noted that $d_i(t)$ and $u_i(t)$ are zero except at $t = (i-1)/2 + k$, $k = 0,1,2,\ldots$, and $d_i'(t)$ and $u_i'(t)$ are zero except at $t = i/2 + k$, $k = 0,1,2,\ldots$ Hence successive non-zero values of any wave are separated by one, i.e., the layer two-way traveltime $\Delta\tau$. If the one-way layer traveltime were being used, the waves would have every other value being zero, and the notation would be even worse.

At any given moment, the four waves at an interface i interact as shown in Figure 3.4. We have

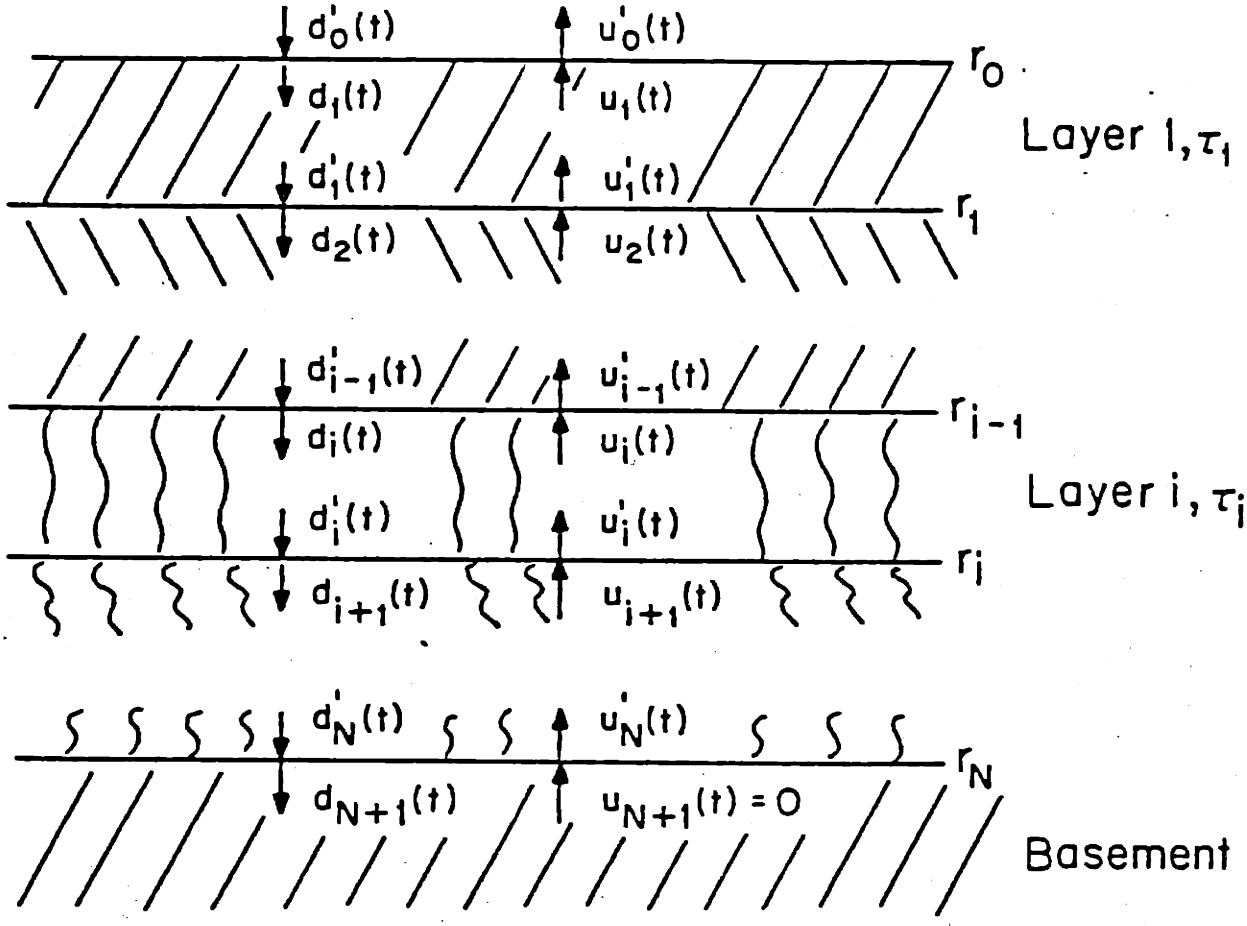

3.3 Notation for upgoing and downgoing waves at the top and bottom of each layer.

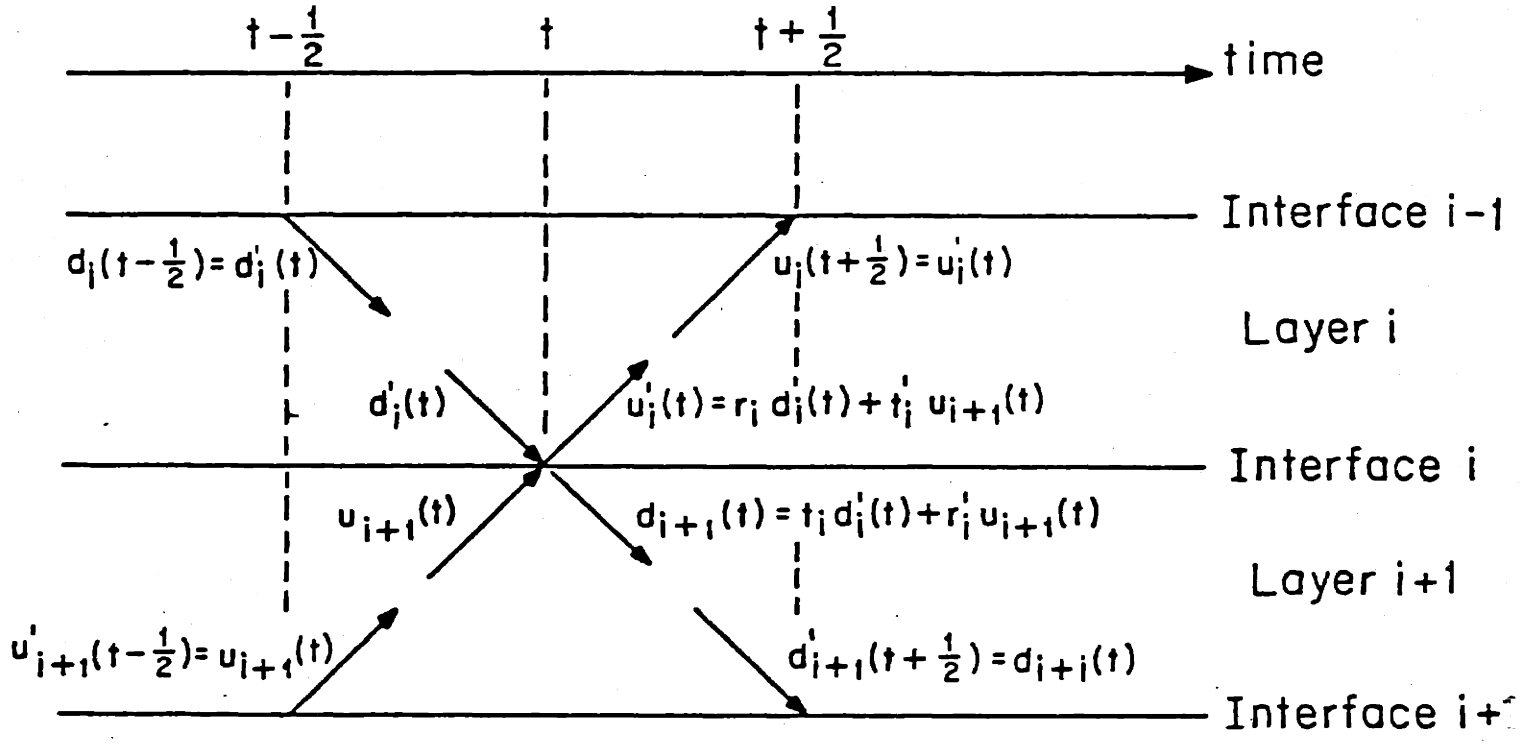

3.4 Interaction of the downgoing and upgoing waves in layers i and i+1.

$$d_{i+1} = t_i d_i' + \bar{r}_i u_{i+1} \tag{3-49a}$$

$$u_i' = r_i d_i' + \bar{t}_i u_{i+1} \tag{3-49b}$$

where r_i, t_i, $\bar{r}_i$, and $\bar{t}_i$ are defined in (3-13) for normalized displacement waves. Equations (3-49) can be rewritten, using (3-13d) and (3-13f), as

$$\begin{bmatrix} u_{i+1} \\ d_{i+1} \end{bmatrix} = \frac{1}{\bar{t}_i} \begin{bmatrix} 1 & -r_i \\ -r_i & 1 \end{bmatrix} \begin{bmatrix} u_i' \\ d_i' \end{bmatrix} \tag{3-50}$$

and defining the layer two-way travel time delay operator z we have, using (3-48)

$$\begin{bmatrix} u_{i+1} \\ d_{i+1} \end{bmatrix} = \frac{1}{z^{\frac{1}{2}} t_i} \begin{bmatrix} 1 & -zr_i \\ -r_i & z \end{bmatrix} \begin{bmatrix} u_i \\ d_i \end{bmatrix} \tag{3-51}$$

A straightforward induction argument similar to that of Aki and Richards (1980, p. 666) shows that for n = 1,2,...N

$$\begin{bmatrix} u_{n+1} \\ d_{n+1} \end{bmatrix} = \frac{1}{z^{n/2}} \begin{bmatrix} M_{11}^n(z) & z^n M_{21}(1/z) \\ M_{21}^n(z) & z^n M_{11}(1/z) \end{bmatrix} \begin{bmatrix} u_1 \\ d_1 \end{bmatrix} \tag{3-52}$$

where $M_{11}(z)$ and $M_{21}(z)$ are polynomials in z having the forms

$$M_{11}^n(z) = \sum_{i=0}^{n} m_{1i}^n z^i/(t_1 t_2 \ldots t_n) \quad , \quad m_{10}^n = 1, \; m_{1n}^n = 0 \tag{3-53a}$$

$$M_{21}^n(z) = \sum_{i=0}^{n} m_{2i}^n z^i/(t_1 t_2 \ldots t_n) \quad , \quad m_{20}^n = -r_n, \; m_{2n}^n = 0 \tag{3-53b}$$

Note that (3-52) defines the discrete state transition matrix, in direct analogy to (2-93). Note that properties analogous to the time-reversal properties (2-98) have been revealed by the induction, and have been used to simplify $M_{12}^n(z)$ and $M_{22}^n(z)$. Note also that the finite order of the polynomials is analogous to the support (2-97) of $M_{11}(x,t)$ and $M_{21}(x,t)$.

The polynomials $M_{11}^n(z)$ and $M_{21}^n(z)$ are generated recursively by the recursions

$$M_{11}^{n+1}(z) = \frac{1}{t_n}\left(M_{11}^n(z) - z r_n M_{21}^n(z)\right) \tag{3-54a}$$

$$M_{21}^{n+1}(z) = \frac{1}{t_n}\left(z M_{21}^n(z) - r_n M_{11}^n(z)\right) \quad . \tag{3-54b}$$

which also follow directly since $[M_{ij}^n(z)]$ is the transition matrix (compare to (2-91)). Equations (3-53) and (3-54) are similar to equations (41) and (42) in Ware and Aki (1969), and to equations (22), (13), and (12) in Berryman and Greene (1980). However, these latter equations were derived for the upgoing (i.e., in <u>decreasing</u> i) transition matrix.

<u>Half-space boundary condition</u>

For an infinite half-space boundary the boundary conditions are

$$\begin{bmatrix} u_1 \\ d_1 \end{bmatrix} = \begin{bmatrix} R(z) \\ 1 \end{bmatrix} \tag{3-55a}$$

$$\begin{bmatrix} u_{N+1} \\ d_{N+1} \end{bmatrix} = \begin{bmatrix} 0 \\ T(z) \end{bmatrix} \tag{3-55b}$$

where

$$R(z) = \sum_{n=0}^{\infty} R_n z^n \tag{3-56a}$$

$$T(z) = \sum_{n=N/2}^{\infty} T_n z^n \tag{3-56b}$$

are constructed from the reflection response sequence at the surface $\{R_n\}$, and the transmission response sequence at the bottom $\{T_n\}$.

The layer matrix in (3-51) has a determinant of unity, hence the propagator matrix in (3-52) also has a determinant of unity. Inserting (3-55) into (3-52), setting n = N, and adding results in

$$z^N(M_{11}^N(1/z) + M_{21}^N(1/z)) + R(z)(M_{11}^N(z) + M_{21}^N(z)) = z^{N/2} T(z) \ . \tag{3-57}$$

Multiplying (3-57) by $\prod_{i=1}^{N} t_i$ and inserting (3-53) and (3-56) results in

$$\sum_{i=0}^{N} z^{N-i}(m_{1i}^N + m_{2i}^N) + \sum_{i=0}^{N} z^i \sum_{j=N-i}^{N} (m_{1,N-j}^N + m_{2,N-j}^N) R_{i+j-N} + O(z^{N+1})$$

$$= (\prod_{j=1}^{N} t_j) \sum_{i=N/2}^{N} z^{N/2+i} T_i + O(z^{N+1})$$

$$= z^N (\prod_{j=1}^{N} t_j) T_{N/2} + O(z^{N+1}), \tag{3-58}$$

where the order of the inner sum of the nested sum has been reversed. Clearly $T_{N/2} = \prod_{j=1}^{N} t_j$, so the right side of (3-58) is just $z^N \prod_{j=1}^{N} (1-r_j^2) + O(z^{N+1})$. Equating coefficients of powers of z on both sides of (3-58) results in the matrix equation

$$\left(I + \begin{bmatrix} 0 & & & R_0 \\ & & & R_1 \\ & & & \vdots \\ R_0 & R_1 & \cdots & R_N \end{bmatrix} \right) \begin{bmatrix} m_{1N}^N + m_{2N}^N \\ \vdots \\ m_{10}^N + m_{20}^N \end{bmatrix} = \begin{bmatrix} 0 \\ \vdots \\ 0 \\ \prod_{j=1}^{N} (1-r_j^2) \end{bmatrix} \qquad (3\text{-}59)$$

which is (70) in Berryman and Greene (1980), and which can be rewritten as

$$\begin{bmatrix} m_{1N}^N + m_{2N}^N \\ \vdots \\ m_{11}^N + m_{21}^N \\ m_{10}^N + m_{20}^N - 1 \end{bmatrix} + \begin{bmatrix} R_0 \\ R_1 \\ \vdots \\ R_N \end{bmatrix} + \begin{bmatrix} 0 & & & R_0 \\ & & & R_1 \\ & & & \vdots \\ R_0 & R_1 & \cdots & R_N \end{bmatrix} \begin{bmatrix} m_{1N}^N + m_{2N}^N \\ \vdots \\ m_{11}^N + m_{21}^N \\ m_{10}^N + m_{20}^N - 1 \end{bmatrix} = \begin{bmatrix} 0 \\ \vdots \\ 0 \\ \prod_{j=1}^{N} (1-r_j^2) - 1 \end{bmatrix} \qquad (3\text{-}60)$$

Equation (3-60) is just a discrete version of the Marchenko integral equation (2-103), in terms of the kernel $m_{1i}^N + m_{2i}^N$ (compare to (2-102)). From (3-53b), and in analogy to (2-104a), we have

$$r_N = - m_{20}^N \quad . \qquad (3\text{-}61)$$

Free surface boundary condition

Here we return to Aki and Richards (1980), pp. 667-669). Now the boundary conditions are

$$\begin{bmatrix} u_1 \\ d_1 \end{bmatrix} = \begin{bmatrix} k(z) \\ 1+k(z) \end{bmatrix} \qquad (3\text{-}62a)$$

$$\begin{bmatrix} u_{N+1} \\ d_{N+1} \end{bmatrix} = \begin{bmatrix} 0 \\ T(z) \end{bmatrix} \qquad (3\text{-}62b)$$

$$k(z) = \sum_{n=0}^{\infty} k_n z^n \tag{3-62c}$$

where $R(z)$ and $T(z)$ are defined by (3-55) and (3-56) and $\{k_n\}$ is the free surface response sequence. Inserting (3-62) in (3-52) with $n = N$ yields

$$\begin{bmatrix} 0 \\ T(z) \end{bmatrix} = \frac{1}{z^{N/2}} \begin{bmatrix} M_{11}^N(z) + z^N M_{21}^N(1/z) & z^N M_{21}^N(1/z) \\ M_{21}^N(z) + z^N M_{11}^N(1/z) & z^N M_{11}^N(1/z) \end{bmatrix} \begin{bmatrix} k(z) \\ 1 \end{bmatrix}. \tag{3-63}$$

Defining the polynomial

$$G(z) \triangleq M_{11}^N(z) + z^N M_{21}^N(1/z) \ , \tag{3-64a}$$

$$= (1/\prod_{j=1}^{N} t_j) \sum_{i=0}^{N} g_i z^i, \ g_i = m_{1i}^N + m_{2,N-i}^N, \ g_0 = 1, \ g_N = -r_N, \tag{3-64b}$$

replacing z with $1/z$ in (3-63a), multiplying by z^N, and adding to (3-63b) yields

$$Z^{-N/2} T(z) = G(\tfrac{1}{z}) \ (1 + k(z) + k(\tfrac{1}{z})) \ . \tag{3-65}$$

Replacing z with $\frac{1}{z}$ in (3-65) shows that $z^{-N/2} T(z) G(z)$ remains unchanged if z is replaced with $\frac{1}{z}$. Since this is a causal polynomial, this is only possible if it is a constant polynomial, and (3-53) and (3-64b) show that this constant is one. Hence we have

$$G(z) = 1/(z^{-N/2} T(z)) \tag{3-66}$$

so that $G(z)$ is the causal and stable deconvolution, inverse, or

whitening filter that outputs the source impulse when the transmission seismogram is fed into it (the $z^{-N/2}$ removes the delay before $\{T_n\}$ becomes non-zero).

Inserting (3-66) into (3-65) we get the important equation

$$1 + k(z) + k(1/z) = T(z)T(1/z) = 1/(G(z)G(1/z)) \qquad (3\text{-}67)$$

which states that the medium response, for a free surface boundary condition, forms one side of the autocorrelation of the transmission seismogram. This famous result is due to Kunetz (1962), and should be compared with (2-149).

Writing out the polynomials in (3-65) using (3-64b) and (3-62c), multiplying by G(1/z), and equating coefficients of negative powers of z to zero (since 1/G(z) is causal by (3-66)) yields the matrix equation

$$\left(2k_o I + \begin{bmatrix} 1 & k_1 & \cdots & k_{N-1} \\ k_1 & & \iddots & \vdots \\ \vdots & \iddots & & k_1 \\ k_{N-1} & \cdots & k_1 & 1 \end{bmatrix}\right) \begin{bmatrix} g_1 \\ g_2 \\ \\ g_N \end{bmatrix} + \frac{1}{\prod_{j=1}^{N} t_j} \begin{bmatrix} k_1 \\ k_2 \\ \vdots \\ k_N \end{bmatrix} = 0 , \qquad (3\text{-}68)$$

and using (3-64) and (3-53) this equation can be rewritten as

$$\begin{bmatrix} k_1 \\ \vdots \\ \vdots \\ k_N \end{bmatrix} \frac{1}{\prod_{j=1}^{N} t_j} + \begin{bmatrix} m_{11}^N + M_{2,N-1}^N \\ m_{12}^N + m_{2,N-2}^N \\ \vdots \\ m_{1N}^N + m_{20}^N \end{bmatrix} + \begin{bmatrix} 2k_0 & k_1 & \cdots & k_{N-1} \\ k_1 & & \iddots & \vdots \\ \vdots & \iddots & & k_1 \\ k_{N-1} & \cdots & k_1 & 2k_0 \end{bmatrix} \begin{bmatrix} m_{11}^N + m_{2,N-1}^N \\ m_{12}^N + m_{2,N-2}^N \\ \vdots \\ m_{1N}^N + m_{20}^N \end{bmatrix} = 0. \qquad (3\text{-}69)$$

Equation (3-69) is a discrete version of the Krein integral equation (2-111), in terms of the kernel $m_{1i}^N + m_{2,N-i}^N$ (compared to (2-110)).

In the continuous medium case, the transmission losses become negligible (see Section 3.4), so $\prod_{j=1}^{N} t_j$ becomes unity. From (3-64b) we have $r_N = -g_N = -(m_{1N}^N + m_{20}^N)$, in analogy to (2-113).

Levinson algorithm

It should not be surprising that the discrete Levinson algorithm can be used to solve the matrix equations (3-60) and (3-68). Indeed, the recursions (3-54) are the Levinson recursions in the form of recursions on the Szego polynomials $M_{11}^n(z)$ and $M_{12}^n(z)$. All that is needed is an "inner product" expression to generate the reflection coefficients, allowing the algorithm to propagate. Equation (52) in Ware and Aki (1969) and equation (21) in Berryman and Greene (1980) are both

$$r_n = \sum_{i=0}^{n-1} k_{n-i} m_{1i}^n \Big/ \prod_{j=0}^{n-1} (1-r_j^2) \tag{3-70}$$

(proved by induction in Appendix A of Ware and Aki, 1969), and this in conjunction with

$$m_{1i}^n = \frac{1}{(1-r_i^2)^{\frac{1}{2}}} (m_{1i}^{n-1} + r_n \, m_{2,i-1}^{n-1}) \tag{3-71a}$$

$$m_{2i}^n = \frac{1}{(1-r_i^2)^{\frac{1}{2}}} (m_{2,i-1}^{n-1} + r_n \, m_{1i}^{n-1}) \,, \quad 1 \leq i \leq n \tag{3-71b}$$

forms the Levinson algorithm for obtaining the reflection coefficients $\{r_n\}$. Note that the sums $m_{1i}^N + m_{2i}^N$ solve the Marchenko-like Hankel matrix system (3-60), while the solution to the Krein-like Toeplitz matrix system (3-68) can be generated from (3-71) and (3-64).

Having obtained discrete analogues to the Marchenko and Krein

integral equations and the Levinson algorithm, we now derive discrete analogues to the layer stripping algorithms of Section 3.2.3.

3.3.2 Layer Stripping Solutions for a Discrete Medium

The layer stripping algorithms for solving the discrete medium problem can be obtained almost immediately from the above development. Recalling (3-51)

$$\begin{bmatrix} u_{i+1} \\ d_{i+1} \end{bmatrix} = \frac{1}{z^{\frac{1}{2}} t_i} \begin{bmatrix} 1 & -zr_i \\ -r_i & z \end{bmatrix} \begin{bmatrix} u_i \\ d_i \end{bmatrix} \tag{3-72}$$

where $t_i = (1-r_i^2)^{\frac{1}{2}}$ from (3-13e). $\begin{bmatrix} u_1 \\ d_1 \end{bmatrix}$ can be initialized using either (3-55) for a half-space boundary or (3-62) for a free surface.

At the leading edge or wave front, there is no upcoming wave from farther below by causality and the initial quiescence of the medium. Hence we may set $u_{i+1} = 0$ in (3-49b), yielding

$$r_i = u_i'/d_i' = u_i(1 + \tfrac{1}{2})/d_i(i - \tfrac{1}{2}) = \left.\frac{u_i}{zd_i}\right|_{z=0} . \tag{3-73}$$

The fast Cholesky algorithm is then, from (3-72) and (3-73),

$$d_{i+1}(t) = \frac{1}{(1-r_i^2)^{\frac{1}{2}}} (d_i(t - \tfrac{1}{2}) - r_i u_i(t + \tfrac{1}{2})) \tag{3-74a}$$

$$u_{i+1}(t) = \frac{1}{(1-r_i^2)^{\frac{1}{2}}} (u_i(t + \tfrac{1}{2}) - r_i d_i(t - \tfrac{1}{2})) \tag{3-74b}$$

$$r_i = u_i(i + \tfrac{1}{2})/d_i(i - \tfrac{1}{2}) \quad . \tag{3-74c}$$

The Schur algorithm (here in its original form as developed by Schur) is (Robinson, 1982)

$$d_{i+1}(z) = \frac{z^{\frac{1}{2}}}{(1-r_i^2)^{\frac{1}{2}}} (d_i - z^{-1} r_i u_i) \tag{3-75a}$$

$$u_{i+1}(z) = \frac{z^{-\frac{1}{2}}}{(1-r_i^2)^{\frac{1}{2}}} (u_i - z r_i d_i) \tag{3-75b}$$

$$r_i = \frac{u_i}{z d_i} \Bigg|_{z = 0} . \tag{3-75c}$$

The dynamic deconvolution algorithm (Robinson, 1982) is obtained by defining

$$R_i(z) = \frac{u_i}{z d_i} \tag{3-76}$$

and noting from (3-75) that $R_i(z)$ satisfies

$$R_{i+1}(z) = \frac{1}{z} \frac{R_i(z) - r_i}{1 - r_i R_i(z)} \tag{3-77a}$$

$$r_i = R_i(0), \tag{3-77b}$$

Note that (3-77a) is a discrete Riccati equation (compare with (3-41)). $R_i(z)$ represents the seismogram that would be obtained if all of the layers 1,2, ... i were stripped off and the remaining portion of the medium were probed with an impulse. Equation (3-77b) simply states that the first reflection from the remaining portion of the medium (Robinson, 1982, refers to it as the "first bounce") is caused by the

reflection coefficient r_i of the next interface. The dynamic deconvolution algorithm is initialized by

$$R_0(z) = R(z) \qquad \text{(half-space boundary)} \tag{3-78a}$$

$$R_0(z) = k(z)/(1+k(z)) \qquad \text{(free surface)} \tag{3-78b}$$

(Note the sign change between (3-43b) and (3-78b); this is caused by the switch from pressure waves to displacement waves.)

The Schur-Cohn stability test is to run the algorithm (3-77), starting with $R_0(z) = f(z)$. Then $|f(z)| < 1$ and $f(z)$ is analytic inside the unit circle if and only if the reflection coefficients all have the property that $|r_i| < 1$. This test is tantamount to the synthesis of a lossless transmission line; the conditions $|f(z)| < 1$ and $|r_i| < 1$ are both statements of the passivity of the line. To see this, recall that each section of the line is implemented by the layer matrix (3-51), which has a determinant of unity. Then, if $|r_i| < 1$, each layer matrix multiplication becomes a lossless rotation, so that the line is lossless. The test is also analogous to the Darlington synthesis of a lossless digital filter. References for all of this are given in Chapter II.

Note that the fast Cholesky algorithm (3-74) does not match the discretized version of the continuous fast Cholesky algorithm presented in (2-25). However, we can easily obtain this form of the fast Cholesky algorithm for the discrete medium problem by making two changes: (1) exchange the roles of the primed and unprimed waves in Figures 3.3 and 3.4, so that the waves in the (revised) fast Cholesky algorithm are the waves at the bottom of each layer; and (2) change from two-way travel time to one-way travel time. Then the wave interactions at an

interface i are described by

$$d'_{i+1} = t_i d_i + \bar{r}_i u'_{i+1} \tag{3-79a}$$

$$u_i = r_i d_i + \bar{t}_i u'_{i+1} \quad . \tag{3-79b}$$

We also have

$$u'_i(t) = u_i(t-1) \tag{3-80a}$$

$$d'_i(t) = d_i(t+1) \tag{3-80b}$$

$$t_i = \bar{t}_i = 1 - r_i^2 \tag{3-80c}$$

where the one-way travel time through each layer is unity and (3-80c) follows from the (continued) use of normalized displacement waves. From (3-79) and (3-80) we get

$$d_{i+1}(t+1) = \frac{1}{(1-r_i^2)^{\frac{1}{2}}} (d_i(t) - r_i u_i(t)) \tag{3-81a}$$

$$u_{i+1}(t-1) = \frac{1}{(1-r_i^2)^{\frac{1}{2}}} (u_i(t) - r_i d_i(t)) \tag{3-81b}$$

$$r_i = u_i(i)/d_i(i) \tag{3-81c}$$

which has the same form as the discretized algorithm, except for the transmission losses and a factor of two in (3-81c). These are discussed in Section 3.4.

It should be noted that Symes and Zimmerman (1982) and Bruckstein et al. (1984) have made detailed numerical studies of the performance of the discrete fast Cholesky algorithm in the presence of

noise and using bandlimited data. The algorithm seems to work quite well for fifty or sixty layers, at which point the conditioning of the problem itself becomes so poor that further inversion by any means would give poor results. Bandlimitation of the data does not affect the algorithm too severely, although the lack of low-frequency components causes problems in reconstructing the trend of the profiles. These results emphasize the comments of Bruckstein and Kailath (1984) that layer stripping methods are NOT inherently inferior to integral equation or matrix methods, as commonly believed. Indeed, a major purpose of Chapters II and III of this thesis is to emphasize that the two approaches are mathematically equivalent, and in fact are dual to each other.

3.4 Relations Between Discrete and Continuous Problems and Solutions

In this section the problems and results of Sections 3.2 and 3.3 are linked. One might intuitively expect the results for a continuous medium to closely match those for a sufficiently finely discretized medium. For the most part this is the case (Gerver, 1970); however, there are some important distinctions. These distinctions are discussed and clarified here, so that the relation between the continuous and discrete problems may be more readily understood.

3.4.1 Discrete to Continuous Transformation

It is a well known development that the two-component wave system inverse scattering problem for a continuous medium can be treated by solving the same problem for a discrete, equal-traveltime medium, and then letting the layer travel time approach zero. This is a common procedure in mechanics; Pusey (1975) employed it in studying the lossless non-uniform transmission line, and Gerver (1970) applied it to the present

problem. Here we quickly sketch over the argument.

Consider a one-dimensional stratified acoustic medium comprised of homogeneous layers, each of which has a thickness proportional to the wave speed within it, so that the one-way traveltime through each layer is Δ. Splitting the medium displacement or pressure in each layer into upgoing and downgoing waves, we have the relations (from (3-74))

$$d_{i+1}(t) = \frac{1}{(1-r_i^2)^{\frac{1}{2}}} (d_i(t-\Delta) - r_i u_i(t+\Delta)) \tag{3-82a}$$

$$u_{i+1}(t) = \frac{1}{(1-r_i^2)^{\frac{1}{2}}} (u_i(t+\Delta) - r_i d_i(t-\Delta)) \tag{3-82b}$$

for waves defined at the top of each layer, and the relations (from (3-81))

$$d_{i+1}(t+\Delta) = \frac{1}{(1-r_i^2)^{\frac{1}{2}}} (d_i(t) - r_i u_i(t)) \tag{3-83a}$$

$$u_{i+1}(t-\Delta) = \frac{1}{(1-r_i^2)^{\frac{1}{2}}} (u_i(t) - r_i d_i(t)) \tag{3-83b}$$

for waves defined at the bottom of each layer. In both cases, the reflection coefficient for normalized displacement waves is

$$r_i = \frac{Z_i - Z_{i+1}}{Z_i + Z_{i+1}} \tag{3-84}$$

while the reflection coefficient for normalized pressure waves is

$$r_i = \frac{Z_{i+1} - Z_i}{Z_{i+1} + Z_i} \; . \tag{3-85}$$

Since the continuous medium results of Section 3.2 were derived using pressure waves, we shall use pressure waves and (3-85) in the sequel.

Now, letting the layer travel time Δ approach zero is tantamount to taking a finer discretization of the medium, i.e., approximating a continuous medium by a stack of thin homogeneous layers. No matter how small Δ is, the relations (3-82), (3-83), and (3-85) all hold; but as $\Delta \to 0$ the equations for the discrete medium approach those for a continuous medium. To see this, note that (3-85) can be written as

$$r_\tau = \frac{Z(\tau+\Delta/2) - Z(\tau-\Delta/2)}{Z(\tau+\Delta/2) + Z(\tau-\Delta/2)} \tag{3-86}$$

where τ is the travel time to the interface i and $Z(\tau)$ is defined in the middle of each layer. If the medium is continuous at τ, we then have

$$r(\tau) \triangleq \lim_{\Delta \to 0} \frac{r_\tau}{\Delta} = \lim_{\Delta \to 0} \frac{Z(\tau+\Delta/2)-Z(\tau-\Delta/2)}{\Delta} \frac{1}{Z(\tau+\Delta/2)+Z(\tau-\Delta/2)} \tag{3-87}$$

$$= \frac{1}{2Z} \frac{dZ}{d\tau}$$

in agreement with (3-35). The reflectivity function $r(\tau)$, defined in this manner, is finite as long as the medium is continuous. A step change in the medium properties results in an impulse in $r(\tau)$.

Using (3-87), rewrite (3-82) as

$$\frac{d_{\tau+\Delta/2}(t) - d_{\tau-\Delta/2}(t-\Delta)/(1-r_\tau^2)^{\frac{1}{2}}}{\Delta} = -\frac{r_\tau}{\Delta} \frac{1}{(1-r_\tau^2)^{\frac{1}{2}}} u_{\tau-\Delta/2}(t+\Delta) \tag{3-88a}$$

$$\frac{u_{\tau+\Delta/2}(t) - u_{\tau-\Delta/2}(t+\Delta)/(1-r_\tau^2)^{\frac{1}{2}}}{\Delta} = -\frac{r_\tau}{\Delta} \frac{1}{(1-r_\tau^2)^{\frac{1}{2}}} u_{\tau-\Delta/2}(t-\Delta) \tag{3-88b}$$

and letting $\Delta \to 0$ yields

$$(\frac{\partial}{\partial \tau} + \frac{\partial}{\partial t})D(\tau,t) = -r(\tau)U(\tau,t) \qquad (3\text{-}89a)$$

$$(\frac{\partial}{\partial \tau} - \frac{\partial}{\partial t})U(\tau,t) = -r(\tau)D(\tau,t) \qquad (3\text{-}89b)$$

in agreement with (3-37a,b). Here the waves $D(\tau,t)$ and $U(\tau,t)$ are simply $d_\tau(t)$ and $u_\tau(t)$, and (3-87) has been used to show that $r_\tau \to 0$.

A similar argument applied to (3-83) also results in (3-89). This is as expected; it shouldn't matter whether the waves are defined at the top of a layer or at its bottom, if the layer thickness is going to zero. However, it does show that $D(\tau,t)$ and $U(\tau,t)$ are well defined, even though there is no physical basis for defining upgoing and downgoing waves in a continuous inhomogeneous medium.

3.4.2 Continuous to Discrete Transformation

From the above results, it might seem that the discrete medium results could be obtained from the continuous medium results by a simple discretization. However, this is not so: the effects of transmission losses and discrete impulsive medium excitations must also be taken into account.

For a simple example of this, consider the discretization of the Marchenko (2-103) and Krein (2-111) integral equations. These result in the matrix equations (3-60) and (3-69), supporting the idea that discretization of the medium is equivalent to discretization of the equations for a continuous medium. However, note that the right side of (3-60) includes a term $(1 - r_i^2) - 1$. This term goes to zero as $0(\Delta^2)$, however it is non-zero for non-zero Δ.

A similar phenomenon is observed in the fast Cholesky algorithm, as would be expected by the mathematical equivalence of the matrix equation and layer stripping approaches. Comparing the algorithm for a discrete

medium (3-81) with the discretized continuous algorithm (2-25), the extra factor $(1-r_i^2)^{\frac{1}{2}}$ is noted. Like the matrix equation term, this factor is $0(\Delta^2)$ and hence is negligible for small Δ. However, it is non-zero for non-zero Δ.

Both of these terms represent transmission losses through the medium. As a propagating wave travels through the medium, it is partially reflected, and loses strength. This is not accounted for in the continuous case, since the reflections are $0(\Delta)$ (from (3-87)), while the transmission losses are $0(\Delta^2)$ (from (3-80c)) and hence are negligible as $\Delta \to 0$. In practical terms, the transmission losses are negligible compared to the reflections for a continuous medium if Δ is sufficiently small. Nevertheless, they should be included by employing (3-81) instead of (2-25) when running the fast Cholesky algorithm on a computer. Note that (3-81) is an orthogonal transformation (i.e., a rotation), and is therefore lossless, while (2-25) is not.

Another difference between (3-81) and (2-25) is the factor of two present in (2-25c) that is not present in (3-81c). This factor results from the effect of a change of time scale on the probing impulse for the continuous medium. The applicable formula is

$$\delta(at) = (1/a)\delta(t) \qquad (3\text{-}90)$$

for a continuous-time impulse (Dirac delta)$\delta(t)$ and constant a. Figuratively, (3-90) states that if the time axis is stretched, a continuous-time impulse becomes weaker, since its constant area is spread over a wider range. When the time axis is stretched by converting the two-way travel time (used in the original discrete medium formulation, hence in (3-81)), to one-way travel time (implicitly used in (2-25)), the impulse becomes weaker. This does not happen for the discrete-time impulse used to obtain (3-81c), hence (3-81c) contains no factor of two. In (2-25c) the weaker reflection from the weaker impulse must be bolstered by a factor of two.

Similar effects will be noted in Chapters IV and VI, in which the expressions for the first reflection (analogous to (2-25c)) will contain factors correcting for variations in the size of the probing impulse caused by variations in the local travel time (i.e., the differential delay time at that depth). These factors disappear in the discrete formulation of these problems, since the discrete-time impulse is unaffected by a change of time scale. Hence the discretized algorithms (to be run on a computer) do not contain these factors.

Berryman and Greene (1980) have pointed out another subtle distinction between the discrete medium solution and the discretized continuous medium solution. From (3-85), the impedances of the discrete medium satisfy

$$Z_{i+1}/Z_i = (1+r_i)/(1-r_i) \tag{3-91}$$

(for normalized pressure waves). However, a formal discrete inverse scattering solution using a discretized Schrodinger equation (Berryman and Greene, 1980) results in

$$Z_{i+1}/Z_i = (1+r_{i-1})/(1-r_i) \ . \tag{3-92}$$

If the medium is continuous, then (3-91) and (3-92) give the same result for the impedance $Z(\tau)$ as $\Delta \to 0$. However, if there is a step change in the medium at τ, then the discrete medium formula (3-91) assigns

$$Z(\tau) \triangleq Z(\tau^+) \tag{3-93}$$

i.e., the value just below the discontinuity, while the discretized continuous formula (3-92) assigns

$$Z(\tau) \triangleq Z(\tau^-)/(1-r_i) = (Z(\tau^-) + Z(\tau^+))/2 \qquad (3\text{-}94)$$

i.e., the arithmetic mean of the values on either side of the discontinuity.

In this chapter the one-dimensional inverse seismic problem at normal incidence has been solved, using both integral equation methods and layer stripping methods. In the next chapter we proceed to the more difficult, but more interesting, one-dimensional problem at non-normal incidence.

REFERENCES FOR CHAPTER III

K. Aki and P.G. Richards, Quantitative Seismology, Theory and Methods, W.H. Freeman and Co., San Francisco, 1980.

J. Berryman and R. Greene, "Discrete Inverse Methods for Elastic Waves in Layered Media," Geophys. 45(2), 213-233 (1980).

A. Bruckstein and T. Kailath, "Inverse Scattering for Discrete Transmission Line Models," Tech. Report, Information Systems Laboratory, Stanford University, 1984.

A. Bruckstein, I. Koltracht, and T. Kailath, "Inverse Scattering with Noisy Data," Tech. Report, Information Systems Laboratory, Stanford University, 1984.

K.P. Bube and R. Burridge, "The One-Dimensional Inverse Problem of Reflection Seismology," SIAM Review 25(4), 497-559 (1983).

A. Bultheel, "Towards an Error Analysis of Fast Toeplitz Factorization," Tech. Report No. TW-44, Applied Mathematics and Programming Division, Katholieke Universiteit Leuven, Belgium, May 1979.

R. Burridge, "The Gel'fand-Levitan, the Marchenko and the Gopinath-Sondhi Integral Equations of Inverse Scattering Theory Regarded in the Context of Inverse Impulse Response Problems," Wave Motion 2, 305-323 (1980).

K. Chadan and P.C. Sabatier, Inverse Problems in Quantum Scattering Theory, Springer-Verlag, New York, 1977.

J.F. Claerbout, "Synthesis of a Layered Medium from its Acoustic Transmission Response," Geophysics 33(2), 264-269 (1968).

J.F. Claerbout, Fundamentals of Geophysical Data Processing, McGraw-Hill, New York, 1976.

J.P. Corones, M.E. Davison, and R.J. Krueger, "Direct and Inverse Scattering in the Time Domain via Invariant Imbedding Equations," J. Acoust. Soc. Am. 74(5), 1535-1541 (1983).

A.P. Dowling and J.E.F. Williams, Sound and Sources of Sound, Halsted Press, New York, 1983.

L.D. Faddeev, "Properties of the S-Matrix of the One-Dimensional Schrodinger Equation," Amer. Math. Soc. Transl., series 2, vol 65, 139-166 (1967).

M.L. Gerver, "The Inverse Problem for the One-Dimensional Wave Equation," Geophys. J.R. astr. Soc. 21, 337-357 (1970).

P. Goupillaud, "An Approach to Inverse Filtering of Near-Surface Layer Effects from Seismic Records," Geophys. 26(6), 754-760 (1961).

S. Gray, "Inverse Scattering for the Reflectivity Function," J. Math. Phys. 24(5), 1148-1151 (1983).

G. Kunetz and I. d'Erceville, "Sur Certaines Propriétés d'une Onde Plane de Compréssion dans un Milieu Stratifié," Ann. Geophysique 18, 351-359 (1962).

R. Newton, "Inversion of Reflection Data for Layered Media: A Review of Exact Methods," Geophys. J.R. astr. Soc. 65, 191-215 (1981).

L. Pusey, "An Innovations Approach to Spectral Estimation and Wave Propagation," Ph.D. Thesis, Dept. of Electrical Engineering and Computer Science, MIT, 1975.

E.A. Robinson, "Spectral Approach to Geophysical Inversion by Lorentz, Fourier, and Radon Transforms," Proc. IEEE 70, 1039-1054 (1982).

F. Santosa and H. Schwetlick, "The Inversion of Acoustical Impedance Profile by Method of Characteristics," Wave Motion 4, 99-110 (1982).

W. Symes, "Stable Solution of the Inverse Reflection Problem for a Smoothly Stratified Medium," SIAM J. Math. Anal. 12(3), 421-453 (1981).

W. Symes and G. Zimmerman, "Experiments in Impedance Profile Inversion Using Noisy and Band-Limited Data," Amoco Production Co. Research Report No. F82-C-3 (1982).

I. Tolstoy and C.S. Clay, Ocean Acoustics, McGraw-Hill, New York, 1966.

J. Ware and K. Aki, "Continuous and Discrete Inverse-Scattering Problems in a Stratified Elastic Medium, Part I: Plane Waves at Normal Incidence," J. Acoust. Soc. Am. 45, 911-921 (1969).

CHAPTER IV

The One-Dimensional Inverse Problem at Non-Normal Incidence

4.1 Introduction

In this chapter the inverse seismic problem for a one-dimensional acoustic layered medium probed by impulsive plane waves at oblique incidence is solved by a layer stripping algorithm. Separate profiles of the density $\rho(z)$ and wave speed $c(z)$ as functions of depth may be obtained from the reflection responses of the medium to obliquely incident plane waves at two different angles of incidence. These responses may be synthesized from the response of the medium to an impulsive point source by utilizing the Radon and Hankel transforms.

The basic results of this chapter are taken from Yagle and Levy (1984). However, we also review the work of Coen (1981), Coen (1982) and Howard (1983), showing how their results relate to the methods of Chapters II and III. A layer stripping algorithm for this experiment performed on a discrete medium is also specified. The Radon and Hankel transforms, which are used to synthesize plane-wave reflection responses from the impulsive point source reflection response, are discussed. Finally, the behavior of medium pressure and displacement at a turning point is analyzed, and a possible way of extending the layer stripping algorithm through the turning point and back up to the surface is discussed. Although most of the latter material is not new, it is important for putting the layer stripping algorithms in the proper

perspective.

The basic problem considered in this chapter is as follows. An acoustic layered medium, whose density $\rho(z)$ and wave speed $c(z)$ are continuous functions of depth alone, is probed by an impulsive plane pressure wave which is incident on the medium at an angle of incidence θ (see Figure 4.1). Although there is no lateral variation in the medium, the medium must of course have a lateral dimension, which was not required by the normal incidence problem of Chapter III. Such a medium is sometimes referred to in the literature as a "1.5 dimensional medium," but this terminology is confusing and will not be adopted here. By probing the medium twice, at two different angles of incidence, the profiles $\rho(z)$ and $c(z)$ are recovered. Two variations on this basic problem are also considered: a discrete medium, in which $\rho(z)$ and $c(z)$ need only be piecewise continuous, and an impulsive point source excitation (see Figure 4.2), which can be related to oblique plane wave excitations by the Radon and Hankel transforms. Either a half-space or free surface boundary condition may be used.

Previous methods for solving this problem have generally employed the integral equation methods of Sections 2.4 and 3.2, applied to a suitably transformed problem. Ware (1969) and Coen (1981) transformed the non-normal incidence problem into a normal incidence problem, and solved the resulting Schrodinger equation with the Gel'fand-Levitan integral equation procedure described in Section 3.2.2. Howard (1983) transformed the non-normal incidence problem into a two-component wave system, which led to a matrix Marchenko integral equation. Coen (1982) showed how the point-source problem can be reduced to the oblique plane wave problem; in fact, this can be done immediately with the Radon transform.

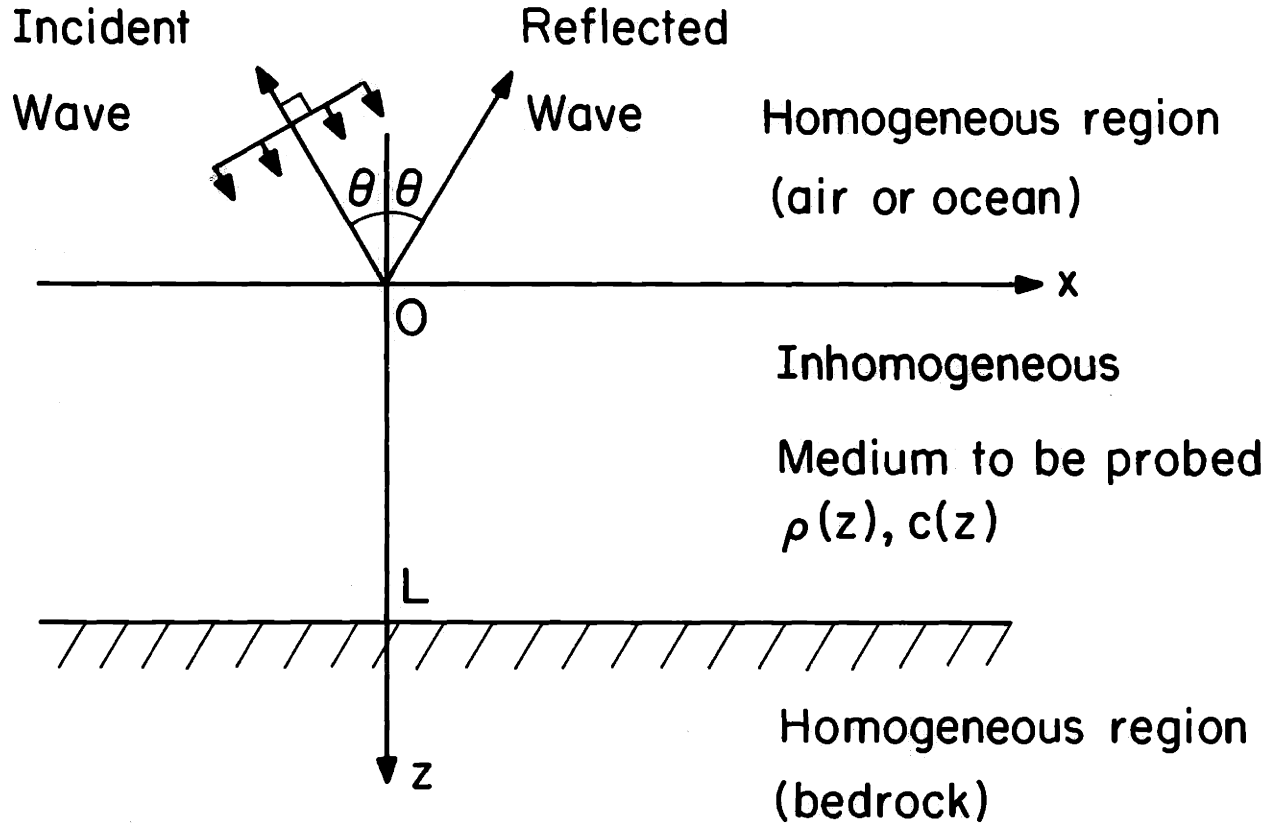

4.1 The non-normal incidence inverse problem.

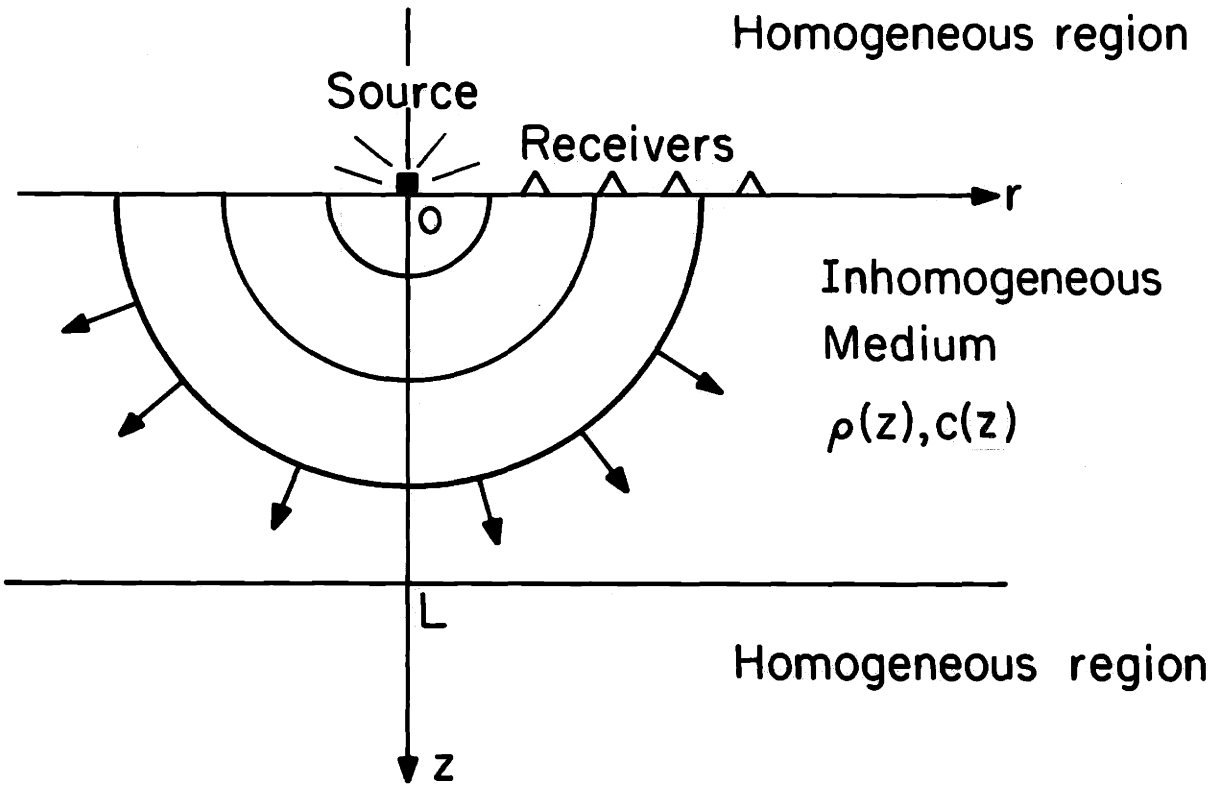

4.2 The point source inverse problem.

A major problem with this approach is that the integral-equation-based techniques are unable to deal with some of the complications endemic to the non-normal incidence problem. The most important of these are turning points, which occur when the local wave speed c(z) has increased to the reciprocal of the slowness p of the probing plane wave. At this point, by Snell's law, the ray paths of the probing plane wave become horizontal and then bend back up to the surface. Since the Schrodinger potential V blows up at a turning point, the Gel'fand-Levitan procedure of Section 3.2.2 cannot be used if a turning point is present. This means that the probing plane wave must be chosen to be nearly vertically incident on the medium, which will lead to small reflections and a poorer signal-to-noise ratio.

Another complication of the problem that can preclude the use of the integral equation methods is a low (wave) speed layer, in which energy can be trapped and propagate as in a waveguide. The energy is transported to such a layer by evanescent (imaginary wavenumber) waves, in a process akin mathematically to quantum mechanical tunneling. Although these "proper" or "trapped" modes can be treated by the integral equation methods, they must be known a priori, which is not possible for an inverse problem.

Layer stripping methods, in contrast, have no problem with these complications. This is in keeping with the layer stripping concept of treating the medium one layer at a time, rather than all at once as in the integral equation methods. A turning point, for example, does not affect a layer stripping algorithm until its depth is reached, at which point the algorithm can go no deeper (below a turning point the propagating waves become evanescent, and probing the medium with

exponentially-decaying waves is an inherently unstable problem). However, an integral equation procedure cannot reconstruct any part of the medium if any other part of it causes difficulties.

There have been very few attempts to apply layer stripping concepts to the non-normal incidence problem for a layered acoustic medium. Carrion et al. (1984) gave recursions for computing the wave speed c_{i+1} and density ρ_{i+1} in a layer from their values ρ_i and c_i in the previous layer and the layer reflection coefficients, but they used a single scattering approximation that neglected all multiple reflections. Carrion (1983) applied the method of characteristics to slant-stacked data and obtain recursions from the midpoint rule for approximating integrals, but these recursions were far more complex than the Levinson or fast Cholesky recursions, and offered no physical insight. The wave speeds were reconstructed by taking differences in arrival times, which is a very unstable procedure.

Summary

In Section 4.2 the inverse problem in which plane waves at oblique incidence are used to probe the medium is discussed. After reviewing and interpreting the results of Ware (1969), Coen (1981), and Howard (1983), the layer stripping algorithm for solving this problem is derived. Then it is shown how a minor modification of the algorithm enables the reconstruction of a discrete ($\rho(z)$ and $c(z)$ piecewise continuous) medium.

In Section 4.3 the inverse problem in which an impulsive point source is used to probe the medium is discussed. The Radon and Hankel transforms are introduced and discussed, and it is shown how these transform point-source data to plane-wave data. Then a layer stripping

algorithm utilizing cylindrical waves, rather than plane waves, is derived.

Finally, in Section 4.4 the behavior of medium pressure and displacement waves at a turning point is analyzed, and the results are used to show how a layer stripping algorithm could be propagated back up to the surface along with the ray paths. This would allow the portion of the data record beyond the two-way travel time to the turning point to be used in the inversion process, and also provide a check on the reconstructed medium.

Two other points should be made. First, there would seem to be a duality between reconstructing the medium from its reflection coefficient $\hat{R}(\omega,\theta)$ specified for all frequencies ω and two angles θ_1 and θ_2 (as is being done in this chapter), and reconstructing it from $\hat{R}(\omega,\theta)$ specified for two frequencies ω_1 and ω_2 and all angles θ. Actually, the duality is between frequency and wavenumber, since $\hat{R}(\omega,\theta)$ is needed for complex angles of incidence (corresponding to probing with evanescent waves) in the second experiment. The first experiment is covered in this chapter; the second experiment is covered in Chapter VII.

The second point concerns sign conventions. In Chapters II and III the standard Fourier sign convention

$$\hat{f}(\omega) = \int_{-\infty}^{\infty} f(t)e^{-j\omega t}\,dt \qquad (4\text{-}1)$$

was used. In much of the geophysical literature, however, the geophysical sign conventions (Aki and Richards, 1980, p. 129)

$$\hat{f}(\omega) = \int_{-\infty}^{\infty} f(t)e^{+j\omega t}\,dt \qquad (4\text{-}2a)$$

$$\hat{g}(k) = \int_{-\infty}^{\infty} g(x)e^{-jkx}\,dx \qquad (4\text{-}2b)$$

are used. The main reason for this convention is that if $f(x,t)$ represents a wave, and $\hat{f}(k,\omega)$ has been obtained by other means, then

$$f(x,t) = (1/4\pi^2) \int_{-\infty}^{\infty}\int_{-\infty}^{\infty} \hat{f}(k,\omega)e^{j(kx-\omega t)} \qquad (4\text{-}3)$$

and $\hat{f}(k,\omega)$ is the amplitude of a wave propagating in the $+x$ direction. However, keeping the usual convention (4-1) merely reverses the direction of the wave, and makes things much easier for non-geophysicists (including the author). Hence the geophysical sign conventions (4-2) will not be used in this thesis.

4.2 Plane Waves at Oblique Incidence

In this section the inverse problem for a layered medium probed by an impulsive plane pressure wave at oblique incidence is solved. First, the integral equation approaches of Ware (1969), Coen (1981), and Howard (1983) are discussed, to put them in perspective relative to the layer stripping algorithm derived next. Finally, a slight modification in the layer stripping algorithm allows a discrete medium to be reconstructed.

4.2.1 Integral Equation Solutions

The methods of Ware (1969), Coen (1981), and Howard (1983) all involve transforming the non-normal incidence problem to the normal incidence problem, and then solving this problem by solving a Marchenko integral equation. As such, these approaches can be considered to be dual to the layer stripping approach (see Chapter II). In addition,

certain aspects of these papers are clarified and related to the transformations used in Section 4.2.2 below.

Ware (1969) starts off with the basic linear equation for medium displacement $\underset{\sim}{u}$, obtained by inserting (3-1a) into (3-1b):

$$\rho \partial^2 \underset{\sim}{u}/\partial t^2 = \nabla(\rho c^2 \nabla \cdot \underset{\sim}{u}) \ . \tag{4-4}$$

Taking the Fourier transform with respect to time and separating into components yields

$$-\rho\omega^2 \hat{u}_x = \rho c^2 \frac{\partial}{\partial x} \left(\frac{\partial \hat{u}_x}{\partial x} + \frac{\partial \hat{u}_z}{\partial z} \right) \tag{4-5a}$$

$$-\rho\omega^2 \hat{u}_z = \frac{\partial}{\partial z} \left(\rho c^2 \left(\frac{\partial \hat{u}_x}{\partial x} + \frac{\partial \hat{u}_z}{\partial z} \right) \right) \tag{4-5b}$$

where $\hat{u}_x(x,z,\omega)$ and $\hat{u}_z(x,z,\omega)$ are the lateral and vertical, respectively, components of displacement. Since the medium properties vary only with depth, the plane wave solutions of (4-5) take the form

$$\hat{u}_z(x,z,\omega) = \hat{U}(z,\omega) e^{j\omega p x} \tag{4-6a}$$

$$\hat{u}_x(x,z,\omega) = \hat{V}(z,\omega) e^{j\omega p x} \tag{4-6b}$$

where $p = \sin\theta_0/c_0$ is the ray parameter for a plane wave incident on the medium at angle of incidence θ_0 from a homogeneous infinite half-space in which the wave speed is c_0.

Inserting (4-6) into (4-5) and eliminating $\hat{V}$ yields

$$\frac{\partial}{\partial z} \left(\frac{\rho c^2}{1 - c^2 p^2} \frac{\partial \hat{U}}{\partial z} \right) + \rho\omega^2 \hat{U} = 0 \ . \tag{4-7}$$

This is not a Schrodinger equation, but may be transformed into a Schrodinger equation by defining $\theta(z)$ by Snell's law

$$\sin \theta(z) = c(z)p \tag{4-8}$$

and employing the Liouville transformations (Courant and Hilbert, 1962), which amount to changing the independent variable z to the vertical travel time

$$\tau(z) \triangleq \int_0^z \frac{\cos \theta(s)}{c(s)} ds = \int_0^z ds/c'(s) \tag{4-9}$$

and the dependent variable $\hat{U}$ to the normalized displacement

$$\hat{\phi}(z,\omega) \triangleq (\rho(z)c(z)/\cos\theta(z))^{\frac{1}{2}} \hat{U}(z,\omega) = Z(z)^{\frac{1}{2}}\hat{U}(z,\omega) \tag{4-10}$$

In (4-9) and (4-10) we have implicitly defined the vertical wave speed $c'(z)$ and impedance $Z(z)$, both of which depend on p. Inserting (4-8) - (4-10) into (4-7) yields the Schrodinger equation

$$\left(\frac{\partial^2}{\partial\tau^2} + \omega^2 - V(\tau,\omega)\right) \hat{\phi}(\tau,\omega) = 0 \tag{4-11}$$

where the potential $V(\tau,\omega)$ is defined as

$$V(\tau,\omega) = \frac{1}{Y} \frac{d^2Y}{d\tau^2} \quad , \quad Y = Z^{\frac{1}{2}} \; . \tag{4-12}$$

Ware (1969) then notes that the Gel'fand-Levitan procedure of Section 3.2.2 can be used to recover $Z(\tau)$. He does not, however, note

that performing this experiment twice, at two different angles of incidence, allows the recovery of $\rho(z)$ and $c(z)$.

Two comments on Ware (1969)'s procedure should be made. First, Ware makes no physical justification for employing the Liouville transformation--why does this work? From a physical point of view, the transformations to the energy-normalized displacement $\hat{\phi}(z,\omega)$ and vertical travel time $\tau(z)$ are evident, in light of Section 3.2.1. From a mathematical point of view, the utility of the Liouville transformation in the present problem is far less obvious. Second, the physical essence of the transformation to a normal-incidence problem is not explained. What is actually happening here is that the progress of the obliquely-incident probing wave along a ray path is being projected onto the vertical depth axis, and the component of the probing wave that is normal to the vertical axis is probing the medium at normal incidence. Thus the problem can be transformed to a normal incidence problem by considering vertical displacement, normalized for vertical energy flux, and treated as a function of vertical travel time, which is precisely the transformation that works.

Coen (1981) similarly obtains the Schrodinger equation (4-11) by utilizing the Liouville transformation; the only difference is that the normalized pressure is used instead of normalized displacement. However, Coen (1981) gives no physical motivation whatever for his mathematics. He does not mention energy-normalized pressure, vertical components of wave speed, or even travel time. We mention here that his inaptly-named "index of refraction" $n(s)$ is actually $\rho_0 c_0/Z(s)$, and the Liouville transformation (11) transforms pressure $\phi(s,\omega)$ to normalized pressure (scaled by $(\rho_0 c_0)^{\frac{1}{2}}$)$g(s,\omega)$, and depth z to vertical travel time (scaled by c_0)ξ.

However, Coen (1981) does employ a useful trick to recover $\rho(z)$ and $c(z)$. By defining an "apparent depth" s by

$$ds/dz = \rho(z)/\rho_o \tag{4-13}$$

and noting that

$$ds/d\tau = Z(\tau)/\rho_o \tag{4-14}$$

he notes that $s(\tau)$ may be obtained by integrating $Z(\tau)$. Then the inverse function $\tau(s)$ is obtained from $s(\tau)$, and $\rho(s)$ and $c(s)$ obtained from $Z(s) = Z(\tau(s))$ for two different angles of incidence. Then $z(s)$ is obtained by integrating (4-13) as

$$z(s) = \int_o^s \frac{\rho_o}{\rho(u)}\, du \tag{4-15}$$

yielding $\rho(z) = \rho(s(z))$ and $c(z) = c(s(z))$. This procedure is similar in spirit to the reconstruction procedure used by Howard (1983), but is much simpler, since Howard (1983)'s procedure, which does not use s, requires the solution of a differential equation. The reason why Coen (1981)'s procedure is simpler than Howard(1983)'s is that Coen (1981) makes use of the fact that $\rho(z)$ is the same for both experiments (although the vertical wave speed $c'(z)$ is not).

Howard (1983) employs an approach different from those of Ware (1969) and Coen (1981). He derives the two-component wave system obtained below (4-30), and proceeds to define Jost solutions for it. This results in the matrix Marchenko equation

$$M(z,\tau) = R(z+\tau)\begin{bmatrix}0\\1\end{bmatrix} - \int_{-z}^{\tau} dy\, R(z+y)\begin{bmatrix}0 & 1\\1 & 0\end{bmatrix} M(y,\tau),\ -\tau \le x \le t \qquad (4\text{-}16)$$

where $R(t)$ is the inverse Fourier transform of the medium reflection coefficient. The reflectivity function $r(\tau)$ is obtained from

$$r(\tau) = 2M_{21}(\tau,\tau) \qquad (4\text{-}17)$$

and $Z(\tau)$ obtained from

$$Z(\tau) = Z(0)\ \exp\{\, 2\int_{o}^{\tau} r(s)ds\,\}\ . \qquad (4\text{-}18)$$

It should be noted here that Howard (1983) incorrectly refers to $(\rho c')^{\frac{1}{2}}$ as the impedance; the true impedance is $\rho c'$. A rather messy reconstruction procedure then yields $\rho(z)$ and $c(z)$ from the results of two experiments at two different angles of incidence.

Howard (1983)'s work is significant because he was able to formulate the non-normal incidence problem as a two-component wave system problem, which is the key step toward deriving a layer stripping algorithm for the problem. This also emphasizes the point of Chapter II that the above integral equation methods are mathematically dual to the layer stripping algorithm derived next.

4.2.2 Layer Stripping Solution for a Continuous Medium

The layer stripping algorithm for the non-normal incidence problem is derived in a manner entirely analogous to that for the normal incidence problem (Section 3.2.3). The major differences are that the resulting algorithm consists of two sets of recursions running in parallel (one for

each of the two experiments), and employs differential updates of $\rho(z)$ and $c(z)$. These updates replace the messy reconstruction procedures of Coen (1981) and Howard (1983).

An impulsive plane pressure wave incident at angle θ from the vertical has the form $\delta(t-z\cos\theta/c_o - x\sin\theta/c_o)$ in the homogeneous half-space $z<0$. In the frequency domain, this is $e^{-j(k_x x + k_z z)}$, where $k_z = \omega\cos\theta/c_o$ and $k_x = \omega\sin\theta/c_o$ are the vertical and horizontal wave numbers and c_o is the wave speed in the half-space. The pressure field for $z<0$ is thus

$$\hat{p}(x,z,\omega,\theta) = (e^{-jk_z z} + \hat{R}(\omega,\theta)e^{jk_z z})e^{-jk_x x} \qquad (4\text{-}19)$$

(compare this to the Schrodinger equation boundary condition (3-21)). This shows that the reflection frequency response $\hat{R}(\omega,\theta)$ in the time domain has the form

$$R(t,x;\theta) = R(t-x\sin\theta/c_o;\theta) \qquad (4\text{-}20)$$

so that theoretically it should only be necessary to measure this response at a single surface point (e.g., $x = 0$). However, in any real-world application it would be a matter of practical necessity to take data for a range of x and filter or stack it to the form (4-20). This is because any real-world impulsive wave could only be locally planar, while the form of (4-20) assumes a plane wave of infinite extent.

Taking Fourier transforms of the basic acoustic equations (3-1), and writing the vector equation (3-1b) as two scalar equations results in

$$\rho(z)\omega^2\hat{u}_x(x,z,\omega) = \partial\hat{p}/\partial x \qquad (4\text{-}21a)$$

$$\rho(z)\omega^2\hat{u}_z(x,z,\omega) = \partial\hat{p}/\partial z \qquad (4\text{-}21b)$$

$$\hat{p}(x,z,\omega) = -\rho(z)c(z)^2\,(\partial\hat{u}_x/\partial x + \partial\hat{u}_z/\partial z) \qquad (4\text{-}21c)$$

where u_x and u_z are the x and z components of the (vector) displacement $\underset{\sim}{u}(x,z,t)$.

Since the medium properties vary only with depth z, the horizontal wave number k_x is preserved, and we may write (following Coen, 1981)

$$\hat{p}(x,z,\omega) = \hat{\psi}(z,\omega)e^{-jk_x x} \quad . \qquad (4\text{-}22)$$

Substituting (4-22) in (4-21b), and then substituting the result in (4-21c) eliminates $\hat{u}_x$ and yields, after some algebra,

$$\hat{p}(x,z,\omega)\,(1-(c(z)^2/c_o^2)\sin^2\theta) = -\rho(z)c(z)^2\partial\hat{u}_z/\partial z \qquad (4\text{-}23)$$

Next, the following substitutions are made:

$$\cos^2\theta(z) = 1 - (c(z)^2/c_o^2)\sin^2\theta \qquad (4\text{-}24)$$

($\theta(z)$ = local angle ray path makes with vertical)

$$c'(z) = c(z)/\cos\theta(z) = \text{local vertical wave speed} \qquad (4\text{-}25)$$

$$\tau(z) = \int_o^z ds/c'(s) = \text{vertical travel time to depth } z \qquad (4\text{-}26)$$

$$Z(\tau) = \rho(\tau)c'(\tau) = \text{effective impedance} \qquad (4\text{-}27)$$

Note that (4-24) follows from Snell's law ($\sin\theta(z)/c(z)$ is constant along

any ray path), and (4-25) defines a local vertical wavenumber $k_z(z) = \omega/c'(z)$. Using (4-24) - (4-27) in (4-23) and (4-21a) yields

$$\partial \hat{p}/\partial \tau = Z\omega^2 \hat{u}_z(\tau,x,\omega) \tag{4-28a}$$

$$\partial \hat{u}_z/\partial \tau = -(1/Z)\hat{p}(\tau,x,\omega) \tag{4-28b}$$

and once again defining the downgoing and upgoing <u>energy-normalized waves</u> (as in (3-33))

$$\hat{v}_1(\tau,x,\omega) = \hat{p}(\tau,x,\omega)/Z^{\frac{1}{2}} + j\omega Z^{\frac{1}{2}}\hat{u}_z(\tau,x,\omega) \tag{4-29a}$$

$$\hat{v}_2(\tau,x,\omega) = \hat{p}(\tau,x,\omega)/Z^{\frac{1}{2}} - j\omega Z^{\frac{1}{2}}\hat{u}_z(\tau,x,\omega) \tag{4-29b}$$

yields the <u>two-component wave system</u>

$$\partial \hat{v}_1/\partial \tau = -j\omega \hat{v}_1 - r(\tau)\,\hat{v}_2 \tag{4-30a}$$

$$\partial \hat{v}_2/\partial \tau = -r(\tau)\,\hat{v}_1 + j\omega \hat{v}_2 \tag{4-30b}$$

with the reflectivity function $r(\tau)$ defined as

$$r(\tau) = \frac{1}{2Z}\frac{dZ}{d\tau} = \frac{1}{2}\frac{d}{d\tau}\log\frac{Z(\tau)}{Z(0)} \,. \tag{4-31}$$

Note that once again the quantities in the two-component wave system (4-30) are the Fourier transforms of the downgoing and upgoing waves, so that once again the <u>vertical</u> motion of the medium is decomposed into upgoing and downgoing waves. Of course, horizontally-travelling waves could not furnish any information on the vertical variation of material parameters. Since these waves have the form defined by equations (2-22)

(i.e., v_1 contains a probing impulse and v_1 and v_2 are causal), all of the algorithms specified in Section 3.2.3 can now readily be identified for the oblique incidence problem.

Now, suppose this oblique incidence experiment were run twice, for two different angles of incidence θ_1 and θ_2. Two different impedances $Z_1(\tau_1)$ and $Z_2(\tau_2)$, as functions of different vertical travel times τ_1 and τ_2, would be obtained. The reconstruction procedures given in Coen (1981) and Howard (1983) could then be used to recover the separate profiles $\rho(z)$ and $c(z)$ from $Z_1(\tau_1)$ and $Z_2(\tau_2)$. However, further consideration of the layer-stripping idea yields the following procedure for recovering $\rho(z)$ and $c(z)$ while the two algorithms are running, obviating the necessity of waiting for the complete impedances $Z_i(\tau_i)$. This procedure is also much simpler than the computationally cumbersome methods of Coen (1981) and Howard (1983).

Let $r_i(z)$ be the reflectivity function associated with the experiment with angle of incidence θ_i $(i = 1,2)$, and let $c_i'(z) = c(z)/\cos\theta_i(z)$ be the associated vertical wave speed. Then

$$r_i(z) = (1/2)(d/dz)\log(\rho(z)\, c_i'(z)) \quad . \tag{4-32}$$

Substituting (4-25) in (4-26) and differentiating with respect to z yields

$$(d/dz)c_i'(z) = (1/\cos^3\theta_i(z))\ (dc(z)/dz) \tag{4-33}$$

Using (4-33), equation (4-32) may be rewritten in matrix form as

$$\begin{bmatrix} r_1(z) \\ r_2(z) \end{bmatrix} = \begin{bmatrix} 1/(2\rho(z)) & 1/(2c(z)\cos^2\theta_1(z)) \\ 1/(2\rho(z)) & 1/(2c(z)\cos^2\theta_2(z)) \end{bmatrix} \begin{bmatrix} (d/dz)\rho(z) \\ (d/dz)c(z) \end{bmatrix} \tag{4-34}$$

Inverting (4-34) yields

$$\begin{bmatrix} (d/dz)\rho(z) \\ (d/dz)c(z) \end{bmatrix} = \frac{\begin{bmatrix} 1/(2c(z)\cos^2\theta_2(z)) & -1/(2c(z)\cos^2\theta_1(z)) \\ -1/(2\rho(z)) & 1/(2\rho(z)) \end{bmatrix} \begin{bmatrix} r_1(z) \\ r_2(z) \end{bmatrix}}{d(z)} \tag{4-35}$$

where

$$d(z) = (\cos^{-2}\theta_2(z) - \cos^{-2}\theta_1(z))/(4\rho(z)c(z)). \tag{4-36}$$

This yields the following recursive algorithm for computing $\rho(z)$ and $c(z)$. Discretizing depth as $z = n\Delta$ (note that time is <u>not</u> discretized) and assuming (for inductive purposes) knowledge of all quantities at depth z, the update procedure is as follows:

$$\cos\theta_i(z) = (1-(c(z)^2/c_o^2)\sin^2\theta_i)^{\frac{1}{2}} \tag{4-37}$$

$$d(z) = (\cos^{-2}\theta_2(z) - \cos^{-2}\theta_1(z))/(4\rho(z)c(z)) \tag{4-38}$$

$$r_i(z) = 2v_2^i(\tau_i, z) \tag{4-39}$$

$$\rho(z+\Delta) = \rho(z) + (r_1(z)/\cos^2\theta_2(z) - r_2(z)/\cos^2\theta_1(z))\Delta/(2c(z)d(z)) \tag{4-40}$$

$$c(z+\Delta) = c(z) + (r_2(z)-r_1(z))\Delta/(2\rho(z)d(z)) \tag{4-41}$$

$$v_1^i(z+\Delta\ ,\ t+\Delta\cos\theta_i(z)/c(z)) = v_1^i(z,t) - r_i\Delta v_2^i(z,t) \tag{4-42}$$

$$v_2^i(z+\Delta,\ t-\Delta\cos\theta_i(z)/c(z)) = v_2^i(z,t) - r_i\Delta v_1^i(z,t) \tag{4-43}$$

$$\tau_i(z+\Delta) = \tau_i(z) + \Delta\cos\theta_i(z)/c(z) \quad . \tag{4-44}$$

At this point all quantities have been updated to depth $z + \Delta$, so the recursion is complete. Note that there are two sets of recursions running in parallel, each one initialized by the data from one of the two experiments ($i = 1,2$).

The reason that the profiles $\rho(z)$ and $c(z)$ can be recovered separately for the oblique incidence problem, but not for the normal incidence problem, is that by running the oblique experiment twice information has been gained along two different ray paths. This option is not available for the normal incidence problem--there is only one choice for the ray path, since this problem is completely one-dimensional.

Along any given ray path Snell's law shows that

$$p = \sin\theta(z)/c(z) = \sin\theta_o/c_o \tag{4-45}$$

so that unless θ is less than the critical angle $\sin^{-1}(c_o/\max c(z))$ $\theta(z)$ will become imaginary at some depth. Physically, this situation results in evanescent waves, in which the pressure field decays exponentially instead of propagating as a wave. The same effect is observed in a waveguide below cutoff. This causes no problems in the layer stripping algorithm until the ray path actually becomes horizontal, prior to turning back up. At this point, called the turning point, the upgoing and downgoing waves lose physical meaning, and the algorithm can go no deeper. However, the method of Coen (1981) requires precritical incidence, or it cannot be used at all. This is because the integral equation method of Coen (1981) involves all of the medium at once, so that

any complication, such as a turning point, ruins it at once. A layer stripping algorithm has no trouble with a turning point until the critical depth is reached, so that all of the medium above the turning point can still be reconstructed.

In Section 4.4 the behavior of the waves at a turning point is analyzed, and it is shown how the waves can be propagated through the turning point and back up to the surface. This allows more of the reflection response data to be used to reconstruct the medium. The evanescent waves below the turning point could furnish information about the medium below the turning point, but there is no practical way to measure these waves from the surface.

4.2.3 Layer Stripping Solution for a Discrete Medium

A slight modification of the above algorithm allows the reconstruction of a discrete medium, in which $\rho(z)$ and $c(z)$ are only required to be piecewise continuous. The modifications consist of incorporating the transmission losses at the medium discontinuities, and altering the updates from a differential form to a discrete form.

The medium being considered has continuous variation of $\rho(z)$ and $c(z)$, with occasional quantum jumps in either or both quantities at discrete levels (hence the term "discrete medium," which is not to be confused with the Goupillaud medium of Chapter III). This is tantamount to letting $\rho(z)$ and $c(z)$ be piecewise continuous. Note that the reflectivity function $r(z)$ will contain an impulse at each level where $\rho(z)$ and $c(z)$ jumps. Hence the differential updates (4-35) will no longer be defined (i.e., will also contain impulses), and the second-order-in-Δ terms neglected in (4-40) and (4-41) will become significant.

The problem is treated by recognizing that the continuous algorithm is in fact always run as a discretized algorithm (viz. (4-37) - (4-44)), so that alterations can be made in this algorithm. Recalling that the reflectivity function r(z) was defined in (3-87) by

$$r(z) = \lim_{\Delta \to 0} \frac{r_z}{\Delta} = \lim_{\Delta \to 0} \frac{1}{\Delta} \frac{Z(z+\Delta) - Z(z)}{Z(z+\Delta) + Z(z)} = \frac{1}{2Z} \frac{dZ}{dz} \tag{4-46}$$

it can be seen that an impulse in r(z) corresponds to a finite, non-zero reflection coefficient r_z and a step change in Z(z). It also can be seen that for small Δ we have

$$r_z \approx r(z)\Delta \approx \frac{Z(z+\Delta) - Z(z)}{Z(z+\Delta) + Z(z)} \tag{4-47}$$

and inverting this yields

$$Z(z+\Delta) \approx Z(z) \frac{1 + r(z)\Delta}{1 - r(z)\Delta} \quad . \tag{4-48}$$

Thus we are synthesizing a discrete medium on which the discrete algorithm operates. The levels where $\rho(z)$ and c(z) jump are now merely levels at which they take bigger jumps than usual.

The new algorithm is now evident. The wave updates (4-42) and (4-43) are modified to include transmission losses by multiplying them by $(1-(r_i(z)\Delta)^2)^{\frac{1}{2}}$; see (3-83). The $\rho(z)$ and c(z) updates (4-40) and (4-41) are replaced by the impedance updates

$$Z_i(z+\Delta) = Z_i(z) \frac{1 + r_i(z)\Delta}{1 - r_i(z)\Delta} \quad , \; i = 1,2 \tag{4-49}$$

from which $\rho(z+\Delta)$ and $c(z+\Delta)$ are obtained using

$$W(z+\Delta) = (Z_2(z+\Delta)/Z_1(z+\Delta))^2 \qquad (4\text{-}50a)$$

$$c(z+\Delta) = [(W(z+\Delta)-1)/(W(z+\Delta)p_2^2-p_1^2)]^{\frac{1}{2}} \qquad (4\text{-}50b)$$

$$\rho(z+\Delta) = Z_i(z+\Delta)\cos\theta_i(z+\Delta)/c(z+\Delta) \quad . \qquad (4\text{-}50c)$$

Equations (4-50) follow immediately from the definition (4-27) of impedance. Note that (4-49) and (4-50) reduce to (4-40) and (4-41) if $r(z)\Delta$ (not just Δ) is sufficiently small.

The extra computation involved in using (4-50) instead of (4-40) and (4-41) is so trivial that in practical applications the discrete algorithm should always be used. The only exception might be in a systolic array implementation, for which the square root extraction in (4-50b) might be too time-consuming (note that the discrete wave updates constitute a rotation, which a CORDIC processor could easily implement in a systolic array). However, for the elastic problem of Chapter VI, the updates for a discrete medium are hopelessly messy, and the differential updates are preferable.

4.3 Impulsive Point Source

The problem considered in this section is that of a layered medium excited by an impulsive point source. Although the medium is still laterally homogeneous, it now occupies three spatial dimensions, with cylindrical symmetry about the z-axis. The point source is located at the origin, and the reflection reponse measured as a function of radial distance r from the source. The situation is illustrated in Figure 4.2.

This problem is related to the non-normal incidence plane wave problem by the Radon and Hankel transforms. After discussing these transforms, the problem is solved by either of two equivalent methods: transformation of the point-source reflection response to non-normal incidence plane wave responses, or a layer stripping algorithm involving cylindrical waves.

4.3.1 The Radon and Hankel Transforms

The Radon transform

The Radon transform is defined as (e.g., Robinson (1982))

$$U(\tau,p) = R[u(x,t)] = \int_{-\infty}^{\infty} u(x,t = \tau+px)dx \qquad (4\text{-}51)$$

where u(x,t) is the displacement or pressure measured on the surface as a function of lateral position x and time t, p is horizontal slowness, and τ is travel time. The Radon transform is thus a line integral along the line $t = \tau + px$, and has the effect of stacking up values of u(x,t) along the line with slope or slant p and intercept τ. For this reason the Radon transform is often called a slant stack.

To see the significance of this, consider an oblique plane wave reflection response moving upward and in the +x direction. Clearly different parts of the plane wave will reach the surface at different times in different places, and the point where the plane wave is touching the surface will move in the +x direction at speed 1/p. Thus the arrival time t of the plane wave at the surface at position x depends not only on the travel time τ of the plane wave, but also on x by

$$t = \tau + px \qquad (4\text{-}52)$$

which is precisely the line on which the Radon transform stacks values of $u(x,t)$.

The physical meaning of the Radon transform is now clear. The Radon transform (4-51) is synthesizing a plane wave response by stacking up those values of $u(x,t)$ which would arise from a plane wave reflection response with slowness p and travel time τ. It thus amounts to continuous beamforming; indeed, (4-51) is simply a continuous sum-of-delays that picks out those ray paths emerging at the angle determined from $\sin\theta = pc_o$. Equation (4-51) functions like a phase-array radar in listening mode, receiving only the response due to a specific plane wave.

It may be shown (by the Sommerfeld integral; see Chapter VII) that the point source experiment is mathematically equivalent to probing the medium in all directions with an infinite number of plane waves of various wavenumbers (some of which are imaginary, corresponding to inhomogeneous plane waves, i.e., evanescent waves). Radon transforming the point source data thus picks out the response due to a certain obliquely incident plane wave, and this response, for two different slownesses, could then be used to initiate the layer stripping algorithm of Section 4.2. Thus, the point source problem is solved by the Radon transform and the layer stripping algorithm for the obliquely-incident plane wave problem.

Taking the Fourier transform with respect to τ of (4-51), changing the order of integration, and noting that a delay of px in the time domain corresponds to multiplication by $e^{-j\omega px} = e^{-jk_x x}$ in the frequency domain yields

$$F_\tau R[u(x,t)] = F_x F_t[u(x,t)]\big|_{k_x = \omega p} \tag{4-53}$$

Again, this shows that the Radon transform is picking out a plane wave response with slowness p. The Fourier dual of (4-53) is

$$F_\tau^{-1} R[\hat{u}(k_x,\omega)] = 2\pi u(x=\omega p,\ t=\omega) \tag{4-54}$$

which shows that knowledge of the Radon transform of $\hat{u}(k_x,\omega)$ for a single value of p is equivalent to knowledge of $\hat{u}(x,t)$ along the slice $x = pt$. This result, called the projection-slice theorem, is a basic result of tomography.

From (4-53) the formula for the inverse Radon transform may be obtained. We have

$$u(x,t) = F_\omega^{-1} F_{k_x=\omega p}^{-1} F_\tau[U(\tau,p)]$$

$$= \frac{1}{(2\pi)^2} \int_{-\infty}^{\infty}\int_{-\infty}^{\infty}\int_{-\infty}^{\infty} U(\tau,p) e^{-j\omega\tau} e^{j\omega px}\, e^{j\omega t}\, d\tau\, |\omega|\, dp\, d\omega$$

$$= \frac{1}{(2\pi)^2} \int_{-\infty}^{\infty}\int_{-\infty}^{\infty}\int_{-\infty}^{\infty} U(\tau,p) e^{j\omega(t-\tau+px)}\, |\omega|\, d\omega d\tau\, dp$$

$$= \frac{1}{2\pi} \int_{-\infty}^{\infty}\int_{-\infty}^{\infty} U(\tau,p) \frac{d}{dt} H[\delta(t-\tau+px)]\, d\tau\, dp$$

$$= \frac{1}{2\pi} \int_{-\infty}^{\infty} \frac{d}{dt} H[U(\tau = t+px,\ p)]\, dp \tag{4-55}$$

where the $|\omega|$ is the Jacobian for changing variables from k_x to p in the

multiple integral, and $H[\cdot]$ represents the Hilbert transform. Note that multiplication by $|\omega| = (j\omega)(-j \operatorname{sgn} \omega)$ in the frequency domain becomes a time derivative and Hilbert transform in the time domain. The inverse Radon transform (4-55) is called a filtered back-projection in tomography, since it amounts to filtering with $|\omega|$ and backprojecting by setting $\tau = t-px$ and integrating over p.

The Hankel transform

The Hankel transform is defined as (Papoulis, 1968)

$$F(\xi) = H[f(r)] = \int_0^\infty f(r)J_0(r\xi)rdr \tag{4-56}$$

where $J_0(\cdot)$ is the Bessel function of the first kind of order zero. The inverse Hankel transform is then

$$f(r) = H^{-1}[F(\xi)] = \int_0^\infty F(\xi)J_0(r\xi)\xi d\xi \ . \tag{4-57}$$

To show the significance of the Hankel transform, let f(x,y) be a circularly symmetric function, so that

$$f(x,y) = f((x^2 + y^2))^{\frac{1}{2}}) = f(r) \tag{4-58}$$

Then the two-dimensional Fourier transform of f(x,y) may be evaluated using polar coordinates. We have

$$F(k_x,k_y) = F(\rho,\phi) = F_x F_y [f(x,y)] = \int_0^\infty \int_0^{2\pi} f(r)e^{-j\rho r\cos(\theta-\phi)}rdrd\theta \tag{4-59}$$

where the cosine addition formula has been used. It is clear from (4-59) that $F(\rho,\phi)$ will not depend on ϕ, i.e., the Fourier transform of a circularly symmetric function is itself circularly symmetric. Using the identity

$$\frac{1}{2\pi}\int_0^{2\pi} e^{-jx\cos\theta}\,d\theta = J_o(x) \quad , \tag{4-60}$$

the radial slice $F(\rho)$ of the circularly symmetric Fourier transform of $f(r)$ is given by

$$F(\rho) = 2\pi\int_0^{\infty} f(r)J_o(\rho r)rdr = 2\pi H[f(r)] \quad . \tag{4-61}$$

Thus the Hankel transform of a function $f(r)$ yields a radial slice of the circularly symmetric Fourier transform of the circularly symmetric function $f(r)$. The above development is due to Mook (1983, p. 27).

Since the reflection response to a point source excitation has circular symmetry, the Hankel transform should be appropriate for synthesizing plane wave response data from point source response data. Indeed, if it is desired to synthesize a plane wave response moving in the +x direction with slowness p, we have

$$F_xF_yF_t\,[u(x,y,t)]\Big|_{\substack{k_x=\omega p\\ k_y=0}} = \int_{-\infty}^{\infty}\int_{-\infty}^{\infty}\int_{-\infty}^{\infty} u(x,y,t)e^{-j\omega(t+px)}dxdydt$$

$$= \int_{-\infty}^{\infty}\int_0^{\infty}\int_0^{2\pi} u(r,t)e^{-j\omega t}e^{-j\omega pr\cos\theta}rd\theta drdt = 2\pi\int_{-\infty}^{\infty}\int_0^{\infty} u(r,t)e^{-j\omega t}J_o(r\omega p)rdrdt$$

$$= 2\pi H F_t[u(r,t)]\Big|_{\xi=\omega p} \quad . \tag{4-62}$$

Thus another way of solving the point source problem is to Hankel transform the reflection response and set $\xi = \omega p$. This synthesizes a plane wave response which can be used to initiate the algorithm of Section 4.2.

Combining (4-53) and (4-62), we have

$$F_\tau R[u] = F_x F_y F_t\ [u]\Big|_{\substack{k_x=\omega p \\ k_y=0}} = HF_t[u]\Big|_{\xi=\omega p} \tag{4-63}$$

showing the relations of the Radon, Hankel, and Fourier transforms to each other. Coen (1982) showed the equality of the first and third terms of (4-63).

The equation $\xi = \omega p$ suggests that ξ is really a radial wavenumber k_r, and $J_o(\omega p r)e^{-j\omega t}$ is a surface wave. Since

$$J_o(k_r r) \simeq \left(\frac{2}{\pi k_r r}\right)^{\frac{1}{2}} \cos\left(k_r r - \frac{\pi}{4}\right) \tag{4-64}$$

$J_o(k_r r)e^{-j\omega t}$ behaves like the sum of incoming and outgoing waves for large r. These surface waves are obtained by setting z = 0 in the expression

$$J_o(k_r r)e^{jk_z z}e^{-j\omega t}\ ,\quad k_z^2 = \omega^2/c_o^2 - k_r^2 \tag{4-65}$$

which represents cylindrical waves. These are fundamental solutions of the wave equation in cylindrical coordinates. In the next section the point source problem is shown to amount to using cylindrical waves to probe the medium, and a layer stripping algorithm embodying the principle is derived.

4.3.2 Layer Stripping Solution

The point source problem depicted in Figure 4.2 was solved by Coen (1982) by transforming it into a non-normal incidence plane wave problem, which could then be solved as in Coen (1981). It has already been shown here that the layer stripping algorithm for the oblique plane wave problem can be used to solve the point source problem by transforming the point source data using either the Radon transform or the Hankel transform. But there should be some way to formulate a layer stripping algorithm that solves the point source problem directly, by probing the medium with cylindrical waves. In this section this algorithm is derived.

Note that probing the medium with cylindrical waves from an impulsive point source makes much more sense physically than does probing it with an infinite oblique plane wave, which cannot exist. Although an impulsive point source is also unphysical, it is a much better model of a real-world experiment.

In order to solve this problem, it will be necessary to define higher-order Hankel transforms. The n^{th} order Hankel transform is defined as (Papoulis, 1968)

$$H_n\{f(r)\} \triangleq \int_0^\infty f(r)J_n(r\xi)r\,dr = F_n(\xi) \tag{4-66}$$

where $J_n(\cdot)$ is the n^{th} order Bessel function. Although Hankel transforms of orders zero and one will be used in the derivation, the final algorithm will contain quantities that involve Hankel transforms of order zero only. In the course of the derivation the properties

$$H_o\{f(r)/r + (\partial/\partial r)f(r)\} = \xi H_1\{f(r)\} \tag{4-67a}$$

$$H_1\{(\partial/\partial r)f(r)\} = -\xi H_o\{f(r)\} \tag{4-67b}$$

will be employed.

Writing the basic acoustic equations (3-1) in cylindrical coordinates, taking Fourier transforms, and noting the circular symmetry of the present problem (no θ-dependence) yields

$$\rho(z)\omega^2\hat{u}_r\ (r,z,\omega) = \partial\hat{p}/\partial r \tag{4-68a}$$

$$\rho(z)\omega^2\hat{u}_z\ (r,z,\omega) = \partial\hat{p}/\partial z \tag{4-68b}$$

$$\hat{p}(r,z,\omega) = -\rho(z)c(z)^2\ (\partial\hat{u}_z/\partial z + \partial\hat{u}_r/\partial r + \hat{u}_r/r) \tag{4-68c}$$

where u_r and u_z are the r and z (depth) components of the (vector) displacement $\underset{\sim}{u}$. Note that the u_θ component of $\underset{\sim}{u}$ does not appear.

Taking Hankel transforms of order zero of (4-68b) and (4-68c), and the Hankel transform of order one of (4-68a) yields

$$\rho(z)\omega^2\hat{U}_r(\xi,z,\omega) = -\xi\hat{P}(\xi,z,\omega) \tag{4-69a}$$

$$\rho(z)\omega^2\hat{U}_z(\xi,z,\omega) = \partial\hat{P}/\partial z \tag{4-69b}$$

$$\hat{P}(\xi,z,\omega) = -\rho(z)c(z)^2\ (\partial\hat{U}_z/\partial z + \xi\hat{U}_r(\xi,z,\omega)) \tag{4-69c}$$

where

$$\hat{U}_r(\xi,z,\omega) = H_1\{\hat{u}_r(r,z,\omega)\} \tag{4-70a}$$

$$\hat{U}_z(\xi,z,\omega) = H_o\{\hat{u}_z(r,z,\omega)\} \tag{4-70b}$$

$$\hat{P}(\xi,z,\omega) = H_o\{\hat{p}(r,z,\omega)\}\ . \tag{4-70c}$$

Eliminating $\hat{U}_r$ from (4-69) yields

$$\rho(z)\omega^2\hat{U}_z(\xi,z,\omega) = \partial\hat{P}/\partial z \tag{4-71a}$$

$$\hat{P}(\xi,z,\omega)(1-(\xi^2/\omega^2)c(z)^2) = -\rho(z)c(z)^2\,\partial\hat{U}_z/\partial z \tag{4-71b}$$

and defining (compare to (4-24) - (4-27))

$$c'(z)^2 = c(z)^2/(1-(\xi^2/\omega^2)c(z)^2) \tag{4-72}$$

$$\tau(z) = \int_o^z ds/c'(s) \tag{4-73}$$

$$Z(\tau) = \rho(\tau)c'(\tau) \tag{4-74}$$

results in the familiar equations (compare to (4-28))

$$\partial\hat{P}/\partial\tau = Z\omega^2\hat{U}_z(\xi,\tau,\omega) \tag{4-75a}$$

$$\partial\hat{U}_z/\partial\tau = -(1/Z)\hat{P}(\xi,\tau,\omega) \quad . \tag{4-75b}$$

Recalling that the Hankel transform of order zero is the two-dimensional Fourier transform of a circularly symmetric function, we may once again define the Hankel-Fourier transforms of the downgoing and upgoing waves (as in (4-29))

$$\hat{V}_1(\xi,\tau,\omega) = \hat{P}(\xi,\tau,\omega)/Z^{\frac{1}{2}} + j\omega Z^{\frac{1}{2}}\hat{U}_z(\xi,\tau,\omega) \tag{4-76a}$$

$$\hat{V}_2(\xi,\tau,\omega) = \hat{P}(\xi,\tau,\omega)/Z^{\frac{1}{2}} - j\omega Z^{\frac{1}{2}}\hat{U}_z(\xi,\tau,\omega) \tag{4-76b}$$

The waves (4-76) satisfy the two-component wave system

$$\partial \hat{V}_1/\partial\tau = -j\omega\hat{V}_1(\xi,\tau,\omega) - r(\tau)\,\hat{V}_2(\xi,\tau,\omega) \tag{4-77a}$$

$$\partial \hat{V}_2/\partial\tau = -r(\tau)\hat{V}_1(\xi,\tau,\omega) + j\omega\hat{V}_2(\xi,\tau,\omega) \tag{4-77b}$$

with the reflectivity function $r(\tau)$ given by

$$r(\tau) = \frac{1}{2Z}\frac{dZ}{d\tau} = \frac{d}{d\tau}\log\frac{Z(\tau)}{Z(0)} \tag{4-78}$$

The forms of the waves used to probe the two-component wave system (4-77) are, in the time-distance domain

$$v_1(r,z,t) = \delta(t-\tau)\delta(r)/r + \tilde{v}_1(r,z,t)1(t-\tau) \tag{4-79a}$$

$$v_2(r,z,t) = \tilde{v}_2(r,z,t)1(t-\tau) \tag{4-79b}$$

where the probing impulse is a roughly cylindrical wave and $\tau = \tau(z)$ (recall that the medium is laterally homogeneous). The Hankel transforms of (4-79), which are the waves actually used in the fast Cholesky algorithm based on (4-77), then have the form (2-22), as desired. Note that letting $\xi = k_x$ in (4-72) results in (4-25), as expected. This choice was noted by Coen (1982).

4.4 Turning Points

4.4.1 Turning Points

A turning point in a layered medium is a depth z_o where the local wave speed $c(z_o)$ has become so great that it equals the reciprocal of the

slowness of the probing plane wave, i.e., $c(z_o) = 1/p$. By Snell's law

$$p = \sin \theta(z)/c(z) \tag{4-80}$$

the ray paths of the probing plane wave are horizontal at a turning point, before turning back up to the surface. The reason for the ray paths turning back to the surface is that the lower part of the probing wave, in the region of higher wave speed, continues to move faster than the upper part. This bends the rays up toward the surface.

The location of a turning point in a layered medium is thus dictated by the ray parameter or slowness p of the probing wave: the steeper the angle of incidence, the deeper the turning point. Indeed, if $c(z) < c_{MAX}$ throughout the medium and the probing angle θ in Figure 4.1 is chosen so that $\theta < \sin^{-1} c_o/c_{MAX}$, then there is no turning point.

Since it depends on the concept of rays, and on Snell's law, turning points as defined above are only defined for the case of geometrical acoustics. This is tantamount to taking $\omega \to \infty$, i.e., the medium must not vary significantly over a wavelength. Another definition of a turning point, as the depth where the character of the solutions of the Schrodinger equation (4-82) below change from oscillatory to exponentially decaying, is useless in the present context since the Schrodinger potential V is unbounded.

In this section we analyze the behavior of the pressure and vertical displacement near a turning point, and then show how these can be used to propagate the layer stripping algorithm of Section 4.2 through a turning point and back up to the surface. This allows more of the

reflection response data to be used in inverting the medium, and provides a check on the $\rho(z)$ and $c(z)$ profiles computed on the way down to the turning point.

WKBJ solution

The expressions obtained for pressure $\hat{p}$ and vertical displacement $\hat{u}$ near a turning point must be matched asymptotically to expressions valid far away from the turning point. More advanced techniques, such as the Langer uniform asymptotic expansion (Nayfeh (1973) is a good treatment) obviate the need of having different expressions in different regions, but we do not consider them here. To derive the expressions valid far away from the turning point, we employ a WKBJ analysis of two Schrodinger equations. The presentation here is based on Ware (1969), although there are many significant departures.

Defining

$$\hat{\pi}(z,\omega) = \hat{p}(z,\omega)/\rho^{\frac{1}{2}}(z) \tag{4-81a}$$

$$\hat{w}(z,\omega) = (\rho(z)c'(z)^2)^{\frac{1}{2}}\ \hat{u}(z,\omega) \tag{4-81b}$$

$$Z(z) = 1/\rho^{\frac{1}{2}}(z) \tag{4-81c}$$

$$Y(z) = (\rho c'(z)^2)^{\frac{1}{2}} \tag{4-81d}$$

it is straightforward to show from the basic equations (4-21) and (4-23) that $\hat{\pi}$ and $\hat{w}$ satisfy the Schrodinger equations

$$\left(\frac{d^2}{dz^2} + \frac{\omega^2}{c'^2} - \frac{1}{Z}\frac{d^2Z}{dz^2}\right)\hat{\pi} = 0 \tag{4-82a}$$

$$\left(\frac{d^2}{dz^2} + \frac{\omega^2}{c'^2} - \frac{1}{Y}\frac{d^2Y}{dz^2}\right)\hat{w} = 0. \tag{4-82b}$$

Since these two equations have the same form, we can treat both of them at once. Choosing the ansatz or trial solution

$$\hat{\pi} = Ae^{j\omega B} \tag{4-83}$$

substituting (4-83) into (4-82a) and writing the real and imaginary parts separately gives, respectively,

$$\ddot{A} - A\omega^2\dot{B}^2 + \frac{\omega^2}{c'^2}A - \frac{\ddot{Z}}{Z}A = 0 \tag{4-84a}$$

$$A\ddot{B} + 2\dot{A}\dot{B} = 0 \tag{4-84b}$$

which in turn yield

$$\dot{B} = \pm\left(\frac{1}{c'^2} - \frac{\ddot{Z}}{\omega^2 Z} + \frac{\ddot{A}}{\omega^2 A}\right)^{\frac{1}{2}} \tag{4-85a}$$

$$A = C/\dot{B}^{\frac{1}{2}} \tag{4-85b}$$

Here $\dot{A} \triangleq \frac{dA}{dz}$ and C is a constant.

Neglecting the third term in (4-85a) and defining

$$\frac{1}{c''} = \left(\frac{1}{c'^2} - \frac{\ddot{Z}}{\omega^2 Z}\right)^{\frac{1}{2}} \simeq \frac{1}{c'} \quad \text{as} \quad \omega \to \infty \tag{4-86}$$

we have for our trial solution

$$\hat{\pi}(z,\omega) = C(c'')^{\frac{1}{2}}e^{\pm j\omega\int_0^z ds/c''(s)} \tag{4-87}$$

or

$$\hat{p}(z,\omega)/(\rho c'')^{\frac{1}{2}} = C_1 e^{j\omega\int_o^z ds/c''(s)} + C_2 e^{-j\omega\int_o^z ds/c''(s)} \qquad (4\text{-}88)$$

for constants C_1 and C_2.

The analysis for $\hat{w}$ is exactly the same through (4-87), yielding

$$(\rho c'')^{\frac{1}{2}}\hat{u}(z,\omega) = C_3 e^{j\omega\int_o^z ds/c''(s)} + C_4 e^{-j\omega\int_o^z ds/c''(s)} \qquad (4\text{-}89)$$

for constants C_3 and C_4.

In the limit as $\omega \to \infty$ (geometrical acoustics), (4-88) and (4-89) become simple decompositions of the energy-normalized pressure and displacement into downgoing and upgoing waves--hardly a surprise. This development shows how much this depends on a slowly varying medium relative to the wavelength of the probing medium. From (4-86), we require

$$\omega >> c'\left(\frac{\ddot{Z}}{Z}\right)^{\frac{1}{2}} \qquad (4\text{-}90)$$

and it is clear there will be trouble at a turning point, where $c' \to \infty$.

Air solution near a turning point

In the limit of geometrical acoustics ($\omega \to \infty$), a turning point has been defined as the depth z_o where $c(z_o) = 1/p$. Then $c'(z_o) \to \infty$ and $1/c'(z_o) = 0$. Let $1/c'(z)^2$ be approximated in the vicinity of the turning point z_o by

$$1/c'(z)^2 = 1/c(z)^2 - p^2 \approx [2p^3 \frac{dc}{dz}(z_o)]\,(z_o - z) \triangleq E(z_o - z) \qquad (4\text{-}91)$$

where E is the (unknown) constant specified in (4-91). Substituting

(4-91) in the Schrodinger equation (4-82a) yields

$$\left(\frac{d^2}{dz^2} + \omega^2 E(z_o - z) - \frac{\ddot{Z}}{Z}\right)\hat{\pi} = 0 \qquad (4\text{-}92)$$

and neglecting the third term in (4-92) for ω large yields the

Airy equation

$$\left(\frac{d^2}{dz^2} + \omega^2 E(z_o - z)\right)\hat{\pi} = 0 \quad . \qquad (4\text{-}93)$$

The solution of this equation involves the Airy function Ai(·), and is

$$\hat{\pi} = C_5 \mathrm{Ai}(-\omega^{2/3} E^{1/3} (z_o - z)) \qquad (4\text{-}94)$$

where C_5 is a constant. The other Airy function, Bi(·), is rejected since it leads to an exponentially growing solution.

Matching asymptotic forms

From Abramowitz and Stegun (1965),

$$\mathrm{Ai}(-y) \simeq \pi^{-\frac{1}{2}} y^{-\frac{1}{4}} \cos\left(\frac{2}{3} y^{\frac{3}{2}} - \frac{\pi}{4}\right) \quad \text{as} \quad y \to \infty \qquad (4\text{-}95)$$

and using this in (4-94) along with (4-81a) results in

$$\hat{p} \simeq C_6 \rho^{\frac{1}{2}} (z_o - z)^{-\frac{1}{4}} \cos\left(\frac{2}{3}\omega E^{\frac{1}{2}} (z_o - z)^{\frac{3}{2}} - \frac{\pi}{4}\right) \qquad (4\text{-}96)$$

for $z << z_o$, i.e., above the turning point. Here C_6 is still another constant, which is related to C_5.

On the other hand, inserting (4-91) in the WKBJ equation (4-88) and taking ω large results in

$$\hat{p} \simeq \rho^{\frac{1}{2}} E^{-\frac{1}{4}}(z_o-z)^{-\frac{1}{4}} \left[C_1 e^{j\omega\tau} e^{j\omega\int_{z_o}^{z} E^{\frac{1}{2}}(z_o-s)^{\frac{1}{2}}ds} + C_2 e^{-j\omega\tau} e^{-j\omega\int_{z_o}^{z} E^{\frac{1}{2}}(z_o-s)^{\frac{1}{2}}ds}\right] \quad (4\text{-}97)$$

$$= \rho^{\frac{1}{2}} E^{-\frac{1}{4}}(z_o-z)^{-\frac{1}{4}} \left[C_1 e^{j\omega\tau} e^{-j\frac{2}{3}\omega E^{\frac{1}{2}}(z_o-z)^{\frac{3}{2}}} + C_2 e^{-j\omega\tau} e^{j\frac{2}{3}\omega E^{\frac{1}{2}}(z_o-z)^{\frac{3}{2}}}\right]$$

where τ is the travel time to the turning point z_o, defined as

$$\tau = \int_o^{z_o} ds/c'(s) \quad . \quad (4\text{-}98)$$

Now, the asymptotic form (4-96) of the Airy solution away from the turning point must match the asymptotic form (4-97) of the WKBJ solution near the turning point. Comparing (4-96) and (4-97) we see that

$$C_1 e^{j\omega\tau} E^{-\frac{1}{4}} = C_6 e^{j\pi/4} \quad (1/2) \quad (4\text{-}99a)$$

$$C_2 e^{-j\omega\tau} E^{-\frac{1}{4}} = C_6 e^{-j\pi/4} \quad (1/2) \quad . \quad (4\text{-}99b)$$

For the experiment in which an oblique plane pressure wave is used to probe the medium, the actual form of $\hat{p}$ is

$$\hat{p}(z,\omega) = (\rho c')^{\frac{1}{2}} \left[e^{-j\omega\int_o^z ds/c'(s)} + \hat{R}_p(\omega) e^{j\omega\int_o^z ds/c'(x)}\right] . \quad (4\text{-}100)$$

Comparing (4-88) and (4-100), and using (4-99), it may be seen that the reflection response $\hat{R}_p(\omega)$ is given by

$$\hat{R}_p(\omega) = C_1/C_2 = e^{-2j\omega\tau}\, e^{j\pi/2} \quad . \tag{4-101}$$

The first term of (4-101) is simply the delay due to the two-way travel time to the turning point. The second term is a phase advance of $\pi/2$, since if ω is negative there is a sign change in the independent variable in (4-94) and (4-95), resulting in $e^{-j\pi/2}$ in (4-101). The phase advance of $\pi/2$ is, in the time domain, a negative Hilbert transform of the source time function.

Comments

There are several comments to be made here. First, the usual definition of a turning point for a Schrodinger equation (for finite ω) is the depth at which the nature of the solution changes from oscillatory to exponentially decaying. For the Schrodinger equation (4-82a), this is where

$$\frac{\omega^2}{c'^2} - \frac{\ddot{Z}}{Z} = \frac{\omega^2}{c''^2} = 0$$

so employing a linear approximation like (4-91) to (4-102) is simply equivalent to replacing c' with c'' throughout. In the limit of high ω c' and c'' become equal. Note in fact that the Airy function Ai(y) is oscillatory for $y < 0$ and exponentially decaying for $y > 0$.

Second, it should be emphasized that (4-101) is the result of a WKBJ analysis, which neglects all internal reflections. It is not true that the amplitude of the reflected signal carries no information about the medium! The purpose of this analysis is simply to discern what happens to a pressure wave passing through a turning point--it gets negative

Hilbert-transformed.

The reflection response of the medium can be separated into two parts: the part before $2\tau_o$, where $2\tau_o$ is the two-way travel time to the turning point; and the part from $2\tau_o$ to $4\tau_o$. The first part of the reflection response is clearly unaffected by the presence of a turning point, since the probing impulse has not penetrated that far into the medium. By causality, it is impossible for the nature of the medium below and ahead of the probing impulse at any time to affect the reflection response of the medium at that time. From $2\tau_o$ to $4\tau_o$, the probing impulse is now essentially probing a mirror image of the medium, and this part of the reflection response reflects this. (Of course, there are also lingering multiple reflections from the downward path, but these have been eliminated by the layer stripping algorithm.) The reflected waves propagate back through the turning point to be measured as the reflection response.

After $2\tau_0$, the transmitted response through the turning point begins to appear at the surface. According to the WKBJ analysis, this transmitted response is simply the negative Hilbert transform of the delayed source excitation. However, this ignores the reflection losses within the medium, which will clearly degrade the transmitted response. Of course, the arrival time of the transmitted response may be used for travel time inversion; however, this is outside the scope of this thesis.

It should also be noted that the result of (4-101), which is the only result we shall actually use in a layer stripping algorithm, is amazingly accurate in practice. Tolstoy and Clay (1966), p. 51) report that for typical frequencies and typical oceanic sound channels, (2-101) is accurate to five significant figures.

Finally, it should be noted how this analysis differs from the usual WKBJ-Airy turning point analysis. The general procedure is to approximate $\omega^2 - V$ by a linear expression, as in (4-91). This will not work on the Schrodinger equation (4-11) considered by Ware (1969) because the potential V(z) blows up at the turning point. Ware (1969) modelled V(z) by a second-order pole and branch point, and obtained a messy result that reduced to (4-101) in the limit $\omega\tau \to \infty$. We have used the Schrodinger equation (4-82a) because its potential does not blow up at the turning point. Unfortunately, the potential of the displacement Schrodinger equation does blow up at the turning point, and a different equation will have to be used for the Airy analysis of that problem.

Displacement

The WKBJ formula for displacement away from the turning point was already derived in (4-89). However, the Airy solution near the turning point will require more work, since $Y = (\rho c'^2)^{\frac{1}{2}}$ blows up there and thus (4-82b) cannot be used.

The displacement equation we shall use near the turning point is

$$\left(\frac{d^2}{dz^2} + \frac{\omega^2}{c'^2} + \left(\frac{2}{c'} \frac{dc'}{dz} + \frac{1}{\rho} \frac{d\rho}{dz} \right) \frac{d}{dz} \right) \hat{u}(z,\omega) = 0 \quad . \qquad (4\text{-}103)$$

In the vicinity of the turning point c'(z) is changing very rapidly, and of course we continue to assume high ω. Hence the fourth term in (4-103) is negligible. Multiplying (4-103) by $1/c'(z)^2$ and using (4-91) gives

$$\left(E(z_o-z)\frac{d^2}{dz^2} + \omega^2E^2(z_o-z)^2 + E\frac{d}{dz}\right)\hat{u}(z,\omega) = 0 \qquad (4\text{-}104)$$

near the turning point z_o.

It turns out that the solution to (4-104) involves the derivative of the Airy function, Ai'(·). To see this, consider the Airy differential equation

$$\frac{d^2f}{dz^2} - zf(z) = 0 \qquad (4\text{-}105)$$

divide by z, differentiate, and multiply by z^2. This gives

$$z\frac{d^3f}{dz^3} - \frac{d^2f}{dz^2} - z^2\frac{df}{dz} = 0 \qquad (4\text{-}106)$$

which is an equation in df/dz having the form (4-104).

Therefore the solution to (4-104) is

$$\hat{u}(z,\omega) = C_7Ai'(-\omega^{\frac{2}{3}}E^{\frac{1}{3}}(z_o-z)) \qquad (4\text{-}107)$$

where C_7 is a constant. From Abramowitz and Stegun (1965)

$$Ai'(-y) \simeq -\pi^{-\frac{1}{2}}y^{\frac{1}{4}}\cos\left(\frac{2}{3}y^{\frac{3}{2}} + \frac{\pi}{4}\right) \quad \text{as } y \to \infty \qquad (4\text{-}108)$$

so the asymptotic form of (4-107) above the turning point is

$$\hat{u}(z,\omega) \simeq C_8(z_o-z)^{\frac{1}{4}}\cos\left(\frac{2}{3}\omega E^{\frac{1}{2}}(z_o-z)^{\frac{3}{2}} + \frac{\pi}{4}\right) \qquad (4\text{-}109)$$

where C_8 is a constant determined by C_7.

On the other hand, the asymptotic form for the WKBJ solution (4-89)

near the turning point is found by inserting (4-91) in (4-89), yielding

$$\hat{u}(z,\omega) \simeq \rho^{-\frac{1}{2}} E^{\frac{1}{4}}(z_o-z)^{\frac{1}{4}}[C_3 e^{j\omega\tau} e^{-j\frac{2}{3}\omega E^{\frac{1}{2}}(z_o-z)^{\frac{3}{2}}} + C_4 e^{-j\omega\tau} e^{j\frac{2}{3}\omega E^{\frac{1}{2}}(z_o-z)^{\frac{3}{2}}}] \tag{4-110}$$

using the same simplications used to produce (4-97).

The asymptotic forms (4-109) and (4-110) must agree, so we have

$$C_3 e^{j\omega\tau} E^{\frac{1}{4}} \rho^{-\frac{1}{2}} = C_8 e^{-j\pi/4} \tag{4-111a}$$

$$C_4 e^{-j\omega\tau} E^{\frac{1}{4}} \rho^{-\frac{1}{2}} = C_8 e^{j\pi/4} \quad , \tag{4-111b}$$

and from (4-89) the reflection response $\hat{R}_u(\omega)$ for the experiment in which an oblique acoustic plane <u>displacement</u> wave is used to probe the medium is given by

$$\hat{R}_u(\omega) = C_3/C_4 = e^{-2j\omega\tau} e^{-j\pi/2} = -\hat{R}_p(\omega) \ . \tag{4-112}$$

Therefore the reflection coefficient for a displacement wave is negative the reflection coefficient for a pressure wave, as expected. This amounts to a <u>phase delay of $\pi/2$</u> as the displacement wave passes through the turning point, which is a <u>Hilbert transform</u> in the time domain.

Again some comments are in order. This is an unusual analysis in that some juggling was required to produce the equations (4-103) and (4-106); it is <u>not</u> just a standard Airy analysis, since it is necessary to isolate the effects of c' blowing up at the turning point. This is much harder to do for displacement than it is for pressure; compare the two Schrodinger equations (4-82a) and (4-82b). Incidentally, it is worth noting that even though the ray paths become horizontal at the turning

point, the vertical displacement $\hat{u}(z_o,\omega)$ does not go to zero.

Of course, it is hardly surprising that the vertical displacement $\hat{u}(z_o,\omega)$ behaves like the derivative of the Airy function, in light of the basic equations (4-21). Indeed, inserting (4-94) and (4-107) into the basic equations (4-21b) and (4-23) for the oblique plane wave problem yields a consistent set of equations if ρ is assumed to have negligible variation in the vicinity of the turning point.

4.4.2 Propagation of the Layer Stripping Algorithm Through a Turning Point

Using the results (4-101) and (4-112), we now show how the layer stripping algorithm can be propagated through a turning point and back up to the surface along the ray path. This allows surface reflection data collected past $2\tau_o$, the two-way travel time to the turning point, to be used in the inversion procedure. The reflection coefficients and profiles of $\rho(z)$ and $c(z)$ computed on the way down can then be checked on the way back up.

The basic idea is to regard the turning point as a "black box" that Hilbert transforms various combinations of the waves and changes the downgoing waves into the upgoing waves, and vice-versa. The only problem is to determine the appropriate time delay as the waves travel through this "box."

The first problem, of course, is to detect a turning point when it is encountered. This presents little difficulty, since $\cos^2\theta(z) = 1 - p^2c(z)^2$ is computed in the course of the algorithm (equation (4-37)). As a turning point is approached, $\theta(z)$ approaches $\pi/2$ as the ray becomes horizontal, and $\cos^2\theta(z)$ goes to zero. Of course, if $1 - p^2c(z)^2 < 0$ then clearly a turning point has been encountered (even

if noise has corrupted the computed c(z), a turning point must be close). However, a better procedure is to set a threshold ε, and decree that if

$$\cos^2 \theta(z_1) = 1 - p^2 c(z_1)^2 \leq \varepsilon^2 \tag{4-113}$$

then a turning point is present at depth z_1.

Of course, if the medium wave speed profile c(z) is such that it increases with depth to approximately $c(z) \approx 1/p$ and then decreases, (4-113) may identify a turning point that is non-existent. This simply represents bad luck in the choice of ray parameter p. The error will be revealed when the $\rho(z)$ and c(z) profiles computed on the way up diverge wildly from those computed on the way down, and the algorithm could simply be rerun with a different choice of p.

The second problem is to determine what happens to the waves as they pass through the turning point. This is where (4-101) and (4-112) are useful. Recall that the downoing wave $\hat{v}_1(z,\omega)$ and upgoing wave $\hat{v}_2(z,\omega)$, which we rename $\hat{D}(z,\omega)$ and $\hat{U}(z,\omega)$ for convenience, are given in (4-29) as

$$\hat{D}(z,\omega) = \hat{p}(z,\omega)/(\rho c')^{\frac{1}{2}} + j\omega(\rho c')^{\frac{1}{2}}\hat{u}(z,\omega) \tag{4-114a}$$

$$\hat{U}(z,\omega) = \hat{p}(z,\omega)/(\rho c')^{\frac{1}{2}} - j\omega(\rho c')^{\frac{1}{2}}\hat{u}(z,\omega) \quad . \tag{4-114b}$$

Now, as these waves pass through the turning point, the pressure is negative Hilbert transformed (4-101) and the displacement, hence the velocity, is Hilbert transformed (4-112). Thus, after passing through the turning point, D(z,t) becomes D'(z,t) and U(z,t) becomes U'(z,t), where

$$D'(z,t) = -H[p/Z^{\frac{1}{2}}] + H[Z^{\frac{1}{2}}v] = -H[U(z,t)] \qquad (4\text{-}115a)$$

$$U'(z,t) = -H[p/Z^{\frac{1}{2}}] - H[Z^{\frac{1}{2}}v] = -H[D(z,t)] \quad . \qquad (4\text{-}115b)$$

In (4-115) $v \overset{\Delta}{=} \partial u/\partial t$ is medium velocity, $Z = \rho c'$ is impedance, and $H[\cdot]$ is the Hilbert transform operator, which is $-j\ SGN(\omega)$ in the frequency domain and has the impulse response $-1/(\pi t)$.

However, after passing through the turning point the downgoing and upgoing waves also become interchanged. The combination of this and (4-115) shows that the net effect of passage through a turning point on the waves in the layer stripping algorithm is a negative Hilbert transform of both waves. This is precisely what would be expected by recalling that the waves (4-114) are really pressure waves, and the turning point acts like a reflection coefficient (4-101).

The final problem is to determine the time delay encountered in passage through the turning point. Recall that the algorithm stops at the depth z_1 where

$$1 - p^2 c(z_1)^2 = \varepsilon^2 \quad . \qquad (4\text{-}116)$$

If the turning point is located at depth $z_o > z_1$, with $\Delta \overset{\Delta}{=} z_o - z_1$ small, then we have, using (4-91)

$$\varepsilon^2 = 1 - p^2 c(z_1)^2 \approx (E/p^2)\,\Delta \quad . \qquad (4\text{-}117)$$

The travel time delay through the turning point is, using (4-91),

$$\Delta\tau = 2\int_{z_1}^{z_o} ds/c'(s) = 2\int_{z_1}^{z_o} E^{\frac{1}{2}}(z_o - s)^{\frac{1}{2}} ds = (4/3)E^{\frac{1}{2}}\Delta^{\frac{3}{2}} \qquad (4\text{-}118)$$

and eliminating the unknown Δ yields

$$\Delta\tau = (4/3)p^3\varepsilon^3/E \quad . \tag{4-119}$$

Note that $\Delta\tau$ varies with the threshold ε as ε^3, and that it is necessary to determine $E = 2p^3 dc(z_o)/dz$ or Δ. E, however, can be estimated from the way c(z) is varying at z_1.

In summary, to extend the layer stripping algorithm through a turning point, use the condition (4-113) to detect a turning point, take the negative Hilbert transform of the waves, and delay them by $\Delta\tau$ in (4-119). Then continue the algorithm back up to the surface, comparing the computed $\rho(z)$ and c(z) profiles with those computed on the way down. This makes use of surface reflection data collected after 2τ, the two-way travel time to the turning point.

In the next chapter the effect of noise on the layer stripping algorithm is discussed, and results of some computer runs of the algorithm on synthetic data presented.

REFERENCES FOR CHAPTER IV

M. Abramowitz and I. Stegun, Handbook of Mathematical Functions, Dover, NY, 1965.

K. Aki and P. Richards, Quantitative Seismology: Theory and Methods, W.H. Freeman and Co., San Francisco, 1980.

P.M. Carrion, "Computation of Velocity and Density Profiles of Acoustic Media with Vertical Inhomogeneities Using the Method of Characteristics Applied to the Slant Stacked Data," Tech. Report, Aldridge Lab. of Applied Geophysics, Columbia University, 1983.

P.M. Carrion, J.T. Kuo, and P.L. Stoffa, "Inversion Method in the Slant Stack Domain Using Amplitudes of Reflection Arrivals," Geophysical Prospecting 32(3), 375-391 (1984).

S. Coen, "Density and Compressibility Profiles of a Layered Acoustic Medium from Precritical Incidence Data," Geophys. 46(9), 1244-1246 (1981).

S. Coen, "Velocity and Density Profiles of a Layered Acoustic Medium from Common Source-Point Data," Geophys. 47(6), 898-905 (1982).

R. Courant and D. Hilbert, Methods of Mathematical Physics, Interscience Publishers, New York, 1962.

M. Howard, "Inverse Scattering for a Layered Acoustic Medium Using the First-Order Equations of Motion," Geophys. 48(2), 163-170 (1983).

D. Mook, "The Numerical Synthesis and Inversion of Acoustic Fields Using the Hankel Transform with Application to the Estimation of the Plane Wave Reflection Coefficient of the Ocean Bottom," Sc.D. Dissertation, Joint MIT/Woods Hole Program in Oceanographic Eng., Jan. 1983.

A. Nayfeh, Perturbation Methods, Wiley and Sons, New York, 1973.

A. Papoulis, Systems and Transforms with Applications in Optics, McGraw-Hill, New York, 1968.

J. Ware, "Scattering and Inverse Scattering Problems in a Continuously-Varying Elastic Medium," Ph.D. Thesis, Dept. of Earth and Planetary Sciences, MIT, Aug. 1969.

A. Yagle and B. Levy, "Application of the Schur Algorithm to the Inverse Problem for a Layered Acoustic Medium," J. Acoust. Soc. Am. 76(1), 301-308 (1984).

CHAPTER V

Performance of the Non-Normal Incidence Inversion Algorithms

5.1 Introduction

In this chapter the results of running the two non-normal incidence inversion algorithms of Chapter IV on a computer are presented. This chapter is not intended to be an exhaustive numerical study of these algorithms. Rather, the purposes of this chapter are to demonstrate that the algorithms do work, and to illustrate some of their strong points and weak points.

The goals of this chapter are threefold: (1) to demonstrate that the algorithms of Chapter IV do indeed reconstruct a layered medium from its synthesized forward response, and still do so in the presence of small amounts of additive noise; (2) to demonstrate some circumstances under which the algorithms break down, and explain how to avoid them; and (3) to develop some minor modifications of the algorithms that improve their performance in the presence of noise. In addition, some other considerations involved in running the algorithms on a computer, such as discretization of time, are discussed. All of the computer programs used in this thesis are given in the Appendix.

5.1.1 Forward vs. Backward Stability

A superficial consideration of the operation of a layer stripping algorithm initiated with noisy data might make it seem as though errors would accumulate rapidly as the medium were penetrated, to the point where the algorithm would quickly break down. However, this is not

the case, as this chapter will show. Note that each step of the discrete algorithm amounts to a Givens rotation of normalized waves (equation (3-86)), so that the waves cannot blow up. Indeed, Bultheel (1979) has shown that the basic fast Cholesky algorithm is numerically stable. And it is important to remember that the layer stripping algorithms are mathematically dual to the integral equation procedures that constitute an alternative to them. Therefore, mathematically, the performance of the integral equation methods used on noisy data is no better than that of the layer stripping methods. So how did dynamic deconvolution methods get the reputation of performing poorly on noisy data? To answer this question requires some discussion of forward vs. backward stability, i.e., the stability of an algorithm vs. the conditioning of the problem to which it is applied.

An inverse problem is defined to be forward stable if a slight perturbation of the data leads to a slight perturbation of the parameters of the reconstructed medium. This is tantamount to requiring continuity of the mapping from the set of admissible data to the set of possible media. This mapping, which is the inverse of the forward problem mapping, is uniquely specified if the inverse problem is well-defined. An inverse problem that is not forward stable is said to be ill-conditioned.

An algorithm is defined to be backward stable if the numerical result of running the algorithm on a given set of data is the same result that would be obtained from an exact run (no roundoff errors, etc.) of the algorithm on a slight perturbation of the given data. Thus, for a forward stable problem, errors inherent in the algorithm are equivalent to a slight perturbation of the data, which in turn results in a slight

perturbation of the reconstructed medium.

These two definitions are taken from Stewart (1973), where the "inverse problem" considered is that of solving the matrix equation $Ax = b$. However, the definitions also apply to the general class of well-defined inverse problems (i.e., those for which a unique solution can be found from the data).

The significance of these two definitions is that they distinguish between the conditioning of a problem and the stability of the algorithm used to solve it. A stable algorithm applied to an ill-conditioned problem (such as inversion of a nearly singular matrix) may give poor results, even though the algorithm itself performs well in general. The fault lies not with the algorithm, but with the decision to use it inappropriately (and there may well be no algorithm that works well on a severely ill-conditioned problem).

This is important in discussing the performance of layer stripping algorithms applied to inverse seismic problems, because the conditioning of an inverse seismic problem gets poorer with increasing depth. Bruckstein et al. (1984) have shown that the condition number c(n) for the one-dimensional discrete normal incidence inverse seismic problem n layers deep is given by

$$c(n) = \prod_{i=1}^{n} \frac{1 + |r_i|}{1 - |r_i|} , \qquad (5\text{-}1)$$

where r_i are the reflection coefficients, assumed to have absolute values less than one, and c(n) is defined as

$$c(n) = ||M_n|| \cdot ||M_n^{-1}|| = \sigma_{max}^{n} / \sigma_{min}^{n} . \qquad (5\text{-}2)$$

Here M_n is a matrix that represents the transmission matrix for the medium, defined by (3-52), and σ_{max}^n and σ_{min}^n are its maximum and minimum singular values. The condition number c(n) is the amplication factor by which a perturbation or error in the data is multiplied to give the perturbation or error in computing r_{n+1} if $\{r_1 \ldots . r_n\}$ are known exactly.

It is clear from (5-1) that c(n) increases with depth n, so that the inverse problem of reconstructing r_n for each n becomes steadily more poorly conditioned. Physically, this can be understood by noting that the medium excitation becomes weaker as it penetrates the medium and suffers reflection losses. In the event of near-total reflection at a level m ($|r_m| \approx 1$), (5-1) shows that c(n) becomes very large for all $n > m$. Cybenko (1980) also derived (5-1) as the condition number of the symmetric Toeplitz matrix of size n that has been inverted after n recursions of the Levinson algorithm.

It is important to remember that the increasing condition number c(n) specified by (5-1) is a property of the inverse problem itself, even in the absence of noise, and applies regardless of the method used to solve it. This explains why layer stripping algorithms perform more poorly as depth increases: the problem is not the accumulation of noise in the algorithm, but the poor conditioning of the inverse problem itself. The same problem is encountered in the use of integral equation or matrix equation methods; however, these methods disguise the variation of the conditioning with depth, since the entire problem for all depths is solved in one huge operation. Layer stripping methods, being layer-recursive, spotlight the problem correctly; the result is an unjust reputation for poor performance.

5.1.2 Previous Work

Numerical work

Previous work on the numerical performance of layer stripping algorithms has all been applied to the one dimensional normal incidence inverse problem, since only for this problem is the layer stripping solution widely known. Bultheel (1979) showed that the fast Cholesky algorithm, the basic layer stripping algorithm for the normal incidence inverse problem (though few seem to know its name), is backward stable by employing an error analysis. Exhaustive numerical studies of this algorithm have been made by Symes and Zimmerman (1982), Bube and Burridge (1983), and Bruckstein et al. (1984), and all are quite favorable. We now summarize their results.

Bube and Burridge (1983) tested what they called the "downward continuation" algorithm against the one-dimensional Born approximation method, and found that the layer stripping algorithm completely outperformed the Born approximation method, due to the inability of the latter to deal with multiple reflections. Bruckstein et al. (1984) found that the fast Cholesky algorithm began to diverge after about fifty layers, since the conditioning of the problem at this depth was so poor that roundoff errors and accumulation errors in the numerical operation of the algorithm were magnified into significant errors in the output. The work of Symes and Zimmerman (1982) tested the algorithm in the presence of noise and bandlimitation of the source and data. Their results were that noise in the seismic band (10-40 Hz) had little effect on the reconstruction of the impedance of the medium for signal-to-noise ratios greater than about five, but the absence of low-frequency data (0-10 Hz) had a significant effect on the reconstruction. This is not surprising,

since the low-frequency response of the medium determines the trend of the impedance profile.

Estimation

If noisy data are to be used, it might seem natural to try to incorporate some sort of estimation procedure into the inversion algorithm. However, attempting to do this for a layer stripping algorithm generally leads to a mess, even for the normal incidence inverse problem. The reason for this is that the resulting estimation problem is very non-linear, as a few recursions of the fast Cholesky algorithm will show. Theriault (1977) derived some Cramer-Rao bounds for the mean-square error of any estimation procedure, and implemented numerically a maximum-likelihood estimator that required the application of a conjugate gradient method maximization at each depth.

The approach of Habibi-Ashrafi and Mendel (1982) is more promising. They employ a layer stripping solution to the discrete normal incidence inverse problem with a suboptimal maximum-likelihood estimation at each depth. Instead of projecting ahead to a specific time to read the next primary reflection, their method searches for the next primary reflection using a matched filter and a transversal equalizing filter, which corrects for wave overlapping effects. This a posteriori approach is in contrast to the a priori (project ahead to a specific, computed time) approach used in this thesis. Some Kalman-filter-like combination of these approaches would be ideal, but it is not clear how this could be done.

The estimator of Habibi-Ashrafi and Mendel (1982) reduces to an a priori project-and-read if the medium excitation is a probing impulse. It is also interesting to note that taking the maximum-likelihood approach as a starting point leads to a layer stripping approach as the optimal

inversion procedure (Habibi-Ashrafi and Mendel, 1982).

If the data are bandlimited, then the inverse problem is ill-posed, since the missing frequency components of the impedance profile cannot be reconstructed. For example, if the data are only specified up to a cutoff frequency, a sinusoidally-varying impedance profile (as a function of travel time) with spatial frequency above the cutoff frequency would be reconstructed as a constant profile. On the other hand, the absence of low-frequency data would result in the loss of low-spatial-frequency (i.e., trend) information about the impedance profile. There is no way around these ambiguities--some additional information is necessary in order to have a unique reconstructed medium.

One approach is the maximum-entropy estimation procedure used by Santosa and Symes (1983). Their approach is to pick the impedance profile with the flattest wave number spectrum that still matches the bandlimited data. However, this amounts to a reformulation of the problem. The layer stripping methods, since they operate in the time domain, simply assume the missing frequency responses to be zero. Any corrections to this must be made on the data itself.

5.1.3 Summary

In Section 5.2 the performance of the algorithms of Chapter IV in the absence of noise is investigated. The main goal of this section is to establish that the various algorithms do in fact work on a computer, even with imperfections in the data generated by the forward problem algorithms. The two forward problem algorithms are discussed and compared, and the performances of the fast Cholesky layer stripping inversion algorithm with continuous medium updates and with discrete

medium updates compared. Some circumstances under which the inversion algorithm breaks down are discussed and investigated. Finally, the Schur and dynamic deconvolution algorithms for the non-normal incidence problem are demonstrated with computers runs.

In Section 5.3 the performance of the fast Cholesky algorithm for the non-normal incidence problem on noisy data is investigated. Random-number-generated noise, uniformly distributed over a prespecified amplitude range, is added to the reflection data before the inversion algorithm is run. The effect this has on the operation of the inversion algorithm is illustrated by a series of runs in which progressively worse signal-to-noise ratios results in progressively poorer performance of the algorithm, as expected.

In Section 5.4 several minor modifications of the fast Cholesky algorithm for the non-normal incidence problem are developed in order to improve its performance in the presence of noise. First, the suggestion of Bruckstein et al. (1984) to set to zero all measured reflection coefficients less than a threshold value determined by the condition number and noise level is adopted. Next, reflection data measured for many different angles of incidence is combined to produce a least-squares fit for the updates of density $\rho(z)$ and wave speed $c(z)$ at each depth. This has two major advantages over least-squares fits of the entire parameter profiles: (1) the problems at each depth are decoupled; and (2) the resulting, more accurate updated parameters are used immediately in the algorithm while it is still running. Both of these modifications are illustrated with computer runs. Finally, a modification that allows a slightly lossy medium to be reconstructed is specified. The losses must be small enough that dispersion of the probing

impulse is negligible.

Section 5.5 then summarizes the results of this chapter. The strong points and weak points of employing layer stripping algorithms are discussed, and some ways in which these algorithms break down are reviewed. A significant advantage of layer stripping inversion procedures over other inversion procedures is the physical interpretations available for almost every aspect of the operation of the algorithm. This makes it much easier to determine when and why an algorithm might break down than is generally the case in numerical analysis.

The computer programs impelemnting these algorithms are all written in FORTRAN, and they are all given in an Appendix to this thesis. These programs were run on a VAX 11/782 minicomputer, and the plots made at the Joint Computer Facility at MIT in 1984.

5.2 Performance of the Algorithms in the Absence of Noise

In this section we present computer runs of the continuous and discrete fast Cholesky layer stripping algorithms for the non-normal incidence inverse problem. Two different forward problem algorithms are used--one based on a time domain (Bremmer series) method, and one based on a frequency domain (reflectivity) method. We show that the inversion algorithms do in fact work, and work well, on high quality (but not perfect) data. Some ways in which the algorithms break down are illustrated and discussed. The idea here is to be illustrative rather than perform exhaustive numerical studies. Computer runs of the Schur and dynamic deconvolution algorithms for the non-normal incidence problem are also given.

5.2.1 Forward Problem Algorithms

Two different forward problem algorithms are used. One, FORI, is a frequency-domain algorithm that uses the reflectivity method (see (Aki and Richards, 1980, p. 393) for a good discussion) and requires an inverse Fourier transform to obtain time responses. The other, BREM, is a time-domain algorithm that computes directly all of the primary and secondary (first-order multiple) reflections, i.e., the first two terms of the Bremmer series for the medium response. Both algorithms have advantages and disadvantages.

FOR1

The reflectivity method used by FOR1 works as follows. It is known that if a layered medium bounded above and below by two infinite, homogeneous half-spaces is probed with an impulse, the downgoing and upgoing waves in the lower half-space will be, respectively, $\hat{T}(\omega)$ and zero . Here $\hat{T}(\omega)$ is the transmission response of the medium, and there is no upgoing wave in the lower half-space by the radiation boundary condition. Thus, if we initialize the waves $\hat{D}_{N+1}(\omega)$ and $\hat{U}_{N+1}(\omega)$ in the lower half-space to one and zero, respectively, and multiply the wave vector $\begin{bmatrix}\hat{D}_{N+1}(\omega)\\ \hat{U}_{N+1}(\omega)\end{bmatrix}$ by the layer matrices for layers N, N-1, ...2, 1 in succession, we get the wave vector

$$\begin{bmatrix}\hat{D}_0(\omega)\\ \hat{U}_0(\omega)\end{bmatrix} = \begin{bmatrix}1/\hat{T}(\omega)\\ \hat{R}(\omega)/\hat{T}(\omega)\end{bmatrix} . \qquad (5\text{-}3)$$

Dividing $\hat{U}_0(\omega)$ by $\hat{D}_0(\omega)$ then gives the medium reflection response $\hat{R}(\omega)$.

In FOR1 the subroutine RECOPP, which is taken from Kind (1976),

implements the above procedure. It is then necessary to take the inverse Fourier transform of $\hat{R}(\omega)$ in order to get the time response R(t). This is accomplished by using an FFT algorithm taken from Oppenheim and Schafer (1975, p. 332) to implement a discrete inverse Fourier transform of $\hat{R}(\omega)$, which is computed at 2^m integer multiples of $\Delta\omega$ by RECOPP. Since R(t) is real, doubling the real part of the discrete inverse Fourier transform gives the desired time response at 2^m integer multiples of $\Delta t = 2\pi/(2^m\Delta\omega)$.

Since the impulse response of a discrete layered medium contains sharp peaks, computing it at discrete time instants runs the risk of missing some of the peaks. To avoid this, and to make the computation of the inverse Fourier transform more stable, the program FOR1 actually computes the integrated impulse response $\hat{R}(\omega)/j\omega$, takes the inverse Fourier transform of this, and then takes differences of the result. This results in the computation of $\{R_n\}$, where

$$R_n = \int_{n\Delta t}^{(n+1)\Delta t} R(t)dt \ . \qquad (5\text{-}4)$$

The major disadvantage in using FOR1 is the inverse Fourier transform required. Since the frequency response is only computed up to $\omega_f = 2^m \Delta\omega = 2\pi/\Delta t$, the resulting computed time response is bandlimited. Indeed, FOR1 actually computes the sinc response of the medium, i.e., the response of the medium to the probing function $(\sin \omega_f t)/\omega_f t$. This results in the peaks in the time response being broadened, or smeared. Since accurate strengths of the primary reflections are essential to the layer stripping algorithms, this is potentially a serious matter. However, the performance of the algorithms did not seem to be excessively hampered

by this. Gibbs phenomenon (side lobes or peaks due to the oscillation of the sinc function) was also observed, but proved to be relatively insignificant.

BREM

In the program BREM the response of the medium is computed directly in the time domain, so that an inverse Fourier transform is not needed. This is indeed a significant improvement over FOR1; since BREM requires much less computation time than FOR1, most of the forward runs in this chapter were performed with BREM. However, the absence of higher-order multiple reflections in the output of BREM was found to be troublesome for large reflection coefficients.

BREM constructs the time response of a layered medium directly in the time domain by ray theory. Each primary reflection is accounted for by computing the two-way travel time to each interface, and assigning to that time in the medium time response a reflection strength proportional to the reflection coefficient at that interface. Second-order multiple reflections are handled similarly, using two nested DO loops to compute them all. The amount of computation required for this is $O(N^3)$, which is manageable. However, computation of the third-order multiple reflections would require $O(N^5)$ operations, and the strength of each such reflection would be proportional to the product of five reflection coefficients. This is so weak that in general it is not worth computing. Thus BREM computes only the first two terms of the Bremmer series of the time response of the layered medium.

Comparison of the performances of FOR1 and BREM

The performances of FOR1 and BREM are most easily compared by running the same inversion algorithm on the outputs of both of them. If

all other factors are equal, the closer the reconstructed medium is to the actual medium, the closer the computed forward response must be to the actual forward response of the medium. Figures 5.1a and 5.1b show the results of computer runs of FOR1 and BREM, both of which were then inverted using the inversion program INVDISC (which is described below in Section 5.2.2). Note that both forward programs (and, of course, the inversion program) performed quite well, since the reconstructed medium almost matches the actual medium.

However, if the number of points at which the frequency and time responses are computed is reduced, FOR1 begins to break down. Figures 5.2a and 5.2b compare FOR1 and BREM on the same medium as Figures 5.1--the only difference is that the medium responses are computed at 256 points instead of 512. Note that FOR1 is breaking down badly while BREM is still working. Figures 5.3a and 5.3b show another cause of breakdown for FOR1 that does not affect BREM--large primary reflections have their peaks smeared by the inverse Fourier transform, so that the reflection coefficients read by the algorithm are too small.

On the other hand, large reflection coefficients can also cause problems for BREM, due to the absence of high-order multiple reflections in BREM's output. Figure 5.4 shows an example of this. The missing higher-order multiple reflections constitute a form of noise, and at the ninth layer the inversion algorithm breaks down.

5.2.2 Inversion Algorithms

Two different layer stripping algorithm computer programs were written. One, INV1, utilized the updates (4-40) - (4-41) for a continuous layered medium. The other, INVDISC, utilized the slightly

depth	cact	ccomp	rhoact	rhocomp	rc1	rc2
0.05	5.0000	4.9992	5.0000	5.0078	0.0007	0.0006
0.10	5.1000	5.1102	4.9000	4.8959	0.0061	0.0145
0.15	5.1000	5.1086	4.9000	4.9049	0.0007	0.0005
0.20	5.2000	5.2122	4.8000	4.8048	0.0060	0.0147
0.25	5.2000	5.2113	4.8000	4.8126	0.0007	0.0006
0.30	5.3000	5.3171	4.7000	4.7096	0.0059	0.0159
0.35	5.3000	5.3173	4.7000	4.7152	0.0006	0.0007
0.40	5.3000	5.2998	4.6000	4.6520	-0.0095	-0.0113
0.45	5.3000	5.3013	4.6000	4.6560	0.0007	0.0008
0.50	5.3000	5.3060	4.5000	4.5430	-0.0115	-0.0111
0.55	5.3000	5.3061	4.5000	4.5498	0.0007	0.0008
0.60	5.4000	5.4058	4.5000	4.5517	0.0161	0.0265
0.65	5.4000	5.4055	4.5000	4.5579	0.0006	0.0006
0.70	5.5000	5.5155	4.5000	4.5648	0.0184	0.0314
0.75	5.5000	5.5119	4.5000	4.5761	0.0007	0.0002
0.80	5.4000	5.4291	4.4000	4.4361	-0.0288	-0.0387
0.85	5.4000	5.4300	4.4000	4.4424	0.0009	0.0009
0.90	5.3000	5.3133	4.3000	4.3626	-0.0277	-0.0400
0.95	5.3000	5.3196	4.3000	4.3606	0.0008	0.0014
1.00	5.2000	5.1918	4.2000	4.2916	-0.0282	-0.0401
1.05	5.2000	5.1939	4.2000	4.2955	0.0008	0.0010
1.10	5.1000	5.1292	4.1000	4.1391	-0.0287	-0.0342
1.15	5.1000	5.1263	4.1000	4.1493	0.0008	0.0005
1.20	5.1000	4.9996	4.1000	4.0995	-0.0259	-0.0356
1.25	5.0000	5.0014	4.0000	4.1027	0.0007	0.0008
1.30	5.0000	5.0009	4.0000	4.1086	0.0006	0.0006
1.35	5.0000	5.0012	4.0000	4.1137	0.0007	0.0007
1.40	5.0000	5.0008	4.0000	4.1196	0.0007	0.0006
1.45	5.0000	5.0006	4.0000	4.1254	0.0007	0.0006
1.50	5.0000	5.0003	4.0000	4.1313	0.0007	0.0007

5.1a Result of running the frequency-domain method forward program FOR1 with the inverse program INVDISC, using 512 points.

n=15 m= 9 dd=0.100 del=0.050 dt=0.00250 p1=0.12 p2=0.15

depth	cact	ccomp	rhoact	rhocomp	r1	rc1	r2	rc2
0.00	5.0000	5.0000	5.0000	5.0000	0.0000	0.0000	0.0000	0.0000
0.05	5.0000	5.0000	5.0000	5.0000	0.0000	0.0000	0.0000	0.0000
0.10	5.1000	5.1000	4.9000	4.9000	0.0055	0.0055	0.0131	0.0131
0.15	5.1000	5.1000	4.9000	4.9000	0.0000	0.0000	0.0000	0.0000
0.20	5.2000	5.2000	4.8000	4.8000	0.0054	0.0054	0.0138	0.0138
0.25	5.2000	5.2000	4.8000	4.8000	0.0000	0.0000	0.0000	0.0000
0.30	5.3000	5.3000	4.7000	4.7000	0.0053	0.0053	0.0146	0.0146
0.35	5.3000	5.3000	4.7000	4.7000	0.0000	0.0000	0.0000	0.0000
0.40	5.3000	5.3000	4.6000	4.6000	-0.0108	-0.0108	-0.0108	-0.0108
0.45	5.3000	5.3000	4.6000	4.6000	0.0000	0.0000	0.0000	0.0000
0.50	5.3000	5.3000	4.5000	4.5000	-0.0110	-0.0110	-0.0110	-0.0110
0.55	5.3000	5.3000	4.5000	4.5000	0.0000	0.0000	0.0000	0.0000
0.60	5.4000	5.4000	4.5000	4.5000	0.0159	0.0159	0.0263	0.0263
0.65	5.4000	5.4000	4.5000	4.5000	0.0000	0.0000	0.0000	0.0000
0.70	5.5000	5.5000	4.5000	4.5001	0.0160	0.0160	0.0277	0.0277
0.75	5.5000	5.5000	4.5000	4.5001	0.0000	0.0000	0.0000	0.0000
0.80	5.4000	5.4001	4.4000	4.3999	-0.0273	-0.0273	-0.0389	-0.0389
0.85	5.4000	5.4000	4.4000	4.4001	0.0000	0.0000	0.0000	0.0000
0.90	5.3000	5.2999	4.3000	4.3001	-0.0274	-0.0274	-0.0377	-0.0377
0.95	5.3000	5.3000	4.3000	4.3000	0.0000	0.0000	0.0000	0.0000
1.00	5.2000	5.2012	4.2000	4.1984	-0.0276	-0.0276	-0.0368	-0.0367
1.05	5.2000	5.2012	4.2000	4.1984	0.0000	0.0000	0.0000	0.0000
1.10	5.1000	5.1013	4.1000	4.0984	-0.0278	-0.0277	-0.0361	-0.0361
1.15	5.1000	5.1018	4.1000	4.0978	0.0000	0.0000	0.0000	0.0000
1.20	5.0000	5.0040	4.0000	3.9954	-0.0280	-0.0279	-0.0356	-0.0354
1.25	5.0000	5.0031	4.0000	3.9966	0.0000	0.0000	0.0000	-0.0001
1.30	5.0000	5.0037	4.0000	3.9956	0.0000	0.0000	0.0000	0.0000
1.35	5.0000	5.0036	4.0000	3.9955	0.0000	0.0000	0.0000	0.0000
1.40	5.0000	5.0043	4.0000	3.9946	0.0000	0.0000	0.0000	0.0001
1.45	5.0000	5.0043	4.0000	3.9942	0.0000	0.0000	0.0000	0.0000
1.50	5.0000	5.0046	4.0000	3.9939	0.0000	0.0000	0.0000	0.0000

5.1b Result of running the time-domain method forward program BREM with INVDISC. Both forward programs work well if 512 points are used.

depth	cact	ccomp	rhoact	rhocomp	rc1	rc2
0.05	5.0000	5.0002	5.0000	5.0122	0.0012	0.0013
0.10	5.1000	5.0996	4.9000	4.9303	0.0073	0.0149
0.15	5.1000	5.0964	4.9000	4.9463	0.0011	0.0009
0.20	5.2000	5.2037	4.8000	4.8493	0.0070	0.0159
0.25	5.2000	5.2025	4.8000	4.8623	0.0011	0.0010
0.30	5.3000	5.2931	4.7000	4.7903	0.0069	0.0153
0.35	5.3000	5.4032	4.7000	4.6387	0.0014	0.0128
0.40	5.3000	5.4139	4.6000	4.5263	-0.0106	-0.0094
0.45	5.3000	5.4043	4.6000	4.5589	0.0020	0.0010
0.50	5.3000	5.4018	4.5000	4.4741	-0.0098	-0.0100
0.55	5.3000	5.2934	4.5000	4.6466	0.0017	-0.0095
0.60	5.4000	5.3301	4.5000	4.7442	0.0162	0.0198
0.65	5.4000	5.3977	4.5000	4.6589	0.0017	0.0088
0.70	5.5000	5.5059	4.5000	4.6545	0.0169	0.0295
0.75	5.5000	5.6876	4.5000	4.4027	0.0018	0.0273
0.80	5.4000	5.5895	4.4000	4.3211	-0.0254	-0.0399
0.85	5.4000	5.4538	4.4000	4.3209	-0.0219	-0.0392
0.90	5.3000	5.3070	4.3000	4.3434	-0.0208	-0.0366
0.95	5.3000	4.8682	4.3000	4.9505	-0.0034	-0.0383
1.00	5.2000	4.7211	4.2000	4.9051	-0.0275	-0.0364
1.05	5.2000	4.7024	4.2000	4.9519	0.0018	0.0008
1.10	5.1000	4.6029	4.1000	4.8362	-0.0273	-0.0326
1.15	5.1000	4.4282	4.1000	5.1162	0.0007	-0.0076
1.20	5.1000	3.8826	4.1000	6.0289	-0.0054	-0.0256
1.25	5.0000	3.8730	4.0000	6.0640	0.0013	0.0010
1.30	5.0000	3.8780	4.0000	6.0700	0.0013	0.0015
1.35	5.0000	3.8820	4.0000	6.0772	0.0013	0.0014
1.40	5.0000	3.8850	4.0000	6.0875	0.0013	0.0014
1.45	5.0000	3.8866	4.0000	6.1008	0.0014	0.0014
1.50	5.0000	3.8904	4.0000	6.1092	0.0013	0.0014

5.2a Result of running FOR1 with INVDISC on the medium used in Figure 5.1, using 256 points.

n=15 m= 8 dd=0.100 del=0.050 dt=0.00500 r1=0.12 r2=0.15

depth	cact	ccomp	rhoact	rhocomp	r1	rc1	r2	rc2
0.00	5.0000	5.0000	5.0000	5.0000	0.0000	0.0000	0.0000	0.0000
0.05	5.0000	5.0000	5.0000	5.0000	0.0000	0.0000	0.0000	0.0000
0.10	5.1000	5.1000	4.9000	4.9000	0.0055	0.0055	0.0131	0.0131
0.15	5.1000	5.1000	4.9000	4.9000	0.0000	0.0000	0.0000	0.0000
0.20	5.2000	5.2000	4.8000	4.8000	0.0054	0.0054	0.0138	0.0138
0.25	5.2000	5.2000	4.8000	4.8000	0.0000	0.0000	0.0000	0.0000
0.30	5.3000	5.3000	4.7000	4.7000	0.0053	0.0053	0.0146	0.0146
0.35	5.3000	5.3000	4.7000	4.7000	0.0000	0.0000	0.0000	0.0000
0.40	5.3000	5.3000	4.6000	4.6000	-0.0108	-0.0108	-0.0108	-0.0108
0.45	5.3000	5.3000	4.6000	4.6000	0.0000	0.0000	0.0000	0.0000
0.50	5.3000	5.3000	4.5000	4.5000	-0.0110	-0.0110	-0.0110	-0.0110
0.55	5.3000	5.3000	4.5000	4.5000	0.0000	0.0000	0.0000	0.0000
0.60	5.4000	5.4000	4.5000	4.5000	0.0159	0.0159	0.0263	0.0263
0.65	5.4000	5.4000	4.5000	4.5000	0.0000	0.0000	0.0000	0.0000
0.70	5.5000	5.5000	4.5000	4.5000	0.0160	0.0160	0.0277	0.0277
0.75	5.5000	5.4999	4.5000	4.5002	0.0000	0.0000	0.0000	0.0000
0.80	5.4000	5.3999	4.4000	4.4001	-0.0273	-0.0273	-0.0389	-0.0389
0.85	5.4000	5.3992	4.4000	4.4011	0.0000	0.0000	0.0000	-0.0001
0.90	5.3000	5.2992	4.3000	4.3010	-0.0274	-0.0274	-0.0377	-0.0377
0.95	5.3000	5.2996	4.3000	4.3005	0.0000	0.0000	0.0000	0.0000
1.00	5.2000	5.1995	4.2000	4.2007	-0.0276	-0.0276	-0.0368	-0.0368
1.05	5.2000	5.1981	4.2000	4.2025	0.0000	0.0000	0.0000	-0.0001
1.10	5.1000	5.0978	4.1000	4.1028	-0.0278	-0.0278	-0.0361	-0.0361
1.15	5.1000	5.0982	4.1000	4.1023	0.0000	0.0000	0.0000	0.0000
1.20	5.0000	4.9977	4.0000	4.0028	-0.0280	-0.0280	-0.0356	-0.0356
1.25	5.0000	4.9981	4.0000	4.0023	0.0000	0.0000	0.0000	0.0000
1.30	5.0000	4.9961	4.0000	4.0049	0.0000	0.0000	0.0000	-0.0001
1.35	5.0000	4.9950	4.0000	4.0063	0.0000	0.0000	0.0000	-0.0001
1.40	5.0000	4.9964	4.0000	4.0042	0.0000	0.0000	0.0000	0.0000
1.45	5.0000	4.9951	4.0000	4.0062	0.0000	0.0000	0.0000	0.0000
1.50	5.0000	4.9966	4.0000	4.0039	0.0000	0.0000	0.0000	0.0001

5.2b Result of running BREM with INVDISC on the medium used in Figure 5.1, using 256 points. FOR1 is breaking down while BREM is still working.

depth	cact	ccomp	rhoact	rhocomp	rc1	rc2
0.10	5.2000	5.1905	4.8000	4.8215	0.0018	0.0071
0.20	5.4000	5.4064	4.6000	4.6174	0.0003	0.0067
0.30	5.5000	5.4746	4.8000	4.8736	0.0338	0.0359
0.40	5.5000	5.4816	4.8000	4.8787	0.0012	0.0014
0.50	5.5000	5.4913	4.8000	4.8815	0.0012	0.0016
0.60	5.7000	5.5613	5.0000	5.2399	0.0422	0.0445
0.70	5.7000	5.6242	5.2000	5.3810	0.0194	0.0215
0.80	5.5000	5.4067	5.4000	5.6246	0.0008	-0.0062
0.90	5.3000	5.1843	5.6000	5.8765	-0.0007	-0.0073
1.00	5.0000	4.8898	5.3000	5.6246	-0.0531	-0.0610
1.10	4.8000	4.8308	5.0000	5.1525	-0.0502	-0.0517
1.20	4.6000	4.6100	4.8000	4.9970	-0.0401	-0.0454
1.30	4.5000	4.6843	4.5000	4.5037	-0.0435	-0.0417
1.40	4.5000	4.6783	4.5000	4.5217	0.0013	0.0012
1.50	4.5000	4.6759	4.5000	4.5362	0.0013	0.0013

5.3a Result of running FOR1 with INVDISC on a more sharply varying medium than the one used in Figures 5.1 and 5.2.

depth	cact	ccomp	rhoact	rhocomp	rc1	rc2
0.10	5.2000	5.2000	4.8000	4.8000	0.0006	0.0061
0.20	5.4000	5.4000	4.6000	4.6000	-0.0010	0.0050
0.30	5.5000	5.5000	4.8000	4.8000	0.0312	0.0343
0.40	5.5000	5.5000	4.8000	4.8000	0.0000	0.0000
0.50	5.5000	5.5000	4.8000	4.8000	0.0000	0.0000
0.60	5.7000	5.7000	5.0000	5.0000	0.0398	0.0464
0.70	5.7000	5.7000	5.2000	5.2000	0.0196	0.0196
0.80	5.5000	5.4998	5.4000	5.4002	-0.0005	-0.0072
0.90	5.3000	5.2997	5.6000	5.6003	-0.0018	-0.0080
1.00	5.0000	4.9996	5.3000	5.3004	-0.0587	-0.0671
1.10	4.8000	4.7998	5.0000	5.0002	-0.0508	-0.0559
1.20	4.6000	4.6011	4.8000	4.7981	-0.0430	-0.0477
1.30	4.5000	4.5026	4.5000	4.4966	-0.0438	-0.0461
1.40	4.5000	4.5024	4.5000	4.4968	0.0000	0.0000
1.50	4.5000	4.5015	4.5000	4.4977	0.0000	0.0000

5.3b Result of running BREM with INVDISC on the medium used in Figure 5.3a. FOR1 has trouble synthesizing the larger primary reflections, while BREM does not.

depth	cact	ccomp	rhoact	rhocomp	rc1	rc2
0.10	5.5000	5.5000	5.5000	5.5000	0.0985	0.1723
0.20	6.0000	6.0000	6.0000	6.0000	0.0907	0.2135
0.30	5.5000	5.5451	5.5000	5.4517	-0.0907	-0.2053
0.40	5.0000	5.0729	5.0000	4.9232	-0.0985	-0.1717
0.50	5.0000	5.0899	5.0000	4.9056	0.0000	0.0022
0.60	5.0000	5.0897	5.0000	4.9063	0.0000	0.0000
0.70	4.5000	4.6191	5.5000	5.3509	-0.0082	-0.0601
0.80	4.0000	4.1681	6.0000	5.7465	-0.0183	-0.0552
0.90	4.0000	3.5158	6.5000	7.4288	0.0400	0.0008
1.00	4.5000	4.1695	7.0000	7.5816	0.0984	0.1371
1.10	4.0000	3.5380	7.0000	7.9433	-0.0619	-0.0998
1.20	3.5000	3.1776	6.5000	8.8867	0.0009	-0.0159
1.30	3.0000	3.2900	6.0000	8.5729	-0.0001	0.0048
1.40	3.0000	3.1303	6.0000	9.0136	-0.0005	-0.0073
1.50	3.0000	3.0826	6.0000	9.1655	0.0005	-0.0015
1.60	3.0000	3.3306	6.0000	8.4063	-0.0035	0.0071
1.70	3.0000	3.4560	6.0000	8.0691	-0.0014	0.0045
1.80	3.0000	3.6155	6.0000	7.7067	0.0003	0.0084
1.90	3.0000	3.7153	6.0000	7.4817	-0.0007	0.0047
2.00	3.0000	3.7111	6.0000	7.4881	-0.0002	-0.0004
2.10	3.0000	3.7230	6.0000	7.4622	-0.0001	0.0006
2.20	3.0000	3.7323	6.0000	7.4410	-0.0001	0.0004
2.30	3.0000	3.7415	6.0000	7.4208	-0.0001	0.0004
2.40	3.0000	3.7574	6.0000	7.3881	0.0000	0.0009
2.50	3.0000	3.7523	6.0000	7.3989	0.0000	-0.0003

5.4 Result of running BREM with INVDISC on a sharply varying medium. The failure of BREM to generate tertiary reflections (second-order multiple reflections) causes errors.

more complicated updates (4-50) for a discrete layered medium. Otherwise, both algorithms were the same. The discrete wave updates (3-83) were used for both algorithms, so that each step of the algorithm would constitute a Givens rotation of the normalized waves. Actually, the effect of transmission losses for the media used in these runs is less than one part in a thousand.

Modification of the algorithms

The results of running these two algorithms showed immediately that one modification was necessary. Although Bultheel (1979) proved that the fast Cholesky algorithm was backward stable, the algorithm used for the non-normal incidence inverse problem is not, strictly speaking, the fast Cholesky algorithm (although the two algorithms are quite similar). The main difference is that the computed wave speed in a layer must be used to project ahead to the arrival time of the next primary reflection. That this is a potential source of instability may be seen as follows.

In running the algorithm on a computer, time, as well as depth, must be discretized. Suppose that the actual arrival time of a primary reflection is $t = (n + \frac{1}{2} - \varepsilon)\Delta t$, where Δt is the discretization time. Then the arrival time of the reflection will be rounded down to $n\Delta t$. Now suppose that due to a slight error in the last reconstructed value of wave speed, the projected time of arrival of this primary reflection (i.e., the time at which the algorithm will look for this reflection) is $t = (n + \frac{1}{2} + \varepsilon)\Delta t$. This time will be rounded up to $(n + 1)\Delta t$, and even though the error in time is only $2\varepsilon\Delta t$, the algorithm will miss this primary reflection.

This instability can be fixed by having the algorithm read the

upgoing wave at not only the projected time $n\Delta t$, but at the previous and following times $(n-1)\Delta t$ and $(n+1)\Delta t$, respectively. Summing these three values of the upgoing wave makes it very unlikely that the primary reflection will be missed, unless the computed wave speed is in considerable error. Summing three values of the upgoing wave also helps compensate for the spreading of the reflected wave itself due to bandlimitation of the computed medium response. Note that there is no danger of adding in a multiple reflection from previous layers, since all of the succeeding multiple reflections from the previous layers have been eliminated by the algorithm.

Figures 5.5 show that this modification works well. BREM was used to generate the forward response of the given medium, and INV1 was used to invert this response, first without the modification (Figure 5.5a), then with it (Figure 5.5b). Note that without the modification the algorithm misses the primary reflection from the sixth interface (the computed reflection coefficient rc2 is zero) and breaks down completely, while with the modification it works fairly well through forty layers.

One problem encountered by employing this modification is worth noting. Near a turning point, the vertical wave speed becomes very large, and the time differences between primary reflections become very small. If the time difference over which the algorithm projects to look for the next primary reflection becomes less than $3\Delta t$, it is possible for the algorithm to read the same primary reflection twice! An example of this double reading is shown in Figure 5.6, in the twelfth and in several succeeding layers.

The conditions under which this double reading becomes possible can be derived as follows. The layer thickness Δz divided by the

n=50 m= 9 dd=0.100 del=0.100 dt=0.00500 r1=0.12 r2=0.15

depth	cact	ccomp	rhoact	rhocomp	r1	rc1	r2	rc2
0.00	5.0000	5.0000	5.0000	5.0000	0.0000	0.0000	0.0000	0.0000
0.10	4.9500	4.9500	5.0000	5.0000	-0.0078	-0.0078	-0.0113	-0.0113
0.20	4.9000	4.9000	5.1000	5.1000	0.0021	0.0021	-0.0013	-0.0013
0.30	4.8000	4.8000	5.2000	5.2000	-0.0059	-0.0059	-0.0122	-0.0122
0.40	4.7000	4.7000	5.3000	5.3000	-0.0061	-0.0061	-0.0119	-0.0119
0.50	4.6500	4.6500	5.4000	5.4000	0.0015	0.0015	-0.0012	-0.0012
0.60	4.6000	4.6000	5.5000	5.5000	0.0014	0.0014	-0.0012	-0.0012
0.70	4.5500	4.5500	5.6000	5.6000	0.0012	0.0012	-0.0013	-0.0013
0.80	4.5000	4.5000	5.7000	5.7000	0.0010	0.0010	-0.0014	-0.0014
0.90	4.4500	4.4500	5.8000	5.8000	0.0009	0.0008	-0.0015	-0.0015
1.00	4.4000	4.4000	5.9000	5.9000	0.0007	0.0007	-0.0016	-0.0016
1.10	4.3500	4.3500	6.0000	6.0000	0.0005	0.0005	-0.0016	-0.0016
1.20	4.3000	4.3000	6.1000	6.1000	0.0003	0.0004	-0.0017	-0.0017
1.30	4.2500	4.2500	6.2000	6.2000	0.0002	0.0002	-0.0018	-0.0018
1.40	4.2000	4.2000	6.3000	6.3000	0.0000	0.0000	-0.0019	-0.0019
1.50	4.2000	4.2000	6.4000	6.4000	0.0079	0.0079	0.0079	0.0079
1.60	4.2000	4.2000	6.5000	6.5000	0.0077	0.0078	0.0077	0.0078
1.70	4.2500	4.2500	6.6000	6.6000	0.0156	0.0156	0.0175	0.0175
1.80	4.3000	4.3000	6.7000	6.6999	0.0154	0.0155	0.0174	0.0174
1.90	4.3500	4.3500	6.8000	6.7998	0.0153	0.0153	0.0174	0.0174
2.00	4.4000	4.3999	6.9000	6.9000	0.0152	0.0152	0.0173	0.0173
2.10	4.4500	4.4500	7.0000	6.9999	0.0151	0.0151	0.0173	0.0173
2.20	4.5000	4.5005	7.1000	7.0983	0.0149	0.0149	0.0173	0.0173
2.30	4.5500	4.5504	7.2000	7.1986	0.0148	0.0148	0.0172	0.0172
2.40	4.5500	4.5510	7.2000	7.1972	0.0000	0.0000	0.0000	0.0000
2.50	4.6000	4.6008	7.3000	7.2979	0.0147	0.0147	0.0172	0.0172
2.60	4.6500	4.6505	7.4000	7.3986	0.0146	0.0146	0.0172	0.0172
2.70	4.7000	4.7004	7.5000	7.4989	0.0145	0.0145	0.0172	0.0172
2.80	4.8000	4.8002	7.4000	7.3997	0.0089	0.0089	0.0147	0.0147
2.90	4.9000	4.9003	7.3000	7.2997	0.0088	0.0088	0.0151	0.0151
3.00	5.0000	5.0003	7.2000	7.2000	0.0087	0.0087	0.0156	0.0156
3.10	5.1000	5.0998	7.1000	7.1010	0.0087	0.0087	0.0162	0.0162
3.20	5.2000	5.1996	7.0000	7.0016	0.0086	0.0086	0.0170	0.0170
3.30	5.2500	5.2496	6.9000	6.9013	0.0007	0.0007	0.0052	0.0052
3.40	5.3000	5.2995	6.8000	6.8016	0.0006	0.0006	0.0054	0.0054
3.50	5.3500	5.3496	6.7000	6.7013	0.0005	0.0005	0.0056	0.0056
3.60	5.4000	5.3452	6.6000	6.7165	0.0004	0.0004	0.0058	0.0000
3.70	5.4500	5.4014	6.5000	6.5975	0.0004	0.0000	0.0060	0.0060
3.80	5.5000	5.4543	6.4000	6.4902	0.0003	0.0003	0.0063	0.0063
3.90	5.5500	5.4526	6.3000	6.4964	0.0002	0.0002	0.0066	0.0000
4.00	5.6000	5.4514	6.2000	6.5006	0.0001	0.0001	0.0069	0.0000
4.10	5.5500	5.4511	6.1000	6.5010	-0.0162	0.0000	-0.0230	0.0000
4.20	5.5000	5.5806	6.0000	6.0347	-0.0163	-0.0163	-0.0227	0.0000
4.30	5.4500	5.5806	5.9000	6.0347	-0.0164	0.0000	-0.0224	0.0000
4.40	5.4000	5.6928	5.8000	5.6279	-0.0165	-0.0165	-0.0222	0.0000
4.50	5.3500	5.6590	5.7000	5.5047	-0.0167	-0.0166	-0.0220	-0.0219
4.60	5.3000	5.6589	5.6000	5.5052	-0.0168	0.0000	-0.0218	0.0000
4.70	5.3500	5.6582	5.5000	5.5071	-0.0011	0.0001	0.0040	0.0000
4.80	5.4000	5.6588	5.4000	5.5061	-0.0012	0.0000	0.0041	0.0001
4.90	5.4000	5.6592	5.4000	5.5057	0.0000	0.0000	0.0000	0.0001
5.00	5.4000	5.6592	5.4000	5.5061	0.0000	0.0000	0.0000	0.0000

5.5a Result of running BREM with INVDISC while reading the reflection coefficient from a single value of the upgoing wave. Errors in the computed wave speeds soon cause the algorithm to miss primary reflections.

n=50 m= 9 dd=0.100 del=0.100 dt=0.00500 r1=0.12 r2=0.15

depth	cact	ccomp	rhoact	rhocomp	r1	rc1	r2	rc2
0.00	5.0000	5.0000	5.0000	5.0000	0.0000	0.0000	0.0000	0.0000
0.10	4.9500	4.9500	5.0000	5.0000	-0.0078	-0.0078	-0.0113	-0.0113
0.20	4.9000	4.9000	5.1000	5.1000	0.0021	0.0021	-0.0013	-0.0013
0.30	4.8000	4.8000	5.2000	5.2000	-0.0059	-0.0059	-0.0122	-0.0122
0.40	4.7000	4.7000	5.3000	5.3000	-0.0061	-0.0061	-0.0119	-0.0119
0.50	4.6500	4.6500	5.4000	5.4000	0.0015	0.0015	-0.0012	-0.0012
0.60	4.6000	4.6000	5.5000	5.5000	0.0014	0.0014	-0.0012	-0.0012
0.70	4.5500	4.5500	5.6000	5.6000	0.0012	0.0012	-0.0013	-0.0013
0.80	4.5000	4.5000	5.7000	5.7000	0.0010	0.0010	-0.0014	-0.0014
0.90	4.4500	4.4500	5.8000	5.8000	0.0009	0.0008	-0.0015	-0.0015
1.00	4.4000	4.4000	5.9000	5.9000	0.0007	0.0007	-0.0016	-0.0016
1.10	4.3500	4.3500	6.0000	6.0000	0.0005	0.0005	-0.0016	-0.0016
1.20	4.3000	4.3000	6.1000	6.1000	0.0003	0.0004	-0.0017	-0.0017
1.30	4.2500	4.2500	6.2000	6.2000	0.0002	0.0002	-0.0018	-0.0018
1.40	4.2000	4.2000	6.3000	6.3000	0.0000	0.0000	-0.0019	-0.0019
1.50	4.2000	4.2000	6.4000	6.4000	0.0079	0.0079	0.0079	0.0079
1.60	4.2000	4.2000	6.5000	6.5000	0.0077	0.0078	0.0077	0.0078
1.70	4.2500	4.2500	6.6000	6.6000	0.0156	0.0156	0.0175	0.0175
1.80	4.3000	4.3001	6.7000	6.6998	0.0154	0.0155	0.0174	0.0175
1.90	4.3500	4.3501	6.8000	6.7997	0.0153	0.0153	0.0174	0.0174
2.00	4.4000	4.4003	6.9000	6.8992	0.0152	0.0152	0.0173	0.0173
2.10	4.4500	4.4505	7.0000	6.9985	0.0151	0.0151	0.0173	0.0173
2.20	4.5000	4.5006	7.1000	7.0983	0.0149	0.0149	0.0173	0.0173
2.30	4.5500	4.5506	7.2000	7.1980	0.0148	0.0148	0.0172	0.0172
2.40	4.5500	4.5510	7.2000	7.1970	0.0000	0.0000	0.0000	0.0000
2.50	4.6000	4.6012	7.3000	7.2965	0.0147	0.0147	0.0172	0.0172
2.60	4.6500	4.6512	7.4000	7.3966	0.0146	0.0146	0.0172	0.0172
2.70	4.7000	4.7010	7.5000	7.4969	0.0145	0.0145	0.0172	0.0172
2.80	4.8000	4.8011	7.4000	7.3968	0.0089	0.0089	0.0147	0.0147
2.90	4.9000	4.9013	7.3000	7.2965	0.0088	0.0088	0.0151	0.0151
3.00	5.0000	5.0012	7.2000	7.1971	0.0087	0.0087	0.0156	0.0156
3.10	5.1000	5.1008	7.1000	7.0981	0.0087	0.0087	0.0162	0.0162
3.20	5.2000	5.2005	7.0000	6.9987	0.0086	0.0086	0.0170	0.0170
3.30	5.2500	5.2505	6.9000	6.8988	0.0007	0.0007	0.0052	0.0052
3.40	5.3000	5.3005	6.8000	6.7988	0.0006	0.0006	0.0054	0.0054
3.50	5.3500	5.3505	6.7000	6.6990	0.0005	0.0005	0.0056	0.0056
3.60	5.4000	5.4003	6.6000	6.5993	0.0004	0.0004	0.0058	0.0058
3.70	5.4500	5.4503	6.5000	6.4993	0.0004	0.0004	0.0060	0.0060
3.80	5.5000	5.5003	6.4000	6.3994	0.0003	0.0003	0.0063	0.0063
3.90	5.5500	5.5502	6.3000	6.2996	0.0002	0.0002	0.0066	0.0066
4.00	5.6000	5.6002	6.2000	6.1997	0.0001	0.0001	0.0069	0.0069
4.10	5.5500	5.5500	6.1000	6.1001	-0.0162	-0.0162	-0.0230	-0.0231
4.20	5.5000	5.5002	6.0000	5.9996	-0.0163	-0.0164	-0.0227	-0.0227
4.30	5.4500	5.4502	5.9000	5.8995	-0.0164	-0.0164	-0.0224	-0.0224
4.40	5.4000	5.4002	5.8000	5.7996	-0.0165	-0.0165	-0.0222	-0.0222
4.50	5.3500	5.3496	5.7000	5.7006	-0.0167	-0.0167	-0.0220	-0.0221
4.60	5.3000	5.2994	5.6000	5.6008	-0.0168	-0.0168	-0.0218	-0.0218
4.70	5.3500	5.3495	5.5000	5.5005	-0.0011	-0.0011	0.0040	0.0040
4.80	5.4000	5.3990	5.4000	5.4015	-0.0012	-0.0012	0.0041	0.0041
4.90	5.4000	5.3992	5.4000	5.4012	0.0000	0.0000	0.0000	0.0000
5.00	5.4000	5.3992	5.4000	5.4013	0.0000	0.0000	0.0000	0.0000

5.5b Result of running BREM with INVDISC while reading the reflection coefficient from three neighboring values of the upgoing wave. This corrects the instability revealed in Figure 5.5a.

depth	cact	ccomp	rhoact	rhocomp	r1	rc1	r2	rc2
0.00	5.0000	5.0000	5.0000	5.0000	0.0000	0.0000	0.0000	0.0000
0.03	5.0000	5.0000	5.0000	5.0000	0.0000	0.0000	0.0000	0.0000
0.05	5.0000	5.0000	5.0000	5.0000	0.0000	0.0000	0.0000	0.0000
0.08	5.0000	5.0000	5.0000	5.0000	0.0000	0.0000	0.0000	0.0000
0.10	5.1000	5.1000	4.9000	4.8997	0.0005	0.0004	0.0032	0.0032
0.13	5.1000	5.1000	4.9000	4.8997	0.0000	0.0000	0.0000	0.0000
0.15	5.1000	5.1000	4.9000	4.8997	0.0000	0.0000	0.0000	0.0000
0.18	5.1000	5.1000	4.9000	4.8997	0.0000	0.0000	0.0000	0.0000
0.20	5.2000	5.2000	4.8000	4.7995	0.0001	0.0001	0.0029	0.0029
0.23	5.2000	5.2000	4.8000	4.7995	0.0000	0.0000	0.0000	0.0000
0.25	5.2000	5.2000	4.8000	4.7995	0.0000	0.0000	0.0000	0.0000
0.28	5.2000	5.2890	4.8000	4.7128	0.0000	0.0000	0.0000	0.0026
0.30	5.3000	5.3862	4.7000	4.6183	-0.0003	-0.0003	0.0026	0.0026
0.33	5.3000	5.3862	4.7000	4.6183	0.0000	0.0000	0.0000	0.0000
0.35	5.3000	5.3862	4.7000	4.6183	0.0000	0.0000	0.0000	0.0000
0.38	5.3000	5.3862	4.7000	4.6183	0.0000	0.0000	0.0000	0.0000
0.40	5.3000	5.3865	4.6000	4.5195	-0.0108	-0.0108	-0.0108	-0.0108
0.43	5.3000	5.0104	4.6000	4.8842	0.0000	0.0000	0.0000	-0.0108
0.45	5.3000	5.0104	4.6000	4.8842	0.0000	0.0000	0.0000	0.0000
0.48	5.3000	5.3941	4.6000	4.4143	0.0000	-0.0110	0.0000	0.0000
0.50	5.3000	5.3938	4.5000	4.3184	-0.0110	-0.0110	-0.0110	-0.0110
0.53	5.3000	5.3938	4.5000	4.3184	0.0000	0.0000	0.0000	0.0000
0.55	5.3000	5.3938	4.5000	4.3184	0.0000	0.0000	0.0000	0.0000
0.57	5.3000	5.7883	4.5000	4.0001	0.0000	0.0000	0.0000	0.0131
0.60	5.4000	5.8721	4.5000	4.0177	0.0101	0.0101	0.0131	0.0131
0.62	5.4000	5.5838	4.5000	4.3304	0.0000	0.0100	0.0000	0.0000
0.65	5.4000	5.5838	4.5000	4.3304	0.0000	0.0000	0.0000	0.0000
0.67	5.4000	5.5838	4.5000	4.3304	0.0000	0.0000	0.0000	0.0000
0.70	5.5000	5.6773	4.5000	4.3379	0.0099	0.0099	0.0131	0.0130
0.72	5.5000	5.7681	4.5000	4.3487	0.0000	0.0099	0.0000	0.0130
0.75	5.5000	5.7681	4.5000	4.3487	0.0000	0.0000	0.0000	0.0000
0.77	5.5000	5.7681	4.5000	4.3487	0.0000	0.0000	0.0000	0.0000
0.80	5.4000	5.6774	4.4000	4.2410	-0.0211	-0.0212	-0.0243	-0.0243
0.82	5.4000	5.5834	4.4000	4.1394	0.0000	-0.0212	0.0000	-0.0243
0.85	5.4000	5.5833	4.4000	4.1390	0.0000	-0.0001	0.0000	-0.0001
0.87	5.4000	5.5833	4.4000	4.1390	0.0000	0.0000	0.0000	0.0000
0.90	5.3000	5.4900	4.3000	4.0370	-0.0216	-0.0216	-0.0246	-0.0246
0.92	5.3000	5.3917	4.3000	3.9423	0.0000	-0.0216	0.0000	-0.0247
0.95	5.3000	5.3898	4.3000	3.9433	0.0000	-0.0001	0.0000	-0.0001
0.97	5.3000	5.3898	4.3000	3.9433	0.0000	0.0000	0.0000	0.0000
1.00	5.2000	5.2936	4.2000	3.8471	-0.0220	-0.0220	-0.0249	-0.0250
1.02	5.2000	5.1919	4.2000	3.7582	0.0000	-0.0221	0.0000	-0.0250
1.05	5.2000	5.1894	4.2000	3.7599	0.0000	0.0000	0.0000	-0.0001
1.07	5.2000	5.1894	4.2000	3.7599	0.0000	0.0000	0.0000	0.0000
1.10	5.1000	5.1870	4.1000	3.7618	-0.0224	0.0000	-0.0253	-0.0001
1.12	5.1000	5.0856	4.1000	3.6726	0.0000	-0.0226	0.0000	-0.0254
1.15	5.1000	5.0853	4.1000	3.6721	0.0000	-0.0001	0.0000	-0.0001
1.17	5.1000	5.0853	4.1000	3.6721	0.0000	0.0000	0.0000	0.0000
1.20	5.0000	5.8154	4.0000	3.0338	-0.0229	-0.0230	-0.0256	0.0000

5.6 Result of running BREM with INVDISC showing the double reading of primary reflections that can occur from the alteration used in Figure 5.5b.

depth	cact	ccomp	rhoact	rhocomp	rc1	rc2
0.10	5.0000	5.0000	5.1000	5.0990	0.0099	0.0099
0.20	5.1000	5.1038	5.1000	5.0939	0.0106	0.0232
0.30	5.2000	5.2075	5.2000	5.1881	0.0201	0.0338
0.40	5.3000	5.3112	5.1000	5.0826	0.0005	0.0154
0.50	5.4000	5.4147	5.0000	4.9777	0.0002	0.0164
0.60	5.5000	5.5182	5.0000	4.9737	0.0099	0.0277
0.70	5.5000	5.5182	5.0000	4.9737	0.0000	0.0000
0.80	5.5000	5.5182	5.0000	4.9736	0.0000	0.0000
0.90	5.4000	5.4247	4.9000	4.8659	-0.0200	-0.0378
1.00	5.3000	5.3313	4.8000	4.7580	-0.0204	-0.0366
1.10	5.2000	5.2378	4.7000	4.6503	-0.0208	-0.0357
1.20	5.1000	5.1448	4.6000	4.5422	-0.0211	-0.0348
1.30	5.0000	5.0526	4.5000	4.4336	-0.0216	-0.0341
1.40	5.0000	5.0538	4.5000	4.4324	0.0000	0.0002
1.50	5.0000	5.0542	4.5000	4.4321	0.0000	0.0001

5.7a Result of running BREM with the continuous medium inversion program INV1 for a fairly smooth medium. This shows INV1 works fairly well for such a medium.

depth	cact	ccomp	rhoact	rhocomp	rc1	rc2
0.10	5.0000	5.0000	5.1000	5.1000	0.0099	0.0099
0.20	5.1000	5.1000	5.1000	5.1000	0.0106	0.0232
0.30	5.2000	5.2000	5.2000	5.2000	0.0201	0.0338
0.40	5.3000	5.3000	5.1000	5.0999	0.0005	0.0154
0.50	5.4000	5.4000	5.0000	4.9999	0.0002	0.0164
0.60	5.5000	5.5000	5.0000	5.0000	0.0099	0.0277
0.70	5.5000	5.5000	5.0000	5.0000	0.0000	0.0000
0.80	5.5000	5.5001	5.0000	4.9999	0.0000	0.0000
0.90	5.4000	5.4001	4.9000	4.8999	-0.0200	-0.0378
1.00	5.3000	5.3000	4.8000	4.8000	-0.0204	-0.0366
1.10	5.2000	5.2002	4.7000	4.6998	-0.0207	-0.0356
1.20	5.1000	5.0997	4.6000	4.6004	-0.0211	-0.0349
1.30	5.0000	4.9986	4.5000	4.5015	-0.0216	-0.0343
1.40	5.0000	4.9978	4.5000	4.5025	0.0000	-0.0001
1.50	5.0000	4.9975	4.5000	4.5028	0.0000	0.0000

5.7b Result of running BREM with INVDISC on the medium used in Figure 5.7a. Both inversion programs work well on fairly smooth media.

depth	cact	ccomp	rhoact	rhocomp	rc1	rc2
0.10	5.2000	5.2000	4.8000	4.8000	0.0006	0.0269
0.20	5.4000	5.4000	4.6000	4.6000	-0.0010	0.0301
0.30	5.5000	5.5000	4.8000	4.8000	0.0312	0.0489
0.40	5.5000	5.5000	4.8000	4.8000	0.0000	0.0000
0.50	5.5000	5.5000	4.8000	4.8000	0.0000	0.0000
0.60	5.7000	5.7000	5.0000	5.0000	0.0398	0.0810
0.70	5.7000	5.7000	5.2000	5.2000	0.0196	0.0196
0.80	5.5000	5.5000	5.4000	5.4000	-0.0005	-0.0419
0.90	5.3000	5.2997	5.6000	5.6009	-0.0017	-0.0357
1.00	5.0000	5.0000	5.3000	5.3005	-0.0587	-0.0995
1.10	4.8000	4.7966	5.0000	5.0043	-0.0508	-0.0738
1.20	4.6000	4.5962	4.8000	4.8046	-0.0429	-0.0627
1.30	4.5000	4.4909	4.5000	4.5100	-0.0438	-0.0532
1.40	4.5000	4.4897	4.5000	4.5113	0.0000	-0.0001
1.50	4.5000	4.4917	**4.5000**	4.5092	0.0000	0.0002

5.8a Result of running BREM with INVDISC on a more sharply varying medium than the one used in Figures 5.7. INVDISC still works well.

depth	cact	ccomp	rhoact	rhocomp	rc1	rc2
0.10	5.2000	5.2161	4.8000	4.7752	0.0006	0.0269
0.20	5.4000	5.4311	4.6000	4.5545	-0.0010	0.0301
0.30	5.5000	5.5328	4.8000	4.7464	0.0312	0.0489
0.40	5.5000	5.5328	4.8000	4.7464	0.0000	0.0000
0.50	5.5000	5.5328	4.8000	4.7464	0.0000	0.0000
0.60	5.7000	5.7472	5.0000	4.9248	0.0398	0.0810
0.70	5.7000	5.7472	5.2000	5.1180	0.0196	0.0196
0.80	5.5000	5.5775	5.4000	5.2775	-0.0005	-0.0419
0.90	5.3000	5.4088	5.6000	5.4317	-0.0018	-0.0358
1.00	5.0000	5.4081	5.3000	5.4323	0.0000	-0.0001
1.10	4.8000	5.4069	5.0000	5.4341	0.0000	-0.0002
1.20	4.6000	5.4052	4.8000	5.4355	0.0000	-0.0003
1.30	4.5000	5.4042	4.5000	5.4367	0.0000	-0.0002
1.40	4.5000	5.4087	4.5000	5.4307	-0.0001	0.0007
1.50	4.5000	5.4122	**4.5000**	5.4247	-0.0002	0.0004

5.8b Result of running BREM with INV1 on the medium used in Figures 5.8a. INV1 now breaks down, as expected.

n=15 m= 9 dd=0.100 del=0.100 dt=0.00250 p1=0.05 p2=0.15

depth	cact	ccomp	rhoact	rhocomp	r1	rc1	r2	rc2
0.00	5.0000	5.0000	5.0000	5.0000	0.0000	0.0000	0.0000	0.0000
0.10	5.2000	5.2000	4.8000	4.8000	0.0006	0.0006	0.0269	0.0269
0.20	5.4000	5.4000	4.6000	4.6000	-0.0010	-0.0010	0.0301	0.0301
0.30	5.5000	5.5000	4.8000	4.8000	0.0312	0.0312	0.0489	0.0489
0.40	5.5000	5.5004	4.8000	4.7996	0.0000	0.0000	0.0000	0.0001
0.50	5.5000	5.5004	4.8000	4.7996	0.0000	0.0000	0.0000	0.0000
0.60	5.7000	5.7003	5.0000	4.9997	0.0398	0.0398	0.0810	0.0810
0.70	5.7000	5.6993	5.2000	5.2007	0.0196	0.0196	0.0196	0.0194
0.80	5.5000	5.4991	5.4000	5.4010	-0.0005	-0.0005	-0.0419	-0.0419
0.90	5.3000	5.2985	5.6000	5.6017	-0.0018	-0.0018	-0.0357	-0.0358
1.00	5.0000	4.9968	5.3000	5.3037	-0.0587	-0.0587	-0.0996	-0.0997
1.10	4.8000	4.7974	5.0000	5.0029	-0.0508	-0.0508	-0.0734	-0.0733
1.20	4.6000	4.6030	4.8000	4.7967	-0.0429	-0.0429	-0.0627	-0.0621
1.30	4.5000	4.5013	4.5000	4.4964	-0.0438	-0.0441	-0.0528	-0.0532
1.40	4.5000	4.5085	4.5000	4.4864	0.0000	-0.0003	0.0000	0.0004
1.50	4.5000	4.5092	4.5000	4.4856	0.0000	0.0000	0.0000	0.0001

5.9a Result of running BREM with INVDISC on the medium used in Figures 5.8, showing the actual (r1, r2) and computed (rc1, rc2) reflection coefficients.

depth	cact	ccomp	rhoact	rhocomp	r1	rc1	r2	rc2
0.00	5.0000	5.0000	5.0000	5.0000	0.0000	0.0000	0.0000	0.0000
0.10	5.2000	5.2161	4.8000	4.7751	0.0006	0.0006	0.0269	0.0269
0.20	5.4000	5.4311	4.6000	4.5544	-0.0010	-0.0010	0.0301	0.0301
0.30	5.5000	5.5328	4.8000	4.7463	0.0312	0.0312	0.0489	0.0489
0.40	5.5000	5.5328	4.8000	4.7463	0.0000	0.0000	0.0000	0.0000
0.50	5.5000	5.5328	4.8000	4.7463	0.0000	0.0000	0.0000	0.0000
0.60	5.7000	5.7472	5.0000	4.9247	0.0398	0.0398	0.0810	0.0810
0.70	5.7000	5.7472	5.2000	5.1178	0.0196	0.0196	0.0196	0.0196
0.80	5.5000	5.5775	5.4000	5.2772	-0.0005	-0.0005	-0.0419	-0.0419
0.90	5.3000	5.4088	5.6000	5.4314	-0.0018	-0.0018	-0.0357	-0.0358
1.00	5.0000	5.4081	5.3000	5.4320	-0.0587	0.0000	-0.0996	-0.0001
1.10	4.8000	5.4069	5.0000	5.4338	-0.0508	0.0000	-0.0734	-0.0002
1.20	4.6000	5.4052	4.8000	5.4351	-0.0429	0.0000	-0.0627	-0.0003
1.30	4.5000	5.4042	4.5000	5.4363	-0.0438	0.0000	-0.0528	-0.0002
1.40	4.5000	5.4087	4.5000	5.4302	0.0000	-0.0001	0.0000	0.0006
1.50	4.5000	5.4122	4.5000	5.4242	0.0000	-0.0002	0.0000	0.0004

5.9b Result of running BREM with INV1 on the medium used in Figures 5.8. Note that even though the reflection coefficients are read perfectly through ten layers, the computed wave speeds and densities are in error, showing that the problem lies in the medium parameter updates.

compensates for the square root extraction required by INVDISC. In the sequel, INVDISC will be used as the inversion algorithm.

Some other comments on the use of these algorithms are appropriate. If FOR1 is being used to generate the medium response, it is important that $t_f = 2^m \Delta t$ be chosen large enough to avoid aliasing when the discrete inverse Fourier transform is taken (recall $\Delta\omega = 2\pi/t_f$). Ganley (1981) recommends choosing t_f to be four to eight times the two-way travel time to the deepest interface. This seems excessive; choosing t_f to be half that size gave satisfactory results. If the source spectrum $\hat{S}(\omega)$ is known, then the impulse response of the medium is the inverse Fourier transform of $\hat{R}(\omega)/\hat{S}(\omega)$, where $\hat{R}(\omega)$ is the medium response to $\hat{S}(\omega)$. This can be used to compensate for the smoothing (low pass filtering) action of the Radon transform. The finite size of the array used to measure the medium response will result in aliasing between wavenumbers, even though the medium response decays to zero with distance; the situation is analogous to the time aliasing problem discussed above, except that the array cannot in general be made big enough to avoid aliasing. However, this will not be a problem in the current experiment as long as the two angles of incidence are widely separated.

5.2.3 Frequency-Domain Layer Stripping Algorithms

The Schur algorithm and dynamic deconvolution versions of the discrete medium layer stripping algorithm can also be used to reconstruct a layered medium. The main feature of these algorithms is that they use frequency-domain data: $\hat{R}(\omega)$, rather than $R(t)$. Thus they avoid the necessity of performing an inverse Fourier transform and its attendant complications.

vertical wave speed $c(z)/\cos\theta(z)$ gives the one-way travel time through the layer. If double this time (the two-way travel time) is less than $3\Delta t$, then a double reading may occur. This condition may be written as

$$\Delta z \cos\theta(z)/(\Delta t\, c(z)) < 3/2 \ , \qquad (5\text{-}5)$$

so that if Δz is too small, Δt too large, or $\cos\theta(z)$ too small (e.g., near a turning point), a double reading may result. The left side of (5-5) was 0.8 when the first double reading of Figure 5.6 occurred.

Double readings can be avoided if care is taken to ensure that (5-5) is never satisfied. An alternative is to monitor the left side of (5-5), and replace the modified read at three neighboring times with a read at a single time whenever (5-5) is satisfied.

Comparison of the performances of INV1 and INVDISC

A comparison of the performances of INV1 and INVDISC reveals exactly what would be expected: both algorithms work well on media with fairly smooth changes, but INV1 breaks down on media with sharp changes. Figures 5.7 show both INV1 and INVDISC satisfactorily inverting a smoothly varying medium. Here INV1 might be preferred since its parameter updates are simpler and do not require a time-consuming square root extraction. Figures 5.8 and 5.9 show INVDISC still working almost perfectly, while INV1 breaks down. Figure 5.9, in particular, shows that INV1 is reading the reflection coefficients correctly, proving that the error lies in the update equations for the medium parameters.

The conclusion is thus that INVDISC works very well on all types of layered media, whether slowly varying or sharply varying, while INV1 breaks down for sharply varying media. This advantage more than

n=12m= 9dd=0.10del=0.10df=1.000p1=0.08p2=0.15

depth	cact	ccomp	rhoact	rhocomp	rc1	rc2
0.10	**5.1000**	**5.1014**	5.1000	5.0993	0.0218	0.0334
0.20	5.2000	5.2067	5.2000	5.1895	0.0211	0.0342
0.30	5.3000	5.3013	5.3000	5.2928	0.0208	0.0336
0.40	5.4000	5.4016	5.4000	5.3960	0.0211	0.0360
0.50	5.5000	5.5003	5.5000	5.4979	0.0205	0.0367
0.60	5.4000	5.3982	5.6000	5.5942	-0.0029	-0.0196
0.70	5.3000	5.2950	5.7000	5.6975	-0.0027	-0.0179
0.80	5.2000	5.1950	5.8000	5.7974	-0.0029	-0.0163
0.90	5.1000	5.0955	5.9000	5.8972	-0.0031	-0.0154
1.00	5.0000	4.9966	6.0000	5.9951	-0.0035	-0.0147
1.10	5.0000	4.9966	6.0000	5.9950	0.0000	0.0000
1.20	5.0000	4.9951	6.0000	5.9979	0.0001	-0.0001
1.30	5.0000	4.9944	6.0000	5.9997	0.0001	0.0000
1.40	5.0000	4.9951	**6.0000**	**5.9988**	**0.0000**	**0.0001**
1.50	**5.0000**	**4.9946**	**6.0000**	**5.9987**	**-0.0001**	**-0.0001**

n=15m= 8dd=0.10del=0.05df=1.000p1=0.15p2=0.12

depth	cact	ccomp	rhoact	rhocomp	rc1	rc2
0.05	5.0000	5.0016	5.0000	5.0019	0.0006	0.0004
0.10	5.1000	5.1081	4.9000	4.8888	0.0133	0.0052
0.15	5.1000	5.1225	4.9000	4.8687	0.0014	0.0002
0.20	5.2000	5.2287	4.8000	4.7558	0.0141	0.0050
0.25	5.2000	5.2373	4.8000	4.7424	0.0007	-0.0001
0.30	5.3000	5.3248	4.7000	4.6526	0.0127	0.0043
0.35	5.3000	5.3104	4.7000	4.6756	-0.0013	0.0002
0.40	5.3000	5.2965	4.6000	4.6284	-0.0086	-0.0073
0.45	5.3000	5.2890	4.6000	4.6466	0.0000	0.0008
0.50	5.3000	5.2930	4.5000	4.5594	-0.0084	-0.0088
0.55	5.3000	5.3073	4.5000	4.5387	0.0014	0.0000
0.60	5.4000	5.3896	4.5000	4.5326	0.0209	0.0124
0.65	5.4000	5.3792	4.5000	4.5456	-0.0013	-0.0002
0.70	5.5000	5.4824	4.5000	4.5120	0.0245	0.0128
0.75	5.5000	5.4855	4.5000	4.5165	0.0014	0.0010
0.80	5.4000	5.3789	4.4000	4.4626	-0.0352	-0.0231
0.85	5.4000	5.4103	4.4000	4.4304	0.0048	0.0014
0.90	5.3000	5.2921	4.3000	4.3838	-0.0363	-0.0241
0.95	5.3000	5.2791	4.3000	4.4224	0.0011	0.0023
1.00	5.2000	5.1351	4.2000	4.4144	-0.0364	-0.0236
1.05	5.2000	5.0926	4.2000	4.4905	-0.0016	0.0019
1.10	5.1000	5.0044	4.1000	4.4453	-0.0255	-0.0188
1.15	5.1000	5.0484	4.1000	4.3873	0.0036	0.0003
1.20	5.1000	5.1175	4.1000	4.2248	-0.0026	-0.0080
1.25	5.0000	5.1376	4.0000	4.1906	0.0007	-0.0009
1.30	**5.0000**	**5.1498**	**4.0000**	4.1701	0.0005	-0.0005
1.35	**5.0000**	**5.1574**	**4.0000**	**4.1579**	**0.0004**	**-0.0003**
1.40	**5.0000**	**5.1614**	**4.0000**	**4.1526**	**0.0003**	**0.0000**

5.10 Result of running FOR1, without its inverse Fourier transform, with the Schur algorithm inversion program SCHUR.

From Chapter III, the Schur algorithm for the discrete medium non-normal incidence inverse problem consists of the set of equations

$$\hat{D}(z+\Delta,\omega) = \hat{D}(z,\omega)e^{-j\omega\Delta/c'(z)} - r(z)\Delta\hat{U}(z,\omega) \tag{5-6a}$$

$$\hat{U}(z+\Delta,\omega) = \hat{U}(z,\omega)e^{j\omega\Delta/c'(z)} - r(z)\,\Delta\,\hat{D}(z,\omega) \tag{5-6b}$$

$$r(z) = \frac{1}{\pi}\int_0^{\infty} e^{j\omega\tau}\hat{U}(z,\omega)d\omega \tag{5-6c}$$

$$\tau(z) = \int_0^z dz/c'(z) \tag{5-6d}$$

$$c'(z) = c(z)/(1-c(z)^2p^2)^{\frac{1}{2}} \tag{5-6e}$$

taken twice (one for each experiment) and the discrete medium parameter updates (4-50). The initial conditions are

$$\hat{D}(0,\omega) = 1 \tag{5-7a}$$

$$\hat{U}(0,\omega) = \hat{R}(\omega) \tag{5-7b}$$

where $\hat{R}(\omega)$ is the frequency response of the layered medium. Note that the complex exponentials in (5-6a) and (5-6b) represent the time delays through the layer in the interval $[z, z+\Delta)$.

The frequency response of the medium was generated by FOR1, and the program SCHUR, implementing (5-6), (4-50), and (5-7), was used to reconstruct the medium. The results of two runs are given in Figures 5.10, and it can be seen that the algorithm functions quite well. The difference in the performances of the two runs seems to be due to the inverse Fourier transforms required to obtain r(z); these transforms are less accurate for 256 points than they are for 512.

Again by analogy to Chapter III, the dynamic deconvolution algorithm for the discrete medium non-normal incidence inverse problem consists of the set of equations

$$\hat{R}(z+\Delta,\omega) = e^{2j\omega\Delta/c'}(\hat{R}(z,\omega) - r(z))/(1 - r(z)\hat{R}(z,\omega)) \qquad (5\text{-}8a)$$

$$r(z) = \frac{1}{\pi}\int_0^{\infty} \hat{R}(z,\omega)d\omega \qquad (5\text{-}8b)$$

taken twice, along with (5-6d), (5-6e) and the discrete medium parameter updates (4-50). The initial condition is

$$\hat{R}(0,\omega) = \hat{R}(\omega) \ . \qquad (5\text{-}9)$$

Note that since the dynamic deconvolution algorithm computes the response $\hat{R}(z,\omega)$ of that portion of the medium below depth z, there is no phase shift in (5-8b).

The frequency response of the medium was again generated by FOR1, and the program DYNDEC, implementing the dynamic deconvolution algorithm, was used to reconstruct the medium. The results of two runs are given in Figures 5.11, and these are comparable to the Schur algorithm results. Since the two methods are mathematically equivalent, this is hardly a surprise. However, the fact that a phase shift (relying on a computed c'(z)) is not present in (5-8b) would seem to make the dynamic deconvolution algorithm preferable to the Schur algorithm.

5.3 Performance of the Algorithm in the Presence of Noise

In this section a series of computer runs shows the effects of

n=12 m= 9	dd=0.10	del=0.10	df=1.000	p1=0.08	p2=0.15	
depth	cact	ccomp	rhoact	rhocomp	rc1	rc2
0.10	5.1000	5.1014	5.1000	5.0993	0.0218	0.0334
0.20	5.2000	5.2081	5.2000	5.1898	0.0213	0.0345
0.30	5.3000	5.3010	5.3000	5.2941	0.0207	0.0333
0.40	5.4000	5.4005	5.4000	5.3941	0.0207	0.0355
0.50	5.5000	5.4971	5.5000	5.4953	0.0202	0.0360
0.60	5.4000	5.3993	5.6000	5.5929	-0.0023	-0.0182
0.70	5.3000	5.3031	5.7000	5.6881	-0.0026	-0.0168
0.80	5.2000	5.2061	5.8000	5.7843	-0.0028	-0.0160
0.90	5.1000	5.1147	5.9000	5.8730	-0.0031	-0.0145
1.00	5.0000	5.0438	6.0000	5.9360	-0.0030	-0.0113
1.10	5.0000	5.0443	6.0000	5.9350	0.0000	0.0000
1.20	5.0000	5.0425	6.0000	5.9376	0.0000	-0.0002
1.30	5.0000	5.0432	6.0000	5.9367	0.0000	0.0001
1.40	5.0000	5.0441	6.0000	5.9353	0.0000	0.0001
1.50	5.0000	5.0432	6.0000	5.9367	0.0000	-0.0001

n=15 m= 8	dd=0.10	del=0.05	df=1.000	p1=0.15	p2=0.12	
depth	cact	ccomp	rhoact	rhocomp	rc1	rc2
0.05	5.0000	5.0016	5.0000	5.0019	0.0006	0.0004
0.10	5.1000	5.1080	4.9000	4.8888	0.0133	0.0052
0.15	5.1000	5.1143	4.9000	4.8818	0.0008	0.0003
0.20	5.2000	5.2201	4.8000	4.7699	0.0141	0.0050
0.25	5.2000	5.2242	4.8000	4.7660	0.0006	0.0002
0.30	5.3000	5.3203	4.7000	4.6665	0.0138	0.0047
0.35	5.3000	5.3126	4.7000	4.6804	-0.0005	0.0003
0.40	5.3000	5.2998	4.6000	4.6246	-0.0093	-0.0080
0.45	5.3000	5.2944	4.6000	4.6388	0.0002	0.0007
0.50	5.3000	5.2931	4.5000	4.5569	-0.0092	-0.0091
0.55	5.3000	5.3075	4.5000	4.5327	0.0010	-0.0004
0.60	5.4000	5.3997	4.5000	4.5179	0.0226	0.0130
0.65	5.4000	5.3935	4.5000	4.5288	-0.0005	0.0002
0.70	5.5000	5.5007	4.5000	4.4865	0.0249	0.0125
0.75	5.5000	5.5100	4.5000	4.4861	0.0026	0.0015
0.80	5.4000	5.4263	4.4000	4.4119	-0.0317	-0.0218
0.85	5.4000	5.4249	4.4000	4.4174	0.0002	0.0004
0.90	5.3000	5.3472	4.3000	4.3601	-0.0273	-0.0189
0.95	5.3000	5.3361	4.3000	4.3761	-0.0011	0.0001
1.00	5.2000	5.3441	4.2000	4.2451	-0.0131	-0.0139
1.05	5.2000	5.3649	4.2000	4.2018	0.0004	-0.0018
1.10	5.1000	5.3579	4.1000	4.2545	0.0044	0.0051
1.15	5.1000	5.3388	4.1000	4.2869	-0.0012	0.0007
1.20	5.1000	5.3873	4.1000	4.1991	0.0025	-0.0026
1.25	5.0000	5.3743	4.0000	4.2044	-0.0029	-0.0015
1.30	5.0000	5.3737	4.0000	4.2065	0.0001	0.0002
1.35	5.0000	5.3700	4.0000	4.2170	0.0003	0.0007
1.40	5.0000	5.3734	4.0000	4.2094	0.0000	-0.0003
1.45	5.0000	5.3717	4.0000	4.2144	0.0001	0.0003
1.50	5.0000	5.3717	4.0000	4.2172	0.0003	0.0003

5.11 Result of running FOR1, without its inverse Fourier transform, with the dynamic deconvolution inversion program DYNDEC.

noise on the discrete layer stripping algorithm for the non-normal incidence inverse problem. As the noise level increases, the performance of the algorithm is degraded, as expected. The algorithm begins to break down badly at a signal-to-noise ratio of about eight, although this threshold varies with the medium being reconstructed.

The program NOISE takes the medium impulse response computed by BREM, adds noise to it, and then runs INVDISC to try to reconstruct the medium from the noisy data. The noise is generated by a center-squaring random number generator, and is evenly distributed over the interval [-xl, xl], where xl is the (inputted) noise maximum amplitude. The signal-to-noise ratio S/N is defined as

$$S/N = 10 \log_{10}\left[\int_o^T R(t)^2 dt \Big/ \int_o^T n(t)^2 dt\right] \quad , \qquad (5\text{-}10)$$

where R(t) is the impulse response of the medium and n(t) is the noise level at time t.

The impulse responses of a thirteen-layer medium at two different angles of incidence were computed using BREM, and NOISE was run for three values of signal-to-noise ratios 48.6, 28.6, and 8.6. Results are plotted in Figures 5.12, 5.13, and 5.14. For each figure, Figure a tabulates the results of the run (for the two angles of incidence), Figures b and c plot these results, and Figures d and e plot both the ideal, noise-free impulse response and (over it) the noisy impulse response from which the inversion is made. This provides a dramatic visual check on the corruption level of the data.

It is evident from Figures 5.12 - 5.14 that the performance of the layer stripping algorithm degrades with noise, as might be expected, and that even at a signal-to-noise ratio of 8.6 the algorithm still does

n=15 m= 8 dd=0.100 del=0.050 dt=0.00500 p1=0.09 p2=0.12 x1=0.3E-04

rms signal= 0.004862 0.005442 rms noise= 0.000018 snr= 48.6 49.5

depth	cact	ccomp	rhoact	rhocomp	r1	rc1	r2	rc2
0.00	5.0000	5.0000	5.0000	5.0000	0.0000	0.0000	0.0000	0.0000
0.05	5.0000	5.0000	5.0000	5.0000	0.0000	0.0000	0.0000	0.0000
0.10	5.2000	5.2012	4.8000	4.7982	0.0044	0.0044	0.0110	0.0110
0.15	5.2000	5.2012	4.8000	4.7982	0.0000	0.0000	0.0000	0.0000
0.20	5.4000	5.4008	4.6000	4.5985	0.0032	0.0031	0.0104	0.0104
0.25	5.4000	5.4008	4.6000	4.5985	0.0000	0.0000	0.0000	0.0000
0.30	5.3000	5.3005	4.7000	4.6985	-0.0014	-0.0014	-0.0052	-0.0052
0.35	5.3000	5.3005	4.7000	4.6985	0.0000	0.0000	0.0000	0.0000
0.40	5.3000	5.3020	4.5000	4.4968	-0.0217	-0.0218	-0.0217	-0.0217
0.45	5.3000	5.3020	4.5000	4.4968	0.0000	0.0000	0.0000	0.0000
0.50	5.3000	5.3025	4.3000	4.2962	-0.0227	-0.0227	-0.0227	-0.0227
0.55	5.3000	5.3025	4.3000	4.2962	0.0000	0.0000	0.0000	0.0000
0.60	5.4000	5.4013	4.2000	4.1976	0.0004	0.0004	0.0041	0.0041
0.65	5.4000	5.4013	4.2000	4.1976	0.0000	0.0000	0.0000	0.0000
0.70	5.5000	5.5003	4.5000	4.4988	0.0465	0.0466	0.0505	0.0505
0.75	5.5000	5.5003	4.5000	4.4988	0.0000	0.0000	0.0000	0.0000
0.80	5.4000	5.4018	4.4000	4.3970	-0.0233	-0.0233	-0.0273	-0.0272
0.85	5.4000	5.4018	4.4000	4.3970	0.0000	0.0000	0.0000	0.0000
0.90	5.3000	5.3020	4.3000	4.2970	-0.0237	-0.0236	-0.0274	-0.0274
0.95	5.3000	5.3042	4.3000	4.2940	0.0000	-0.0001	0.0000	0.0000
1.00	5.2000	5.2049	4.2000	4.1929	-0.0240	-0.0241	-0.0276	-0.0276
1.05	5.2000	5.2049	4.2000	4.1929	0.0000	0.0000	0.0000	0.0000
1.10	5.1000	5.1030	4.1000	4.0948	-0.0244	-0.0244	-0.0278	-0.0278
1.15	5.1000	5.1030	4.1000	4.0948	0.0000	0.0000	0.0000	0.0000
1.20	5.0000	5.0031	4.0000	3.9952	-0.0248	-0.0248	-0.0280	-0.0280
1.25	5.0000	5.0031	4.0000	3.9952	0.0000	0.0000	0.0000	0.0000
1.30	5.0000	5.0031	4.0000	3.9952	0.0000	0.0000	0.0000	0.0000
1.35	5.0000	5.0031	4.0000	3.9952	0.0000	0.0000	0.0000	0.0000
1.40	5.0000	5.0031	4.0000	3.9952	0.0000	0.0000	0.0000	0.0000
1.45	5.0000	5.0031	4.0000	3.9952	0.0000	0.0000	0.0000	0.0000
1.50	5.0000	5.0031	4.0000	3.9952	0.0000	0.0000	0.0000	0.0000

5.12a Result of running BREM with NOISE, which adds noise to the results of BREM and then uses INVDISC on the noisy data. Here a high SNR is used.

5.12b Plots of the actual (2) and reconstructed (3) wave speeds.

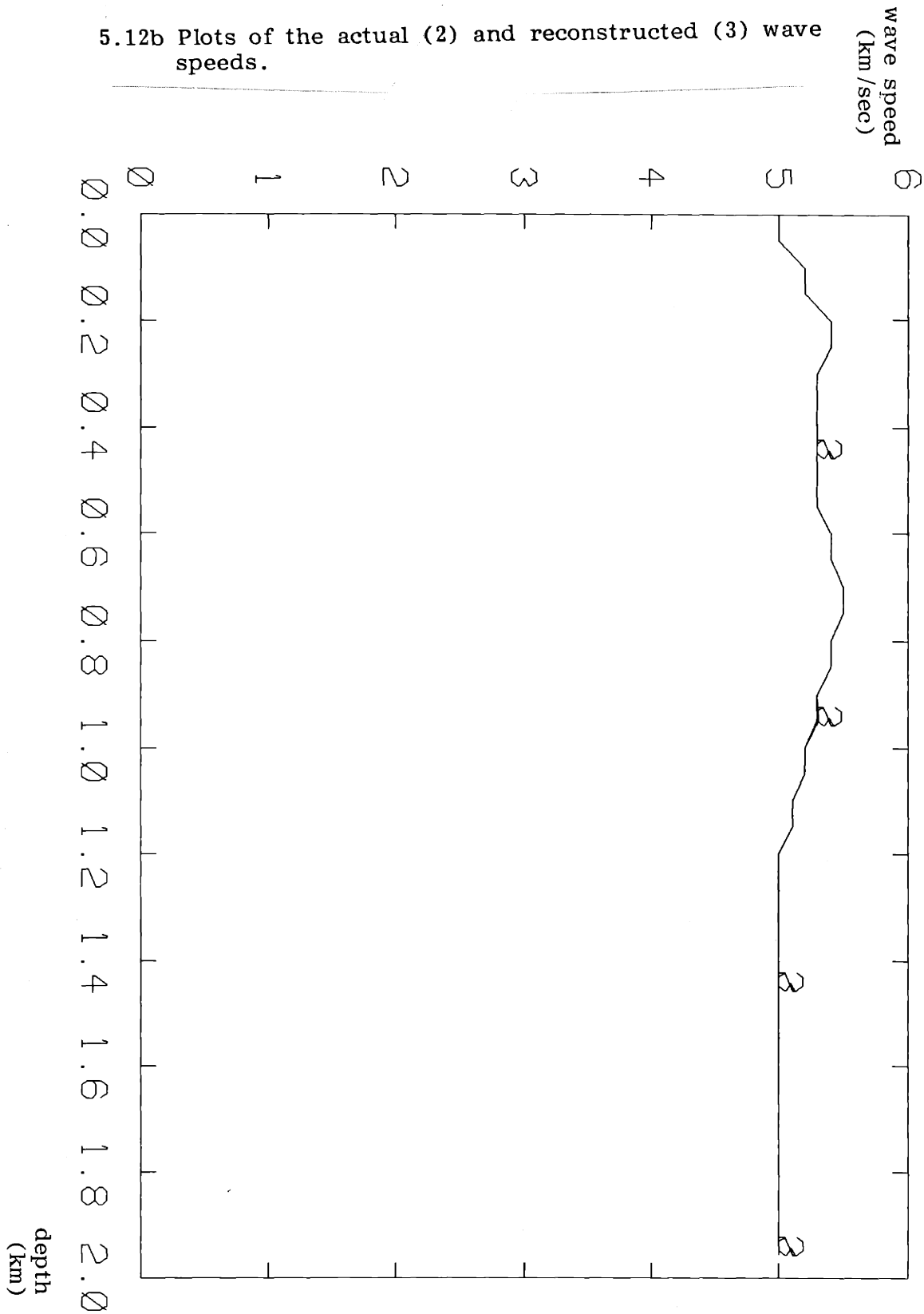

5.12c Plots of the actual (4) and reconstructed (5) densities.

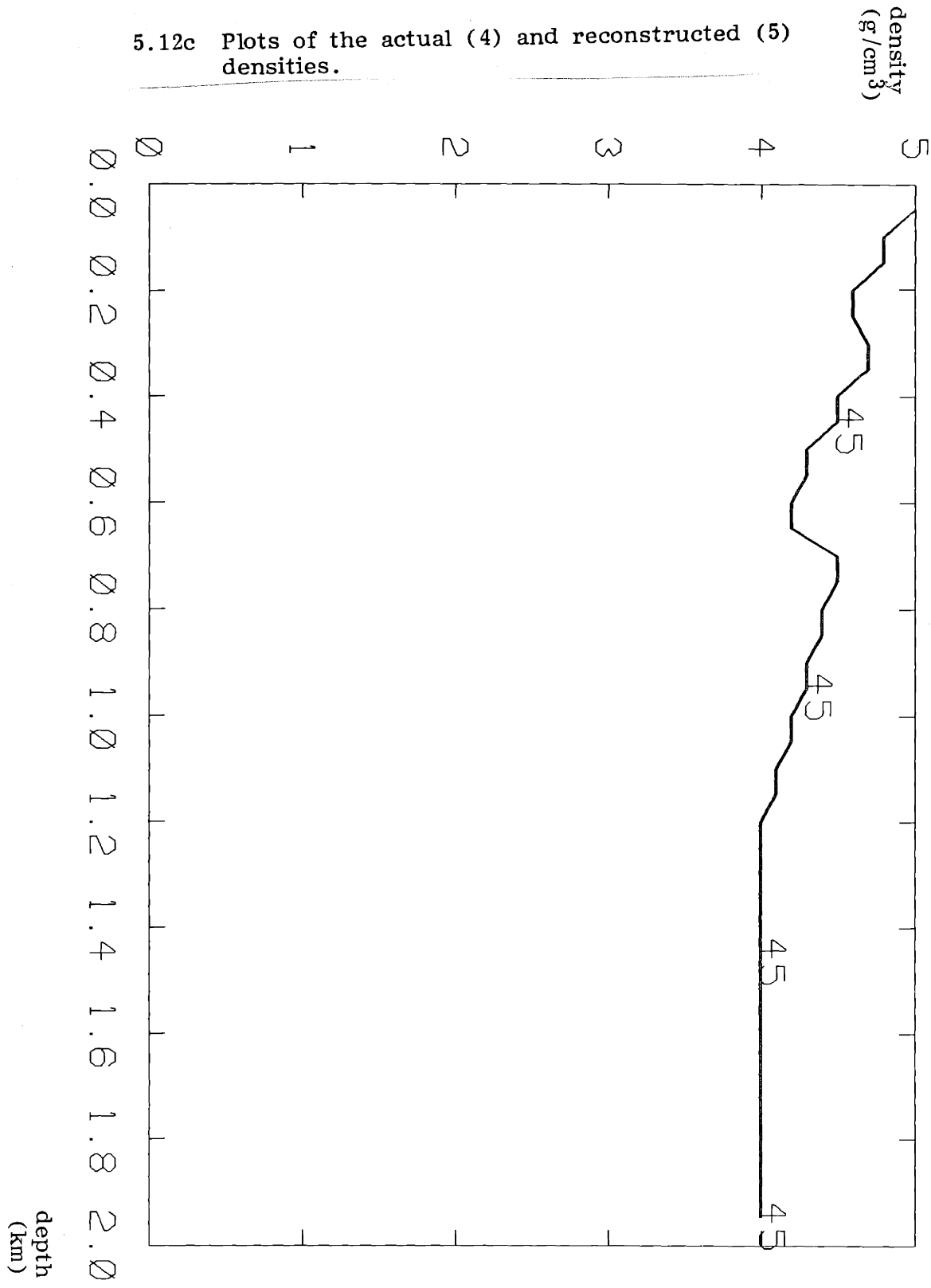

5.12d Plot of the noisy waveform used as data for INVDISC, for p = p1.

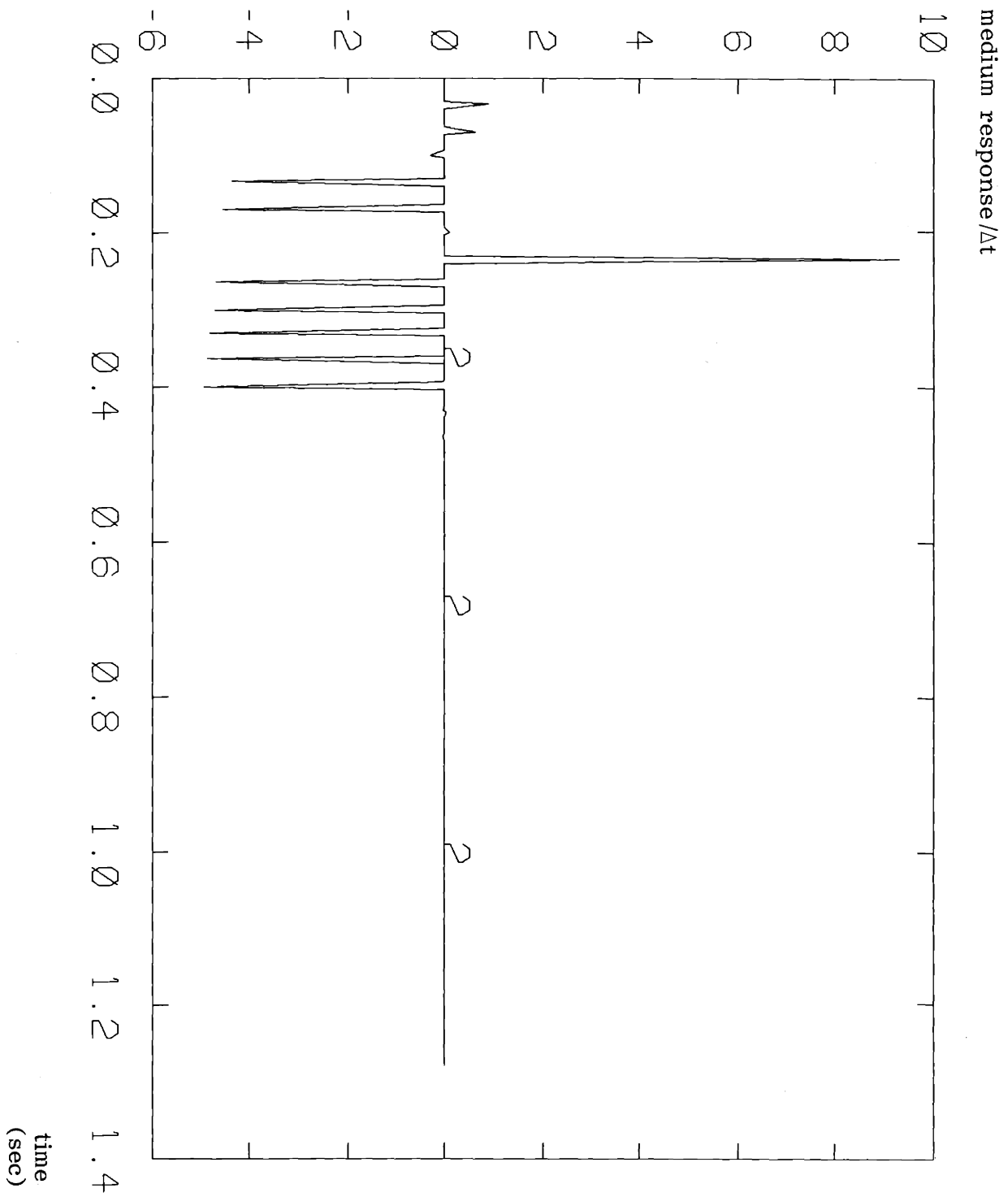

5.12e Plot of the noisy waveform used as data for INVDISC, for p = p2.

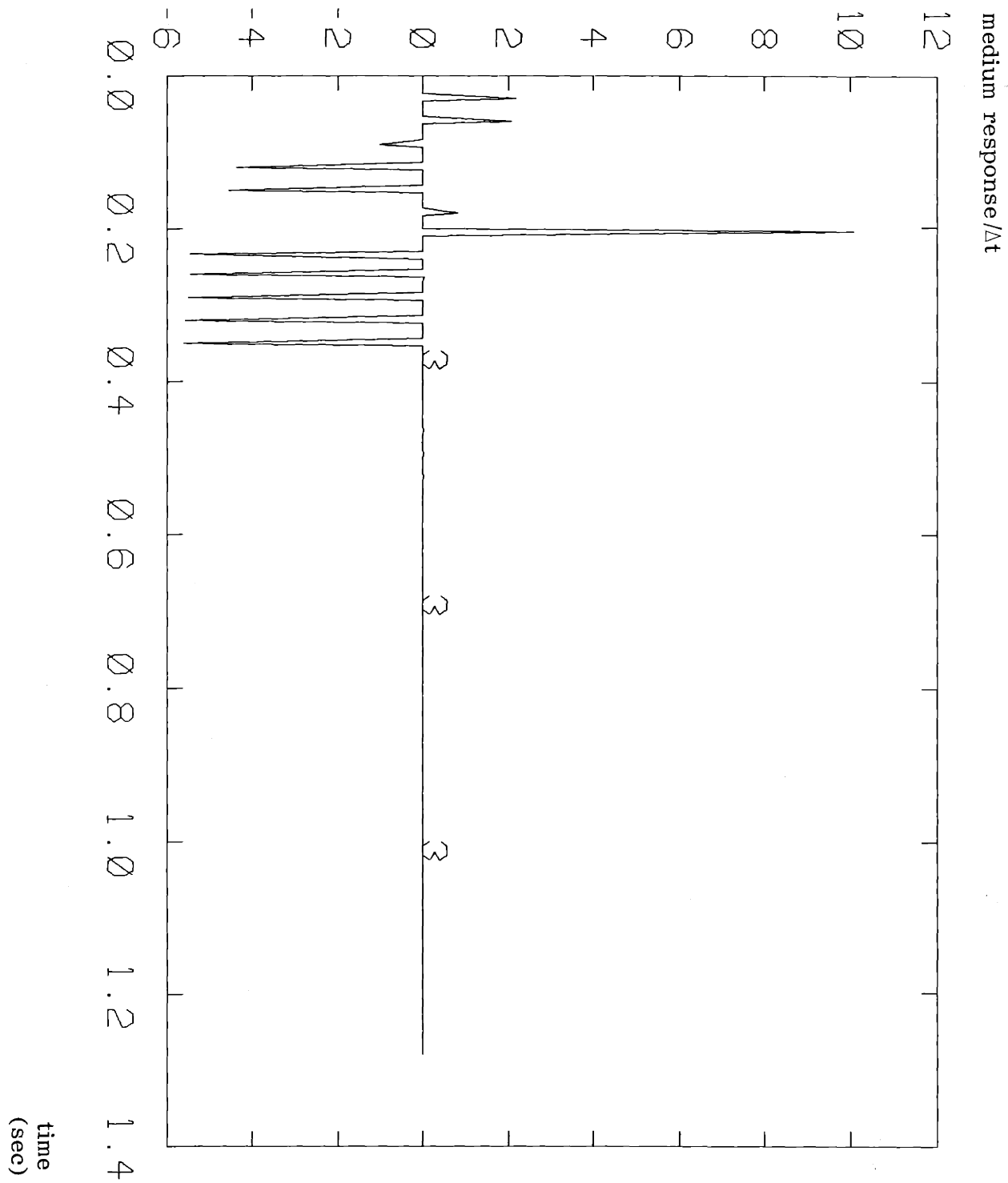

n=15 m= 8 dd=0.100 del=0.050 dt=0.00500 r1=0.09 r2=0.12 x1=0.3E-03
rms signal= 0.004862 0.005442 rms noise= 0.000182 snr= 28.6 29.5

depth	cact	ccomp	rhoact	rhocomp	r1	rc1	r2	rc2
0.00	5.0000	5.0000	5.0000	5.0000	0.0000	0.0000	0.0000	0.0000
0.05	5.0000	5.0000	5.0000	5.0000	0.0000	0.0000	0.0000	0.0000
0.10	5.2000	5.2124	4.8000	4.7824	0.0044	0.0041	0.0110	0.0111
0.15	5.2000	5.2124	4.8000	4.7824	0.0000	0.0000	0.0000	0.0000
0.20	5.4000	5.4084	4.6000	4.5852	0.0032	0.0029	0.0104	0.0100
0.25	5.4000	5.4084	4.6000	4.5852	0.0000	0.0000	0.0000	0.0000
0.30	5.3000	5.3053	4.7000	4.6852	-0.0014	-0.0017	-0.0052	-0.0056
0.35	5.3000	5.3053	4.7000	4.6852	0.0000	0.0000	0.0000	0.0000
0.40	5.3000	5.3194	4.5000	4.4683	-0.0217	-0.0220	-0.0217	-0.0215
0.45	5.3000	5.3194	4.5000	4.4683	0.0000	0.0000	0.0000	0.0000
0.50	5.3000	5.3249	4.3000	4.2621	-0.0227	-0.0229	-0.0227	-0.0227
0.55	5.3000	5.3249	4.3000	4.2621	0.0000	0.0000	0.0000	0.0000
0.60	5.4000	5.4241	4.2000	4.1606	0.0004	0.0000	0.0041	0.0038
0.65	5.4000	5.4241	4.2000	4.1606	0.0000	0.0000	0.0000	0.0000
0.70	5.5000	5.5131	4.5000	4.4724	0.0465	0.0468	0.0505	0.0504
0.75	5.5000	5.5131	4.5000	4.4724	0.0000	0.0000	0.0000	0.0000
0.80	5.4000	5.4297	4.4000	4.3529	-0.0233	-0.0236	-0.0273	-0.0269
0.85	5.4000	5.4297	4.4000	4.3529	0.0000	0.0000	0.0000	0.0000
0.90	5.3000	5.3432	4.3000	4.2383	-0.0237	-0.0238	-0.0274	-0.0271
0.95	5.3000	5.3650	4.3000	4.2092	0.0000	-0.0008	0.0000	0.0000
1.00	5.2000	5.2724	4.2000	4.0984	-0.0240	-0.0246	-0.0276	-0.0280
1.05	5.2000	5.2724	4.2000	4.0984	0.0000	0.0000	0.0000	0.0000
1.10	5.1000	5.1555	4.1000	4.0160	-0.0244	-0.0245	-0.0278	-0.0286
1.15	5.1000	5.1555	4.1000	4.0160	0.0000	0.0000	0.0000	0.0000
1.20	5.0000	5.0624	4.0000	3.9131	-0.0248	-0.0245	-0.0280	-0.0276
1.25	5.0000	5.0624	4.0000	3.9131	0.0000	0.0000	0.0000	0.0000
1.30	5.0000	5.0624	4.0000	3.9131	0.0000	0.0000	0.0000	0.0000
1.35	5.0000	5.0624	4.0000	3.9131	0.0000	0.0000	0.0000	0.0000
1.40	5.0000	5.0624	4.0000	3.9131	0.0000	0.0000	0.0000	0.0000
1.45	5.0000	5.0624	4.0000	3.9131	0.0000	0.0000	0.0000	0.0000
1.50	5.0000	5.0624	4.0000	3.9131	0.0000	0.0000	0.0000	0.0000

5.13a Result of running BREM with NOISE for a moderate SNR.

5.13b Plots of the actual (2) and reconstructed (3) wave speeds.

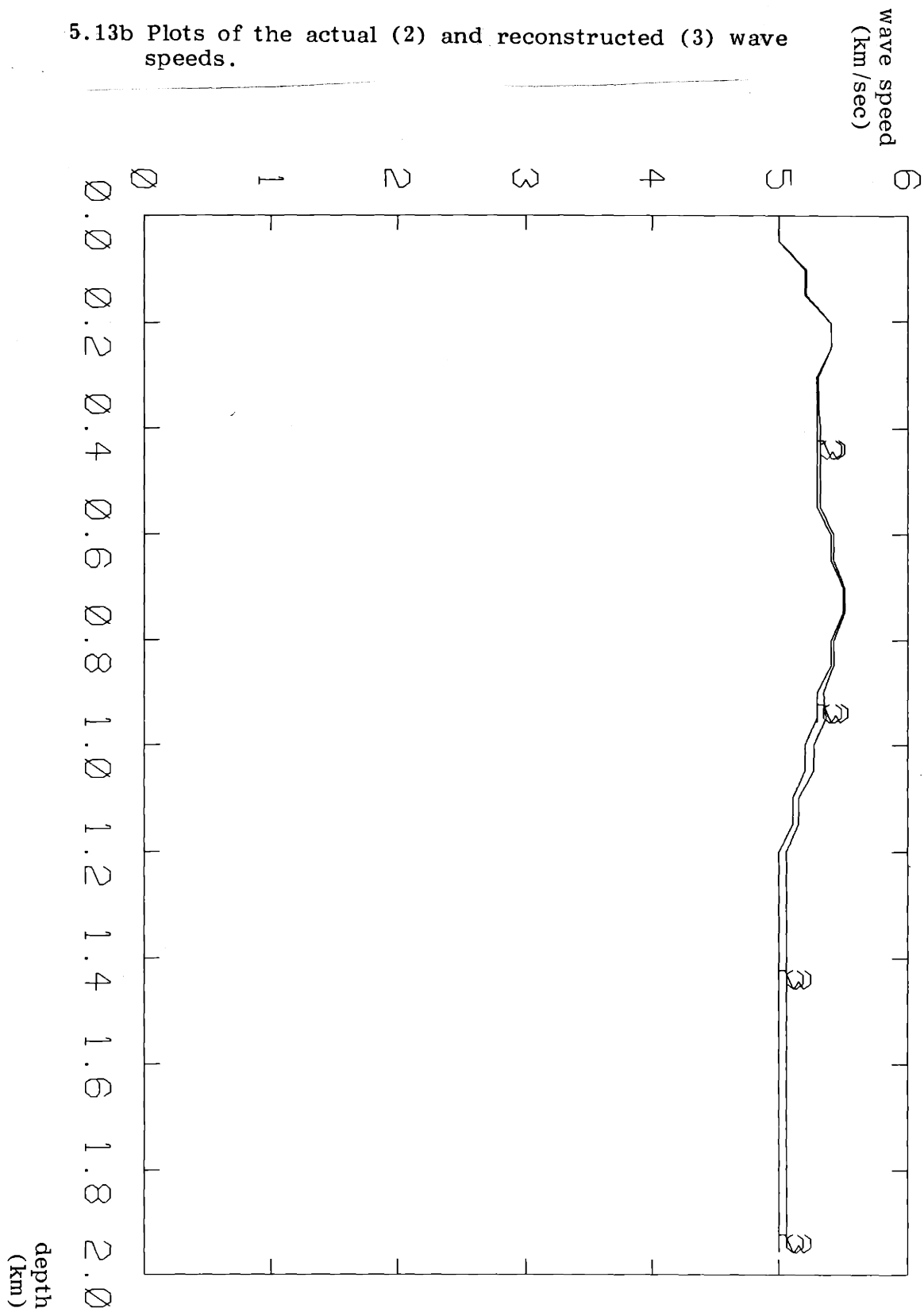

5.13c Plots of the actual (4) and reconstructed (5) densities.

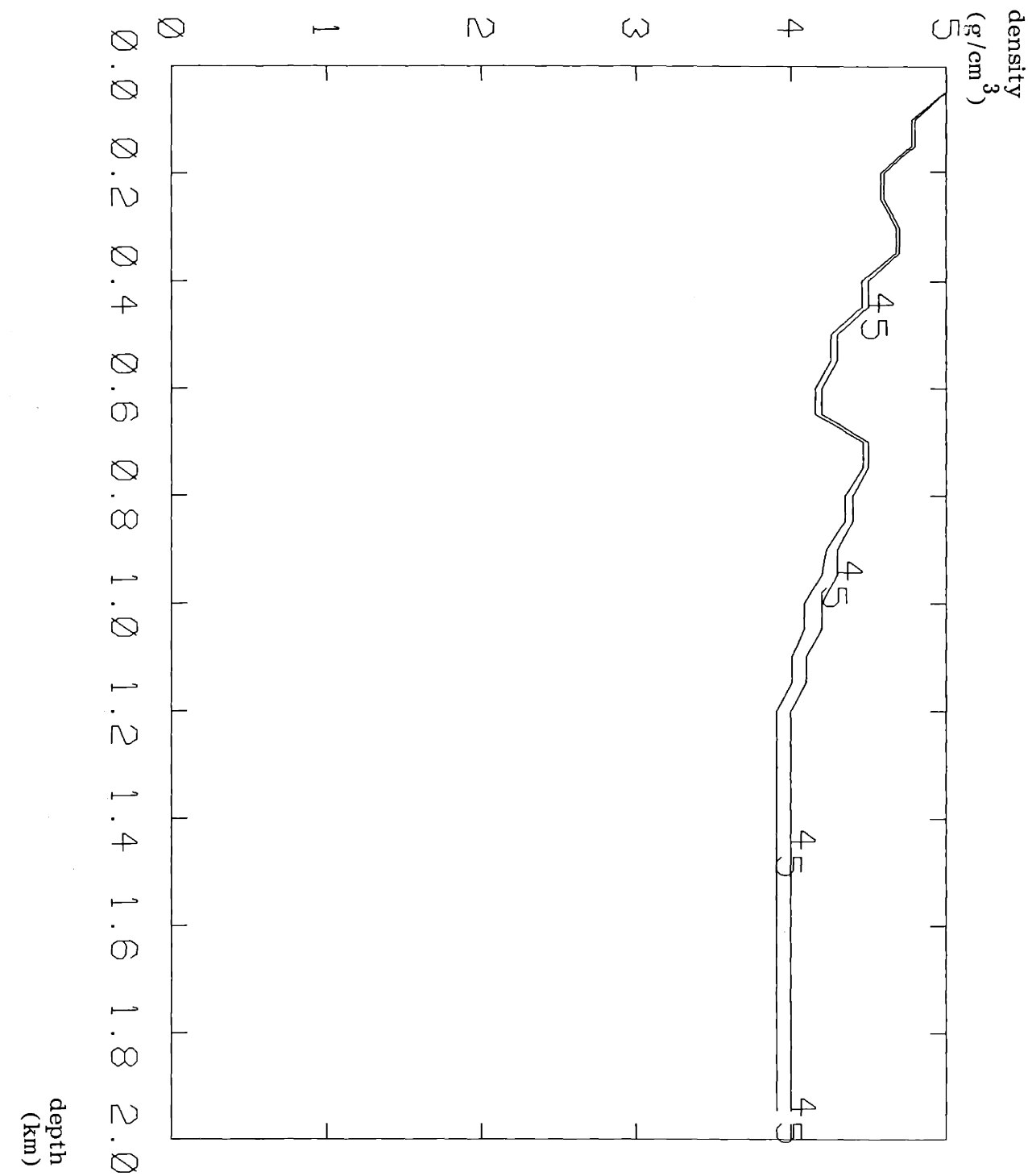

5.13d Plots of the noiseless (3) and noisy (4) wave forms used as data for INVDISC, for p = p1.

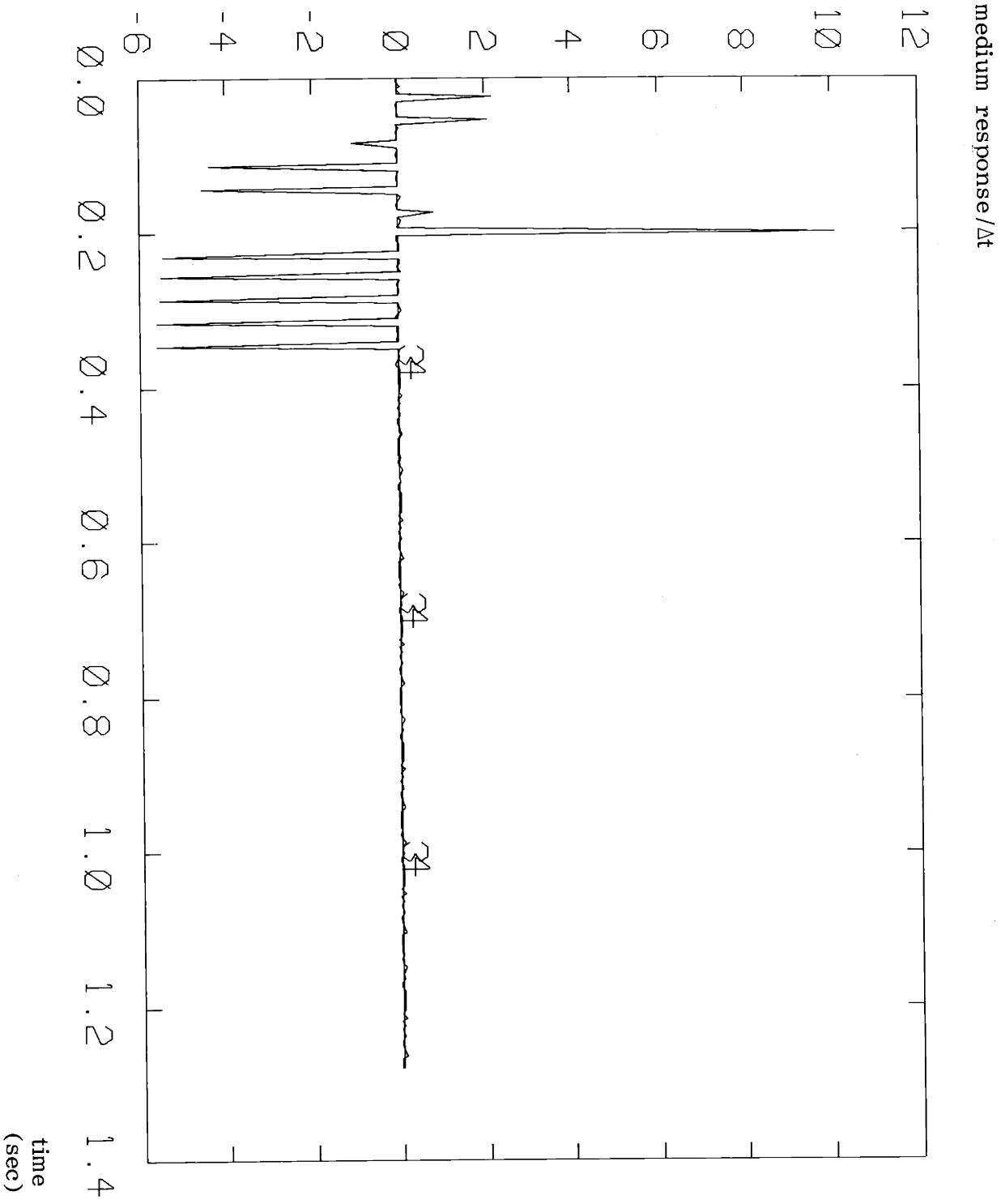

5.13e Plots of the noiseless (1) and noisy (2) wave forms used as data for INVDISC, for p = p2.

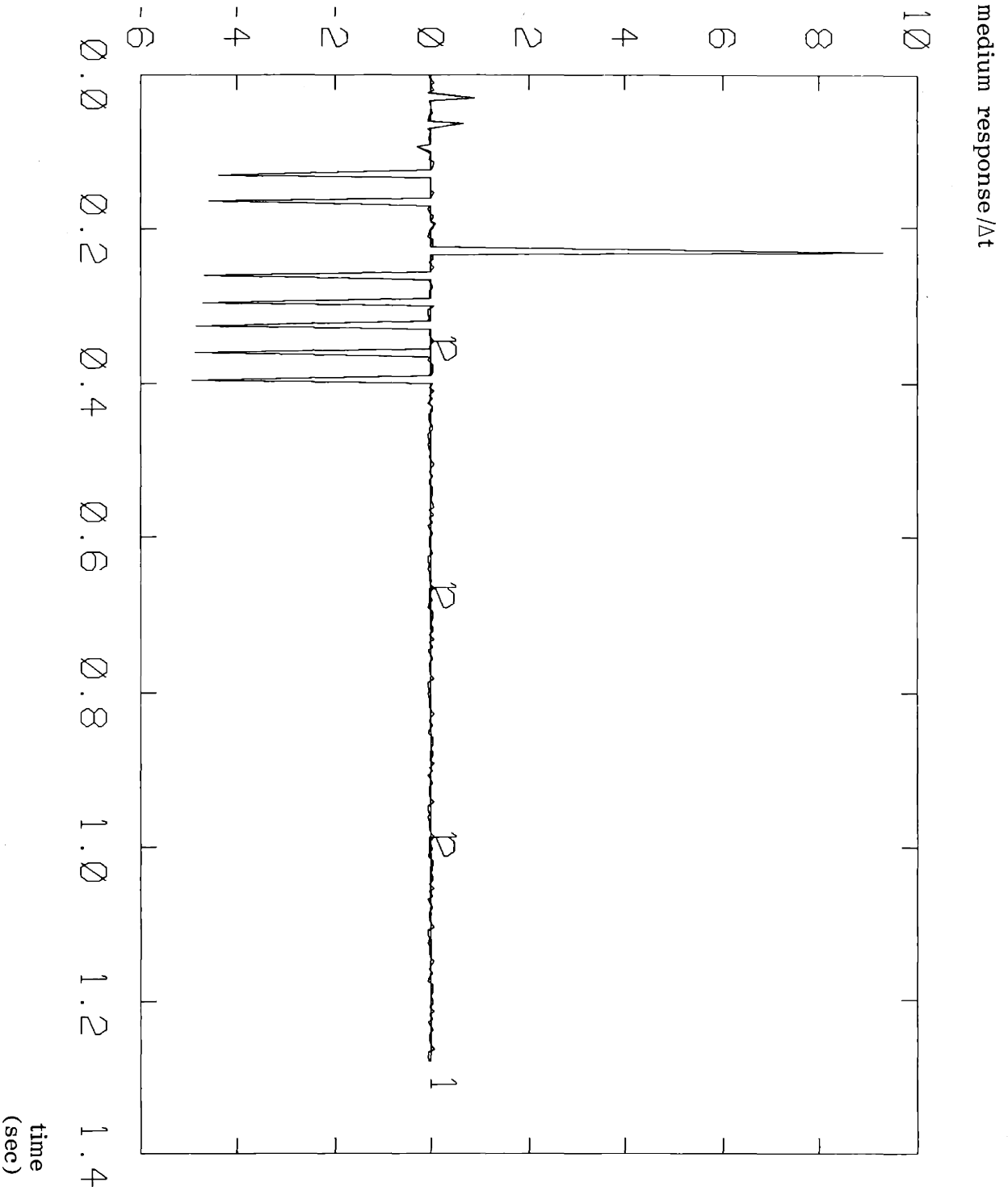

n=15 a= 8 dd=0.100 del=0.050 dt=0.00500 p1=0.09 p2=0.12 x1=0.3E-02

rms signal= 0.004862 0.005442 rms noise= 0.001817 snr= 8.6 9.5

depth	cact	ccomp	rhoact	rhocomp	r1	rc1	r2	rc2
0.00	5.0000	5.0000	5.0000	5.0000	0.0000	0.0000	0.0000	0.0000
0.05	5.0000	5.0000	5.0000	5.0000	0.0000	0.0000	0.0000	0.0000
0.10	5.2000	5.3533	4.8000	4.5824	0.0044	0.0000	0.0110	0.0120
0.15	5.2000	5.3533	4.8000	4.5824	0.0000	0.0000	0.0000	0.0000
0.20	5.4000	5.5226	4.6000	4.3986	0.0032	0.0000	0.0104	0.0066
0.25	5.4000	5.5226	4.6000	4.3986	0.0000	0.0000	0.0000	0.0000
0.30	5.3000	5.2671	4.7000	4.6798	-0.0014	0.0000	-0.0052	-0.0098
0.35	5.3000	5.2671	4.7000	4.6798	0.0000	0.0000	0.0000	0.0000
0.40	5.3000	5.3956	4.5000	4.3216	-0.0217	-0.0242	-0.0217	-0.0194
0.45	5.3000	5.3956	4.5000	4.3216	0.0000	0.0000	0.0000	0.0000
0.50	5.3000	5.3886	4.3000	4.1400	-0.0227	-0.0223	-0.0227	-0.0226
0.55	5.3000	5.3886	4.3000	4.1400	0.0000	0.0000	0.0000	0.0000
0.60	5.4000	5.3886	4.2000	4.1400	0.0004	0.0000	0.0041	0.0000
0.65	5.4000	5.3886	4.2000	4.1400	0.0000	0.0000	0.0000	0.0000
0.70	5.5000	5.4269	4.5000	4.5336	0.0465	0.0500	0.0505	0.0515
0.75	5.5000	5.4269	4.5000	4.5336	0.0000	0.0000	0.0000	0.0000
0.80	5.4000	5.4865	4.4000	4.2411	-0.0233	-0.0261	-0.0273	-0.0238
0.85	5.4000	5.4865	4.4000	4.2411	0.0000	0.0000	0.0000	0.0000
0.90	5.3000	5.4333	4.3000	4.0840	-0.0237	-0.0253	-0.0274	-0.0274
0.95	5.3000	5.4333	4.3000	4.0840	0.0000	0.0000	0.0000	0.0000
1.00	5.2000	5.4704	4.2000	3.7990	-0.0240	-0.0317	-0.0276	-0.0302
1.05	5.2000	5.4704	4.2000	3.7990	0.0000	0.0000	0.0000	0.0000
1.10	5.1000	5.1239	4.1000	3.9459	-0.0244	-0.0234	-0.0278	-0.0359
1.15	5.1000	5.1239	4.1000	3.9459	0.0000	0.0000	0.0000	0.0000
1.20	5.0000	4.9904	4.0000	3.9043	-0.0248	-0.0219	-0.0280	-0.0262
1.25	5.0000	4.9904	4.0000	3.9043	0.0000	0.0000	0.0000	0.0000
1.30	5.0000	4.9904	4.0000	3.9043	0.0000	0.0000	0.0000	0.0000
1.35	5.0000	4.9904	4.0000	3.9043	0.0000	0.0000	0.0000	0.0000
1.40	5.0000	4.9904	4.0000	3.9043	0.0000	0.0000	0.0000	0.0000
1.45	5.0000	4.9904	4.0000	3.9043	0.0000	0.0000	0.0000	0.0000
1.50	5.0000	4.9904	4.0000	3.9043	0.0000	0.0000	0.0000	0.0000

5.14a Result of running BREM with NOISE for a low SNR.

5.14b Plots of the actual (2) and reconstructed (3) wave speeds.

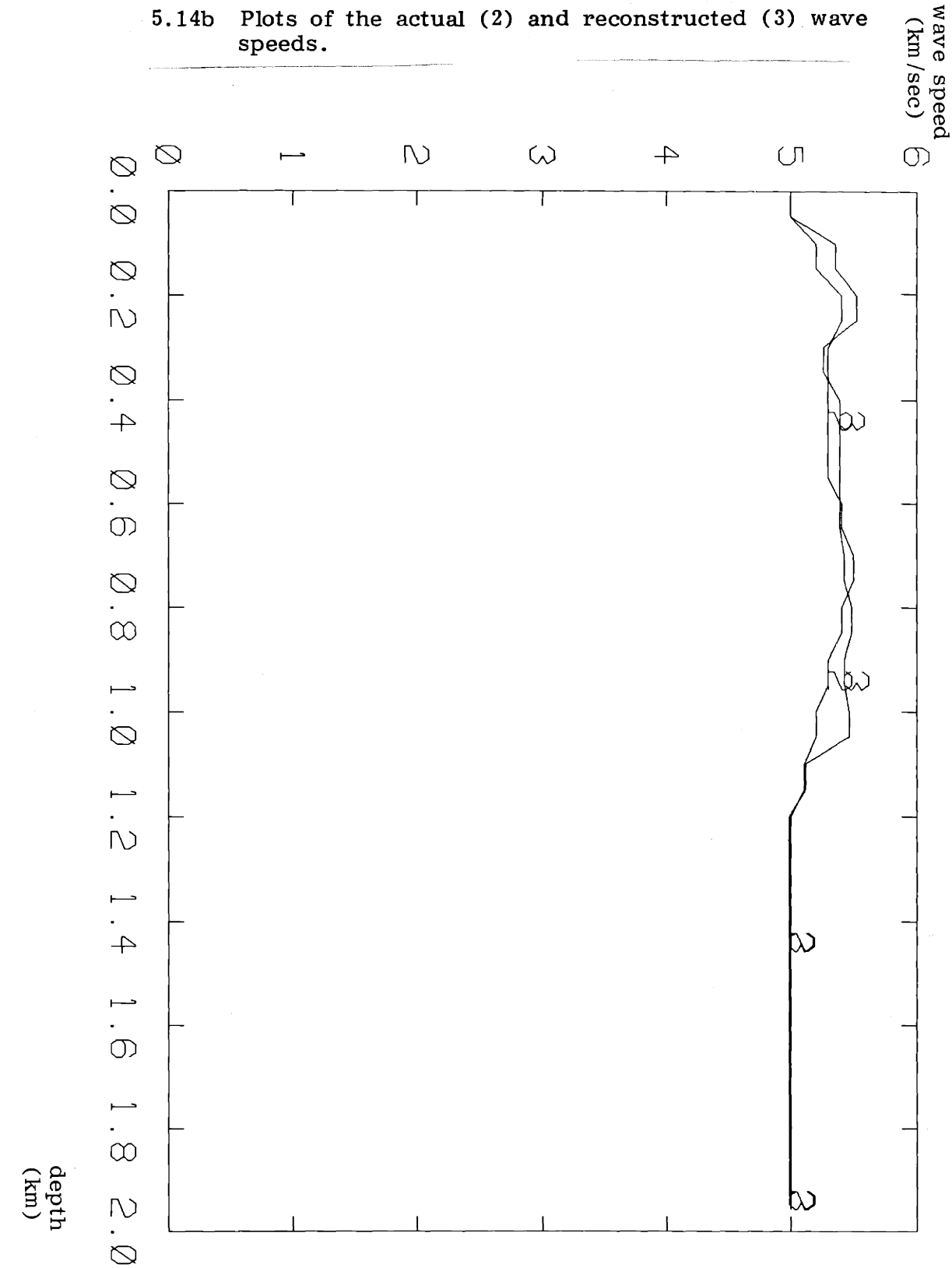

5.14c Plots of the actual (4) and reconstructed (5) densities.

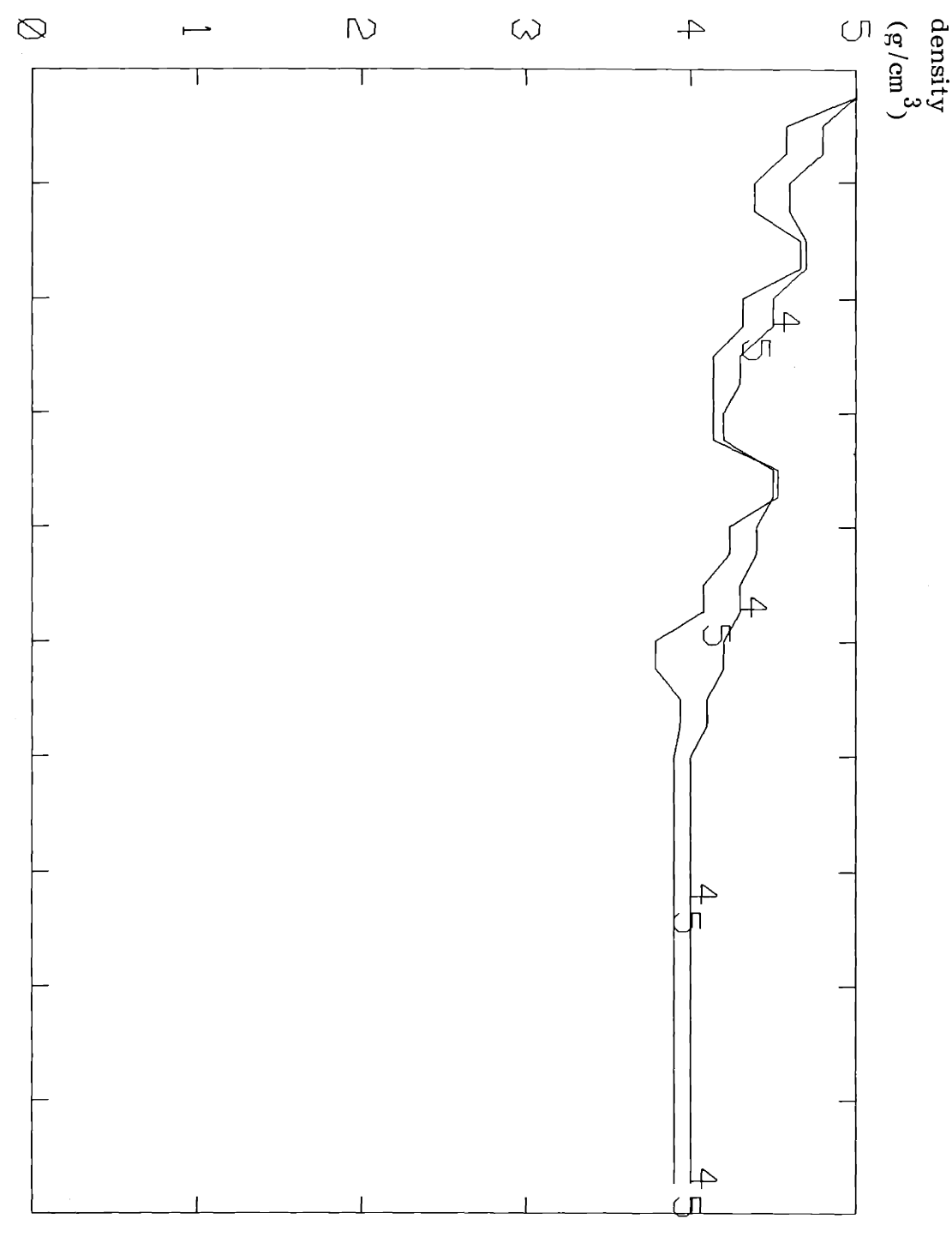

5.14d Plots of the noiseless (3) and noisy (4) wave forms used as data for INVDISC, for p = p1.

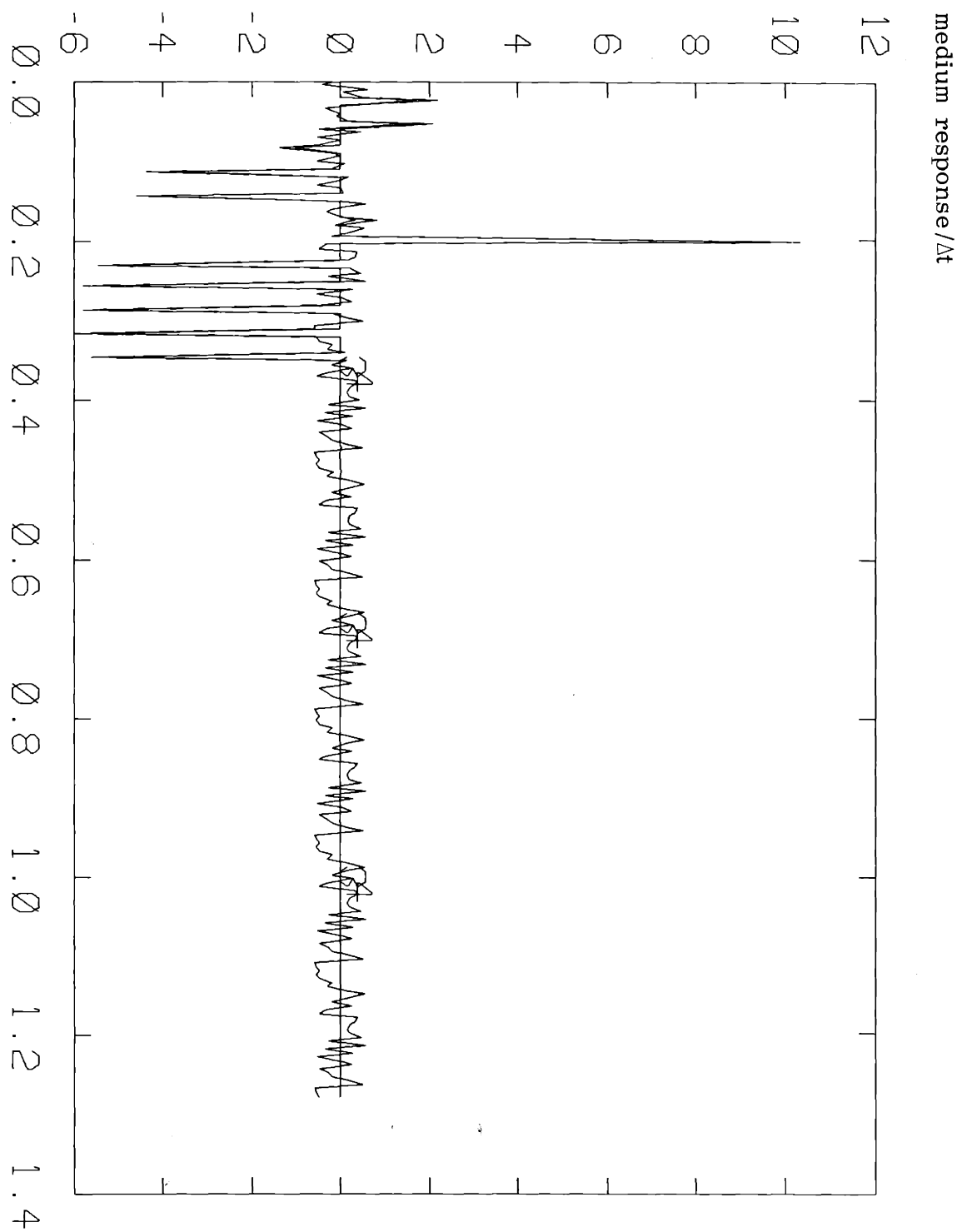

5.14e Plots of the noiseless (1) and noisy (2) wave forms used as data for INVDISC, for p = p2.

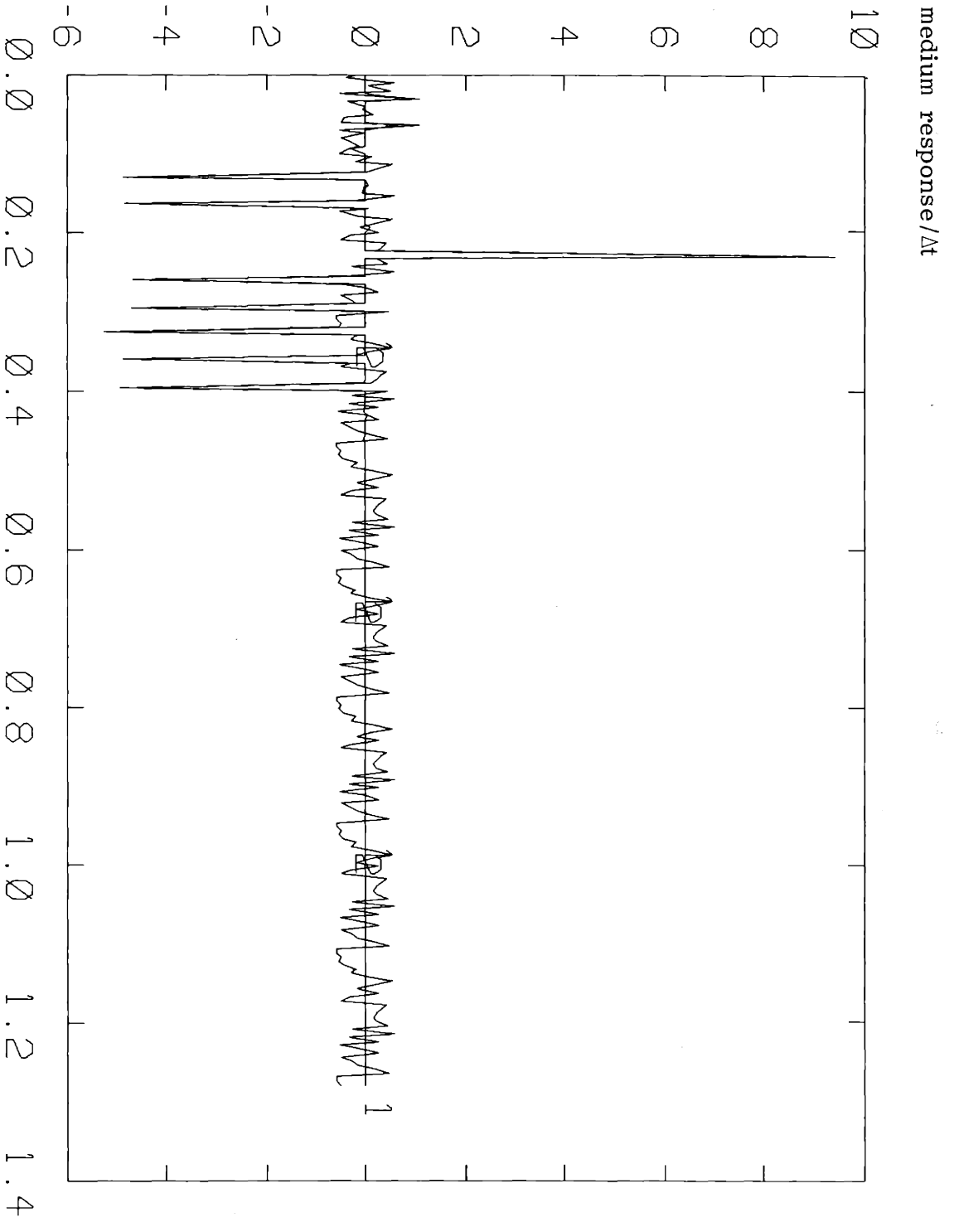

a reasonable job of reconstructing the medium. More dramatic results are available; Figure 5.15 shows the results of a computer run on the same medium with S/N = 7.6 and 5.1. The algorithm does not work well, but in view of the low S/N its performance is surprisingly good.

Generally speaking, the layer stripping algorithm works very well at S/N ratios above 20, works moderately well for S/N ratios between 8 and 20, and starts to break down at a S/N ratio of 8. High angles of incidence, corresponding to wide-angle reflections, help since this makes the reflection coefficients larger, increasing the strength of the reflection response. However, this can result in having problems with double readings and post-critical incidence.

The particular medium and values of noise greatly influence matters in the S/N range of 8-20, since one noisy primary reflection can lead to computation of an incorrect wave speed, projection to the wrong time for the next reflection, and misreadings of consequence reflections. Below a S/N value of 8 or so, the algorithm breaks down after about 10-15 layers, where the conditioning of the problem becomes poor.

It should be kept in mind that the layer stripping algorithm considered here is <u>not</u> the true fast Cholesky algorithm investigated by Symes and Zimmerman (1982) and Bruckstein et al. (1984). Those works considered the inverse problem at <u>normal</u> incidence, for which the goal is merely reconstruction of the impedance profile as a function of travel time. Since there was never any need to project ahead to a computed time to read the next primary reflection, the consequences of a misreading were not as dire as in the present algorithm. This is why those works reported results that were more impressive (though not excessively so) than those reported here.

n=15 m= 8 dd=0.100 del=0.050 dt=0.00500 p1=0.15 p2=0.12 xl=0.5E-02
rms signal= 0.007291 0.005442 rms noise= 0.003028 snr= 7.6 5.1

depth	cact	ccomp	rhoact	rhocomp	r1	rc1	r2	rc2
0.00	5.0000	5.0000	5.0000	5.0000	0.0000	0.0000	0.0000	0.0000
0.05	5.0000	5.0000	5.0000	5.0232	0.0000	0.0023	0.0000	0.0023
0.10	5.2000	5.1877	4.8000	4.8581	0.0269	0.0276	0.0110	0.0127
0.15	5.2000	5.2138	4.8000	4.7847	0.0000	-0.0012	0.0000	-0.0035
0.20	5.4000	5.4718	4.6000	4.4445	0.0301	0.0308	0.0104	0.0041
0.25	5.4000	5.4218	4.6000	4.5117	0.0000	-0.0063	0.0000	-0.0005
0.30	5.3000	5.3553	4.7000	4.4912	-0.0155	-0.0201	-0.0052	-0.0129
0.35	5.3000	5.3249	4.7000	4.5013	0.0000	-0.0068	0.0000	-0.0037
0.40	5.3000	5.2330	4.5000	4.4775	-0.0217	-0.0260	-0.0217	-0.0172
0.45	5.3000	5.2365	4.5000	4.4366	0.0000	-0.0037	0.0000	-0.0040
0.50	5.3000	5.2874	4.3000	4.1697	-0.0227	-0.0182	-0.0227	-0.0230
0.55	5.3000	5.2540	4.3000	4.2195	0.0000	-0.0025	0.0000	0.0007
0.60	5.4000	5.3695	4.2000	4.0616	0.0145	0.0107	0.0041	-0.0008
0.65	5.4000	5.3219	4.2000	4.1620	0.0000	-0.0003	0.0000	0.0046
0.70	5.5000	5.4524	4.5000	4.4012	0.0621	0.0628	0.0505	0.0487
0.75	5.5000	5.3775	4.5000	4.5262	0.0000	-0.0063	0.0000	0.0020
0.80	5.4000	5.1988	4.4000	4.5798	-0.0389	-0.0397	-0.0273	-0.0224
0.85	5.4000	5.1769	4.4000	4.6713	0.0000	0.0045	0.0000	0.0064
0.90	5.3000	5.0504	4.3000	4.5587	-0.0377	-0.0422	-0.0274	-0.0320
0.95	5.3000	5.1024	4.3000	4.4675	0.0000	0.0021	0.0000	-0.0020
1.00	5.2000	5.0792	4.2000	4.2357	-0.0368	-0.0321	-0.0276	-0.0303
1.05	5.2000	4.6577	4.2000	4.7775	0.0000	-0.0328	0.0000	-0.0056
1.10	5.1000	4.7388	4.1000	4.5654	-0.0361	-0.0056	-0.0278	-0.0101
1.15	5.1000	4.5090	4.1000	4.6671	0.0000	-0.0369	0.0000	-0.0249
1.20	5.0000	4.4860	4.0000	4.6838	-0.0356	-0.0029	-0.0280	-0.0018
1.25	5.0000	4.1673	4.0000	5.2653	0.0000	-0.0052	0.0000	0.0081
1.30	5.0000	3.7421	4.0000	6.0910	0.0000	-0.0102	0.0000	0.0034
1.35	5.0000	4.0236	4.0000	5.5290	0.0000	0.0065	0.0000	-0.0021
1.40	5.0000	4.1247	4.0000	5.2681	0.0000	-0.0044	0.0000	-0.0079
1.45	5.0000	4.4142	4.0000	4.7516	0.0000	0.0059	0.0000	-0.0056
1.50	5.0000	4.6862	4.0000	4.2761	0.0000	0.0033	0.0000	-0.0101
1.55	5.0000	4.6490	4.0000	4.3827	0.0000	0.0045	0.0000	0.0065
1.60	5.0000	4.6493	4.0000	4.3667	0.0000	-0.0017	0.0000	-0.0018
1.65	5.0000	4.4286	4.0000	4.7533	0.0000	-0.0030	0.0000	0.0078
1.70	5.0000	4.2095	4.0000	5.1299	0.0000	-0.0056	0.0000	0.0034
1.75	5.0000	4.0582	4.0000	5.3353	0.0000	-0.0101	0.0000	-0.0046
1.80	5.0000	4.3492	4.0000	4.8194	0.0000	0.0066	0.0000	-0.0044
1.85	5.0000	4.2999	4.0000	4.8985	0.0000	-0.0017	0.0000	0.0003
1.90	5.0000	4.7303	4.0000	4.1725	0.0000	0.0080	0.0000	-0.0127
1.95	5.0000	4.8948	4.0000	3.9396	0.0000	0.0070	0.0000	-0.0031
2.00	5.0000	4.9680	4.0000	**3.8634**	**0.0000**	0.0066	0.0000	0.0017

5.15 Result of running BREM with NOISE for a low SNR, showing how the algorithm breaks down after 20 layers.

However, it is not necessary to deal with the algorithm only in its present form. In the next section we consider some modifications of the algorithm designed to improve its performance in noise.

5.4 Modifications of the Algorithm for Dealing with Noisy Data

5.4.1 Zeroing Out Reflection Coefficients Using the Condition Number

One problem with the layer stripping algorithm as it stands is that the reading of the reflection coefficients from the data is a completely a posteriori process. Although the algorithm cannot provide an a priori estimate of the next reflection coefficient, it can provide a measure of accuracy of its measurement: the condition number c(n) of the inverse problem at the depth $z = n\Delta$ in question. As noted by Bruckstein et al. (1984), the condition number for the normal incidence inverse problem is given by (5-1). Furthermore, an error analysis given in Bruckstein et al. (1984) for the normal incidence inverse problem with a free surface boundary condition reveals that the error in reading the nth reflection coefficient can be bounded by c(n-1), as

$$|r_n - \hat{r}_n| \leq 2\varepsilon\, c(n-1) + O(\varepsilon^2) = 2\varepsilon \prod_{i=1}^{n-1} \frac{1+|r_i|}{1-|r_i|} + O(\varepsilon^2) , \qquad (5\text{-}11)$$

where ε is the maximum noise strength and the r_i have absolute values less than one.

Bruckstein et al. (1984) point out that by symmetry the roles of the read and actual reflection coefficients can be interchanged, i.e., r_n can be considered the data and $\hat{r}_n$ the actual value. This means that the possible error in reading $\hat{r}_n$ can be bounded by the following bound

computed from the previous read reflection coefficients

$$|r_n - \hat{r}_n| \leq 2\varepsilon \prod_{i=1}^{n-1} \frac{1+|\hat{r}_i|}{1-|\hat{r}_i|} + O(\varepsilon^2) \quad , \tag{5-12}$$

which can be computed as the layer stripping algorithm runs. Since the two-component wave system (4-30) for the non-normal incidence inverse problem has the same form as the wave system (3-34) for the normal incidence inverse problem, these results all carry over into the non-normal incidence inverse problem. Of course, the reflection coefficients themselves have different values, but that is irrelevant.

Even equation (5-12) would seem to be of little help, since we have no a priori notion of what r_n is. However, for a true discrete layered medium, with a small Δ chosen, it would be expected that most of the reflection coefficients would be zero, and that the non-zero reflection coefficients, particularly at high angles of incidence, would be quite large (on the order of 0.1 or so). In this situation, it makes sense to incorporate these a priori notions into the algorithm by setting values of $\hat{r}_n$ less in absolute value than the bound in (5-12) to zero. This serves to eliminate much of the observation noise, and should improve the performance of the algorithm. Of course, this also may eliminate some weak primary reflections and their succeeding multiples, but these are generally buried in the noise anyway.

Bruckstein et al. (1984) report that incorporating this modification into the fast Cholesky algorithm for the normal incidence inverse problem considerably improves its performance. Certainly for a medium consisting of relatively thick (compared to Δ) layers of sharply varying properties this modification should help. However, for relatively smoothly varying media with layer thicknesses less than about 4Δ, results are mixed.

Figures 5.16 show the results of running the layer stripping algorithm with and without this modification on the response of a medium whose layer thicknesses are 4Δ, at S/N = 8.7 and 9.7. Note that without this modification the noise has more opportunities to degrade the algorithm and it breaks down at the twelfth layer. With the modification it works well through eighteen layers. Figures 5.17, showing the effect of the modification on a medium with a mixture of strong and weak reflections at S/N = 13.8 and 16.9, shows how the modification smooths out the reconstructed profiles. On the other hand, Figures 5.18 show the modification leading to a worse reconstruction, due to the suppression of several weak primary reflections.

In summary, it seems that setting measured reflection coefficients less than the threshold (5-12) to zero improves the performance of the algorithm if Δ is much less than a typical layer thickness, since this eliminates much of the noise. On the other hand, if Δ is greater than about one-third of a typical layer thickness, the noise suppression due to this modification becomes minimal, and suppression of weak primary reflections tends to worsen the performance of the algorithm. The decision of whether or not to use this modification must be made on the basis of a priori knowledge about the general nature of the medium. In any case, monitoring the threshold (5-12) gives some notion of the reliability of the reconstruction at each depth.

5.4.2 Use of Reflection Responses at More Than Two Angles of Incidence

In the layer stripping algorithm, the response of the medium is stacked at two values of slowness p (i.e., computed at two angles of incidence), since this suffices to compute the updates of the two parameters $\rho(z)$ and $c(z)$. However, it is possible to compute the medium

n=16 m= 9 dd=0.100 del=0.025 dt=0.00250 p1=0.05 p2=0.10 x1=0.5E-02
rms signal= 0.008274 0.009316 rms noise= 0.003046 snr= 8.7 9.7

depth	cact	ccomp	rhoact	rhocomp	r1	rc1	r2	rc2
0.00	5.0000	5.0000	5.0000	5.0000	0.0000	0.0000	0.0000	0.0000
0.03	5.0000	5.0000	5.0000	5.0000	0.0000	0.0000	0.0000	0.0000
0.05	5.0000	5.0000	5.0000	5.0000	0.0000	0.0000	0.0000	0.0000
0.08	5.0000	5.0000	5.0000	5.0000	0.0000	0.0000	0.0000	0.0000
0.10	6.0000	5.8923	4.0000	4.0762	-0.0130	-0.0135	0.0192	0.0147
0.13	6.0000	5.8923	4.0000	4.0762	0.0000	0.0000	0.0000	0.0000
0.15	6.0000	5.8923	4.0000	4.0762	0.0000	0.0000	0.0000	0.0000
0.18	6.0000	5.8923	4.0000	4.0762	0.0000	0.0000	0.0000	0.0000
0.20	6.0000	5.8923	4.0000	4.0762	0.0000	0.0000	0.0000	0.0000
0.23	6.0000	5.8923	4.0000	4.0762	0.0000	0.0000	0.0000	0.0000
0.25	6.0000	5.8923	4.0000	4.0762	0.0000	0.0000	0.0000	0.0000
0.28	6.0000	5.8923	4.0000	4.0762	0.0000	0.0000	0.0000	0.0000
0.30	6.0000	5.8057	4.5000	4.6442	0.0588	0.0571	0.0588	0.0539
0.33	6.0000	5.8057	4.5000	4.6442	0.0000	0.0000	0.0000	0.0000
0.35	6.0000	5.8057	4.5000	4.6442	0.0000	0.0000	0.0000	0.0000
0.38	6.0000	5.8057	4.5000	4.6442	0.0000	0.0000	0.0000	0.0000
0.40	6.0000	5.9983	5.0000	4.9558	0.0526	0.0503	0.0526	0.0574
0.43	6.0000	5.9983	5.0000	4.9558	0.0000	0.0000	0.0000	0.0000
0.45	6.0000	5.9983	5.0000	4.9558	0.0000	0.0000	0.0000	0.0000
0.48	6.0000	6.3234	5.0000	4.5515	0.0000	-0.0134	0.0000	0.0000
0.50	5.5000	5.9788	5.0000	4.3354	-0.0474	-0.0552	-0.0649	-0.0693
0.53	5.5000	5.9788	5.0000	4.3354	0.0000	0.0000	0.0000	0.0000
0.55	5.5000	5.9788	5.0000	4.3354	0.0000	0.0000	0.0000	0.0000
0.57	5.5000	5.9788	5.0000	4.3354	0.0000	0.0000	0.0000	0.0000
0.60	5.0000	5.2526	5.0000	4.5652	-0.0511	-0.0444	-0.0657	-0.0687
0.62	5.0000	5.2526	5.0000	4.5652	0.0000	0.0000	0.0000	0.0000
0.65	5.0000	5.2526	5.0000	4.5652	0.0000	0.0000	0.0000	0.0000
0.67	5.0000	5.2526	5.0000	4.5652	0.0000	0.0000	0.0000	0.0000
0.70	4.0000	6.3594	6.0000	3.4197	-0.0263	-0.0400	-0.0487	0.0000
0.72	4.0000	5.1096	6.0000	4.3402	0.0000	0.0000	0.0000	-0.0441
0.75	4.0000	5.1096	6.0000	4.3402	0.0000	0.0000	0.0000	0.0000

5.16a Result of running BREM with NOISE using the condition number modification.

n=16 m= 9 dd=0.100 del=0.025 dt=0.00250 p1=0.05 p2=0.10 xl=0.5E-02
rms signal= 0.008274 0.009316 rms noise= 0.003046 snr= 8.7 9.7

depth	cact	ccomp	rhoact	rhocomp	r1	rc1	r2	rc2
0.00	5.0000	5.0000	5.0000	5.0000	0.0000	0.0000	0.0000	0.0000
0.03	5.0000	4.7037	5.0000	5.4409	0.0000	0.0098	0.0000	0.0023
0.05	5.0000	4.5263	5.0000	5.6528	0.0000	-0.0012	0.0000	-0.0053
0.08	5.0000	4.6774	5.0000	5.3920	0.0000	-0.0063	0.0000	-0.0028
0.10	6.0000	5.9886	4.0000	3.9616	-0.0130	-0.0211	0.0192	0.0187
0.13	6.0000	5.9318	4.0000	3.9588	0.0000	-0.0056	0.0000	-0.0077
0.15	6.0000	5.6675	4.0000	4.1933	0.0000	0.0039	0.0000	-0.0056
0.18	6.0000	5.8482	4.0000	4.0321	0.0000	-0.0025	0.0000	0.0039
0.20	6.0000	5.7861	4.0000	4.0773	0.0000	-0.0002	0.0000	-0.0025
0.23	6.0000	5.7732	4.0000	4.0928	0.0000	0.0007	0.0000	0.0002
0.25	6.0000	5.9794	4.0000	3.9003	0.0000	-0.0049	0.0000	0.0027
0.28	6.0000	7.0442	4.0000	3.2745	0.0000	0.0042	0.0000	0.0552
0.30	6.0000	7.0385	4.5000	3.6549	0.0588	0.0544	0.0588	0.0541
0.33	6.0000	6.9864	4.5000	3.7447	0.0000	0.0079	0.0000	0.0048
0.35	6.0000	6.9323	4.5000	3.8147	0.0000	0.0048	0.0000	0.0017
0.38	6.0000	6.7323	4.5000	3.9945	0.0000	0.0065	0.0000	-0.0044
0.40	6.0000	6.9653	5.0000	4.2304	0.0526	0.0479	0.0526	0.0607
0.43	6.0000	7.8079	5.0000	3.6928	0.0000	-0.0018	0.0000	0.0583
0.45	6.0000	7.9586	5.0000	3.5544	0.0000	-0.0078	0.0000	0.0061
0.48	6.0000	7.9864	5.0000	3.5669	0.0000	0.0038	0.0000	0.0065
0.50	5.5000	8.0636	5.0000	3.4875	-0.0474	-0.0055	-0.0649	0.0023
0.53	5.5000	8.5205	5.0000	2.8938	0.0000	-0.0600	0.0000	-0.0047
0.55	5.5000	8.8368	5.0000	2.4742	0.0000	-0.0558	0.0000	-0.0042
0.57	5.5000	8.8349	5.0000	2.4877	0.0000	0.0026	0.0000	0.0022
0.60	5.0000	8.3719	5.0000	2.6797	-0.0511	0.0041	-0.0657	-0.0671
0.62	5.0000	7.6584	5.0000	2.9684	0.0000	-0.0019	0.0000	-0.0742
0.65	5.0000	7.6200	5.0000	2.9959	0.0000	0.0017	0.0000	-0.0014
0.67	5.0000	7.5473	5.0000	3.0655	0.0000	0.0059	0.0000	0.0002
0.70	4.0000	7.9035	6.0000	2.6585	-0.0263	-0.0441	-0.0487	-0.0139
0.72	4.0000	7.8057	6.0000	2.6974	0.0000	-0.0001	0.0000	-0.0090
0.75	4.0000	7.7405	6.0000	2.6988	0.0000	-0.0047	0.0000	-0.0103

5.16b Result of running BREM with NOISE without the condition number modification. In this case the modification improves the performance of INVDISC.

n=16 m= 8 dd=0.100 del=0.050 dt=0.00500 p1=0.15 p2=0.10 x1=0.1E-02

rms signal= 0.005995 0.004159 rms noise= 0.000853 snr= 16.9 13.8

depth	cact	ccomp	rhoact	rhocomp	r1	rc1	r2	rc2
0.00	5.0000	5.0000	5.0000	5.0000	0.0000	0.0000	0.0000	0.0000
0.05	5.0000	5.0000	5.0000	5.0000	0.0000	0.0000	0.0000	0.0000
0.10	5.1000	5.1274	4.9000	4.8337	0.0131	0.0128	0.0032	0.0000
0.15	5.1000	5.1274	4.9000	4.8337	0.0000	0.0000	0.0000	0.0000
0.20	5.2000	5.2061	4.8000	4.7795	0.0138	0.0134	0.0029	0.0048
0.25	5.2000	5.2061	4.8000	4.7795	0.0000	0.0000	0.0000	0.0000
0.30	5.3000	5.3111	4.7000	4.6751	0.0146	0.0154	0.0026	0.0028
0.35	5.3000	5.3111	4.7000	4.6751	0.0000	0.0000	0.0000	0.0000
0.40	5.3000	5.3111	4.7000	4.6751	0.0000	0.0000	0.0000	0.0000
0.45	5.3000	5.3111	4.7000	4.6751	0.0000	0.0000	0.0000	0.0000
0.50	5.2000	5.2015	4.6000	4.5917	-0.0358	-0.0365	-0.0239	-0.0234
0.55	5.2000	5.2015	4.6000	4.5917	0.0000	0.0000	0.0000	0.0000
0.60	5.1000	5.0965	4.5000	4.4960	-0.0351	-0.0358	-0.0242	-0.0244
0.65	5.1000	5.0965	4.5000	4.4960	0.0000	0.0000	0.0000	0.0000
0.70	5.0000	5.0179	4.4000	4.3589	-0.0345	-0.0338	-0.0245	-0.0259
0.75	5.0000	5.0179	4.4000	4.3589	0.0000	0.0000	0.0000	0.0000
0.80	4.9000	4.9238	4.3000	4.2411	-0.0340	-0.0350	-0.0249	-0.0263
0.85	4.9000	4.9238	4.3000	4.2411	0.0000	0.0000	0.0000	0.0000
0.90	4.8000	4.8233	4.2000	4.1379	-0.0337	-0.0345	-0.0252	-0.0258
0.95	4.8000	4.8233	4.2000	4.1379	0.0000	0.0000	0.0000	0.0000
1.00	4.7000	4.6869	4.3000	4.2941	-0.0096	-0.0107	-0.0018	0.0000
1.05	4.7000	4.6869	4.3000	4.2941	0.0000	0.0000	0.0000	0.0000
1.10	4.7000	4.6869	4.3000	4.2941	0.0000	0.0000	0.0000	0.0000
1.15	4.7000	4.6869	4.3000	4.2941	0.0000	0.0000	0.0000	0.0000
1.20	4.8000	4.7574	4.4000	4.4341	0.0329	0.0310	0.0251	0.0257
1.25	4.8000	4.7574	4.4000	4.4341	0.0000	0.0000	0.0000	0.0000
1.30	4.9000	4.8654	4.5000	4.5330	0.0331	0.0344	0.0247	0.0256
1.35	4.9000	4.8654	4.5000	4.5330	0.0000	0.0000	0.0000	0.0000
1.40	5.0000	4.9669	4.5000	4.5368	0.0225	0.0231	0.0134	0.0140
1.45	5.0000	4.9669	4.5000	4.5368	0.0000	0.0000	0.0000	0.0000
1.50	5.0000	4.9669	4.5000	4.5368	0.0000	0.0000	0.0000	0.0000

5.17a Result of running BREM with NOISE using the condition number modification.

n=16 m= 8 dd=0.100 del=0.050 dt=0.00500 p1=0.15 p2=0.10 x1=0.1E-02
rms signal= 0.005995 0.004159 rms noise= 0.000853 snr= 16.9 13.8

depth	cact	ccomp	rhoact	rhocomp	r1	rc1	r2	rc2
0.00	5.0000	5.0000	5.0000	5.0000	0.0000	0.0000	0.0000	0.0000
0.05	5.0000	5.0000	5.0000	4.9862	0.0000	-0.0014	0.0000	-0.0014
0.10	5.1000	5.1152	4.9000	4.8483	0.0131	0.0128	0.0032	0.0013
0.15	5.1000	5.1124	4.9000	4.8488	0.0000	-0.0006	0.0000	-0.0003
0.20	5.2000	5.1922	4.8000	4.7931	0.0138	0.0134	0.0029	0.0048
0.25	5.2000	5.1940	4.8000	4.7959	0.0000	0.0007	0.0000	0.0005
0.30	5.3000	5.3001	4.7000	4.6897	0.0146	0.0154	0.0026	0.0028
0.35	5.3000	5.3140	4.7000	4.6613	0.0000	0.0005	0.0000	-0.0012
0.40	5.3000	5.3156	4.7000	4.6586	0.0000	0.0001	0.0000	-0.0001
0.45	5.3000	5.3008	4.7000	4.6857	0.0000	-0.0009	0.0000	0.0009
0.50	5.2000	5.1900	4.6000	4.6035	-0.0358	-0.0365	-0.0239	-0.0234
0.55	5.2000	5.1906	4.6000	4.6014	0.0000	-0.0001	0.0000	-0.0001
0.60	5.1000	5.0846	4.5000	4.5069	-0.0351	-0.0358	-0.0242	-0.0244
0.65	5.1000	5.0935	4.5000	4.4984	0.0000	0.0012	0.0000	0.0003
0.70	5.0000	5.0148	4.4000	4.3615	-0.0345	-0.0338	-0.0245	-0.0259
0.75	5.0000	5.0143	4.4000	4.3500	0.0000	-0.0014	0.0000	-0.0014
0.80	4.9000	4.9200	4.3000	4.2327	-0.0340	-0.0350	-0.0249	-0.0263
0.85	4.9000	4.9117	4.3000	4.2517	0.0000	0.0004	0.0000	0.0011
0.90	4.8000	4.8102	4.2000	4.1494	-0.0337	-0.0345	-0.0252	-0.0258
0.95	4.8000	4.8159	4.2000	4.1332	0.0000	-0.0007	0.0000	-0.0012
1.00	4.7000	4.7007	4.3000	4.2507	-0.0096	-0.0107	-0.0018	-0.0016
1.05	4.7000	4.6675	4.3000	4.3115	0.0000	0.0001	0.0000	0.0026
1.10	4.7000	4.6604	4.3000	4.3342	0.0000	0.0011	0.0000	0.0016
1.15	4.7000	4.6235	4.3000	4.3963	0.0000	-0.0006	0.0000	0.0020
1.20	4.8000	4.6974	4.4000	4.5350	0.0329	0.0310	0.0251	0.0257
1.25	4.8000	4.7026	4.4000	4.5260	0.0000	0.0001	0.0000	-0.0003
1.30	4.9000	4.8149	4.5000	4.6208	0.0331	0.0344	0.0247	0.0256
1.35	4.9000	4.8179	4.5000	4.6281	0.0000	0.0014	0.0000	0.0012
1.40	5.0000	4.9230	4.5000	4.6379	0.0225	0.0242	0.0134	0.0152
1.45	5.0000	4.9379	4.5000	4.6245	0.0000	0.0019	0.0000	0.0006
1.50	5.0000	4.9874	4.5000	4.5397	0.0000	0.0019	0.0000	-0.0026

5.17b Result of running BREM with NOISE without the condition number modification. Again the modification improves the performance of INVDISC.

n=16 m= 8 dd=0.100 del=0.050 dt=0.00500 p1=0.15 p2=0.10 x1=0.1E-02

rms signal= 0.005995 0.004159 rms noise= 0.000606 snr= 19.9 16.7

depth	cact	ccomp	rhoact	rhocomp	r1	rc1	r2	rc2
0.00	5.0000	5.0000	5.0000	5.0000	0.0000	0.0000	0.0000	0.0000
0.05	5.0000	5.0000	5.0000	5.0000	0.0000	0.0000	0.0000	0.0000
0.10	5.1000	5.1116	4.9000	4.8746	0.0131	0.0133	0.0032	0.0021
0.15	5.1000	5.1116	4.9000	4.8746	0.0000	0.0000	0.0000	0.0000
0.20	5.2000	5.2367	4.8000	4.7162	0.0138	0.0139	0.0029	0.0000
0.25	5.2000	5.2367	4.8000	4.7162	0.0000	0.0000	0.0000	0.0000
0.30	5.3000	5.3527	4.7000	4.5748	0.0146	0.0145	0.0026	0.0000
0.35	5.3000	5.3527	4.7000	4.5748	0.0000	0.0000	0.0000	0.0000
0.40	5.3000	5.3527	4.7000	4.5748	0.0000	0.0000	0.0000	0.0000
0.45	5.3000	5.3527	4.7000	4.5748	0.0000	0.0000	0.0000	0.0000
0.50	5.2000	5.2643	4.6000	4.4647	-0.0358	-0.0349	-0.0239	-0.0238
0.55	5.2000	5.2643	4.6000	4.4647	0.0000	0.0000	0.0000	0.0000
0.60	5.1000	5.1632	4.5000	4.3760	-0.0351	-0.0350	-0.0242	-0.0234
0.65	5.1000	5.1632	4.5000	4.3760	0.0000	0.0000	0.0000	0.0000
0.70	5.0000	5.0501	4.4000	4.3032	-0.0345	-0.0352	-0.0245	-0.0234
0.75	5.0000	5.0501	4.4000	4.3032	0.0000	0.0000	0.0000	0.0000
0.80	4.9000	4.9736	4.3000	4.1709	-0.0340	-0.0332	-0.0249	-0.0258
0.85	4.9000	4.9736	4.3000	4.1709	0.0000	0.0000	0.0000	0.0000
0.90	4.8000	4.8755	4.2000	4.0773	-0.0337	-0.0332	-0.0252	-0.0245
0.95	4.8000	4.9066	4.2000	4.0216	0.0000	0.0000	0.0000	-0.0027
1.00	4.7000	4.8492	4.3000	4.0566	-0.0096	-0.0083	-0.0018	-0.0034
1.05	4.7000	4.7417	4.3000	4.1764	0.0000	-0.0087	0.0000	0.0000
1.10	4.7000	4.7417	4.3000	4.1764	0.0000	0.0000	0.0000	0.0000
1.15	4.7000	4.7417	4.3000	4.1764	0.0000	0.0000	0.0000	0.0000
1.20	4.8000	4.3490	4.4000	4.9097	0.0329	0.0000	0.0251	0.0264
1.25	4.8000	4.3490	4.4000	4.9097	0.0000	0.0000	0.0000	0.0000
1.30	4.9000	4.4982	4.5000	4.9312	0.0331	0.0323	0.0247	0.0231
1.35	4.9000	4.4982	4.5000	4.9312	0.0000	0.0000	0.0000	0.0000
1.40	5.0000	4.6493	4.5000	4.8380	0.0225	0.0217	0.0134	0.0114
1.45	5.0000	4.6493	4.5000	4.8380	0.0000	0.0000	0.0000	0.0000
1.50	5.0000	4.6493	4.5000	4.8380	0.0000	0.0000	0.0000	0.0000

5.18a Result of running BREM with NOISE using the condition number modification.

n=16 m= 8 dd=0.100 del=0.050 dt=0.00500 ρ1=0.15 ρ2=0.10 ×1=0.1E-02
rms signal= 0.005995 0.004159 rms noise= 0.000606 snr= 19.9 16.7

depth	cact	ccomp	rhoact	rhocomp	r1	rc1	r2	rc2
0.00	5.0000	5.0000	5.0000	5.0000	0.0000	0.0000	0.0000	0.0000
0.05	5.0000	5.0000	5.0000	5.0046	0.0000	0.0005	0.0000	0.0005
0.10	5.1000	5.1116	4.9000	4.8791	0.0131	0.0133	0.0032	0.0021
0.15	5.1000	5.1079	4.9000	4.8853	0.0000	-0.0002	0.0000	0.0001
0.20	5.2000	5.2164	4.8000	4.7662	0.0138	0.0139	0.0029	0.0020
0.25	5.2000	5.2215	4.8000	4.7469	0.0000	-0.0008	0.0000	-0.0014
0.30	5.3000	5.3275	4.7000	4.6305	0.0146	0.0145	0.0026	0.0015
0.35	5.3000	5.3107	4.7000	4.6581	0.0000	-0.0014	0.0000	0.0008
0.40	5.3000	5.3083	4.7000	4.6536	0.0000	-0.0011	0.0000	-0.0008
0.45	5.3000	5.3007	4.7000	4.6623	0.0000	-0.0010	0.0000	0.0000
0.50	5.2000	5.2076	4.6000	4.5561	-0.0358	-0.0349	-0.0239	-0.0238
0.55	5.2000	5.2091	4.6000	4.5454	0.0000	-0.0008	0.0000	-0.0010
0.60	5.1000	5.1071	4.5000	4.4519	-0.0351	-0.0350	-0.0242	-0.0239
0.65	5.1000	5.1181	4.5000	4.4335	0.0000	0.0005	0.0000	-0.0006
0.70	5.0000	5.0001	4.4000	4.3658	-0.0345	-0.0352	-0.0245	-0.0234
0.75	5.0000	4.9847	4.4000	4.3951	0.0000	-0.0002	0.0000	0.0013
0.80	4.9000	4.9036	4.3000	4.2655	-0.0340	-0.0332	-0.0249	-0.0258
0.85	4.9000	4.9034	4.3000	4.2584	0.0000	-0.0009	0.0000	-0.0009
0.90	4.8000	4.8136	4.2000	4.1541	-0.0337	-0.0321	-0.0252	-0.0245
0.95	4.8000	4.8615	4.2000	4.0788	0.0000	0.0013	0.0000	-0.0027
1.00	4.7000	4.7736	4.3000	4.1574	-0.0096	-0.0096	-0.0018	-0.0023
1.05	4.7000	4.7506	4.3000	4.1904	0.0000	-0.0010	0.0000	0.0008
1.10	4.7000	4.7533	4.3000	4.1828	0.0000	-0.0003	0.0000	-0.0005
1.15	4.7000	4.7345	4.3000	4.2119	0.0000	-0.0005	0.0000	0.0009
1.20	4.8000	4.8023	4.4000	4.3594	0.0329	0.0318	0.0251	0.0264
1.25	4.8000	4.7763	4.4000	4.3864	0.0000	-0.0025	0.0000	-0.0004
1.30	4.9000	4.8889	4.5000	4.4565	0.0331	0.0325	0.0247	0.0231
1.35	4.9000	4.8984	4.5000	4.4461	0.0000	0.0009	0.0000	0.0001
1.40	5.0000	5.0144	4.5000	4.4047	0.0225	0.0215	0.0134	0.0108
1.45	5.0000	5.0264	4.5000	4.3854	0.0000	0.0006	0.0000	-0.0006
1.50	5.0000	5.0318	4.5000	**4.3817**	**0.0000**	0.0008	0.0000	0.0003

5.18b Result of running BREM with NOISE without the condition number modification. In this case the modification hampers the performance of the algorithm.

response at more than two angles of incidence, resulting in an overdetermined system for the two updates at each depth, and then use a least-squares fit. This can be done as follows.

If the medium response is computed for m different values $p_1 \ldots p_m$ of slowness p, i.e., m different angles of incidence ($\theta_i = \sin^{-1} p_i c_o$, i = 1 ... m), then running m copies of the wave updates (4-42) - (4-43) will result in the computation of m different reflectivity functions ($r_i(z)$, i = 1 ... m), which are related to the medium parameter updates by

$$\begin{bmatrix} r_1(z) \\ \vdots \\ r_m(z) \end{bmatrix} = \frac{1}{2} \begin{bmatrix} 1/\rho(z) & 1/(c(z)\cos^2\theta_1(z)) \\ \vdots & \vdots \\ 1/\rho(z) & 1/(c(z)\cos^2\theta_m(z)) \end{bmatrix} \begin{bmatrix} (d/dz)\ \rho(z) \\ \\ (d/dz)\ c(z) \end{bmatrix} . \qquad (5\text{-}13)$$

Note that (5-13) reduces to (4-34) for m = 2, as it should.

The overdetermined system (5-13) can be written as

$$\underline{r}(z) = M(z) \begin{bmatrix} (d/dz)\ \rho(z) \\ \\ (d/dz)\ c(z) \end{bmatrix} \qquad (5\text{-}14)$$

and it is well-known that the minimum square error solution to (5-14) is given by

$$\begin{bmatrix} (d/dz)\ \rho(z) \\ \\ (d/dz)\ c(z) \end{bmatrix} = (M^T M)^{-1} M^T \underline{r}(z) \qquad (5\text{-}15)$$

After discretization, (5-15) becomes

$$\rho(z+\Delta) = \rho(z) + \frac{2\Delta\rho(z)}{DET(z)}\left(\sum_{i=1}^{m}\cos^{-4}\theta_i(z)\sum_{j=1}^{m}r_j(z) - \sum_{j=1}^{m}r_j(z)\cos^{-2}\theta_j(z)\sum_{i=1}^{m}\cos^{-2}\theta_i(z)\right) \tag{5-16a}$$

$$c(z+\Delta) = c(z) + \frac{2\Delta c(z)}{DET(z)}\left(-\sum_{i=1}^{m}\cos^{-2}\theta_i(z)\sum_{j=1}^{m}r_j(z) + m\sum_{i=1}^{m}r_i(z)\cos^{-2}\theta_i(z)\right) \tag{5-16b}$$

where

$$DET(z) \triangleq m\sum_{i=1}^{m}\cos^{-4}\theta_i(z) - \left(\sum_{j=1}^{m}\cos^{-2}\theta_j(z)\right)^2 . \tag{5-17}$$

The results of this modification were tested by computing the reflection responses of a layered medium at five different angles of incidence using the program MULTFOR, adding noise, and then running five copies of the wave updates (4-42) - (4-43) together with the medium parameter updates (5-16) and the condition number modification. The program MULT1 does all this. Results are tabulated in Figure 5.19a, and are rather dramatic: the algorithm works quite well, even though the data has S/N = 1, 1.5, 2.6, 4.8, and 8.3! Note that the condition number modification is a big help. For comparison, NOISE was run on the data with the two highest S/N. The results, shown in Figure 5.19b, are much poorer.

For a discrete medium with sharp variation at interfaces, the continuous updates can no longer be used, and the least-squares fit of the updated parameters becomes a very complicated non-linear problem. An easier procedure is simply to compute updated parameters for each pair of reflection coefficients, and then average them. If m different

n=18 m= 9 nm= 5 dd=0.100 del=0.050 dt=0.00250 x1=0.2E-02
values of r are 0.05 0.08 0.11 0.14 0.16

snr=	1.0	1.5	2.6	4.8	8.3			
depth	cact	ccomp	rhoact	rhocomp	r1	rc1	r2	rc2
0.00	5.0000	5.0000	5.0000	5.0000	0.0000	0.0000	0.0000	0.0000
0.05	5.0000	5.0171	5.0000	4.9532	0.0000	0.0000	0.0000	-0.0044
0.10	5.0500	5.0894	5.0500	4.9684	0.0103	0.0101	0.0109	0.0055
0.15	5.0500	5.0952	5.0500	4.9489	0.0000	0.0000	0.0000	0.0000
0.20	5.1000	5.1432	5.1000	5.0232	0.0102	0.0118	0.0108	0.0140
0.25	5.1000	5.1432	5.1000	5.0232	0.0000	0.0000	0.0000	0.0000
0.30	5.1500	5.1578	5.1500	5.1305	0.0101	0.0124	0.0107	0.0097
0.35	5.1500	5.1531	5.1500	5.1298	0.0000	0.0000	0.0000	0.0000
0.40	5.2000	5.2021	5.1000	5.0711	0.0003	0.0000	0.0010	0.0000
0.45	5.2000	5.2021	5.1000	5.0711	0.0000	0.0000	0.0000	0.0000
0.50	5.2500	5.2386	5.0500	5.0323	0.0002	0.0000	0.0009	0.0000
0.55	5.2500	5.2386	5.0500	5.0323	0.0000	0.0000	0.0000	0.0000
0.60	5.3000	5.3030	5.0000	4.9591	0.0001	0.0000	0.0008	0.0000
0.65	5.3000	5.2977	5.0000	4.9788	0.0000	0.0000	0.0000	0.0000
0.70	5.3500	5.3544	4.9500	4.9172	0.0000	0.0000	0.0007	0.0000
0.75	5.3500	5.3544	4.9500	4.9172	0.0000	0.0000	0.0000	0.0000
0.80	5.4000	5.4141	4.9000	4.8256	-0.0001	0.0000	0.0006	-0.0047
0.85	5.4000	5.3944	4.9000	4.8512	0.0000	0.0000	0.0000	0.0000
0.90	5.4500	5.4231	4.8500	4.8421	-0.0002	0.0000	0.0005	0.0000
0.95	5.4500	5.4282	4.8500	4.8219	0.0000	0.0000	0.0000	0.0000
1.00	5.5000	5.4691	4.8000	4.7980	-0.0003	0.0000	0.0005	0.0000
1.05	5.5000	5.4691	4.8000	4.7980	0.0000	0.0000	0.0000	0.0000
1.10	5.4500	5.4042	4.7500	4.7583	-0.0102	-0.0142	-0.0109	-0.0102
1.15	5.4500	5.4042	4.7500	4.7583	0.0000	0.0000	0.0000	0.0000
1.20	5.4000	5.3487	4.7000	4.7198	-0.0103	-0.0075	-0.0110	-0.0128
1.25	5.4000	5.3487	4.7000	4.7198	0.0000	0.0000	0.0000	0.0000
1.30	5.3500	5.3235	4.6500	4.6331	-0.0104	-0.0126	-0.0110	-0.0142
1.35	5.3500	5.3235	4.6500	4.6331	0.0000	0.0000	0.0000	0.0000
1.40	5.3000	5.2867	4.6000	4.5764	-0.0105	-0.0073	-0.0111	-0.0098
1.45	5.3000	5.2867	4.6000	4.5764	0.0000	0.0000	0.0000	0.0000
1.50	5.2500	5.2183	4.5500	4.5272	-0.0106	-0.0116	-0.0112	-0.0134
1.55	5.2500	5.2183	4.5500	4.5272	0.0000	0.0000	0.0000	0.0000
1.60	5.2000	5.1663	4.5000	4.4664	-0.0107	-0.0124	-0.0113	-0.0105
1.65	5.2000	5.1663	4.5000	4.4664	0.0000	0.0000	0.0000	0.0000
1.70	**5.2000**	**5.1663**	**4.5000**	**4.4664**	**0.0000**	**0.0000**	**0.0000**	**0.0000**
1.75	**5.2000**	**5.1897**	**4.5000**	**4.4120**	**0.0000**	**-0.0050**	**0.0000**	**-0.0050**

5.19a Result of running MULTFOR, which runs BREM using several different angles of incidence, with MULT1, which adds noise and uses a least-squares fit to compute the updated wave speed and density at each depth. Note the low SNR's.

r3	rc3	r4	rc4	r5	rc5
0.0000	0.0000	0.0000	0.0000	0.0000	0.0000
0.0000	-0.0046	0.0000	0.0000	0.0000	0.0000
0.0121	0.0171	0.0148	0.0144	0.0190	0.0218
0.0000	-0.0048	0.0000	0.0000	0.0000	0.0000
0.0121	0.0136	0.0149	0.0184	0.0194	0.0210
0.0000	0.0000	0.0000	0.0000	0.0000	0.0000
0.0120	0.0144	0.0149	0.0156	0.0198	0.0139
0.0000	0.0000	0.0000	-0.0044	0.0000	0.0000
0.0023	0.0000	0.0053	0.0051	0.0105	0.0090
0.0000	0.0000	0.0000	0.0000	0.0000	0.0000
0.0022	0.0000	0.0054	0.0064	0.0110	0.0065
0.0000	0.0000	0.0000	0.0000	0.0000	0.0000
0.0022	0.0000	0.0055	0.0080	0.0115	0.0128
0.0000	0.0052	0.0000	0.0000	0.0000	0.0000
0.0021	0.0055	0.0055	0.0000	0.0121	0.0149
0.0000	0.0000	0.0000	0.0000	0.0000	0.0000
0.0021	0.0000	0.0057	0.0000	0.0128	0.0132
0.0000	0.0000	0.0000	0.0000	0.0000	-0.0054
0.0020	0.0060	0.0058	0.0084	0.0136	0.0078
0.0000	-0.0056	0.0000	0.0000	0.0000	0.0000
0.0020	0.0067	0.0059	0.0080	0.0144	0.0118
0.0000	0.0000	0.0000	0.0000	0.0000	0.0000
-0.0124	-0.0090	-0.0163	-0.0208	-0.0249	-0.0292
0.0000	0.0000	0.0000	0.0000	0.0000	0.0000
-0.0125	-0.0087	-0.0162	-0.0204	-0.0240	-0.0229
0.0000	0.0000	0.0000	0.0000	0.0000	0.0000
-0.0125	-0.0101	-0.0161	-0.0134	-0.0232	-0.0188
0.0000	0.0000	0.0000	0.0000	0.0000	0.0000
-0.0126	-0.0153	-0.0160	-0.0136	-0.0225	-0.0182
0.0000	0.0000	0.0000	0.0000	0.0000	0.0000
-0.0126	-0.0154	-0.0159	-0.0203	-0.0219	-0.0278
0.0000	0.0000	0.0000	0.0000	0.0000	0.0000
-0.0127	-0.0164	-0.0158	-0.0174	-0.0214	-0.0230
0.0000	0.0000	0.0000	0.0000	0.0000	0.0000
0.0000	0.0000	0.0000	0.0000	0.0000	0.0000
0.0000	0.0000	0.0000	0.0000	0.0000	0.0000

n=18 m= 9 dd=0.100 del=0.050 dt=0.00250 p1=0.14 p2=0.16 x1=0.2E-02
res signal= 0.002173 0.003228 rms noise= 0.001218 snr= 5.0 8.5

depth	cact	ccomp	rhoact	rhocomp	r1	rc1	r2	rc2
0.00	5.0000	5.0000	5.0000	5.0000	0.0000	0.0000	0.0000	0.0000
0.05	5.0000	5.0000	5.0000	5.0000	0.0000	0.0000	0.0000	0.0000
0.10	5.0500	5.0659	5.0500	5.0072	0.0148	0.0137	0.0190	0.0193
0.15	5.0500	5.0659	5.0500	5.0072	0.0000	0.0000	0.0000	0.0000
0.20	5.1000	5.0799	5.1000	5.1457	0.0149	0.0164	0.0194	0.0177
0.25	5.1000	5.0799	5.1000	5.1457	0.0000	0.0000	0.0000	0.0000
0.30	5.1500	5.1304	5.1500	5.1806	0.0149	0.0135	0.0198	0.0182
0.35	5.1500	5.1304	5.1500	5.1806	0.0000	0.0000	0.0000	0.0000
0.40	5.2000	5.1708	5.1000	5.1588	0.0053	0.0061	0.0105	0.0101
0.45	5.2000	5.1708	5.1000	5.1588	0.0000	0.0000	0.0000	0.0000
0.50	5.2500	5.2514	5.0500	5.0356	0.0054	0.0044	0.0110	0.0133
0.55	5.2500	5.2514	5.0500	5.0356	0.0000	0.0000	0.0000	0.0000
0.60	5.3000	5.3367	5.0000	4.8586	0.0055	0.0000	0.0115	0.0107
0.65	5.3000	5.3367	5.0000	4.8586	0.0000	0.0000	0.0000	0.0000
0.70	5.3500	5.4064	4.9500	4.7157	0.0055	0.0000	0.0121	0.0099
0.75	5.3500	5.3723	4.9500	4.7856	0.0000	0.0000	0.0000	-0.0050
0.80	5.4000	5.4632	4.9000	4.6002	0.0057	0.0000	0.0128	0.0140
0.85	5.4000	5.4632	4.9000	4.6002	0.0000	0.0000	0.0000	0.0000
0.90	5.4500	5.5425	4.8500	4.4398	0.0058	0.0000	0.0136	0.0144
0.95	5.4500	5.5425	4.8500	4.4398	0.0000	0.0000	0.0000	0.0000
1.00	5.5000	5.5814	4.8000	4.4194	0.0059	0.0066	0.0144	0.0145
1.05	5.5000	5.5814	4.8000	4.4194	0.0000	0.0000	0.0000	0.0000
1.10	5.4500	5.6469	4.7500	4.1601	-0.0163	-0.0150	-0.0249	0.0000
1.15	5.4500	5.5401	4.7500	4.3706	0.0000	0.0000	0.0000	-0.0234
1.20	5.4000	5.6301	4.7000	4.0343	-0.0162	-0.0193	-0.0240	0.0000
1.25	5.4000	5.4986	4.7000	4.2844	0.0000	0.0000	0.0000	-0.0271
1.30	5.3500	5.4986	4.6500	4.2844	-0.0161	0.0000	-0.0232	0.0000
1.35	5.3500	5.3374	4.6500	4.5954	0.0000	0.0000	0.0000	-0.0249
1.40	5.3000	5.3374	4.6000	4.5954	-0.0160	0.0000	-0.0225	0.0000
1.45	5.3000	5.1680	4.6000	4.9300	0.0000	0.0000	0.0000	-0.0199
1.50	5.2500	5.1680	4.5500	4.9300	-0.0159	0.0000	-0.0219	0.0000
1.55	5.2500	4.8735	4.5500	5.5368	0.0000	0.0000	0.0000	-0.0250
1.60	5.2000	5.1158	4.5000	4.8397	-0.0158	-0.0198	-0.0214	0.0000
1.65	5.2000	5.1158	4.5000	4.8397	0.0000	0.0000	0.0000	0.0000
1.70	5.2000	5.1158	4.5000	4.8397	0.0000	0.0000	0.0000	0.0000
1.75	5.2000	5.1158	4.5000	4.8397	0.0000	0.0000	0.0000	0.0000

5.19b Result of running BREM with NOISE, for comparison with 5.19a.

angles of incidence are used, this gives m(m-1)/2 updated parameters to average. The program MULTINV implements this procedure.

This modification was tested on a discrete medium for five different angles of incidence. Results are tabulated in Figure 5.20. This procedure does not work as well as the least-squares fit, but certainly it helps.

5.4.3 Reconstruction of Slightly Lossy Media

Still another modification of the layer stripping algorithm allows the reconstruction of a slightly lossy medium. However, the absorption of the medium must be small enough that the effects of dispersion in spreading out the probing impulse can be neglected. This assumption must break down at great depths, although a shallow portion of the medium can be reconstructed despite this breakdown.

Absorption losses in the medium are generally modelled by allowing the wave speed c(z) to be complex (e.g., Aki and Richards, 1980; Ganley, 1981). The reason for this can be seen as follows. Let

$$c(z) = c_r(z) + jc_i(z) \quad , \quad c_i(z) << c_r(z) \quad , \tag{5-18}$$

and note that the phase shift $e^{-j\omega\Delta/c(z)}$, representing the travel time delay through a layer of thickness Δ, becomes

$$e^{-j\omega\Delta/c} = e^{-j\omega\Delta(c_r - jc_i)/|c|^2} \approx e^{-j\omega\Delta/c_r}\, e^{-\omega\Delta c_i/|c|^2} \quad . \tag{5-19}$$

Equation (5-19) shows that the complex wave speed (5-18) can be interpreted as resulting in the usual time delay specified by $c_r(z)$, and an attenuation specified by $c_i(z)$ and $c_r(z)$. The quality Q, whose

n=18 m= 9 nm= 5 dd=0.100 del=0.050 dt=0.00250 x1=0.2E-02
values of p are 0.05 0.08 0.11 0.14 0.16
snr= 1.0 1.5 2.6 4.8 8.3

depth	cact	ccomp	rhoact	rhocomp	r1	rc1	r2	rc2
0.00	5.0000	5.0000	5.0000	5.0000	0.0000	0.0000	0.0000	0.0000
0.05	5.0000	4.9689	5.0000	5.0346	0.0000	0.0000	0.0000	-0.0044
0.10	5.0500	5.0689	5.0500	4.9968	0.0103	0.0070	0.0109	0.0055
0.15	5.0500	5.0511	5.0500	5.0175	0.0000	0.0000	0.0000	0.0000
0.20	5.1000	5.1193	5.1000	5.0631	0.0102	0.0118	0.0108	0.0140
0.25	5.1000	5.1193	5.1000	5.0631	0.0000	0.0000	0.0000	0.0000
0.30	5.1500	5.1314	5.1500	5.1799	0.0101	0.0124	0.0107	0.0097
0.35	5.1500	5.1314	5.1500	5.1799	0.0000	0.0000	0.0000	0.0000
0.40	5.2000	5.1652	5.1000	5.1460	0.0003	0.0000	0.0010	0.0000
0.45	5.2000	5.1652	5.1000	5.1460	0.0000	0.0000	0.0000	0.0000
0.50	5.2500	5.1937	5.0500	5.1185	0.0002	0.0000	0.0009	0.0000
0.55	5.2500	5.1615	5.0500	5.1657	0.0000	0.0000	0.0000	-0.0054
0.60	5.3000	5.2070	5.0000	5.1238	0.0001	0.0000	0.0008	0.0000
0.65	5.3000	5.2250	5.0000	5.1016	0.0000	0.0000	0.0000	0.0000
0.70	5.3500	5.2780	4.9500	5.0489	0.0000	0.0000	0.0007	0.0000
0.75	5.3500	5.2780	4.9500	5.0489	0.0000	0.0000	0.0000	0.0000
0.80	5.4000	5.2390	4.9000	5.1118	-0.0001	0.0000	0.0006	-0.0044
0.85	5.4000	5.3115	4.9000	4.9570	0.0000	-0.0053	0.0000	0.0000
0.90	5.4500	5.3115	4.8500	4.9570	-0.0002	0.0000	0.0005	0.0000
0.95	5.4500	5.3214	4.8500	4.9532	0.0000	0.0000	0.0000	0.0000
1.00	5.5000	5.3214	4.8000	4.9532	-0.0003	0.0000	0.0005	0.0000
1.05	5.5000	5.2562	4.8000	5.0121	0.0000	0.0000	0.0000	0.0000
1.10	5.4500	5.2562	4.7500	5.0121	-0.0102	0.0000	-0.0109	0.0000
1.15	5.4500	5.1489	4.7500	5.1161	0.0000	0.0000	0.0000	0.0000
1.20	5.4000	5.1489	4.7000	5.1161	-0.0103	0.0000	-0.0110	0.0000
1.25	5.4000	5.0641	4.7000	5.2292	0.0000	0.0000	0.0000	-0.0053
1.30	5.3500	5.0023	4.6500	5.2941	-0.0104	0.0000	-0.0110	0.0000
1.35	5.3500	4.9148	4.6500	5.3839	0.0000	0.0000	0.0000	0.0000
1.40	5.3000	4.8246	4.6000	5.4853	-0.0105	0.0000	-0.0111	0.0000
1.45	5.3000	4.9299	4.6000	5.2143	0.0000	-0.0137	0.0000	-0.0111
1.50	5.2500	4.8715	4.5500	5.2759	-0.0106	0.0000	-0.0112	0.0000
1.55	5.2500	4.9984	4.5500	5.0109	0.0000	-0.0124	0.0000	-0.0105
1.60	5.2000	5.0073	4.5000	5.0063	-0.0107	0.0000	-0.0113	0.0000
1.65	5.2000	5.0073	4.5000	5.0063	0.0000	0.0000	0.0000	0.0000
1.70	5.2000	5.0794	4.5000	4.8754	0.0000	-0.0050	0.0000	0.0000
1.75	5.2000	5.0794	4.5000	4.8754	0.0000	0.0000	0.0000	0.0000

5.20 Result of running MULTFOR with MULTINV, which adds noise and averages the updated wave speeds and densities computed by using the discrete medium updates on every pair of experiments.

r3	rc3	r4	rc4	r5	rc5
0.0000	0.0000	0.0000	0.0000	0.0000	0.0000
0.0000	-0.0046	0.0000	0.0000	0.0000	0.0000
0.0121	0.0171	0.0148	0.0144	0.0190	0.0218
0.0000	-0.0048	0.0000	0.0000	0.0000	0.0000
0.0121	0.0158	0.0149	0.0185	0.0194	0.0210
0.0000	0.0000	0.0000	0.0000	0.0000	0.0000
0.0120	0.0144	0.0149	0.0170	0.0198	0.0139
0.0000	0.0000	0.0000	0.0000	0.0000	0.0000
0.0023	0.0000	0.0053	0.0050	0.0105	0.0078
0.0000	0.0000	0.0000	0.0000	0.0000	0.0000
0.0022	0.0000	0.0054	0.0051	0.0110	0.0063
0.0000	0.0000	0.0000	0.0000	0.0000	0.0000
0.0022	0.0000	0.0055	0.0075	0.0115	0.0118
0.0000	0.0051	0.0000	0.0000	0.0000	0.0000
0.0021	0.0058	0.0055	0.0000	0.0121	0.0155
0.0000	0.0000	0.0000	0.0000	0.0000	0.0000
0.0021	0.0000	0.0057	0.0000	0.0128	0.0000
0.0000	0.0000	0.0000	0.0000	0.0000	-0.0059
0.0020	0.0000	0.0058	0.0000	0.0136	0.0000
0.0000	-0.0060	0.0000	0.0000	0.0000	0.0129
0.0020	0.0000	0.0059	0.0000	0.0144	0.0000
0.0000	0.0000	0.0000	0.0000	0.0000	-0.0292
-0.0124	0.0000	-0.0163	0.0000	-0.0249	0.0000
0.0000	0.0000	0.0000	-0.0202	0.0000	-0.0227
-0.0125	0.0000	-0.0162	0.0000	-0.0240	0.0000
0.0000	0.0000	0.0000	-0.0134	0.0000	0.0000
-0.0125	0.0000	-0.0161	0.0000	-0.0232	-0.0215
0.0000	-0.0154	0.0000	-0.0158	0.0000	0.0000
-0.0126	0.0000	-0.0160	0.0000	-0.0225	-0.0276
0.0000	-0.0147	0.0000	0.0000	0.0000	0.0000
-0.0126	0.0000	-0.0159	-0.0191	-0.0219	0.0000
0.0000	0.0000	0.0000	0.0000	0.0000	0.0000
-0.0127	0.0051	-0.0158	0.0000	-0.0214	0.0000
0.0000	0.0000	0.0000	0.0000	0.0000	0.0000
0.0000	0.0000	0.0000	0.0000	0.0000	0.0000
0.0000	0.0000	0.0000	0.0000	0.0000	0.0000

reciprocal is defined as the fraction of energy lost per unit cycle due to absorption, divided by 2π, is then specified by

$$1/Q(z) = (\Delta E/E)/2\pi = 2c_i(z)/|c(z)| \ . \qquad (5\text{-}20)$$

The assumption that Q is independent of frequency is generally tenable for seismic frequencies (0.001 - 100 Hz) (Aki and Richards, 1980, p. 170).

However, in the attenuation factor in (5-19), it is clearly necessary to replace ω with $|\omega|$ if negative frequencies are to be considered (note that this makes (5-19) conjugate symmetric, so that its inverse Fourier transform is real). This means that the inverse Fourier transform of (5-19) is not causal. In general, this problem must be removed by letting c vary with frequency (Aki and Richards, 1980, p. 171). Therefore, an absorbing medium is necessarily dispersive, and if an impulse is used to probe the medium, it will become dispersed. Thus the layer stripping algorithm would seem to be inapplicable to lossy media.

However, if Q is large and the medium is only slightly lossy, then it is also only slightly dispersive. The dispersive relations covering the behavior of $c(\omega)$ often depend logarithmically on ω; the relation

$$c(\omega_1)/c(\omega_2) = 1 + \log(\omega_1/\omega_2)/\pi Q \qquad (5\text{-}21)$$

works well and is often used (Aki and Richards, 1980, p. 177). Further, the effects of dispersion of the probing impulse will not be apparent at shallow depths, since the impulse has not had time to disperse significantly. Most importantly, the use of a layer stripping

algorithm ensures that the disperson of the impulse at great depths will not affect the reconstruction of the medium at shallow depths. The conclusion is that a modified layer stripping algorithm should be able to reconstruct the shallow layers of a high-Q, slightly lossy medium.

Since the only change in the inverse problem is that the wave speed c(z) is now complex, the alterations to the layer stripping algorithm are minor. The equations for the reflection coefficients and impedances are unaltered (Ganley, 1981), although these quantities are now complex. The major change is that since the reflection coefficients are complex and depend on the sign of ω, the Schur algorithm must be used in place of the fast Cholesky algorithm.

The complete algorithm consists of two sets of wave updates

$$\hat{D}_k(z+\Delta,\omega) = \hat{D}_k(z,\omega)e^{-j\omega\Delta/c'_k(z)}e^{-\omega\Delta c_i/(c'_k(z))^2} - r_k(z)\Delta\,\hat{U}_k(z,\omega) \qquad (5\text{-}22a)$$

$$\hat{U}_k(z+\Delta,\omega) = \hat{U}_k(z,\omega)e^{j\omega\Delta/c'_k(z)}e^{\omega\Delta c_i/(c'_k(z))^2} - r_k(z)\,\Delta\,\hat{D}_k(z,\omega) \qquad (5\text{-}22b)$$

$$r_k(z)\Delta = \lim_{\omega\to\infty} 2j\omega e^{j\omega\tau_k}\,\hat{U}_k(z,\omega) \quad , \quad k = 1,\ 2,\ \omega \geq 0 \qquad (5\text{-}22c)$$

initiated using the two reflection responses $\hat{R}_k(\omega)$ by

$$\hat{D}_k(0,\omega) = 1 \qquad (5\text{-}23a)$$

$$\hat{U}_k(0,\omega) = \hat{R}_k(\omega) \ , \qquad k = 1,\ 2 \ , \qquad (5\text{-}23b)$$

and the set of parameter updates

$$Z_k(z+\Delta) = \frac{1 + r_k(z)\Delta}{1 - r_k(z)\Delta} Z_k(z) , \quad k = 1, 2 \tag{5-24}$$

$$U(z) = \cos^2\theta_2(z)/\cos^2\theta_1(z) = (Z_1(z)/Z_2(z))^2 \tag{5-25}$$

$$c_r(z) = [(U(z) - 1)/(U(z)p_1^2 - p_2^2)]^{\frac{1}{2}} \tag{5-26}$$

$$c_k'(z) = c_r(z)/(1 - c_r(z)^2 p_k^2)^{\frac{1}{2}} \tag{5-27}$$

$$\rho(z) = \mathrm{Re}[Z_k(z)]/c_k'(z) \tag{5-28}$$

$$c_i(z) = \mathrm{Im}[Z_k(z)]c_r(z)/(\rho(z)c_k'(z)) \tag{5-29}$$

$$\tau_k(z+\Delta) = \tau_k(z) + \Delta/c_k'(z), \quad k = 1, 2 . \tag{5-30}$$

Note that although Z_1 and Z_2 are both complex, their ratio is real. It should also be noted that we are able to recover three medium parameter profiles $\rho(z)$, $c_r(z)$, and $c_i(z)$ from only two reflection responses $\hat{R}_1(\omega)$ and $\hat{R}_2(\omega)$. This is possible because the profile $c_i(z)$ manifests itself as the imaginary parts of $r_k(z)$ and $Z_k(z)$, which were previously constrained to be real.

It may seem as though the introduction of a complex wave speed should make the reflection time responses $R_k(t)$ complex. However, this is not the case, since the imaginary part of the wave speed $c_i(z)$ is implicitly multiplied by SGN ω. This correction made (5-19) conjugate symmetric in ω, so that its inverse Fourier transform is real but non-causal. A similar effect holds for the reflection time responses $R_k(t)$. Note that since the probing excitation is no longer causal, it is hardly surprising that the $R_k(t)$ are also no longer causal.

It should be noted that since $c_i(z)$ is implicitly multiplied by SGN ω, the simple multiplications of $r(z)$ times the waves in the frequency domain become convolutions involving the Hilbert transform in the time domain. This is why the Schur algorithm, which only uses non-negative frequencies, must be used instead of the fast Cholesky algorithm, which has a very complicated form for this problem. Recall that (5-22c) requires only that the reflection responses at each depth be strictly proper (see Chapter III), which is still true.

5.5 Summary

The primary goal of this chapter was to demonstrate that the layer stripping algorithms work in the presence of small amounts of noise. Since this has been demonstrated, the application of noise reduction techniques such as beamforming should allow the algorithm to work on noisy data. The modifications of Section 5.4, especially the use of reflection data at many angles of incidence, should also help considerably.

If the signal-to-noise ratio is low (less than eight), then it may be expected that the layer stripping algorithm will break down at the depth at which the conditioning of the inverse problem becomes so poor that the noise overwhelms it. In this event, there is probably little choice but to use deconvolution-type methods that treat the reconstruction of the medium as a problem in modelling a random process by an AR (autoregressive) filter. This amounts to a reformulation of the inverse problem, and thus lies outside the scope of this thesis. The algorithms given in this thesis produce exact reconstructions in the limit as $\Delta \to 0$, so they would be preferable in situations where noise levels are low.

The weak point of the layer stripping algorithms is of course their

susceptibility to imperfect data. However, part of the reason for this is their layer-recursive nature, which makes the inverse problem solved at each recursion steadily more poorly conditioned. This loss of conditioning with depth must be experienced by any inversion process, but is often disguised by the machinery of the process, rather than illuminated by it as it is for the layer stripping algorithms. Band-limitation of the source and data also causes problems, but again there is no way around this without reformulation of the problem. The only major fault inherent in the algorithms themselves is the catastrophic nature of their breakdown when it does occur.

The strong points of the layer stripping algorithms are as follows. First, of course, is that they provide an exact solution as $\Delta \to 0$. Second is their great simplicity, which lends itself to fast processing on a computer. Third is their physical interpretability, providing a physical insight into the inversion process that other inversion methods in general cannot match. Reasons for the algorithm breaking down often carry with them a physical interpretation that makes them much easier to visualize and perhaps solve.

The results of this chapter can be summarized as follows. The time-domain foward problem program BREM was found to be preferable to the frequency-domain forward problem program FOR1, since the former did not require an inverse Fourier transform and its attendant complications. The continuous-medium inversion program INV1 broke down when applied to discrete media, as expected, while the discrete medium inversion program INVDISC continued to work satisfactorily. This more than compensated for the more complicated updates (including a square root extraction) required by INVDISC.

The inversion algorithm tended to work quite well for several layers, until the steadily increasing error in the computed wave speed caused the algorithm to project ahead to the wrong time and miss the next primary reflection, at which point the algorithm broke down. The a posteriori methods of Habibi-Ashrafi and Mendel (1982) are better at preventing this, although much more computation is required, and there is still a chance of missing a weak primary reflection. The algorithm still worked when noise was added to the data, although the greater the noise level, the shallower the depth at which the algorithm broke down, as expected.

Some modifications for improving the performance of the algorithm on noisy data were developed. The first modification consisted of setting to zero all measured reflection coefficients below a varying threshold determined by the condition number of the problem at each depth. This proved quite effective for discrete media composed of layers several times thicker than the discretization depth Δ. However, it could also lead to worse results for more continuously varying media, whose weak reflection coefficients could be mistakenly suppressed as noise. The other modification consisted of using reflection data at several different angles of incidence to perform a least-squares fit for the updated medium parameters at each depth.

The problem of determining the profiles of $\rho(z)$ and $c(z)$ for a layered acoustic medium by probing it with impulsive plane waves and measuring the reflection response has now been quite thoroughly covered, as far as layer stripping inversion methods are concerned. We now proceed to a more complicated generalization of this problem--that of determining the parameter profiles for an elastic medium from its reflection responses.

REFERENCES FOR CHAPTER V

K. Aki and P. Richards, Quantitative Seismology: Theory and Methods, W.H. Freeman and Co., San Francisco, 1980.

A. Bruckstein, I. Koltracht, and T. Kailath, "Inverse Scattering with Noisy Data," Tech. Report, Information Systems Laboratory, Stanford University, 1984.

K.P. Bube and R. Burridge, "The One-Dimensional Inverse Problem of Reflection Seismology," SIAM Review 25(4), 497-559 (1983).

A. Bultheel, "Towards an Error Analysis for Fast Toeplitz Factorization," Report No. TW 44, Applied Mathematics and Programming Division, Katholieke Universiteit Leuven (Belgium), May 1979.

G. Cybenko, "The Numerical Stability of the Levinson-Durbin Algorithm for Toeplitz Systems of Equations," SIAM J. Sci. Stat. Comput. 1(3), 303-319 (1980).

D.C. Ganley, "A Method for Calculating Synthetic Seismograms Which Include the Effects of Absorption and Dispersion," Geophysics 46(8), 1100-1107 (1981).

F. Habibi-Ashrafi and J. Mendel, "Estimation of Parameters in Lossless Layered Media Systems," IEEE Trans. A.C. AC-27(1), 31-48 (1982).

R. Kind, "Computation of Reflection Coefficients for Layered Media," J. Geophysics 42, 191-200 (1976).

A.V. Oppenheim and R.W. Schafer, Digital Signal Processing, Prentice-Hall, Englewood Cliffs, NJ, 1975.

F. Santosa and W. Symes, "Inversion of the Impedance Profile from Band-limited Data," Preprint, 1983.

G. Stewart, Introduction to Matrix Computations, Academic Press, NY, 1973.

W. Symes and G. Zimmerman, "Experiments in Impedance Profile Inversion Using Noisy and Band-Limited Data," Amoco Production Co. Research Report No. F82-C-3 (1982).

K.B. Theriault, "Accuracy Bounds for Normal-Incidence Acoustic Structure Estimation," Ph.D. Thesis, Dept. of Electrical Engineering and Computer Science, MIT, August 1977.

CHAPTER VI

The Inverse Problem for a One-Dimensional Elastic Medium

6.1 Introduction

In this chapter the inverse seismic problem for a one-dimensional elastic layered medium probed by impulsive plane waves at oblique incidence is solved by a layer stripping algorithm. Separate profiles of the Lamé parameters $\lambda(z)$ and $\mu(z)$ and the density $\rho(z)$ as functions of depth may be obtained from the P - to - P, P - to - SV, and SV - to - SV reflection responses of the medium. Alternative choices for the data to initiate the algorithm are discussed in Section 6.3.2.

The basic results of this chapter are taken from Yagle and Levy (1985). However, those results are supplemented by a dynamic deconvolution inversion procedure for an elastic medium. Some alternative formulations of the layer stripping algorithm that allow the reconstruction of an elastic medium when it is probed from a fluid half-space are also given. This is clearly applicable to probing the sea bottom from the ocean above it. Finally, some comments on discrete elastic media, collected from a variety of sources, are made.

Problem formulation

The basic problem considered in this chapter is as follows. An elastic layered medium, which supports the propagation of both compressional (P) waves and shear (S) waves, is parametrized completely by the continuous profiles of the Lamé parameters $\lambda(z)$ and $\mu(z)$ and the density $\rho(z)$. The medium is isotropic and laterally homogeneous,

waves at oblique incidence. This procedure allowed recovery of the parameter profiles by solving Marchenko integral equations, but it sidestepped the issue of P-SV mode conversions. Blagoveshchenskii (1967) exhibited several integral equations whose solutions yielded the parameter profiles as functions of travel times; by combining the Gel'fand–Levitan inverse scattering method with the solution of a Volterra equation, Carroll and Santosa (1982) were able to recover the parameter profiles as functions of depth. Baker (1982) solved the related problem of reconstructing radially varying parameters by using spherical harmonics and Marchenko integral equations.

Kennett and Illingworth (1981) used propagator matrices to propagate upgoing and downgoing P and SV waves between various depths. The waves were expressed by a generalization of the Langer uniform approximation (involving Airy functions), which is tantamount to neglecting all multiple reflections and wave interconversions (i.e., a single scattering approximation). Although their inversion procedure is very complicated, it does incorporate multiple turning points nicely. Frasier (1969) attempted to use matrix methods to solve the discrete elastic problem, but the different wave speeds for P and S waves cause problems in defining a Goupillaud medium model, and his solution is necessarily only an approximation.

Clarke (1984) and Shiva and Mendel (1983) have recently given algorithms that utilize the layer-stripping principle. However, their algorithms are far more complicated than the algorithm of this chapter. Clarke (1984) requires the iterative solution (using Newton's method for solving equations) of several equations at each step of the algorithm in order to update the medium parameters. His numerical example

and has a lateral dimension, so that it may be probed at oblique incidence. The medium is probed with an impulsive plane P wave at oblique incidence, and its P - to - P and P - to - SV reflection responses measured. The medium is then probed again with an impulsive plane SV wave at oblique incidence, and its SV - to - SV reflection response measured. Either a half-space or a free surface boundary condition may be used at the surface.

This problem is far more complex than the acoustic problem considered in Chapter IV because there is interconversion between P and SV waves as the inhomogeneous medium is penetrated. Thus instead of having two waves with continuous coupling between them, there are four waves with continuous coupling between each pair of waves. Due to various symmetries, the couplings can be parametrized by three reflectivity functions and an interconversion transmissivity function. In the operation of the layer stripping algorithm, the three reflectivity functions are recovered from the three surface reflection responses or traces (i.e., seismograms), $\lambda(z)$, $\mu(z)$, and $\rho(z)$ are computed, and the layer stripping algorithm is then propagated to the next depth. Complications are introduced by the different wave speeds for P and S waves, so the algorithm is much more than a simple generalization of the algorithms of Chapter IV.

Previous work

Previous work on this elastic problem has yielded methods of solution that are computationally arduous to implement. For example, Coen (1981) solved this problem by employing solutions to the acoustic problem for the separate cases of P and SV impulsive plane waves at normal incidence, which are decoupled for a layered medium, and of SH

consists of only six layers, perhaps as a result of the complexity of his algorithm. He also assumes that the P - to -SV and SV - to -SV reflectivity functions are independent of the P-wave speed, and that the P - to - P reflectivity function depends only on the P-wave speed. The algorithm of Shiva and Mendel (1983) requires the solution of a cubic equation at each step, and some more algebra to update the medium parameters. In addition, they employ maximum-likelihood estimation to look for the next set of first reflections, which yield the reflectivity functions. This a posteriori approach is in contrast to the much simpler a priori approach of the algorithm of this chapter, in which the times of the first reflections are projected.

The reason that the layer stripping algorithms of Clarke (1984) and Shiva and Mendel (1983) are so complicated is that these papers assume the medium is discrete. Here, it is assumed that the medium is continuous, which allows the use of differential updates of the medium parameters. The computational results of Section 6.4 indicate that this assumption is generally workable, and that the vastly more complicated discrete updates may not be worth the amount of work they require.

It should be noted that there is no single procedure for solving the elastic problem that is analogous to the Gel'fand-Levitan procedure of Section 3.2.2. This is because the different wave speeds of P and S waves makes it impossible to formulate the elastic problem as a matrix Schrodinger equation, to which the Gel'fand-Levitan procedure could be applied.

Summary

In Section 6.2 the layer stripping algorithm for a continuous elastic medium is derived, specified, and physically interpreted. The algorithm

is more than a simple generalization of the algorithms of Chapter IV, since the different wave speeds of P and S waves complicates matters immensely. Indeed, there are no simple integral equation methods for solving the elastic problem that take into account wave conversions, for this reason.

In Section 6.3 some alternative formulations of the algorithm are presented. First, a dynamic deconvolution algorithm involving a matrix Riccati equation is derived. Next, the problem of probing an elastic medium from an acoustic (i.e., liquid) half-space is solved using a different version of the layer stripping algorithm. Note that for this problem the elastic medium cannot be probed with S waves, and the reflected response of S waves cannot be measured, since the liquid half-space does not support shear stresses. This problem has an obvious application in probing the sea bottom from the ocean above it. Finally, some comments are made on discrete elastic media, in order to show the relations between acoustic medium results and their elastic medium generalizations.

In Section 6.4 the results of a computer run on a twenty-layer medium are presented. The forward problem reflection responses were generated using the reflectivity method, and an inverse Fourier transform taken. This introduces errors into the synthesized responses in the form of bandlimiting, aliasing, and Gibb's phenomenon, but the layer stripping algorithm nevertheless works satisfactorily.

Some basic concepts of elastic wave propagation

The two basic equations for a linear elastic medium in the absence of sources are the momentum relation (compare to Newton's second law of motion, F = ma)

$$\rho \partial^2 u_i / \partial t^2 = \sum_j \partial \tau_{ij} / \partial x_j \qquad (6\text{-}1)$$

and Hooke's law

$$\tau_{ij} = c_{ijpq} e_{pq} \quad , \qquad (6\text{-}2)$$

where τ_{ij} represents an element of the symmetric stress tensor, e_{pq} represents an element of the symmetric strain tensor, and u_i is the component of displacement in the direction x_i (Aki and Richards, 1980). Suppose all deformations of the medium are adiabatic, so that a strain energy function can be defined, and the medium is isotropic. Then, due to various symmetries, the tensor c_{ijpq}, which contains 81 elements, is actually a function of just two quantities, since it has the form

$$c_{ijpq} = \lambda \delta_{ij} \delta_{pq} + \mu(\delta_{ip}\delta_{jq} + \delta_{iq}\delta_{jp}), \qquad (6\text{-}3a)$$

$$\delta_{ij} = \begin{cases} 1 \text{ if } i = j \\ 0 \text{ if } i \neq j \end{cases} . \qquad (6\text{-}3b)$$

The quantities λ and μ are called the Lamé parameters. Along with the density ρ, these quantites completely specify the medium: other quantities such as bulk modulus, can be specified in terms of λ and μ (Aki and Richards, 1980).

Unlike an acoustic or liquid medium, an elastic medium can support shear stresses, since $\mu \neq 0$. This means that an elastic medium can support two types of propagating waves: P waves, which are physically the same as acoustic waves, and travel at a wave speed

$$\alpha = ((\lambda + 2\mu)/\rho)^{\frac{1}{2}} \quad ; \tag{6-4}$$

and S waves, in which the wave displacement is perpendicular to the direction of propagation (which clearly requires shear stress), and which travel at a wave speed

$$\beta = (\mu/\rho)^{\frac{1}{2}} \quad . \tag{6-5}$$

Note that P waves always travel faster than S waves. In fact, the notations "P" and "S" come from the fact that the first or Primary body wave from an earthquake is always a P wave, while a Secondary arrival is an S wave. Also note that S waves can be polarized in any direction perpendicular to the ray path. S waves are generally decomposed into components in the vertical plane (SV waves) and the horizontal plane (SH waves). For a layered medium, in which λ, μ, and ρ are functions of depth only, the SH waves are decoupled from the P and SV waves (Aki and Richards, 1980). At normal incidence, the P and SV waves are also decoupled. Coen (1981) used these facts in order to solve the inverse problem for an elastic medium using the Gel'fand-Levitan procedure. Since the SH waves are completely independent of the P and SV waves, we shall disregard them for the remainder of this chapter.

6.2 Layer Stripping Solution for a Continuous Elastic Medium

In this section we derive and specify the layer stripping algorithm that solves the inverse problem for a continuous layered elastic medium. The resulting algorithm is very simple computationally, and lends much physical insight into the inversion process.

The problem considered is as follows. A continuous, lossless, layered elastic medium is probed, in separate experiments, with impulsive plane P and SV waves, and the P - to - P, P - to - SV, and SV - to - SV reflection responses of the medium are measured (note that the P - to - SV and SV - to - P responses are identical). The angles of incidence θ_p and θ_s are chosen (i.e., the data are slant-stacked) so that the slowness p for both incident plane waves is the same, i.e.,

$$p = \sin \theta_p / \alpha(0) = \sin \theta_s / \beta(0) \quad . \tag{6-6}$$

The goal is to recover the profiles $\lambda(z)$, $\mu(z)$, and $\rho(z)$, which characterize the medium completely.

Although the reflection response is defined for a half-space boundary condition, a free surface boundary condition may also be used. In this case, the reflection response may be synthesized from the surface traces (seismograms) by inverting the formulae (Frasier, 1969)

$$V_H = \frac{\sin\theta_p}{Z_p^{\frac{1}{2}}} (DP + UP) + \frac{\cos \theta_s}{Z_s^{\frac{1}{2}}} (US + DS) \tag{6-7a}$$

$$V_V = \frac{-\cos \theta_p}{Z_p^{\frac{1}{2}}} (UP - DP) + \frac{\sin \theta_s}{Z_s^{\frac{1}{2}}} (US - DS) \tag{6-7b}$$

where $V_H(t)$ and $V_V(t)$ are the horizontal and vertical velocity traces; DP, UP, DS, and US are the amplitudes of the downgoing and upgoing P and SV waves; and

$$Z_p = \rho a \cos \theta_p \tag{6-8a}$$

$$Z_s = \rho\beta\cos\theta_s \tag{6-8b}$$

are the P- and SV-wave impedances at the surface. Inverting (6-7) for the two experiments gives, for the P-wave experiment,

$$\hat{R}_{pp}(\omega) = Z_p^{\frac{1}{2}}/(b_p\cos(\theta_p-\theta_s))(\sin\theta_s\hat{v}_H(\omega)-\cos\theta_s\hat{v}_V(\omega)+b_p\cos(\theta_p+\theta_s)/Z_p) \tag{6-9a}$$

$$\hat{R}_{ps}(\omega) = Z_s^{\frac{1}{2}}/(b_p\cos(\theta_p-\theta_s))(\cos\theta_p\hat{v}_H(\omega)+\sin\theta_p\hat{v}_V(\omega)-b_p\sin 2\theta_p/Z_p) \tag{6-9b}$$

and inverting (6-7) for the SV-wave experiment gives

$$\hat{R}_{sp}(\omega) = Z_p^{\frac{1}{2}}/(b_s\cos(\theta_p-\theta_s))(\sin\theta_s\hat{v}_H(\omega)-\cos\theta_s\hat{v}_V(\omega)-b_s\sin 2\theta_s/Z_s) \tag{6-10a}$$

$$\hat{R}_{ss}(\omega) = Z_s^{\frac{1}{2}}/(b_s\cos(\theta_p-\theta_s))(\cos\theta_p\hat{v}_H(\omega)+\sin\theta_p\hat{v}_V(\omega)-b_s\cos(\theta_p+\theta_s)/Z_s) \tag{6-10b}$$

where b_p and b_s are the strengths of the incident P and SV excitations.

It should also be noted that the algorithm may be run concurrently with many different values of slowness p from a single point source experiment. In this case, the updated medium parameters at each depth from each run may be averaged, and the averaged values then used in the algorithms. This reduces the effect of noise in the data, as discussed in Chapter V. Furthermore, the desired responses for P and SV excitations could be obtained by an appropriate superposition of

the responses to a P-wave source and to a mixed, P- and SV-wave source. Other possibilities of using data for several different values of slowness p are noted in Section 6.3.2.

We now define the following quantities:

$$\alpha(z) = ((\lambda(z) + 2\mu(z))/\rho(z))^{\frac{1}{2}} = \text{local P-wave velocity} \tag{6-11a}$$

$$\beta(z) = (\mu(z)/\rho(z))^{\frac{1}{2}} = \text{local S-wave velocity} \tag{6-11b}$$

$$\sin \theta_p(z) = \alpha(z)p = \text{sine of local angle between P-wave ray and vertical} \tag{6-11c}$$

$$\sin \theta_s(z) = \beta(z)p = \text{sine of local angle between S-wave ray and vertical} \tag{6-11d}$$

$$\alpha'(z) = \alpha(z)/\cos \theta_p(z) = \text{local vertical P-wave velocity} \tag{6-11e}$$

$$\beta'(z) = \beta(z)/\cos \theta_s(z) = \text{local vertical S-wave velocity.} \tag{6-11f}$$

We also define the vector

$$\underset{\sim}{g}(t,x,z) = \begin{bmatrix} u_x(t,x,z) \\ u_z(t,x,z) \\ \tau_{zx}(t,x,z) \\ \tau_{zz}(t,x,z) \end{bmatrix} \tag{6-12}$$

where u_x and u_z are the horizontal and vertical components of the displacement, and where τ_{zx} and τ_{zz} are the horizontal and vertical tractions on an element perpendicular to the z axis.

An impulsive plane wave $\underset{\sim}{b}_0\delta(t-px-qz)$ is used to probe the elastic medium. Here $\delta(\cdot)$ denotes the Dirac delta function, and q is the

vertical ray parameter just below the surface (for a free surface), or in the homogeneous half-space above the medium. The Fourier transform of this plane wave is $(\underset{\sim}{b}_0 \exp -j\omega qz)\exp -j\omega px$. Since the horizontal ray parameter p is independent of depth, we may write the Fourier transform of the vector (6-12) for $z > 0$ (inside the medium) as

$$\hat{\underset{\sim}{g}}(\omega,x,z) = \hat{\underset{\sim}{f}}(\omega,z)\exp -j\omega px \quad . \tag{6-13}$$

From Aki and Richards (1980, p. 269) and Kennett (1983, p. 26), the propagation of seismic waves in an inhomogeneous, layered, continuous elastic medium is described by

$$d\hat{\underset{\sim}{f}}/dz = A(z)\hat{\underset{\sim}{f}}(\omega,z) \tag{6-14}$$

where

$$A(z) = \begin{bmatrix} 0 & -j\omega p & 1/\mu & 0 \\ -j\omega p\,\lambda/(\lambda+2\mu) & 0 & 0 & 1/(\lambda+2\mu) \\ 4\omega^2 p^2 \mu(\lambda+\mu)/(\lambda+2\mu) - \rho\omega^2 & 0 & 0 & -j\omega p\,\lambda/(\lambda+2\mu) \\ 0 & -\rho\omega^2 & -j\omega p & 0 \end{bmatrix} \tag{6-15}$$

Next, we diagonalize equation (6-14), defining upgoing and downgoing P and SV waves. Appropriate weightings of the eigenvectors of A(z) will be necessary to put equation (6-14) into a form suitable for

a fast algorithm.

Transformation to upgoing and downgoing waves

It is well-known (e.g., Kennett et al., 1978) that changing variables in equation (6-14) from $\hat{\underset{\sim}{f}}(\omega,z)$ to $R(z)\hat{\underset{\sim}{f}}(\omega,z)$, where $R(z)$ is the matrix of row eigenvectors of $A(z)$, diagonalizes equation (6-14) into upgoing and downgoing waves. In the present context it will be necessary to weight the row eigenvectors of $A(z)$ in order to obtain a recursive algorithm. Thus we define

$$\hat{\underset{\sim}{w}}(\omega,z) = X(z)R(z)\hat{\underset{\sim}{f}}(\omega,z) \tag{6-16}$$

where X is a diagonal matrix whose elements weight the row eigenvectors of $A(z)$. We may then write

$$\hat{\underset{\sim}{f}}(\omega,z) = R^{-1}X^{-1}\hat{\underset{\sim}{w}}(\omega,z) = CX^{-1}\hat{\underset{\sim}{w}}(\omega,z) \tag{6-17}$$

where $C(z) = R(z)^{-1}$ is the matrix of column eigenvectors of $A(z)$.

Taking the partial derivative of equation (6-17) with respect to z and premultiplying by XR yields

$$d\hat{\underset{\sim}{w}}/dz = [\Lambda - (X(RdC/dz)X^{-1} + X(d/dz(X^{-1})))]\hat{\underset{\sim}{w}} \tag{6-18}$$

where

$$\Lambda = RAC = \text{diag}[-j\omega/\alpha', \ -j\omega/\beta', \ j\omega/\alpha' \ , \ j\omega/\beta']. \tag{6-19}$$

We now choose the elements of the diagonal matrix X so that the

(diagonal) term $X(d/dz)X^{-1} = -(d/dz)\log X$ zeroes the diagonal elements of $X(RdC/dz)X^{-1}$. This is straightforward, and the result is

$$X = \mathrm{diag}[(\alpha\rho\cos\theta_p)^{\frac{1}{2}}, (\beta\rho\cos\theta_s)^{\frac{1}{2}}, (\alpha\rho\cos\theta_p)^{\frac{1}{2}}, (\beta\rho\cos\theta_s)^{\frac{1}{2}}]. \quad (6\text{-}20)$$

We recognize the components of X as the square roots of the P-wave and SV-wave impedances. Hence weighting the components of $R\hat{\underset{\sim}{f}}$ by these quantities normalizes the energy fluxes moving upwards and downards. Although this transformation was noted by Chapman (1974), it is interesting that searching for a form suitable for a fast algorithm leads automatically to the energy normalization (6-20).

Inserting equation (6-20) in equation (6-18) results in

$$d\hat{\underset{\sim}{w}}/dz = \begin{bmatrix} -j\omega/\alpha' & -t_c & -r_p & -r_c \\ t_c & -j\omega/\beta' & -r_c & -r_s \\ -r_p & -r_c & j\omega/\alpha' & -t_c \\ -r_c & -r_s & t_c & j\omega/\beta' \end{bmatrix} \hat{\underset{\sim}{w}} \quad (6\text{-}21)$$

where

$$r_p(z) = (1/2 - 2\beta^2p^2)(d/dz)\log\rho(z) - 4\beta^2p^2\,(d/dz)\log\beta(z)$$

$$+ 1/(2-2\alpha^2p^2)(d/dz)\log\alpha(z) \quad (6\text{-}22a)$$

$$r_c(z) = -(p/2)(\alpha'\beta')^{\frac{1}{2}}((1-2\beta^2p^2 + 2\beta^2/\alpha'\beta')(d/dz)\log\rho(z)$$

$$-(4\beta^2p^2 - 4\beta^2/\alpha'\beta')(d/dz)\log\beta(z)) \qquad (6\text{-}22b)$$

$$r_s(z) = -(1/2 - 2\beta^2p^2)(d/dz)\log\rho(z)$$

$$-(1/(2-2\beta^2p^2) - 4\beta^2p^2)(d/dz)\log\beta(z) \qquad (6\text{-}22c)$$

$$t_c(z) = (p/2)(\alpha'\beta')^{\frac{1}{2}}((1-2\beta^2p^2 - 2\beta^2/\alpha'\beta')(d/dz)\log\rho(z)$$

$$-(4\beta^2p^2 + 4\beta^2/\alpha'\beta')(d/dz)\log\beta(z)) \qquad (6\text{-}22d)$$

and the quantities in equations (6-22) have the following interpretations:

$r_p(z)$ = reflectivity function for a reflected P wave generated by a P wave;

$r_c(z)$ = reflectivity function for a reflected wave generated by a wave of the opposite type;

$r_s(z)$ = reflectivity function for a reflected SV wave generated by an SV wave;

$t_c(z)$ = transmissivity function for a transmitted wave generated by a wave of the opposite type.

We use notations similar to those of Chapman (1974) and Kennett and Illingworth (1981). The physical meaning of the reflectivity functions is illustrated in Figure 6.1, which describes an infinitesimal section of a lattice filter structure which implements the elastic wave equation (6-21). Note that the elementary delay elements $D_p \triangleq \exp - j\omega\Delta/\alpha'(z)$ and $D_s \triangleq \exp -j\omega\Delta/\beta'(z)$ appearing in Figure 6.1 vary with depth. The lattice structure of Figure 6.1 can be viewed as a generalization of the lattice structure of Figure 2.1.

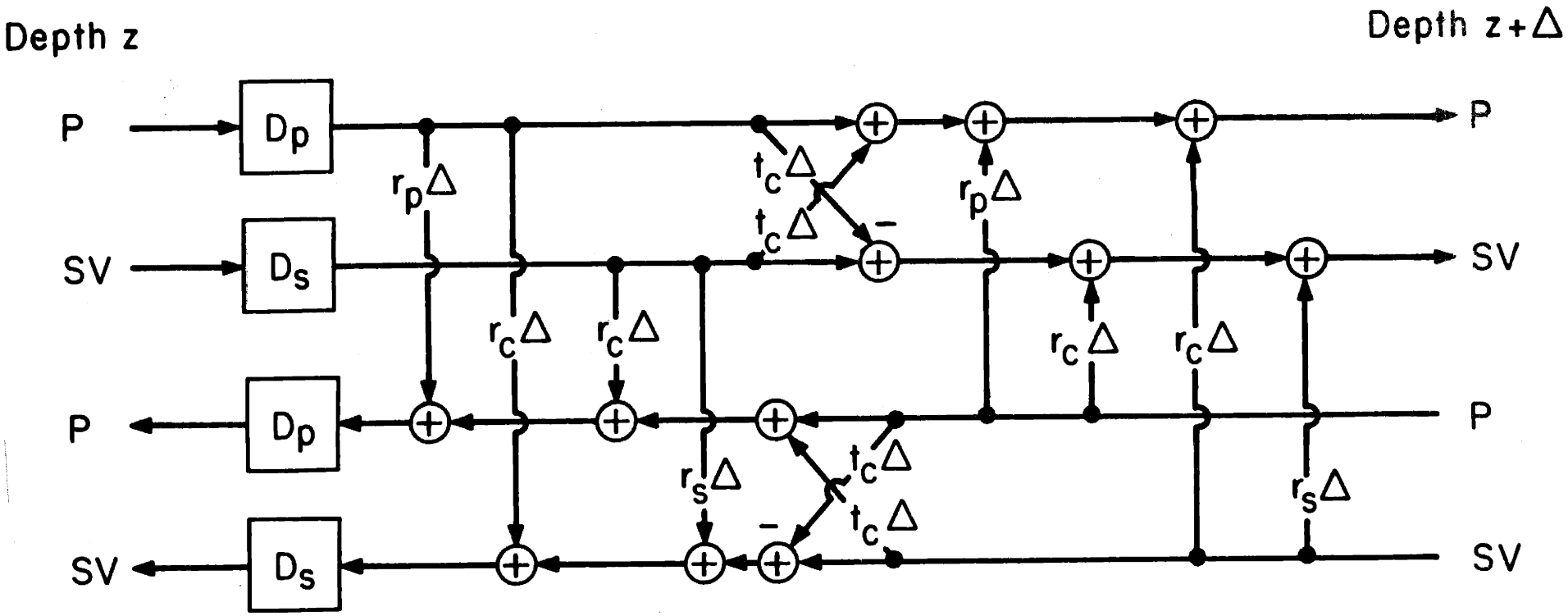

6.1 An infinitesimal section of the ladder filter which implements the elastic wave equation.

Next, we use the transformed equation (6-21) to obtain a fast inversion algorithm.

Inversion algorithm

Recall that the first experiment consisted of probing the medium with a planar impulsive P wave. Since the first component of $\hat{\underset{\sim}{w}}(\omega,z)$ corresponds to a downgoing P wave, we may write its inverse Fourier transform $\underset{\sim}{w}(t,z)$ as

$$\underset{\sim}{w}(t,z) = \begin{bmatrix} b_p \delta(t-\tau_p(z)) \\ 0 \\ 0 \\ 0 \end{bmatrix} + \begin{bmatrix} w_1(t,z) \\ w_2(t,z) \\ w_3(t,z) \\ w_4(t,z) \end{bmatrix} 1(t - \tau_p(z)) \qquad (6\text{-}23)$$

where

$$\tau_p(z) = \int_0^z d\ell/\alpha'(\ell) \qquad (6\text{-}24)$$

denotes the vertical travel time for P waves, and

$$1(t) = \begin{cases} 1 \text{ for } t \geq 0 \\ 0 \text{ for } t < 0 \end{cases} \qquad (6\text{-}25)$$

is the unit step function. The second term in (6-23) reflects the causality of the excitation: there can be no wave at depth z until the excitation has had time to reach depth z.

Taking the inverse Fourier transform of equation (6-21), inserting the expression (6-23), and equating coefficients of $\delta(t-\tau_p)$ yields

$$r_p(z) = 2w_3(\tau_p(z),z)/(\alpha'(z)b_p) \tag{6-26a}$$

$$r_c(z) = w_4(\tau_p(z),z)(1/\alpha'(z) + 1/\beta'(z))/b_p \quad . \tag{6-26b}$$

Now, for the second experiment, the excitation is a downgoing, impulsive SV wave. Since the second component of $\underset{\sim}{w}(t,z)$ corresponds to such a wave, we have for this experiment

$$\underset{\sim}{w}(t,z) = \begin{bmatrix} 0 \\ b_s\delta(t-\tau_s(z)) \\ 0 \\ 0 \end{bmatrix} + \begin{bmatrix} w_1(t,z) \\ w_2(t,z) \\ w_3(t,z) \\ w_4(t,z) \end{bmatrix} \tag{6-27}$$

where the waves $w_i(t,z)$ have the form

$$w_i(t,z) = n_i(t,z)1(t-\tau_p(z)) + q_i(t,z)1(t-\tau_s(z)) \tag{6-28}$$

and where the vertical travel time for SV waves has been defined as

$$\tau_s(z) = \int_0^z d\ell/\beta'(\ell) \quad . \tag{6-29}$$

Note that the form of equation (6-28) differs from that of equation (6-23). This is because in the SV experiment the impulsive excitation (an SV wave) does not coincide with the wavefront (a P wave). In the P experiment both of these were P waves and hence coincided.

Proceeding as above, we obtain ($q_i(z)$ is defined in equation (6-28))

$$r_c(z) = q_3(\tau_s(z),z)(1/\alpha'(z) + 1/\beta'(z))/b_s \tag{6-30a}$$

$$r_s(z) = 2q_4(\tau_s(z),z)/(\beta'(z)b_s) \quad . \tag{6-30b}$$

The importance of equations (6-26) and (6-30) is that they permit computation of the reflectivity functions at any depth provided the waves $\underset{\sim}{w}(t,z)$ are known at that depth.

Next, equations (6-22a-c) are written as a matrix equation:

$$\begin{bmatrix} r_p(z) \\ r_c(z) \\ r_s(z) \end{bmatrix} = M(z) \begin{bmatrix} (d/dz) & \log\ \rho(z) \\ (d/dz) & \log\ \beta(z) \\ (d/dz) & \log\ \alpha(z) \end{bmatrix} \tag{6-31}$$

where

$$M(z) = \begin{bmatrix} 1/2 - 2\beta^2p^2 & -4\beta^2p^2 & 1/(2-2\alpha^2p^2) \\ -\ell(1-2\beta^2p^2 + 2\beta^2/(\alpha'\beta')) & \ell(4\beta^2p^2 - 4\beta^2/(\alpha'\beta')) & 0 \\ -(1/2 - 2\beta^2p^2) & -(1/(2-2\beta^2p^2) - 4\beta^2p^2) & 0 \end{bmatrix} \tag{6-32}$$

and

$$\ell(z) = (p/2)(\alpha'\beta')^{\frac{1}{2}} \quad . \tag{6-33}$$

Inverting (6-32) gives

$$\begin{bmatrix} (d/dz)\ \log\ \rho(z) \\ (d/dz)\ \log\ \beta(z) \\ (d/dz)\ \log\ \alpha(z) \end{bmatrix} = N(z)/m(z) \begin{bmatrix} r_c(z) \\ r_s(z) \\ r_p(z) \end{bmatrix} \tag{6-34}$$

where

$$N(z) = \begin{bmatrix} -(1/(2-2\beta^2p^2) - 4\beta^2p^2) & -\ell(4\beta^2p^2 - 4\beta^2/(\alpha'\beta')) & 0 \\ 1/2 - 2\beta^2p^2 & -\ell(1-2\beta^2p^2 + 2\beta^2/(\alpha'\beta')) & 0 \\ -\dfrac{(1-\alpha^2p^2)(4\beta^2p^2-1)}{2(1-\beta^2p^2)} & -4\ell(1-\alpha^2p^2)(\beta^2p^2 + \beta^2/(\alpha'\beta')) & 2m(1-\alpha^2p^2) \end{bmatrix} \tag{6-35}$$

and

$$m(z) \triangleq (\det M(z))(2-2\alpha^2 p^2)$$

$$= \ell[1/2 - 3\beta^2 p^2 - \beta^2/(\alpha'\beta') + 2\beta^4 p^4 + 2\beta^4 p^2/(\alpha'\beta')]/(1-\beta^2 p^2). \quad (6\text{-}36)$$

Equations (6-34) function as update equations for $\rho(z)$, $\beta(z)$, and $\alpha(z)$. Note that $\rho(z)$ and $\beta(z)$ are updated solely from $r_c(z)$ and $r_s(z)$, and then $r_p(z)$ is used to update $\alpha(z)$. From these three parameters, any other parameter of interest (e.g., $\lambda(z)$ and $\mu(z)$) may be quickly found. Chapman (1974, p. 67) gives equations similar to equations (6-31); however, Chapman's equations involve too many quantities ($\mu, \rho, \beta, \alpha'$, and β') and require the unobservable transmission coefficient t_c. Thus, they are unsuitable as update equations.

We have now specified all of the equations of the algorithm, in differential form. The algorithm consists of equation (6-21), twice (one for the experiment involving excitation by P waves; one for excitation by SV waves) for updating the up- and down-going waves; equations (6-26) and (6-30) for computing the reflectivity functions; equations (6-34) - (6-36) for updating the material parameters $\rho(z)$, $\beta(z)$, and $\alpha(z)$; and equation (6-22d) for computing the transmissivity function $t_c(z)$ required to complete the matrix in equation (6-21). We then immediately have, for each z,

$$\mu(z) = \beta^2(z)\rho(z) \quad (6\text{-}37a)$$

$$\lambda(z) = (\alpha^2(z) - 2\beta^2(z))\rho(z). \quad (6\text{-}37b)$$

Next, the algorithm is discretized in order to clarify the recursions and specify in what order quantities should be computed.

Discretization

The depth coordinate z is discretized by $z = n\Delta$, where n is a positive integer and Δ is the discretization length. The time coordinate t may also be discretized, but its discretization is independent of that of z.

Initialization

It is assumed that all material parameters (λ, μ, ρ, and hence α, β, α', and β') are known at the earth's surface. If we are assuming a free surface, the waves at the surface are determined by measuring the velocity components over time, for both the P and SV experiments, and using (6-9) and (6-10). If the medium is probed from a half-space, the upgoing waves are initialized by the inverse Fourier transforms of the appropriate reflection responses. Since only the smooth parts of the waves need be propagated in the algorithm, the downgoing waves are initialized to zero.

Recursion

We start off with knowledge of $\alpha(z)$, $\beta(z)$, $\rho(z)$, $\alpha'(z)$, $\beta'(z)$ as well as that of all up- and down-going waves at depth z, from the previous iteration. Let $\underset{\sim}{w}^{P}(t,z)$ represent the waves in the P-wave source experiment, and $\underset{\sim}{w}^{S}(t,z)$ represent the waves in the S-wave source experiment. For convenience, we identify the dimensionless quantities

$$B(z) = \beta^2(z)p^2 = \sin^2\theta_s(z) \qquad (6\text{-}38a)$$

$$G(z) = \beta^2(z)/(\alpha'(z)\beta'(z)) = (1/2)\sin 2\theta_s \cot \theta_p \ . \qquad (6\text{-}38b)$$

Then, taking the inverse Fourier transform of equation (6-21) and

employing a simple forward difference approximation to the various derivatives in the differential form of the algorithm yields the following recursive algorithm:

1) Computation of the reflectivity functions. From equations (6-26) and (6-30),

$$r_p(z) = 2w_3^p(\tau_p(z),\ z)/(\tilde{b}_p\Delta) \tag{6-39a}$$

$$r_c(z) = 2w_4^p(\tau_p(z),\ z)/(\tilde{b}_p\Delta) \tag{6-39b}$$

$$r_s(z) = 2(w_4^s(\tau_s(z)^+,z) - w_4^s(\tau_s(z)^-,z))/(\tilde{b}_s\Delta). \tag{6-39c}$$

where $\tilde{b}_p = b_p\alpha'(z)/\Delta$ and $\tilde{b}_s = b_s\beta'(z)/\Delta$ are the strengths of the discretized continuous impulses.

Upon going from continuous time to discrete time, the continuous-time impulse $b_i\delta(t)$ becomes a discrete-time impulse of height b_i/D_i, where D_i is the differential delay time at depth z for wave type i (see Figure 6.1). Since the impulse has been spread out over the time interval D_i, its height must be b_i/D_i in order to maintain its area b_i. For a P→P reflection $D_p = \Delta/\alpha'(z)$. For a P→S reflection the two-way delay is $D_p + D_s$, hence the one-way delay is half of this, or $(\Delta/2)(1/\alpha'(z) + 1/\beta'(z))$. Equations (6-26) and (6-30) are thus modified to (6-39).

2) Computation of auxiliary quantities. From equations (6-36) and (6-38),

$$B(z) = \beta^2(z)p^2 \tag{6-40}$$

$$G(z) = \beta^2(z)/(\alpha'(z)\beta'(z)) \tag{6-41}$$

$$m(z) = (1/2 - 3B - G + 2B^2 + 2BG)\ell/(1-B) \tag{6-42}$$

$$t_c(z) = -\ell(1/2 - 3B + G + 2B^2 - 2BG)r_c(z)/((1-B)m(z)) + 2Br_s(z)/m(z) \tag{6-43}$$

where $\ell(z)$ is defined as above.

3) Update of material parameters. From equations (6-34) - (6-35),

$$\rho(z+\Delta) = \rho(z) - \rho(z)((1/(2-2B) - 4B)r_c(z) + 4\ell(B-G)r_s(z))\Delta/m(z) \tag{6-44}$$

$$\beta(z+\Delta) = \beta(z) - \beta(z)((2B-1/2)r_c(z) + \ell(1-2B+2G)r_s(z))\Delta/m(z) \tag{6-45}$$

$$\alpha(z+\Delta) = \alpha(z) + \alpha(z)(1-\alpha^2(z)p^2)(2r_p(z) - ((2B-1/2)/(1-B)m(z))r_c(z) - \ell(4(B+G)/m(z))r_s(z))\Delta \tag{6-46}$$

$$\alpha'(z+\Delta) = \alpha(z+\Delta)/(1-\alpha^2(z+\Delta)p^2)^{\frac{1}{2}} \tag{6-47}$$

$$\beta'(z+\Delta) = \beta(z+\Delta)/(1-\beta^2(z+\Delta)p^2)^{\frac{1}{2}} \quad . \tag{6-48}$$

4) Wave update. From the inverse Fourier transforms of equation (6-21),

$$w_1(t+\Delta/\alpha'(z),\ z+\Delta) = w_1(t,z) - (t_c(z)w_2(t,z) + r_p(z)w_3(t,z) + r_c(z)w_4(t,z))\Delta \tag{6-49a}$$

$$w_2(t+\Delta/\beta'(z),\ z+\Delta) = w_2(t,z) - (-t_c(z)w_1(t,z) + r_c(z)w_3(t,z) + r_s(z)w_4(t,z))\Delta \tag{6-49b}$$

$$w_3(t-\Delta/\alpha'(z),\ z+\Delta) = w_3(t,z) - (r_p(z)w_1(t,z) + r_c(z)w_2(t,z) + t_c(z)w_4(t,z))\Delta \tag{6-49c}$$

$$w_4(t-\Delta/\beta'(z),\ z+\Delta) = w_4(t,z) - (r_c(z)w_1(t,z) + r_s(z)w_2(t,z) - t_c(z)w_3(t,z))\Delta \qquad (6\text{-}49d)$$

and these same recursions are used for both $\underset{\sim}{w}^P(t,z)$ and $\underset{\sim}{w}^S(t,z)$.

At this point, we have obtained $\rho(z+\Delta)$, $\alpha(z+\Delta)$, $\beta(z+\Delta)$, $\alpha'(z+\Delta)$ $\beta'(z+\Delta)$, and all eight waves at depth $z+\Delta$. Hence the recursion is complete. Each step in the recursion can be implemented as one stage or section of a ladder-type filter, which can be regarded as a more complex version of the lattice filter commonly encountered in spectral estimation theory. A typical section of this ladder filter is illustrated in Figure 6.1. The downgoing P and SV waves at depth z enter the filter section at the upper left, interact with each other, are reflected (due to the inhomogeneity of the medium), and exit at the upper right, now at depth $z+\Delta$. Upgoing P and SV waves undergo a similar experience in the lower half of the filter. Note how this filter illustrates the physical meaning of the reflectivity functions $r_p(z)$, $r_c(z)$ and $r_s(z)$, and of the transmissivity function $t_c(z)$.

The recursions of the waves in z and t, given by equations (6-49), are slightly complicated, so the recursion patterns are illustrated in Figures 6-2a and 6-2b. We start off knowing the waves at depth z for all time, and wish to find the waves at depth $z+\Delta$. Although the simultaneous time and depth updates may make it seem as though information at early times is being lost, recall that by causality there can be no wave at depth z until the initial excitation has had time to reach depth z. Thus there is no information to lose at the early times.

The algorithm that we have described above for reconstructing $\rho(z)$, $\lambda(z)$ and $\mu(z)$ works even if some turning points exist for the P and SV

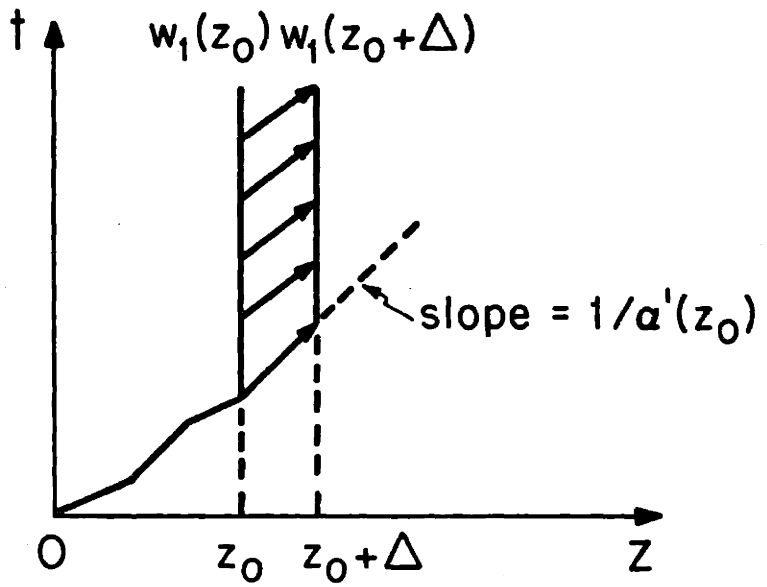

6.2a Recursion pattern for updating the downgoing waves.

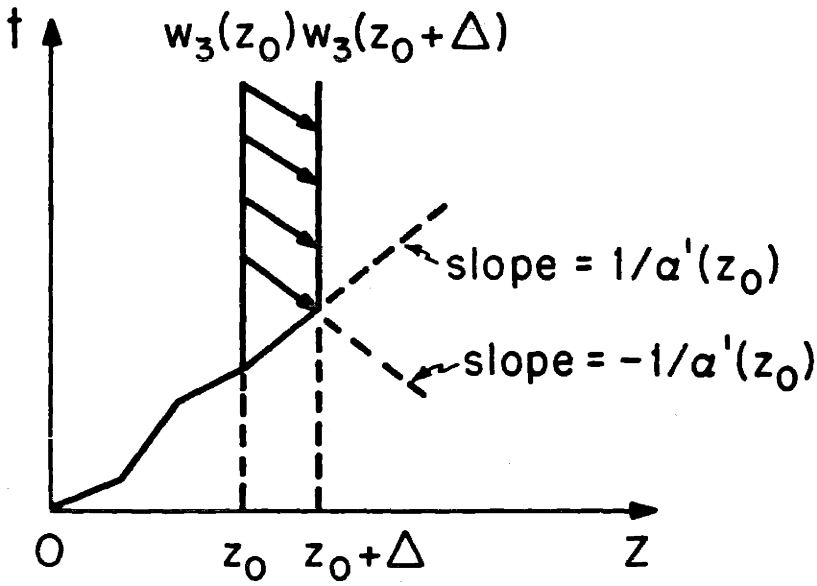

6.2b Recursion pattern for updating the upgoing waves.

waves propagating through the elastic medium. However, in this case ρ, λ and μ can only be reconstructed up to the depth z_p where the ray path for the P wave becomes horizontal. Note that along rays associated with the P and SV waves

$$\sin \theta_p(z)/\alpha(z) = \sin \theta_s(z)/\beta(z) = p = \text{constant} \qquad (6\text{-}50)$$

so that unless $\alpha(z) < 1/p$ for all z (in which case we have also $\beta(z) < 1/p$), the angle $\theta_p(z)$ will become imaginary at some depth z_p. Physically, this situation results in evanescent waves where the waves decay exponentially with depth. This causes no problem in the reconstruction algorithm until $z = z_p$, at which point $\alpha'(z) \to \infty$. Then, the waves $\underset{\sim}{w}^p(z,t)$ and $\underset{\sim}{w}^s(z,t)$ cannot be propagated further, and the material parameters are reconstructed only up to depth z_p.

Comments

The algorithm, of course, works on a layer stripping principle. At each depth, the first reflections in three of the four upgoing waves (P and SV for each of the two experiments) yield the reflectivity functions $r_p(z)$, $r_c(z)$ and $r_s(z)$. The transmissivity function $t_c(z)$, which is not a transmission loss but a coupling between two waves moving in the same direction, is then computed using (6-22d). All eight waves are then propagated down to the next depth. Complications are introduced since the SV first reflection arrives after the P first reflection, and must be separated out from the downgoing P wave. However, the elastic layer stripping algorithm is basically a generalization of the algorithm of Chapter IV, with some complications added.

However, if the waves $\underset{\sim}{\hat{w}}$ are written out using definition (6-16), the result is

$$\hat{w}_{\substack{1\\3}} = Z_p^{\frac{1}{2}}\left[\sin^2\theta_s\left(\frac{\hat{u}_x}{\sin\theta_p} \mp \frac{\hat{u}_z}{\sin\theta_s}\right) \pm \frac{\hat{u}_z}{2\cos\theta_p} - \frac{ip}{2\omega\rho}\left(\frac{\hat{\tau}_{zx}}{\cos\theta_p} \pm \frac{\hat{\tau}_{zz}}{\sin\theta_s}\right)\right. \tag{6-51a}$$

$$\hat{w}_{\substack{2\\4}} = Z_s^{\frac{1}{2}}\left[\sin^2\theta_s\left(\frac{\hat{u}_x}{\cos\theta_s} \pm \frac{\hat{u}_z}{\sin\theta_s}\right) + \frac{\hat{u}_x}{2\cos\theta_s} - \frac{ip}{2\omega\rho}\left(\frac{\hat{\tau}_{zx}}{\sin\theta_s} \mp \frac{\hat{\tau}_{zz}}{\cos\theta_s}\right)\right. \tag{6-51b}$$

where the upper signs are used for the downgoing waves and the lower signs for the upgoing waves. These certainly don't look like physically interpretable waves. However, they may be simplified to

$$\hat{w}_{\substack{1\\3}} = Z_p^{-\frac{1}{2}}(\hat{\tau}_{zz}\cos\theta_p \pm \hat{\tau}_{zx}\sin\theta_p) \pm j\omega Z^{\frac{1}{2}}\frac{\hat{u}_z}{\cos\theta_p} = Z_p^{-\frac{1}{2}}\hat{\tau}_p \pm j\omega Z_p^{\frac{1}{2}}\hat{u}_p \tag{6-52a}$$

$$\hat{w}_{\substack{2\\4}} = Z_s^{-\frac{1}{2}}(\hat{\tau}_{zx}\cos\theta_s \mp \hat{\tau}_{zz}\sin\theta_s) \mp j\omega Z^{\frac{1}{2}}\frac{\hat{u}_z}{\sin\theta_s} = Z_s^{-\frac{1}{2}}\hat{\tau}_s \pm j\omega Z_s^{\frac{1}{2}}\hat{u}_s \tag{6-52b}$$

where $\hat{\tau}_p$ and $\hat{u}_p$ are stress and displacement in the direction of propagation and $\hat{\tau}_s$ and $\hat{u}_s$ are stress and displacement <u>perpendicular</u> to the direction of propagation. Here we have used the relations

$$\hat{u}_p = \pm\,\hat{u}_z/\cos\theta_p = \hat{u}_x/\sin\theta_p \tag{6-53a}$$

$$\hat{\tau}_p = \hat{\tau}_{zx}\sin\theta_p \pm \hat{\tau}_{zz}\cos\theta_p \tag{6-53b}$$

$$\hat{u}_s = \mp\,\hat{u}_z/\sin\theta_s = \hat{u}_x/\cos\theta_s \tag{6-53c}$$

$$\hat{\tau}_s = \hat{\tau}_{zx}\cos\theta_s \mp \hat{\tau}_{zz}\sin\theta_s \tag{6-53d}$$

in both (6-51) and (6-52).

The waves in (6-52) look much more like the choices made in

Chapters III and IV. If the medium is locally homogeneous, they simplify even further to energy-normalized displacements. This matches the choices made by Frasier (1969) and Shiva and Mendel (1983) for a discrete medium composed of homogeneous layers.

It should also be noted that if the medium is discretized, i.e., modelled as a welded stack of thin, homogeneous layers with material parameters varying only between different layers, then RdC/dz may be interpreted as a scattering matrix for the layer at depth z. To see this, replace $(d/dz) \log \rho(z) = (d/dz)\rho(z)/\rho(z)$ by the discrete approximation $\Delta\rho(z)/\rho(z)$, and do the same for $\beta(z)$ and $\alpha(z)$. Then equations (6-22) become the reflection and transmission coefficients at an interface (Aki and Richards, 1980, p. 153). Thus discretization of the algorithm is equivalent to a physical discretization of the medium.

6.3 Alternative Formulations of the Algorithm

In this section some other layer stripping algorithms for inverse problems for elastic media are given. First, a dynamic deconvolution algorithm, involving a matrix Riccati equation, is specified for the problem considered above. Next, a layer stripping algorithm is derived for the problem in which an elastic medium is probed from an overlying liquid ($\mu = 0$) half-space. Since shear waves cannot propagate through a liquid, only the P - to - P reflection response is available for this problem. Finally, some comments on discrete elastic media are made to tie this chapter closer to Chapter III.

6.3.1 Dynamic Deconvolution

The dynamic deconvolution algorithm for the elastic problem is quite easy to derive. Let the matrix reflection coefficient $S(z,\omega)$ relating

the downgoing P and SV waves to the upgoing P and SV waves be defined by

$$\begin{bmatrix} UP \\ US \end{bmatrix} = S \begin{bmatrix} DP \\ DS \end{bmatrix} \tag{6-54}$$

where DP, DS, UP, and US are the amplitudes of the downgoing and upgoing P and SV waves, respectively. For convenience, rewrite (6-21) as

$$\frac{d}{dz} \left[\begin{array}{c} DP \\ DS \\ \hline UP \\ US \end{array}\right] = \left[\begin{array}{c|c} J_1 & -R \\ \hline -R & J_2 \end{array}\right] \left[\begin{array}{c} DP \\ DS \\ \hline UP \\ US \end{array}\right] \tag{6-55}$$

where

$$R = \begin{bmatrix} r_p & r_c \\ r_c & r_s \end{bmatrix}, \quad J_1 = \begin{bmatrix} -j\omega/\alpha' & -t_c \\ t_c & -j\omega/\beta' \end{bmatrix}, \quad J_2 = \begin{bmatrix} j\omega/\alpha' & -t_c \\ t_c & j\omega/\beta' \end{bmatrix}. \tag{6-56}$$

Then, taking the derivative of (6-54) with respect to z yields

$$\frac{d}{dz}\begin{bmatrix} UP \\ US \end{bmatrix} = -R\begin{bmatrix} DP \\ DS \end{bmatrix} + J_2\begin{bmatrix} UP \\ US \end{bmatrix} = \left(\frac{d}{dz}S\right)\begin{bmatrix} DP \\ DS \end{bmatrix} + S\frac{d}{dz}\begin{bmatrix} DP \\ DS \end{bmatrix}$$

$$= \left(\frac{d}{dz}S\right)\begin{bmatrix} DP \\ DS \end{bmatrix} + SJ_1\begin{bmatrix} DP \\ DS \end{bmatrix} - SR\begin{bmatrix} UP \\ US \end{bmatrix}, \tag{6-57}$$

and inserting (6-54) and collecting terms gives

$$\left(\frac{d}{dz}S + SJ_1 - J_2S + R - SRS\right)\begin{bmatrix} DP \\ DS \end{bmatrix} = \begin{bmatrix} 0 \\ 0 \end{bmatrix}, \tag{6-58}$$

and noting that (6-58) must hold for any set of waves $\begin{bmatrix} DP \\ DS \end{bmatrix}$ finally results in the matrix Riccati equation

$$\frac{d}{dz}S = J_2 S - S J_1 - R + SRS \quad . \tag{6-59}$$

Note that in the high frequency case, where the transmissivity function t_c becomes negligible, (6-59) becomes

$$\frac{d}{dz}S = j\omega\begin{bmatrix} 1/\alpha' & 0 \\ 0 & 1/\beta' \end{bmatrix} S + j\omega S \begin{bmatrix} 1/\alpha' & 0 \\ 0 & 1/\beta' \end{bmatrix} - R + SRS \quad . \tag{6-60}$$

A Riccati equation similar to (6-59) was derived by Wilcox (1964) for the electric wave propagation problem on two non-uniform, coupled transmission lines. Thus it is not surprising that a similar equation applies to the somewhat similar problem of seismic wave propagation in an elastic medium.

Since $S(z,\omega)$ is strictly proper, we have (compare to (3-42))

$$R = \lim_{\omega \to \infty} j\omega \left(S \begin{bmatrix} 1/\alpha' & 0 \\ 0 & 1/\beta' \end{bmatrix} + \begin{bmatrix} 1/\alpha' & 0 \\ 0 & 1/\beta' \end{bmatrix} S \right) \tag{6-61}$$

and the dynamic deconvolution algorithm consists of (6-59), (6-61), the initial condition

$$S(0,\omega) = \begin{bmatrix} \hat{R}_{pp}(\omega) & \hat{R}_{ps}(\omega) \\ \hat{R}_{sp}(\omega) & \hat{R}_{ss}(\omega) \end{bmatrix} , \tag{6-62}$$

and (6-22d) for computing t_c from R. The Riccati equation (6-59) is propagated in z, recovering R at each depth from (6-61). The medium parameter updates (6-34) - (6-36) are used to obtain $\alpha(z)$, $\beta(z)$ and $\rho(z)$.

6.3.2 Elastic Medium with an Overlying Liquid Half-Space

In this problem an elastic medium is probed from an overlying liquid

half-space. This is clearly applicable to the problem of probing the ocean floor from the ocean above it. The difficulty, of course, is that since the liquid does not support shear stresses and shear waves, it is impossible to measure $\hat{R}_{ps}$ and $\hat{R}_{ss}$. Nevertheless, it is still possible to reconstruct the profiles $\lambda(z)$, $\mu(z)$, and $\rho(z)$ from $\hat{R}_{pp}$ alone, if $\hat{R}_{pp}$ is obtained for <u>three</u> different values of slowness p.

We assume first that the transition from liquid to solid medium is a gradual, continuous transition. This is in fact the situation at the bottom of the ocean--the interface between the water and ooze is gradual. If this is the case, then the continuous medium parameter updates may still be used. Writing (6-22a) for $p = p_1, p_2, p_3$ and arranging the results into a matrix, we have

$$\begin{bmatrix} r_{p_1}(z) \\ r_{p_2}(z) \\ r_{p_3}(z) \end{bmatrix} = \begin{bmatrix} (1/2-2\beta^2 p_1^2) & -4\beta^2 p_1^2 & 1/(2-2\alpha^2 p_1^2) \\ (1/2-2\beta^2 p_2^2) & -4\beta^2 p_2^2 & 1/(2-2\alpha^2 p_2^2) \\ (1/2-2\beta^2 p_3^2) & -4\beta^2 p_3^2 & 1/(2-2\alpha^2 p_3^2) \end{bmatrix} \begin{bmatrix} (d/dz)\log\ \rho(z) \\ (d/dz)\log\ \beta(z) \\ (d/dz)\log\ \alpha(z) \end{bmatrix}$$

$$= \begin{bmatrix} m_{11} & m_{12} & m_{13} \\ m_{21} & m_{22} & m_{23} \\ m_{31} & m_{32} & m_{33} \end{bmatrix} \begin{bmatrix} (d/dz)\log\ \rho(z) \\ (d/dz)\log\ \beta(z) \\ (d/dz)\log\ \alpha(z) \end{bmatrix} . \qquad (6\text{-}63)$$

Inverting (6-63) yields the update equations

$$\rho(z+\Delta) = \rho(z) + [(m_{22}m_{33}-m_{23}m_{32})r_{p_1}(z)-(m_{12}m_{33}-m_{13}m_{32})r_{p_2}(z) + (m_{12}m_{23}-m_{22}m_{13})r_{p_3}(z)]\cdot \Delta/d(z) \qquad (6\text{-}64a)$$

$$\beta(z+\Delta) = \beta(z)+[-(m_{21}m_{33}-m_{23}m_{31})r_{p_1}(z) + (m_{11}m_{33}-m_{31}m_{13})r_{p_2}(z) - (m_{11}m_{23}-m_{13}m_{21})r_{p_3}(z)]\cdot\Delta/d(z) \quad (6\text{-}64b)$$

$$\alpha(z+\Delta) = \alpha(z)+[(m_{21}m_{32}-m_{31}m_{22})r_{p_1}(z) - (m_{11}m_{32}-m_{31}m_{12})r_{p_2}(z) + (m_{11}m_{22}-m_{12}m_{21})r_{p_3}(z)]\cdot\Delta/d(z) \quad (6\text{-}64c)$$

$$d(z) = \text{DET } M(z) = m_{11}(m_{22}m_{33}-m_{23}m_{32})-m_{12}(m_{21}m_{33}-m_{23}m_{31}) + m_{13}(m_{21}m_{32}-m_{22}m_{31}). \quad (6\text{-}64d)$$

The layer stripping algorithm works as follows. The upgoing and downgoing P waves are initialized using the P - to - P reflection response $\hat{R}_{pp}(\omega)$ for each of the three slowness values p_1, p_2 and p_3. The upgoing and downgoing SV waves are initialized to zero. Three copies of the wave update equations (6-49) (one for each of p_1, p_2, and p_3), the parameter update equations (6-64), the reflectivity function equation (6-39a), and the equation (6-22d) for t_c constitute the algorithm. At each depth z, the reflection data for p_1, p_2, and p_3 yield $r_{p_1}(z)$, $r_{p_2}(z)$, and $r_{p_3}(z)$, which are used to update $\rho(z)$, $\beta(z)$, and $\alpha(z)$ to $z+\Delta$ by (6-64). After t_c has been obtained by (6-22d), the twelve waves (in three groups of four) can be updated to $z+\Delta$ by (6-49). At this point all quantities have been updated to $z+\Delta$ and the recursion is complete.

Note that in the liquid half-space β and $d\beta/dz$ are both zero, and the updates (6-64) reduce to the updates (4-35) for the acoustic problem. Then, at the interface, $d\beta/dz$ becomes non-zero since $\beta(z+\Delta)$ is non-zero. How does the algorithm "know" when $\beta(z)$ becomes non-zero? If $\beta(z)$ is zero, the system of equations (6-63) is an overdetermined but

consistent version of the system (4-35), since there are now three reflectivity functions instead of two. When the values of the reflectivity functions take on values such that the system (6-63) is no longer consistent, it can only be because $\beta(z)$ is now non-zero. Downgoing and upgoing SV waves are introduced by the coupling terms r_c and t_c.

Of course, this algorithm could also be used in place of the algorithm in Section 6.2. The main disadvantage of this algorithm is that the reflection response must be synthesized for three different values of p instead of only one. And after all, the SV wave responses can be measured just as easily as the P wave responses (see (6-10)). However, this algorithm does have the advantage of not requiring two separate experiments utilizing P and SV wave sources. If this is a problem, there is still another option: measure the P - to - P and P - to - SV reflection responses for <u>two</u> values of slowness p. Then use

$$\begin{bmatrix} r_{p_1}(z) \\ r_{p_2}(z) \\ r_{c_1}(z) \\ r_{c_2}(z) \end{bmatrix} = \begin{bmatrix} (\tfrac{1}{2}-2\beta^2 p_1^2) & -4\beta^2 p_1^2 & 1/(2-2\alpha^2 p_1^2) \\ (\tfrac{1}{2}-2\beta^2 p_2^2) & -4\beta^2 p_2^2 & 1/(2-2\alpha^2 p_2^2) \\ -\ell_1(1-2\beta^2 p_1^2+2\beta^2/(\alpha'_1\beta'_1)) & \ell_1(4\beta^2 p_1^2-4\beta^2/(\alpha'_1\beta'_1)) & 0 \\ -\ell_2(1-2\beta^2 p_2^2+2\beta^2/(\alpha'_2\beta'_2)) & \ell_2(4\beta^2 p_2^2-4\beta^2/(\alpha'_2\beta'_2)) & 0 \end{bmatrix} \begin{bmatrix} (d/dz)\log \rho \\ (d/dz)\log \beta \\ (d/dz)\log \alpha \end{bmatrix} \tag{6-65}$$

where $\ell_i(z)$ is defined by (6-33) and $\alpha'_i(z)$ and $\beta'_i(z)$ clearly depend on p_i. Omitting any row of (6-65) and inverting the resulting 3 x 3 matrix as before using (6-64) yields a recursive algorithm. This algorithm consists of (6-64), in which the m_{ij} are now defined by (6-65) (with one row missing), for medium parameter updates, and two copies of the wave update equations (6-49) (one for each of p_1 and p_2). The missing row from (6-65) is also available as a consistency check.

However, if the solid-liquid interface is not gradual and continuous, but sudden and sharp (like the bottom of a swimming pool), then the discrete expressions for the reflection coefficients must be used. These expressions, given in Aki and Richards (1980, p. 150), are exact in that they are accurate across large jumps in $\rho(z)$, $\beta(z)$ and $\alpha(z)$, but are far too complex to be practical in a fast algorithm. So let us consider the case where the discrete expressions are only used once, at the solid-liquid interface, and the continuous expressions (6-22) are used thereafter. If ρ_o, α_o, and $\beta_o = 0$ are the known values of $\rho(z)$, $\beta(z)$, and $\alpha(z)$ just above the interface, and ρ_1, β_1, and α_1 are the unknown values just below the interface, then we have the following result. Define q_{p_i} by

$$q_{p_i} = (1/\alpha_o^2 - p_i^2)^{\frac{1}{2}}(1 - r_{p_i})/(1 + r_{p_i}), \quad i = 1, 2, 3 \qquad (6\text{-}66)$$

and note that q_{p_i} is known from the data. Then solve the two (highly) non-linear simultaneous equations

$$[(1-2\beta_1^2 p_i^2)/(1/\alpha_1^2 - p_i^2)^{\frac{1}{2}} + 4\beta_1^4 p_i^2 (1/\beta_1^2 - p_i^2)^{\frac{1}{2}}]q_{p_i} = \rho_o/\rho_1 = \text{constant},$$

$$i = 1, 2, 3 \qquad (6\text{-}67)$$

in α_1 and β_1 for α_1 and β_1. Then ρ_1 follows immediately. Once α_1, β_1, and ρ_1 have been obtained, use the previous continuous algorithm to reconstruct the rest of the medium.

Since the equations (6-67) need only be solved once, this algorithm could prove workable in a situation with a known sharp solid-liquid interface. However, the required solution of (6-67) is not an appealing prospect, numerically.

6.3.3 Some Comments on Discrete Elastic Media

It has already been remarked that the layer stripping algorithms specified by Clarke (1984) and Shiva and Mendel (1983) are far more complex than the comparatively simple algorithm of Section 6.2, since these algorithms assume a discrete medium for which $\lambda(z)$, $\mu(z)$, and $\rho(z)$ are piecewise constant. Further, the different wave speeds of P and SV waves seems to rule out a matrix Schordinger equation - Gel'fand-Levitan-integral equation solution procedure. On this basis, it might seem that there are relatively few connections between discrete elastic media and the discrete acoustic media considered in Chapter III.

However, this is not the case. Indeed, a surprising number of basic results of Chapter III generalize to the case of a discrete elastic medium, and some of these results have implications for the continuous elastic medium algorithm. To aid in understanding how the elastic medium is a generalization of the acoustic medium, we now quickly sketch over some results of Chapter III that generalize to the case of a discrete elastic medium. Most of these results are due to Frasier (1969).

Let DP_n, DS_n, UP_n, and US_n be the downgoing and upgoing energy-normalized displacement waves, respectively, at the top of layer n, and let DP'_n, DS'_n, UP'_n, and US'_n be corresponding waves at the bottom of layer n (see Figure 6.3). Then we have the scattering relation

$$\begin{bmatrix} DP_{n+1} \\ DS_{n+1} \\ UP'_n \\ US'_n \end{bmatrix} = \begin{bmatrix} t_{pp} & t_{sp} & r'_{pp} & r'_{sp} \\ t_{ps} & t_{ss} & r'_{ps} & r'_{ss} \\ r_{pp} & r_{sp} & t'_{pp} & t'_{sp} \\ r_{ps} & r_{ss} & t'_{ps} & t'_{ss} \end{bmatrix} \begin{bmatrix} DP'_n \\ DS'_n \\ UP_{n+1} \\ US_{n+1} \end{bmatrix} \tag{6-68}$$

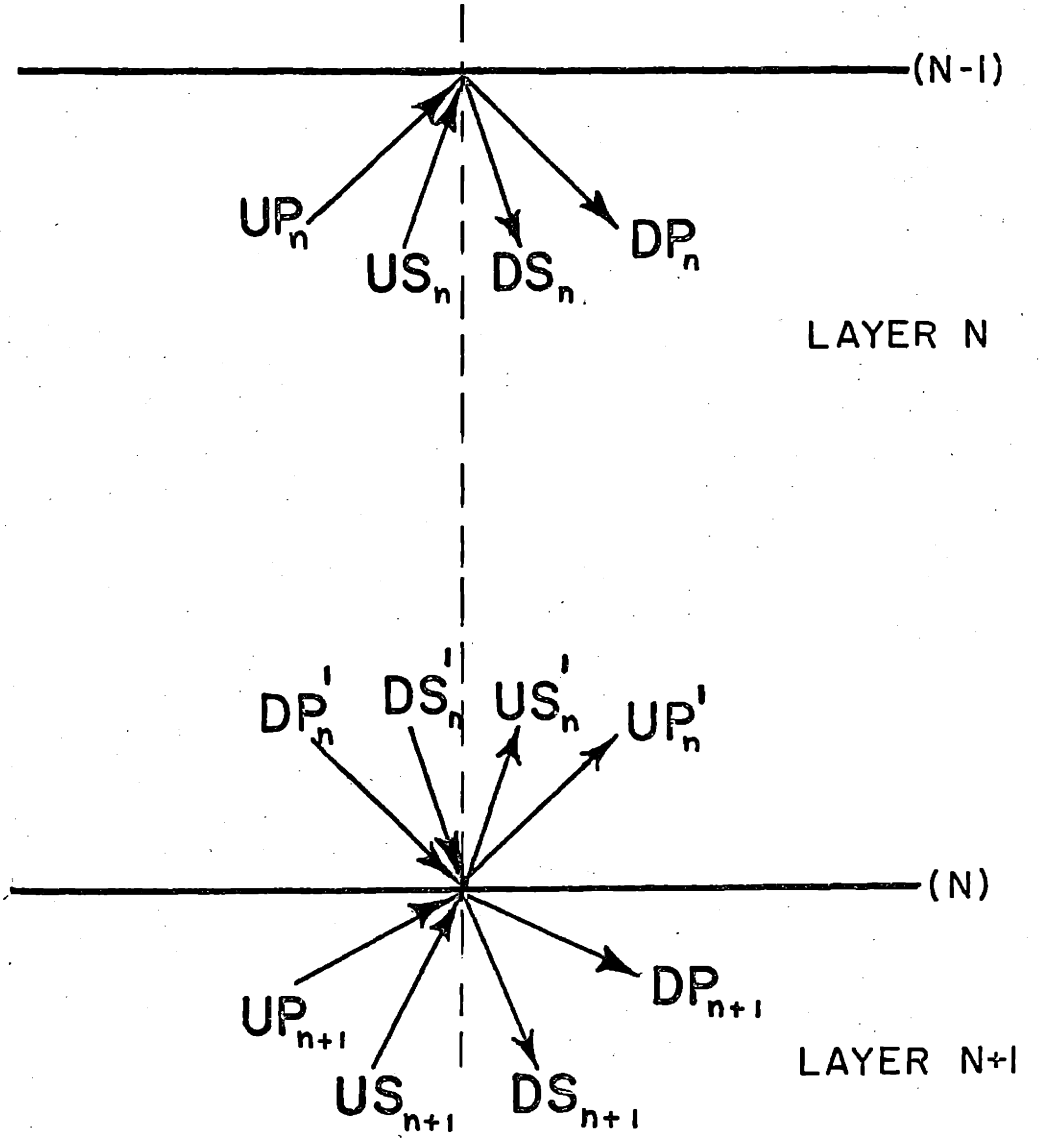

6.3 Wave notations for downgoing and upgoing P and SV waves in a discrete elastic medium.

where r_{ij} and t_{ij} are the reflection and transmission coefficients for waves incident from above, and r'_{ij} and t'_{ij} are the coefficients for waves incident from below. Rearranging (6-68) gives

$$\begin{bmatrix} I & -R'_n \\ 0 & T'_n \end{bmatrix} \begin{bmatrix} d_{n+1} \\ u_{n+1} \end{bmatrix} = \begin{bmatrix} T_n & 0 \\ -R_n & I \end{bmatrix} \begin{bmatrix} d'_n \\ u'_n \end{bmatrix} \tag{6-69}$$

where

$$R_n = \begin{bmatrix} r_{pp} & r_{sp} \\ r_{ps} & r_{ss} \end{bmatrix}, \; T_n = \begin{bmatrix} t_{pp} & t_{sp} \\ t_{ps} & t_{ss} \end{bmatrix}, \; d_n = \begin{bmatrix} DP_n \\ DS_n \end{bmatrix}, \; u_n = \begin{bmatrix} UP_n \\ UP_n \end{bmatrix} \tag{6-70}$$

and the primed matrices are defined similarly. We then have

$$\begin{bmatrix} d_{n+1} \\ u_{n+1} \end{bmatrix} = \begin{bmatrix} T_n - R'_n T'^{-1}_n R_n & R'_n T'^{-1}_n \\ -T'^{-1}_n R_n & T'^{-1}_n \end{bmatrix} \begin{bmatrix} d'_n \\ u'_n \end{bmatrix} \tag{6-71}$$

and using the facts that R_n and R'_n are symmetric and (Frasier, 1969)

$$T'_n = T_n^T \tag{6-72a}$$

$$T_n R_n + R'_n T_n = 0 \tag{6-72b}$$

$$T_n^T T_n + R_n^T R_n = I \tag{6-72c}$$

we get the surprisingly simple result

$$\begin{bmatrix} d_{n+1} \\ u_{n+1} \end{bmatrix} = T'^{-1}_n \begin{bmatrix} I & -R_n \\ -R_n & I \end{bmatrix} \begin{bmatrix} d'_n \\ u'_n \end{bmatrix}. \tag{6-73}$$

Equation (6-73) looks just like the 2 x 2 layer matrix equation (3-50). However, the quantities in (6-73) are matrices. Thus if the elastic problem layer stripping algorithm is to be used on a discrete elastic medium, with the medium parameter updates given in Clarke (1984), the continuous medium wave updates (6-49) should be replaced by (6-73) (with appropriate time delays), a fact missed by Clarke (1984).

It should also be noted that the relations (6-72), which Frasier (1969) derived from the continuity of unnormalized normal stress and displacement at the interface, are simply a statement of the unitarity of the scattering matrix (6-68). The relations (6-72) should be compared to the corresponding relations in Chapter II. The unitary scattering matrix considered by Kennett et al. (1978) is the matrix in (6-68) premultiplied by $\begin{bmatrix} 0 & I \\ I & 0 \end{bmatrix}$.

To show that (6-73) reduces to (6-49) for a continuous medium as the layer thickness Δ approaches zero, recall that the reflectivity and transmissivity functions are defined by

$$r_p(z) = \lim_{\Delta \to 0} r_{pp}/\Delta \tag{6-74}$$

and similarly for the other functions. From (6-72c) it is clear that t_{pp} and t_{ss} are both $1+ 0(\Delta^2)$. The layer matrix (6-73) then becomes, for small Δ,

$$T'^{-1}\begin{bmatrix} I & -R_n \\ -R_n & I \end{bmatrix} = \begin{bmatrix} 1 & t_c\Delta \\ -t_c\Delta & 1 \end{bmatrix}^{-1} \begin{bmatrix} I & -R\Delta \\ -R\Delta & I \end{bmatrix} + 0(\Delta^2)$$

$$= \begin{bmatrix} 1 & -t_c\Delta \\ t_c\Delta & 1 \end{bmatrix}\begin{bmatrix} I & -R\Delta \\ -R\Delta & I \end{bmatrix} + 0(\Delta^2) = \begin{bmatrix} 1 & -t_c\Delta & -r_p\Delta & -r_c\Delta \\ t_c\Delta & 1 & -r_c\Delta & -r_s\Delta \\ -r_p\Delta & -r_c\Delta & 1 & -t_c\Delta \\ -r_c\Delta & -r_s\Delta & t_c\Delta & 1 \end{bmatrix} + 0(\Delta^2) \tag{6-75}$$

where $R \triangleq \begin{bmatrix} r_p & r_c \\ r_c & r_s \end{bmatrix}$ and we have used (Aki and Richards, 1980, p. 150)

$$r_{ps} = r_{sp} \tag{6-76a}$$

$$t_{ps} = t'_{sp} \cong t_c \Delta \tag{6-76b}$$

$$t_{sp} = t'_{ps} \cong -t_c \Delta \quad . \tag{6-76c}$$

The matrix (6-75) matches the wave updates (6-49).

Frasier (1969) then proceeds to define a delay matrix

$$Z_n = \begin{bmatrix} z^{\ell_n} & 0 \\ 0 & z^{m_n} \end{bmatrix} \tag{6-77}$$

where the travel time through the layer is $\ell_n \Delta$ for for P waves and $m_n \Delta$ for S waves. Of course, this is incorrect, although the error goes to zero along with Δ. Using (6-77) and (6-73) gives

$$\begin{bmatrix} d_{n+1} \\ u_{n+1} \end{bmatrix} = T'^{-1}_n \begin{bmatrix} Z_n^{-1} & -R_n Z_n \\ -R_n Z_n^{-1} & Z_n \end{bmatrix} \begin{bmatrix} d_n \\ u_n \end{bmatrix} \tag{6-78}$$

in analogy to (3-51). Frasier (1969) then derives many other results analogous to those of Chapter III, including a matrix equation, Levinson recursions, and a generalization of the Kunetz result (3-67). However, all of these results rely on the inaccurate time discretization specified by (6-77).

6.4 Computational Results

The algorithm was tested by running it on the synthesized impulse

response of a twenty-layer medium. The variation of medium parameters from one layer to another was made small (around 2%) in order to simulate a continuous layered medium. This is important, since the differential updates assume a continuously varying medium; the algorithm cannot handle sharp changes in medium properties unless the step size Δ is made smaller in such regions. The medium velocities and step size Δ are in units of km/sec and km., respectively, and the density is relative to that of water.

The response of the medium to impulsive plane P and SV waves was generated in the frequency domain using the reflectivity method (Aki and Richards, 1980, p. 393). A FORTRAN program given by Kind (1976) was used to compute the plane wave transfer functions R_{pp}, R_{ps}, and R_{ss} at 512 frequency points (integer multiples of 0.78 Hz). Each of these was divided by $j2\pi f$, and a discrete inverse Fourier transform was taken. This synthesized sample step responses; taking differences and dividing by the discretization time Δt = 0.005s yielded the discretized impulse responses. Careful attention must be paid to signs in going from potential reflection responses to velocity reflection responses (see Aki and Richards, 1980, p. 191).

The impulse responses, scaled by $1/\Delta t$ for convenience, are plotted in Figures 6.4. Although the responses were computed for t = 0 up to t = 2.565 seconds to avoid aliasing problems, the responses beyond t = 1.3 seconds were essentially zero and are not shown. Note that the peaks corresponding to strong primary reflections are smeared out. This is due in part to the use of a DFT, which is this case is tantamount to bandpass filtering the data with a filter with pass band 0.78 Hz - 400 Hz. Since the strengths of the primary reflections are especially

6.4a P → P impulse response, scaled by $1/\Delta t$ for convenience.

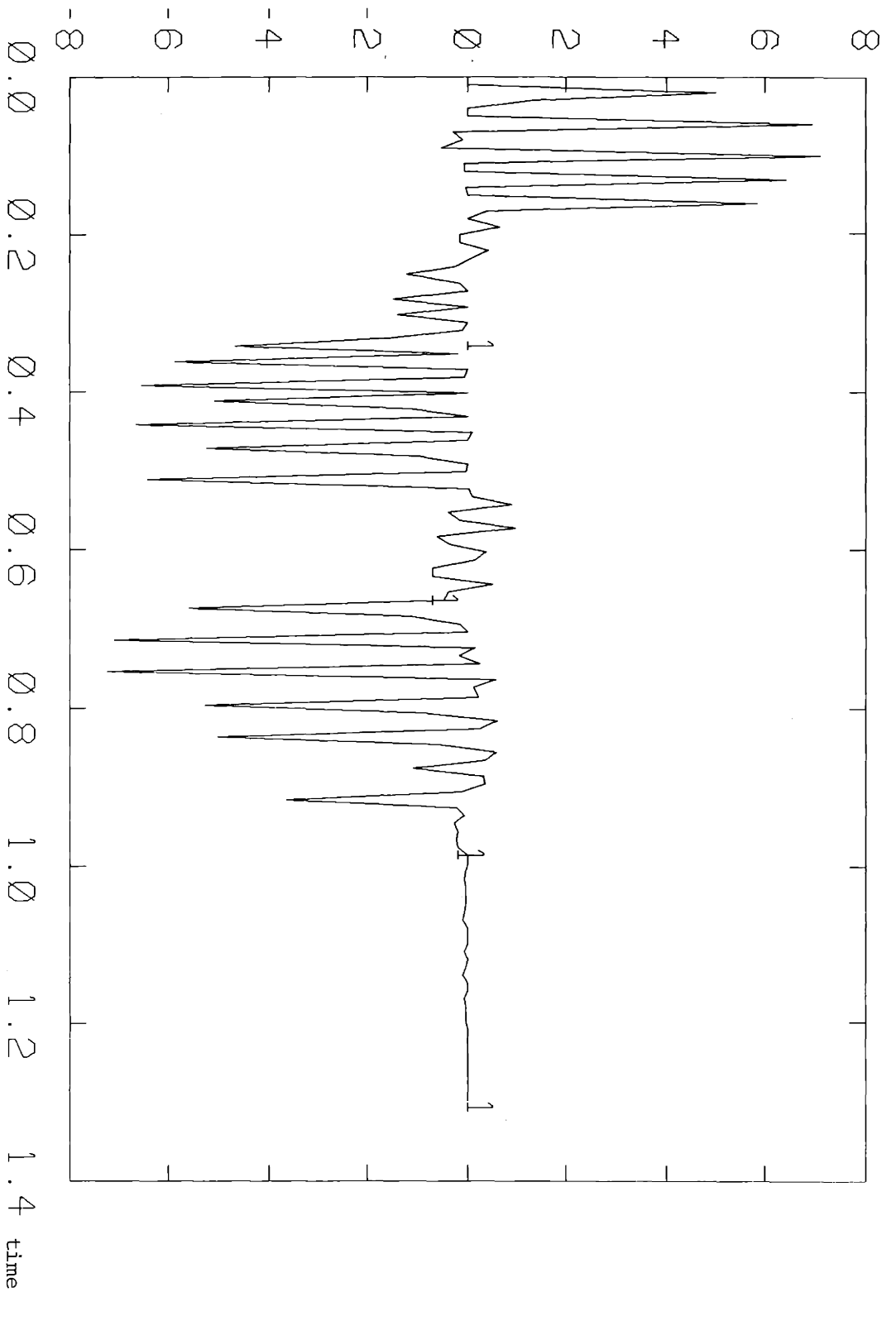

6.4b P→S impulse response, scaled by 1/Δt for convenience.

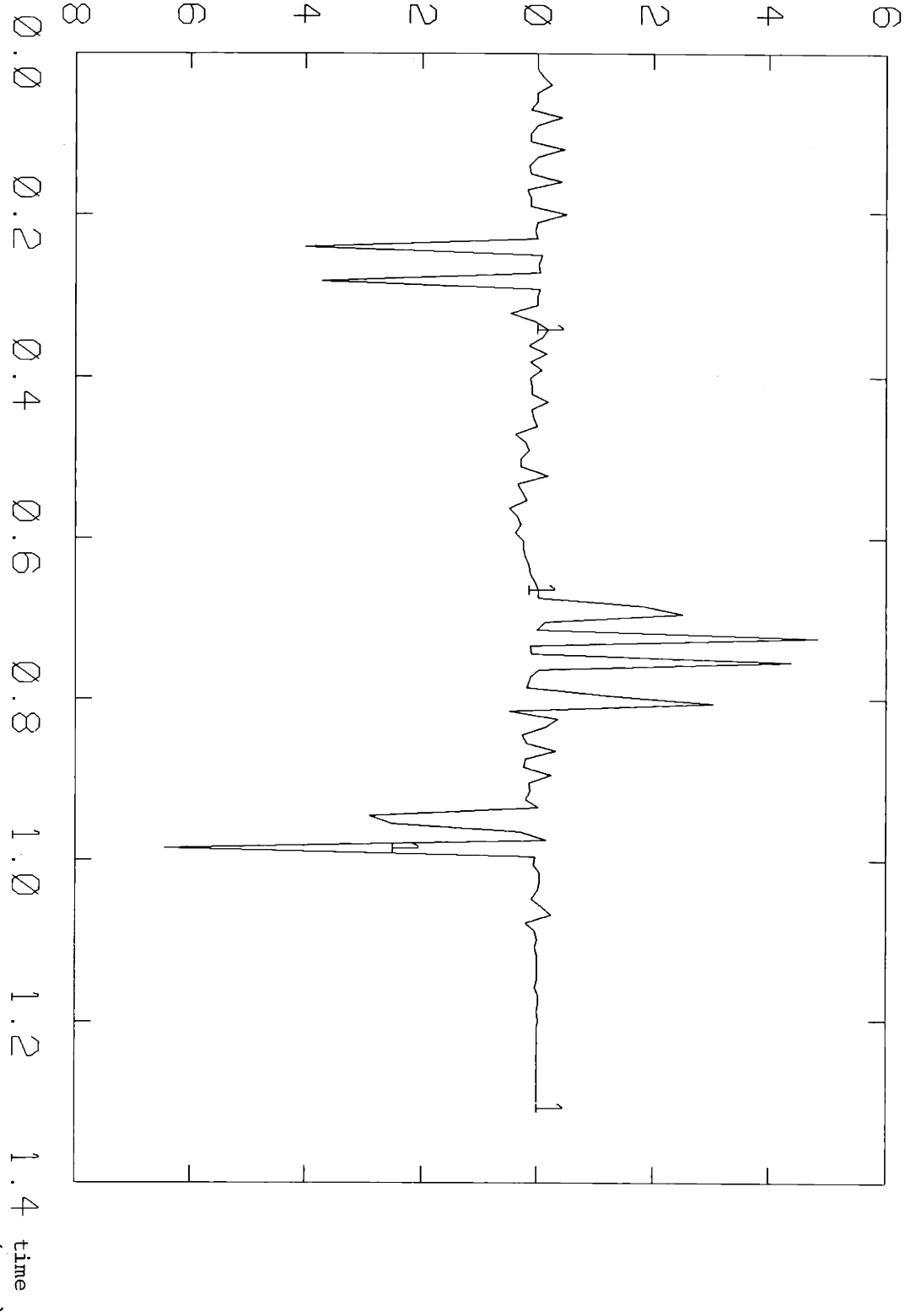

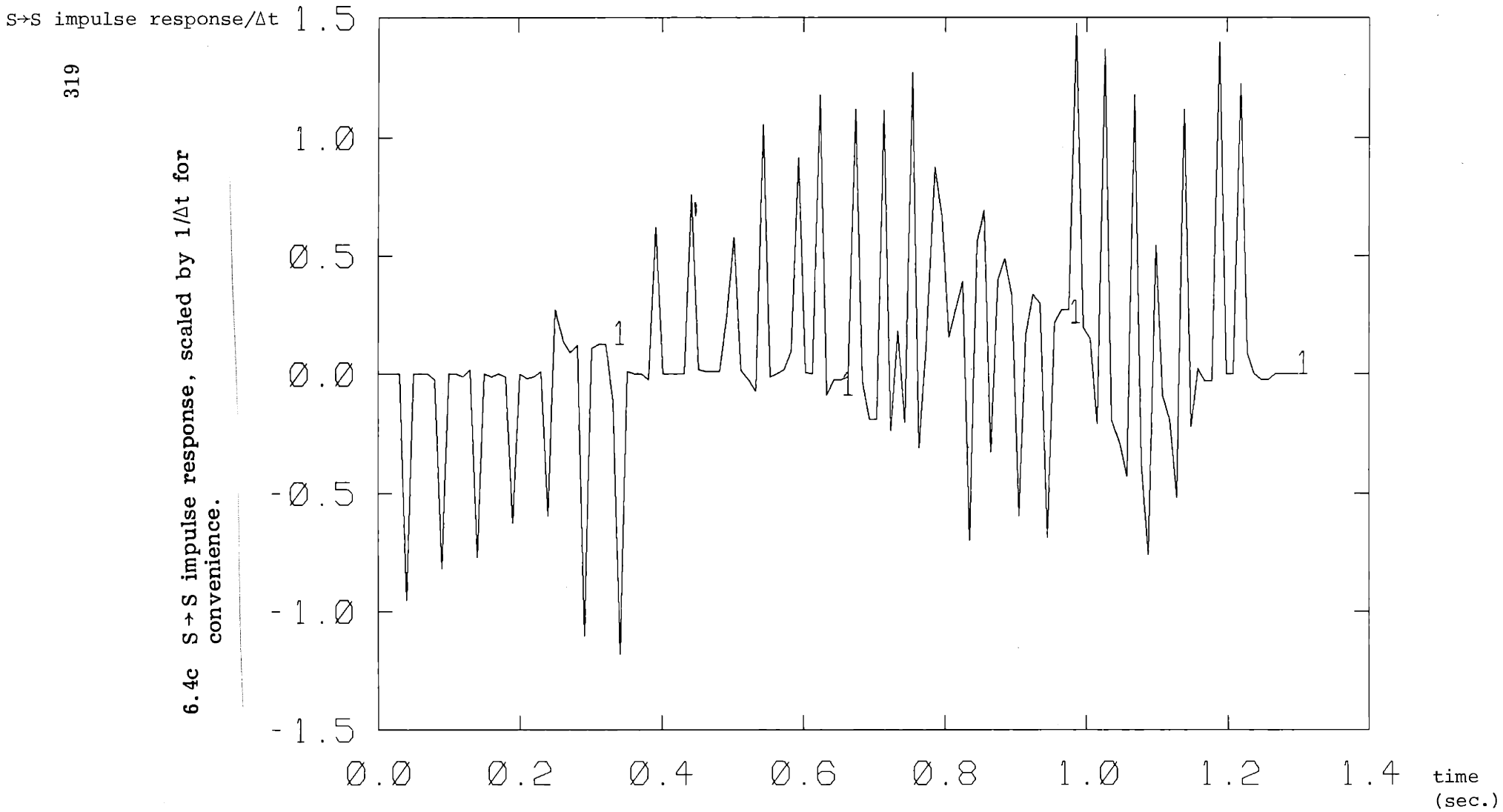

6.4c S → S impulse response, scaled by 1/Δt for convenience.

important to the algorithm, this smearing might be expected to hamper its performance. However, this evidently did not happen.

The impulsive plane wave responses were then used to initialize the upgoing P and SV waves, and the algorithm was run on a VAX-11/782 computer. Results are plotted in Figure 6.5, and the computer output is given in Figure 6.6. It can be seen that the agreement between the actual and algorithm-generated medium parameter profiles is quite good, with less than 5% error everywhere.

It should be noted that the algorithm was not tested under perfect conditions. Bandlimiting of the frequency response resulted in the time response being smeared over two or three samples, and the medium itself was discrete, so that some error may be expected in the update equations. Nevertheless, the algorithm performed quite well.

The algorithm was also tested on the six-layer medium on which Clarke (1984) demonstrated his algorithm. The computer output is given in Figure 6.7. It should be emphasized that this medium varies sharply at each interface, which would be expected to cause difficulties for the algorithm, since it was designed for a smoothy varying medium. However, the algorithm does not perform too badly, and certainly the computation required is much less than that required by Clarke's (1984) algorithm.

In this chapter the simple layer stripping concept presented in Chapters II and III has been generalized to a 4 x 4 system, with many more couplings between waves and three parameters to reconstruct instead of one. In the next chapter the concept of layer stripping is generalized still further, with a completely different physical interpretation.

6.5a Comparison between actual and computed P wave speed profiles (2 = actual, 3 = computed).

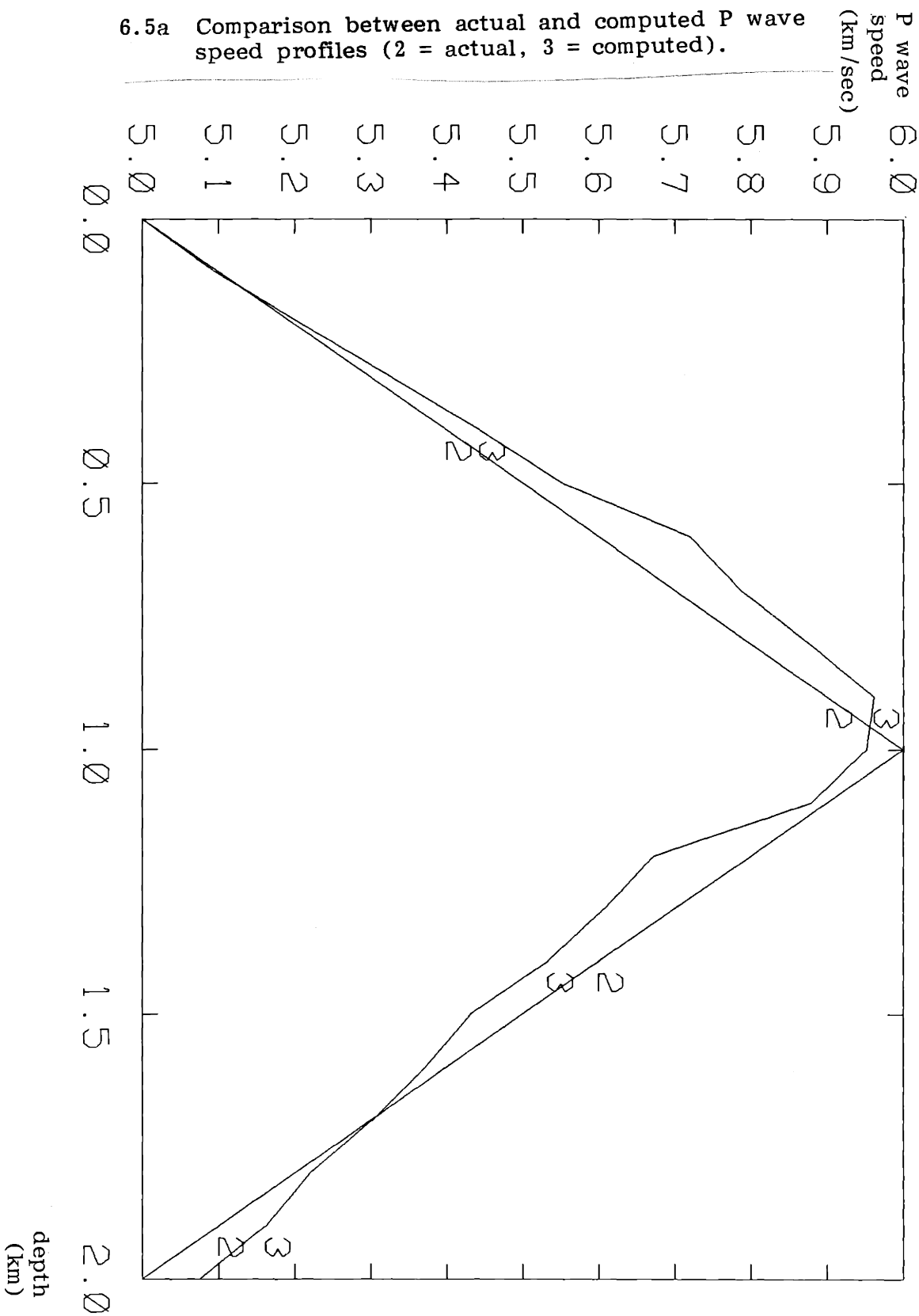

6.5b Comparison between actual and computed SV wave speed profiles (4 = actual, 5 = computed).

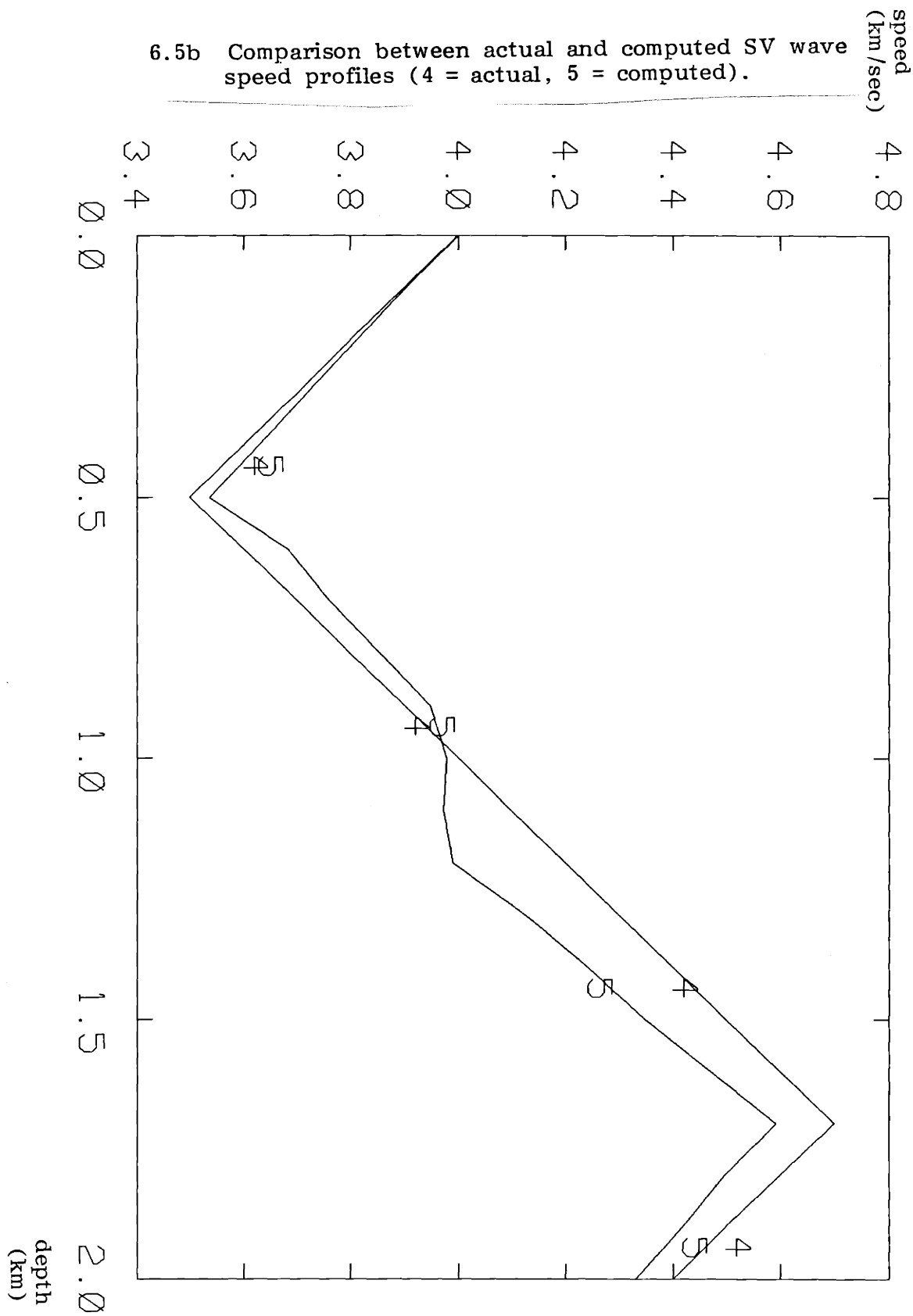

6.5c Comparison between actual and computed density profiles (6 = actual, 7 = computed).

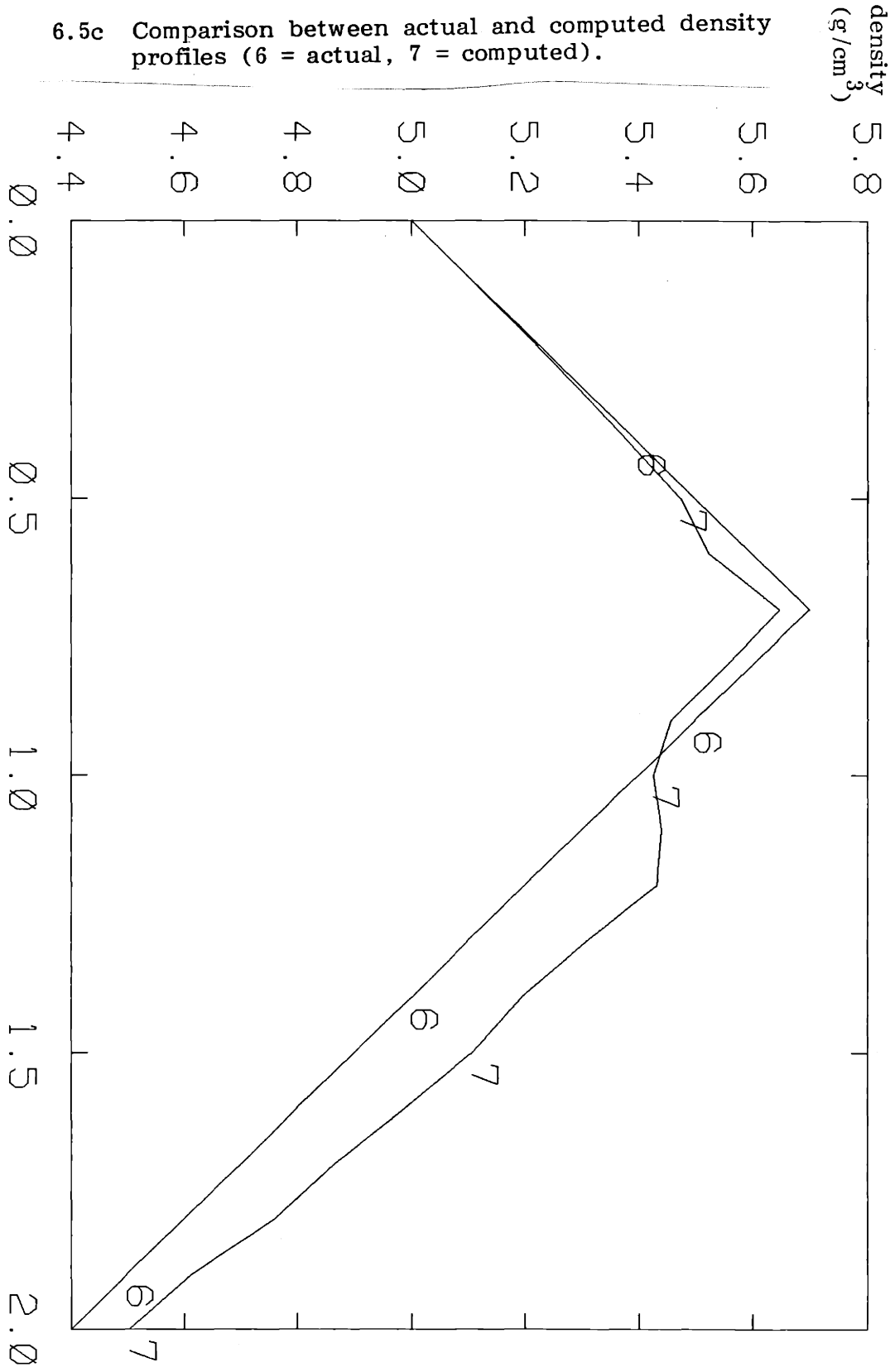

6.6 Computer output of a run of the layer stripping algorithm on a smoothly varying medium (p = 0.1).

depth	aact	acomp	bact	bcomp	rhoact	rhocomp	rp	rc	rs	tc
0.10	5.100	5.09969	3.900	3.90031	5.100	5.09993	0.0320	0.00180	0.0047	0.0164
0.20	5.200	5.21051	3.800	3.81041	5.200	5.19570	0.03332	0.00180	0.0042	0.0156
0.30	5.300	5.32851	3.700	3.71691	5.300	5.29210	0.03337	0.00200	0.0038	0.0157
0.40	5.400	5.44591	3.600	3.62931	5.400	5.38300	0.03231	0.00190	0.0032	0.0146
0.50	5.500	5.55351	3.500	3.53541	5.500	5.47490	0.03171	0.00250	0.0028	0.0156
0.60	5.600	5.72131	3.600	3.68041	5.600	5.52310	0.00361	0.01911	0.0051	0.0261
0.70	5.700	5.78911	3.700	3.77591	5.700	5.64840	0.00241	0.01821	0.0060	0.0157
0.80	5.800	5.87841	3.800	3.85621	5.600	5.55570	0.00651	0.00221	0.0031	0.0163
0.90	5.900	5.96241	3.900	3.94871	5.500	5.45610	0.00701	0.00071	0.0038	0.0155
1.00	6.000	5.96521	4.000	3.97761	5.400	5.42680	0.00691	0.00021	0.0012	0.0049
1.10	5.900	5.88101	4.100	3.97381	5.300	5.43930	0.00821	0.00071	0.0005	0.0005
1.20	5.800	5.67291	4.200	3.99641	5.200	5.43130	0.03091	0.00151	0.0005	0.0041
1.30	5.700	5.60951	4.300	4.12731	5.100	5.30811	0.03331	0.00251	0.0055	0.0225
1.40	5.600	5.53421	4.400	4.24091	5.000	5.19421	0.03191	0.00121	0.0056	0.0194
1.50	5.500	5.43371	4.500	4.34651	4.900	5.10671	0.03341	0.00261	0.0051	0.0186
1.60	5.400	5.37341	4.600	4.47121	4.800	4.98961	0.03231	0.00161	0.0068	0.0217
1.70	5.300	5.30301	4.700	4.59261	4.700	4.86671	0.03341	0.00021	0.0072	0.0208
1.80	5.200	5.22011	4.600	4.49691	4.600	4.75651	0.00501	0.02231	0.0027	0.0250
1.90	5.100	5.14251	4.500	4.41921	4.500	4.61521	0.00351	0.02481	0.0002	0.0225
2.00	5.000	5.07601	4.400	4.33971	4.400	4.50591	0.00181	0.02261	0.0006	0.0234
2.10	4.900	4.99471	4.300	4.24021	4.300	4.39141	0.00021	0.02361	0.0004	0.0234
2.20	4.800	4.77821	4.400	4.24191	4.200	4.38701	0.02791	0.00031	0.0002	0.0001

6.7 Computer output of a run of the layer stripping algorithm on the layered medium used in Clarke (1984) (p = 0.4).

depth	aact	acomp	bact	bcomp	rhoact	rhocomp	rp	rc	rs	tc
1.00	1.750	1.7500	1.000	1.0000	1.200	1.2000	0.0000	0.0000	0.0000	0.0000
2.00	1.850	1.8535	1.100	1.0982	1.400	1.3705	0.0207	-0.0938	-0.0212	-0.0718
3.00	1.900	1.9073	1.100	1.0977	1.700	1.6299	0.0542	-0.0923	-0.0217	-0.0046
4.00	1.850	1.8589	1.050	1.0470	1.600	1.5257	-0.0020	0.0411	0.0003	0.0383
5.00	1.950	1.9811	1.150	1.1659	1.900	1.7736	0.0181	-0.1047	-0.0134	-0.0862
6.00	2.000	2.0142	1.200	1.2098	2.100	1.9562	-0.0036	-0.0573	0.0020	-0.0363
7.00	2.100	2.0692	1.250	1.2598	2.200	2.0464	0.0016	-0.0286	0.0103	-0.0409
8.00	2.100	2.0728	1.250	1.2601	2.200	2.0488	0.0025	-0.0006	0.0001	-0.0003
9.00	2.100	2.0730	1.250	1.2606	2.200	2.0483	-0.0003	0.0001	0.0001	-0.0004
10.00	2.100	2.0729	1.250	1.2604	2.200	2.0484	0.0001	0.0000	-0.0001	0.0002

REFERENCES FOR CHAPTER VI

K. Aki and P.G. Richards, Quantitative Seismology, Theory and Methods, W.H. Freeman and Co., San Francisco, 1980.

G. A. Baker, "Solutions of an Inverse Elastic-Wave Scattering Problem," J. Acoust. Soc. Am. 71, 785-789 (1982).

A.S. Blagoveshchenskii, "The Inverse Problem in the Theory of Seismic Wave Propagation," in Topics in Mathematical Physics v. 1, pp. 55-67, ed. by M.S. Birman, Consultants Bureau, NY, 1967.

R. Carroll and F. Santosa, "On the Complete Recovery of Geophysical Data," Math. Meth. in the Appl. Sci. 4, 33-73 (1982).

C.H. Chapman, "Generalized Ray Theory for an Inhomogeneous Medium," Geophys. J.R. astr. Soc. 36, 673-704 (1974).

T.J. Clarke, "Full Reconstruction of a Layered Elastic Medium from P-SV Slant-Stack Data," Geophys. J.R. astr. Soc. 78(3), 775-793 (1984).

S. Coen, "On the Elastic Profiles of a Layered Medium, Part I. Plane-Wave Sources," J. Acoust. Soc. Am. 70, 172-175 (1981).

C.W. Frasier, "Discrete-Time Solution of Plane P-SV Waves in a Plane Layered Medium," Ph.D. Thesis, Dept. of Earth and Planetary Sciences, MIT, May 1969.

B.L.N. Kennett, Seismic Wave Propagation in Stratified Media, Cambridge University Press, Cambridge, 1983.

B.L.N. Kennett and M.R. Illingworth, "Seismic Waves in a Stratified Half Space, Part III. Piecewise Smooth Models," Geophys. J.R. astr. Soc. 66, 633-675 (1981).

B.L.N. Kennett, N.J. Kerry, and J.H. Woodhouse, "Symmetries in the Reflection and Transmission of Elastic Waves," Geophys. J.R. astr. Soc. 52, 215-229 (1978).

R. Kind, "Computation of Reflection Coefficients for Layered Media," J. Geophys. 42, 191-200 (1976).

M. Shiva and J.M. Mendel, "Non-Normal Incidence Inversion: Existence of Solution," Geophysical Prospecting 31, 888-914 (1983).

C.H. Wilcox, "Electric Wave Propagation on Non-Uniform Coupled Transmission Lines," SIAM Review 6(2), 148-165 (1964).

A. Yagle and B. Levy, "A Layer-Stripping Solution of the Inverse Problem for a One-Dimensional Elastic Medium" to appear in Geophysics 50(3), March 1985.

CHAPTER VII

The Inverse Problem for a Layered Acoustic Medium Probed by Spherical Harmonic Waves

7.1 Introduction

In this chapter we consider the same layered acoustic medium dealt with in Chapter IV, but we make a change in the excitation with which the medium is probed. Instead of using an obliquely-incident impulsive plane wave, or impulsive cylindrical waves from a point source to probe the medium, we use harmonic, single-frequency waves from a point source. By performing this experiment twice, at two different source frequencies, it is possible to recover the profiles of density $\rho(z)$ and wave speed $c(z)$ as functions of depth.

The basic results of this chapter are taken from Yagle and Levy (1984). However, dynamic deconvolution versions of the two layer stripping algorithms presented in that paper are also given here. In addition, the inverse resistivity problem, in which the resistivity profile of the earth as a function of depth is recovered from current and potential measurements made at the earth's surface, is solved using a layer stripping algorithm. This problem turns out to be mathematically analogous to the acoustic problem with a rigid surface and constant wave speed; hence its inclusion in this chapter. The layer stripping algorithm for the inverse resistivity problem is taken from Levy (1984).

In Chapter IV the profiles $\rho(z)$ and $c(z)$ were recovered by measuring the reflection response $\hat{R}(\omega,\theta)$ for all frequencies ω (this is

tantamount to obtaining the impulse response of the medium) and two different angles of incidence θ. In this chapter we consider the dual problem of recovering $\rho(z)$ and $c(z)$ from measurement of $\hat{R}(\omega,k_r)$ for two frequencies ω and all lateral wave numbers $k_r = \omega \sin \theta/c(o)$. Note that it is necessary to obtain $\hat{R}(\omega,\theta)$ for complex angles of incidence θ. These angles, corresponding to values of k_r greater than $\omega/c(o)$, are associated with probing the medium with evanescent, exponentially-decaying waves. In theory, knowledge of this post-critical response is necessary in order to solve the inverse problem exactly. In practice, there are some situations in which this response has little influence on the reconstructed profiles. This point will be discussed further as we proceed.

Basic Problem

The basic problem considered in this chapter is as follows. A continuous layered, laterally homogeneous medium is probed by a point harmonic source emitting sinusoidal spherical waves. The reflection response of the medium is measured as a function of radial distance from the source. By performing this experiment twice, at two different source frequencies, it is possible to recover the separate profiles of the density $\rho(z)$ and local speed of sound $c(z)$ as functions of depth z. The inverse problem is to recover these profiles from measurement of the reflection response of the medium.

Two different configurations of this problem are considered. For the first configuration, the inhomogeneous medium to be probed is bounded above and below by infinite, homogeneous half-spaces. The point pressure harmonic source is located in the upper half-space, whose medium parameters ρ_0 and c_0 are assumed known, and the pressure reflection

response of the inhomogeneous medium is measured in this half-space. In the second configuration, the inhomogeneous medium is bounded above by a free surface. The point pressure harmonic source is located just below the surface, and the medium acceleration at the free surface is measured. Fast algorithm solutions to each of these inverse problems are obtained. One algorithm is illustrated by means of a simple analytical example, and the other is illustrated by a computer run on synthetic data.

The technique of using a harmonic (CW) source to probe a layered medium has been used in ocean acoustics by Frisk et al. (1981). Here the medium being probed is the sediment at the ocean bottom. A typical experimental set-up is illustrated in Figure 7.1. A pulsed, CW source is towed behind a ship, and hydrophones are used to measure the reflection response of the sea floor. The hydrophones are connected to DIBOS (digital buoy system) receivers consisting of a quadrature demodulator, digitizer, and cassette recorder. In the experiment performed by Frisk et al. (1981) over the Hatteras abyssal plain, the battery-powered source emitted a four-second burst at 220 Hz. every fourteen seconds, while being towed at 0.5 knots. The four-second burst was long enough to achieve a sinusoidal steady state. In general, the experiment takes place over a range of up to 10 km, and interest in the inhomogeneous sea bottom (well-modelled by a layered medium since it is formed by sedimentary processes) centers on the first 400 m.

Previous work

Coen (1982) solved the free surface configuration of this inverse

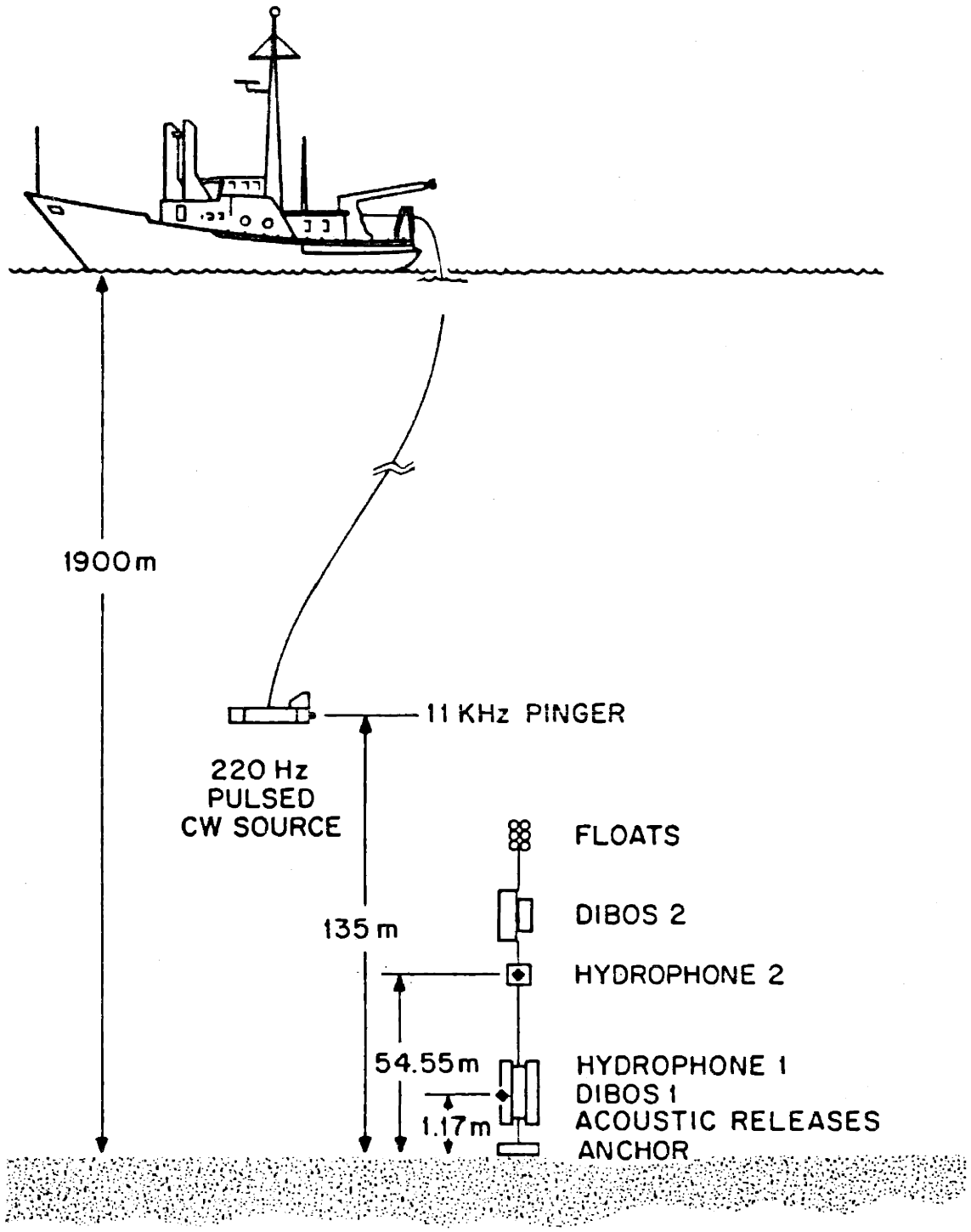

7.1 Experimental set-up for the inverse problem.

problem by employing the Gel'fand-Levitan method of Weidelt (1972) to solve the inverse scattering problem for the resulting Schrodinger-like equation (equation (7-5) in this chapter). His procedure requires two inverse Laplace transforms (part of the Weidelt (1972) procedure), and the solution of two Marchenko integral equations, with c(z) and a differential equation for $\rho(z)$ being obtained from the resulting potentials. The assumption of post-critical incidence ($c(z) \leq c(0)$ for all z) is also required. Stickler (1983) solved the half-space configuration by using trace methods (Deift and Trubowitz, 1979) to solve the inverse scattering problem for the resulting Schrodinger equation (equation (7-8) in this chapter). This requires the solution of a nonlinear differential equation and also requires that there be no trapped modes. Trapped modes are square-integrable solutions corresponding to a wave-guide-like effect, which can arise in low-velocity zones.

In both of these approaches methods of mathematical physics are used to solve the inverse scattering problem. This leads to additional assumptions (post-critical incidence, no trapped modes) being required, and prevents insight into the workings of the inversion procedure.

Summary

In Section 7.2 the half-space configuration of the two-frequencies inverse seismic problem is formulated as a Schrodinger equation inverse scattering problem, as in Stickler (1983), and solved using the fast algorithm developed for Schrodinger equation inverse scattering problems presented in Section 2.3.5. This algorithm is simpler than the trace formula method used by Stickler (1983), since there is no need to generate Jost solutions of the Schrodinger equation numerically. A dynamic deconvolution version of this algorithm is also presented.

In Section 7.3 the free surface configuration of this problem is formulated as a Schrodinger-like equation, as in Coen (1982), and solved using a variation of the fast algorithm for direct recovery of Schrodinger equation potentials presented in Section 2.3.5. This algorithm replaces the Marchenko integral equation whose solution is required in Coen (1982). However, an inverse Laplace transform is still necessary. The necessity of an inverse Laplace transform of the reflection data for the free surface problem is tied to the use of post-critical data; since exponentially-decaying evanescent waves are being used to probe the medium, there seems to be no way to avoid the inherent instability of the inverse Laplace transformation. The dynamic deconvolution version of this algorithm does not require an inverse Laplace transform, but does require another unstable operation.

In Section 7.4 the two fast algorithms are illustrated in action. The half-space algorithm is run on a computer to solve the inverse problem from synthetically generated data. The free surface algorithm is illustrated by a simple analytical example in which numbers that would be generated by a computer are replaced by actual analytical expressions for the waves, reflection response, potential, etc. The example is in fact the same example Coen (1982) used to illustrate his solution procedure for this problem.

Finally, in Section 7.5 the inverse resistivity problem is briefly described and then solved using a layer stripping algorithm due to Levy (1984). The relevance of this problem to this chapter stems from the fact that the inverse resistivity problem is mathematically analogous to the two-frequencies acoustic medium inverse problem with a rigid surface and constant wave speed $c(z)$. This rather surprising analogy allowed

the method of images interpretation of the inverse resistivity problem inversion procedure to be applied to the two-frequencies acoustic medium inverse problem as well.

This last point is particularly important, since the physical interpretation of the algorithms of this chapter is considerably different from that of previous chapters. In this chapter, the layer stripping concept is used in a novel way. Instead of generating upgoing and downgoing waves as functions of time at each depth, the layer stripping algorithm generates a continuous distribution of image sources as functions of a fictitious depth coordinate, at each depth. These image sources synthesize the medium's sinusoidal steady-state response at each depth. The strength of the first non-zero image source (analogous to the first reflection discussed in earlier chapters) yields information about the medium at the current depth and allows the algorithm to be propagated to the next depth. Note that in addition to its computational simplicity, all quantities in the algorithm have physical interpretations, which allows considerable insight into the workings of the inversion process. This could be useful for interpreting the causes of numerical difficulties caused by the physics of the experiment. Note also that it is not necessary to assume the absence of trapped modes, or that the experiment be restricted to pre- or post-critical incidence.

7.2 The Half-Space Problem

7.2.1 Formulation of the Problem

The problem considered in this section is as follows. A continuous layered medium, laterally homogeneous, is bounded above and below by two infinite homogeneous half-spaces. A point pressure harmonic source

is located in the upper half-space, and is used to probe the layered medium with sinusoidal spherical pressure waves. The pressure reflection response of the layered medium in the sinusoidal steady state is measured in the upper half-space as a function of radial distance r from the source. The situation is illustrated in Figure 7.2. The goal is to recover the profiles $\rho(z)$ and $c(z)$ of the layered medium by performing this experiment twice, at two different source frequencies.

The medium behavior is assumed to be described by the basic linear equations for fluids (3-1), which are

$$\rho \frac{\partial^2 \underset{\sim}{u}}{\partial t^2} = - \nabla p \qquad (7\text{-}1a)$$

$$p = - \rho c^2 \nabla \cdot \underset{\sim}{u} \ . \qquad (7\text{-}1b)$$

Here $\underset{\sim}{u}$ is medium displacement and p is pressure (negative isotropic stress). Noting the cylindrical symmetry of the problem and the assumption that the medium is in the sinusoidal steady state, a Fourier transform with respect to time t is followed by Hankel transforms of order zero of (7-1b) and the z-component of (7-1a), and by a Hankel transform of order one of the r-component of (7-1a). This combination Fourier-Hankel transform is sometimes called the Fourier-Bessel transform. The result is

$$\hat{p} = - \rho c^2 \left(\frac{d}{dz} \hat{u}_z + \xi \hat{u}_r \right) \qquad (7\text{-}2a)$$

$$\rho \omega^2 \hat{u}_r = - \xi \hat{p} \qquad (7\text{-}2b)$$

$$\rho \omega^2 \hat{u}_z = \frac{d\hat{p}}{dz} \qquad (7\text{-}2c)$$

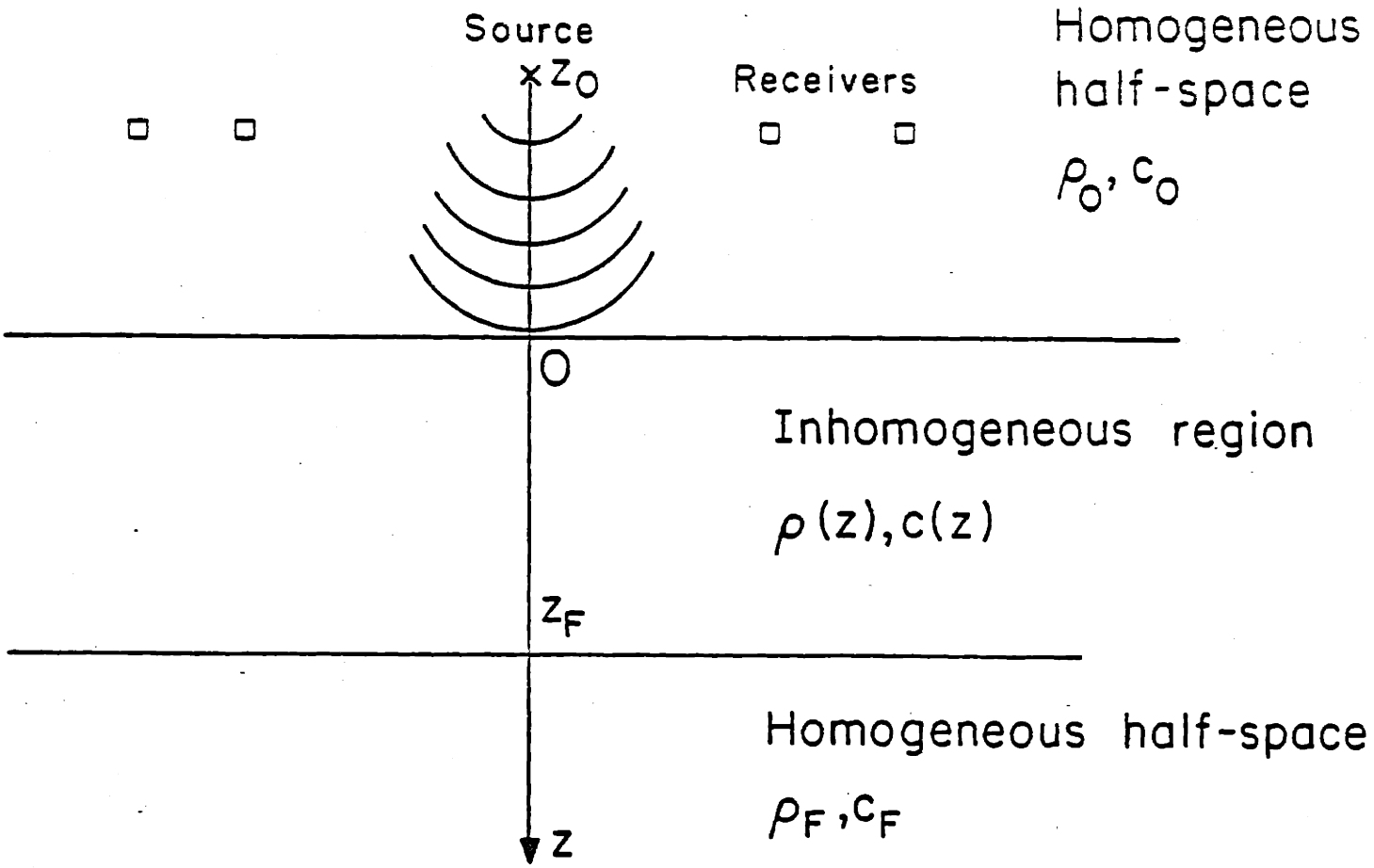

7.2 The half-space inverse problem.

where

$$\hat{p}(\xi,z,\omega) = H_0 F[p(r,z,t)] \tag{7-3a}$$

$$\hat{u}_z(\xi,z,\omega) = H_0 F[u_z(r,z,t)] \tag{7-3b}$$

$$\hat{u}_r(\xi,z,\omega) = H_1 F[u_r(r,z,t)]. \tag{7-3c}$$

Since the sinusoidal steady state is assumed, the time dependence for the quantities (7-3) is $e^{-j\omega t}$. Since cylindrical symmetry is assumed, ξ is the lateral wavenumber k_r.

Eliminating $\hat{u}_r$ and $\hat{u}_z$ from (7-3) and defining the normalized pressure

$$\hat{\pi}(\xi,z,\omega) = \hat{p}/\sqrt{\rho} \tag{7-4}$$

yields the Schrodinger-like equation

$$\left(\frac{d^2}{dz^2} - \xi^2 - V_\xi\right)\hat{\pi} = 0 \tag{7-5}$$

where the potential V_ξ is given by

$$V_\xi(z,\omega) = Z''/Z - \omega^2/c(z)^2 \quad . \tag{7-6}$$

Here $Z = 1/\sqrt{\rho}$ and the double prime denotes the second derivative with respect to z. Note that (7-5) is <u>not</u> a true Schrodinger equation, since the energy term $-\xi^2$ is always negative. The equation (7-5) was derived by Coen (1982) for the free surface inverse problem.

A true Schrodinger equation can be written using the vertical

wavenumber k_z, defined by

$$k_z = (\omega^2/c_0^2 - \xi^2)^{\frac{1}{2}} \tag{7-7}$$

where c_0 is the (known) speed of sound in the upper half space. From (7-5) we have

$$(\frac{d^2}{dz^2} + k_z^2 - V_k)\hat{\pi} = 0 \tag{7-8}$$

where

$$V_k(z,\omega) = \omega^2/c_0^2 - \omega^2/c(z)^2 + Z''/Z \quad . \tag{7-9}$$

The equation (7-8) was derived by Stickler (1983) for the half-space problem.

For the half-space problem the Schrodinger equation (7-8) is used with the boundary conditions.

$$\hat{\pi}(\xi,z,\omega) = \hat{\pi}((\omega^2/c_0^2 - k_z^2)^{\frac{1}{2}},z,\omega) = \begin{cases} (e^{-jk_z(z-z_o)} + R(k_z,\omega)e^{jk_z(z+z_o)})/jk_z, \\ \qquad\qquad z_o < z < 0 \\ (T(k_z,\omega)e^{-jk_F(z-z_o)})/jk_z, \quad z > z_F \end{cases} \tag{7-10}$$

Here the sources and receivers are located at $z = z_o < 0$, $R(k_z,\omega)$ is the (measured) plane wave reflection coefficient, $T(k_z,\omega)$ is the (unknown) plane wave transmission coefficient, and $k_F = (\omega^2/c(z_F)^2 - \xi^2)^{\frac{1}{2}}$ is the vertical wavenumber in the lower half space. These boundary

conditions amount to a radiation condition--it is assumed that there are no upward travelling pressure waves in the lower half space. Note that the reflected wave seems to arise from an image source located at $z = -z_o$. This accounts for the change in sign of z_o.

The form of (7-10), in particular the factor $1/jk_z$, can be obtained by considering the Sommerfeld integral

$$(e^{j\omega R/c})/R = \int_o^\infty (1/jk_z)e^{-jk_z|z|}J_o(k_r r)k_r dk_r \tag{7-11a}$$

$$R \triangleq (r^2 + z^2)^{\frac{1}{2}} \quad . \tag{7-11b}$$

This integral decomposes a monochromatic spherical wave into a superposition of cylindrical waves of varying wavenumbers. The advantage of this is that the response of the layered medium to a spherical wave can now be written as the superposition of the responses to cylindrical waves (Aki and Richards (1980), p. 200). Thus we may write

$$\begin{aligned} p(r,z,\omega)/\sqrt{\rho_o} &= \int_o^\infty (1/jk_z)e^{-jk_z(z-z_o)}\, J_o(k_r r)k_r dk_r \\ &+ \int_o^\infty (1/jk_z)R(k_z,\omega)e^{jk_z(z+z_o)}\, J_o(k_r r)k_r dk_r, \quad z_o < z < 0 \end{aligned} \tag{7-12}$$

where the pressure field has been written as the sum of an incident field due to the source and a scattered field due to the layered medium. Since cylindrical waves are being used, the plane wave reflection coefficient $R(k_z,\omega)$ expresses the response of the layered medium. Recognizing the two integrals in (7-12) as inverse Hankel transforms, it is seen that taking the Hankel transform of (7-12) immediately yields (7-10).

It should be noted that Stickler (1983) uses Jost solutions to the Schrodinger equation (7-8) and obtains the factor $1/jk_z$ from a Wronskian. Here the origin of this factor is explained in a different, more familiar

setting. It should also be noted that the inverse problem represented by equations (7-8) and (7-10) can be solved given knowledge of $R(k_z,\omega)$ for either all ω and two k_z/ω or all k_z and two ω. Mathematical physics solutions to these dual problems may be found in Coen (1982) and Stickler (1983), respectively, while layer stripping fast algorithm solutions may be found in Chapter IV and the following section of this chapter.

A comment on the measurement of $R(k_z,\omega)$ is also in order. Note that $R(k_z,\omega)$ is obtained from the Hankel transform of the pressure reflection response, which is a function of the lateral wavenumber ξ. This means that $R(k_z,\omega)$ is known only on the positive imaginary k_z axis (corresponding to post-critical incidence), and on the positive real k_z axis as far as ω/c_0 (see Figure 7.3). Stickler (1983) has pointed out that $R(k_z,\omega)$ may be obtained for $k_z > \omega/c_0$ from its values on the imaginary axis by using a complex procedure due to Van Winter (1971). He also remarks that his numerical results indicate that the contribution of $R(k_z,\omega)$ for $k_z > \omega/c_0$ seems to be negligible for real-world problems. Our own results (Section 7.4) seem to confirm this. It should also be noted that the physical measurement of the pressure reflection response is a far from trivial problem. Mook (1983) is a good source on the subject; see also Frisk et al. (1980).

7.2.2 Layer Stripping Solution of the Half-Space Problem

In this section a procedure taken from Section 2.3.5 is used to obtain a layer stripping, fast algorithm solution to the inverse problem represented by equations (7-8) and (7-10). An interesting physical interpretation of the operation of the algorithm is also provided.

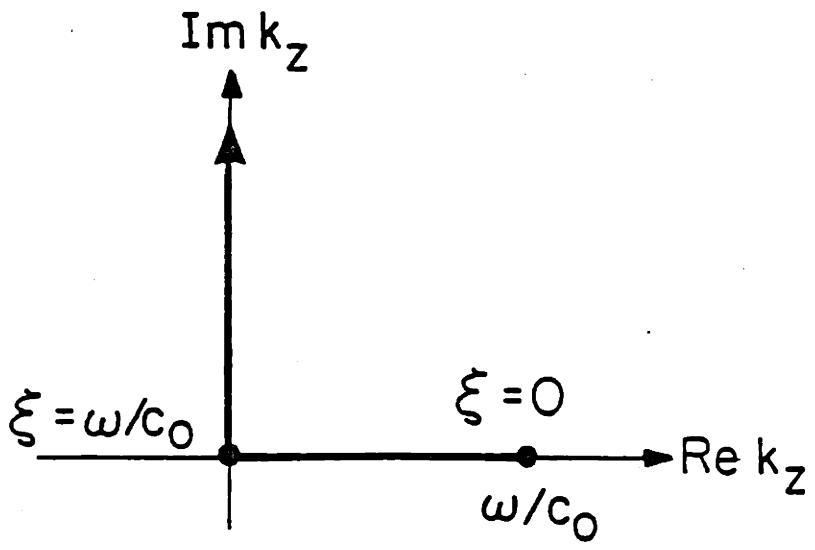

7.3 Regions where $R(k_z)$ may be computed from data.

Define the reflectivity function $r(z,\omega)$ as the solution of the following differential equation (the Miura transform)

$$r^2 - \frac{dr}{dz} \triangleq V_k(z,\omega) \tag{7-13}$$

where $r(0,\omega)$ will be specified later and ω is a parameter. Define the potential V_ψ by

$$r^2 + \frac{dr}{dz} \triangleq V_\psi(z,\omega) \tag{7-14}$$

and let $\hat{\psi}(\xi,z,\omega)$ solve the auxiliary Schrodinger equation

$$\left(\frac{d^2}{dz^2} + k_z^2 - V_\psi\right)\hat{\psi} = 0 \tag{7-15}$$

with boundary conditions

$$\hat{\psi}(\xi,z,\omega) = \hat{\psi}((\omega^2/c_o^2 - k_z^2)^{\frac{1}{2}},z,\omega) = \begin{cases} (e^{-jk_z(z-z_o)} - R(k_z,\omega)e^{jk_z(z+z_o)})/jk_z, & z<0 \\ (T(k_z,\omega)e^{-jk_F(z-z_o)})/jk_z & z>z_F . \end{cases} \tag{7-16}$$

Now define

$$\hat{D}(k_z,z,\omega) \triangleq (\hat{\pi} + \hat{\psi})/2 \tag{7-17a}$$

$$\hat{U}(k_z,z,\omega) \triangleq (\hat{\pi} - \hat{\psi})/2 \quad . \tag{7-17b}$$

Then, $\hat{D}$ and $\hat{U}$ satisfy the coupled system of differential equations

$$\frac{d}{dz}\begin{bmatrix}\hat{D}\\ \hat{U}\end{bmatrix} = \begin{bmatrix}-jk_z & -r\\ -r & jk_z\end{bmatrix}\begin{bmatrix}\hat{D}\\ \hat{U}\end{bmatrix} \quad . \tag{7-18}$$

To see this, note that taking the derivative of (7-18) with respect to z decouples (7-18) into the two Schrodinger equations (7-8) and (7-15).

Multiplying (7-18) by jk_z and taking the inverse Fourier transform with respect to k_z yields the coupled wave system

$$(\frac{\partial}{\partial z} + \frac{\partial}{\partial \zeta})\overset{\vee}{D}(z,\zeta) = -r(z)\overset{\vee}{U}(z,\zeta) \tag{7-19a}$$

$$(\frac{\partial}{\partial z} - \frac{\partial}{\partial \zeta})\overset{\vee}{U}(z,\zeta) = -r(z)\overset{\vee}{D}(z,\zeta) \tag{7-19b}$$

where

$$\overset{\vee}{D}(z,\zeta) \overset{\Delta}{=} F_{k_z}^{-1}[jk_z\hat{D}(k_z,z)] \tag{7-20a}$$

$$\overset{\vee}{U}(z,\zeta) \overset{\Delta}{=} F_{k_z}^{-1}[jk_z\hat{U}(k_z,z)] \tag{7-20b}$$

i.e., the inverse Fourier transform has taken k_z into the fictitious depth coordinate ζ, and the parametric dependence on ω has been dropped. The system (7-19) is referred to as a coupled wave system since $\overset{\vee}{D}$ and $\overset{\vee}{U}$ can be interpreted as waves in z and ζ propagating through the inhomogeneous layered medium. The inhomogeneity of the layered medium is expressed by the reflectivity function r(z), which causes portions of each wave to be reflected into the other wave. In the upper half-space equation (7-13) shows that r(z) = 0, which makes the wave nature of $\overset{\vee}{D}$ and $\overset{\vee}{U}$ apparent. Although it is not yet clear what these waves are, i.e., how they could be interpreted physically, this will soon be made clear.

The initial conditions for the system (7-19) are obtained from the boundary conditions (7-10) and (7-16) for $\hat{\pi}$ and $\hat{\psi}$, and also equations (7-17) and (7-20). They are:

$$\overset{\vee}{D}(0,\zeta) = \delta(\zeta) \tag{7-21a}$$

$$\overset{\vee}{U}(0,\zeta) = \overset{\vee}{R}(\zeta) \tag{7-21b}$$

where $\delta(\cdot)$ is the unit impulse function and $\overset{\vee}{R}(\zeta)$ is the inverse Fourier transform of $\hat{R}(k_z)$. The forms of the system (7-19) and initial conditions (7-21) make it clear that $\overset{\vee}{D}(z,\zeta)$ and $\overset{\vee}{U}(z,\zeta)$ have the general forms

$$\overset{\vee}{D}(z,\zeta) = \delta(\zeta-z) + \overset{\vee}{D}_o(z,\zeta)1(\zeta-z) \tag{7-22a}$$

$$\overset{\vee}{U}(z,\zeta) = \overset{\vee}{U}_o(z,\zeta)1(\zeta-z) \tag{7-22b}$$

where $1(\cdot)$ is the unit step function. This expresses a causality principle--at a given depth z both waves are zero until $\zeta \geq z$, i.e., until the "wavefront" passes.

The Layer Stripping Algorithm

Substituting the forms (7-22) into the system (7-19) yields

$$r(z) = 2\overset{\vee}{U}(z,z+). \tag{7-23}$$

The smooth parts $\overset{\vee}{D}_o(z,\zeta)$ and $\overset{\vee}{U}_o(z,\zeta)$ of the waves (7-22) can now be propagated using (7-19), yielding r(z) by (7-23). This is of course the fast Cholesky algorithm, and while the derivation of it has been familiar, the setting is not. The algorithm is initialized using the initial conditions (7-21), which requires only the inverse Fourier transform of $R(k_z)$.

Note that $r(0)$ is now specified by equations (7-21b) and (7-23) as $2\overset{\vee}{R}(0)$.

The layer stripping algorithm yields $r(z)$, from which $V_k(z)$ can immediately be obtained by using (7-13). By running the experiment twice, at two different source frequencies ω_1 and ω_2, the two potentials $V_k(z,\omega_1)$ and $V_k(z,\omega_2)$ are obtained. We then have, using (7-9),

$$1/c(z)^2 = 1/c_o^2 - (V_k(z,\omega_1) - V_k(z,\omega_2))/(\omega_1^2-\omega_2^2) \tag{7-24a}$$

$$Z''/Z = (\omega_2^2 V_k(z,\omega_1) - \omega_1^2 V_k(z,\omega_2))/(\omega_2^2-\omega_1^2) \tag{7-24b}$$

and the differential equation (7-24b) can then be solved for $Z = 1/\sqrt{\rho}$. Note in particular that if the profile $\rho(z)$ is smooth, the initial conditions for (7-24b) are $Z(0) = 1/\sqrt{\rho_o}$ and $Z'(0) = 0$. Otherwise, knowledge of $\rho'(0)$ is required.

If z and ζ are discretized by $z = n\Delta$ and $\zeta = m\Delta$, where m and n and positive integers and Δ is the discretization length, then a forward difference approximation to the partial derivatives in the coupled system yields the following explicit form of the layer stripping algorithm:

$$\overset{\vee}{D}(z+\Delta,\ \zeta+\Delta) = \overset{\vee}{D}(z,\zeta) - r(z)\,\Delta\,\overset{\vee}{U}(z,\zeta) \tag{7-25a}$$

$$\overset{\vee}{U}(z+\Delta,\ \zeta-\Delta) = \overset{\vee}{U}(z,\zeta) - r(z)\,\Delta\,\overset{\vee}{D}(z,\zeta) \tag{7-25b}$$

$$r(z+\Delta) = 2\overset{\vee}{U}(z+\Delta,\ z+\Delta). \tag{7-25c}$$

The recursion patterns for $\overset{\vee}{D}$ and $\overset{\vee}{U}$ are illustrated in Figures 7.4a and 7.4b. We start off knowing the waves at z for all ζ, and wish to update them to $z+\Delta$ for all ζ. Although the forms of the recursions may make it seem as though some information is being lost, recall that by causality

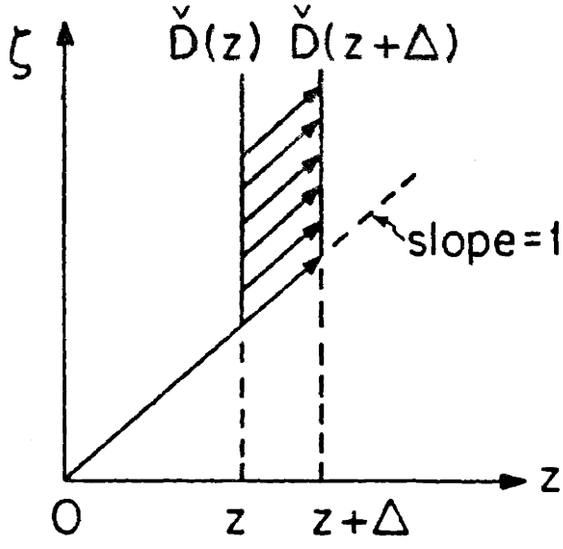

7.4a Recursion pattern for updating the downgoing waves.

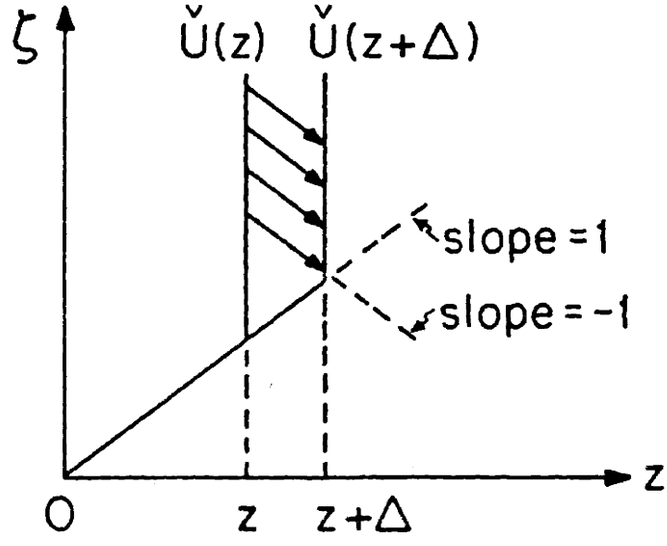

7.4b Recursion pattern for updating the upgoing waves.

and $\overset{\vee}{D}(z,\zeta)$ and $\overset{\vee}{U}(z,\zeta)$ are causal, in that both are zero if $\zeta < z$.

In equation (7-26) the normalized pressure $\pi(r,z)$ has been written as a superposition of contributions due to a continuous distribution of point sources along the (fictitious) ζ axis. The strength of the point source at ζ is $\overset{\vee}{\pi}(z,\zeta)d\zeta$. Each source emits a spherical wave which travels in a (fictitious) medium with constant sound speed c_0. This is illustrated for a single element of the continuous distribution $\overset{\vee}{\pi}(z,\zeta)$ of sources in Figure 7.5. Similar interpretations hold for $\overset{\vee}{\psi}$, $\overset{\vee}{D}$, and $\overset{\vee}{U}$. Note that the origin of the ζ axis corresponds to the depth z on the z axis.

Thus the layer stripping algorithm is decomposing the medium response at each depth into a superposition of responses due to image sources, located in a (fictitious) medium of constant speed of sound c_0 and distributed along a (fictitious) depth coordinate ζ. The causality of $\overset{\vee}{D}$, $\overset{\vee}{U}$, $\overset{\vee}{\pi}$, and $\overset{\vee}{\psi}$ is due to the fact that an image source is never located within the medium wherein it is to simulate a response; it is always "in the looking glass," so to speak. Thus any image source that is supposed to simulate a medium response at depth z must be located deeper than z in the fictitious ζ-axis medium, i.e., $\overset{\vee}{\pi}(z,\zeta) = 0$ unless $\zeta > z$. This corresponds to a depth deeper than 2z on the z-axis, which is as expected since the image source is an image of the actual source, which is located at the surface. This image source causality replaces the time causality (i.e., the medium response at a given depth is zero until the probing impulsive plane wave has had time to reach that depth) generally used in layer stripping algorithms, but unavailable in the present problem since the sinusoidal steady state is assumed.

it is known that both waves are zero for $\zeta < z$. It should also be noted that equations (7-13) and (7-24b) can be approximated by differences, so that if the two layer stripping algorithms initiated by $\overset{\vee}{R}(\zeta,\omega_1)$ and $\overset{\vee}{R}(\zeta,\omega_2)$ are run concurrently, $\rho(z)$ and $c(z)$ may be outputted immediately, reducing considerably the amount of storage required.

Physical Interpretation of the Layer Stripping Algorithm

Although the layer stripping algorithm consisting of equations (7-19) and (7-23) could certainly be run without any physical understanding of the quantities involved, a major advantage of layer stripping algorithms is that the inversion procedure can generally be interpreted in physical terms. This is helpful in interpreting any unusual behavior or results of the algorithm. Thus we now give a physical interpretation of the algorithm and its operation. To make things clearer, let the source and measuring devices both be located at $z = 0$.

Defining $\overset{\vee}{\pi}(z,\zeta)$ in the same manner as $\overset{\vee}{D}$ and $\overset{\vee}{U}$ (equation (7-20)) and using the Sommerfeld integral (7-11), we have for the normalized pressure frequency response $\pi(z,r,\omega)$ at the source frequency ω:

$$\pi(z,r) = H^{-1}[\overset{\vee}{\pi}(z,\xi)] = H^{-1}[(1/jk_z) \int_{-\infty}^{\infty} \overset{\vee}{\pi}(z,\zeta)e^{-jk_z\zeta}\, d\zeta]$$

$$= \int_z^{\infty} \overset{\vee}{\pi}(z,\zeta)H^{-1}[(1/jk_z)e^{-jk_z\zeta}]d\zeta = \int_z^{\infty} \overset{\vee}{\pi}(z,\zeta)(1/R)e^{j\omega R/c_o}\, d\zeta \qquad (7\text{-}26)$$

where

$$R = \sqrt{r^2 + \zeta^2} \qquad (7\text{-}27)$$

and the lower limit of the integral has been replaced by z because

$$\overset{\vee}{\pi}(z,\zeta) = \overset{\vee}{D}(z,\zeta) + \overset{\vee}{U}(z,\zeta) \qquad (7\text{-}28)$$

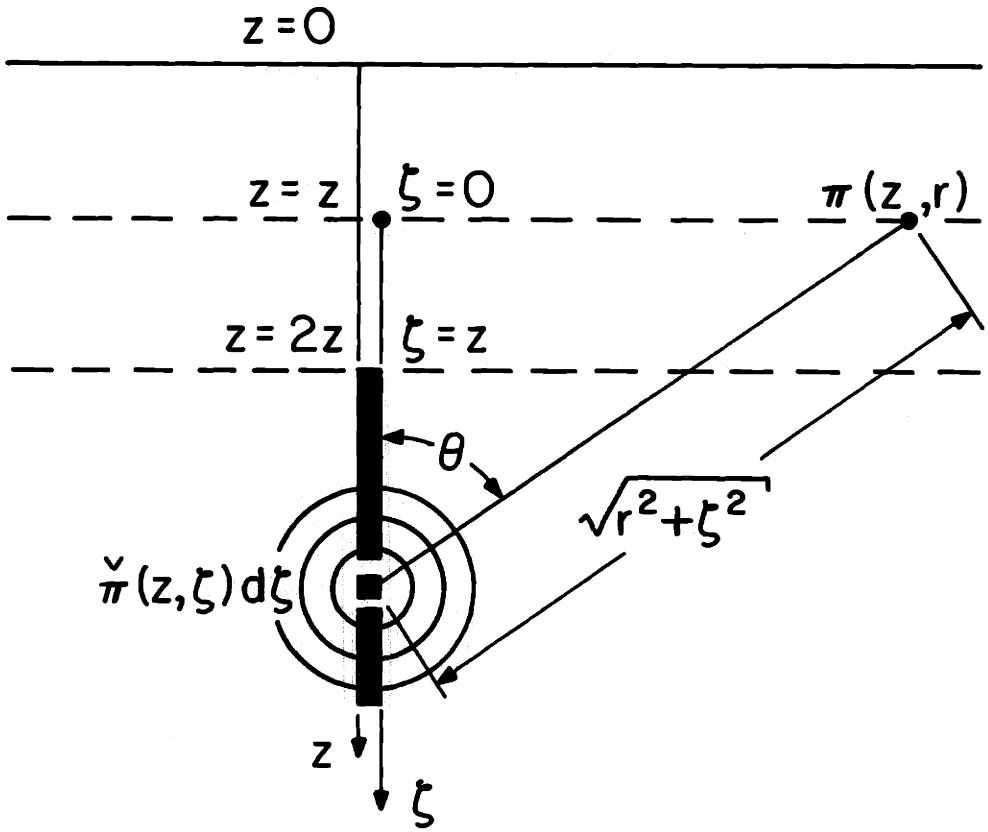

7.5 $\overset{\vee}{\pi}(z,\zeta)$ interpreted as a sequence of image sources emitting spherical waves.

The advantage of this decomposition into image sources is that the first image source (i.e., the first non-zero value of $\check{U}(z,\zeta)$, which is $\check{U}(z,z+)$) clearly has the responsibility of simulating the primary reflection from depth z. This image source should thus have strength r(z)/2, since the actual measured response must travel down from the source to depth z and then back up, while the image source response need only travel up from depth 2z to depth z, where the response is to be simulated. This immediately gives equation (7-23), which is comparable to the usual layer stripping property that the first arrival from depth z is the primary reflection from that depth, and its strength thus gives the value of the reflectivity function r(z) at that depth. Since multiple reflections must be accounted for, the image source distributions are non-zero in general for all $\zeta > z$; however, they quickly decay toward zero since the higher the order of a multiple reflection, the weaker the reflection.

In the particular case of a constant sound speed medium, i.e., $c(z) = c_0$, equation (7-13) can be solved to give an explicit formula for r(z)

$$r(z) = -\ (1/Z)(dZ/dz) \tag{7-29}$$

which can be immediately integrated to give

$$\rho(z) = \rho_0 \exp\ (2 \int_0^z r(u)du) \quad . \tag{7-30}$$

This avoids the necessity of computing r'(z) to obtain the potential $V_k(z)$ in (7-13), and also avoids the differential equation (7-24b) for Z. It would be a great convenience if a closed-form expression for r(z)

could be obtained for the general case of varying c(z), but there seems to be no closed-form solution to the Riccati equation (7-13).

Dynamic deconvolution algorithm

The dynamic deconvolution algorithm associated with this fast Cholesky algorithm may be derived quickly. Defining the reflection coefficient $\hat{R}_k(k_z,z,\omega)$ for the portion of the medium beneath depth z as

$$\hat{R}_k(k_z,z,\omega) \stackrel{\Delta}{=} \hat{U}(k_z,z,\omega)/\hat{D}(k_z,z,\omega) \tag{7-31}$$

we have from (7-18) the Riccati equation

$$\frac{d}{dz}\hat{R}_k(k_z,z,\omega) = 2jk_z\hat{R}_k - r(1 - \hat{R}_k^2) \tag{7-32}$$

and from (7-23) and the final value theorem

$$r(z) = \lim_{k_z\to\infty} 2jk_z\hat{R}_k \quad . \tag{7-33}$$

The algorithm is initialized using

$$\hat{R}_k(k_z,0,\omega) = \hat{R}(k_z,\omega) \quad . \tag{7-34}$$

This algorithm has the usual interpretation of defining a new, smaller, inverse scattering problem at each depth z. The reflection data at each depth are contained in $\hat{R}_k(k_z,z,\omega)$, and the problem support is reduced at each step from $[z,\infty)$ to $[z+\Delta,\infty)$.

The equation (7-33) for obtaining r(z) from $\hat{R}_k(k_z,z,\omega)$ for large k_z can be interpreted physically as follows. A large value of k_z corresponds to probing the medium at normal incidence with a very

short wavelength. For such a short wavelength, only the very top of the medium, whose inhomogeneity is contained in r(z) (recall the problem support is $[z,\infty)$), will affect the reflection response--the rest of the medium is effectively too far away. Hence the high-wavenumber behavior of $\hat{R}_k(k_z,z,\omega)$ should contain information about the reflectivity function for waves in z and ζ, viz, r(z), as (7-33) shows.

A similar interpretation can be applied to (3-42) of the normal-incidence inverse problem dynamic deconvolution algorithm. Here the short wavelength corresponds to a high value of ω, since the waves are in z and t rather than in z and ζ.

7.3 The Free Surface Problem

In this section the second configuration of the inverse problem is formulated, and a fast algorithm solution derived. Instead of being bounded by two infinite half-spaces, the inhomogeneous layered medium is bounded above by a free surface (pressure release surface) at z = 0, ana is assumed to extend to infinite depth. The point pressure harmonic source is located at the origin, just below the free surface, and the acceleration of the medium at the free surface is measured. The situation is illustrated in Figure 7.6. The goal is once again to reconstruct the profiles $\rho(z)$ and c(z) by performing the experiment twice, at two different source frequencies. The depth to which the medium profiles are reconstructed is limited in a practical sense by the strength of the source relative to the ambient noise at that frequency.

Coen (1982) solved this problem by using a Gel'fand-Levitan-type procedure due to Weidelt (1972) to solve the Schrodinger-like equation (7-5). Coen's method requires two inverse Laplace transforms, the

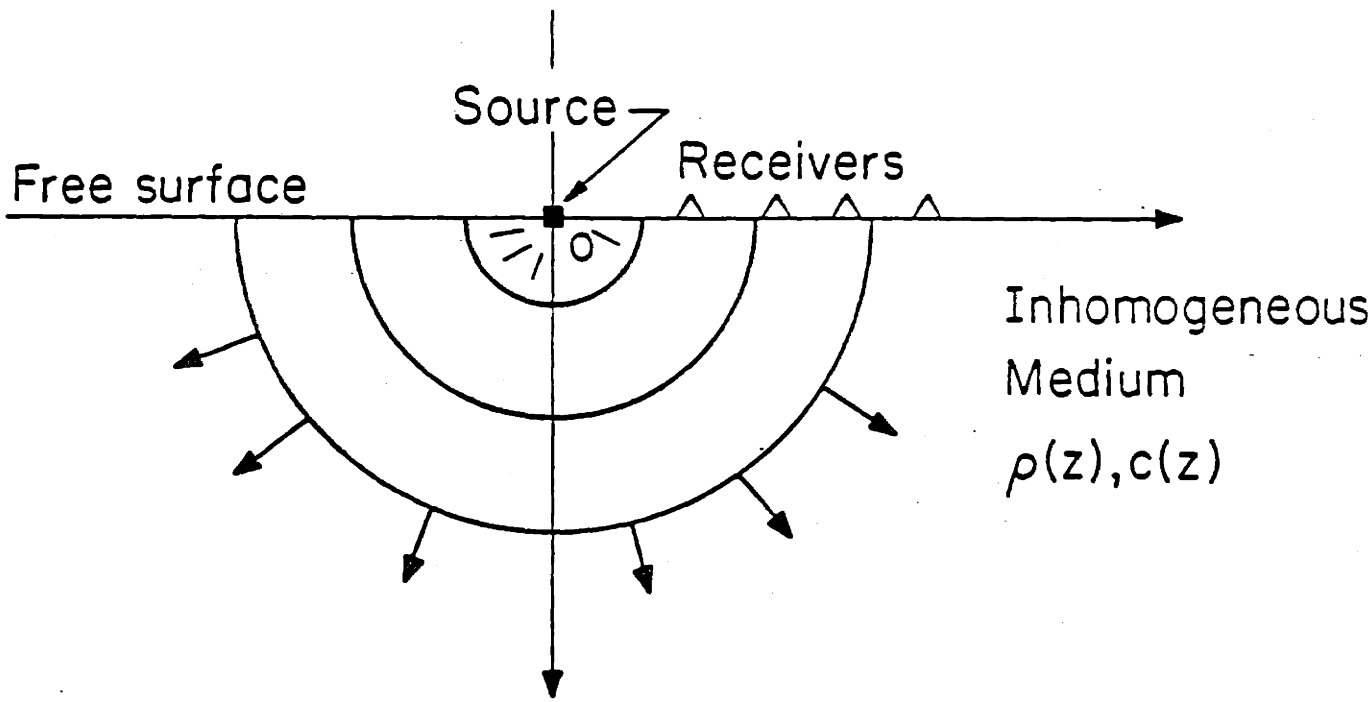

7.6 The free surface inverse problem.

solution of two Marchenko integral equations, and the assumption of post-critical incidence (i.e., $c(z) \geq c(0)$)--a most restrictive assumption. The present method does not require post-critical incidence and uses a fast algorithm directly on the basic equations of the problem, bypassing the necessity of setting up and solving an integral equation. Unfortunately, an inverse Laplace transform, or solution of an equivalent integral equation, is still necessary in preprocessing the data. On physical grounds this seems to be unavoidable, since Coen (1982) has pointed out that the use of any post-critical data requires probing the medium with evanescent waves, which will lead to an unstable inversion for large depths since the probing wave decays exponentially with depth.

Since k_z is imaginary for post-critical incidence, and since some post-critical data must be used, we now work with the lateral wavenumber ξ. Recall the Schrodinger-like equation (7-5), which is

$$\left(\frac{d^2}{dz^2} - \xi^2 - V_\xi\right)\hat{\pi} = 0 . \tag{7-35}$$

Define a new quantity $\hat{\phi}(\xi,z,\omega)$ by

$$\begin{aligned}\hat{\phi}(\xi,z,\omega) &\triangleq \left(\frac{d}{dz}+\xi\right)\hat{\pi} = \omega^2\sqrt{\rho}\,(\hat{u}_z-\hat{u}_r) - (1/2\rho)(d\rho/dz)\hat{\pi} \\ &= \sqrt{\rho}\,(\hat{a}_r-\hat{a}_z) - (1/2\rho)(d\rho/dz)\hat{\pi}\end{aligned} \tag{7-36}$$

where the $\hat{a}_i$ are appropriate Hankel transforms (see equations (7-3b) and (7-3c)) of the medium acceleration components and equations (7-2b) and (7-2c) have been used to interpret $\hat{\phi}$. Equation (7-5) can then be written as the coupled system

$$\frac{d}{dz}\begin{bmatrix}\hat{\pi}\\ \hat{\phi}\end{bmatrix} = \begin{bmatrix}-\xi & 1\\ V_\xi & \xi\end{bmatrix}\begin{bmatrix}\hat{\pi}\\ \hat{\phi}\end{bmatrix} . \tag{7-37}$$

The initial conditicns at the free surface z = 0 are

$$\hat{\pi}(\xi,0,\omega) = H[b\delta(r)/r] = b \tag{7-38a}$$

$$\hat{\phi}(\xi,0,\omega) = -\sqrt{\rho(0)}\ \ \hat{a}_z(\xi,0,\omega) \tag{7-38b}$$

where the source term $[b\delta(r)/r]$ has been included in the $\hat{\pi}$ initial condition and $b\sqrt{\rho(0)}$ is the strength of the harmonic source in units of pressure. Note that the radial acceleration $\hat{a}_r$ vanishes on the free surface.

Since the measured quantities (accelerations) now have dimensions, the strength of the source must now be specified, unlike the previous problem in which the dimensionless reflection response was measured.

Comparing the coupled system (7-37) with the coupled system (7-18) of the previous problem, it seems we are stymied. Since the diagonal elements are real instead of imaginary, an inverse Fourier transform with respect to ξ is not appropriate. However, a similar system has been encountered in considering the inverse resistivity problem (see Section 7.5) and following an approach similar to that treatment we define

$$\overset{\vee}{\pi}(z,\zeta) \triangleq L_\xi^{-1}[\hat{\pi}(\xi,z)] \tag{7-39a}$$

$$\overset{\vee}{\phi}(z,\zeta) \triangleq L_\xi^{-1}[\hat{\phi}(\xi,z)] \tag{7-39b}$$

i.e., the inverse Laplace transform has taken ξ into ζ, and the parametric dependence on ω has been dropped.

Taking the inverse Laplace transform of equation (7-37) yields

$$(\frac{\partial}{\partial z} + \frac{\partial}{\partial \zeta}) \overset{\vee}{\pi}(z,\zeta) = \overset{\vee}{\phi}(z,\zeta) \tag{7-40a}$$

$$(\frac{\partial}{\partial z} - \frac{\partial}{\partial \zeta}) \overset{\vee}{\phi}(z,\zeta) = V_{\zeta} \overset{\vee}{\pi}(z,\zeta) \tag{7-40b}$$

with the initial conditions (from equations (7-38))

$$\overset{\vee}{\pi}(0,\zeta) = b\delta(\zeta) \tag{7-41a}$$

$$\overset{\vee}{\phi}(0,\zeta) = -\sqrt{\rho(0)}\, L^{-1}[\hat{a}_z(\xi,0)] \tag{7-41b}$$

As before, the forms of the system (7-40) and initial conditions (7-41) make it clear that $\overset{\vee}{\pi}(z,\zeta)$ and $\overset{\vee}{\phi}(z,\zeta)$ have the forms

$$\overset{\vee}{\pi}(z,\zeta) = b\delta(\zeta - z) + \overset{\vee}{\pi}_0(z,\zeta)1(\zeta - z) \tag{7-42a}$$

$$\overset{\vee}{\phi}(z,\zeta) = \overset{\vee}{\phi}_0(z,\zeta)1(\zeta - z) \tag{7-42b}$$

(note that equation (7-40a) shows that $\overset{\vee}{\phi}$ will <u>not</u> contain an impulse) so that $\overset{\vee}{\pi}$ and $\overset{\vee}{\phi}$ both obey a causality principle, as before.

<u>The Layer Stripping Algorithm</u>

Substituting the forms (7-42) into the system (7-40) yields

$$V_{\xi}(z) = -2\overset{\vee}{\phi}(z,z+)/b \tag{7-43}$$

and the system (7-40) and condition (7-43) together form a layer stripping algorithm that recursively generates the potential $V_{\xi}(z)$. The update patterns for $\overset{\vee}{\pi}$ and $\overset{\vee}{\phi}$ are again given by Figures 7.4a and 7.4b, respectively.

By running the experiment twice, at two different source frequencies ω_1 and ω_2, the two potentials $V_\xi(z,\omega_1)$ and $V_\xi(z,\omega_2)$ are obtained. We then have, from equation (7-6),

$$c(z) = [(\omega_2^2 - \omega_1^2)/(V_\xi(z,\omega_1) - V_\xi(z,\omega_2))]^{\frac{1}{2}} \tag{7-44a}$$

$$Z''/Z = (\omega_2^2 V_\xi(z,\omega_1) - \omega_1^2 V_\xi(z,\omega_2))/(\omega_2^2 - \omega_1^2) \tag{7-44b}$$

and the differential equation (7-44b) can then be solved for $Z = 1/\sqrt{\rho}$.

Two comments are in order here. First, the initial conditions (7-41) for the layer stripping algorithm require that the medium acceleration data be Hankel transformed and then inverse Laplace transformed. These two operations may be replaced by the solution of an integral equation derived below. Second, the coupled system (7-40) describes anisotropic scattering, since the "reflectivity functions" 1 and V_ξ are different for waves travelling in different directions. However, by utilizing the layer stripping algorithm in this form, the necessity of differentiating r(z) in equation (7-13) is avoided.

Physical Interpretation of the Layer Stripping Algorithm

The layer stripping algorithm for the solution of the free surface inverse problem also has the physical interpretation of constructing distributions of image sources that simulate the response of the medium at each depth. There are, however, some differences from the previous interpretation. In addition, an integral equation is derived that offers an alternative to the necessity of Hankel and inverse Laplace transformation of the data prior to use of the layer stripping algorithm.

Since $\hat{\phi}$, determined from the data, is used to initialize the algorithm

we write (dropping the parametric dependence on ω)

$$\phi(r,z) = H^{-1}[\hat{\phi}(\xi,z)] = H^{-1}[\int_0^\infty \overset{\vee}{\phi}(z,\zeta)e^{-\xi\zeta}d\zeta]$$

$$= \int_0^\infty \overset{\vee}{\phi}(z,\zeta)H^{-1}[e^{-\xi\zeta}]d\zeta = \int_0^\infty \overset{\vee}{\phi}(z,\zeta)(\zeta/(\zeta^2+r^2)^{\frac{3}{2}})d\zeta$$

$$= \int_0^\infty \overset{\vee}{\phi}(z,\zeta)\cos\theta(\zeta,r)/(\zeta^2+r^2)d\zeta \quad , \qquad (7\text{-}45)$$

where θ is shown in Figure 7.5.

Thus $\phi(r,z)$ can be written as a superposition of fields due to a continuous distribution $\overset{\vee}{\phi}(z,\zeta)$ of image sources distributed along the fictitious depth coordinate ζ. Note that the image sources no longer generate spherical waves; each source generates a field that drops off inversely with the square of the distance from the source. The vertical components of the fields at radius r are then integrated to get ϕ. This is consistent with the interpretation of ϕ as a measurement of vertical acceleration. The comments made in Section 7.2 on causality and interpretation of the first non-zero source as yielding information about the medium still hold, with two changes. First, the information about the medium is now the downgoing reflectivity function, which happens to be the potential $V_\xi(z)$ (see equation (7-43)). Second, the necessity of maintaining zero pressure on the free surface away from the source implies that a mirror image of the distribution of pressure image sources must exist <u>above</u> the free surface, i.e., $\overset{\vee}{\pi}(z,\zeta)$ is an <u>odd</u> function of ζ (since the image sources above the surface must have opposite sign to maintain zero pressure at $z = 0$). Since the free surface acts as a mirror itself, these additional sources do not affect the interpretation in any way.

The interpretation given by equation (7-45) allows an alternate means of initializing the layer stripping algorithm from the data. Setting z = 0 in equation (7-45) and taking the inverse Hankel transform of equation (7-38b) yields

$$\phi(r,0,\omega) = -\sqrt{\rho(0)}\, a_z(r,0,\omega) = \int_0^\infty \overset{\vee}{\phi}(0,\zeta)(\zeta/(\zeta^2+r^2)^{\frac{3}{2}})d\zeta \quad . \tag{7-46}$$

This integral equation may be solved for $\overset{\vee}{\phi}(0,\zeta)$, which is then used to initialize the algorithm. Solving this integral equation may be preferable to Hankel transforming and then inverse Laplace transforming the data, depending on how the data were obtained.

Dynamic deconvolution algorithm

A dynamic deconvolution algorithm may be associated with the free surface layer stripping algorithm as follows. Defining the reflection coefficient

$$R_\xi(\xi,z,\omega) \overset{\Delta}{=} \hat{\phi}(\xi,z,\omega)/\hat{\pi}(\xi,z,\omega) \quad , \tag{7-47}$$

we have from (7-37) the Riccati equation

$$\frac{d}{dz} R_\xi(\xi,z,\omega) = 2\xi R_\xi + V_\xi - R_\xi^2 \tag{7-48}$$

and from (7-43) and the final value theorem for Laplace transforms,

$$V_\xi(z,\omega) = \underset{\xi\to\infty}{\text{LIM}} -2\xi R_\xi(\xi,z,\omega) \quad . \tag{7-49}$$

The algorithm is initiated using

$$R_\xi(\xi,0,\omega) = -\hat{a}_z(\xi,0,\omega)/(b\rho(0)^{\frac{1}{2}}) \quad . \tag{7-50}$$

The equation (7-49) for obtaining $V_\xi(z,\omega)$ from $R_\xi(\xi,z,\omega)$ for large ξ can be interpreted physically as follows. Probing the medium for large values of the lateral wavenumber ξ amounts to probing the medium with evanescent waves, since ξ is greater than any possible value of $\omega/c(z)$ and thus the local vertical wavenumber

$$k_z(z) = (\omega^2/c(z)^2 - \xi^2)^{\frac{1}{2}} \tag{7-51}$$

is imaginary. Since ξ is large, $jk_z(z)$ is large and negative, and the evanescent waves decay very quickly with z. In the limit as $\xi \to \infty$, the waves sense nothing but the reflectivity function at the surface z. Since the reflectivity function for the downgoing $\hat{\pi}$ wave is V_ξ, the high-ξ behavior of $\hat{R}_\xi$ determines V_ξ. This argument is taken from Frisk (1979).

7.4 Simple Illustrations of the Algorithms

We give two quantitative examples of the algorithms in action. The first example is a very simple analytical example due to Coen (1982) for the free surface problem. An analytical example is used to avoid problems in numerically computing the inverse Laplace transform. In this example, actual analytic expressions for $\overset{\vee}{\pi}(z,\zeta)$ and $\overset{\vee}{\phi}(z,\zeta)$ are obtained and shown to satisfy the coupled system (7-40) as well as the condition (7-43). Hence a computer run of the algorithm would have generated the same values. In the second example an actual computer run of the algorithm for the half-space problem is made on synthetic data generated using the reflectivity method by a program due to Kind (1976). Results are

excellent, confirming that the bandlimitation of the vertical wavenumber k_z by ω/c_0 is not a serious problem for realistic numbers.

7.4.1 Free Surface Problem -- Analytic Example

This example is due to Coen (1982). Let the profiles be given by

$$c(z) = c_0; \ \rho(z) = \rho_0/(1 + hz)^2 \quad . \tag{7-52}$$

Since $Z = 1/\sqrt{\rho}$, we then have

$$V_\xi(z,\omega) = -\omega^2/c_0^2 \tag{7-53}$$

and $\hat{\pi}(\xi,z,\omega)$ satisfies

$$\left(\frac{d^2}{dz^2} - \xi^2 + \omega^2/c_0^2\right)\hat{\pi} = 0 \ . \tag{7-54}$$

The solution that satisfies the boundary condition (7-38a) and the radiation condition is

$$\hat{\pi}(\xi,z,\omega) = b \exp\left[-(\xi^2 - \omega^2/c_0^2)^{\frac{1}{2}} z\right] \quad . \tag{7-55}$$

Using

$$\begin{aligned} L[I_0(a(t^2-z^2)^{\frac{1}{2}})1(t-z)] &= (\exp(-z(s^2-a^2)^{\frac{1}{2}}))/(s^2-a^2)^{\frac{1}{2}} \\ &= (-1/zs)(d/ds)\exp(-z(s^2-a^2)^{\frac{1}{2}}) \end{aligned} \tag{7-56}$$

where $I_0(\cdot)$ is the modified Bessel function of the first kind of order

zero we have that

$$\overset{\vee}{\pi}(z,\zeta) = L^{-1}[\hat{\pi}(\xi,z)] = bz(1/\zeta)(d/d\zeta)I_0((\omega/c_0)(\zeta^2-z^2)^{\frac{1}{2}})1(\zeta-z)$$

$$= b\delta(\zeta-z) + (bz\omega/c_0)I_1((\omega/c_0)(\zeta^2-z^2)^{\frac{1}{2}})/(\zeta^2-z^2)^{\frac{1}{2}}1(\zeta-z) \qquad (7\text{-}57)$$

and

$$\overset{\vee}{\phi}(z,\zeta) = (\frac{\partial}{\partial z} + \frac{\partial}{\partial \zeta})\overset{\vee}{\pi}(z,\zeta) = (b\omega/c_0)I_1((\omega/c_0)(\zeta^2-z^2)^{\frac{1}{2}})/(\zeta^2-z^2)^{\frac{1}{2}}1(\zeta-z)$$

$$+ bz\omega/c_0(\zeta-z)\,[(I_0((\omega/c_0)(\zeta^2-z^2)^{\frac{1}{2}})(\omega/c_0)/(\zeta^2-z^2) - 2I_1((\omega/c_0)(\zeta^2-z^2)^{\frac{1}{2}})$$

$$/(\zeta^2-z^2)^{\frac{3}{2}}]1(\zeta-z). \qquad (7\text{-}58)$$

Now, the surface data will consist of

$$\hat{\phi}(\xi,0,\omega) = (\frac{d}{dz} + \xi)\hat{\pi}(\xi,z,\omega)\,|_{z=0} = b(\xi - (\xi^2-\omega^2/c_0^2)^{\frac{1}{2}}) \qquad (7\text{-}59)$$

as well as

$$c(0) = c_0;\ \rho(0) = \rho_0;\ d\rho(0)/dz = -2\rho_0 h\ . \qquad (7\text{-}60)$$

Thus the inversion problem is to reconstruct the profiles $\rho(z)$ and $c(z)$ from the surface data (7-59) and (7-60). Taking the inverse Laplace transform (analytically!) of (7-59) yields

$$\overset{\vee}{\phi}(0,\zeta) = (b\omega/c_0)I_1(\omega\zeta/c_0)/\zeta 1(\zeta)\ . \qquad (7\text{-}61)$$

and of course it is known that

$$\overset{\vee}{\pi}(0,\zeta) = b\delta(\zeta) \quad . \tag{7-62}$$

The initial conditions (7-61) and (7-62) are used to initiate the layer stripping algorithm consisting of equations (7-40) and (7-43). Propagation of the algorithm will yield, in numerical form, $\overset{\vee}{\pi}(z,\zeta)$ and $\overset{\vee}{\phi}(z,\zeta)$, which are specified analytically by equations (7-57) and (7-58).

At each depth the potential V_ξ is being reconstructed using

$$V_\xi(z,\omega) = -\, 2\overset{\vee}{\phi}(z,z+)/b = -\, (2/b) \lim_{\zeta \to z} \overset{\vee}{\phi}(z,\zeta) = -\, \omega^2/c_0^2 \tag{7-63}$$

where we have used

$$\lim_{x \to 0} I_1(x)/x = 1/2 \quad . \tag{7-64}$$

Then, using equations (7-44) yields

$$c(z) = c_0 \tag{7-65a}$$

$$Z''/Z = 0 \tag{7-65b}$$

and (7-65b) is integrated to get

$$Z(z) = 1/\sqrt{\rho(z)} = C_1 + C_2 z \tag{7-66}$$

which implies

$$\rho(z) = 1/(C_1 + C_2 z)^2 \tag{7-67}$$

where the constants of integration C_1 and C_2 are obtained from (7-60). Thus the profiles (7-52) have been recovered.

The dynamic deconvolution algorithm applied to this problem works as follows. We have from (7-55) that

$$\hat{\phi}(\xi,z,\omega) = (\frac{d}{dz} + \xi)\hat{\pi} = (\xi - (\xi^2 - \omega^2/c_0^2)^{\frac{1}{2}})\hat{\pi} \tag{7-68}$$

which agrees with (7-59) at the surface z = 0. The reflection coefficient $R_\xi(\xi,z,\omega)$ is then

$$R_\xi = \hat{\phi}/\hat{\pi} = \xi - (\xi^2 - \omega^2/c_0^2)^{\frac{1}{2}} \tag{7-69}$$

and a simple substitution shows that R_ξ as defined in (7-69) does indeed satisfy the Riccati equation (7-48). Hence the dynamic deconvolution algorithm recursively generates the R_ξ in (7-69), with V_ξ obtained from (7-49) as

$$V_\xi = \underset{\xi \to \infty}{\text{LIM}} -2\xi R_\xi = \underset{\xi \to \infty}{\text{LIM}} -2\xi(\xi - (\xi^2 - \omega^2/c_0^2)^{\frac{1}{2}}) = -\omega^2/c_0^2 \tag{7-70}$$

Then $\rho(z)$ and $c(z)$ are recovered as was done using (7-65) - (7-67).

7.4.2 Half-Space Problem -- Computer Run

A reflectivity method computer program due to Kind (1976) was employed to generate reflection coefficients for various wavenumbers for a fifteen-layer medium at two different source frequencies 20 Hz and 30 Hz. The density profile, in units of specific gravity, was a variation from 1.4 to 2.0 and back down to 1.4 in steps of 0.1, in order to simulate a continuous medium. The sound speed was held constant at 2 km/sec., and the step size Δ was 50 m. The thickness of the inhomogeneous medium was 1.3 km (13 layers, each 100 m thick).

The inverse Fourier transforms required by equation (7-21b) were implemented using a 512-point FFT, and the algorithm was run on a VAX-11/782 computer. The differential equation (7-24b) was solved recursively as the algorithm proceeded, using a simple difference scheme to implement the second derivative. Despite the simplistic numerical implementation, the resulting reconstruction was extremely accurate. Figure 7.7 shows the close agreement between the actual and reconstructed density profiles; the largest error is 1.5%. The reconstructed sound speed profile was correct to five decimal places. Apparently band-limitation of $R(k_z)$ by ω/c_0 is not a serious problem for realistic data.

It is worth noting that the experiment could be run for several source frequencies and the various computed ρ and c updates could be averaged and then reinserted into all of the concurrently running algorithms at each depth. This averaging could reduce the effect of noise in the data.

7.5 The Inverse Resistivity Problem

7.5.1 Formulation of the Problem

In this section we formulate the inverse resistivity problem for direct current measurements, and solve it using a layer stripping algorithm. The relevance of this problem to this chapter stems from the fact that this problem is mathematically analogous to the inverse problem for an acoustic medium probed at two frequencies, if the wave speed c(z) is constant and a rigid surface boundary condition is assumed. Since c(z) is constant, probing at one frequency suffices, and this frequency is in fact $\omega = 0$ (DC). This rather surprising fact allowed the method of images interpretation of the inverse resistivity problem algorithm to be applied to the inverse problem for an acoustic medium as well. The results of

7.7 Comparison between actual and computed density profiles (2 = actual, 3 = computed).

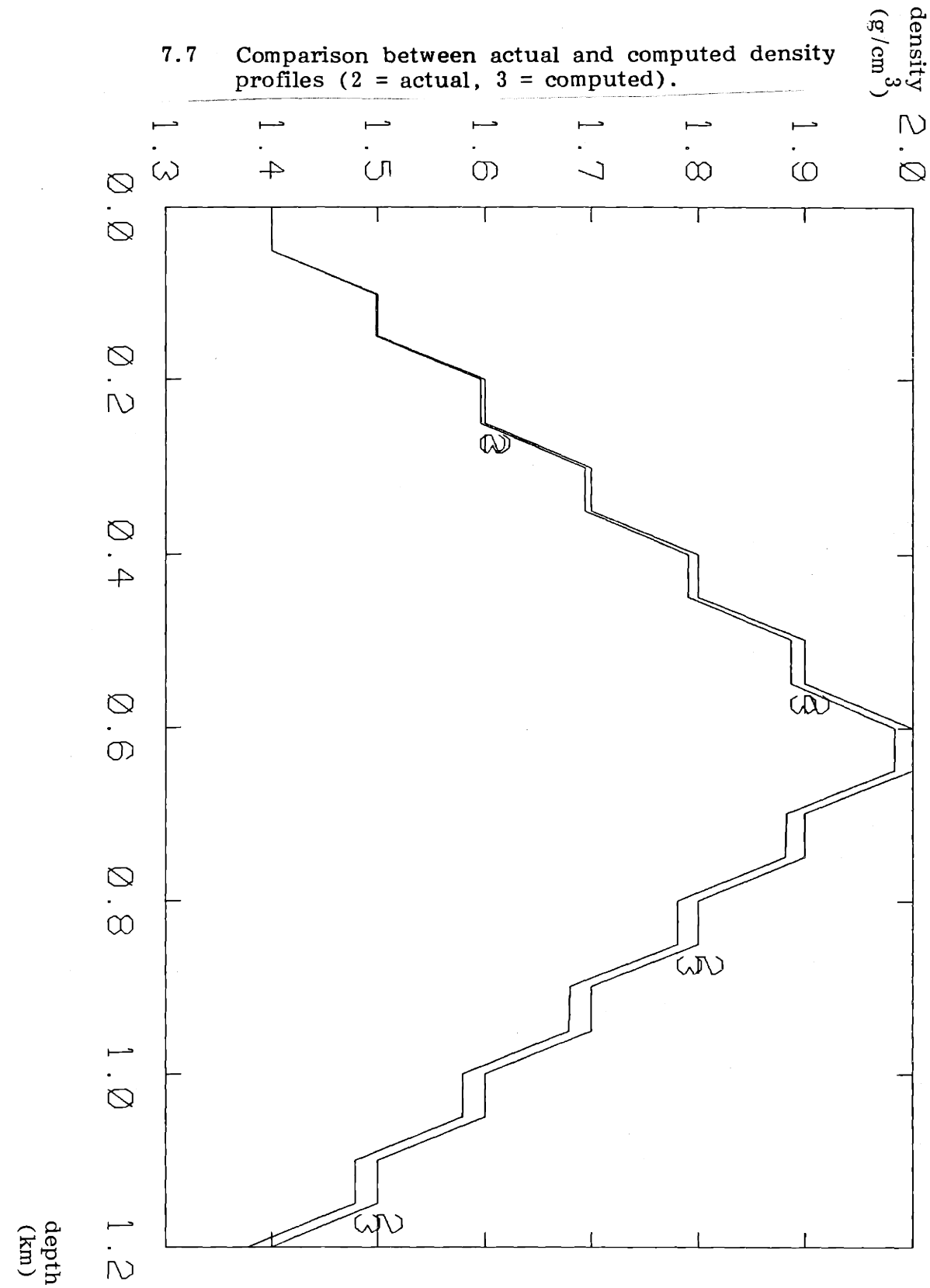

this section are taken from Levy (1984).

The inverse resistivity problem with direct current measurements is formulated as follows. The earth is assumed to be a layered medium characterized by its conductivity $\sigma(z)$, which varies only with depth (conductivity is the reciprocal of resistivity). Some direct current I is introduced into the medium at the origin, and the electrical potential $v(z = 0, r)$ is measured at the earth's surface. The object is to reconstruct $\sigma(z)$ from $v(0,r)$. A somewhat more realistic version of this problem, in which the Schlumberger electrode configuration is used to measure the apparent resistivity $-(\partial v/\partial r)/(I/2\pi r^2)$, is also considered in Levy (1984).

Details of past work on this problem are given in Levy (1984); however, three references are worth noting. Coen and Yu (1981) used the transformation procedure of Weidelt (1972) in order to solve this problem by the Gel'fand-Levitan procedure; this method requires an inverse Laplace transform and solution of a Marchenko integral equation, and bears a marked similarity to the method of Coen (1982) for solving the inverse problem for an acoustic medium probed at two frequencies. Kunetz and Rocroi (1970) derived a fast algorithm for solution of the discrete inverse resistivity problem; although they did not recognize it as such, their algorithm was in fact the Levinson algorithm for solving the discretized Marchenko equation. Pekeris (1940) derived the discrete version of the dynamic deconvolution Riccati equation (7-97) below; the recursion of Pekeris (1940) is in fact identical to the recursion (3-77) used for the Schur-Cohn stability test. It should be evident how these methods are linked together by the results of Chapters II and III of this thesis.

Mathematical formulation of the problem

From Ohm's law and the law of conservation of charge, the basic equations of the inverse resistivity problem are

$$\underset{\sim}{i}(z,r) = \sigma(z)\,\nabla v(z,r) \tag{7-71a}$$

$$\nabla\cdot\underset{\sim}{i}(z,r) = 0 \tag{7-71b}$$

where $v(z,r)$ is electrical potential and $\underset{\sim}{i}(z,r)$ is current density. Since current I is being introduced at the origin, the vertical component of current density at the surface is given by

$$i_z(0,r) = -\,(I/2\pi)\,\delta(r)/r \quad . \tag{7-72}$$

Equation (7-72), along with the measured potential $v(0,r)$ at the surface, constitute the boundary condtions for (7-71).

Comparing (7-71) and (3-1), it is seen immediately that the basic equations of the inverse resistivity problem are mathematically analogous to those for the inverse problem for a layered acoustic medium. The analogous quantities are pressure and potential, medium acceleration and negative current density, and density and resistivity, with wave speed fixed at unity. (Note that since direct current measurements are being used, the probing frequency $\omega = 0$ and $\partial^2 v/\partial t^2 = 0$.) The boundary condition (7-72) is analogous to requiring a fixed or rigid surface, except at the impulsive source, and measuring the pressure response at the surface of the medium.

With this analogy in mind, we simply repeat the transformations used earlier in this chapter. We define (in analogy to (7-3))

$$\hat{v}(z,\xi) = H_o[v(z,r)] \tag{7-73a}$$

$$\hat{i}_z(z,\xi) = H_o[i_z(z,r)] \tag{7-73b}$$

$$\hat{i}_r(z,\xi) = H_1[i_r(z,r)] \tag{7-73c}$$

(Fourier transforms are of course unnecessary, since there is no time dependence). The normalized potential (compare to (7-4))

$$\hat{\phi}(z,\xi) = \sigma(z)^{\frac{1}{2}}\hat{v}(z,\xi) \tag{7-74}$$

satisfies the Schrodinger-like equation (compare to (7-5))

$$\left(\frac{d^2}{dz^2} - \xi^2 - V_\phi\right)\hat{\phi}(z,\xi) = 0 \tag{7-75}$$

where V_ϕ is defined as (compare to (7-6) and recall $\omega = 0$)

$$V_\phi(z) = Y''/Y, \quad Y = \sigma(z)^{\frac{1}{2}} \quad . \tag{7-76}$$

Now, the reflectivity function k(z) can be defined again by the Miura transform (7-13) as

$$k^2 - \frac{dk}{dz} \triangleq V_\phi(z) \ , \tag{7-77}$$

but from (7-76) we can now immediately write k(z) as (compare to (7-29))

$$k(z) = -\frac{1}{Y}\frac{dY}{dz} = -\frac{1}{2\sigma}\frac{d\sigma}{dz} \quad . \tag{7-78}$$

This makes things much easier, since we now know that the auxiliary Schrodinger-like equation analogous to (7-15)

$$\left(\frac{d^2}{dz^2} - \xi^2 - V_\chi\right)\hat{\chi}(z,\xi) = 0 \tag{7-79}$$

where V_χ is defined as in (7-14) by

$$k^2 + \frac{dk}{dz} \triangleq V_\chi(z) \tag{7-80}$$

is in fact satisfied by

$$\hat{\chi}(z,\xi) = -\hat{i}_z(z,\xi)/(\xi\sigma(z)^{\frac{1}{2}}) \quad . \tag{7-81}$$

Thus the downgoing and upgoing waves defined in analogy to (7-17)

$$\hat{D}(z,\xi) = (\hat{\phi} + \hat{\chi})/2 = (\sigma(z)^{\frac{1}{2}}\hat{v}(z,\xi) - \hat{i}_z(z,\xi)/(\xi\sigma(z)^{\frac{1}{2}}))/2 \tag{7-82a}$$

$$\hat{U}(z,\xi) = (\hat{\phi} - \hat{\chi})/2 = (\sigma(z)^{\frac{1}{2}}\hat{v}(z,\xi) + \hat{i}_z(z,\xi)/(\xi\sigma(z)^{\frac{1}{2}}))/2 \tag{7-82b}$$

satisfy the coupled system of differential equations

$$\frac{d}{dz}\begin{bmatrix}\hat{D}\\ \hat{U}\end{bmatrix} = \begin{bmatrix}-\xi & -k(z)\\ -k(z) & \xi\end{bmatrix}\begin{bmatrix}\hat{D}\\ \hat{U}\end{bmatrix} \quad . \tag{7-83}$$

In comparing (7-82) with the waves (3-33), it should be recalled that medium acceleration is analogous to negative vertical current density. This accounts for the change of sign.

Levy (1984) shows how a scattering matrix can be defined for the system (7-83) by taking the analytic continuation of the scattering matrix defined for $\xi = jk$. This requires that k(z) have compact support, i.e., the medium is bounded below by a homogeneous half-space. However, this assumption is not required by the algorithms to follow.

7.5.2 Solution by Fast Algorithms

Fast Cholesky algorithms

The coupled system (7-83) has real elements along the diagonal, so an inverse Fourier transform is not appropriate. However, this situation was encountered in the system (7-37) for the free surface problem, so we know what to do. Defining (in analogy to (7-39))

$$\overset{\vee}{D}(z,\zeta) = L^{-1}[\xi \hat{D}(z,\xi)] \tag{7-84a}$$

$$\overset{\vee}{U}(z,\zeta) = L^{-1}[\xi \hat{U}(z,\xi)] \quad , \tag{7-84b}$$

we see that $\overset{\vee}{D}$ and $\overset{\vee}{U}$ satisfy the two-component wave system

$$(\partial/\partial z + \partial/\partial\zeta)\overset{\vee}{D}(z,\zeta) = -k(z)\overset{\vee}{U}(z,\zeta) \tag{7-85a}$$

$$(\partial/\partial z - \partial/\partial\zeta)\overset{\vee}{U}(z,\zeta) = -k(z)\overset{\vee}{D}(z,\zeta) \quad . \tag{7-85b}$$

However, in order to define the fast Cholesky algorithm for (7-85), it is still necessary to show that $\overset{\vee}{D}(z,\zeta)$ contains a leading impulse, as in (7-22). This can be done as follows. The potential v(z,r) can be expressed as

$$v(z,r) = \frac{I}{2\pi\sigma(0)}\left(\frac{1}{(z^2 + r^2)^{\frac{1}{2}}} + 2h(z,r)\right) \tag{7-86}$$

where the first term of (7-86) is the potential of a homogeneous medium with conductivity $\sigma(0)$ (to see this, note that the radial component of current density is $I/(2\pi(r^2 + z^2))$ and use (7-71a)), and the second term of (7-86) is the perturbation due to the inhomogeneity of the actual medium. Taking the Hankel transform of order zero of (7-86) gives

$$\hat{v}(0,\xi) = \frac{I}{2\pi\sigma(0)}\left(\frac{1}{\xi} + 2\hat{h}(0,\xi)\right) \tag{7-87}$$

and taking the Hankel transform of order zero of (7-72) yields, with

(7-82),

$$\hat{D}(0,\xi) = \frac{I}{2\pi\sigma^{\frac{1}{2}}(0)} \left(\frac{1}{\xi} + \hat{h}(0,\xi)\right) \tag{7-88a}$$

$$\hat{U}(0,\xi) = \frac{I}{2\pi\sigma^{\frac{1}{2}}(0)} \hat{h}(0,\xi) \quad . \tag{7-88b}$$

Multiplying by ξ and taking the inverse Laplace transform, we finally get

$$\overset{\vee}{D}(0,\zeta) = \frac{I}{2\pi\sigma^{\frac{1}{2}}(0)} \left(\delta(\zeta) + \overset{\vee}{h}(\zeta)\right) \tag{7-89a}$$

$$\overset{\vee}{U}(0,\zeta) = \frac{I}{2\pi\sigma^{\frac{1}{2}}(0)} \overset{\vee}{h}(\zeta) \tag{7-89b}$$

where $\overset{\vee}{h}(\zeta) \overset{\Delta}{=} L^{-1}[\xi\hat{h}(0,\xi)]$.

Thus we have shown that the downgoing wave $\overset{\vee}{D}(0,\zeta)$ at the surface does indeed contain a leading impulse, and the fast Cholesky algorithm, consisting of (7-85) and

$$k(z) = 2\overset{\vee}{U}(z,z+) \quad , \tag{7-90}$$

can be used to reconstruct $k(z)$ and hence $\sigma(z)$. The initial conditions for the fast Cholesky algorithm are

$$\overset{\vee}{D}(0,\zeta) = \overset{\vee}{U}(0,\zeta) = \overset{\vee}{h}(\zeta) = L^{-1}[\xi H_o[h(0,r)]] \tag{7-91}$$

where $h(0,r)$ is obtained from the measured $v(0,r)$ using (7-86).

The initial conditions (7-91) are recognized as those for a free surface (compare to (3-16)). This is not surprising; the air above the earth's surface is effectively an insulator ($\sigma(z) = 0$ for $z < 0$), so that the upward traveling current $i_z(0,r)$ is reflected back down into the

earth. Indeed, the earth's surface might well be considered a "current release surface," in analogy to a pressure release surface. The actual analogy here, of course, is to an "acceleration-release" or rigid surface, since current density is analogous to medium acceleration.

The physical interpretation of the fast Cholesky algorithm (7-85), (7-90), and (7-91) follows from noting that

$$v(z,r) = H_o^{-1}[\hat{v}(z,\xi)] = H_o^{-1}[\frac{1}{\xi}\int_o^\infty \overset{\vee}{v}(z,\zeta)e^{-\xi\zeta}\,d\zeta]$$

$$= \int_o^\infty \overset{\vee}{v}(z,\zeta)\; H_o^{-1}[\frac{1}{\xi}\,e^{-\xi\zeta}]\;d\zeta = \int_o^\infty \overset{\vee}{v}(z,\zeta)\,\frac{d\zeta}{(\zeta^2+r^2)^{\frac{1}{2}}} \qquad (7\text{-}92)$$

which also may be obtained from the definition (4-57) of the inverse Hankel transform and the identity

$$\int_o^\infty e^{-\xi t}J_o(\xi r)d\xi \;=\; 1/(t^2+r^2)^{\frac{1}{2}}\quad . \qquad (7\text{-}93)$$

Equation (7-92) shows that the potential $v(z,r)$ at the current depth at which the algorithm is operating is being written as the superposition of current sources of strengths $2\pi\sigma(0)\overset{\vee}{v}(z,\zeta)d\zeta/I$ distributed along a fictitious depth axis ζ. According to Maxwell's method of images, the potential $v(z,r)$ in a layered inhomogeneous medium can be written as a superposition of potentials due to fictitious current sources that are images of the actual point current source at the surface. These sources are always "in the looking glass," i.e., they are not in that portion of the medium whose potential they are trying to simulate. Thus they must always be located deeper than depth z. (A mirror image distribution of current sources must also exist in the other "looking-glass," i.e., above the free surface, in order to maintain $i_z(0,r) = 0$. This

means that $\overset{\vee}{h}(z,\zeta)$ is actually an even function in ζ, but we ignore the "anticausal" part above the free surface.)

The fact that the image sources must always be located deeper than z, i.e., $z < \zeta$, amounts to a causality condition that replaces the temporal causality used for the fast Cholesky algorithms in Chapters III and IV. Also note that the first or uppermost source, at $\zeta = z+$, clearly has the responsibility of accounting for the medium inhomogeneity at z+, which is characterized by k(z). This accounts for the first reflection condition (7-90). The ways in which these concepts may be applied to the analogous but more difficult (since c(z) also varies) inverse problem for a layered acoustic medium should be evident.

Dynamic deconvolution algorithm

Defining the reflection coefficient for the medium below depth z

$$R(z,\xi) = \hat{U}(z,\xi)/\hat{D}(z,\xi) \tag{7-94}$$

we note from the system (7-83) that $R(z,\xi)$ satisfies the Riccati equation

$$\frac{d}{dz}R(z,\xi) = 2\xi R - k(z)(1-R^2) \tag{7-95}$$

and k(z) can be obtained from $R(z,\xi)$ using

$$k(z) = \underset{\xi \to \infty}{\text{LIM}} \; 2\xi R(z,\xi) \tag{7-96}$$

since $R(z,\xi)$, being the analytic continuation of a strictly proper function R(z,jk), is itself strictly proper (Levy, 1984, p. 13). $R(z,\xi)$ is initialized from

$$R(0,\xi) = \hat{U}(0,\xi)/\hat{D}(0,\xi) = \xi\hat{h}(0,\xi)/(1+\xi\hat{h}(0,\xi)), \tag{7-97}$$

where $\hat{h}(0,\xi)$ is defined by the Hankel transform of (7-86).

The discrete version of (7-95) - (7-97), to be applied to a discrete layered medium, was proposed by Pekeris (1940). Pekeris's formula in lieu of (7-95) was

$$R_{i+1}(\xi) = e^{2\xi\Delta}\,(R_i(\xi) - k_i)/(1 - k_i R_i(\xi)) \tag{7-98}$$

where Δ is the layer thickness. This formula should be compared with equations (2-32) and (3-77a).

The major disadvantage of the dynamic deconvolution algorithm is the unstable computation (7-96). A major advantage of it is that the data need not be inverse Laplace transformed, which is also an unstable operation. Using (7-92), the combination Hankel transform-inverse Laplace transform required by (7-91) to initialize the fast Cholesky algorithm may be combined into the solution of the integral equation

$$h(0,r) = \int_0^\infty \overset{\vee}{h}(0,\zeta)\,\frac{d\zeta}{(\zeta^2+r^2)^{\frac{1}{2}}} \tag{7-99}$$

which is analogous to (7-46).

7.5.3 The Inverse Problem of Determining Reservoir Transmissivities

As a final note to show again that the problems and solutions covered in this chapter have widespread applicability, we quickly show that the inverse problem of determining aquifer transmissivities is mathematically equivalent to the inverse resistivity problem.

The inverse transmissivity problem is to determine the transmissivity T of an aquifer or reservoir from measurement of the change h in hydraulic head resulting from a source or sink q (of known strength) in the flow rate of the liquid in the reservoir. This liquid could, for example,

be water in an aquifer or petroleum in an underground reservoir. Typically, fluid is pumped from the reservoir at a well, the flow rate q (the sink term) at the well is monitored, and the hydraulic head h is measured on top of the reservoir. The reconstructed transmissivity T is a function of the depth, viscosity and density of the fluid at each point, and thus yields information about the condition and accessibility of the liquid in the reservor.

The basic equation for this problem are the conservation of fluid relation and the definition of mass flow rate $\underset{\sim}{J}$

$$q = \nabla \cdot \underset{\sim}{J} \tag{7-100a}$$

$$\underset{\sim}{J} = T \nabla h \tag{7-100b}$$

where equation (7-100b) simply states that fluid flow is caused by a gradient in head acting through a resistance 1/T (compare this to Ohm's law). Comparing (7-100) and (7-71), the mathematical analogy to this problem to the inverse resistivity problem is clear. Mass flow rate $\underset{\sim}{J}$ is analogous to current density $\underset{\sim}{i}$, head h is analogous to potential v, and transmissivity T is analogous to conductivity σ. Reflection shows that these analogies make sense physically as well.

This means that in the one-dimensional problem, in which the reservoir is treated as a huge pipe whose cross-sectional area varies with distance (not unlike the inverse problem for determining the shape of the human vocal tract; see Chapter II), the problem can be formulated as an inverse scattering problem and solved as was just done for the inverse resistivity problem. Wilson (1983) formulated the problem in this way, but did not propose a solution.

In this chapter the layer stripping concept has been used in a novel way to solve an inverse problem to which, at first glance, the layer stripping concept seems inapplicable. In the next chapter, layer stripping is applied to the most difficult problem of all--that of higher-dimensional media.

REFERENCES FOR CHAPTER VII

K. Aki and P. Richards, Quantitative Seismology: Theory and Methods, W.H. Freeman and Co., San Francisco, 1980.

S. Coen, "Velocity and Density Profiles of a Layered Acoustic Medium from Common Source-Point Data," Geophys. 47(6), 898-905 (1982).

S. Coen and M. W-H. Yu, "The Inverse Problem of the Direct Current Conductivity Profile of a Layered Earth," Geophysics 46 (12), 1702-1713 (1981).

P. Deift and E. Trubowitz, "Inverse Scattering on the Line," Comm. Pure, Applied Math. 32(2), 121-251 (1979).

G. Frisk, "Inhomogeneous Waves and the Plane-Wave Reflection Coefficient," J. Acoust. Soc. Am. 66(1), 219-234 (1979).

G.V. Frisk, A.V. Oppenheim, and D.R. Martinez, "A Technique for Measuring the Plane-Wave Reflection Coefficient of the Ocean Bottom," J. Acoust. Soc. Am. 68, 602-612 (1980).

G.V. Frisk, J.A. Doutt, and E.E. Hays, "Bottom Interaction of Low-Frequency Acoustic Signals at Small Grazing Angles in the Deep Ocean," J. Acoust. Soc. Am. 69, 84-94 (1981).

R. Kind, "Computation of Reflection Coefficients for Layered Media," J. Geophysics 42, 191-210 (1976).

G. Kunetz and J.P. Rocroi, "Traitement Automatique des Sondages Electriques," Geophys. Prospecting 18, 157-198 (1970).

B. Levy, "Layer by Layer Reconstruction Methods for the Earth Resistivity from Direct Current Measurements," Tech. Report LIDS-P-1388, Laboratory for Information and Decision Systems, MIT (1984).

D. Mook, "The Numerical Synthesis and Inversion of Acoustic Fields Using the Hankel Transform with Application to the Estimation of the Plane Wave Reflection Coefficient of the Ocean Bottom," D.Sc. Dissertation, Joint MIT/Woods Hole Program in Oceanographic Eng., January 1983.

C.L. Pekeris, "Direct Method of Interpretation in Resistivity Prospecting," Geophysics 5(1), 31-42 (1940).

D. Stickler, "Inverse Scattering in a Stratified Medium," J. Acoust. Soc. Am. 74(3), 994-1005 (1983).

C. van Winter, "Fredholm Equations on a Hilbert Space of Analytic Functions," Trans. Am. Math. Soc. 162, 103-139 (1971).

P. Weidelt, "The Inverse Problem of Geomagnetic Induction," Zeitschrift für Geophysik 38, 257-289 (1972).

W.H. Wilson, "An Inverse Scattering Approach to the Pressue Transient Analysis of Petroleum Reservoirs," in Conference on Inverse Scattering: Theory and Applications, ed. by J.B. Bednar, R. Redner, E. Robinson, and A. Weglein, pp. 170-180, SIAM, Philadelphia, 1983.

A. Yagle and B. Levy, "A Fast Algorithm Solution of the Inverse Problem for a Layered Acoustic Medium Probed by Spherical Harmonic Waves," to appear in J. Acoust. Soc. Am.

CHAPTER VIII

Higher Dimensional Inverse Seismic Problems

8.1 Introduction

In this chapter the inverse seismic problem in dimensions higher than one is considered. The medium being probed is no longer required to be layered or laterally homogeneous--the density and wave speed are now functions of two or three spatial variables, e.g., $\rho(x,z)$ and $c(x,z)$, or $\rho(x,y,z)$ and $c(x,y,z)$. The goal is to reconstruct ρ and/or c by measuring the response of the medium to an impulsive plane pressure wave.

To clarify matters, some terminology is introduced. The dimension of an inverse problem is defined as the number of spatial variables on which the quantities of interest (ρ and c) depend. Thus, the two-dimensional (2-D) problem is the inverse problem of determining $\rho(x,z)$ and $c(x,z)$ from surface measurements of the displacement $u(x, z=0, t)$, and the three-dimensional (3-D) problem is the inverse problem of determining $\rho(x,y,z)$ and $c(x,y,z)$ from surface measurements of the displacement $u(x, y, z=0, t)$.

Note that the dimension of a problem need not be the same as the dimension of the medium in which it is defined--a problem of given dimension can be embedded in a medium of higher dimension. For example, the non-normal incidence problem described in Chapter IV is a 1-D problem embedded in a 2-D medium, while the point-source problem of that same chapter is a 1-D problem embedded in a 3-D medium. This terminology will make nomenclature in this chapter much easier.

Higher-dimensional inverse seismic problems are much more difficult than the one-dimensional problems that have been considered so far in this thesis. Indeed, the general 3-D problem of reconstructing $\rho(x,y,z)$ and $c(x,y,z)$ exactly from surface measurements is at present an open problem. While this most difficult problem is not solved here, for reasons to be given later, layer stripping algorithms that are in some ways improvements over existing solution methods are given for several higher-dimensional inverse problems. These include the reconstruction of $\rho(x,y,z)$ with constant wave speed, reconstruction of $c(x,z)$ with constant density, and reconstruction of $\rho(x,z)$ and $c(x,z)$, all from the medium response to a plane wave at normal incidence in the first two cases and at oblique incidence in the third case.

Previous work

Generalizing 1-D results and techniques to the 2-D and 3-D problems has proven to be very difficult. Most of the solution procedures have in some way employed the Born approximation, which is essentially a weak scattering assumption requiring that the medium parameters vary slowly. Mathematically, the Born approximation can be specified as follows. Suppose we wish to recover the potential $V(\underset{\sim}{x})$ of the Schrodinger equation

$$(\nabla^2 + k^2 - V(\underset{\sim}{x}))\psi(\underset{\sim}{x},k) = 0 \qquad (8\text{-}1)$$

from measurements of the scattered field $\psi_s(\underset{\sim}{x},k)$. As an example of this problem, note that if ρ is constant and $c = c(\underset{\sim}{x})$ in the Fourier transforms of the basic acoustic equations (3-1)

$$\hat{p} = -\rho c^2 \nabla \cdot \hat{\underset{\sim}{u}} \tag{8-2a}$$

$$\rho \omega^2 \hat{\underset{\sim}{u}} = \nabla \hat{p} \tag{8-2b}$$

then p solves the Schrodinger-like equation

$$(\nabla^2 + k^2 - k^2(1 - c_o^2/c(\underset{\sim}{x})^2))\hat{p} = 0 \tag{8-3}$$

Here $k \triangleq \omega/c_o$ and c_o is the wave speed in the far field, where it is constant. The k^2 multiplying the potential can easily be accommodated in the following procedure.

Writing the Schrodinger equation (8-1) as

$$(\nabla^2 + k^2)\psi = V\psi \tag{8-4}$$

and treating $V\psi$ as a source term, it may be seen that ψ solves the Lippmann-Schwinger integral equation

$$\psi(\underset{\sim}{x}) = e^{j\underset{\sim}{k}\cdot\underset{\sim}{x}} + \int d\underset{\sim}{y}\ G(\underset{\sim}{x},\underset{\sim}{y})V(\underset{\sim}{x})\psi(\underset{\sim}{y}) \tag{8-5}$$

where $G(\underset{\sim}{x},\underset{\sim}{y})$ is the Green's function for the wave equation (8-4) and $e^{i\underset{\sim}{k}\cdot\underset{\sim}{x}}$ is the incident probing plane wave in the direction $\underset{\sim}{k}$ ($k = |\underset{\sim}{k}|$). Equation (8-5) may be solved by repeatedly inserting it into itself, producing an infinite series. Now, suppose we truncate this series after two terms, which amounts to a linearization. Then we have

$$\psi(\underset{\sim}{x}) = e^{j\underset{\sim}{k}\cdot\underset{\sim}{x}} + \int d\underset{\sim}{y}\ G(\underset{\sim}{x},\underset{\sim}{y})V(\underset{\sim}{x})e^{j\underset{\sim}{k}\cdot\underset{\sim}{y}} \tag{8-6}$$

This truncation can also be viewed as approximating the field $\psi(\underset{\sim}{y})$

inside the integral by the incident field $e^{j\underset{\sim}{k}\cdot\underset{\sim}{y}}$, which is to say that the incident field has been unaffected by the weak scattering losses it suffers while passing through the inhomogeneous medium. By any of the above names, the approximation of (8-5) by (8-6) is the Born approximation.

In the 1-D case, equation (8-6) becomes a simple Fourier transform, and $V(\underset{\sim}{x})$ may be obtained by taking the inverse Fourier transform with respect to k of the backscattered field $\psi(\underset{\sim}{x},k) - e^{j\underset{\sim}{k}\cdot\underset{\sim}{x}}$. In higher dimensions, things become more complicated, although Cohen and Bleistein (1979) have solved the 2-D problem. The tomographic approach of Devaney (1984) is also a Born approximation method.

The major problems with using the Born approximation are as follows. First, it is an approximation, requiring slow variation of ρ and c, and thus is fundamentally inexact. Second, Born approximation inversion methods require that measurements be taken in the far field, which is generally not possible for inverse seismic experiments on land. Third, Born approximation inversion methods are generally only applicable if density is constant (or if wave speed is constant and density is varying). This limits the scope of problems to which it can be applied. Finally, the Born approximation is by definition a single scattering approximation, so that multiple reflections are interpreted as primary reflections. This leads to errors beyond those made due to the basic assumption of a slowly varying medium.

The other approach to solving higher-dimensional inverse problems is migration, which can be very effective if the medium consists of several homogeneous regions separated by non-horizontal interfaces. The basic approach of migration is to image a particular point in the

medium by beamforming. A properly weighted sum of delays applied to data from various sensing positions will have the effect of a collective focus on the point being imaged (see Section 4.3). The strength of the reflection, of course, indicates the amount of scattering due to medium inhomogeneity taking place at that point. The major problem with migration is the wavefield extrapolation or back propagation, to determine which point in the medium is being imaged. This requires knowledge of $c(\underset{\sim}{x})$ along the ray paths, and often the wave speed is simply taken to be constant. This of course leads to errors. Berkhout (1982) is a good treatment on migration and wavefield extrapolation.

Raz (1982) has proposed a migration-like technique that involves a distorted-wave Born model. Various assumptions are made, including a straight-ray approximation between scattering and observation points. Results of a numerical 2-D inversion are presented, and a 3-D procedure proposed. Clayton and Stolt (1981) used the WKBJ approximation (see Section 4.4), which is tantamount to assuming that energy is propagating along rays, as in geometrical optics.

Newton (1980) has described a general 3-D inverse scattering problem solution that reconstructs a Schrodinger potential from a scattering amplitude given as a function of energy and directions of incident and scattered particles. Solution of a generalized Marchenko integral equation is required, as is the behavior of the scattering amplitude for particles of very high incident energy. And it is not clear how this method might be adapted to yield both $\rho(x,y,z)$ and $c(x,y,z)$ from the scattering amplitude.

Morawetz and Kriegsmann (1983) have proposed an iterative scheme in which an initial guess at a 2-D potential $V(x,y)$ is iteratively refined.

In the numerical examples presented for a 1-D inverse potential problem, up to thirteen iterations were required, and also some smoothing to prevent numerical instability. The computations and memory required for 2-D inversion are admitted to be enormous.

Finally, Symes (1983) showed how layer stripping ideas could be applied to higher-dimensional inverse problems. The problem solved by Symes (1983) was that of reconstructing the density $\rho(x,z)$ of a medium with constant wave speed, which is the 2-D version of the problem considered in Section 8.2. Symes's approach was to reconstruct the medium layer by layer by solving a Schrodinger equation in the lateral variable x to obtain the lateral dependence of density ρ at each depth. This approach is not nearly as simple and physically interpretable as the algorithm of Section 8.2.

Well-posedness of higher dimensional inverse problems

Most methods for solving higher-dimensional inverse problems, including tomographic methods (e.g., Devaney, 1984) and the generalized Gel'fand-Levitan method of Newton (1980), require as data the scattering amplitude or generalized reflection coefficient for probing particles for all energies incident from all directions. For the 3-D problem, this means that the measured data is a function of five parameters, one describing the energy of the probing particle, two describing the direction from which the particle is incident, and two describing in which direction the strength of the scattering field is being measured. Using spherical coordinates, this may be written as

$$A = A(k, \theta_{inc}, \phi_{inc}, \theta_{obs}, \phi_{obs}) . \qquad (8\text{-}7)$$

On the other hand, the potential whose reconstruction from the scattering amplitude A is desired is a function of three parameters

$$V = V(r, \theta, \phi) . \tag{8-8}$$

If the probing takes place using an incident plane wave, the energy k^2 is replaced by frequency, but otherwise the situation is the same.

Equations (8-7) and (8-8) show that the 3-D inverse scattering problem formulated as above is overdetermined; a function of five variables is being used to determine a function of three variables. This means that the 3-D inverse scattering problem as formulated above is ill-posed. This is true because a slight perturbation in the data $A(k, \theta_{inc}, \phi_{inc}, \theta_{obs}, \phi_{obs})$ may result in data that is inadmissible, i.e., corresponds to no potential $V(r, \theta, \phi)$. Indeed, since any potential V can give rise to only one scattering amplitude A (the ambiguity due to bound states does not arise in higher dimensions according to Newton (1980, p. 1698)), the set of admissible scattering amplitudes, i.e., those amplitudes A which actually arise from some potential V, are of measure zero in the space of possible scattering amplitudes. Thus this inverse problem is ill-conditioned: any small perturbation in the data (due, for example, to noisy observations) may lead to the failure of any potential reconstruction method, since there is no longer any potential to reconstruct. Of course, the problem may be regularized by adding noise a priori to the observations, and regarding any perturbation from the set of admissible data as being due to that noise, regardless of its actual cause (e.g., model failure). However, we do not consider that approach in this thesis.

It should be noted here, however, that the inverse problems proposed and solved in this chapter are all well-posed. Indeed, the algorithms themselves show that the problems are well-posed: a slight perturbation of the data simply leads to a slight perturbation of the reconstructed medium, since the reconstructed medium parameters depend in a continuous (but complicated) way on the observed data, as may be seen from the equations. The fact that the layer stripping algorithms do not require knowledge of the scattering amplitude for all incident and observation angles accounts for the well-posedness of these problems.

Summary

In Section 8.2 the 3-D inverse problem of determining the density $\rho(x,y,z)$ for a medium with constant wave speed c from measurement of the medium response to a plane wave at normal incidence is formulated and solved using a layer stripping algorithm. This turns out to be a fairly straightforward application of the layer stripping principle. The 2-D versions of this problem and solution first appeared in Yagle (1983).

In Section 8.3 the 2-D inverse problem of determining the wave speed $c(x,z)$ for a medium with constant density ρ using the same measurements as in Section 8.2 is formulated and solved. This problem turns out to be much more difficult than the problem of Section 8.2, since the varying wave speed results in the wave front no longer being planar. The wave speed is still determined along the wave front, but in this problem it is necessary to track the wave front and translate the reconstructed wave speeds along it into a function $c(x,z)$. The algorithm can handle caustics and turning points within the medium,

although of course the wave speed cannot be reconstructed beyond a turning point.

In Section 8.4 the non-normal incidence problem and algorithm of Section 4.2 are generalized to a 2-D problem and algorithm. The goal is to reconstruct $\rho(x,z)$ and $c(x,z)$ from measurements of the medium's responses to two plane waves moving in the y-direction and incident at two different angles. It is also noted that the result of Chapter III, viz. the impedance $\rho c(\tau)$ as a function of travel time τ can be reconstructed from the normal incidence plane wave response, can be generalized to higher dimensions. The impedance $\rho c(\tau)$ is reconstructed as a function of travel time along a ray path.

8.2 Reconstruction of $\rho(x,y,z)$ for Constant Wave Speed

The problem considered in this section is as follows. An acoustic isotropic medium for which the wave speed $c(x,y,z) = c_o$ is constant but the density $\rho(x,y,z)$ varies continuously with all spatial variables is probed at normal incidence with a plane wave from the homogeneous half-space $z < 0$. The medium's vertical acceleration $a_z(x,y,o,t)$ and pressure $p(x,y,o,t)$ are known at the surface; two combinations of them are fixed by the nature of the probing plane wave and the boundary condition at the surface. For example, if a sinusoidal plane pressure wave is used to probe the medium and a rigid surface is assumed, we have

$$p(x,y,o,t) = b\cos(\omega t + \phi)1(t) + R(x,y,t)1(t) \qquad (8\text{-}9a)$$

$$a_z(x,y,o,t) = 0 \qquad (8\text{-}9b)$$

where b is the strength of the wave, ω the frequency, and ϕ a phase

shift. In this case the data is $R(x,y,t)$.

Since a function of three variables $R(x,y,t)$ is being used to determine a function of three variables $\rho(x,y,z)$, the problem is not overdetermined. Since the wave speed $c(x,y,z) = c_o$ is constant, there are of course no turning points, and there are no caustics since the probing wave is a plane wave. Indeed, the wave front at any time t is a horizontal plane wave at depth $z = c_o t$. This makes the layer stripping algorithm for this problem much simpler than the one to follow in Section 8.3.

To solve this problem, we use the method of characteristics of Section 2.3.5. The basic acoustic equations (3-1) for this problem take the form

$$\partial^2 p/\partial t^2 = -\rho c_o^2(\partial a_x/\partial x + \partial a_y/\partial y + \partial a_z/\partial z) \tag{8-10a}$$

$$\partial p/\partial x = -\rho a_x \tag{8-10b}$$

$$\partial p/\partial y = -\rho a_y \tag{8-10c}$$

$$\partial p/\partial z = -\rho a_z \ , \tag{8-10d}$$

where a_x, a_y, and a_z are the respective components of the medium acceleration. Inserting (8-10b) and (8-10c) in (8-10a) eliminates a_x and a_y, leaving

$$\partial a_z/\partial z = [\partial^2 p/\partial x^2 + \partial^2 p/\partial y^2 - (1/c_o^2)(\partial^2 p/\partial t^2)]/\rho - [(\partial \rho/\partial x)(\partial p/\partial x) + (\partial \rho/\partial y)(\partial p/\partial y)]/\rho^2 \tag{8-11a}$$

$$\partial p/\partial z = -\rho a_z \ . \tag{8-11b}$$

Now, for any type of probing acoustic wave, we have

$$p(x,y,z,t) = \tilde{p}(x,y,z,t)\,1(t-\tau) \tag{8-12a}$$

$$v_z(x,y,z,t) = \tilde{v}_z(x,y,z,t)\,1(t-\tau) \tag{8-12b}$$

where v_z is the vertical component of medium velocity, τ is the vertical travel time z/c, and $\tilde{p}$ and $\tilde{v}_z$ are smooth functions. Equations (8-12) are a statement of causality--the medium at any point is at rest until the wavefront has passed that point. Note that for an acoustic wave p and v_z must have the same type of discontinuity at the wave front; indeed, in a homogeneous medium $p = Zv_z$, where Z is the impedance.

Taking the partial derivative of (8-12b) with respect to time gives

$$a_z(x,y,z,t) = \tilde{v}_z(x,y,z,t)\,\delta(t-\tau) + \tilde{a}_z(x,y,z,t)1(t-\tau)\ , \tag{8-13}$$

where $\tilde{a}_z \overset{\Delta}{=} \partial\tilde{v}_z/\partial t$.

Inserting (8-12a) and (8-13) into (8-11b) and equating the coefficients of $\delta(\cdot)$ on both sides gives

$$\rho(x,y,z)c_o = \tilde{p}(x,y,z,\tau)/\tilde{v}_z(x,y,z,\tau) \tag{8-14}$$

Inserting (8-12a) and (8-13) into (8-11a) and equating the coefficients of $\dot{\delta}(\cdot)$ also gives (8-14). However, equating the coefficients of $\delta(\cdot)$ gives the additional condition

$$\partial\tilde{v}_z(x,y,z,\tau)/\partial z = \tilde{a}_z(x,y,z,\tau)/c_o - (2/\rho c_o^2)(\partial/\partial t)\tilde{p}(x,y,z,\tau) \tag{8-15}$$

The layer stripping algorithm thus consists of (8-11) for updating

$\tilde{v}_z(x,y,z,\tau)$ in depth (note that the entire time function $\tilde{v}_z(x,y,z,t)$ is not updated; only its $t = \tau$ value), and (8-14) for computing $\rho(x,y,z)$ at the updated depth. At each depth, these updates are performed for all x, y, and t, point-by-point.

Note that the extra condition (8-15) is necessary in order to use (8-14) to recover $\rho(x,y,z)$. It is unfortunate that $\tilde{a}_z$, rather than $\tilde{v}_z$, must be used in the updates (8-11), since the additional condition (8-15) is now required. However, an attempt to formulate the algorithm using p and v_z exclusively leads to terms of the form $\partial^2 v_z/\partial z \partial t$, which are clearly inadmissible.

Note that the condition (8-14) is essentially an impedance reconstruction taking place in a higher dimensional problem (compare (8-14) to (2-78)). Also note that the partial derivatives with respect to x and y can all be eliminated by taking Fourier transforms with respect to these variables. This results in the recovery of $\rho(k_x, k_y, z)$, which is then inverse Fourier transformed to get $\rho(x,y,z)$. However, this would introduce a plethora of convolution integrals. A Fourier transform with respect to t would eliminate the partial derivatives with respect to t, but would require that (8-14) be replaced by

$$\rho(x,y,z)c_o = \lim_{\omega \to \infty} \hat{p}(x,y,z,\omega)/\hat{v}_z(x,y,z,\omega) \qquad (8\text{-}16)$$

which is also not a desirable numerical operation.

Finally, this algorithm is simple because the wave front, along which the reconstruction takes place, is a simple plane whose location $z = c_o t$ is known at all times. This is a direct consequence of the assumption of a constant wave speed throughout the medium. When this assumption is

relaxed, as it is in the next two sections, considerable effort must go into tracking the wave front, and the algorithms become more complex.

8.3 Reconstruction of c(x,z) for Constant Density

The problem considered in this section is formulated in the exact same way that the problem of Section 8.2 is formulated, except that now the density $\rho(x, z) = \rho_o$ is constant and the wave speed c(x,z) varies, and the problem is now a 2-D problem. However, this means that the wave front is no longer planar, and the inverse problem algorithm must not only reconstruct c(x,z), but must track the wave front, and convert the values of c reconstructed along the wave front into functions of x and z. These additional tasks are accomplished by a variation of 2-D ray tracing that could be referred to as wave front tracing.

Change of coordinates

Once again, the basic approach is to use the method of characteristics of Section 2.3.5. However, we now make a change of coordinates from (x,z) to (s,e), which are time-varying curvilinear coordinates defined so that s is normal to the wave front and e is tangent to it (see Figure 8.1). The initial wave front is assumed to be planar and coinciding with the surface; other excitations will lead to different coordinates (s, e). These new coordinates are further defined as coinciding with the x and z coordinates, respectively, at t = 0, and as undergoing no scale or length changes as time varies. Thus the coordinates (s,e) amount to a simple rotation of the coordinates (x,z), and this rotation varies continuously with t. The coordinates (s,e) are discussed in Aki and Richards (1980, p. 94).

It is important to recognize that there are no scale changes in

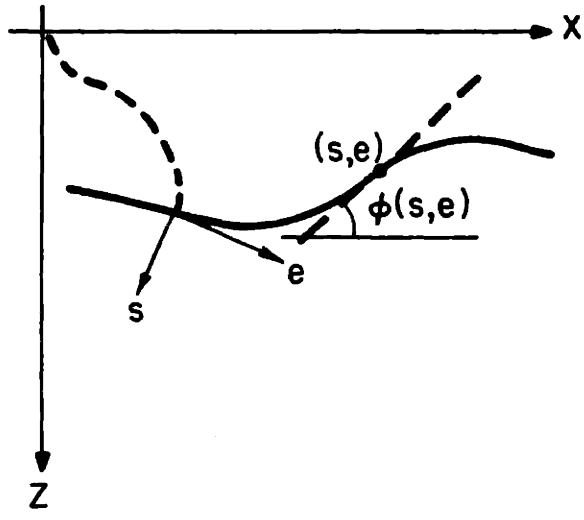

8.1 Definition of coordinates s and e.

changing from the coordinates (x,z) to (s,e), since it is these scale changes that account for the complexity of the general formulae for divergence, curl, and gradient expressed in curvilinear coordinates. For example, the change from the rectangular coordinates (x,y) to the polar coordinates (r,s), where $s = r\theta$, amounts to a rotation through an angle θ, and then scaling the s coordinate by r. No such scale change takes place in the present problem, so the basic acoustic equations (8-10) become simply

$$\partial^2 p/\partial t^2 = -\rho_o c^2(\partial a_s/\partial s + \partial a_e/\partial e) \qquad (8\text{-}17a)$$

$$\partial p/\partial e = -\rho_o a_e \qquad (8\text{-}17b)$$

$$\partial p/\partial s = -\rho_o a_s \qquad (8\text{-}17c)$$

where a_s and a_e are the respective s and e components of the medium acceleration and $\rho(x,z) = \rho_o$ is constant.

Now, the coordinate s represents the arc length along a ray path, and e picks out both a point on the wave front and the ray path leading from the corresponding surface point to that point. Here we use the term "ray paths" to mean the characteristic curves associated with the characteristic surface, which is the wave front. This means that the ray paths are defined as the orthogonal complements to the family of surfaces consisting of the wave front locations for various values of t. Note that although these ray paths are defined in the same way that rays are defined in WKBJ theory, there is an important distinction. Here we are <u>not</u> assuming that energy is propagated from point to point in the medium along rays; we are simply using them to reference

locations within the medium. This explains the use of the term "ray path" rather than ray to emphasize this difference.

Thus the ray paths are defined by the propagation of the wave front, and constitute a simple grid (although a rather twisted one) for specifying locations within the medium. The location of the wave front at any time t is specified by the equation

$$\tau(s,e) = \int_o^s d\sigma/c(\sigma,e) = t \qquad (8\text{-}18)$$

where $\tau(s,e)$ is the travel time. Note that $\tau(s,e)$ depends only on s on the wave front, since the wave front has the property (8-18) at all points. Of course s varies along the wave front, since some ray paths pass through faster portions of the medium than others, and thus travel farther in time t. Defining τ undoes this variation of s.

The point of all this is to show that on the wave front (which is the only place the equations are actually used), a change of variables from s to τ amounts to a simple scaling of $\partial p/\partial s$ and $\partial a_s/\partial s$ by $\partial\tau/\partial s = 1/c$. If we make this change and also define

$$\pi(\tau,e,t) = p(\tau,e,t)/\rho_o \qquad (8\text{-}19)$$

equations (8-17) become, on the wave front,

$$\partial^2\pi/\partial t^2 = -c^2(\partial a_e/\partial e) - c(\partial a_\tau/\partial\tau) \qquad (8\text{-}20a)$$

$$\partial\pi/\partial e = -a_e \qquad (8\text{-}20b)$$

$$\partial\pi/\partial\tau = -ca_\tau \ . \qquad (8\text{-}20c)$$

Layer stripping algorithm

Inserting (8-20b) into (8-20a) and eliminating a_e yields

$$\partial a_\tau/\partial\tau = c(\partial^2\pi/\partial e^2 - (\partial^2\pi/\partial t^2)/c^2) \qquad (8\text{-}21a)$$

$$\partial\pi/\partial\tau = - ca_\tau \quad . \qquad (8\text{-}21b)$$

Now we use the method of characteristics. For any type of probing acoustic wave, we have

$$\pi(\tau,e,t) = \tilde{\pi}(\tau,e,t)1(t-\tau) \qquad (8\text{-}22a)$$

$$v_\tau(\tau,e,t) = \tilde{v}_\tau(\tau,e,t)1(t-\tau) \qquad (8\text{-}22b)$$

where v_τ is the τ-component of the medium velocity. Equations (8-22) have the same forms as (8-12), and do so for the same reasons.

Proceeding as with (8-13) - (8-15), we find that equating coefficients of $\delta(\cdot)$ and $\dot{\delta}(\cdot)$ when (8-22) are substituted into (8-21) results in

$$c(\tau,e) = \tilde{\pi}(\tau,e,\tau)/\tilde{v}_\tau(\tau,e,\tau) \qquad (8\text{-}23a)$$

$$(\partial/\partial\tau)\tilde{v}_\tau(\tau,e,\tau) = \tilde{a}_\tau(\tau,e,\tau) - (2/c)(\partial/\partial t)\tilde{\pi}(\tau,e,\tau) \quad . \qquad (8\text{-}23b)$$

Note once again that the additional condition (8-23b) is required in order to make use of the impedance reconstruction (8-23a).

The layer stripping algorithm thus consists of (8-21) for updating π and v_τ in τ, and (8-23) for obtaining $c(\tau,e)$. The algorithm is quite similar to that of Section 8.2, with the updates taking place point by point for all e and t along the wave front, the wave speed $c(\tau,e)$

being reconstructed along the wave front, and the wave front then propagated forward in τ. The only problem is that $c(\tau,e)$ must somehow be translated into $c(x,z)$. This can be done concurrently with the layer stripping algorithm, as we now show.

Wave front tracing

Let $\phi(\tau,e)$ be the angle between a tangent to the wavefront at the point (τ,e) and the (horizontal) x-axis (see Figure 8.1). Clearly the wavefront will advance locally in the direction $\phi - 90°$.

Now, ϕ is of course a function of e, unless the medium is homogeneous. But ϕ changes with τ due to variation of the wave speed c along the wavefront--without such variation, the wavefront would retain its shape. This allows the derivation of an update equation for ϕ. From Figure 8.2, we have

$$\tan(\phi(\tau+\delta\tau,e) - \phi(\tau,e)) = (c(\tau,e+\delta e) - c(\tau,e))\delta\tau/\delta e \qquad (8\text{-}24)$$

and letting $\delta\tau$ and δe go to zero yields

$$\partial\phi(\tau,e)/\partial\tau = \partial c(\tau,e)/\partial e \quad . \qquad (8\text{-}25)$$

This equation is an update equation for ϕ, since $c(\tau,e)$ is assumed to be known at τ for all e, hence $\partial c/\partial e$ may be computed (although this computation is not very stable).

Now, suppose the coordinates (x,z) associated with the point (τ,e) are known for all e. When τ is incremented by Δ, these coordinates will change slightly, by amounts δx and δz. But clearly

$$\delta x(\tau,e) = c(\tau,e)\ \Delta \sin\phi(\tau,e) \qquad (8\text{-}26a)$$

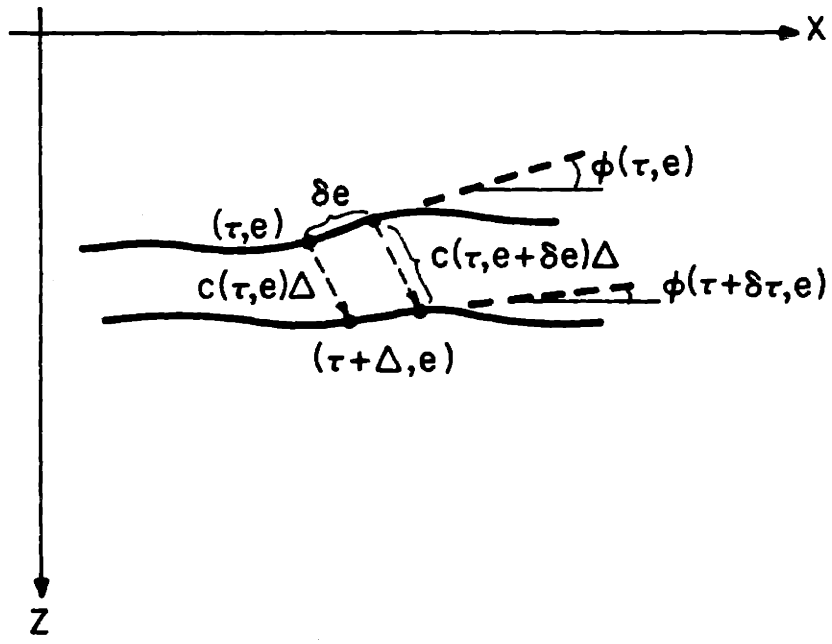

8.2 Derivation of update equation for ϕ.

$$\delta z(\tau,e) = c(\tau,e)\ \Delta \cos \phi(\tau,e). \qquad (8\text{-}26b)$$

This allows c(x,z) to be computed recursively, as follows:

Given: $c(\tau,e)$, $x(\tau,e)$, $z(\tau,e)$, $\cos \phi(\tau,e)$, $\sin \phi(\tau,e)$.
Update all quantities in τ. Each step is done for all e.

(1) Update $\cos \phi$ from $\partial(\cos \phi)/\partial \tau = -(\sin \phi)\partial c/\partial e$ (8-27)

(2) Update $\sin \phi$ from $\partial(\sin \phi)/\partial \tau = (\cos \phi)\,\partial c/\partial e$ (8-28)

(3) Update x and z from (8-26)

(4) Update $c(\tau,e)$ by the algorithm (8-21) - (8-23)

(5) Update $c(\tau + \Delta,e)$, $x(\tau + \Delta,e)$, $z(\tau + \Delta,e)$ as c(x,z). This is quite suitable for plotting.

Note that (8-25) has been used in (8-27) and (8-28), and that $\phi(0,e)$ is initialized to zero.

It might seem that generalizing this algorithm to an inverse 3-D problem algorithm that would reconstruct c(x,y,z) would require the trivial addition of another coordinate e_2, so that (x,y,z) becomes (s,e_1,e_2), where e_1 and e_2 specify a ray and a location on the wave front. However, Aki and Richards (1980, p. 95) have pointed out that it is not possible to select such coordinates so that e_1 and e_2 are always orthogonal in general inhomogeneous media. The reason for this is that in such media a given ray is no longer confined to a single plane, but may twist around like a corkscrew (Aki and Richards, 1980, p. 100). Thus rays can twist around each other, and if (e_1,e_2) is assigned to a single ray and also to the point on the wave front through which the ray passes, the angle between e_1 and e_2 will in general change with time and the wave front. Since e_1 and e_2 are no longer orthogonal, the equations corresponding to (8-17) will become vastly more complicated. Thus, it

seems unlikely that layer stripping methods can be used to solve 3-D inverse problems.

However, there are still several salient points to the above 2-D algorithm. First, of course, is that it is an exact method, unlike the Born approximation methods. Second, it is not ill-posed, unlike methods that require the scattering amplitude of the medium for all angles. Third, it does not require the assumption of high frequencies, geometrical seismics, and energy propagation along rays, as do WKBJ and ray tracing methods. For this reason, the algorithm can handle caustics, which are points where rays are focused and intersect. WKBJ methods have difficulty with caustics, since the geometrical spreading function is zero at a caustic, which makes the amplitude blow up. The layer stripping algorithm encounters caustics as cusps in the wave front, but the arc length e around the cusp is still defined. The angle $\phi(\tau,e)$ is discontinuous in e at a cusp, but this presents no problem.

The only assumptions being made in the use of the layer stripping algorithm are the validity of the basic equations (8-10) and the concept of causality, which manifests itself in the assumption that there is in fact a wave front. The wave front traces out orthogonal complements (the ray paths) as time advances. Also, it is necessary to assume that ρ and c are smooth functions, so that the various partial derivatives in the algorithm are all well defined.

8.4 Generalizations of One-Dimensional Results to Higher Dimensions

In this section it is shown how the basic results for the 1-D problems examined in Chapters III and IV generalize to higher dimensions. First, the non-normal incidence problem and algorithm of Chapter IV are each

generalized a full dimension. The present algorithm recovers $\rho(x,z)$ and $c(x,z)$ separately from the reflection responses of the medium to two impulsive plane waves travelling in the y-direction and incident at two different angles. Next, the well-known result noted in Chapter III that only the impedance $\rho c(\tau)$ as a function of travel time τ can be recovered from the response of a layered medium to a plane wave at normal incidence is generalized. For the 2-D problem, it is shown how the impedance $\rho c(\tau)$ as a function of travel time along rays can be recovered from the medium's response to a plane wave at normal incidence.

8.4.1 The Two-Dimensional Non-Normal Incidence Problem

Here the non-normal incidence problem and algorithm of Chapter IV which resulted in recovery of the separate profiles $\rho(z)$ and $c(z)$ is generalized a full dimension. Recall that in the problem given in Chapter IV impulsive plane pressure waves were incident upon a 2-D medium with 1-D material parameter variation, viz. $\rho(z)$ and $c(z)$. Running this experiment twice, at two different angles of incidence, allowed the recovery of $\rho(z)$ and $c(z)$ separately. A generalization of this experiment will now allow $\rho(x,z)$ and $c(x,z)$ to be recovered separately.

The problem set-up is as described in Chapter IV, only now $\rho(x,z)$ and $c(x,z)$ are functions of one lateral coordinate as well as depth, and the impulsive plane wave now has a normal lying in the y-z plane, where y is the other lateral coordinate. This may be visualized as a horizontal stack of identical inhomogeneous plates, with the normal to the impulsive plane wave having components in the direction of the stacking and in the direction of increasing depth. This problem is often

referred to as the $2\frac{1}{2}$ dimensional problem.

Recall the basic acoustic equations (8-10)

$$\partial^2 p/\partial t^2 = - \rho c^2 (\partial a_x/\partial x + \partial a_y/\partial y + \partial a_z/\partial z) \tag{8-29a}$$

$$- \rho a_x = \partial p/\partial x \tag{8-29b}$$

$$- \rho a_y = \partial p/\partial y \tag{8-29c}$$

$$- \rho a_z = \partial p/\partial z \quad . \tag{8-29d}$$

Proceeding as in Chapter IV, the fact that $\rho(x,z)$ and $c(x,z)$ do not vary with y means that if the medium is subject to an impulsive plane wave whose Fourier transform for $z < 0$ (above the surface) is $e^{-j(k_x x + k_y y + k_z z)}$, then the wave number k_y will not vary with x and z either above the surface or below it. Hence the Fourier transform of the pressure takes the form

$$\hat{p}(x,y,z,\omega) = \hat{\psi}(x,z,\omega)\, e^{-jk_y y} = \hat{\psi}(x,z,\omega)\, e^{-j\omega y \sin\theta_i/c_0} \tag{8-30}$$

where θ_i is the angle of incidence for the plane wave and c_0 is the (homogeneous) wave speed for $z < 0$ (above the surface).

Taking Fourier transforms of (8-29) with respect to t, substituting (8-30), defining

$$\cos^2 \theta_i(x,z) = 1 - c(x,z)^2 \sin^2 \theta_i/c_0^2 \quad , \tag{8-31}$$

and converting back to the time domain yields, in analogy to (4-23),

$$(\partial^2 p/\partial t^2) \cos^2 \theta_i(x,z) = - \rho c^2 (\partial a_x/\partial x + \partial a_z/\partial z) \quad . \tag{8-32}$$

Note that $\theta_i(x,z)$ can be interpreted as the angle between the tangent to the actual ray path at a point (x,y,z) and its projection on the x-z plane. Compare this to $\theta(z)$ in (4-24), which was the angle between the tangent to the ray path at depth z and the z-axis. Equation (8-32) shows that the problem has been reduced from a 2-D problem embedded in a 3-D medium to a 2-D problem embedded in a 2-D medium.

Since the partial derivatives in (8-29) and (8-32) constitute a gradient and divergence, respectively, they must (taken collectively) be independent of the choice of coordinates. Thus we may change from x and z to the time-varying curvilinear coordinates s and e, where s is normal to the (2-D) wave front and e is tangent to it, as before. Note that these coordinates will be the same for both experiments.

Writing (8-29) and (8-32) in terms of s and e yields

$$(\partial^2 p/\partial t^2) \cos^2 \theta_i(s,e) = - \rho c^2 (\partial a_s/\partial s + \partial a_e/\partial e) \qquad (8\text{-}33a)$$

$$- \rho a_s = \partial p/\partial s \qquad (8\text{-}33b)$$

$$- \rho a_e = \partial p/\partial e \qquad (8\text{-}33c)$$

where a_s and a_e are the components of acceleration in the appropriate directions. Eliminating a_e gives

$$(\partial^2 p/\partial t^2) \cos^2 \theta_i(s,e) = - \rho c^2 (\partial a_s/\partial s) + c^2 \partial^2 p/\partial e^2 - (c^2/\rho)(\partial \rho/\partial e)(\partial p/\partial e) \qquad (8\text{-}34)$$

and defining the travel times

$$d\tau/ds = 1/c(s,e) \qquad (8\text{-}35)$$

$$d\tau_i/d\tau = \cos \theta_i(s,e) \quad , \quad i = 1, 2 \qquad (8\text{-}36)$$

for two experiments with initial angles of incidence θ_1 and θ_2 allows the pressure and medium velocity to be written in the forms (compare to (8-22))

$$v_s^i(\tau,e,t) = \tilde{v}_s^i(\tau,e,t)\ 1(t-\tau_i) \tag{8-37a}$$

$$p^i(\tau,e,t) = \tilde{p}^i(\tau,e,t)\ 1(t-\tau_i) \tag{8-37b}$$

where p^i is the pressure field resulting from the experiment at angle of incidence θ_i, and similarly for v_s^i.

Proceeding once again as with (8-13) - (8-15), we substitute (8-35) - (8-37) into (8-34) and (8-33b) and equate coefficients of $\delta(\cdot)$ and $\dot{\delta}(\cdot)$. This results in

$$\rho c(\tau,e)/\cos\theta_i(\tau,e) = \tilde{p}^i(\tau,e,\tau_i)/\tilde{v}_s^i(\tau,e,\tau_i) \tag{8-38a}$$

$$(\partial/\partial\tau)\tilde{v}_s^i(\tau,e,\tau_i) = \tilde{a}_s(\tau,e,\tau_i) - (2\cos\theta_i(\tau,e)/(\rho c))(\partial/\partial t)\tilde{p}^i(\tau,e,\tau_i) \tag{8-38b}$$

which should be compared to (8-23).

Equations (8-33b), (8-34) - (8-36), and (8-38) taken together thus constitute a differential algorithm for computing $\rho(\tau,e)$ and $c(\tau,e)$, with the update taking place as an increment in the ray path travel time τ. The algorithm may be summarized as follows:

Given: $p^i(\tau,e,t)$, $a_s^i(\tau,e,t)$, $\rho(\tau,e)$, $c(\tau,e)$, $\cos\theta_i(\tau,e)$, $v_s^i(\tau,e,\tau_i)$
$\tau_i(\tau,e)$, $i = 1,2$.

Update all quantities in τ.

Each step is done pointwise for all e and t.

(1) Update p^i : $\partial p^i/\partial\tau = -\rho c\, a_s^i$ (8-39)

(2) Update a_s^i : $\partial a_s^i/\partial\tau = -[(\partial^2 p^i/\partial t^2)\cos^2\theta_i(\tau,e) - c^2\partial^2 p^i/\partial e^2 + (c^2/\rho)(\partial\rho/\partial e)(\partial p^i/\partial e)]/(\rho c)$ (8-40)

(3) Update v_s^i: $\partial v_s^i/\partial\tau = a_s^i(\tau,e,\tau_i) - (2\cos\theta_i(\tau,e)/(\rho c))\partial/\partial t)p^i(\tau,e,\tau_i)$ (8-41)

(4) Update τ_i : $\partial\tau_i/\partial\tau = \cos\theta_i(\tau,e)$ (8-42)

(5) Compute U : $U(\tau^+,e) = \left[\frac{p^2}{v_s^2}(\tau^+,e,t=\tau_2^+)\Big/\frac{p^1}{v_s^1}(\tau^+,e,t=\tau_1^+)\right]^2$ (8-43)

(6) Compute c : $c(\tau^+,e) = c_0[(U-1)/(U\sin^2\theta_2 - \sin^2\theta_1)]^{\frac{1}{2}}$ (8-44)

(7) Compute $\cos\theta_i$: $\cos\theta_i(\tau^+,e) = [1 - c(\tau^+,e)^2/c_0^2\sin^2\theta_i]^{\frac{1}{2}}$ (8-45)

(8) Compute ρ: $\rho(\tau^+,e) = p^1(\tau^+,e,t=\tau_1^+)\cos\theta_1(\tau^+,e)/c(\tau^+,e)$. (8-46)

This algorithm bears a marked resemblance to the corresponding algorithm (4-37) - (4-44), and it is not difficult to see why. In the 1-D offset problem algorithm updates similar to those above were carried out as the planar projected wave front advanced from depth z to depth $z + \Delta$. In the 2-D offset problem the projected wave front is no longer a flat plane, but is described at time t by the equation $\tau(x,z) = t$. Hence the increment occurs in ray path travel time τ, which by definition is the same for all rays, i.e., all along the wave front. When τ is incremented, the wave front advances slightly, and (8-39) - (8-46) generate $\rho(\tau + \Delta,e)$ and $c(\tau + \Delta,e)$. The wave front tracing procedure (8-26) - (8-28) can then be used to generate $\rho(x,z)$ and $c(x,z)$ for each τ, i.e., throughout the medium.

8.4.2 The Two-Dimensional Normal Incidence Problem

It is known (see Chapter III) that for the 1-D inverse seismic problem

in which an impulsive plane wave is normally incident on a 1-D medium, and the upgoing wave at the surface measured, then the only information about the medium that can be reconstructed exactly is the impedance as a function of travel time, viz. $\rho c(\tau)$. How might this result generalize to higher dimensions?

Rewriting equations (8-17) in terms of displacement $\underset{\sim}{u}$ rather than acceleration $\underset{\sim}{a}$, we have

$$p = - \rho c^2 \, (\partial u_s/\partial s + \partial u_e/\partial e) \tag{8-47a}$$

$$\partial p/\partial s = - \rho \, \partial^2 u_s/\partial t^2 \tag{8-47b}$$

$$\partial p/\partial e = - \rho \, \partial^2 u_e/\partial t^2 \tag{8-47c}$$

where u_s and u_e are components of displacement in the appropriate directions. Now, in the 1-D case changing variables from depth to travel time resulted in a set of equations entirely in terms of the impedance $\rho c(\tau)$, which allowed recovery of this quantity by layer-stripping. Unfortunately, this is <u>not</u> possible for (8-47), since e would also have to be differentially scaled by c, and this brings in other terms. And as long as ρ and c are present separately in these equations, there is no way they can be propagated from knowledge (from the first reflection) of their product ρc alone.

The solution here is to recognize an implicit feature of the 1-D inverse seismic problem: Since the problem takes place along a single vertical ray path, only acoustic (i.e., P-wave) wave propagation along this path need be considered. In the 2-D case, this is tantamount to considering only acoustic wave propagation along a ray path. From the nature of acoustic wave propagation, this means that u_e is negligible

(Aki and Richards, 1980, p. 95). (Note that this assumption would simplify the algorithms of the preceding sections.) With this assumption, equations (8-47) become

$$p = - \rho c^2 \, \partial u_s / \partial s \tag{8-48a}$$

$$\partial p / \partial s = - \rho \, \partial^2 u_s / \partial t^2 \tag{8-48b}$$

which have the same form as the basic 1-D equations. Defining outgoing and incoming waves as

$$O(s,e,t) = p / \sqrt{\rho c} + \sqrt{\rho c} \;\; \partial u_s / \partial t \tag{8-49a}$$

$$I(s,e,t) = p / \sqrt{\rho c} - \sqrt{\rho c} \;\; \partial u_s / \partial t \tag{8-49b}$$

and assuming an impulse present in the outgoing wave yields the fast Cholesky equations of the 1-D problem

$$(\partial / \partial \tau + \partial / \partial t) \; O(\tau,e,t) = - \; r(\tau,e) \; I(\tau,e,t) \tag{8-50a}$$

$$(\partial / \partial \tau - \partial / \partial t) \; I(\tau,e,t) = -r(\tau,e) \; O(\tau,e,t) \tag{8-50b}$$

$$r(\tau,e) = 2I(\tau,e,\tau) \tag{8-50c}$$

now applied along each ray (i.e., for each e). Thus instead of reconstructing $\rho c(\tau)$, we now reconstruct $\rho c(\tau,e)$.

A variation on the 1-D problem provides for pure shear wave propagation, with $\rho c(\tau)$ again being reconstructed. For the 2-D problem, we simply neglect u_s instead of u_e. Since (8-47) are symmetric in u_s and u_e, the result is once again a fast Cholesky algorithm which reconstructs $\rho c(\tau,e)$.

As in the 1-D problem, some sort of non-normal incidence experiment, involving the medium responses to impulsive plane waves at two different angles of incidence, is necessary in order to reconstruct ρ and c separately, and as functions of x and z. The 2-D non-normal incidence problem where the normal to the plane wave lies in the (y,z) plane was solved in the previous section. More desirable would be a solution to the 2-D problem where the normal to the plane wave lies in the (x,z) plane (so that all of the action takes place in this plane), but there seems to be no way to relate the different wave front histories resulting from the two experiments to each other.

In this chapter some progress has been made in applying layer stripping ideas to higher dimensional problems. The results included workable algorithms for reconstructing $\rho(x,y,z)$ with wave speed constant and $c(x,z)$ with density constant from normal incidence data, and $\rho(x,z)$ and $c(x,z)$ from non-normal incidence data. In addition, a familiar 1-D result has been generalized to a 2-D result. However, the complex geometry of a wave front in a medium in which the wave speed varies with x, y, and z makes it seem unlikely that layer stripping algorithms can be derived for general 3-D problems.

REFERENCES FOR CHAPTER VIII

K. Aki and P.G. Richards, Quantitative Seismology, Theory and Methods, W.H. Freeman and Co., San Francisco, 1980.

A.J. Berkhout, Seismic Migration, Elsevier, Amsterdam, 1982.

R.W. Clayton and R.H. Stolt, "A Born-WKBJ Inversion Method for Acoustic Reflection Data," Geophysics 46(11), 1559-1567 (1981).

J. K. Cohen and N. Bleistein, "Velocity Inversion Procedure for Acoustic Waves," Geophysics 44(6), 1077-1087 (1979).

A.J. Devaney, "Geophysical Diffraction Tomography," IEEE Trans. Geoscience and Remote Sensing GE-22(1), 3-13 (1984).

C. Morawetz and G. Kriegsmann, "The Calculations of an Inverse Potential Problem," SIAM J. Appl. Math. 43(4), 844-854 (1983).

R.G. Newton, "Inverse Scattering. II. Three Dimensions," J. Math. Phys. 21(7), 1698-1715 (1980).

R. Raz, "A Procedure for Multidimensional Inversion of Seismic Data," Geophysics 47(10), 1422-1430 (1982).

W. Symes, "An Inversion Method for a Three-Dimensional Wave Equation Problem," presented at the Workshop on Computational Methods in Ill-Posed and Inverse Problems, Cornell University, July 1983.

A. Yagle, "Notes on Layer Stripping Solutions of Higher Dimensional Inverse Seismic Problems," Tech. Report # LIDS-P-1347, Laboratory for Information and Decision Systems, MIT (1983).

CHAPTER IX

Conclusion

9.1 Summary

In this thesis the concept of layer stripping has been applied to a wide variety of inverse seismic problems. The goal of this thesis, which was to show that layer stripping could lead to fast algorithms for the solutions of many more inverse problems than has been generally realized, has thus been accomplished.

Prior to this thesis, virtually all applications of the layer stripping concept were made solely to the one-dimensional inverse problem at normal incidence. The resulting dynamic deconvolution algorithms were generally considered to be entirely unrelated to the usual integral equation (for continuous media) or matrix equation (for discrete media) methods for solving this problem, and it was also generally believed that such algorithms would quickly blow up due to the accumulation of noise within them.

The work of Bruckstein et al. (1983) showed that layer stripping algorithms are in fact closely related to the integral/matrix equation methods, and that their simplicity and physical interpretability are in fact closely related. Furthermore, the breakdown of such algorithms after a large number of layers is due more to the poor conditioning of the inverse problem at those depths than to any fault in the algorithms themselves, as noted in Bruckstein et al. (1984). Computer runs of the algorithms on synthetic data in Symes and Zimmerman (1982) and Bube and Burridge (1983) showed that the algorithms were numerically better

behaved than had previously been suspected. But throughout all of this, attention was still focused on the one-dimensional inverse problem at normal incidence.

In this thesis the scope of applicability of layer stripping has proven to be much wider than just this one problem. To mark this in detail, the results of this thesis are now reviewed.

In Chapter II the general symmetric two-component wave system inverse scattering problem was defined and shown to be solved by a coterie of layer stripping algorithms. The fast Cholesky algorithm involved leftgoing and rightgoing waves in the time domain, the Schur algorithm involved these same waves in the frequency domain, and the dynamic deconvolution algorithm involved the reflection coefficient for the unknown part of the medium. These three mathematically equivalent algorithms all reconstructed the scattering medium using the principle of causality: the first reflection from the medium at any depth gave the value of the reflectivity function at that depth. All three algorithms only require $0(N^2)$ computations to reconstruct the medium, hence they may be considered fast algorithms.

Also in Chapter II, two coupled fast Cholesky algorithms (or two coupled Schur or dynamic deconvolution algorithms) were shown to solve the inverse scattering problem for an asymmetric two-component wave system, and other fast algorithms for reconstructing the potential of a Schrodinger equation were derived.

Various integral equation methods of solving these problems were also derived, and a fast algorithm (the Krein-Levinson algorithm) was shown to solve these integral equations by exploiting the Toeplitz or Hankel structure of their kernels. The relations between the layer

stripping fast algorithms, which reconstruct the medium and the waves in it directly, and the Krein-Levinson fast algorithm, which solves the integral equations for reconstructing the medium, were discussed in detail. The results of Chapter II were illustrated with three examples: the non-uniform transmission line without losses; the non-uniform line with losses; and the linear least-squares estimation of a stationary stochastic process.

The results of Chapter II were further illustrated by the results of Chapter III, which collected together a wide variety of methods for solving the one-dimensional inverse seismic problem at normal incidence. Layer stripping solutions for both discrete and continuous media were derived, and integral and matrix solutions for, respectively, continuous and discrete media were also derived. This illustrated dramatically the duality between the two approaches, as discussed in Chapter II.

In Chapter IV the one-dimensional inverse seismic problem involving impulsive plane waves obliquely incident on a layered medium was considered. Fast, layer stripping algorithms were derived for both discrete and continuously varying media. The difference between the two algorithms lay in the update equations for the medium parameters, which were more complicated for a discrete medium. Although the additional complexity is trivial for this problem, the additional complexity of the discrete medium parameter updates for an elastic medium increases the complexity of that algorithm to the point where it is no longer a fast algorithm. A layer stripping solution for an impulsive point source excitation, involving probing with cylindrical waves, and a procedure for propagating the layer stripping algorithms through a turning point, in order to use more of the reflection response data, were also given.

In Chapter V the performance of the layer stripping algorithms of Chapter IV on synthetically generated data was investigated. In the absence of noise, the continuous and discrete medium algorithms, and their Schur and dynamic deconvolution counterparts, performed quite well. The continuous medium parameter updates did not work well when applied to a discrete medium, as expected.

Several modifications of the layer stripping algorithms for use with noisy data were discussed. These included the use of a threshold based on the condition number for zeroing false reflection coefficients, and the use of reflection data at several angles of incidence to compute a least-squares fit for the updated medium parameters at each depth. The former modification proved to be useful for thickly layered media in which many of the reflection coefficients are zero, while the latter modification proved to be very useful in general. The effect of noise on the performance of the algorithm was illustrated with a series of plots for three different signal-to-noise ratios; the algorithm does in fact work in the presence of small amounts of additive noise.

In Chapter VI the two sets of 2 x 2 systems of coupled equations used for the preceding problem are generalized to two 4 x 4 systems of coupled equations for the elastic problem. This is necessary because there are now four different types of waves propagating through the medium: up- and down-going P and S waves. And all of these waves couple to one another.

Fortunately, symmetries in the couplings between different wave types imply that these couplings can be described by three reflectivity functions and one transmissivity function. And the transmissivity function can be determined from the three reflectivity functions. Thus there are

three reflectivity functions and three quantities of interest: the Lamé parameters $\lambda(z)$ and $\mu(z)$; and the density $\rho(z)$. These quantities are differentially related, so that update equations for $\lambda(z)$, $\mu(z)$, and $\rho(z)$ in terms of the reflectivity functions can be obtained.

However, obtaining the reflectivity functions themselves requires that two experiments be run: One with an impulsive P wave source and one with an impulsive S wave source. This is because the determination of the P-P reflectivity function requires an impulsive downgoing P excitation, while determination of the S-S reflectivity function requires an impulsive downgoing S excitation. Hence two interconnected 4 x 4 systems (one for each experiment) are needed.

Other complications are introduced by the different wave speeds of P and S waves, which necessitates different time discretization for P and S waves at each depth. Still, a good understanding of the algorithm may be had by carefully studying Figure 6.1, which shows the interactions between the various waves and how the algorithm updates all four waves from one depth to the next.

It is interesting to note that the transformation to up- and down-going P and S waves was made purely with the derivation of a fast algorithm in mind. Nevertheless, the unique transformation that "diagonalizes" the basic system matrix A(z) in (6-15) to the desired form also normalizes the up- and down-going waves with respect to energy. That this energy normalization can be obtained without any a priori attention to conservation ideas is interesting.

In addition, a dynamic deconvolution form of this 4 x 4 system of coupled equations was derived, and the subsidiary problem of probing an elastic medium from a liquid half-space (so that no S-wave excitations

or measurements of the elastic medium are possible) was solved by probing for three different values of slowness p instead of only one. The basic elastic layer stripping algorithm was tested on synthetic data, and proved to work quite well.

In Chapter VII the layer stripping methodology was applied in a novel way. The inverse problem considered in this chapter was that of reconstructing a layered medium from measurement of its response to a harmonic excitation at two frequencies and all wavenumbers. Note that this problem, which is discussed in Frisk et al. (1981), is dual to that of Chapter IV, in which the layered medium was reconstructed from measurement of its response for all frequencies and two slownesses. Since no impulsive excitation is involved, and all measurements are taken in the sinusoidal steady state, there would seem to be no causality condition for a layer stripping algorithm to exploit.

Nevertheless, a layer stripping algorithm for solving this problem was obtained. In this algorithm, the "waves" are continuous sequences of image sources that simulate the response of the unknown portion of the medium. The causality principle exploited by the algorithm is the necessity of all image sources lying in the unknown part of the medium, outside the region in which they are to simulate a response.

Fast algorithms for two different formulations of this problem (free surface and half-space boundary conditions) were derived using the layer stripping methodology. In addition, the layer stripping solution of Levy (1984) for the mathematically analogous inverse resistivity problem was also presented.

Finally, layer stripping fast algorithm solutions of several higher-dimensional inverse seismic problems were derived in Chapter VIII. For

these problems, the density $\rho(x,z)$ and wave speed $c(x,z)$ are allowed to vary laterally with x as well as with depth z. The first problem considered was to reconstruct a 3-D density $\rho(x,y,z)$ for a medium in which the wave speed c was assumed to be constant throughout. The assumption of a constant wave speed means that the impulsive wave front, along which the reconstruction of ρ takes place, has the simplest possible form: a flat impulsive plane wave moving straight downward at known velocity. This algorithm is intended more to be illustrative of the application of the layer-stripping idea to higher-dimensional problems than to be a practical algorithm.

The second problem considered was that of reconstructing $c(x,z)$ in a medium with constant density. This problem is much more difficult than the first problem, since the variation of $c(x,z)$ means that the shape of the wave front becomes complicated. This makes the problem much harder, and necessitates a form of differential ray tracing in order to interpret the updated quantity as $c(x,z)$.

Next, the offset problem of Chapter IV is generalized a full dimension. Now $\rho(x,z)$ and $c(x,z)$ are to be reconstructed by measuring the response to an impulsive plane pressure wave obliquely incident in the y-direction, for two angles of incidence. Reconstruction of ρ and c again takes place along the wavefront, and again differential ray tracing is necessary to recover $\rho(x,z)$ and $c(x,z)$.

Finally, the 1-D result on reconstruction of the impedance $\rho c(\tau)$ is generalized to higher dimensions. The generalized result is that the impedance can be reconstructed along the wave fronts (or alternately, along the rays), but converting this information into something useful seems to be difficult, considering the paucity of the available information.

9.2 Suggestions for Further Research

There are several avenues along which further research on the application of layer stripping concepts to inverse seismic problems could proceed. In this section we note some of these avenues, and identify several specific topics on which further research is needed.

The most pressing need for further research lies in the area of adapting the various algorithms to function better in the presence of noise. The modifications discussed in Chapter V constitute a start in this direction, but more improvements are needed if the algorithms are to be successful in reconstructing a medium from real-world data. This is particularly important for overcoming the popular conception that layer stripping algorithms do not work on noisy data.

A particularly promising possibility is that of combining the *a priori* approach used in this thesis, in which the updated, computed wave speed is used to project ahead to the computed time at which the next primary reflection should occur, with the *a posteriori* approach used by Habibi-Ashrafi and Mendel (1982), in which a maximum likelihood search for the next primary reflection is carried out using a matched filter. There are advantages and disadvantages to both approaches; a Kalman-filter-like combination of both *a priori* and *a posteriori* information may well prove to be worth the extra computation such a combination would require.

Other possibilities for dealing with noise in the data include incorporating *a priori* knowledge about the medium into the inversion process (this was done in a crude way with the condition number modification of Chapter V, which works best if it is known *a priori* that most of the medium reflection coefficients are zero) and modelling

the medium itself as a random process. However, the inverse problem of estimating a random medium is so difficult that any resulting algorithm might well experience too many numerical difficulties for it to be practical. Incorporating a priori knowledge about the medium is particularly important when the data are bandlimited, as they must always be in real life.

Another avenue of research consists of determining how breakdowns in the assumed model of the medium affects the performance of the algorithms. There is of course no such thing as a truly layered medium; interfaces between layers need not be entirely horizontal. The effect of the presence of small scatterers (e.g., small rocks) within the medium can be modelled crudely as noise, but large inhomogeneities have a separate effect that cannot be passed off. Slowly varying lateral inhomogeneities also affect the medium response by making it a more complicated function of lateral position. Note that all of these departures from the assumed model can be detected by noting how the measured medium response departs from its expected form (e.g., for a plane wave response, $R(x,t) = R(t-x \sin\theta/c_o)$), but how should this be compensated?

A final avenue of research consists of further theoretical extensions of the application of layer stripping ideas to inverse seismic problems. The results of Chapter VII show that layer stripping ideas may be applicable to an inverse problem in wholly unexpected ways. The solution of other higher dimensional inverse seismic problems, in particular the general 3-D problem, may well be possible by layer stripping methods utilized in such an unusual way. The generalized Gel'fand-Levitan approach of Newton (1980) would seem to be a logical

starting point for investigating this topic. Another problem worth investigating is that of reconstructing a medium directly from its transmission response, which might lead to an algorithm for reconstructing a lossy medium better than the one of Chapter V.

REFERENCES FOR CHAPTER IX

A. Bruckstein, B. Levy and T. Kailath, "Differential Methods in Inverse Scattering," Tech. Report, Information Systems Laboratory, Stanford University, 1983.

A.M. Bruckstein, I. Koltracht, and T. Kailath, "Inverse Scattering with Noisy Data," Tech. Report, Information Systems Laboratory, Stanford University, 1984.

K.P. Bube and R. Burridge, "The One-Dimensional Inverse Problem of Reflection Seismology," SIAM Review 25(4), 497-559 (1983).

G.V. Frisk, J.A. Doutt, and E.E. Hays, "Bottom Interaction of Low-Frequency Acoustic Signals at Small Grazing Angles in the Deep Ocean," J. Acoust. Soc. Am. 69, 84-94 (1981).

F. Habibi-Ashrafi and J. Mendel, "Estimation of Parameters in Lossless Layered Media Systems," IEEE Trans. A.C. AC-27(1), 31-48 (1982).

B. Levy, "Layer by Layer Reconstruction Methods for the Earth Resistivity from Direct Current Measurements," Tech. Report # LIDS-P-1388, Laboratory for Information and Decision Systems, MIT, 1984.

R.G. Newton, "Inverse Scattering. II. Three Dimensions," J. Math. Physics 21(7), 1698-1715 (1980).

W. Symes and G. Zimmerman, "Experiments in Impedance Profile Inversion Using Noisy and Band-Limited Data," Amoco Production Co. Research Report No. F82-C-3 (1982).

APPENDIX

Computer Programs

In this Appendix all of the computer programs used to obtain the numerical results of Chapters V - VII are given. The programs are listed in alphabetical order by their names. A brief description of each program is supplied below.

The programs are all written using standard FORTRAN. Input parameters common to all of the programs are as follows:

n = number of layers (including upper and lower half-spaces)

m = $\log_2$ (number of points at which the time and/or frequency response of the medium is computed). m = 9 corresponds to 512 points.

dd = thickness of each layer

del = discretization length Δ

dt = discretization time Δt

p1, p2 = slownesses = $\sin \theta_o / c_o$

a(i) = wave speed in layer i

rho(i) = density in layer i

b(i) = S wave speed in layer i, for ELAS and INVELAS

freq1, freq2 = probing source frequencies, for FORFREQ and INVFREQ

Program Descriptions

BREM: Forward problem program that computes the impulse response of a layered medium directly in the time domain by computing the first two terms of the Bremmer series.

DYNDEC: Reconstructs a layered medium from its frequency responses by using the dynamic deconvolution algorithm.

ELAS: Forward problem program that computes the P→P, P→SV, and SV→SV impulse responses of a layered elastic medium using the reflectivity method (subroutine RECOPS) and inverse Fourier transforms (subroutine FFT).

FOR1: Forward problem program that computes the impulse response of a layered acoustic medium using the reflectivity method (subroutine RECOPP) and an inverse Fourier transform (subroutine FFT).

FORFREQ: Forward problem program that computes the response of a layered medium for two frequencies and all wavenumbers using the reflectivity method (subroutine RECOPP).

INVDISC: Reconstructs a layered medium from its impulse responses by using the fast Cholesky algorithm and discrete medium parameter updates.

INVELAS: Reconstructs a layered elastic medium from its P→P, P→SV, and SV→SV impulse responses by using the algorithm of Section 6.2.

INVFREQ: Reconstructs a layered medium from its response at two frequencies and all wavenumbers using the algorithm of Section 7.2.

INV1: Reconstructs a layered medium from its impulse responses by using the fast Cholesky algorithm and continuous medium parameter updates.

MULTFOR: Forward problem program that computes the impulse response of a layered medium as does BREM, but does so for nm (input parameter) angles of incidence instead of just two.

MULT1: Reconstructs a layered medium from its impulse responses at nm angles of incidence, using a least-squares fit to compute the updated medium parameters (using the continuous medium parameter updates) at each depth.

MULTINV: Reconstructs a layered medium from its impulse responses at nm angles of incidence, by computing updated medium parameters (using the discrete medium parameter updates) for each pair of reflection coefficients, and then averaging the results, at each depth.

NOISE: Takes the impulse response of a layered medium, adds uniformly distributed noise to it (xl = maximum noise amplitude), and then reconstructs the medium using INVDISC. The condition number modification of Section 5.4 is activated by inputting ic = 1.

SCHUR: Reconstructs a layered medium from its frequency responses by using the Schur algorithm.

Program Lists

Program BREM

```
      dimension a(50),rho(50),dt1(50),dt2(50),r1(50),r2(50),tr1(50),tr2
      dimension uw1(1024),uw2(1024)                                    (50)
      read(5,10) n,m,dd,del,dt,p1,p2
10    format(2i,5f)                                                  422
      read(5,11) (a(i),rho(i),i=1,n)
11    format(2f)
      m=2**m
      do 77 i=1,m
      uw1(i)=0.
      uw2(i)=0.
77    continue
      tr1(1)=1.
      tr2(1)=1.
      t11=1.
      t12=1.
      t1=0.
      t2=0.
      z1=a(1)*rho(1)/sqrt(1.-a(1)*a(1)*p1*p1)
      z2=a(1)*rho(1)/sqrt(1.-a(1)*a(1)*p2*p2)
      do 1 i=2,n
c     dt1(i) is 2-way traveltime thru layer i for exp't 1
      dt1(i-1)=2.*dd*sqrt(1.-a(i)*a(i)*p1*p1)/a(i)
      dt2(i-1)=2.*dd*sqrt(1.-a(i)*a(i)*p2*p2)/a(i)
      rho(i-1)=rho(i)
1     continue
c     compute reflection coefficients
      do 2 i=1,n-2
      r1(i)=(rho(i+1)/dt1(i+1)-rho(i)/dt1(i))/(rho(i+1)/dt1(i+1)+rho(i)
     +(i))                                                          /dt1
      r2(i)=(rho(i+1)/dt2(i+1)-rho(i)/dt2(i))/(rho(i+1)/dt2(i+1)+rho(i)
     +(i))                                                          /dt2
c     compute 2-way transmission coefficients
      tr1(i+1)=1.-r1(i)*r1(i)
      tr2(i+1)=1.-r2(i)*r2(i)
2     continue
c     do primaries
      do 3 i=1,n-2
      t1=t1+dt1(i)/dt
      t2=t2+dt2(i)/dt
      t11=t11*tr1(i)
      t12=t12*tr2(i)
      uw1(int(t1+0.5))=r1(i)/dt*t11
      uw2(int(t2+0.5))=r2(i)/dt*t12
3     continue
c     do secondaries
      do 4 n1=2,n-2
      do 5 n2=1,n1-1
      do 6 n3=n2+1,n-2
      nmin=min0(n1,n3)
      nmax=max0(n1,n3)
      t1=0.
      t2=0.
      t11=1.
      t12=1.
      do 7 i=1,nmax
      t1=t1+dt1(i)/dt
      t2=t2+dt2(i)/dt
      t11=t11*tr1(i)
      t12=t12*tr2(i)
      if((i.le.n2).or.(i.gt.nmin)) go to 7
      t1=t1+dt1(i)/dt
      t2=t2+dt2(i)/dt
      t11=t11*tr1(i)
```

```
      t12=t12*tr2(i)
7     continue
      if(int(t1).ge.m)go to 6
      uw1(int(t1+0.5))=uw1(int(t1+0.5))-r1(n1)*r1(n2)*r1(n3)/dt*t11
      if(int(t2).ge.m)go to 6
      uw2(int(t2+0.5))=uw2(int(t2+0.5))-r2(n1)*r2(n2)*r2(n3)/dt*t12
6     continue
5     continue
4     continue
      do 78 i=1,n-2
      z1=z1*(1.+r1(i))/(1.-r1(i))
      z2=z2*(1.+r2(i))/(1.-r2(i))
      write(8,79)a(i+1),rho(i),r1(i),r2(i),z1,z2
79    format(1x,6f10.5)
78    continue
      do 8 i=1,m
      time=time+dt
8     write(7,12) time,uw1(i),uw2(i)
12    format(1x,f7.4,f15.6,4x,f15.6)
      call exit
      end
```

```
      dimension a(50),rho(50),d(50)
      complex rc1(1025),rc2(1025),dtau1,dtau2
c     set ic=0 to skip forward part; read from device #7.
c     set ic=1 to generate forward response and then solve from it.
      read(5,10)n,m,dd,del,df,p1,p2,ic
10    format(2i,5f,i)
      read(5,20)(a(i),rho(i),i=1,n)
20    format(2f)
      write(6,21)n,m,dd,del,df,p1,p2
21    format(1x,'n=',i2,2x,'m=',i2,2x,'dd=',f4.2,2x,'del=',f4.2,2x,
     +'df=',f5.3,2x,'p1=',f4.2,2x,'p2=',f4.2)
      do 1 i=1,n
1     d(i)=dd
      pie=3.1415926536
      m2=2**m
      if(ic.ne.0)go to 53
      read(7,52)(rc1(i),rc2(i),i=1,m2)
      go to 54
53    do 2 i=1,m2
      freq=freq+df
      call recopp(n,a,rho,d,p1,freq,rc1(i))
      call recopp(n,a,rho,d,p2,freq,rc2(i))
      write(7,52)rc1(i),rc2(i)
52    format(1x,4f10.4)
2     continue
54    ac1=a(1)/sqrt(1.-a(1)*a(1)*p1*p1)
      ac2=a(1)/sqrt(1.-a(1)*a(1)*p2*p2)
      z1=rho(1)*ac1
      z2=rho(1)*ac2
      write(6,51)
51    format(3x,'depth',6x,'cact',5x,'ccomp',4x,'rhoact',3x,'rhocomp',4x,
     +'rc1',9x,'rc2')
      do 3 i=1,int(dd/del*n)+5
      dep=dep+del
      sum1=0.
      sum2=0.
      omeg=0.
      do 4 j=1,m2
      omeg=omeg+2.*pie*df
      dtau1=cmplx(0.,2.*omeg*del/ac1)
      dtau2=cmplx(0.,2.*omeg*del/ac2)
      rc1(j)=cexp(dtau1)*(rc1(j)-cmplx(r1,0.))/(1.-rc1(j)*cmplx(r1,0.))
      rc2(j)=cexp(dtau2)*(rc2(j)-cmplx(r2,0.))/(1.-rc2(j)*cmplx(r2,0.))
      sum1=sum1+real(rc1(j))
      sum2=sum2+real(rc2(j))
4     continue
      r1=sum1/m2
      r2=sum2/m2
      z1=z1*(1.+r1)/(1.-r1)
      z2=z2*(1.+r2)/(1.-r2)
      u=z1*z1/z2/z2
      ac=sqrt((u-1.)/(u-p2*p2/p1/p1))/p1
      ac1=ac/sqrt(1.-ac*ac*p1*p1)
      ac2=ac/sqrt(1.-ac*ac*p2*p2)
      rhoc=(z1/ac1+z2/ac2)/2.
```

```
      l=min0(int(dep/dd)+2,n)
      write(6,50)dep,a(l),ac,rho(l),rhoc,r1,r2
50    format(1x,f7.2,6f10.4)
3     continue
      call exit
      end
      subroutine recopp(n,a,rho,d,u,freq,rpp)
      dimension a(n),rho(n),d(n)


      complex rpp,ni,nip,roi,roip,m21,m22,e2,e1,e
      d(1)=0.
      pi=3.1415926536
      omega=2.*pi*freq
      om2=omega*omega
      xk=omega*u
      xk2=xk*xk
      m22=cmplx(1.,0.)
      m21=cmplx(0.,0.)
      do 170 j=1,n
      i=n-j+1
      arg=om2/(a(i)*a(i))-xk2
      if(arg.gt.0.)ni=cmplx(sqrt(arg),0.)
      if(arg.le.0.)ni=cmplx(0.,-sqrt(-arg))
      roi=cmplx(rho(i),0.)
      if(i.eq.n)go to 171
      e1=nip*roi
      e2=ni*roip
      e=cexp(ni*cmplx(0.,2.*d(i)))
      e1=e1*(m21+m22)
      e2=e2*(m21-m22)
      m21=e1+e2
      m22=e*(e1-e2)
      rmax=cabs(m22)
      rm=cabs(m21)
      if(rm.gt.rmax)rmax=rm
      e1=cmplx(1./rmax,0.)
      m22=m22*e1
      m21=m21*e1
171   nip=ni
      roip=roi
170   continue
      rpp=-m21/m22
      return
      end
```

```
      subroutine fft(x,m)
      complex x(1024),u,w,t
      n=2**m
      pi=3.1415926536
      do 20 l=1,m
      le=2**(m+1-l)
      le1=le/2
      u=cmplx(1.,0.)
      w=cmplx(cos(pi/float(le1)),sin(pi/float(le1)))
      do 20 j=1,le1
      do 10 i=j,n,le
      ip=i+le1
      t=x(i)+x(ip)
      x(ip)=(x(i)-x(ip))*u
10    x(i)=t
20    u=u*w
      nv2=n/2
      nm1=n-1
      j=1
      do 30 i=1,nm1
      if(i.ge.j)go to 25
      t=x(j)
      x(j)=x(i)
      x(i)=t
25    k=nv2
26    if(k.ge.j)go to 30
      j=j-k
      k=k/2


      go to 26
30    j=j+k
      return
      end
```

```
      dimension a(50),b(50),rho(50),d(50)
      dimension upp(1024),ups(1024),usp(1024),uss(1024)
      complex rpp(1024),rps(1024),rsp(1024),rss(1024),om
      read(5,10)n,m,dd,del,dt,p
10    format(2i,4f)
      read(5,20)(a(i),b(i),rho(i),i=1,n)
20    format(3f)
      do 1 i=1,n
1     d(i)=dd
      pie=3.1415926536
      m2=2**m
      m22=2*m2
      tfin=m2*dt
      df=1./tfin
      acp=1.-a(1)*a(1)*p*p
      bcp=1.-b(1)*b(1)*p*p
      e=sqrt(a(1)/b(1))*sqrt(sqrt(bcp/acp))
      do 2 i=1,m22-1
      freq=freq+df
      call recops(n,a,b,rho,d,p,freq,rpp(i+1),rps(i+1),rss(i+1),rsp(i+1))
      om=cmplx(0.,freq)*2.*pie
      rpp(i+1)=rpp(i+1)/om
      rps(i+1)=rps(i+1)/om
      rsp(i+1)=rsp(i+1)/om
      rss(i+1)=rss(i+1)/om
      if(i.lt.m2)go to 2
      rpp(i+1-m2)=rpp(i+1-m2)+rpp(i+1)
      rps(i+1-m2)=rps(i+1-m2)+rps(i+1)
      rsp(i+1-m2)=rsp(i+1-m2)+rsp(i+1)
      rss(i+1-m2)=rss(i+1-m2)+rss(i+1)
2     continue
      call fft(rpp,m)
      call fft(rps,m)
      call fft(rsp,m)
      call fft(rss,m)
      upp(1)=2.*real(rpp(1))*df
      usp(1)=-2.*real(rps(1))*df*e
      ups(1)=2.*real(rsp(1))*df/e
      uss(1)=-2.*real(rss(1))*df
      do 3 i=1,m2
      time=time+dt
      upp(i+1)=2.*real(rpp(i+1))*df
      usp(i+1)=-2.*real(rps(i+1))*df*e
      ups(i+1)=2.*real(rsp(i+1))*df/e
      uss(i+1)=-2.*real(rss(i+1))*df
      upp(i)=(upp(i+1)-upp(i))/dt-dcpp
      usp(i)=(usp(i+1)-usp(i))/dt-dcsp
      ups(i)=(ups(i+1)-ups(i))/dt-dcps
      uss(i)=(uss(i+1)-uss(i))/dt-dcss
      dcpp=upp(1)
      dcsp=usp(1)
      dcps=ups(1)
      dcss=uss(1)
      write(7,30)time,upp(i),usp(i),ups(i),uss(i)
30    format(1x,f7.4,f15.6,3f19.6)
3     continue
      call exit
      end
      subroutine recops(n,a,b,rho,d,u,freq,rpp,rps,rss,rsp)
      dimension a(n),b(n),rho(n),d(n)
      complex t1,t2,t3,t4,t5,rpp,rps,rss,rsp,det,cn,cns,t53,t63
     +,t11,t21,t31,t51,t61,t12,t15,t32,t45,t42,t35,t62,t65,t13,t23,t33
      pi=3.1415926536
```

```
      omes=2.*pi*freq
      c=1./u
      rk=omes*u
      n1=n-1
      com=c*omes
      u2=u*u
      c2=c*c
      rk2=rk*rk
      om2=omes*omes
      s=b(n)
      p=a(n)
      rro=rho(n)
      s2=s*s
      p2=p*p
      arsp=1.-c2/p2
      arss=1.-c2/s2
      if(arsp.ge.0.)cn=cmplx(0.,-rk*sqrt(arsp))
      if(arsp.lt.0.)cn=cmplx(rk*sqrt(-arsp),0.)
      if(arss.lt.0.)cns=cmplx(rk*sqrt(-arss),0.)
      if(arss.ge.0.)cns=cmplx(0.,-rk*sqrt(arss))
      r1=2.*rk2-om2/s2
      rpp=cn*cns
      t1=cmplx(-s2*s2*rro/(om2+om2),0.)*(cmplx(4.*rk2,0.)*rpp+
     +cmplx(r1*r1,0.))
      t2=cmplx(0.,0.5)*cn
      t3=cmplx(0.,-s2*u/(2.*omes))*(cmplx(r1,0.)+rpp+rpp)
      t4=cmplx(0.,-0.5)*cns
      t5=cmplx(-1./(2.*rro*om2),0.)*(rpp+cmplx(rk2,0.))
      tr1=real(t1)
      ti1=aimag(t1)
      tr2=real(t2)
      ti2=aimag(t2)
      tr3=2.*real(t3)
      ti3=2.*aimag(t3)
      tr4=real(t4)
      ti4=aimag(t4)
      tr5=real(t5)
      ti5=aimag(t5)
      if(n.lt.3)go to 2000
      do 1000 j=2,n1
      i=n-j+1
      s=b(i)
      s2=s*s
      p=a(i)
      p2=p*p
      thk=rk*d(i)
      arsp=1.-c2/p2
      if(arsp.ge.0.)go to 190
      ra=sqrt(-arsp)
      p=thk*ra
      sp=sin(p)
      cp=cos(p)
      x=ra*sp
180   arss=1.-c2/s2
      if(arss.ge.0.)go to 200
      rb=sqrt(-arss)
      q=thk*rb
      sq=sin(q)
      cq=cos(q)
      z=sq*rb
      go to 210
190   ra=-sqrt(arsp)
      ep=0.5*exp(thk*ra)
```

```
            em=0.25/ep
            sp=ep-em
            cp=ep+em
            x=-sp*ra
            go to 180
200         rb=-sqrt(argg)
            ep=0.5*exp(thk*rb)
            em=0.25/ep
            sq=ep-em
            cq=ep+em
            z=-sq*rb
210         w=sp/ra
            y=sq/rb
            s1=-2.*s2*u2
            s2=s1+1.
            e1=cp*cq
            e2=1.-e1
            e3=w*y
            e4=x*z
            e5=w*cq
            e6=y*cp
            r1=com*rho(i)
            r2=1./r1
            r3=r1*s1
            r4=r1*s2
            f1=e2+e3
            f2=f1*r2
            s16=-r2*(f2+(e2+e4)*r2)
            s13=-r3*s16+f2
            f3=s1*f1+e3
            f4=r3*s13+f3
            s31=r3*f4+f3*r4
            s11=e1-f4
            s33=f4+0.5
            s61=-r3*s31-r4*(e3*r4+f3*r3)
            s15=-r2*(e5+z*cp)
            s23=-r3*s15+e5
            s21=-r3*s23-r4*e5
            s12=r2*(e6+x*cq)
            s32=-r3*s12-e6
            s51=-r3*s32+r4*e6
            s22=e1
            s25=z*w
            s52=x*y
            tr11=tr1*s11+tr2*s21-ti3*s31+tr4*s51+tr5*s61
            ti11=ti1*s11+ti2*s21+tr3*s31+ti4*s51+ti5*s61
            tr22=tr1*s12+tr2*s22-ti3*s32+tr4*s52+tr5*s51
            ti22=ti1*s12+ti2*s22+tr3*s32+ti4*s52+ti5*s51
            tr33=-ti1*s13-ti2*s23+tr3*s33-ti4*s32-ti5*s31
            ti33=tr1*s13+tr2*s23+ti3*s33+tr4*s32+tr5*s31
            tr44=tr1*s15+tr2*s25-ti3*s23+tr4*s22+tr5*s21
            ti44=ti1*s15+ti2*s25+tr3*s23+ti4*s22+ti5*s21
            tr5=tr1*s16+tr2*s15-ti3*s13+tr4*s12+tr5*s11
            ti5=ti1*s16+ti2*s15+tr3*s13+ti4*s12+ti5*s11
            tr1=tr11
            ti1=ti11
            tr2=tr22
            ti2=ti22
            tr3=2.*tr33
            ti3=2.*ti33
            tr4=tr44
            ti4=ti44
            rmax=abs(tr5)
```

```
      if(rmax.lt.abs(ti5)) rmax=ti5
      if(rmax.lt.abs(ti4)) rmax=ti4
      if(rmax.lt.abs(ti3)) rmax=ti3
      if(rmax.lt.abs(ti2)) rmax=ti2
      if(rmax.lt.abs(ti1)) rmax=ti1
      if(rmax.lt.abs(tr4)) rmax=tr4
      if(rmax.lt.abs(tr3)) rmax=tr3
      if(rmax.lt.abs(tr2)) rmax=tr2
      if(rmax.lt.abs(tr1)) rmax=tr1
      rmax=1./rmax
      tr1=tr1*rmax
      tr2=tr2*rmax
      tr3=tr3*rmax
      tr4=tr4*rmax
      tr5=tr5*rmax
      ti1=ti1*rmax
      ti2=ti2*rmax
      ti3=ti3*rmax
      ti4=ti4*rmax
      ti5=ti5*rmax
1000  continue
2000  continue
      p=a(1)
      p2=p*p
      s=b(1)
      s2=s*s
      rro=rho(1)
      arss=1.-c2/s2
      arsp=1.-c2/p2
      if(arsp.ge.0.) cn=cmplx(0.,-rk*sqrt(arsp))
      if(arsp.lt.0.) cn=cmplx(rk*sqrt(-arsp),0.)
      if(arss.lt.0.) cns=cmplx(rk*sqrt(-arss),0.)
      if(arss.ge.0.) cns=cmplx(0.,-rk*sqrt(arss))
      rm=rro*s2
      rl=rk2+rk2-om2/s2
      rpp=cn*cns
      rm2=rm*rm
      rl2=rl*rl
      t11=cmplx(-rk2,0.)
      t13=t11+rpp
      t11=t11-rpp
      t21=cmplx(0.,rro*om2)
      t51=t21*cn
      t21=-t21*cns
      t31=cmplx(0.,-rm*rk*rl)
      rss=cmplx(0.,2.*rm*rk)*rpp
      t33=t31+rss
      t31=t31-rss
      t61=cmplx(-rm2*rl2,0.)
      rss=cmplx(4.*rk2*rm2,0.)*rpp
      t63=t61+rss
      t61=t61-rss
      t23=cmplx(0.,rm*(2.*rk2-rl))
      t53=t23*cn
      t23=t23*cns
      t12=cmplx(rk+rk,0.)
      t15=t12*cns
      t12=t12*cn
      t32=cmplx(0.,4.*rm*rk2)
      t45=t32*cns
      t32=t32*cn
      t42=cmplx(0.,2.*rm*rl)
      t35=t42*cns
```

```
      t42=t42*cn
      t62=cmplx(4.*rm2*rl*rk,0.)
      t65=t62*cns
      t62=t62*cn
      t1=cmplx(tr1,ti1)
      t2=cmplx(tr2,ti2)
      t3=cmplx(tr3,ti3)
      t4=cmplx(tr4,ti4)
      t5=cmplx(tr5,ti5)
      det=t1*t11+t2*t21+t3*t31+t4*t51+t5*t61
      det=cmplx(1.,0.)/det
      rss=t1*t13+t2*t23+t3*t33+t4*t53+t5*t63
      rss=-rss*det
      rpp=-t1*t13-t2*t21-t3*t33+t4*t51-t5*t63
      rpp=rpp*det
      t3=t3*cmplx(0.5,0.)
      rps=t1*t12+t3*t32+t3*t42+t5*t62
      rps=-rps*det
      rsp=t1*t15+t3*t35+t3*t45+t5*t65
      rsp=rsp*det
      return
      end
      subroutine fft(x,m)
      complex x(1024),u,w,t
      n=2**m
      pi=3.1415926536
      do 20 l=1,m
      le=2**(m+1-l)
      le1=le/2
      u=cmplx(1.,0.)
      w=cmplx(cos(pi/float(le1)),sin(pi/float(le1)))
      do 20 J=1,le1
      do 10 i=J,n,le
      ip=i+le1
      t=x(i)+x(ip)
      x(ip)=(x(i)-x(ip))*u
10    x(i)=t
20    u=u*w
      nv2=n/2
      nm1=n-1
      J=1
      do 30 i=1,nm1
      if(i.se.J) so to 25
      t=x(J)
      x(J)=x(i)
      x(i)=t
25    k=nv2
26    if(k.se.J) so to 30
      J=J-k
      k=k/2
      so to 26
30    J=J+k
      return
      end
```

Program FOR1

```
      dimension a(50),rho(50),d(50)
      dimension uw1(1025),uw2(1025)
      complex rp1(1025),rp2(1025)
      read(5,10)n,m,dd,del,dt,p1,p2
10    format(2i,5f)
      read(5,20)(a(i),rho(i),i=1,n)
20    format(2f)
      do 1 i=1,n
1     d(i)=dd
      pie=3.1415926536
      m2=2**m
      tfin=m2*dt
      df=1./tfin
      do 2 i=1,m2-1
      freq=freq+df
      call recopp(n,a,rho,d,p1,freq,rp1(i+1))
      call recopp(n,a,rho,d,p2,freq,rp2(i+1))
      rp1(i+1)=rp1(i+1)/(cmplx(0.,freq)*2.*pie)
      rp2(i+1)=rp2(i+1)/(cmplx(0.,freq)*2.*pie)
2     continue
      call fft(rp1,m)
      call fft(rp2,m)
      uw1(1)=2.*real(rp1(1))*df
      uw2(1)=2.*real(rp2(1))*df
      do 3 i=1,m2
      time=time+dt
      uw1(i+1)=2.*real(rp1(i+1))*df
      uw2(i+1)=2.*real(rp2(i+1))*df
      uw1(i)=(uw1(i+1)-uw1(i))/dt
      uw2(i)=(uw2(i+1)-uw2(i))/dt
      write(7,30)time,uw1(i),uw2(i)
30    format(1x,f7.4,f15.6,4x,f15.6)
3     continue
      call exit
      end
      subroutine recopp(n,a,rho,d,u,freq,rpp)
      dimension a(n),rho(n),d(n)
      complex rpp,ni,nip,roi,roip,m21,m22,e2,e1,e
      d(1)=0.
      pi=3.1415926536
      omega=2.*pi*freq
      om2=omega*omega
      xk=omega*u
      xk2=xk*xk
      m22=cmplx(1.,0.)
      m21=cmplx(0.,0.)
      do 170 j=1,n
      i=n-j+1
      arg=om2/(a(i)*a(i))-xk2
      if(arg.gt.0.)ni=cmplx(sqrt(arg),0.)
      if(arg.le.0.)ni=cmplx(0.,-sqrt(-arg))
      roi=cmplx(rho(i),0.)
      if(i.eq.n)go to 171
      e1=nip*roi
      e2=ni*roip
```

```
      e=cexp(ni*cmplx(0.,2.*d(i)))
      e1=e1*(m21+m22)
      e2=e2*(m21-m22)
      m21=e1+e2
      m22=e*(e1-e2)
      rmax=cabs(m22)
      rm=cabs(m21)
      if(rm.gt.rmax)rmax=rm
      e1=cmplx(1./rmax,0.)
      m22=m22*e1
      m21=m21*e1
171   nip=ni
      roip=roi
170   continue
      rpp=-m21/m22
      return
      end
      subroutine fft(x,m)
      complex x(1024),u,w,t
      n=2**m
      pi=3.1415926536
      do 20 l=1,m
      le=2**(m+1-l)
      le1=le/2
      u=cmplx(1.,0.)
      w=cmplx(cos(pi/float(le1)),sin(pi/float(le1)))
      do 20 j=1,le1
      do 10 i=j,n,le
      ip=i+le1
      t=x(i)+x(ip)
      x(ip)=(x(i)-x(ip))*u
10    x(i)=t
20    u=u*w
      nv2=n/2
      nm1=n-1
      j=1
      do 30 i=1,nm1
      if(i.ge.j)go to 25
      t=x(j)
      x(j)=x(i)
      x(i)=t
25    k=nv2
26    if(k.ge.j)go to 30
      j=j-k
      k=k/2
      go to 26
30    j=j+k
      return
      end
```

```
      dimension a(50),rho(50),d(50)
      dimension uw1(1025),uw2(1025)
      complex rp1(1025),rp2(1025)
      read(5,10)n,m,dd,freq1,freq2
10    format(2i,3f)
      read(5,20)(a(i),rho(i),i=1,n)
20    format(2f)
      do 1 i=1,n
1     d(i)=dd
      pie=3.1415926536
      m2=2**m
      fmin=min(freq1,freq2)
      dk=fmin/a(1)/m2
      dt=a(1)/fmin/2.
      zk=0.
      do 2 i=1,m2-1
      zk=zk+dk
      p1=sqrt(1.-zk*zk*a(1)*a(1)/freq1/freq1)/a(1)
      p2=sqrt(1.-zk*zk*a(1)*a(1)/freq2/freq2)/a(1)
      call recopp(n,a,rho,d,p1,freq1,rp1(i+1))
      call recopp(n,a,rho,d,p2,freq2,rp2(i+1))
2     continue
      call fft(rp1,m)
      call fft(rp2,m)
      uw1(1)=2.*real(rp1(1))*dk
      uw2(1)=2.*real(rp2(1))*dk
      do 3 i=1,m2
      time=time+dt
      uw1(i+1)=2.*real(rp1(i+1))*dk
      uw2(i+1)=2.*real(rp2(i+1))*dk
      write(7,30)time,uw1(i),uw2(i)
30    format(1x,f7.4,f15.6,4x,f15.6)
3     continue
      call exit
      end
      subroutine recopp(n,a,rho,d,u,freq,rpp)
      dimension a(n),rho(n),d(n)
      complex rpp,ni,nip,roi,roip,m21,m22,e2,e1,e
      d(1)=0.
      pi=3.1415926536
      omega=2.*pi*freq
      om2=omega*omega
      xk=omega*u
      xk2=xk*xk
      m22=cmplx(1.,0.)
      m21=cmplx(0.,0.)
      do 170 j=1,n
      i=n-j+1
      ars=om2/(a(i)*a(i))-xk2
      if(ars.gt.0.)ni=cmplx(sqrt(ars),0.)
      if(ars.le.0.)ni=cmplx(0.,-sqrt(-ars))
      roi=cmplx(rho(i),0.)
      if(i.eq.n)go to 171
      e1=nip*roi
      e2=ni*roip
      e=cexp(ni*cmplx(0.,2.*d(i)))
      e1=e1*(m21+m22)
      e2=e2*(m21-m22)
      m21=e1+e2
```

```
      m22=e*(e1-e2)
      rmax=cabs(m22)
      rm=cabs(m21)
      if(rm.gt.rmax)rmax=rm



      e1=cmplx(1./rmax,0.)
      m22=m22*e1
      m21=m21*e1
171   nip=ni
      roip=roi
170   continue
      rpp=-m21/m22
      return
      end
      subroutine fft(x,m)
      complex x(1024),u,w,t
      n=2**m
      pi=3.1415926536
      do 20 l=1,m
      le=2**(m+1-l)
      le1=le/2
      u=cmplx(1.,0.)
      w=cmplx(cos(pi/float(le1)),sin(pi/float(le1)))
      do 20 j=1,le1
      do 10 i=j,n,le
      ip=i+le1
      t=x(i)+x(ip)
      x(ip)=(x(i)-x(ip))*u
10    x(i)=t
20    u=u*w
      nv2=n/2
      nm1=n-1
      j=1
      do 30 i=1,nm1
      if(i.ge.j)go to 25
      t=x(j)
      x(j)=x(i)
      x(i)=t
25    k=nv2
26    if(k.ge.j)go to 30
      j=j-k
      k=k/2
      go to 26
30    j=j+k
      return
      end
```

```
      dimension a(50),rho(50)
      dimension dw1(1024),dw2(1024),uw1(1024),uw2(1024)
      read(5,10)n,m,dd,del,dt,p1,p2
10    format(2i,5f)
      read(5,20)(a(i),rho(i),i=1,n)
20    format(2f)
      m=2**m
      do 4 i=1,m
      read(7,30)time,uw1(i),uw2(i)
30    format(1x,f7.4,f15.6,4x,f15.6)
      dw1(i)=0.
      dw2(i)=0.
4     continue
      ac=a(1)
      rhoc=rho(1)
      s1=0.
      s2=0.
      kts1=0
      kts2=0
      t11=1.
      t12=1.
      dep=0.
      z1=a(1)*rho(1)/sqrt(1.-a(1)*a(1)*p1*p1)
      z2=a(1)*rho(1)/sqrt(1.-a(1)*a(1)*p2*p2)
      write(6,40)
40    format(1x,'depth',8x,'cact',5x,'ccomp',4x,'rhoact',3x,'rhocomp'
     +'rc1',9x,'rc2')                                                  ,4x,
      do 5 i=1,m
      dep=dep+del
      acp1=1.-ac*ac*p1*p1
      acp2=1.-ac*ac*p2*p2
      if((acp1.le.0.).or.(acp2.le.0.))call exit
      s1=s1+2.*del/dt*sqrt(acp1)/ac
      s2=s2+2.*del/dt*sqrt(acp2)/ac
      ks1=int(s1-kts1+0.5)
      ks2=int(s2-kts2+0.5)
      kts1=kts1+ks1
      kts2=kts2+ks2
      t11=t11*sqrt(1.-rc1*rc1)
      t12=t12*sqrt(1.-rc2*rc2)
      kmax=max0(kts1,kts2)
      if(kmax.ge.m)call exit
      do 6 k=1,m-kmax+1
      temp1=(dw1(k)-rc1*uw1(k))/sqrt(1.-rc1*rc1)
      temp2=(dw2(k)-rc2*uw2(k))/sqrt(1.-rc2*rc2)
      uw1(k)=(uw1(k)-rc1*dw1(k))/sqrt(1.-rc1*rc1)
      uw2(k)=(uw2(k)-rc2*dw2(k))/sqrt(1.-rc2*rc2)
      dw1(k)=temp1
      dw2(k)=temp2
6     continue
```

```
      rc1=(uw1(ks1-1)+uw1(ks1)+uw1(ks1+1))*dt/tl1
      rc2=(uw2(ks2-1)+uw2(ks2)+uw2(ks2+1))*dt/tl2
      do 7 k=1,m-kmax+1
      uw1(k)=uw1(k+ks1)
      uw2(k)=uw2(k+ks2)
7     continue
      z1=z1*(1.+rc1)/(1.-rc1)
      z2=z2*(1.+rc2)/(1.-rc2)
      u=z1*z1/z2/z2
      ac=(sqrt((u-1.)/(u-p2*p2/p1/p1)))/p1
      rhoc1=z1*sqrt(1.-ac*ac*p1*p1)/ac
      rhoc2=z2*sqrt(1.-ac*ac*p2*p2)/ac
      rhoc=(rhoc1+rhoc2)/2.


      l=min0(int(dep/dd)+2,n)
      write(6,50)dep,a(1),ac,rho(1),rhoc,rc1,rc2
50    format(1x,f7.2,6f10.4)
5     continue
      call exit
      end
```

Program INVELAS

```
      dimension a(50),b(50),rho(50)
      dimension dpp(1024),upp(1024),dsp(1024),usp(1024)
      dimension dps(1024),ups(1024),dss(1024),uss(1024)
      read(5,10)n,m,dd,del,dt,p
10    format(2i,4f)
      read(5,20)(a(i),b(i),rho(i),i=1,n)
20    format(3f)
      m2=2**m
      m22=2*m2
      do 4 i=1,m2
      read(7,30)time,upp(i),usp(i),ups(i),uss(i)
30    format(1x,f7.4,f15.6,3f19.6)
4     continue
      ac=a(1)
      bc=b(1)
      rhoc=rho(1)
      tlp=1.
      tls=1.
      write(6,40)
40    format(1x,'depth',2x,'aact',2x,'acomp',2x,'bact',2x,'bcomp',2x,
     +'rhoact',2x,'rhocomp',4x,'rp',5x,'rc',5x,'rs',5x,'tc')
      do 5 i=1,m2
      dep=dep+del
      aa=ac*ac*p*p
      bb=bc*bc*p*p
      acp=1.-aa
      bcp=1.-bb
      if((acp.le.0.).or.(bcp.le.0.))call exit
      s=bc*sqrt(acp*bcp)/ac
      x=sqrt(bb/s)/2.
      det=(0.5-3.*bb-s+2.*bb*bb+2.*bb*s)*x/bcp
      tp=tp+2.*del/dt*sqrt(acp)/ac
      ts=ts+2.*del/dt*sqrt(bcp)/bc
      tm=tm+del/dt*(sqrt(acp)/ac+sqrt(bcp)/bc)
      kdp=int(tp-ktp+0.5)
      kds=int(ts-kts+0.5)
      kdm=int(tm-ktm+0.5)
      ktp=ktp+kdp
      kts=kts+kds
      ktm=ktm+kdm
      tlp=tlp*sqrt(1.-rp*rp-rc*rc-tc*tc)
      tls=tls*sqrt(1.-rs*rs-rc*rc-tc*tc)
      if(kts.ge.m2)call exit
```

```
      do 6 k=1,m2-kts+1
      temp1=dpp(k)-tc*dsp(k)-rp*upp(k)-rc*usp(k)
      temp2=dsp(k)+tc*dpp(k)-rc*upp(k)-rs*usp(k)
      temp3=upp(k)-rp*dpp(k)-rc*dsp(k)-tc*usp(k)
      temp4=usp(k)-rc*dpp(k)-rs*dsp(k)+tc*upp(k)
      dpp(k)=temp1
      dsp(k)=temp2
      upp(k)=temp3
      usp(k)=temp4
      temp1=dps(k)-tc*dss(k)-rp*ups(k)-rc*uss(k)
      temp2=dss(k)+tc*dps(k)-rc*ups(k)-rs*uss(k)
      temp3=ups(k)-rp*dps(k)-rc*dss(k)-tc*uss(k)
      temp4=uss(k)-rc*dps(k)-rs*dss(k)+tc*ups(k)
      dps(k)=temp1
      dss(k)=temp2
      ups(k)=temp3
      uss(k)=temp4
6     continue
      rp=(upp(kdp-1)+upp(kdp)+upp(kdp+1))*dt/tlp
      rc1=(usp(kdm-1)+usp(kdm)+usp(kdm+1))/tlp



      rc2=(ups(kdm-1)+ups(kdm)+ups(kdm+1))/tls
      rc=(rc1+rc2)*dt/2.
      rs=(uss(kds-1)+uss(kds)+uss(kds+1))*dt/tls
      tc=-(0.5-3.*bb+s-2.*bb*s+2.*bb*bb)/(det*bcp)*x*rc+2.*bb/det*rs
      do 7 k=1,m2-ktp+1
      upp(k)=upp(k+kdp)
      ups(k)=ups(k+kdm)
      usp(k)=usp(k+kdm)
      uss(k)=uss(k+kds)
7     continue
      ac=ac-((2.*bb-0.5)*rc/bcp+4.*x*(bb+s)*rs-2.*det*rp)*ac*acp/det
      bc=bc-((2.*bb-0.5)*rc+x*(1.-2.*bb+2.*s)*rs)*bc/det
      rhoc=rhoc-((0.5/bcp-4.*bb)*rc+4.*(bb-s)*x*rs)*rhoc/det
      l=min0(int(dep/dd)+2,n)
      write(6,50)dep,a(1),ac,b(1),bc,rho(1),rhoc,rp,rc,rs,tc
50    format(1x,f5.2,f6.3,f7.4,f6.3,f7.4,f8.3,5f7.4)
5     continue
      call exit
      end
```

Program INVFREQ

```
      dimension a(50),rho(50)
      dimension dw1(1024),dw2(1024),uw1(1024),uw2(1024)
      read(5,10)n,m,dd,freq1,freq2
10    format(2i,3f)
      read(5,20)(a(i),rho(i),i=1,n)
20    format(2f)
      m=2**m
      pie=3.1415926536
      fmin=min(freq1,freq2)
      dt=a(1)/fmin/2.
      f1sq=freq1*freq1
      f2sq=freq2*freq2
      do 4 i=1,m
      read(7,30)time,uw1(i),uw2(i)
30    format(1x,f7.4,f15.6,4x,f15.6)
      dw1(i)=0.
      dw2(i)=0.
4     continue
      t11=1.
      t12=1.
      kt=0
      dep=0.
      z=1./sqrt(rho(1))
      ztemp=z
      r1temp=0.
      r2temp=0.
      write(6,40)
40    format(1x,'depth',8x,'cact',5x,'ccomp',4x,'rhoact',3x,'rhocomp'
     +'rc1',9x,'rc2')
      do 5 i=1,m
      kt=kt+1
      dep=dep+dt
      t11=t11*sqrt(1.-rc1*rc1)
      t12=t12*sqrt(1.-rc2*rc2)
      do 6 k=1,m-kt+1
      temp1=(dw1(k)-rc1*uw1(k))/sqrt(1.-rc1*rc1)
      temp2=(dw2(k)-rc2*uw2(k))/sqrt(1.-rc2*rc2)
      uw1(k)=(uw1(k)-rc1*dw1(k))/sqrt(1.-rc1*rc1)
      uw2(k)=(uw2(k)-rc2*dw2(k))/sqrt(1.-rc2*rc2)
      dw1(k)=temp1
      dw2(k)=temp2
6     continue
      rc1=uw1(1)*dt/t11
      rc2=uw2(1)*dt/t12
      do 7 k=1,m-kt+1
      uw1(k)=uw1(k+1)
      uw2(k)=uw2(k+1)
7     continue
```

```
      v1=rc1*rc1-(rc1-r1temp)
      v2=rc2*rc2-(rc2-r2temp)
      r1temp=rc1
      r2temp=rc2
      ac=1./sqrt(1./(a(1)*a(1))-(v1-v2)/((f1sq-f2sq)*dt*dt))
      zplus=((f2sq*v1-f1sq*v2)/(f2sq-f1sq)+2.)*z-ztemp
      rhoc=1./(z*z)
      ztemp=z
      z=zplus
      l=min0(int(dep/dd)+2,n)
      write(6,50)dep,a(l),ac,rho(l),rhoc,rc1,rc2
50    format(1x,f7.2,6f10.4)
      if(l.eq.n)call exit
5     continue
      call exit


      end
```

Program INV1

```
      dimension a(50),rho(50)
      dimension dw1(1024),dw2(1024),uw1(1024),uw2(1024)
      read(5,10)n,m,dd,del,dt,p1,p2
10    format(2i,5f)
      read(5,20)(a(i),rho(i),i=1,n)
20    format(2f)
      m2=2**m
      do 4 i=1,m2
      read(7,30)time,uw1(i),uw2(i)
30    format(1x,f7.4,f15.6,4x,f15.6)
4     continue
      ac=a(1)
      rhoc=rho(1)
      t11=1.
      t12=1.
      write(6,40)
40    format(1x,'depth',8x,'cact',5x,'ccomp',4x,'rhoact',3x,'rhocomp'
     +'rc1',9x,'rc2')
      do 5 i=1,m2
      dep=dep+del
      acp1=1.-ac*ac*p1*p1
      acp2=1.-ac*ac*p2*p2
      if((acp1.le.0.).or.(acp2.le.0.))call exit
      s1=s1+2.*del/dt*sqrt(acp1)/ac
      s2=s2+2.*del/dt*sqrt(acp2)/ac
      ks1=int(s1-kts1+0.5)
      ks2=int(s2-kts2+0.5)
      kts1=kts1+ks1
      kts2=kts2+ks2
      t11=t11*sqrt(1.-rc1*rc1)
      t12=t12*sqrt(1.-rc2*rc2)
      kmax=max0(kts1,kts2)
      if(kmax.ge.m2)call exit
      do 6 k=1,m2-kmax+1
      temp1=(dw1(k)-rc1*uw1(k))/sqrt(1.-rc1*rc1)
      temp2=(dw2(k)-rc2*uw2(k))/sqrt(1.-rc2*rc2)
      uw1(k)=(uw1(k)-rc1*dw1(k))/sqrt(1.-rc1*rc1)
      uw2(k)=(uw2(k)-rc2*dw2(k))/sqrt(1.-rc2*rc2)
      dw1(k)=temp1
      dw2(k)=temp2
6     continue
      rc1=(uw1(ks1-1)+uw1(ks1)+uw1(ks1+1))*dt/t11
      rc2=(uw2(ks2-1)+uw2(ks2)+uw2(ks2+1))*dt/t12
      do 7 k=1,m2-kmax+1
      uw1(k)=uw1(k+ks1)
      uw2(k)=uw2(k+ks2)
7     continue
      ac=ac+2.*ac*(rc2-rc1)*acp1*acp2/(acp1-acp2)
      rhoc=rhoc+2.*rhoc*(rc1*acp1-rc2*acp2)/(acp1-acp2)
      l=min0(int(dep/dd)+2,n)
      write(6,50)dep,a(l),ac,rho(l),rhoc,rc1,rc2
50    format(1x,f7.2,6f10.4)
5     continue
      call exit
      end
```

```
      dimension a(50),rho(50),dt1(50,5),r(50,5),tr(50,5)
      dimension uw(1024,5),p(5),tl(5),t(5),nrand(5)
      read(5,10) n,m,nm,dd,del,dt,xl,ic
10    format(3i,4f,i)
      read(5,13) (p(i),i=1,5),(nrand(i),i=1,5)
13    format(5f,5i)
      read(5,11) (a(i),rho(i),i=1,n)
11    format(2f)
      m=2**m
      do 77 J=1,nm
      tr(i,J)=1.
      tl(J)=1.
      t(J)=0.
      do 77 i=1,m
      uw(i,J)=0.
77    continue
      do 1 i=2,n
      rho(i-1)=rho(i)
      do 1 J=1,nm
c     dt1(i,J) is 2-way traveltime thru layer i for exp't J
      dt1(i-1,J)=2.*dd*sqrt(1.-a(i)*a(i)*p(J)*p(J))/a(i)
1     continue
c     compute reflection coefficients
      do 99 J=1,nm
      do 2 i=1,n-2
      r(i,J)=(rho(i+1)/dt1(i+1,J)-rho(i)/dt1(i,J))/(rho(i+1)/dt1(i+1,J
     ++rho(i)/dt1(i,J))
c     compute 2-way transmission coefficients
      tr(i+1,J)=1.-r(i,J)*r(i,J)
2     continue
c     do primaries
      do 3 i=1,n-2
      t(J)=t(J)+dt1(i,J)/dt
      tl(J)=tl(J)*tr(i,J)
      uw(int(t(J)+0.5),J)=r(i,J)/dt*tl(J)
3     continue
c     do secondaries
      do 4 n1=2,n-2
      do 5 n2=1,n1-1
      do 6 n3=n2+1,n-2
      nmin=min0(n1,n3)
      nmax=max0(n1,n3)
      t(J)=0.
      tl(J)=1.
      do 7 i=1,nmax
      t(J)=t(J)+dt1(i,J)/dt
      tl(J)=tl(J)*tr(i,J)
      if((i.le.n2).or.(i.gt.nmin)) go to 7
      t(J)=t(J)+dt1(i,J)/dt
      tl(J)=tl(J)*tr(i,J)
7     continue
      if(int(t(J)).ge.m)go to 6
      uw(int(t(J)+.5),J)=uw(int(t(J)+.5),J)-r(n1,J)*r(n2,J)*r(n3,J)/dt
6     continue                                                    +tl(J)
5     continue
4     continue
99    continue
      write(8,79) ((r(i,J),J=1,5),i=1,n-2)
79    format(1x,5f10.5)
      write(7,12) ((uw(i,J),J=1,5),i=1,m)
12    format(1x,5f19.6)
                                          call exit
                                          end
```

```
      dimension a(50),rho(50),r(50,5),rd(5),rc(5),p(5),sn(5),s(5),z(5),st(5)
      dimension dw(1024,5),uw(1024,5),xsig(5),xnoz(5),snr(5),acp(5)
      dimension temp(5),ks(5),kts(5),t1(5),nrand(5),xk(5),enr(5),nrand1(5)
      read(5,10)n,m,nm,dd,del,dt,xl,ic
10    format(3i,4f,i)
c   ic=1 if want rc(i) zeroed using condition no.; ic=0 suppresses this.
      read(5,12)(p(i),i=1,5),(nrand(i),i=1,5)
12    format(5f,5i)
      write(6,11)n,m,nm,dd,del,dt,xl
11    format(1x,'n=',i2,2x,'m=',i2,2x,'nm=',i2,2x,'dd=',f5.3,2x,'del=',f5.3
     +,2x,'dt=',f7.5,2x,'xl=',e7.1)
      write(6,13)(p(j),j=1,5)
13    format(1x,'values of p are',5f6.2)
c   a(1)=a(2) and rho(1)=rho(2),so no instantaneous reflections.
      read(5,20)(a(i),rho(i),i=1,n)
20    format(2f)
      read(8,51)((r(i,j),j=1,5),i=1,n-2)
51    format(1x,5f10.5)
      m=2**m
      do 1 j=1,5
      xsig(j)=0.
      xnoz(j)=0.
      xk(j)=2.*xl
      nrand1(j)=nrand(j)
1     continue
      do 4 i=1,m
      read(7,30)(uw(i,j),j=1,5)
30    format(1x,5f19.6)
      do 4 j=1,nm
      dw(i,j)=0.
      xsig(j)=xsig(j)+uw(i,j)*uw(i,j)*dt*dt
      st(j)=(1.e-4)*int(float(nrand(j)*nrand(j))/100.)
      st(j)=st(j)-float(int(st(j)))
      nrand(j)=int(st(j)*(1.e4))
      if(st(j).lt.(1.e-3)) nrand(j)=nrand1(j)
      sn(j)=(st(j)-0.5)*2.*xl
      uw(i,j)=uw(i,j)+sn(j)/dt
      xnoz(j)=xnoz(j)+sn(j)*sn(j)
4     continue
```

```
      ac=a(1)
      rhoc=rho(1)
      dep=0.
      l=2
      do 2 j=1,nm
      s(j)=0.
      kts(j)=0
      tl(j)=1.
      snr(j)=10.*alog10(xsig(j)/xnoz(j))
2     continue
      write(6,39)(snr(j),j=1,5)
39    format(1x,'snr=',5f6.1)
      write(6,40)
40    format(1x,'depth',2x,'cact',4x,'ccomp',3x,'rhoact',2x,'rhocomp',3x
     +,'r1',5x,'rc1',6x,'r2',6x,'rc2',5x,'r3',5x,'rc3',6x,'r4',6x,'rc4'
     +,5x,'r5',6x,'rc5')
      do 5 i=1,m
      write(6,50)dep,a(l),ac,rho(l),rhoc,(rd(k),rc(k),k=1,5)
50    format(1x,f5.2,14f8.4)
      dep=dep+del
      do 8 j=1,nm
      acp(j)=1.-ac*ac*p(j)*p(j)
      if(acp(j).le.0.)call exit
      s(j)=s(j)+2.*del/dt*sqrt(acp(j))/ac



      ks(j)=int(s(j)-kts(j)+0.5)
      kts(j)=kts(j)+ks(j)
      tl(j)=tl(j)*sqrt(1.-rc(j)*rc(j))
      if(kts(j).ge.m)call exit
      if(dep.gt.((n+5)*dd))call exit
      do 6 k=1,m-kts(j)+1
      temp(j)=(dw(k,j)-rc(j)*uw(k,j))/sqrt(1.-rc(j)*rc(j))
      uw(k,j)=(uw(k,j)-rc(j)*dw(k,j))/sqrt(1.-rc(j)*rc(j))
      dw(k,j)=temp(j)
6     continue
```

```
      rc(j)=(uw(ks(j)-1,j)+uw(ks(j),j)+uw(ks(j)+1,j))*dt/tl(j)
      if(ic.eq.0)go to 17
      if(abs(rc(j)).lt.xk(j)) rc(j)=0.
      xk(j)=xk(j)*(1.+abs(rc(j)))/(1.-abs(rc(j)))
17    do 7 k=1,m-kts(j)+1
7     uw(k,j)=uw(k+ks(j),j)
8     continue
      acp2=0.
      acp4=0.
      acpr=0.
      rt=0.
      do 18 j=1,nm
      acp2=acp2+1./acp(j)
      acp4=acp4+1./acp(j)/acp(j)
      acpr=acpr+rc(j)/acp(j)
      rt=rt+rc(j)
18    continue
      det=nm*acp4-acp2*acp2
      rhoc=rhoc+2.*rhoc/det*(acp4*rt-acp2*acpr)
      ac=ac+2.*ac/det*(nm*acpr-rt*acp2)
      ll=min0(int(dep/dd+0.0001)+2,n)
      do 9 j=1,nm
9     rd(j)=r(l-1,j)
      if(ll.ne.1)go to 53
      do 19 j=1,nm
19    rd(j)=0.
53    l=ll
5     continue
      call exit
      end
```

Program MULTINV

```
      dimension a(50),rho(50),r(50,5),rd(5),rc(5),s(5),sn(5),z(5),t(5)
      dimension dw(1024,5),w(1024,5),xsis(5),xnoz(5),snr(5),esp(5)
      dimension tem2(5),ks(5),kts(5),t1(5),nrand(5),xk(5),enr(5),nrand1(5)
      read(5,10)nu,m,dd,del,dt,xlic
   10 format(3i4,4f,1)
      ic=1 if want rc(i) zeroed using condition no.# ic=0 suppresses this.
      read(5,12)(a(i),i=1,5),(nrand(i),i=1,5)
   12 format(5f,5i)
      write(6,11)nu,m,dd,del,dt,xl
   11 format(1x,'n=',i2,2x,'m=',i2,2x,'nm=',i2,2x,'dd=',f5.3,2x,'del=',f5.3
     +,2x,'dt=',f7.5,2x,'xl=',e7.1)
      write(6,13)(a(j),j=1,5)
   13 format(1x,'values of P are',5f6.2)
      a(1)=a(2) and rho(1)=rho(2),so no instantaneous reflections.
      read(5,20)(a(i),rho(i),i=1,nu)
   20 format(2f)
      read(8,51)((r(i,j),j=1,5),i=1,n-2)
   51 format(1x,5f10.5)
      m=2**m
      do 1 j=1,5
      xsis(j)=0.
      xnoz(j)=0.
      xk(j)=2.**x1
      nrand1(j)=nrand(j)
    1 continue
      do 4 i=1,m
      read(7,30)(uw(i,j),j=1,5)
   30 format(1x,5f19.9)
      do 4 j=1,nu
      dw(i,j)=0.
      xsis(j)=xsis(j)+uw(i,j)*uw(i,j)*dt*dt
      st(j)=(1.e-4)*int(float(nrand(j)*nrand(j))/100.)
      st(j)=st(j)-float(int(st(j)))
      nrand(j)=int(st(j)*1.e4)
      if(st(j).lt.0.5)nrand(j)=nrand1(j)
      sn(j)=(st(j)-0.5)**2**1
      uw(i,j)=uw(i,j)+sn(j)*dt
      xnoz(j)=xnoz(j)+sn(j)
    4 continue
```

```
      ac=a(1)
      rhoc=rho(1)
      dep=0.
      xerr=0.
      l=2
      do 2 j=1,nm
      s(j)=0.
      kts(j)=0
      tl(j)=1.
      z(j)=a(i)*rho(1)/sqrt(1.-a(1)*a(1)*p(j)*p(j))
      snr(j)=10.*alog10(xsig(j)/xnoz(j))
2     continue
      write(6,39)(snr(j),j=1,5)
39    format(1x,'snr=',5f6.1)
      write(6,40)
40    format(1x,'depth',2x,'cact',4x,'ccomp',3x,'rhoact',2x,'rhocomp',3x
     +,'r1',5x,'rc1',6x,'r2',6x,'rc2',5x,'r3',5x,'rc3',6x,'r4',6x,'rc4'
     +,5x,'r5',6x,'rc5')
      do 5 i=1,m
      write(6,50)dep,a(1),ac,rho(1),rhoc,(rd(k),rc(k),k=1,5)
50    format(1x,f5.2,14f8.4)
      dep=dep+del
      do 8 j=1,nm
      acp(j)=1.-ac*ac*p(j)*p(j)



      if(acp(j).le.0.)call exit
      s(j)=s(j)+2.*del/dt*sqrt(acp(j))/ac
      ks(j)=int(s(j)-kts(j)+0.5)
      kts(j)=kts(j)+ks(j)
      tl(j)=tl(j)*sqrt(1.-rc(j)*rc(j))
      if(kts(j).ge.m)go to 99
      if(dep.gt.((n+5)*dd))go to 99
      do 6 k=1,m-kts(j)+1
      temp(j)=(dw(k,j)-rc(j)*uw(k,j))/sqrt(1.-rc(j)*rc(j))
      uw(k,j)=(uw(k,j)-rc(j)*dw(k,j))/sqrt(1.-rc(j)*rc(j))
      dw(k,j)=temp(j)
6     continue
```

```
      rc(j)=(uw(ks(j)-1,j)+uw(ks(j),j)+uw(ks(j)+1,j))*dt/tl(j)
      if(ic.eq.0)go to 17
      if(abs(rc(j)).lt.xk(j)) rc(j)=0.
      xk(j)=xk(j)*(1.+abs(rc(j)))/(1.-abs(rc(j)))
17    do 7 k=1,m-kts(j)+1
7     uw(k,j)=uw(k+ks(j),j)
      z(j)=z(j)*(1.+rc(j))/(1.-rc(j))
8     continue
      ac=0.
      rhoc=0.
      do 18 j=1,nm-1
      do 18 k=j+1,nm
      u=z(j)*z(j)/z(k)/z(k)
      act=(sqrt((u-1.)/(u-p(k)*p(k)/p(j)/p(j))))/p(j)
18    ac=ac+act
      ac=ac*2./nm/(nm-1)
      do 16 j=1,nm
16    rhoc=rhoc+z(j)*sqrt(1.-ac*ac*p(j)*p(j))/ac
      rhoc=rhoc/nm
      ll=min0(int(dep/dd+0.0001)+2,n)
      do 9 j=1,nm
9     rd(j)=r(l-1,j)
      if(ll.ne.1)go to 53
      do 19 j=1,nm
19    rd(j)=0.
53    l=ll
      do 29 j=1,nm
29    xerr=xerr+(s(l)-ac)*(s(l)-ac)
5     continue
99    do 49 j=1,nm
49    enr(j)=10.*alog10(xerr/xnoz(j)*2./i)
      write(6,52)(enr(j),j=1,5)
52    format(1x,'enr=',5f8.3)
      call exit
      end
```

```
      dimension a(50),rho(50),r1(50),r2(50)
      dimension dw1(1024),dw2(1024),uw1(1024),uw2(1024)
      read(5,10)n,m,dd,del,dt,p1,p2,xl,ic,nrand
10    format(2i,6f,2i)
c     ic=1 if want rci zeroed using condition no.; ic=0 suppresses this.
      write(6,11)n,m,dd,del,dt,p1,p2,xl
11    format(1x,'n=',i2,2x,'m=',i2,2x,'dd=',f5.3,2x,'del=',f5.3,2x,
     +'dt=',f7.5,2x,'p1=',f4.2,2x,'p2=',f4.2,2x,'xl=',e7.1)
c     a(1)=a(2) and rho(1)=rho(2),so no instantaneous reflections.
      read(5,20)(a(i),rho(i),i=1,n)
20    format(2f)
      read(8,51)(r1(i),r2(i),i=1,n-2)
51    format(1x,2f10.5)
      m=2**m
      xsis1=0.
      xsis2=0.
      xnoz=0.
      xerr1=0.
      xerr2=0.
      xk1=2.*xl
      xk2=2.*xl
      l=2
      do 4 i=1,m
      read(7,30)time,uw1(i),uw2(i)
30    format(1x,f7.4,f15.6,4x,f15.6)
      dw1(i)=0.
      dw2(i)=0.
      xsis1=xsis1+uw1(i)*uw1(i)*dt*dt
      xsis2=xsis2+uw2(i)*uw2(i)*dt*dt
      st=1.e-4*int(float(nrand*nrand)/100.)
      st=st-float(int(st))
      nrand=int(st*1.e4)
      sn=(st-0.5)*2.*xl
      temp1=uw1(i)
      temp2=uw2(i)
      uw1(i)=uw1(i)+sn/dt
      uw2(i)=uw2(i)+sn/dt
      write(9,54)temp1,uw1(i),temp2,uw2(i)
54    format(1x,4f18.6)
      xnoz=xnoz+sn*sn
4     continue
      ac=a(1)
      rhoc=rho(1)
      s1=0.
      s2=0.
      kts1=0
      kts2=0
      tl1=1.
      tl2=1.
      dep=0.
      z1=a(1)*rho(1)/sqrt(1.-a(1)*a(1)*p1*p1)
      z2=a(1)*rho(1)/sqrt(1.-a(1)*a(1)*p2*p2)
      rms1=sqrt(xsis1/m)
      rms2=sqrt(xsis2/m)
      rmsn=sqrt(xnoz/m)
      snr1=10.*alog10(xsis1/xnoz)
      snr2=10.*alog10(xsis2/xnoz)
      write(6,39)rms1,rms2,rmsn,snr1,snr2
39    format(1x,'rms signal=',2f10.6,2x,'rms noise=',f10.6,2x,'snr=',
      write(6,40)                                                  2f6.1)
40    format(1x,'depth',2x,'cact',4x,'ccomp',4x,'rhoact',3x,'rhocomp'
     +'r1',4x,'rc1',4x,'r2',4x,'rc2')                              ,2x,
      do 5 i=1,m
```

```
      write(6,50)dep,s(1),ac,rho(1),rhoc,rd1,rc1,rd2,rc2
50    format(1x,f5.2,8f8.4)
      dep=dep+del
      acp1=1.-ac*ac*p1*p1
      acp2=1.-ac*ac*p2*p2
      if((acp1.le.0.).or.(acp2.le.0.))call exit
      s1=s1+2.*del/dt*sqrt(acp1)/ac
      s2=s2+2.*del/dt*sqrt(acp2)/ac
      ks1=int(s1-kts1+0.5)
      ks2=int(s2-kts2+0.5)
      kts1=kts1+ks1
      kts2=kts2+ks2
      tl1=tl1*sqrt(1.-rc1*rc1)
      tl2=tl2*sqrt(1.-rc2*rc2)
      kmax=max0(kts1,kts2)
      if(kmax.ge.m)go to 99
      if(dep.gt.((n+5)*dd)) go to 99
      do 6 k=1,m-kmax+1
      temp1=(dw1(k)-rc1*uw1(k))/sqrt(1.-rc1*rc1)
      temp2=(dw2(k)-rc2*uw2(k))/sqrt(1.-rc2*rc2)
      uw1(k)=(uw1(k)-rc1*dw1(k))/sqrt(1.-rc1*rc1)
      uw2(k)=(uw2(k)-rc2*dw2(k))/sqrt(1.-rc2*rc2)
      dw1(k)=temp1
      dw2(k)=temp2
6     continue
      rc1=(uw1(ks1-1)+uw1(ks1)+uw1(ks1+1))*dt/tl1
      rc2=(uw2(ks2-1)+uw2(ks2)+uw2(ks2+1))*dt/tl2
      if(ic.eq.0) go to 8
      if(abs(rc1).lt.xk1)rc1=0.
      if(abs(rc2).lt.xk2)rc2=0.
      xk1=xk1*(1.+abs(rc1))/(1.-abs(rc1))
      xk2=xk2*(1.+abs(rc2))/(1.-abs(rc2))
8     do 7 k=1,m-kmax+1
      uw1(k)=uw1(k+ks1)
      uw2(k)=uw2(k+ks2)
7     continue
      z1=z1*(1.+rc1)/(1.-rc1)
      z2=z2*(1.+rc2)/(1.-rc2)
      u=z1*z1/z2/z2
      ac=(sqrt((u-1.)/(u-p2*p2/p1/p1)))/p1
      rhoc1=z1*sqrt(1.-ac*ac*p1*p1)/ac
      rhoc2=z2*sqrt(1.-ac*ac*p2*p2)/ac
      rhoc=(rhoc1+rhoc2)/2.
      l1=min0(int(dep/dd+0.0001)+2,n)
      rd1=r1(l-1)
      rd2=r2(l-1)
      if(l1.ne.l)go to 53
      rd1=0.
      rd2=0.
53    l=l1
      xerr1=xerr1+(rd1-rc1)*(rd1-rc1)
      xerr2=xerr2+(rd2-rc2)*(rd2-rc2)
5     continue
99    rmse1=sqrt(2.*xerr1/i)
      rmse2=sqrt(2.*xerr2/i)
      enr1=20.*alog10(rmse1/rmsn)
      enr2=20.*alog10(rmse2/rmsn)
      write(6,52)rmse1,rmse2,rmsn,enr1,enr2
52    format(1x,'rms error=',2f10.6,2x,'rms noise=',f10.6,2x,'enr='
     1                                                    ,2f8.3)
      call exit
      end
```

Program SCHUR

```
      dimension a(50),rho(50),d(50)
      complex u1(1025),u2(1025),d1(1025),d2(1025),temp1,temp2
c     set ic=0 to skip forward part; read from device #7.
c     set ic=1 to generate forward response and then solve from it.
      read(5,10)n,m,dd,del,df,p1,p2,ic
10    format(2i,5f,i)
      read(5,20)(a(i),rho(i),i=1,n)
20    format(2f)
      write(6,21)n,m,dd,del,df,p1,p2
21    format(1x,'n=',i2,'m=',i2,'dd=',f4.2,'del=',f4.2,'df=',f5.3,
     +'p1=',f4.2,'p2=',f4.2)
      do 1 i=1,n
1     d(i)=dd
      pie=3.1415926536
      m2=2**m
      if(ic.ne.0)go to 53
      read(7,52)(u1(i),u2(i),i=1,m2)
      go to 54
53    do 2 i=1,m2
      freq=freq+df
      call recopp(n,a,rho,d,p1,freq,u1(i))
      call recopp(n,a,rho,d,p2,freq,u2(i))
      d1(i)=cmplx(1.,0.)
      d2(i)=cmplx(1.,0.)
      tau1=0.
      tau2=0.
      write(7,52)u1(i),u2(i)
52    format(1x,4f10.4)
2     continue
54    ac1=a(1)/sqrt(1.-a(1)*a(1)*p1*p1)
      ac2=a(1)/sqrt(1.-a(1)*a(1)*p2*p2)
      z1=rho(1)*ac1
      z2=rho(1)*ac2
      write(6,51)
51    format(3x,'depth',6x,'cact',5x,'ccomp',4x,'rhoact',3x,'rhocomp'
     +'rc1',9x,'rc2')
      do 3 i=1,int(dd/del*n)+5
      dep=dep+del
      tau1=tau1+del/ac1
      tau2=tau2+del/ac2
      sum1=0.
      sum2=0.
      omes=0.
      do 4 j=1,m2
      omes=omes+2.*pie*df
      temp1=d1(j)*cexp(-cmplx(0.,omes*del/ac1))-cmplx(r1,0.)*u1(j)
      temp2=d2(j)*cexp(-cmplx(0.,omes*del/ac2))-cmplx(r2,0.)*u2(j)
      u1(j)=u1(j)*cexp(cmplx(0.,omes*del/ac1))-cmplx(r1,0.)*d1(j)
      u2(j)=u2(j)*cexp(cmplx(0.,omes*del/ac2))-cmplx(r2,0.)*d2(j)
      d1(j)=temp1
      d2(j)=temp2
      sum1=sum1+real(cexp(cmplx(0.,omes*tau1))*u1(j))
      sum2=sum2+real(cexp(cmplx(0.,omes*tau2))*u2(j))
4     continue
```

```
      r1=sum1/m2
      r2=sum2/m2
      z1=z1*(1.+r1)/(1.-r1)
      z2=z2*(1.+r2)/(1.-r2)
      u=z1*z1/z2/z2
      ac=sqrt((u-1.)/(u-p2*p2/p1/p1))/p1
      ac1=ac/sqrt(1.-ac*ac*p1*p1)
      ac2=ac/sqrt(1.-ac*ac*p2*p2)
      rhoc=(z1/ac1+z2/ac2)/2.



      l=min0(int(dep/dd)+2,n)
      write(6,50)dep,a(1),ac,rho(l),rhoc,r1,r2
50    format(1x,f7.2,6f10.4)
3     continue
      call exit
      end
      subroutine recopp(n,a,rho,d,u,freq,rpp)
      dimension a(n),rho(n),d(n)
      complex rpp,ni,nip,roi,roip,m21,m22,e2,e1,e
      d(1)=0.
      pi=3.1415926536
      omega=2.*pi*freq
      om2=omega*omega
      xk=omega*u
      xk2=xk*xk
      m22=cmplx(1.,0.)
      m21=cmplx(0.,0.)
      do 170 j=1,n
      i=n-j+1
      ars=om2/(a(i)*a(i))-xk2
      if(ars.gt.0.)ni=cmplx(sqrt(ars),0.)
      if(ars.le.0.)ni=cmplx(0.,-sqrt(-ars))
      roi=cmplx(rho(i),0.)
      if(i.eq.n)go to 171
      e1=nip*roi
      e2=ni*roip
      e=cexp(ni*cmplx(0.,2.*d(i)))
      e1=e1*(m21+m22)
      e2=e2*(m21-m22)
      m21=e1+e2
      m22=e*(e1-e2)
      rmax=cabs(m22)
      rm=cabs(m21)
      if(rm.gt.rmax)rmax=rm
      e1=cmplx(1./rmax,0.)
      m22=m22*e1
      m21=m21*e1
171   nip=ni
      roip=roi
170   continue
      rpp=-m21/m22
      return
      end
```

```
      subroutine fft(x,m)
      complex x(1024),u,w,t
      n=2**m
      pi=3.1415926536
      do 20 l=1,m
      le=2**(m+1-l)
      le1=le/2
      u=cmplx(1.,0.)
      w=cmplx(cos(pi/float(le1)),sin(pi/float(le1)))
      do 20 J=1,le1
      do 10 i=J,n,le
      ip=i+le1
      t=x(i)+x(ip)
      x(ip)=(x(i)-x(ip))*u
10    x(i)=t
20    u=u*w
      nv2=n/2
      nm1=n-1
      j=1
      do 30 i=1,nm1


      if(i.ge.J)go to 25
      t=x(J)
      x(J)=x(i)
      x(i)=t
25    k=nv2
26    if(k.ge.J)go to 30
      J=J-k
      k=k/2
      go to 26
30    J=J+k
      return
      end
```